NASA-TM-108002

P. 387

Space Life Sciences Symposium:

Three Decades of Life Science Research in Space

(NASA-TM-108002) SPACE LIFE SCIENCES SYMPOSIUM: THREE DECADES OF LIFE SCIENCE RESEARCH IN SPACE Abstracts only (NASA) 387 p

N93-70388

Unclas

Z9/51 0124706

Washington, D.C.
June 21–26, 1987

Abstracts

Sponsored by:
Office of Space Science and Applications
National Aeronautics and Space Administration
Cosponsors:
Aerospace Medical Association
American Astronautical Society
Baylor College of Medicine
National Institutes of Health
Universities Space Research Association

DEDICATION

Philip C. Johnson, Jr., M.D.
1924—1987

The sudden death of Phil Johnson on May 24, 1987, leaves a void in the hearts of his friends and colleagues as well as in the NASA Life Sciences Program. As Chief Scientist of the Medical Sciences Division at Johnson Space Center, Phil's biomedical research spanned the Gemini, Apollo, Skylab and Shuttle programs. Author of more than 200 scientific publications and recipient of numerous awards, his work toward a better understanding of man's adaptation to the space environment represents a significant contribution to science. In the present symposium, he was the author of two papers and was to have chaired the Immunology and Hematology panel. As a teacher, a physician, and a friend, he will be sorely missed by all. We respectfully dedicate this volume to his memory.

Organization of the Abstract Volume:

The volume is divided into two sections: Poster Sessions and Parallel Sessions. Within the Poster division, abstracts are grouped according to discipline and within the discipline are grouped alphabetically by the first author. In the Parallel division, the grouping is first by the day of the week, then by discipline sessions, then by first author.

Changes made after the Abstract volume went to press may result in differences between the Abstract volume and the Program; in these cases the Program should take precedence. In some cases, what was to be a session for oral presentation was revised to become a Panel discussion. If the participants had already submitted an abstract, those abstracts are included herein in order to familiarize the reader with the individual's recent research.

Finally, abstracts received after the volume was already assembled appear in a supplementary section at the end of the book.

Table of Contents

Poster Sessions:

BIOSPHERICS 2
CELSS 8
EXOBIOLOGY 28
SPACE BIOLOGY 38
SPACE BIOMEDICINE 59

Parallel Sessions:

CALCIUM AND BONE PHYSIOLOGY I 140
CARDIOPULMONARY PHYSIOLOGY I 142
DECOMPRESSION SICKNESS 148
IMMUNOLOGY AND HEMATOLOGY (PANEL) 156
MUSCULOSKELETAL SYSTEM 160
SPACE STATION ENVIRONMENTAL FACTORS 178
CELL BIOLOGY (PANEL) 184
MICRO-G: UNDERSTANDING G-RECEPTORS (PANEL) 192
CARDIOPULMONARY PHYSIOLOGY II (PANEL) 198
FLUIDS AND ELECTROLYTES (PANEL) 202
NEUROSCIENCE I 204
NEUROSCIENCE II (PANEL) 216
PLANTS AND GRAVITY I (PANEL) 224
PLANTS AND GRAVITY II (PANEL) 224
CALCIUM AND BONE PHYSIOLOGY II 226
CREW FACTORS (PANEL) 234
LIFE SCIENCE AND THE SPACE STATION 240
SPACE STATION CREW FACTORS (PANEL) 244
BIOMASS PRODUCTION I 246
BIOMASS PRODUCTION II 256
EXOBIOLOGY I 260
EXOBIOLOGY II 270
HUMAN FACTORS I 286
HUMAN FACTORS II 296
CELSS SYSTEMS ENGINEERING 300
CELSS TECHNOLOGY 304
BIOSPHERICS I 314
BIOSPHERICS II 326
EXOBIOLOGY III 336
EXOBIOLOGY IV 346
BIOSPHERICS III 358
EXOBIOLOGY V 362
EXOBIOLOGY VI 378

Acknowledgments:

This volume represents the work of a large number of dedicated individuals and reflects the broad scope of research by the Life Sciences investigators from a variety of institutions. Their interest in participating in the conference and reporting on these important investigations is appreciated. The efforts of the Discipline Scientists at NASA Headquarters in organizing such broadly based activities into a coherent Symposium program are likewise acknowledged. Finally, the Symposium organizers wish to thank those responsible for the actual production of the volume: the staff at the Universities Space Research Association's Division of Space Biomedicine and the Lunar and Planetary Institute's Production Services Department.

Poster Sessions

CHARACTERIZATION OF THE THERMAL PROPERTIES OF PRESCRIBED WILDLAND FIRES USING THERMAL INFRARED REMOTE SENSING AND CORRELATION TO NUTRIENT MOBILIZATION DUE TO COMBUSTION

J. A. Brass[1], V. G. Ambrosia[2], and P. Riggan[3]
[1]*Ecosystem Science and Technology Branch, NASA/Ames Research Center, Mail Stop 242-4, Moffett Field, California 94035,* [2]*TGS Technology, Inc., NASA/Ames Research Center, Moffett Field, California 94035, and* [3]*USDA/Forest Fire Service, Riverside Fire Laboratory, Riverside, California*

The combustion of biomass during wildland fires plays an important mobilizing role in the earth's biogeochemical cycles. Fires are a major source of many tropospheric trace gases, but the cumulative extent of such contributions is not well known. The occurrence of fire also leads to increases in soil loss through erosion, to stream sedimentation, and to the conversion of organic material into loosely bound inorganic forms that are subject to leaching and surface losses by water and wind. The nutrients volatilized by wildland fires are redistributed to surrounding ecosystems and can act as an indirect source of fertilization. These and other effects of the combustion of biomass, and the ubiquitous extent of fire worldwide, make fire a very important process in global cycles of key elements such as nitrogen.

Emitted and reflected radiation related to physical characteristics of wildland fires and their fuels are determinants of the consequences of fire. The combustion temperature, rate of spread of the fire front and the duration of heating of the surface are related to (1) losses of vegetation cover and subsequent exposure to incident solar radiation, (2) production of surface ash and fixed carbon affecting the absorptivity of the surface, and (3) production of volatilization products, particulates and trace gases. Classification of fuel type and quantification of the amount of fuel, before and after the fire, are major determinants of the amount of organic material volatilized. Monitoring of the smoke plume during and following the fire are important to understand the effects on atmospheric and plume transmission, are related to the trace gas loadings, and to the downwind disposition of the plume material. These emitted thermal and reflected visible-infrared properties are amenable to measurement by remote sensing, especially if frequent data acquisition is possible during the fire.

A research effort to quantitatively measure and monitor the emitted and reflectance characteristics of fires and their fuels was conducted as part of a large cooperative research experiment in the chaparral ecosystems of the Los Angeles Basin. A large number of interested scientists and resource managers from the USDA/Forest Service, the U. S. Environmental Protection Agency, the California Department of Forestry, the California Air Resources Board, the University of Washington, UCLA, the Desert Research Laboratory and the Los Angeles County Fire Department were joined by scientists from NASA/Ames Research Center and Langley Research Center. Their combined efforts made the prescribed fire at Lodi Canyon in the San Gabriel Mountains north of the Los Angeles area the most intensively studied wildland fire in history. The prescribed fire was planned by the Angeles National Forest to reduce wildland fire hazards in the San Dimas Experimental Forest. They planned to burn up to 1200 acres of mature chaparral vegetation having a fuel loading of from 3.5 to 11 kg/m^2 (21 year old *ceanothus*). Using helitorches carried on helicopters, the fire was ignited on December 12, 1986. During the fire many different aircraft were sampling various characteristics of the plume, while overhead the NASA U-2 acquired data from the Daedalus Airborne Thematic Mapper (ATM) sensor, passing over the active fire every ten minutes. The ATM has two thermal channels with variable gain settings, one of which was set up for lower temperatures and the other for the expected high temperatures of the active fire front. A real time data link from the U-2 to the ground allowed the Ames scientists to demonstrate the potential for continuous fire behavior monitoring by displaying the thermal and other channels continuously on a color monitor located near the fire site.

Active fire front temperatures emitted enough radiation to saturate all near and middle infrared channels of the ATM. Because of this saturation, the highest temperature recorded was 400° C when

ground sensors recorded temperatures recorded temperatures of 750-800° C. The low gain thermal sensor did not saturate, but temperature measurements calculated from the thermal channels tended to be too low relative to those measured directly on the ground. We determined that the calibration of the thermal channels was non-linear, tending to become asymptotic at higher temperatures, and was not well represented by the fairly low temperature range standard carried onboard the scanner (up to 50° C). A black-body source with a large aperture and a range up to 1000° C is being investigated to permit a complete calibration before the next mission. The frequent repeat flights by the U-2 allowed us to develop a sequence of synoptic images in which the plume did not obscure the thermal features underneath and permitted the calculation of the rate and direction of fire spread. Previous knowledge of the spatial distribution of the fuel composition coupled with the rate of spread to determine fire duration and fire intensity has been related to the types and amounts of gases volatilized as measured by other researchers. The spectral properties of the ash layer after the fire have been related to both the intensity and the age of the fuel burned. Where the fire was particularly intense, the heated soils often stayed above ambient temperature for up to four hours (as determined by the ATM data). This long duration heating has been related to increased destruction of the biomass above and below ground and to the subsequent loss of nutrients through post-fire volatilization and to erosion.

These studies, still in their initial stages, have indicated the important role remote sensing can play in understanding the consequences of biomass combustion. Work is in progress to relate the emitted and reflective characteristics observed for the Lodi Canyon burn to the many other fire variables collected by the other investigators. The shortcomings of existing remote sensing systems, airborne or satellite, for quantitative monitoring of wildland fires have been examined. These data are also being combined with data from the NOAA Advanced Very High Resolution Radiometer, acquired on the same day, to evaluate those coarser resolution data as an eventual means to extrapolate observations globally. ■

EVALUATION OF ENVIRONMENTAL RESOURCES AT JOHN F. KENNEDY SPACE CENTER USING GEOGRAPHIC INFORMATION DATA MANAGEMENT AND REMOTE SENSING

C. R. Hinkle[1], M. J. Provancha[1], P. A. Schmalzer[1], J. A. Provancha[1], C. R. Hall[1], W. M. Knott[2], and A. M. Koller[2]
[1]The Bionetics Corporation and [2]NASA/KSC Biomedical Operations and Research Office, John F. Kennedy Space Center, Florida 32899

INTRODUCTION

The National Aeronautics and Space Administration in assuming responsibility for the management of John F. Kennedy Space Center (KSC) operations, must ensure that appropriate actions are taken to prevent, control, and abate all environmental pollution with respect to federal facilities and all activities under the control of the agency. Under the John F. Kennedy management instruction KMI 8800.6A (1979) the Biomedical Operations and Research Office (MD) has been charged with "investigating, interpreting, and predicting physical, chemical, and biological impacts on the surrounding environment for all KSC operations." In accordance with this directive, MD in conjunction with other government agencies, universities, and contractors has conducted over the past decade several baseline environmental surveys and ecological studies primarily designed to assess impacts of KSC operations. The data from the baseline studies have served as the basis for developing a long range Environmental Monitoring and Research Program to establish the capability and database necessary to meet the defined mission.

Central to the KSC long-range monitoring and research program has been the utility of remotely sensed data and geographic information management techniques. These techniques provide the information necessary not only to assess environmental impacts after the fact, but also to move toward the predictive mode of assessment before the fact. This paper describes a part of that effort specifically

related to the use of geographic information management for analysis of impacts to environmental resources.

PROJECT IMPLEMENTATION

The vegetation of the 56000 ha KSC reserve was mapped by photointerpretation of low altitude, false-color infrared imagery; ground reconnaissance included the establishment of 315 permanent vegetation sampling transects. Also aerial transects with a helicopter were used to verify mapped boundaries. A total of twenty-seven vegetation types and several resource categories were interpreted from the imagery, and these were digitized at a pixel resolution of 0.051 ha. The geographic information database has been used to produce variable-scale maps of resources (from single master-planning sheets at a scale of 1:9600 to composite maps at a scale of 1:63000) depending on user needs. The complete system will contain parameters that include watershed boundaries, storm water drainage, soil types, water quality data, habitat suitability information, and other ecological information for increasing the interpretive and predictive capability of the users for management, planning, monitoring, or research needs.

Future efforts will include the use of satellite and low altitude thematic mapper data (1) for comparison with low altitude infrared imagery for assessment of environmental resources, and (2) as a means to periodically update the geographic information database. The utility of these and other environmental data from KSC represents a valuable resource not only for local site management decisions, but also for the establishment of long-term ecological data for research purposes that have regional as well as global implications for understanding and evaluating environmental problems. ■

MALARIA, A VECTOR BORNE DISEASE, ADDRESSABLE BY REMOTE SENSING

L. Legters, B. Wood and P. D. Sebesta

[1]Department of Epidemiology, Uniformed Services University of the Health Sciences, Bethesda, Maryland 20814, [2]TGS, NASA/Ames Research Center, Moffett Field, California 94035, and [3]Ecosystems Science and Technology Branch, NASA/Ames Research Center, Moffett Field, California 94035

The World Health Organization (WHO) has defined the dramatic increase of the vector-borne disease, malaria, over the past decade. In 1982, WHO estimated 250 million malaria cases globally with 46% of the world's population living where malaria currently exists and an additional 18% living where malaria could exist. Worldwide it is estimated that some 92 to 98 million new cases occur annually (WHO 1986a; 1986b). The global problem of malaria has been called "one of the greatest scourges of mankind, possibly having killed more humans than any other infectious disease" (NASA CR-129822, 1972). The disease is spreading for two primary reasons. The disease burden is increasing and malaria is spreading geographically because malaria control resources are scarce and costly. In some cases the control programs have been interrupted due to prohibitive costs or changing governmental priorities. Underlying these major problems are difficulties imposed by insecticide resistance on the part of the malaria vectors and drug resistance on the part of the malaria parasites in the human blood stream. To date no effective vaccines are available. A predictive model of vector-borne disease driven by the timely supplied information from remote sensing instruments from aircraft and spacecraft will provide health scientists with the information about the potential for malaria outbreaks. This information will enable these scientists to more effectively use their scare and costly resources to reduce death and suffering. This will lead to higher productivity in developing nations. The need is immediate, the goals are obtainable, and the costs are modest. ■

REFERENCES

WHO. 1986a. WHO Expert Committee on Malaria. 18th report. Tech. Rpt. Ser. No. 735. World health organization, Geneva.

WHO 1986b. World malaria situation. 1984. Wld. Hlth. Statis. Quart. 39: 171-205. World health organization.

Public Health Applications of Remote Sensing of the Environment, Univ. of Texas, 1972, (NASA CR-129822).

A COMPARISON OF RELATIONSHIPS BETWEEN LEAF AREA INDEX AND THEMATIC MAPPER DATA ACROSS THREE REGIONS OF THE WESTERN U. S. CONIFEROUS BIOME

D. L. Peterson[1], S. W. Running[2], M. A. Spanner[3], and L. Pierce[2]
[1]*Ecosystem Science and Technology Branch, NASA/Ames Research Center, Mail Stop 242-4, Moffett Field, California 94035,* [2]*School of Forestry, University of Montana, Missoula, Montana,* [3]*TGS Technology, Inc., NASA/Ames Research Center, Moffett Field, California 94035*

Theoretical considerations of radiation transport in plant canopies predict that variations in the leaf area index (LAI, one-sided leaf surface area projected per unit ground area) would be uniquely related to spectral reflectance of solar radiation. For example, there should be a positive relationship between LAI and near infrared reflectance due to strong scattering by the leaves in the canopy. Conversely, there should be a strong inverse relationship between variations in LAI and reflected red and shortwave infrared radiation, regions of absorption by chlorophyll and foliar water respectively. Furthermore, ratios of measurements made in these spectral regions contrasting an absorption and a scattering phenomenon, such as the ratio of near infrared to red reflectance, should be positively related to LAI. These relationships have been consistently observed in crop and grass canopy studies. The research reported here summarizes the relationships between the LAI of temperate coniferous forests from throughout the western United States and data acquired from the Thematic Mapper on the Landsat satellite.

Seventy-three forest plots from three regions of the western U. S. coniferous biome were measured on the ground and the measurements were used with allometric equations based on the tree diameter at breast height to estimate LAI. The observed range in LAI is from 0.6 to over 16 with almost a continuous variation in between. Plots were placed across west-central Oregon, in Sequoia National Park in the southern Sierra-Nevada Mountains of California, and the Seeley-Swan Basin of the northwest Montana Rockies.

A systematic protocol using lake radiances and simulation codes for atmospheric scattering were used to reduce the effects of additive path radiance and transmission which differed between the three regions. After these corrections to the data, the remaining effects of differences in solar zenith angle and topographic slope and aspect were removed from each data point.

The earlier analyses of data from the Oregon transect contained several surprising results. That study attempted to develop a data set with a large range in LAI (0.6-15.4 m^2/m^2) while maintaining a closed canopy condition. In that way, variations due to background could be minimized while insights could be gained about the overstory. Atmospheric effects were systematically removed by spectral measurement of targets near the surface coordinated with the same from the aircraft (Spanner, *et al.*, 1984; Running, *et al.*, 1986). Consistent with physical expectations, the reflectance measured in the red region was inversely related to LAI but the asymptote for this log-linear relationship was much higher, about LAI = 6-8, than expected. Contrary to physical expectations, virtually no relationship was found between LAI and the near infrared reflectance; the infrared signal was practically constant across this LAI range. However, a strong positive relationship was found between LAI and the ratio of the near infrared and red bands, the 4/3 ratio. This was explained by the strong inverse relationship of band 3 and the co-variation of bands 3 and 4 at higher LAI values. The log-linear relationship explained 91% of the variation and was slowly asymptotic at about LAI = 8-10, higher than expected. The atmospheric correction changed the slope of the relationship by three-fold and improved the sensitivity of the relationship by about 40% (Peterson, *et al.*, 1987).

Research at Sequoia National Park involved several additional tasks not required in Oregon. First, allometric equations relating diameter at breast height (DBH) or sapwood basal area (SBA) to other physical characteristics of the two fir species, *Abies magnifica* (red fir) and *A. concolor* (white fir), did not exist. Twenty-four trees across the expected diameter range were felled in nearby Sequoia National Forest (part of a harvesting plan) and were carefully measured for many properties. Allometric equations were developed (Westman and Rundel, 1987) to permit the estimation of LAI and other tree characteristics from individual field tree measurements. The analysis of a large data set acquired by Nate Stephenson of Cornell University for a gradient analysis of the Park was used to explore the

Thematic Mapper data for the Park. Variations in canopy closure were determined to be the major source of variation in the radiance data and the relationships were somewhat insensitive to community type. An inverse relationship was found between total basal area of the sampled plots and the ratio of the TM bands 5 to 4, the shortwave (1.55 microns) and near infrared. Twenty-nine new plots were sampled in Sequoia covering the entire range of LAI conditions encountered there (1-11.4).

An additional 28 plots were sampled in Montana with an LAI range of 1-11.3. Many of the same species are encountered in Montana and Oregon, but the distribution tends toward *Pinus contorta* (lodgepole pine), *Pseudotsuga menzeisii* (Douglas fir) and *Larix occidentalis* (western larch). The Lodgepole pine stands can carry a low LAI under very dense closed canopy conditions.

The analysis of the combine data sets from Oregon, Montana and Sequoia have refined our interpretations of the LAI and radiance relationships at a regional scale. The inverse relation between the red region and LAI (also, between the shortwave infrared and LAI) is asymptotic at about an LAI = 4. This result is more in line with experimental results from other plant canopies and with theoretical expectations. There is greater variability in the data which is primarily due to variations in canopy closure with widely different background conditions (from grass and brush understories to bare granite and dark forest floor litter layers). As the canopy closure decreases, the reflectance signal generally increases because nearly all background conditions in the red are brighter than the highly absorbing overstory foliage. For example, for a series of eight plots in Sequoia of roughly the same LAI = 7-8, there was a consistent increase in red reflected radiance (from 0.4 to 1.4 mW/cm^2-st-micron) as the canopy closure decreased from greater than 90% to 25-50% exposing more of the bright granite and darker litter material.

The combined data for the near infrared radiance values indicated that there was no general apparent relationship with LAI. The radiance values varied from 4 to 10 mW/cm^2- ster-micron. However, when only the 11 plots with a consistently determined closed canopy condition (>90%) were examined, a strong positive relationship was found. Only by combining plots from all three regions could we satisfy both a closed canopy condition and still produce a range in LAI values from 2.7 to 15.4. The linear regression explained 84% of the variance. The remaining plots had canopy closures that varied from less than 25% to 89%. The trend in these remaining plots was opposite to the >90% positive relationship. There are four general classes of overstory/canopy closure/background in the remaining data. Many of the plots from Sequoia that fell below the >90% regression line are characterized as old growth stands with very large overstory trees and a sparse understory or heavily shadowed grey background. Several stands from Montana were comparable to these and were also below the line. More open canopies with generally lower leaf area indices tend to have higher values of infrared reflectance than the >90% line. These plots included a number of plantations and were characterized by bright backgrounds and understory of brush or grasses. Two plots from Oregon of intermediate LAI contained a significant proportion of broadleaf trees which contributed to an elevated infrared signal. These results indicate the importance of determining canopy closure and background conditions in conifer forests so that a protocol can be developed to remove the background effects from the infrared signal.

Various band combinations have been examined including the infrared/red ratio and the normalized difference of the infrared and red bands. There is a positive relationship between LAI and the 4/3 ratio, but the scatter in the data is greatly increased over the Oregon results. When only the closed canopy plots are considered, the relationship is strongly positive, becoming asymptotic at about LAI = 8-10. The scatter in the entire data set tended to mimic the relationships found in the near infrared data. These data confirm the high variability in forest data at the scale of the Thematic Mapper (30 × 30 m), whereas the Oregon data represent the average of four plots over an entire stand for each point. When data are aggregated over several points or over geographic proximity, the variance in the 4/3 ratio and LAI relationship is reduced substantially. Normalized difference values tend to reach an asymptotic value of about 0.8 at LAI = 5-6. This value is about 0.3 higher than values recorded for uncorrected TM data and equivalent to values for broadleaf canopies. Thus, methods using the integrated normalized difference vegetation index over the growing season would generally underestimate the true value by about 40% if the data are not corrected.

This research has shown that variations in coniferous forest LAI at regional levels is related to canopy reflectance of solar radiation in the visible and infrared regions. However, one needs to know more than

just the value of the LAI to interpret the data. Variations in background and canopy closure, and, atmospheric and terrain effects must be accounted for to explain across regional variations in the radiance data of the Thematic Mapper. Research is continuing in Montana to develop a consistent method to account for these variations. ■

PROJECT DI-MOD (PREDICTIVE MODELING OF VECTOR-BORNE DISEASE) PHASE I, CALIFORNIA

R. K. Washino, B. Wood, and P. D. Sebesta
[1]*Department of Entomolgy, University of California, Davis, California 95616,* [2]*TGS, NASA/Ames Research Center, Moffett Field, California 94035, and* [3]*Ecosystems Science and Technology Branch, NASA/Ames Research Center, Moffett Field, California 94035*

In California, a single malaria vector, *Anopheles freeborni* is found throughout much of the state. At the present the Plasmodium phase of the transmission cycle is absent. However, this does not inhibit studying the vector or developing a model of vector population dynamics. The existence of field data over the past decade combined with NASA overflights over the same study area of northern California has provided a unique opportunity for undertaking research into data integration and predictive disease model development. During 1985, aircraft-based remotely sensed data was coordinated with field investigations by researchers from the University of California at Davis (UCD) over a portion of the study area on a weekly basis between June and October of 1985. A key objective has been to identify the relationship between the anopheline population dynamics in rice fields and the environmental variables which have been studied by researchers at UCD. The second objective has been to show which of these environmental variables can be remotely sensed and can provide quantitative indicators of future anopheline mosquito populations. Preliminary results show direct positive correlations between specific vegetation reflectance characteristics of rice fields as detected by a thematic mapper simulator (TMS) from NASA'S's ER-2 aircraft and anopheline larval counts as documented by field research teams from UCD. The primary focus of Phase I will be the development of a predictive model of vector population dynamics for the rice-growing region in California. This model can then be applied as a bridge to the goals of DI-MOD Phase II which will utilize NASA technology to study and model environmental variables that influence the prevalence and distribution of endemic malaria vectors in tropical and subtropical regions. The Phase II model could possibly be driven from data collected from the NASA Space Station which orbits over 90% of the world's endemic malarial regions or be monitored by co-orbiting and polar orbiting platforms. ■

MANAGEMENT STRATEGIES UNDER UNCERTAINTY: A DEMONSTRATION OF LFGG ROBUST CONTROL IN A CELSS SCENARIO

A. L. Blackwell, C. C. Blackwell, R. Kila, and T. Vecera
Department of Mechanical Engineering, The University of Texas at Arlington, Arlington, Texas

The economic advantage of utilizing a life support system that consists, at least partially, of a bioregenerative system has been demonstrated for several manned missions planned by NASA for the next several decades [4]. This advantage was estimated from the costs of initially launching the system payload and subsequently transporting the payloads for resupply of the life support system. The control system algorithm for a bioregenerative life support system (BLSS) is realized with a suitably selected and organized system of components with appropriately matched dynamic properties. Proposed designs comprise a system of processors, material storage reservoirs, and set-point controllers (regulators) [6, 8]. The sizing of some of these components, and consequent payload mass launch and transportation cost advantage, is dependent in part upon the excess capacity needed to accommodate variations in the dynamics of such a system about the designed operating points.

Several models and computer simulations of a BLSS have been developed for the purpose of investigating the dynamics of its operation [1, 6, 8]. These studies have included: investigations of system operation under various nominal operating conditions, system operation under uncertain conditions, and system operation under component failure. The most complex BLSS simulation model [6] describes the dynamics of a completely closed system, tracking the flows and transformation of Carbon, Hydrogen, Oxygen, and Nitrogen throughout the CELSS. The system model consists of five processors, nine storage reservoirs, and seven set-point controllers with separate atmospheres for the plant growth module and for the crew compartment.

It has been noted that management strategies developed for biological resource systems, a class of systems which include a BLSS, should be designed to accommodate the inevitable uncertainties which exist in our knowledge of the processes and parameters which govern the system dynamics [2]. For a BLSS, these basic uncertainties may be augmented by additional variations in the functional response of the biological components caused by exposure to elements of the extraterrestrial environment. This variation may result in deterioration in performance of the control system to less desirable or unacceptable levels of deviation from the system set-points. Further, it is likely that only very limited data will be available to describe the altered functional response of the components.

In recent years, research has been focused on the development of control strategies which produce system performance robust to uncertainties in disturbances, parameters, dynamics, and/or functional forms of the model of the components of the system, where only the possible sizes of these variations are known. One of these, the Lyapunov Function Gradient Generated (LFGG) robust control theory guarantees "practical stability" if certain conditions are satisfied. This means that we are assured of the existence of a control strategy, which is a function of the system state, and which will drive the system state into and maintain it within an acceptable region of the nominal (undisturbed) equilibrium state, regardless of the time history of all combinations of the uncertainties. The utility of the theory has been illustrated for control of models of economic and ecological as well as engineering systems [3, 5 and references therein, 7] and has been demonstrated in laboratory systems.

In this presentation, the results of the application of LFGG robust control to a highly simplified version of the BLSS model described in [6] are described. We have adapted a portion of that model, generously provided to us by the authors, to explore the application of the theory to a CELSS scenario and to illustrate the performance of the system using the LFGG robust control. ■

REFERENCES:
1. Averner, M.M. 1981. An approach to the mathematical modelling of a controlled ecological life support system. NASA CR-166331.
2. Blackwell, A.L. 1987. Examination of institutional structures in multiple resource, multiple management systems: A control theoretic approach. In T.T. Vincent and J.M. Skowronski, eds. Modeling and management of resources under uncertainty. Lecture Notes in Biomathematics, Springer-Verlag, NY. (In press)
3. Corless, M., and G. Leitmann. 1985. Adaptive long-term management of some ecological systems subject to uncertain disturbances. p3-29 in G. Feichtinger, ed. Optimal Control Theory and Economic Analysis 2. Elsevier Science Publishers B.V. (North Holland). 664 p.
4. Gustan, E., and T. Vinopal. 1982. Controlled ecological life support system: Transportation analysis. NASA CR- 166420.
5. Lee, C.S., and G. Leitmann. 1983. On optimal long term management of some ecological systems subject to uncertain disturbance. Int. J. System Science 14(8):979.
6. Rummel, J.D., and T. Volk. 1986. A modular BLSS simulation model. Adv. in Space Res. (In press)
7. Schapiro, S., and R. Lamberson. Determination of an optimal harvesting policy for a discrete logistic population model with environmental uncertainties. Unpublished manuscript.
8. Stahr, J.D., D.M. Auslander, R.C. Spear, and G.E. Young. 1982. An approach to the preliminary evaluation of closed ecological life support system (CELSS) scenarios and control strategies. NASA CR-166368.

CONCEPTS FOR A COMMERCIAL SPACE-BASED PLANT GROWTH UNIT

R. J. Bula, R. B. Corey, S. J. Volkweiss, and T. W. Tibbitts
Wisconsin Center for Space Automation and Robotics, University of Wisconsin, 1357 University Avenue, Madison, Wisconsin 53706

The NASA-sponsored Center for Space Automation and Robotics, University of Wisconsin-Madison, is involved in the development of a commercial, automated, space-based plant growth unit that could become a component of a CELSS. This is one of three currently active projects of the center. The plant growth unit, as currently planned is being conceptualized around the requirements needed to provide continuous production of potatoes over an area of 10 m^2 (plant production from this area would provide one-half the daily caloric requirement per person). The intent is to develop concepts that are sufficiently generic in nature that the plant growth unit could be adapted for growing other higher plant species and be effectively scaled up to a size that would support a crew of 6 to 8 people.

Commercial organizations will be involved in translating these concepts into designs and hardware construction. Such organizations will thus be involved in the subsystem or component development, flight-testing of these components, construction of space-based demonstration units, and eventually construction of operational plant growth units.

This project is directed toward conceptualizing a total plant growing system that involves 11 subsystems as shown in Figure 1. Major effort will be directed toward subsystems with technological requirements that have not been previously elaborated. This includes principally those subsystems that are critical to sustaining plant growth in space. From the group shown in Figure 1, the subsystems that will receive major attention will be the plant culture, nutrient supply, irradiation, sanitation and automation and robotics.

Initial activity of this project has been directed toward development of concepts for the plant culture and nutrient supply subsystems. This report will discuss the current status of concepts for these systems. A major constraint in the conceptual development of the plant growth unit has been that the

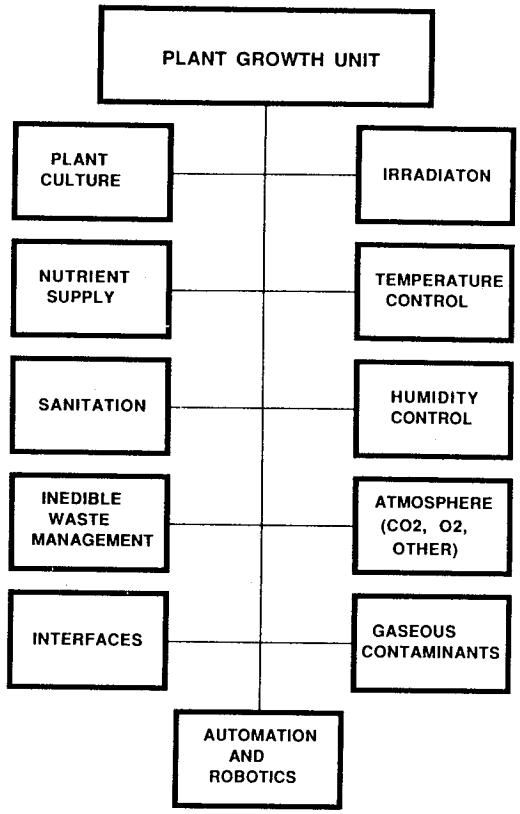

Figure 1. Subsystems of a space-based plant growth unit.

space environment would necessitate operation of the unit under conditions of microgravity or weightlessness (MacElroy *et al.*, 1985). This space environmental condition imposes a critical requirement on concepts that may be proposed for supplying nutrient solution to the plant roots. Unique technologies will need to be used to provide adequate aeration under weightlessness for maintenance of effective root functioning (Wright, 1984).

We are proposing to use a rooting medium in contact with a solid porous material, such as stainless steel, surrounding a cavity through which the nutrient solution would be circulated. The nutrient solution would be circulated under suction through the cavity surrounded by the porous material. The suction would be at a level that would leave the large pores of the rooting medium filled with air, but enough of the smaller pores filled with solution to maintain hydraulic conductivity sufficient to replace water removed by the plants. Under these conditions, the plant root zone would be in a non-saturated condition thereby providing aeration to the roots. Since the liquid would be under suction, it could not escape from the root zone into the atmosphere around the plants. The advantages of using stainless steel include: (1) no consumables involved since it could be cleaned and recycled, (2) sufficiently rigid to withstand the suction required to circulate the nutrient solution, and (3) porosity and pore size can be defined during fabrication and these characteristics maintained over an indefinite period of usage. The desired characteristics of the porous material such as pore size, porosity, and shape of the cavity are under study.

Maintenance of the proper ion concentrations in the nutrient solution is another important function required in an effective plant growth unit. We are proposing the use of ion-exchange materials for maintaining the correct concentration of ions in the nutrient solution as suggested by Corey and Combs (1987) and Checkai *et al.* (1987). The only analytical component required would be an electrical conductivity sensor for control of the total ionic strength of the nutrient solution. The ionic strength would be replenished from a reservoir containing the essential chemicals. Water lost from the nutrient solution through plant transpiration would be replaced from a water reservoir based on a volume

sensing device. The ion-exchange materials that provide the best long-term ion regulation for a space-based system will be selected from a number of materials presently under investigation.

The Wisconsin Center for Space Automation and Robotics provides a unique opportunity for bringing together various academic disciplines and commercial interests to design and construct plant growth units for use in space. We are certain that this Center can contribute new technology for CELSS development and at the same time contribute new technology for use in terrestrial systems. This work was performed in the Wisconsin Center for Space Automation and Robotics at the University of Wisconsin-Madison and supported in part by NASA under grant NAG-W975 and by a consortium of industrial sponsors. ■

REFERENCES:

Checkai, R.T., L.L. Hendricksen, R.B.Corey, and P.A. Helmke. 1987. A method for controlling the activities of free metal, hydrogen, and phosphate ions in hydroponic solutions using ion-exchange and chelating resins. Plant and Soil. (In Press).

Corey, R.B., and S.M. Combs. 1987. Control of nutrient concentrations in plant growth media. Plant and Soil. (In Press).

MacElroy, R.D., D.T. Smernoff, and H. Klein. 1985. Life Support systems in space travel. (Topical Session of XXVth COSPAR meeting, Graz, Austria). NASA CP-2378.

Wright, B.D. 1984. A hydroponic method for plant growth in microgravity. 35th Congress of the International Astronautical Federation. Lausanne, Switzerland, October 7-13, 1984.

EFFECTS OF STATIC VS. FLOWING ATMOSPHERES ON PLANT GROWTH IN THE SPACE SHUTTLE PLANT GROWTH UNIT

M. D. Cuellar and C. A. Mitchell
Department of Horticulture, Purdue University, West Lafayette, Indiana 47907

A non-flight-qualified version of the Plant Growth Unit (PGU) was used to conduct plant growth and gas analysis studies as a function of atmospheric turnover rate. The cavity of the PGU contained enough space to insert 6 atmospherically-separated plant growth containers (PGCs), although only the center 4 spaces were used due to a drastic reduction in irradiance from the fluorescent lamp bank in the PGU at the two end positions. The base of each 5 × 23 × 19-cm PGC was lined with rockwool substrate pre-soaked with half-strength Hoagland's no. 1 nutrient solution, pH 6.0.

Twelve uniform seeds of mungbean (*Phaseolus aureus* Rosb. cv. Berken) were planted among the rockwool fibers in each PGC before attaching the transparent lexan lid to the base. Plants were grown for 7 days from seeding at 26.0 ± 0.5°C and a continuous phytosynthetic photon flux (400-700 nm) of 105-115 μmol s^{-1} m^{-2} over the 4 center positions at the level of rockwool in the PGCs.

Shoots of mungbeans growing in a static atmosphere had the same fresh and dry weights as those growing in PGCs with atmosphere turning over at 1 liter h^{-1}, but stem length and specific water content of shoot tissues was much less in the static system. Leaves assumed a pronounced "droop" position in the closed chambers. Atmosphere flowing at 1 or 5 liters h^{-1} through a PGC enhanced stem length and leaf area but decreased node and internode diameter. Traps containing $KMnO_4$ or $Hg(ClO_4)_2$ within sealed PGCs negated many effects of atmospheric closure on growth. Ethylene gas was not present at detectable levels when 1-ml samples of the 2-liter PGC headspace atmosphere were taken after 7 days of plant growth. However, after release from trapping in a small volume of $Hg(ClO_4)_2$ for 7 days, enough C_2H_4 was recovered from PGCs containing plants to half-saturate the growth inhibition response of many plants and free C_2H_4 accumulated to that concentration ($\geq$ 0.1 μl l^{-1}) in the headspace. thus, $Hg(ClO_4)_2$ must have been a strong sink competing with rockwool, nutrient solution, chamber walls, and/or plant tissue in attracting C_2H_4 to the trap. Wherever C_2H_4 goes (or stays) in sealed PGCs, it is not detectable by direct headspace analysis but has physiological effects on the contained plants.

Even in the flowing-atmosphere mode, CO_2 level increased 1.7 to 4-fold in PGCs for the first 3 days following seeding, after which CO_2 declined for the duration of the 7-day growth period, reflecting the transition from net respiration to net photosynthesis during seedling development. Carbon dioxide level in sealed chambers approached what likely was the CO_2 compensation point at the very low PPF currently available in this system. Atmosphere turnover rates exceeding the maximum tested in this study (2.5 chamber volumes h^{-1}) would be required to prevent large swings in CO_2 content resulting from plant gas exchange, but might begin to dehumidify the headspace or desiccate the plant growth medium.

Use of unfiltered cabin air is not a viable option to ventilate individual PGCs in the Shuttle or Space Station because the high levels of CO_2 expected could be phytotoxic and might contain trace levels of volatile contaminants. The current version of PGU and subsequent generations should be designed with careful consideration for control of atmospheric composition as well as other major environmental parameters impacting plant growth.

Research supported in part by NASA grant NSG 7278. ■

IMPLEMENTATION OF THE CELSS BREADBOARD PROJECT

W. M. Knott
MD-RES, Life Sciences Research Office, Biomedical Operations and Research Office, John F. Kennedy Space Center, Florida 32899

INTRODUCTION

The CELSS Breadboard Project is NASA's first attempt to develop a functioning bioregenerative life support system at a scale sufficient to assess our capability to build and operate such a system given current technology. The primary module being developed at this time is for biomass production using primarily higher plants. A modified 7.5 m × 3.5 m steel hypobaric chamber is the focus of this effort and will function as the atmospherically sealed biomass production facility for this project. Environmental control, nutrient delivery, condensate water recycling, and atmospheric control subsystems are being designed and/or constructed as part of this chamber facility. The Biomass Production Chamber (BPC) is currently being evaluated for basic environmental control and plant growth capabilities, and designs are nearly complete on nutrient delivery and atmospheric subsystems to be installed during July and August of this year. The BPC is scheduled to be thoroughly baselined in late 1987, with and without plants, and crop research will be initiated the first of 1988. Initial crop studies will last for at least two years, at the conclusion of which the chamber will be enhanced (based on operational results) to improve its biomass production capacity.

PROJECT IMPLEMENTATION

The effort required to construct the BPC was organized according to approaches used for most NASA construction projects. Several NASA and contractor organizations were involved: the Engineering Development Directorate as the primary design group, the Biomedical Operations and Research Office as the user, several support contractors that work for one or the other of these two directorates, and scientific experts outside the NASA organization assisting in the development of design requirements. Drawings and requirement documents were developed, design reviews were held at specified intervals, and construction was completed through a combined effort of contractor and NASA personnel. The operational philosophy impressed upon this team required that the facility be continuously evolving and that the initial configuration was only the start, not the finish.

Implementation of the research and technology development aspects of this project have followed a similar approach to that used for construction. Considerable effort had been spent in developing an expert work force along with methods to grow plants in a manner compatible with hydroponic subsystems applicable to growing plants in space. Research and technology development are conducted in conventional plant growth chambers or in laboratories. Areas of emphasis have included

nutrient maintenance, germination techniques, and plant support and nutrient delivery equipment; future direction will be toward robotics, instrument monitoring, and expert interactive controls. Tasks required to prepare each new crop for inclusion in the BPC will be conducted in a similar manner throughout the life of the project.

Food processing and the waste management modules will be evaluated as laboratory activities conducted in association with the BPC. The modules will be sized to satisfy the requirements of the biomass production module. Mass and energy fluxes through each of these modules will be monitored and evaluated continuously. Even though these modules will not be atmospherically united with the BPC, their operation will yield data required to design a human- tended facility that will have all three modules within a common atmosphere. The construction of such a facility, the next major step in the CELSS Program, is scheduled for mid- 1990.

The Breadboard Project has introduced into the CELSS Program a goal-oriented approach with definite deliverables produced according to a designated schedule. Applied objectives are being addressed by an in-house NASA/contractor team that will continue to expand in numbers and expertise as the CELSS Program grows. Such an in-house team, working in parallel with research groups extramural to NASA, is essential to the completion of a CELSS that will sustain humans in space during long periods of habitation in a cost effective and timely manner. ■

EFFECTS OF CLOSURE ON NATURAL ECOSYSTEM STRUCTURE AND DYNAMICS

B. Maguire, Jr.
Department of Zoology, The University of Texas at Austin, Austin, Texas 78712

INTRODUCTION

When major portions of ecosystems can be isolated from the remainder of the world, both biologically and with respect to material flows, tools of considerable power towards gaining better understanding of ecosystem function may be provided. In any practical enclosed ecosystem, except for those which are both naturally isolated and very simple (as in endolitic microbial systems, especially those of Antarctica), closure always results in the exclusion of some species populations (especially when some species are large or particularly demanding of environmental resources). These exclusions may affect the function of the system, but appropriate choice of system (and perhaps manipulative substitution for these effects) can eliminate or ameliorate the problem.

The kinds of ecological dynamics which are most effectively approachable through the use of enclosed natural ecosystems can roughly be divided into 4 groups:

1. Those which require closure-excluded (or reduced) physical dynamics (wind, for example), and/or "buffering" pools of needed materials which are larger than those within the enclosure (carbon dioxide, for example). The importance of these physical dynamics and pools can be qualitatively and quantitatively evaluated by the provision of the excluded component(s) at appropriate levels.

2. Those which involve larger scale ecological dynamics than are includable in an enclosure, but dynamics which can be experimentally imposed on or simulated in enclosed ecosystems. For example, many of the results of predation, competition, dispersal, and so on, can be especially effectively observed as these are experimentally set at various levels by manipulation; resultant effects on the dynamics and structure of the enclosed natural ecosystems then are observed.

3. When the stochastic interactions between the larger world and an ecosystem are reduced to the minimum provided by closure, subsequent control of the levels of environmental factors, and control of inputs and outflows of matter and energy between the system and the rest of the world provide powerful tools. These can be used to study the internal dynamics of the ecosystems, the responses of ecosystems to various levels of natural environmental conditions, and/or to the effects of toxins and other "unnatural" perturbations.

4. Enclosed ecosystems provide the only tools with which to determine, both qualitatively and quantitatively, what minimal interchanges of matter and energy are required between a (piece of an) ecosystem and the remainder of the world if the normal function of that ecosystem is to be sustained.

Fundamental characteristics of enclosed ecosystems which will interact to affect their postclosure dynamics and structure include especially (a) enclosure size, (b) the physical and chemical characteristics established initially in the enclosure, (c) the nature of the ecosystem (portion) which is enclosed, and (d) biological and physico-chemical manipulations following closure. Very few experiments on really enclosed ecosystems have been carried out because of the difficulties in achieving reasonable postclosure longevity and normality.

Only Maguire and Folsome and his students have reported quantitative results from long-term observations of completely closed (portions of) ecosystems. Maguire's 1980 data concerned the great effect of size of enclosed (glass sealed) aliquants of the microscopic (micro-crustacea and smaller) part of 3 different aquatic communities (two of which had very few larger members of the "entire" ecosystem than the micro-crustacea). In addition to the great increase in rate of the disappearance of micro-crustacea from the systems as a function of decrease in aliquant size, there was a very large effect of the nature of the community which was enclosed. Micro-crustacean activity ceased fairly rapidly in enclosed ecosystems from a sewage stabilization pond, moderately rapidly in those from a small permanent pond, and very slowly from those from an isolated, ephemeral pool (all of these are freshwater systems). Kearns and Folsome (1981), Takano, Folsome, and Karl (1983), and Obenhuber and Folsome (1984) observed that marine, mostly prokaryotic (partial) ecosystems developed and maintained above-atmosphere levels of oxygen for up to 8 years, that ATP tended to increase and to oscillate with a period of about 50 days in these systems, and that the eukaryote/prokaryote ratio also increases after closure.

Botkin *et al* (1979), Slobodkin *et al* (1980), and Maguire *et al* (1980) discuss theoretical aspects of ecosystem closure, its problems, advantages, and suggest descriptors for them.

MATERIALS AND METHODS

Data reported below were derived from two experiments in which fresh water aquatic communities were enclosed to different degrees and subjected to additional manipulation. In one experiment, nineteen 10- gallon aquaria were submersed except for about 5 cm "freeboard" in a pond (where light and temperature were very similar to what they were in the pond), and were filled with water from that pond; equal amounts of pond bottom sediment were added to each. Three were fertilized (N,P, and N+P) and sealed (glass top attached with silicone sealant), and half of the remaining aquaria were sealed closed while the other half were left open (2 cm "air spaces" were left between the top of these aquaria and the covering glass). Half of the aquaria were provided with a single fish as one of the inhabitants (small, equal sized males of *Gambusia affinis*), and all visible amphipods were removed from half and added equally to the other half of the aquaria. Four of the aquaria were broken during the April 11 to Aug. 12 experimental period (some of the sealed ones by explosion brought on by the thermal expansion of the contents which occurred during this period). The attempt to eliminate amphipods from half of the aquaria was not successful because, as we learned later, small individuals and/or eggs escaped our search. The data are number of taxa observed, number per liter, pH, and methyl orange and phenolphthalein alkalinity endpoints four months after closure.

In the second experiment, 250 ml of the natural communities of small fresh water aquatic organisms, micro-crustacea and smaller in size, from a sewage stabilization pond, from a small permanent pond, and from an ephemeral pond were placed in each of a number of 500 ml erlenmeyer flasks. Some were closed by melting the glass, others were tightly stoppered with neoprene stoppers, and the others were protected from infalling dust and from over-rapid evaporation by transparent polystyrene cups which were inverted over their tops. Some were fertilized and others not. One half of the flasks were placed in east windows where they received sunlight directly all morning, and the other half were placed in north windows which received direct sunlight for only very brief periods during the longest days of the year. The data presented are counts of number of taxa (of micro- metazoa, protozoa, and algae (including cyanobacteria) observed to be alive four years after the experiment was started.

RESULTS AND CONCLUSIONS

Summarized data (significant with the Wilcoxon T test) from the four month aquarium experiment are:

	Open aquaria	Closed aquaria	Signif.	Pond
mean # of taxa	38.0	30.7	$p<0.05$ 60	
mean # of organisms	404.3×10^6/L	134×10^6/L	$p<0.01$	753×10^6
mean pH	8.38	9.17	$p\sim0.05$	7.2
mean ml to endpoint - phenolphthalein	0.85	1.91	$p\sim0.01$	9.0
mean ml to endpoint - methyl orange	6.26	2.14	$p\sim0.01$	25.5

As can be seen from this table, there was considerable decrease in both number of taxa and number of individual organisms per ml in the experimental aquaria such that the open aquaria contained fewer than did the open pond, and the closed aquaria contained significantly fewer than those which were open to the atmosphere. This kind of decrease is very commonly observed following closure, and is, as illustrated here, more pronounced as the degree of closure is increased. The pond had the advantage that it had low but constant inflow of well water which had a pH of 6.8, and phenolphthalein and methyl orange alkalinities of 0.0 and 31.5, respectively. This reflects the higher carbon dioxide and bicarbonate levels of the well water, and shows that they are reduced, probably largely through photosynthetic uptake of the carbon dioxide. The progressively higher pHs and the changes in the alkalinity end points illustrate that as closure increased there was increased modification of the ecosystem's chemical characteristics (and lowering of carbon dioxide availability) by its biota. It well may be that this progressive decrease (from pond to open to closed aquaria) in level of carbon dioxide for photosynthesis is a major reason for the progressive decrease in the number of taxa and the number of individuals per unit volume which was observed. Counteracting this effect is one of the obvious next experimental steps to be taken.

In the other experiment reported here, 250 ml samples of communities, including organisms of the size of micro- crustacea and smaller, were kept in 500 ml erlenmeyer flasks which were placed about 10 cm from large east or north facing windows. They were in a heated, air conditioned building so that their temperatures were greatly moderated over what they would have been outside. These flasks were either sealed with a neoprene stopper, or by melting the flask's glass, or they had transparent dust cover, evaporation-inhibiting cups inverted over their tops. The communities represented were: BT, from the small permanent pond in which the above aquarium experiment was performed; WC, from a sewage stabilization pond (which periodically became anoxic so that there were no fish or other large organisms in it), and MF, from a shallow, rock-bottomed ephemeral pool. Only in BT were there normally larger organisms within the natural community (and in the aquarium experiment discussed above, the presence of a fish [in half of the aquaria] appeared to make little difference). The average numbers of still-living taxa after 4 years in this experiment (only eukaryotes and cyanobacteria were counted) are:

	Amt of closure	BT	ME	WC
E window	Glass seal	0.60	0.00	2.60
	Stopper	0.65	0.16	2.85
	Dust cover	2.40	3.00	1.75
N window	Glass seal	0.40	0.20	4.20
	Stopper	1.40	0.67	3.00
	Dust cover	1.52	4.00	2.83

It is clear that there was a statistically larger number of taxa surviving in the north than in the east windows. I surmise that this is because the light intensity was lower there, and therefore the ecosystems exposed to it could not drive themselves into fatal nutrient depletion as rapidly. In the BT and MF systems, there was a decrease in the number of surviving taxa with increase in degree of closure, but in WC, the situation was nearly perfectly the reverse. Rotifers were observed in 11 out of the 20 stoppered WC flasks, and not counting these rotifers, the average number of survivors was the same (2.45 vs 2.44). ■

REFERENCES

Botkin, D.B., B. Maguire, Jr., B. Moore III, H.J. Morowitz, and L.B. Slobodkin. 1979. Closed regenerative life support systems for space travel: Their development poses fundamental questions for ecological science. (COSPAR) Life Sciences and Space Research. 17:3-12.

Kearns, E.A. and C.E. Folsome. 1981. Measurement of biological activity in materially closed microbial ecosystems. BioSystems. 14:205-209.

Maguire, B. Jr. 1980. Some patterns in post-closure ecosystem dynamics (failure). pp. 319-332 in Microcosms in Ecological Research. J.P.Giesy, ed. Department of Energy, CONF-781101-15.

Maguire, B. Jr., L.B. Slobodkin, H.J. Morowitz, B. Moore III, and D.B. Botkin. 1980. A new paradigm for the examination of closed ecosystems. pp. 30-68 in Microcosms in Ecological Research. J.P. Giesy, ed. ibid.

Obenhuber, D.C. and C.E. Folsome. 1984. Eucaryote/procaryote ratio as an indicator of stability for closed ecological systems. BioSystems. 16:291-296.

Slobodkin, L.B., D. B. Botkin, B. Maguire, Jr., B. Moore III, and H. Morowitz. 1980. On the epistemology of ecosystem analysis. pp. 497-507 in Estuarine Perspectives. V.S. Kennedy, ed. Academic

Takano, C.T., C.E. Folsome, and D.M. Karl. 1983. ATP as a biomass indicator for closed ecosystems. BioSystems. 16:75-78.

ORBITAL LIGHT/DARK CYCLE EFFECTS ON PLANT GROWTH

R. C. Morrow, R. J. Bula, and T. W. Tibbits
University of Wisconsin-Madison, Madison, Wisconsin 53706

The direct use of solar irradiation for plant growth has often been proposed in designs of space station-based controlled ecological life support systems (CELSS). A potential difficulty exists for maintaining plants within these systems, for structures in low earth orbit (LEO) receive a light/dark cycle of only 90 minutes duration (60 minutes light and 30 minutes dark). Previous reports identify a variety of detrimental effects on plant growth when light/dark cycles have been shortened below the 24-hour terrestrial cycle. These include reduced dry matter production (1,2,3,4,5), reduced chlorophyll content (2,3,4,5), decreased stem elongation (3,4,5), and reduced leaf development (4,5). The most extreme effects were often observed with light/dark cycles similar to the LEO light/dark cycle. The purpose of this study was to determine the effects of this cycle on the growth of three CELSS candidate species: lettuce, wheat, and potatoes.

Three cultivars of lettuce, three cultivars of wheat, and four cultivars of potatoes (see Table 1 for cultivars) were grown in large controlled-environment rooms at the University of Wisconsin Biotron. The orbital (60/30) treatment consisted of 60 minutes of irradiance provided by cool white fluorescent lamps at a level of 400 $\upsilon mol\ s^{-1} m^{-2}$, followed by 30 minutes of darkness. The comparison treatment was a terrestrial (16/8) light/dark cycle, with 16 hours of light at 400 $\upsilon mol\ s^{-1} m^{-2}$ followed by 8 hours of darkness. Both treatments provided equivalent total irradiance over a 24 hour period. Plants were grown in peat-vermiculite and maintained at a temperature of 18°C and a relative humidity of 70 percent.

Lettuce plants harvested at 4 weeks showed a moderate reduction in total dry weight under the 60/30 cycle compared to the 16/8 cycle (Table 1). Of the three lettuce cultivars, Salad Bowl appeared to be

SPECIES AND CULTIVAR	TOTAL SHOOT DRY WT (g/plant) LIGHT/DARK CYCLE	
	16hr L/8hr D	60 min L/30 min D
Lactuca sativa - lettuce		
Waldmann's Green	5.42±0.77	3.74±0.92
Grand Rapids	2.59±0.32	1.88±0.57
Salad Bowl	3.34±0.68	3.14±1.15
Triticum aestivum - wheat		
Freemont	102.5±0.3	88.0±8.2
Yecora Rojo	82.4±4.8	86.5±9.4
Olescens Dwarf	58.1±3.6	50.7±3.8
Solanum tuberosum - potato		
Norland	138.4±18.9	47.5±8.8
Russet Burbank	107.7±15.9	55.4±13.8
Denali	101.8±4.5	36.2±0.8
Kennebec	89.7±14.0	30.0±3.0

Table 1. Comparison of total biomass production by plants grown under an orbital (60min/30min) light/dark cycle versus those grown under a terrestrial (16hr/8hr) light/dark cycle.

the cultivar least sensitive to this effect. The 60/30 cycle plants showed a much greater biomass reduction during the first cycle of the experiment than the second. This suggests that the LEO light/dark cycle is borderline for normal lettuce growth and that slight variations in other environmental conditions might cause major reductions in yield.

Wheat plants were harvested at 8 weeks and showed only slight growth reductions under the 60/30 cycle in terms of total biomass production (Table 1). Although plants were not grown to maturity, the cultivars Freemont and Yecora Rojo began heading 2 days later, and Olescens Dwarf 2 days earlier under the 60/30 cycle compared to the 16/8 cycle.

Potatoes showed the most severe growth reduction under a 60/30 cycle (Table 1). All the cultivars tested exhibited a nearly 50 percent reduction in total shoot biomass. At the end of eight weeks, tuberization under the 60/30 cycle was initiated in all cultivars except for Norland, though tuberization was reduced compared to the 16/8 treatment. Under the 16/8 cycle, all cultivars initiated tuberization. Stomatal measurements on potato leaves grown under the 60/30 cycle showed that stomates remained relatively closed throughout the entire light/dark cycle. It is not known whether such stomatal closure would restrict CO_2 uptake sufficiently to account for the differences observed between treatments. Plants grown under the 60/30 cycle also showed a marked reduction in chlorophyll levels compared to those grown under the 16/8 cycle, suggesting a possible inhibition of photosynthesis in addition to the stomatal effects.

These observations indicate that if crop plants are to be grown successfully in a CELSS under a LEO light/dark cycle, environmental conditions of the plant growth unit may have to be modified to achieve acceptable levels of productivity. When the physiological basis for the observed plant responses are more clearly defined, it should be possible to determine exactly what modifications will need to be made.

This work was performed in the Wisconsin Center for Space Automation and Robotics at the University of Wisconsin-Madison and is supported in part by NASA under grant NAG-W975 and by a consortium of industrial sponsors. ■

REFERENCES

1. Berry, W., T. Hoshizaki, and A. Ulrich. 1986. The effect of ultradian and orbital cycles on plant growth in controlled ecological life support systems: CELSS '85. NASA Ames Research Center, Moffett Field, CA. NASA TM-88215:565- 576.
2. Bonde,E.K. 1956. Further studies on the effects of various cycles of light and darkness on the growth of tomato and cocklebur plants. Physiol. Plant. 9:51-59.
3. Bonde, E.K. 1955. The effects of various cycles of light and darkness on the growth of tomato and cocklebur plants. Physiol. Plant. 8:913-923.
4. Garner, W.W. and H.A. Allard. 1931. Effect of abnormally long and short alterations of light and darkness on growth and development of plants. J. Agric. Res. 42:629-651.
5. Takano, T., K. Inada, and J. Takanashi. 1987. Trickle water and feeding systems in plant culture and light-dark cycle effects on plant growth. XXVI COSPAR-86 Proceedings, Toulouse, France. Pergamon Journals, LTD.

DESIGN STUDIES FOR REGENERATIVE LIFE-SUPPORT SYSTEMS

C. O. Patterson
Department of Biology, Texas A&M University, College Station, Texas 78743

For long-duration missions and for permanent bases beyond low-Earth orbit, regenerative life-support systems may offer advantages in terms of weight, volume, and power savings. An interdisciplinary team has been formed through the Space Research Center (SRC) at Texas A&M University, with the goal of studying the practicality of closed environmental life-support systems. We are attempting to understand what scientific, engineering, and technological problems must be solved to approach total atmosphere regeneration, water reclamation, waste management, and food production. Our team is composed of faculty, graduate students, and research professionals from the Departments of Agricultural Engineering, Biology, Chemistry, Chemical Engineering, Industrial Engineering, Mechanical Engineering and SRC staff. By bringing together a large group of investigators with diverse research interests and expertise, it has been possible to take a "fresh-eyes" approach to questions of how best to support life in space for extended time. Our work has been supported by NASA-Johnson Space Center.

Our working hypothesis envisions a space qualified system which employs combinations of biological, chemical, and physical components operating in series and in parallel, or perhaps redundantly. Figure 1 depicts schematically a possible functional layout of such a system. Chemical and physical systems offer the advantages of simplicity of design, more precisely defined parameters of operation, and easy "switch on - switch off" functioning. Biological systems, although more complex and information-rich, offer the advantages of operation at low temperatures and pressures, integration of atmospheric regeneration, water purification, and food production within a single component and the straightforward production of the stereo-isomers of carbohydrates and amino acids which humans require for nutrition. We see necessary roles for all of these systems. As a prelude to total regeneration of all life support needs, we are also considering alternatives including limited resupply and disposal. This is appropriate due to the facts that current NASA planning calls for some resupply, that there is a lack of detailed data on which to base practical food requirement scenarios, and that there is a likelihood that some resupply will provide highest efficiencies given current technologies.

We begin our system design with human metabolic parameters. An adequate human diet must supply energy (Kcal or joules), amino acids, fatty acids, and certain vitamins and minerals. The diet must include as major components carbohydrates, proteins, fats, and fiber. Energy content of food may be calculated: $E = 16{,}760\ C_t + 22{,}626\ P_t + 39{,}386\ F_t$, where E = joules/gm food, C_t = gm carbohydrates/gm food, P_t = gm protein/gm food, and F_t = gm fat/gm food.

Then, rate of food metabolism may be calculated as $R_{food,m} = M/E$, where $R_{food,\ m}$ = gm food processed/second and M = power output in watts.

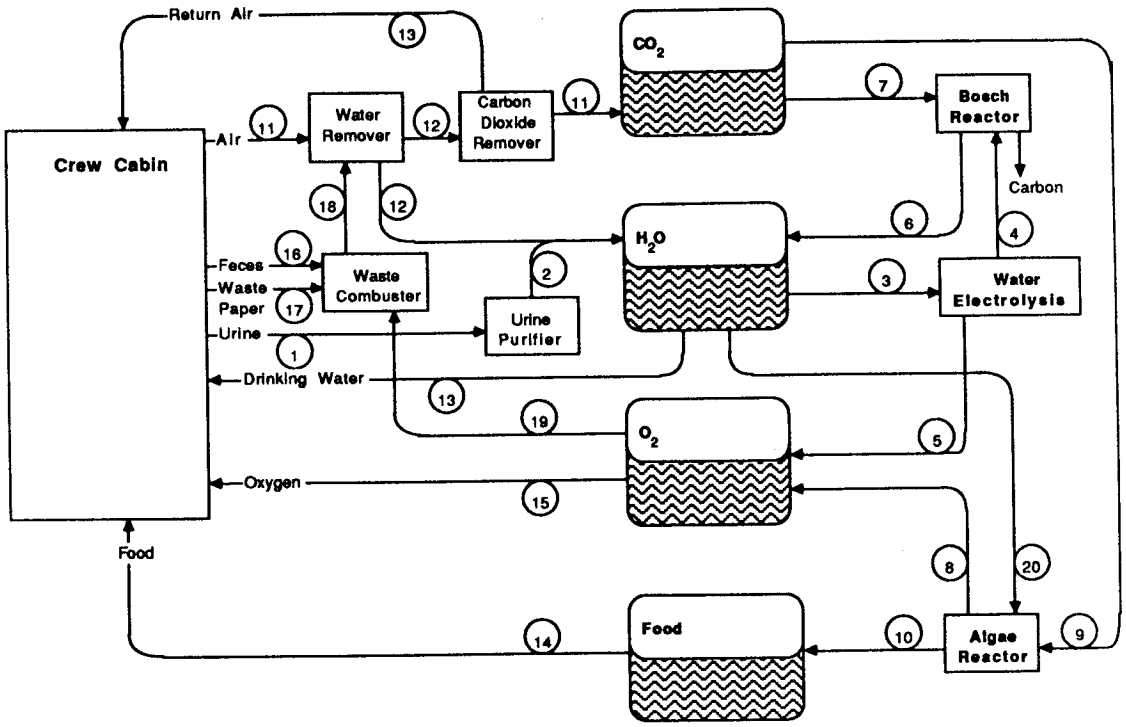

Figure 1. Functional Layout for CELSS.

Since virtually all human output appears as heat, we can thus obtain working numbers for environmental cooling requirements.

In addition, we can calculate rates of CO_2 production:

$$R^{human}_{CO_2} = [1.467\ C_t + 1.544\ P_t = 2.809\ F_t]\ R_{food,m}$$

and O_2 consumption

$$R^{human}_{O_2} = [0.67\ C_t + 1.332\ P_t + 2.860\ F_t]\ R_{food,m}$$

and rate of H_2O production

$$R^{human}_{H_2O} = [0.6\ C_t + 0.521\ P_t + 1.085\ F_t]\ R_{food,m}$$

Similar equations have been developed for rates of food consumption (removal from stores), rate of feces production, feces composition, rate of water loss by breathing (influenced by temperature and relative humidity), rate of urine production, etc. Knowing feces production rate and composition, it is possible to calculate O_2 consumption for waste combustion, CO_2 from combustion, H_2O from combustion (for biological, chemical, and physical modules). These values, plus those above, allow us to begin calculating weight, volume, and power requirements for biological, chemical, and physical systems to regenerate atmosphere, purify water, and produce food. We assume for these calculations the use of a Bosch reactor, photosynthetic algal reactor, and an electrolysis system. Optimal sizes of the regenerative modules are calculated, based on a 4-person crew. These numbers will then be used to develop a detailed, realistic simulation program, using object-oriented programming methodology, which will introduce heterogeneity and stochastic variation into the system to test its stability and limitations.

We also assume that initial processing of wastes will involve thermal combustion. In cooperation with General Electric, we have obtained access to a waste management- water recover system (the RITE System). The RITE System is a completely integrated system capable of processing wastes from a 4-person crew (urine, feces, wash water, food waste, and non-metallic trash). It has been successfully tested in continuous runs of more than 180 days duration. We have installed the RITE System in our laboratory and reactivated it. We are now investigating techniques and hardware for integrating the

RITE System with electrochemical systems for atmosphere regeneration and with biological (photosynthetic) systems for atmosphere regeneration and food production. The numerical analyses described above guide us in experimental manipulation of the hardware modules, while results from the experiments allow us to refine the numerical simulations. ■

ECOLOGICAL THEORY AND INTEGRATED TOXICITY TESTING: TWO APPLICATIONS OF CELSS TECHNOLOGY

K. W. Scott
Division of Biological Sciences, University of Texas at Austin, Austin, Texas 78712

Controlled Ecological Life Support System (CELSS) technology is used in a dual approach: 1) to test ecological theories concerning structure, complexity and stability of controlled ecosystems, and 2) to use an integrated toxicity testing approach to test the effects of perturbations on terrestrial community dynamics. An example of this using the herbicide bromacil and its effects on an agroecosystem-based community is being undertaken. This report summarizes the results of the first phase of the study dealing with CELSS design and baseline information.

Ecosystem stability is recognized as an important characteristic of natural communities. Stability is the inherent capacity of a system to tolerate or resist change caused by outside influences (Ricklefs, 1979). The community assembly, environmental components and their interactions, or, the structure of an ecosystem, determines its stability to a given perturbation or stress condition. The structure and structural dynamics (function) of an ecosystem determines its ability to buffer stress(es) and return the system to a given steady state, while reducing the oscillations in a stable system, or oscillating at repeating equal frequencies in a neutrally stable system. The tendency of a system to restore itself to a particular condition (a stable equilibrium) after a perturbation, is referred to as the system's resiliency.

While stability and structure may be inherent in complex natural ecosystems (presumably because of the results of coevaluation), rebuilt or artificial ecosystems usually have a more simple and forced structure and therefore may frequently possess less stability. Drastically disturbed land and Controlled Ecological Life Support Systems (CELSS) are good examples of rebuilt and artificial systems. While structure (both abiotic and biotic) is recognized as an important factor in reconstruction of drastically disturbed land, far less is known about how structure effects a CELSS and its stability. The issue of stability within CELSS has been identified by several authors (Moore *et al.*, 1979; Maguire *et al.*, 1980; Martello, 1986) but has received very little experimental attention. In closed and partially closed systems the question arises: what degree and kind of structure is required to keep an ecosystem functioning at a given stable steady state (at an ecological equilibrium)? Ideally one would like to be able to measure certain simple properties of an ecosystem (like a CELSS) before they are perturbed, and then on the basis of the results, be able to predict how gently or violently the system will respond to a disturbance (Harte, 1974). The systems response would depend on the systems structure and the type and duration of stress.

Stress may be caused by abiotic factors (*i.e.*, environmental conditions or toxic substances) or ecological factors (*i.e.*, competition or predation). In a CELSS, physiological stresses to a crop caused by abiotic factors will be minimized by careful control of the environmental conditions. However the control of ecological stresses, such as interspecific competition by bacteria and plants, or parasitism of plants by bacteria or fungi, will be difficult. Keeping CELSS completely free of bacteria and fungi is both difficult (impossible) and impractical (Nelson 1986, Maguire 1980). Therefore ecological as well as some physical stresses (*i.e.*, lack of gravity in space) will be present in CELSS crop systems. CELSS community stability and its' response to stresses will depend upon CELSS physical and biological structure.

This study used reconstructed terrestrial microcosms (CELSS units) to examine the effects of altering the degree and type of structure has on the stability of a specifically defined terrestrial ecosystem. The goal is to find out how much the structure of an ecosystem determines its ability to buffer given

stress(es) and return to predetermined defined physiological steady state after the perturbation. The degree of structure is altered by changing the growing substrate (physical structure) and microfloral community (biological structure) of the starting simple vascular plant-based agroecosystem. Stress will be induced on the system by a photosynthesis-inhibiting herbicide.

A secondary objective of this study is to use CELSS technology as a simple system for (terrestrial) multispecies toxicity testing. More importantly, this information will be used in an integrated approach to toxicity testing. Current environmental toxicity testing protocols deal with single species bioassay systems; more specifically, physiologic and abundance attributes of organism and population levels (Van Voris *et al.*, 1986). Such tests ignore the community and ecosystem level of interaction and complexity. It is realized that single species tests are not sufficient in determining a compounds' effects on a complex community or ecosystem, which consists of many levels of biotic and abiotic interactions. Ecosystem level evaluations, however, are very difficult to design, implement and interpret, and generally lack (a) validated test protocols, (b) replicable test systems, (c) reproducible results and (d) cost effective techniques (Van Voris *et al.* 1986). This study used simple, reproducible, controlled-environment experiments to compare the effects that a test substance (and its degradation products) has on the components of biologically related simple single-species systems (wheat only) and more complex multispecies systems (wheat and microflora).

The present program includes a series of experimental treatments, each with a different degree of ecosystem structure (physical and/or biological). An experimental treatment run consists of three basic pieces: properties and hardware identical in all microcosms, treatment differences (*i.e.*, differences in ecosystem structure), and the induced stress.

Properties similar to all microcosms include: the environments, provided by materially closed/energetically open CELSS units (modified from Maguire, unpublished); input materials (*i.e.*, water, air, nutrients); the stress target, vascular plants (dwarf wheat); and related measurements. Treatment differences are rooting substrate (*i.e.*, "soil"), and its' microcommunity. By changing the growing substrate and the microflora, a given ecosystems' structure can be altered from simple to complex (physically, biologically, or both). Three growing substrate are being used: (1) synthetic, sterile, and chemically inert fiberglass plug (Grodon), (2) a high-clay, high-organic-matter chernozem (udic borol) topsoil, and (3) a low-clay, low-organic-matter luvisol (alfisol) topsoil. The microfloral community, consisting of soil fungi, alga, and bacteria are controlled by sterilization, introduction, and reintroduction techniques.

To test the stability of a particular ecosystem and its' treatment, one half of the microcosms in a run are being stressed at a physiological point in the plant by the systemic substituted uracil herbicide, bromacil (5-bromo-3- *sec*-butyl-6-methyluracil). The effects that increasing the ecosystems' structural complexity by increasing the abundance and species richness of the microfloral community (biological structure), and increasing the absorbance capacity of the rooting substrate (physical structure), has on the bromacil and the bromacil's effects upon the vascular plants, are being measured. This will assist in determining whether the increase in structural complexity assists or hinders an ecosystems' resiliency and the wheat's ability to resist the applied stress. Measurement of some of the ecosystem's dynamic (functional) parameters (*i.e.*, Assimilatory and Respiratory Quotients: AQ and RQ) are done at intervals throughout the experiment. As well, parameters (*i.e.*, plant weight, soil characteristics, microfloral community, and bromacil analysis) at the end of an experimental run, help determine the response of the given ecosystem.

To understand the mechanisms of the effects of ecological stress or physiological stress on the stability of a given ecosystem (CELSS or natural) the behaviour and fate of the stress component in the system must be understood. In this study four factors governing the fate and behaviour of bromacil in the microcosms are (i) the chemical structure and physical properties of the herbicide, (ii) the chemical and physical properties of the soils, (iii) environmental conditions, (Gerstl and Yaron, 1983), and (iv) biological properties (interactions) of the herbicide (Scott, 1986). Therefore, proper analysis of the effect of the stress on this (or any) microcosms requires an adequate baseline of information concerning the four factors listed above. Baseline information for chemical and physical properties of bromacil will be presented. Some of the physico-chemical properties of the substrates are presented in Table 1. These include soil texture and absorption isotherms constants from bromacil and individual substrate. Physiological properties of bromacil and results of single species assays (including vascular plants; blue-

TABLE 1 **Some properties of the soils used in this study**

SOIL TYPE	Luvisol (Orthic Gray)	Chernozem (Calcareous Eluviated Black)	Grodon
PROPERTIES			
Texture	Silt loam	Clay loam	Spun fiberglass
Sand %	23.0	21.0	-
Silt %	60.0	49.0	-
Clay %	17.0	30.0	-
Org. Mat. %	7.9	10.9	-
CEC meq/100g	24.5	44.3	UD
pH	5.6	8.1	-
BROMACIL ADSORPTION CONSTANTS			
K	0.77	1.73	UD
n	0.51	0.97	UD

*UD-Undetermined

green alga, *Anacystis nidulans*, and fungi) will also be presented. The baseline information is also used in integrated toxicity testing to compliment the multispecies bioassays run in the CELSS units. ■

REFERENCES

Gerstl, Z. and Yaron, B. 1983. Behaviour of bromacil and napromide in soils: I. Adsorption and degradation. Soil Sci. Soc. Am. J. 47:474-478.

Harte, J. 1979. Ecosystem Stability and Distribution of community matrix eigenvalues. In: Theoretical Systems Ecology, ed Halfon, E., Academic Press.

Moore III, B., Kaufmann, R., Mason, R. and Wolf, S. 1980. Biological problems and experimental program for a controlled ecological life support system. NASA.

Nelson, B. 1986. The role of plant disease in the development of controlled ecological life support systems, in MacElroy, R.D., Martello, N.V., Smernoff, D.T. eds. Controlled Ecological Life Support Systems: CELSS '85 Workshop, NASA TM 88215.

Maguire, B., Jr. 1980. Literature review of human carried microbes interaction with plants. NASA CR-166330, 185 p.

Maguire, B. Jr., Slobodkin, LB., Morowitz, H.J., Moore, B. III, and Botkin, D.B. 1980. A new paradigm for the examination of close ecosystems. In: Microcosoms in Ecological Research. ed Giesy, J.P., Jr., U.S. Technical Information Center, U.S. Department of Energy, Symposium Series 52 (CONF-7811101).

Martello, N.V. 1986. Development of space technology for ecological habitats, in MacElroy, R.D., Martello, N.V., Smernoff, D.T. eds. Controlled Ecological Life Support Systems: CELSS '85 Workshop, NASA TM 88215.

Ricklefs, R.E. 1980. Ecology 2nd ed. Chiron Press Inc. New York.

Scott, K.W. 1986. Laboratory and Greenhouse Studies for the rehabilitation of bromacil contaminated soils, Annual report 1985/1986. Unpublished report prepared for NOVA, AN ALBERTA CORPORATION.

Van Voris, P., Tolle, D.A., Arthur, M.F., Chesson, J. 1985 Terrestrial Microcosoms: Applications, validations, and cost-benefit analysis. In: Cairns, J., Jr. Multispecies Toxicity Testing. Pergamon Press N.Y., N.Y.

ATMOSPHERIC EXCHANGE SYSTEM HARDWARE DEVELOPMENT

M.G. Timm[1], B.D. Yost[1], W.R. Munsey[2], and W.M. Knott[3]
[1]*The Bionetics Corporation,* [2]*NASA/Cargo Project Office, John F. Kennedy Space Center, Florida 32899,*
[3]*NASA/Biomedical Operations and Research Office, John F. Kennedy Space Center, Florida 32899*

An Atmospheric Exchange System (AES) is currently under development at Kennedy Space Center to support the Chromosomes and Plant Cell Division in Space (CHROMEX) middeck experiment. The AES will allow for the flow of air through the Plant Growth Chambers (PGCs) of the Plant Growth Unit (PGU), the primary experiment carrier for CHROMEX. The AES is designed to scrub ambient air from the middeck to remove selected organic and inorganic contaminates, reduce the ambient CO_2 level to between 300 and 1500 parts per million, and deliver the scrubbed air to four PGCs at a minimum flow rate of one liter per hour per PGC. After circulation through the PGCs, the air is returned to the cabin. As currently designed, the AES utilizes existing PGU/PGC interfaces, thus requiring no hardware modifications for AES subcomponent attachment. The AES is battery operated, which minimizes required orbiter interfaces. To reduce the possibility of microbial contamination, a 0.22 micron filter is installed downstream of the pump, and all components downstream of the filter are steam autoclavable. Air is delivered to the PGCs in a parallel fashion to provide equal air distribution to all PGCs and to further reduce the possibility of cross contamination between PGCs. Currently, prototype development and evaluations are ongoing at KSC and at the Principal Investigator's laboratory, State University of New York at Stony Brook. Prototype evaluations include PGU fit checks, filter efficiency, air flow, battery life, and preliminary hardware certification testing, as well as plant growout studies. ■

GROWTH OF PLANTS AND PLANT TISSUE CULTURES IN SIMULATED LUNAR SOIL—IMPLICATIONS FOR A LUNAR BASE CELSS

S. Venketeswaran[1] and D. L. Henninger[2]
[1]*Biology Department, University of Houston, Houston, Texas 77004, and* [2]*NASA/Johnson Space Center, Mail Code SN12, Houston, Texas 77058*

INTRODUCTION

Plant tissue culture techniques are very useful for growing many agricultural and herbaceous plants, particularly vegetable plants, which constitute one of the major groups of food plants for man. Hydroponic food cultivation of tomato and lettuce are two familiar examples which have been successfully grown under strictly controlled conditions and routinely used as food by man. The food technology required for long-term space missions warrants the welcome need of such natural foods in addition to other available more processed foods, and should consider the possibilities of raising plants for human consumption. Particularly, it is appropriate to visualize the possibility of growing higher plants on a lunar base CELSS (12). This paper describes growth of plants and plant tissue cultures in the presence of simulated lunar soils, terrestrial basalts or natural glasses. If plant cells can be grown in such inclusions and substrates, their effect on growth and development can be studied and used as base line data for growing higher plants on a lunar base CELSS. Since plant tissue culture systems have several advantages and plants form a major bioregenerative life support system, lunar-based agriculture can perform a vital role in providing food, landscape and other psychological aspects for future manned missions to the moon, Space Station and manned interplanetary exploration.

ADVANTAGES OF PLANT TISSUE CULTURE SYSTEMS

These are ideal for establishing baseline information on growth of plants, *viz.*, (a) they are easy to grow in well-defined nutrient culture media; (b) they can be grown initially and for long periods of time under total aseptic conditions (free of bacteria and other living forms); and, (c) they can be grown as

"clones" and propagated in large numbers (in millions) at lower costs, space and time and eventually adapted to conventional methods of planting, particularly on the lunar base which is free of microbiological population.

BACKGROUND

The following diagram illustrates a simple Biological Life Support System (BLSS) which can be conveniently employed and suggested for space missions (1).

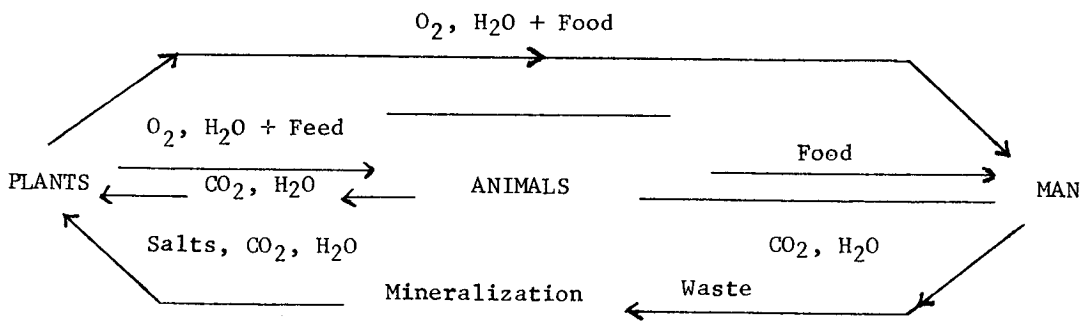

Various modifications to this simple system can be made or have been suggested (2). In such systems, obviously higher plants play a dominant role. Some investigations have been carried out in the US and many more in the USSR to examine the utilization of higher plants as mans' food source in space (2,12). In particular, there is some information on artificial plant cultivation (hydroponics, aeroponics and other methods) as applied to BLSS using substrate and nonsubstrate techniques (2,4). Further, the social psychology of man warrants that along with astronaut's foodstuffs which are packaged, it will be ideal to have in addition some natural products, *viz.*, fresh vegetables, fruits, etc. Such a list has been recommended (8).

Previous investigations in NASA's Botany Program during the Apollo missions for quarantine studies between 1967-75 at the NASA/Johnson Space Center were initiated and carried out from this laboratory using tissue culture aseptic methods. Many of the plant species selected for the Apollo mission were selected, tested and grown under tissue culture conditions at the University of Houston (13,14).

GENERAL PLAN OF WORK

Simulated lunar soils (based on the composition of the lunar regolith and its parent bedrock), zeolites and other "synthesized soils", samples of terrestrial basalts, natural glasses and other volcanic glasses will be dusted directly or incorporated into nutrient culture media suitable for plant cell growth and differentiation. Three main tissue culture techniques (3) are used: (1) seed germination, seed development and other related growth are carried out directly on the simulated lunar soils using them as a solid supporting medium and if necessary, will be saturated with other essential plant nutrients; (2) established actively-growing undifferentiated tissue masses are sprinkled or subcultured with simulated lunar soils and other addenda in solid media (jelled with agar); and, (3) the finely-powdered samples are dispersed in liquid media and innoculated with suspensions of plant cells and maintained on a shaker at 60 rpm. Various concentrations of the addends are tested. Emphasis is placed on tissues that can be grown on completely-defined synthetic media.

PLANT MATERIALS

The following higher plants are investigated and have been selected on the basis of projected diets of plant species which approach characterization of life support systems and previous background information of growth in tissue culture (10,14).

Tomato	Spinach	Carrot	Soybean
Wheat/Corn	Pine	Lettuce	Tobacco

Attention is focused on representatives of gymnosperms, dicots, and monocots. All these materials can be easily handled for this purpose under sterile conditions. Their growth period to a fair-sized seedling state is within a 3- week period and later transfer to a greenhouse. Data of growth are obtained at routine intervals with photographs.

Carrot	Corn/Rice	Tobacco	Fern
Soybean	Tomato	Pine	Marchantia

CULTURE MEDIA

The composition and mineral contents of the tissue culture media employed are described in literature (5,7,9,15). Analyses of the mineral contents of the lunar rocks from Apollo missions are available (11).

GROWTH ANALYSES

Data will be obtained on growth rate in media containing various test addends, mitotic rate (wherever possible), morphogenetic (differentiation) potential of tissues (wherever possible), cytology, histology and ultrastructure. Detailed analyses will include: (1) wet and dry weight on a time scale over a 4-5 week period; (2) cell packed volume (solid culture) and settled tissue volume (liquid culture); (3) populations of cells/unit weight or unit volume using cell counts; (4) protein contents on weight and per cell bases; (5) number of colonies/plate and (6) seedling height, number of leaves and other parameters.

RESULTS & SIGNIFICANCE

Our preliminary results have indicated that simulated lunar soils do not appear to have any inhibitory effects on growth of plants using tissue culture systems. It is of importance to determine whether these simulated addends are incorporated directly into the cells or whether there is interaction between nutrient elements in the culture medium. A number of additional experiments are planned towards the answer of several important considerations.

The concept of growing higher plants on a lunar base CELSS as part of the bioregenerative life support system has received considerable attention. The results of Apollo 11 and 12 quarantine studies (14) and subsequent observations after the following missions, demonstrated that higher plants and tissue cultures can survive and grow in the presence of lunar soil, and some plants even showed increased vigor in growth, pigmentation, etc. These encouraging results indicated that more baseline data is needed for growing plants on the lunar regolith and particularly on the choice of plants and how they can be grown and propagated on the lunar base. Studies are aimed to determine whether a "soil" derived from the lunar regolith (6) can be "synthesized" through chemical treatments, weathering or even through biodegradation. But with the unavailability of enough Apollo regolith and soil for follow-up studies, the next best alternative will be to use simulated lunar soils. This paper describes such studies and procedures with additional significance.

Supported by NASA Contract No. NAG-9-214 from JSC, Houston. ■

REFERENCES:

1. Biological Life Support System. 1975 In: Foundations of Space Biology and Medicine—Joint USA/USSR Pub. III, pp. 247-308; 280.
2. Controlled Ecological Life Support System (CELSS). 1985. NASA Conf. Publ 2378.
3. Dixon, R.A. 1985. Plant Cell Culture-A practical approach. IRL Press. pp. 1-236.
4. Foundations of Space Biology and Medicine-Joint USA/USSR Pub. III. 1975. pp. 1-386.
5. Gamborg, O.L, R.A. Miller & K. Ojima. 1968. Exp. Cell Res. 50:151-158.
6. Henninger, D.L., C.W. Lagle, D.W. Mung. 1986. Personal Communication.
7. Hoagland, D.R. 1923. In: Plants in Action. 1956. W.H. Freeman, San Francisco.
8. Jones, W.L. 1975. In: Foundations of Space Biology and Medicine - Joint USA/USSR Pub. III, pp. 247-273.
9. Murashige, T. & F. Skoog. 1962. Physiol. Plant. 15: 473- 497.
10. Olson, R.L., E.A. Gustan & T.J. Vinopal. 1985 In: CELSS, NASA Conf. Pub. #2378.
11. NASA Reference Publication 1057. 1980. pp. 1-120.

12. Tibbits, T.W. & D.K. Alford. 1982. CELSS. NASA CP-2231.
13. Venketeswaran, S. 1973. Final Report, NASA Contract NAS- 10947.
14. Walkinshaw, C.H., C.W. Sweet, S. Venketeswaran & W.H. Horne. 1970. Bioscience 20: 1297.
15. White, P.R. 1963. The Ronald Press Co., New York.

PRODUCTIVITY AND COST TRADE-OFFS OF VARIOUS ENVIRONMENTS FOR GROWING POTATOES IN A CELSS

R. M. Wheeler and T. W. Tibbitts
Department of Horticulture, University of Wisconsin, Madison, Wisconsin 53706

Physiological studies of the potato plant (*Solanum tuberosum L.*) have demonstrated that both tuber and shoot development are strongly affected by environmental factors such as photoperiod, temperature, irradiance level, and CO_2 level. In addition, responses to these factors can vary among different cultivars. With the selection of the potato as a potential crop for controlled ecological life support systems (CELSS), it has become important to determine the ranges and combination of these factors that give the best productivity given the variable constraints of environmental regulation, cropping time, and growing area in the CELSS.

Results from our studies at the University of Wisconsin Biotron point to the following trends for potato growth and tuber yield in controlled environments: tuber development is promoted by cool temperatures (<20°C), high irradiance levels (≥400 υmol m^{-2} s^{-1} PPF, *i.e.*, 1/5 to 1/4 full sunlight) and elevated CO_2 levels (> 350 ppm). Clearly, it may be difficult to continuously maintain the optimum levels of all of these factors; thus, certain environmental and energy trade-offs will have to be made. For example, tuber yields obtained under a 12-h light, 12-h dark photoperiod can be substantially increased by using continuous irradiation (*i.e.*, a 24-h photoperiod), but the production per unit irradiance is greater under the 12-h photoperiod (Table 1). In such a case, the CELSS farmer faces different

Table 1. Tuber dry weight yield and energy efficiency of "Norland" potatoes grown under 12- and 24-h photoperiods.

Photoperiod	Tuber Yield*	Energy Efficiency†
(hrs)	(g DW/m^2)	(g DW/MJ)
12	2860	1.47
24	3955	1.02

*Plants spaced five per m^2 and harvested at 148 days.
†Assuming 304 W (304 J s^{-1}) electrical power per m^2 of growing area to provide an irradiance level of 400 μmol m^{-2} s^{-1} PPF from high pressure sodium lamps.

management scenarios for growing potatoes. For example, (1) if electrical lighting is used, and electrical energy is relatively unlimited, but growing space and time are critical, long photoperiods and high irradiance levels would be preferable—the more irradiation, the greater the productivity; (2) If electrical energy for lighting is restricted, but growing space and time are not, short photoperiods would be preferable because of the higher irradiant energy conversion. For the same amount of electrical energy needed to continuously irradiate a unit area (*i.e.*, a 24-h photoperiod), two units of area could be irradiated alternately using a 12-h photoperiod, thereby increasing the total yield.

Complete management of CELSS crops must also incorporate the constraints and costs of regulating factors other than photoperiod and irradiance level. For example, elevated CO_2 levels (*e.g.*, 1000 ppm) can accelerate photosynthetic rates and overall plant growth, and our studies have shown that this is most effective when total irradiance levels are limited, *e.g.*, shorter photoperiods. Thus high CO_2 can partially substitute for high amounts of irradiation. In most CELSS scenarios, once the system is "primed" and operational, CO_2 will most likely be cheap to provide in comparison to electrical power for lighting. However, it is conceivable that the CELSS may initially be carbon-limited and maintaining adequate CO_2 levels may be costly. Likewise, temperature regulation in the growing area must be considered. Under a 24-h photoperiod, temperatures should be kept near 16°C to sustain tuber development, while under a 12-h photoperiod, temperatures near 20°C are sufficient. Consequently, higher cooling costs may be incurred when long photoperiods are utilized. ■

EVALUATION OF NEW CANDIDATE CROP SPECIES FOR CELSS

D. L. Bubenheim and C. A. Mitchell
Department of Horticulture, Purdue University, West Lafayette, Indiana 47907

Research in the food production group of the CELSS program at Purdue University emphasizes yield optimization of candidate species grown in controlled environments. We presently are evaluating the yield optimization potential of crops not utilized thus far for CELSS. These crops are being selected for potential to provide appropriate food and energy value necessary for a restricted vegetarian diet and to complement present candidate species (wheat, potato, sweet potato, soybean, and lettuce).

"New" candidate species include oilseed crops such as peanut, rapeseed, and safflower, and low-fat protein crops such as cowpea, snap/dry bean, and sugar/shell pea. These candidate species have been characterized for flowering response to photoperiod and supplemental photosynthetic photon flux (PPF) in a greenhouse, and their growth habit evaluated as a function of these treatments. Rapeseed and safflower responded as typical long-day plants. Safflower was the only long-day plant to respond to increased PPF by flowering earlier. Flowering of pea was day neutral, but pea did flower earlier under high PPF than under low PPF regardless of photoperiod. Bean and peanut cultivars tested responded as short-day plants, but flowering of some peanut cultivars was hastened by high PPF. Cowpea also responded as a short-day plant with regard to flowering, and a determinate cultivar exhibiting compact growth habit has been identified for seed production in further controlled environment studies. Because of the highly-nutritive foliage and vigorous vegetative growth of cowpea, we will evaluate the food value of entire vegetative plants grown in optimizing environments. Total plant dry weight at flowering was greatest when grown under high-PPF conditions regardless of photoperiod. We currently are investigating potential biomass production by cowpea for several harvest strategies (one-time harvest of vegetative plant parts vs. combinations of partial defoliation, periodic seed harvest, and/or one- time, final harvest of mature seeds).

Rapeseed and safflower responded well to greenhouse conditions, and evaluation of these crops will progress to the growth chamber with acquisition of dwarf cultivars. Plant height, especially for the rapeseed cultivars used thus far, is the major obstacle for controlled environment use.

Development of a hydroponic system providing a rhizosphere environment suitable for pegging of peanuts is necessary before this crop can be included in growth chamber optimization. The yield potential of cowpea and pea in seed production systems will be readily evaluated in growth chamber environments.

Research supported in part by NASA-Ames Cooperative Agreement NCC2-100. ■

CHEMICAL AND SPECTROSCOPIC CHARACTERIZATION OF A SUITE OF MARS SOIL ANALOGS

L.M. Coyne[1], A. Banin[2], J.B. Orenberg[3], G.C. Carle[4], S. Chang[4] and T.W. Scattergood[5]
[1]San Jose State University, San Jose, California 95192 [2]Hebrew University, Rehovot, 76.100 Israel [3]San Francisco Sate University, San Francisco, California 94132 [4]NASA/Ames Research Center, Moffett Field, California 94035 [5]State University of New York at Stony Brook, Stony Brook, New York 11794

The National Aeronautics and Space Administration has begun preparations for the flight of the Mars Observer Mission in the early 1990's. This mission has several objectives: 1) to determine the global elemental and mineralogical character of the surface material; 2) to determine the spatial and temporal distribution, abundance, sources, and sinks of volatile material and dust; and 3) to explore the structure and circulation of the Martian atmosphere. These determinations will principally be made using a visual and infrared mapping spectrometer and a gamma-ray spectrometer. In order to evaluate those science objectives for this mission which are of importance to exobiology and to interpret the results of the mission, specifically reflectance spectra of the surface, an advance ground-based study is being conducted on a usefully limited suite of Mars Soil Analog Materials (MarSAM) intended to stimulate the aeolian material that presumably covers much of the surface of Mars. A series of variably proportioned iron/calcium smectite clays have been prepared from a typical montmorillonite clay using the Banin method (Banin, 1973). Evidence has been obtained which supports the premise that these materials provide an exciting and unique model soil system for the Martian surface in that they are consistent with the constraints imposed by the Viking surface elemental analyses, the reflectance data obtained by various spacecraft instruments and ground-based telescopes, and the chemical reactivity measured by one of the Viking 'biology' experiments, the Labeled Release experiment. The modified clays also show evidence for a previously uninvestigated association between two structural moieties, surface iron and stored electronic energy, that are probably involved in catalytic properties of clays.

Whether or not clays are important constituents of the aeolian material is an important question for several reasons. First, the Viking surface analyses are consistent with clays constituting a significant portion of the Martian soil, but no information concerning the actual mineralogy could be obtained. Second, the presence of clays would be highly suggestive of abundant water on Mars existing sometime in the past. Third, only part of the water that is tied up in the clay structure would have been detected by the Viking instruments or remote observations and, hence, there could be much more water present on Mars than was found. Fourth, clays would be expected to contribute to the surface reactivity to a degree disproportionately greater than their abundance. Fifth, clays have a number of special properties which would suggest that they have the capacity to store significant amounts of electronic energy which may affect both the reflectance properties of the clays and their surface reactivity, particularly in the presence of penetrating radiation (e.g. radioactivity or cosmic rays) or mechanical and frictional stresses (Coyne, 1985). Finally, clays are of particular interest to the exobiology community because of the role that they may have played in any surface chemistry and because of the hypothesis that clays may have been prototypic life forms providing templates for the prebiotic origin of simple life (Cairns-Smith, 1982).

A more specific hypothesis (Banin and Rishpon, 1978) that significant amounts of iron on Mars may have been associated with the postulated surface clays adds further interest to the search for clays on Mars. Reflectance spectra of the Martian surface are not consistent with spectra of known crystalline iron oxides. Among several possible explanations for the weak iron absorption in the Martian spectra is that the iron may occur as both surface and structural cations in smectite clays. The absorption due to iron in both of these loci would be anticipated to be lower than expected based on overall iron abundance. Thus, as much as 33% of the Martian surface iron could be accommodated in clays. Also, iron as a surface constituent of a clay produces catalytic activity (for the decomposition of organic

acids) which corresponds more closely to that found by Viking than does the iron in palagonite, another model for the Martian soil.

We discuss here the effect of increasing exchangeable iron on a diverse set of chemical and spectroscopic properties of our suite of clays. In order to chemically characterize the MarSAM and to compare them with the Martian soil studied by Viking, our clays were analyzed for their major and minor elemental compositions by X-ray fluorescence and ion-coupled plasma techniques. The results of these analyses confirmed the compositional integrity of the materials after modification and the desired changes in iron (and calcium) content produced by the Fe-Ca exchange.

Initial results of the measurements of diffuse reflectance of the MarSAM are shown in Figure 1 (The spectra are offset for clarity). For comparison, a spectrum of a Martian high albedo region (Mccord, *et al.*,1977) is also shown in the Figure. Qualitatively, the match of the Martian spectrum with that of the 100% exchanged iron clay is quite striking, although not perfect. Iron is manifested most notably in the charge transfer region at wavelengths shorter than about 0.7 μm, however, absorptions of iron are also found at longer wavelengths. It should be noted that for this initial work, the clays were measured in room air and, hence, probably contained more adsorbed water than may be appropriate for the Martian soil. This additional water could explain the differences in the spectra for wavelengths longer than about 1.4 μm.

REFLECTANCE SPECTRA OF MONTMORILLONITE CLAYS WITH VARIOUS LEVELS OF IRON SUBSTITUTION AND OF A BRIGHT REGION ON MARS

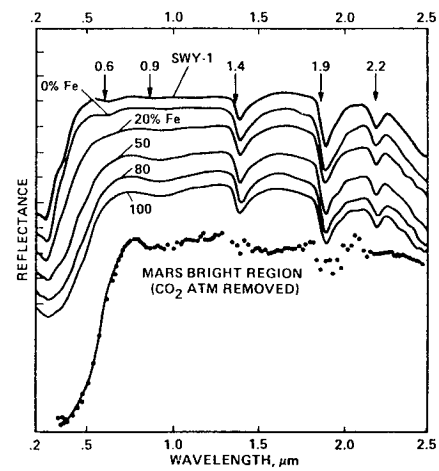

Figure 1.

Results of initial studies on the relationship between surface iron and surface activity in simulations of the Viking Labeled Release experiment are shown in Figure 2. The profiles of chemical activity, as

DECOMPOSITION OF SODIUM FORMATE BY MARTIAN SOIL (VIKING LABELED RELEASE EXPERIMENT) AND BY THREE IRON-CALCIUM MONTMORILLONITE CLAYS AT TWO MOISTURE CONTENTS

Figure 2.

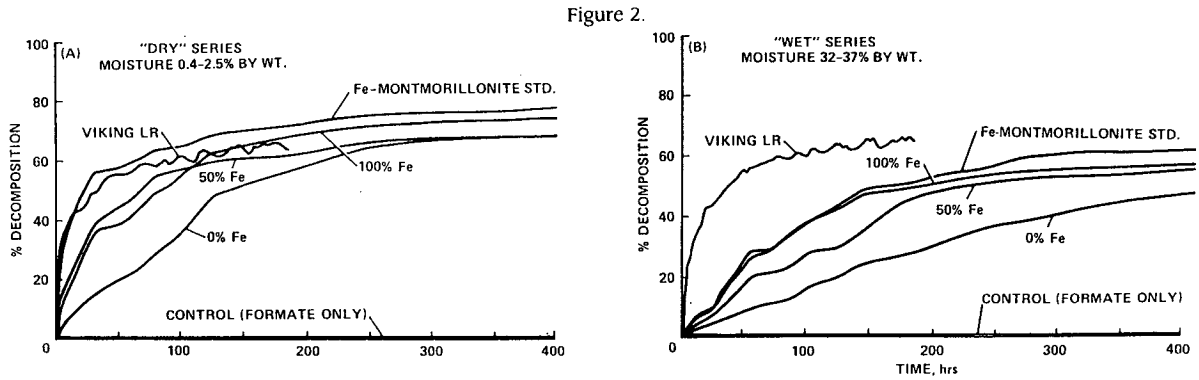

measured by the decomposition of sodium formate with time, are reasonably similar between the clays and the Martian soil. Note that the best match to the Viking LR results (from Levin and Straat, 1976) is obtained with the MarSAM containing the highest amount of iron and th smallest amount of water. This particular clay also showed the best compositional agreement with the Martian soil as determined by Viking.

In Figure 3, the dependence of stored energy content, as evidence by thermoluminescence, on amount of surface iron of natural and electronically excited materials is shown (Coyne and Banin, 1986).

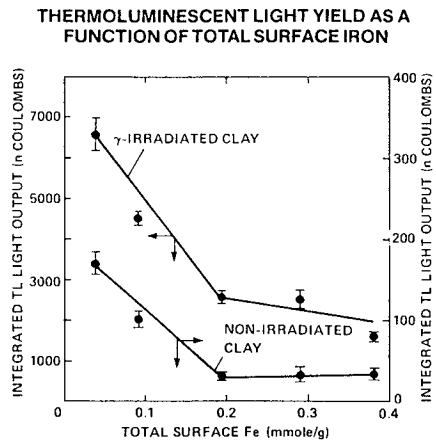

Figure 3.

Note that marked changes in the light output form both the irradiated and non-irradiated clays occurs at about 0.2 mmole/g of surface iron, which corresponds to roughly 50% of the exchangeable cations. Non-linear behavior with increasing surface iron was also found for at least three other properties of the clays. The distribution of surface iron between exchangeable and acid-extractable fractions, the surface paramagnetism, and the surface chemical activity also exhibited non-linear increases with increasing surface iron. Of particular note is that changes in all of these properties appeared to level off at about the same amount of surface iron, that is, where iron accounts for about 50% of the exchange capacity of the clay.

We conclude that the surface iron has a complex and hitherto uninvestigated impact on the catalytic and spectroscopic properties of clays and on the ability of these materials to store energy. Such energy has been hypothesized to be an an important structural moiety with respect to catalytic activity and spectral properties (Coyne and Banin, 1986).We believe that the MarSAM that we are investigating provide an exciting, unique, and appropriate model for the Martian aeolian material and that study of these MarSAM will reveal new insights into the catalytic activity of clay minerals. Also, these and future studies of the properties of suitably modified clays will provide a data base necessary for the proper interpretation of much of the reflectance spectra to be obtained by the Mars Observer, and that all of this information will be useful in determining the properties, past and present, of the soils on Mars. ■

REFERENCES

Banin, A.: 1973, 'Quantitative ion exchange process for clays,' U.S. Patent 3,725,528.
Banin, A. and Rishpon, J.: 1978, *Life Sci. and Spa. Res.*, XVII, 59.
Cairns-Smith, A.G.: 1982, *The Genetic Takeover and the Mineral Origin of Life*, Cambridge University Press, Cambridge.
Coyne, L.M. and Banin, A.: 1986, *Clays and Clay Minerals*, 34, 645.
Coyne, L.M.: *Origins of Life*, 15, 161. Levin, G.V. and Straat, P.A.: 1976, *Origins of Life*, 7, 293.
Mccord, T.B., Huguenin, R.L., Mink, D., and Pieters, C.: 1977, *Icarus*, 31,25.

KINETIC ANALYSIS OF THE TEMPLATE EFFECT IN RIBOOLIGOGUANYLATE ELONGATION

A. Kanavarioti[1] and D. H. White[2]
[1]*Life Sciences Division/Planetary Biology Branch, NASA/Ames Research Center, Moffett Field, California 94035 and* [2]*Chemistry Department, University of Santa Clara, Santa Clara, California 95053*

Template-directed reactions based on nucleotides are the only successful model known to date, where synthesis of complementary oligonucleotides occurs and during the process information transfer is achieved. Studies of these types of reactions may provide a key to understanding the nonenzymatic synthesis of nucleic acids in prebiotic evolution.

In this context we have undertaken a complete kinetic analysis of the template-directed oligoguanylate synthesis originated by Orgel and coworkers (Inoue and Orgel, 1982 and 1983). The reaction of guanosine 5'-phospho-2-methylimidazolide (2-MelmpG), the activated monomer, with all 3'-5' linked riboolígoguanylates (designated n^3 with n = 7-12) was studied in the presence or absence of the complementary template, polycytidylic acid (poly(C)). Conditions were chosen where poly(C) and 2-MelmpG are in large excess over the oligoguanylate. In the absence of the template at 37°C, the reaction leads to three isomeric oligomers that are elongated by one monomer unit. They are the 3'-5' linked, $(n+1)^3$, the 2'-5' linked, $(n+1)^2$, and the pyrophosphate product, $(n+1)^P$, formed in an approximate ratio 1:2:5. In the presence of the template the reaction is 20-fold faster and yields products n+1, n+2, n+3, etc., (See Figures 1 and 2) as long as 2-MelmpG is available (Kanavarioti, 1986). Most importantly, the formation of the natural n^3 isomer is enhanced selectively by 140-fold at 37°C, whereas under the same conditions the formation of the n^2 isomers is inhibited and the formation of the n^P is enhanced

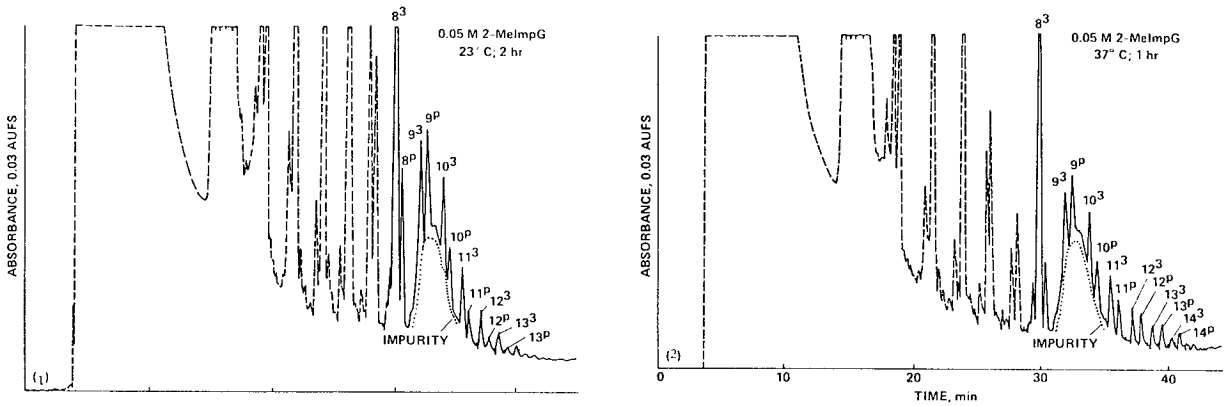

Figures 1 & 2. High performance liquid chromatography (HPLC) elution profiles of the reaction products of 0.05 M 2-MelmpG with an oligoguanylate 8^3 (90% pure) in the presence of 0.03 M poly(C); unreacted oligomer and elongation products are shown by solid line; oligomerization products of 2-MelmpG by dashed line. The impurity (dotted line) comes from 2-MelmpG. Figure 1: 2 hr incubation, 23°C; Figure 2:1 hr, 37°C.

only by 4-fold. Semiquantitative observations allow the conclusion that this selective enhancement of the natural over both other isomers is temperature-dependent and increases with decreasing temperature. For example, at 1°C only the n^3 isomers were detected (See Figure 3). Initial rates for the disappearance of oligoguanylates were determined at 1°C, 23°C and 37°C. It was found that the pseudo-first order rate constant for the template-directed oligoguanylate elongation is proportional to the 2-MelmpG concentration and that higher concentrations of the activated monomer favor the formation of n^P isomers both in the absence and in the presence of the template.

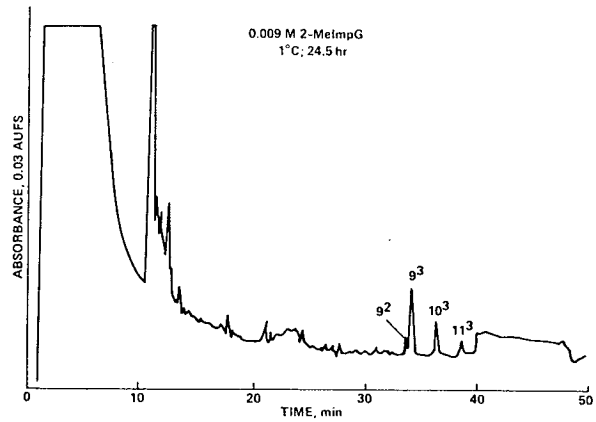

Figure 3: HPLC elution profiles of the reaction products of 0.009 M 2-MelmpG with an oligoguanylate 9^3 (80% pure with 9^2 being the impurity) in the presence of 0.03 M poly(C) after 24.5 hr incubation at 1°C.

The results support the following conclusions: (a) Lower temperatures, *i.e.*, close to freezing, selectively favor isomerically pure products, which incidentally are the natural ones. This may be due to a much tighter association between template and oligonucleotide at the growing ends of the latter with decreasing temperature. Thus, it seems that at low temperatures the present chemical system mimics its biological counterpart with respect to selectivity. It is then inferred from these studies that temperatures close to freezing may have been more conducive to the chemical evolution of selected, isomerically pure systems before the development of enzymes. (b) The observation that higher monomer concentration increases the formation of the n^p isomer is surprising. It is not clear why selectivity in this synthesis of one isomer over another would be dependent on 2-MelmpG concentration. The relationship between the concentration of the reactants and product selectivity is an important one in view of the rather limited amounts of starting materials plausibly present in the prebiotic environment and merits further investigation. (c) Finally, one might have expected that the efficiency of reaction is due to a strong binding that forces the reactants together in a stable complex and thereby induces the reaction. It is well established that the complex poly(C)·n^3 is very stable (Miles and Frazier, 1982). Contrary to expectation though, the linear dependence of the template-directed elongation rate constant on 2-MelmpG concentration implies that the association of the monomer in the ternary complex poly(C)·n^3·2-MelmpG is weak and transient, a conclusion which is also supported by infrared data (Miles and Frazier, 1982). Hence we expect that any parameter which stabilizes this ternary reaction complex may enhance the rate accordingly. The search for such complex-stabilizing parameters could therefore lead to even more efficient template-directed reactions. ■

REFERENCES

Inoue, T. and Orgel, L.E.: 1982, J. Mol. Biol. 162, 201- 217.
Inoue, T. and Orgel, L.E.: 1983, Science 219, 859-862.
Kanavarioti, A.: 1986, Origins of Life 17, 85-103.
Miles, H.T. and Frazier, J.: 1982, J. Mol. Biol. 162, 219- 230.

NITROGEN AS AN EXAMPLE OF MICROBE ATMOSPHERE INTERACTIONS AND THE EVOLUTION OF BIOGEOCHEMICAL CYCLES

R. L. Mancinelli and C. P. McKay
Solar System Exploration Branch, Mail Stop 239-12, NASA/Ames Research Center, Moffett Field, California 94035

Nitrogen and the nitrogen cycle are integral parts of not only biogeochemistry, but also of life itself. Nitrogen is an essential element of such biologically important molecules as proteins, purines and pyrimidines, etc. Biological transformations of nitrogen within the biosphere are primarily carried out only by certain procaryotic organisms. Consequently, the evolution of the metabolic processes capable of carrying out these transformations is of primary interest, and is fundamental to understanding not only the evolution of organisms on earth, but also to the development of the biogeochemical cycles. This in turn will also yield valuable information regarding the development of ecosystems within the biosphere, as well as a clearer understanding of basic ecological principles.

Primarily two approaches to hypothesizing upon the evolution of biogeochemical cycles have been taken, *i.e.*, an ecological approach, or a biochemical approach. The ecological approach makes use of three basic facts of microorgansims: (1) organisms are opportunistic and consume simple, readily available nutrients first; (2) organisms will consume all of one type of nutrient until it has been depleted; (3) organisms will only evolve more complex successful metabolic pathways through natural selection when all available nutrients for the existing pathway are depleted. The biochemical approach makes use of the fact that biochemical pathways progressed, or evolved, from the simple to the complex, and that the commonality across phylogenetic lines reflects common ancestry and early evolution of such things as fermentation pathways. In addition, the homology of particular enzymes among different genera and kingdoms has been used as a means for arguing for the common ancestry of biochemical pathways employing those enzymes.

Three basic stages of evolution of the N-cycle are considered:
(1) Pre-biological chemical reactions which set the stage for evolution of the metabolic pathways of the first organisms by providing the necessary substrates for energy and biomass production.
(2) Pre-Cambrian microbe-environment interactions, which occurred under anaerobic conditions and ended with the advent of an aerobic atmosphere.
(3) Cambrian to present day microbe-environment interactions, which occurred after the advent of an aerobic atmosphere.

We present a theory of evolution regarding the important aspects of the biogeochemical nitrogen cycle by linking and correlating atmospheric development with biological evolution. The pre-biological earth's environment, primarily the atmosphere, by supplying the compounds for growth *i.e.*, the substrates for the first primitive enzymes, defined the limits of the first metabolic pathway, and thereby outlined the course for the origin and early evolution of life on this planet. This led to the emergence of certain metabolic pathways at particular times within the history of the biosphere. The interaction between the atmosphere and the evolving biota yielded a particular series of events which we postulate led to the following sequence of nitrogen metabolism and cycling: Ammonification → Denitrification → Nitrification → Nitrogen fixation. ■

MULTIPLEX GAS CHROMATOGRAPHY: A NOVEL ANALYTICAL TECHNIQUE FOR SOLAR SYSTEM EXPLORATION

J. R. Valentin[1], G. C. Carle[1], J. B. Phillips[2]
[1]*NASA-Ames Research Center, Moffett Field, California 94035;* [2]*Department of Chemistry and Biochemistry, Southern Illinois University at Carbondale, Carbondale, Illinois 62901*

Gas chromatography is a powerful technique for the analysis of gaseous mixtures. It has been successfully employed in the analysis of planetary atmospheres [Oyama, V.I. and B.J. Berdahl (1977). The Viking Gas Exchange Experiment Results from Chryse and Utopia Surface Samples, J. of Geophys. Res., *82,* 4669-4676. Oyama, V.I., G.C. Carle, F. Woeller, J.B. Pollack, R.T. Reynolds, and R.A. Craig (1980a) Pioneer Venus Gas Chromatography of the Lower Atmosphere of Venus, J. of Geophys. Res., *85,* 7891-7902.]. It is also a major analytical technique with a great many applications on Earth. Some limitations still exist in this technique. One of the most serious limitations is the time required to perform a determination. For example, only a limited time is available to a probe passing through a planetary atmosphere. This is because in conventional chromatography, an additional injection of sample into the carrier gas stream cannot be made until the preceding sample has finished passing through the system. Consequently, in conventional chromatography, no information is obtained on the chemical composition of an atmosphere between the points where the injections have been made. One example of this limitation was clearly illustrated during the Pioneer Venus mission where information on the chemical composition of the atmosphere of Venus was obtained only at three different altitudes while the probe was descending. A second limitation of conventional chromatography is detector sensitivity which is constrained by the sample volume limitations of the column. Only a relatively small volume of sample may be introduced into the column, then, this sample is further diluted by the carrier gas during the chromatographic process. Therefore, in order to make trace-level measurements, sensitive and usually sophisticated detectors must be employed. Finally, a consumable carrier gas is usually required, even when the sample itself is gaseous.

In multiplex gas chromatography [Phillips, J.B. (1980) Multiplex Gas Chromatography, Anal. Chem., *45,* 468A-478A.], however, rapid multiple sample injections are made into the carrier gas stream. A new sample may be taken every few seconds without having to wait for one determination to be finished before taking a new sample. Because of this, every point of the chromatographic signal contains information about the entire chromatogram. A second advantage of multiplex chromatography is an improvement in both sensitivity and detection limit which makes the use of less sophisticated detectors practical. Finally, multiplex gas chromatography is not limited to conventional injection valve techniques. In addition, a wide variety of chemical modulation techniques can be used. Some of those are chemically selective, and selective modulation is potentially as valuable as selective detection [Valentin, J.R., Carle, G.C., Phillips, J.B. (1985b) Determination of Methane in Ambient Air by Multiplex Gas Chromatography, Anal. Chem., *57,* 1035-1039. Valentin, J.R., Carle, G.C., Phillips, J.B. (1983) Concentration Modulation by Thermal Decomposition for Multiplex Gas Chromatography, J. High Resolut. Chromatogr. and Chromatogr. Comm., *6,* 621-622]. Because of the way the sample is introduced into the system, the output signal is not interpretable by the observer (Figure 1). By the application of deconvolution techniques like cross-correlation, the technique used in this work, the equivalent of a chromatogram is obtained from this output.

Figure 1. Multiplex GC Output.

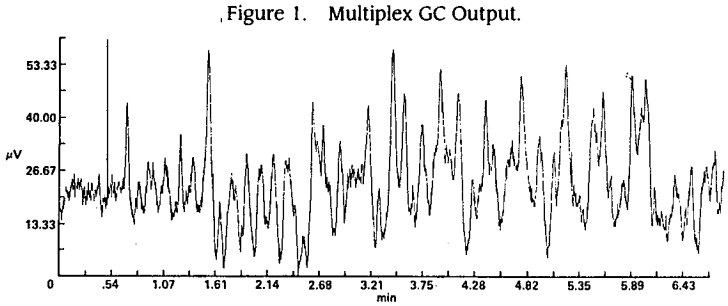

In order to efficiently perform multiplex gas chromatography experiments in the laboratory and on board future space craft, skills, equipment, and computer software are being developed. Three new techniques for generating chemical concentration signals were demonstrated. In all of them, the need for a separate gas stream as the carrier was avoided through the use of a chemical modulator at the head of the column to directly modulate a sample stream. The first technique involved generating a chemical concentration signal by thermal desorption from a stationary phase [Valentin, J.R., Carle, G.C., and Phillips, J.B. (1982) A non-mechanical Chemical Concentration Modulator for Multiplex Gas Chromatography, J. High Resolut. Chromatogr. and Chromatogr. Comm., *5*, 269–271.] Only those components adsorbed by this stationary phase were modulated leaving the other components unchanged in the gas stream. An improvement of 100 fold in detection limits was achieved. A difference in signal intensity was observed to be related to adsorbent capacity (Figure 2). The second technique

Figure 2.

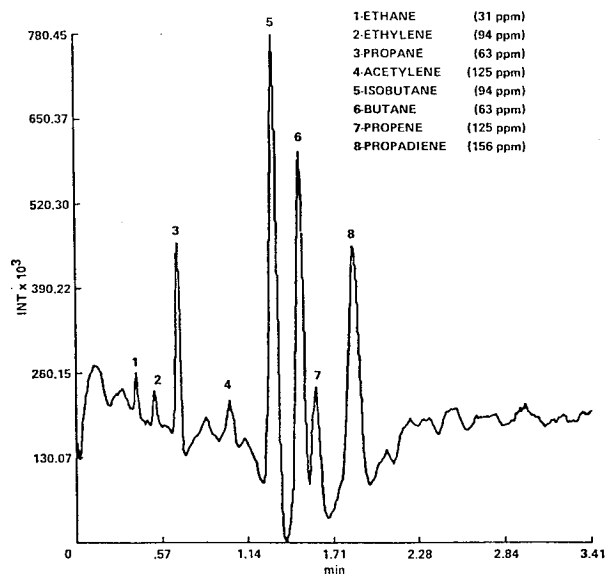

involved modulating a sample by thermal decomposition. Removing thermally unstable components from the gas stream resulted in a chromatogram containing vacancies rather than peaks (Figure 3). With a test sample containing ten components, only four were modulated resulting in a chromatogram containing four vacancies. Similar to the first modulator developed, an improvement in sensitivity of

Figure 3.

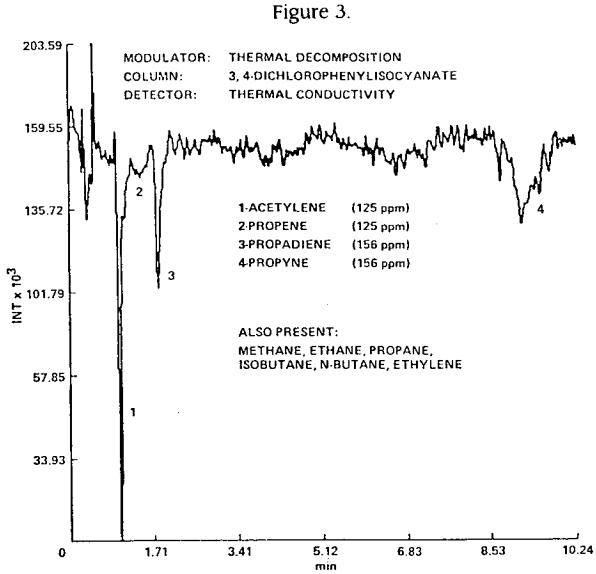

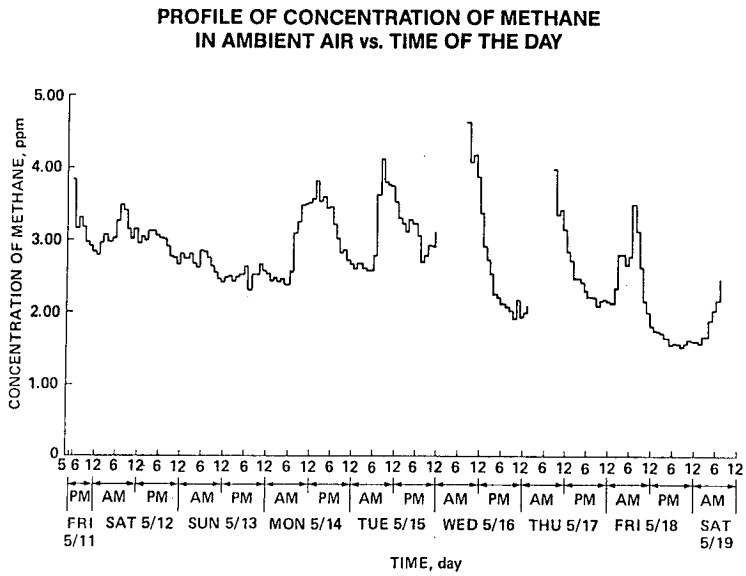

Figure 4. Methane Concentration Profile.

100-fold was demonstrated [Valentin, J.R. (January 1985) Multiplex Gas Chromatography for Use in Space Craft, NASA Tech Mem 86668.].

Finally, the analysis of an environmental sample by multiplex chromatography was accomplished by employing catalytic modulation for the determination of methane in ambient air. A modest gas chromatograph which used air as the carrier gas was modified by adding a silver oxide modulator that selectively catalyzed the decomposition of methane in air. The resulting analytical system required no consumables beyond power. A profile of the methane concentration in the laboratory was obtained for an eight day period. During this period, the methane concentration varied with an approximately daily period from a low comparable to accepted values of ambient methane concentrations to a high substantially above this concentration (Figure 4). These variations indicate the presence of some local source or sources for methane. This work demonstrated the utility of a simple multiplex gas chromatograph for the analysis of an atmospheric sample. This technique should be applicable to other trace components in air as well as in other planetary atmospheres. ■

FLIGHT INSTRUMENTS FOR TRACE GAS AND VAPOR ANALYSIS

F. H. Woeller, D. R. Kojiro, and N. Takeuchi
Solar System Exploration Branch, NASA/Ames Research Center, Moffett Field, California 94035

The continuing development of trace gas and vapor analysis presently centers around gas chromatography and the highly sensitive and universally responsive metastable ionization detector.

The laboratory at NASA-Ames has strengthened the suitability of the method for spaceflight. Complemental deployment of gas chromatographs and mass spectrometers can be advocated, while tandem systems incorporating both seem to reduce the overall system capability and reliability. Both methods also lack the ability to identify and quantitate certain reactive species such as Sulfur-oxides and higher Nitrogen-oxides. The measurement of the latter currently must remain reserved to spectroscopic methods.

The approach at NASA-Ames involved first the verification that the metastable ionization detector can be quite dependable. It is more rugged and lighter, and requires no mass balast or alternately, less

complex temperature controls, than theristor detectors. Real-time sensitivities of 20 ppb for essentially any analyte, are firmly achievable. The functional theory of the detector is still highly disputed, and ongoing studies at Ames seek to establish a model that reconciles seemingly contradictory observations that have been reported in the literature. Recent progress has been made in the construction of a micro-cavity ionization detector capable of operating at less than 2scc/minute (one-tenth the carrier gas consumption of commercial designs).

Ultraclean assembly of the gas chromatograph is a prerequisite for proper function of the ionization detector. Fortuitously, this requirement is automatically met when instruments are assembled for flight. Extensive studies at NASA-Ames have been devoted to the synthesis of zero-bleed materials for separation columns. Other efforts are directed at the study of low-flow dynamics for packed columns in order to take proper advantage of the progress in regard to the micro-detector. Another large effort is directed towards securing sources for helium carrier gas that exceeds present research grade standards.

Automated sample acquisition for gas and vapor analysis are based on the successful designs for the Viking and Pioneer-Venus missions. ■

EXAMINATION OF A CONTROLLED ANIMAL NUTRIENTS DELIVERY SYSTEM FOR USE IN SPACEFLIGHT

A.H. Battles[1], L.M. Kalla[1], J.L. Moyer[1], B.R. Stevens[2], M.T. Lang[1], W.M. Knott[3], and W.R. Munsey[4]
[1]The Bionetics Corporation, [2]The University of Florida, [3]NASA Biomedical Operations and Research Office, John F. Kennedy Space Center, Florida 32899, and [4]NASA Cargo Projects Office, John F. Kennedy Space Center, Florida 32899

A purified diet formulation, based on the AIN-76A, in powder form was selected for incorporation into a 65% moisture diet for laboratory rats to evaluate the diet form for consistency, nutrient content, sterility, shelf life, ease of delivery, animal performance, and suitability for spaceflight. To achieve the desired consistency for flight and ground applications, the diet was formulated using wheat gluten (32%) and gellan gum (3%) in place of casein and cellulose, respectively, in the AIN-76A formulation. Weanling male, Sprague-Dawley, specific pathogen free rats were fed irradiation sterilized high moisture diet with and without water *ad libitum* over a 28-day period and compared to rats fed the same diet in pellet form (irradiated) with *ad libitum* water. In addition, rats were fed standard AIN-76A diet in pellet form (both non- irradiated and irradiated) with water *ad libitum*. Each dietary treatment was fed to ten rats. Preliminary analyses indicated no significant differences between rats fed the high moisture diet with and without water *ad libitum*, indicating the high moisture diet form alone is capable of supplying all nutrients including water. Dietary wastage of the high moisture diet in the animal's cage was minimal, thus allowing accurate measurement of nutrient consumption; conversely, greater than 10% of the pellet form diets was noted as wastage. The high moisture diet consistency (high surface tension) appeared to be suitable for controlled delivery in microgravity. It was also shown that high moisture and pellet diets were adequately sterilized by irradiation and that the packaging techniques maintained diet sterility for at least an eight-week period. A delivery system for the high moisture diet form is under development for use in future ground and flight testing. ■

THE *DICTYOSTELIUM* LIFE CYCLE: A SENSITIVE GAUGE OF CELLULAR AND ORGANISMIC RESPONSE TO GRAVITY

M. A. Benjaminson
Dept. of Microbiology, New York College of Osteopathic Medicine, Old Westbury, New York 11568

Dictyostelium discoideum is an eucaryotic organism which bridges the gap between the unicellular and the multicellular states. Starting as isolated, free-living, actively feeding amebae, which unite to form a multicellular migratory form called, descriptively, a slug, the life cycle of this organism is completed when the differentiated cells of the slug reorganize to form an erect, rigid structure, topped with spores, called a sorocarp. The spores, when released to a favorable environment, will produce single amebae capable of recapitulating this entire sequence of events. A series of complex cell surface phenomena and intercellular syntheses have emerged as important factors in the complex genetic/humoral/environmental interactions which play dominant roles in the life cycle. Because it is a microcosm of phylogeny, has a short life cycle and has emerged as an excellent genetic model for the study of growth, differentiation, maturation and longevity on both the cellular and organismic levels, the author chose to investigate its responses to the environment of space.

Two wild type strains of *D. discoideum*, the "CB" and "ATCC", were studied. They were both fed a nonmucoid strain of *E. coli*. To evaluate the sensitivity of the *D. discoideum* life cycle to orientation of the solid agar substrate on which they are grown, cultures of both strains begun as either spores or amebae were raised in an inverted position (agar surface down), or, as controls, with the agar surface facing up. For both strains grown in an inverted position, the life cycle was completed more quickly than in the controls. Also, the two strains differed from each other in the length of time they took to complete their respective life cycles. Observations on the inverted plates showed that, in contrast to the case of the controls, slugs did not migrate, but rather, underwent reorganization *in situ*, to form sorocarps. This served as the first clue that slug migration is gravity sensitive.

To evaluate the sensitivity of the *D. discoideum* life cycle to altered gravity, centrifugation and clinostating (which simulates microgravity) were used. Altered gravity effects on cultures begun from spores or amebae are expressed by the sorocarp to slug (So/Sl) ratio. This measure of the speed of conversion from slug to sorocarp is an index of rate of development. Chronic 3g centrifugation of ATCC wild type cultures for 7 days, when spore-initiated, gave an So/Sl ratio of 0.44 as compared with 0.17 at 1g. When started with amebae, a 3g So/Sl ratio of 9.44 to one of 0.26 at 1g, was observed. This indicated that 3g accelerates development. Clinostat treatment of the ameba-initiated CB strain for 96 hrs. yielded an So/Sl ratio of 0.15 as compared with a 1g ratio of 0.3. ATCC, treated the same way, gave an So/Sl ratio of 2, in contrast to 6 at 1g (Fig. 1). Thus, ATCC completes its life cycle in less time than

Figure 1. Summary of Effects of Simulated Altered g

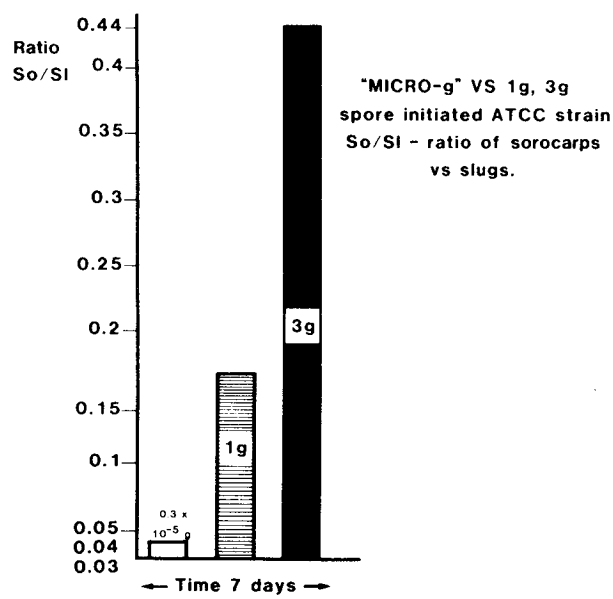

CB and, for both strains, clinostating decreases the rate of development. Clinostated ATCC slugs migrated an average distance of 12.2 mm. These data imply that the rate of development increases directly with increased g force and that the chronology of the life cycle has a genetic component. They also suggest that the rate of expenditure of stored energy during slug migration, is a gravity sensitive phenomenon.

Further evidence for the sensitivity of slug migration to forces encountered in the space environment is found in the response of *D. discoideum* to constant simulated sunlight. Here, again, slug migration appears to be a sensitive phenomenon, with sorocarp production occurring more rapidly in light-exposed cultures than in controls grown in the dark. Furthermore, maturation rate differences are seen between CB and ATCC wild types, as before.

Periodic cellulose production marks *Dictyostelium* stages. To establish a basis for relative quantitation, *in situ*, its deposition in sequentially differentiating stages of *D. discoideum* was followed with FITC-cellulase. Cellulase is conjugated to FITC or another suitable fluorescent compound and the excess dye

Figure 2. Migrating Slug and Slime Tube Stained with FITC- Cellulase

removed by column chromatography or ultrafiltration. Specimens were stained as whole mounts and mounted in buffered glycerine and examined with a fluorescence microscope. We verified that,cellulose occurs in the slime tube of the migrating slug stage, in the slug sheath and the sorocarp and its spores (Figs. 2, 3, 4). When the intact slugs were stained with FITC-cellulase, the internal cells did not fluoresce, but the enveloping sheath did. Younger slugs fluoresced less intensely than older ones. Slugs which culminate without migrating may not produce a slime sheath. In spore development, fluorescence intensity increased with maturation. Thus, FITC-cellulase specifically stains *in situ* cellulose, and allows for qualitative estimates of the relative amounts of cellulose in stained structures. These are based on fluorescence intensity and foreshadow quantitation. Sequential microphoto-fluorometric measurements of the relative staining intensity of the cellulose-containing structures of *D. discoideum*, as

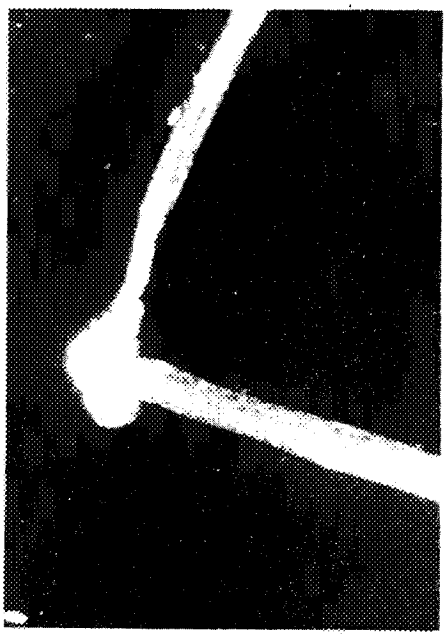

Figure 3.

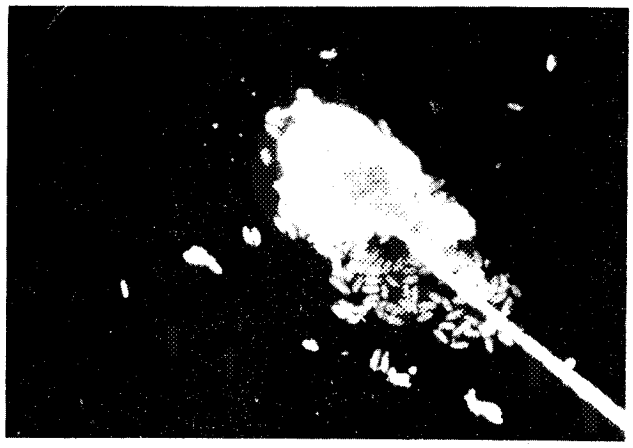

Figure 4.

morphogenesis progresses, are applicable to the study of the relationships between the quantity of cellulose laid down during specific stages in the life cycle and the rates of energy expenditure as they carry with alterations in gravity, sunlight and other components of the environment of space. Video-linked fluorescent cellulase microscopy has been used by the author for studies of other cell systems, apple and onion cells. There is no doubt that similar instrumentation can be used for continuous monitoring of the *D. discoideum* life cycle and record the progress of cellulose deposition. Such a system lends itself to both automation and remote viewing and recording.

The *D. discoideum* life cycle is a good model for the study of the effects of space-related phenomena on the level of both organism and individual cell. Its study has provided data linking gravity, maturation, longevity (and possible energy expenditure). The genome appears to exercise ultimate control over these interrelationships under the experimental conditions we have studied. ■

AMPHIBIAN FERTILIZATION AND DEVELOPMENT IN MICROGRAVITY

S. D. Black[1], S. M. Swales[2], H. M. Mack[2], H. J. Ginoza[2] and K. A. Souza[2]
[1]*Department of Molecular Biology, University of California, Berkeley, California 94720 and* [2]*Life Science Division, NASA/Ames Research Center, Moffett Field, California 94035*

INTRODUCTION

Gravity and centrifugal force have long been known to affect amphibian development. For example, eggs held in position and inclined 90° to the gravity vector will form the dorsal structures of the body axis from the uppermost side of the egg. This topography is seen even if the sperm entry point side (the prospective ventral side in control eggs) of the egg is uppermost. Thus, gravity can be used to experimentally override the normal mechanisms that specify the position of the dorsal structures relative to the sperm entry point. However, it is not known if gravity has a role in normal development, where the egg is free to rotate inside a fluid-filled membrane. We will attempt to determine whether or not gravity has a role in normal development by fertilizing and monitoring the development of *Xenopus laevis* eggs in microgravity.

EXPERIMENTAL DESIGN

Our experiment is scheduled for the Space Shuttle-Spacelab J mission in 1991. About 24 hours prior to launch, four female frogs will be placed in a damp, foam-lined box through which air is circulated,

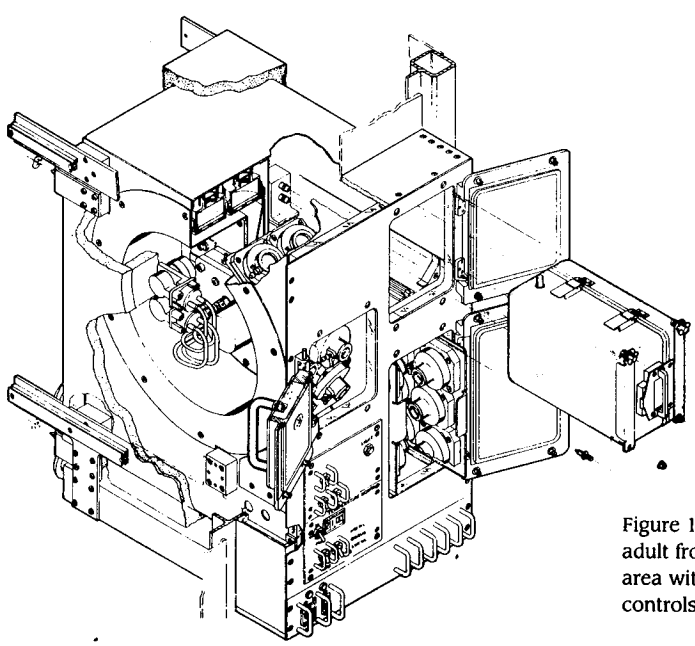

Figure 1. Frog Environmental Unit. Upper right: adult frog box; lower right: microgravity stowage area with egg chambers; left centrifuge and controls.

and a sperm suspension will be prepared. The frogs in their box will be placed in the Frog Environmental Unit (FEU—see Fig. 1), which is integral with the pressurized Spacelab module. During the second day of flight, the frogs will be injected with human chorionic gonadotropin to induce ovulation. Approximately 16 hours after injection, eggs from each frog will be evaluated for fertilizability and general quality. Eggs will be covered with activated sperm suspension and 15 eggs from each frog will be placed on each of two egg baskets (Fig. 2). The egg baskets will then be inserted into egg chambers (Fig. 2) and 50 ml of dilute amphibian Ringer's solution added. One of the two chambers from each frog will be left at microgravity while the other chamber will be placed on the FEU centrifuge and rotated at 1 g. Forty minutes after insemination, the eggs will be examined under a dissecting microscope and video system. On the basis of percent fertilization and egg quality, a prime frog will be selected.

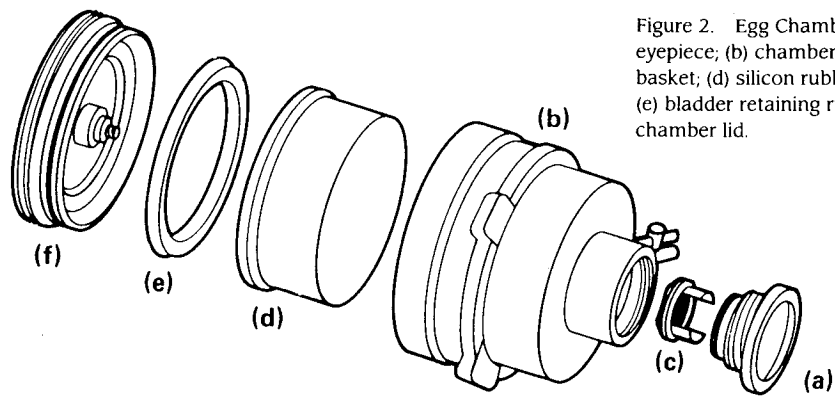

Figure 2. Egg Chamber. (a) eyepiece; (b) chamber body; (c) egg basket; (d) silicon rubber bladder; (e) bladder retaining ring; (f) chamber lid.

Using eggs from the prime frog, 22 egg chambers will be loaded. Ten chambers will be incubated at 1 g on the FEU centrifuge, and 12 will be incubated at microgravity. Eggs in some chambers will be fixed at several important stages of development, namely the 2-4 cell stage, gastrula, neurula, and swimming tadpole stages (approximately 100 hours old); these specimens will be analyzed cytologically after the flight. Tadpoles in 13 egg chambers will be returned unfixed and will be examined for abnormal swimming behavior; some will then be fixed for electron microscopic study of the vestibular system, and some will be raised to sexual maturity and mated to determine if there are multigenerational effects of microgravity on development.

Of the egg chambers that will be fixed, three will be used to determine the sperm entry point-neural plate topography. A payload specialist will use forceps to orient eggs so that the animal hemispheres will be visible through the eyepiece or chamber lid. After the eggs are fertilized, the payload specialist will record the position of the visible sperm entry point for each egg; when the eggs have developed to the neural plate stage, the payload specialist will record the position of the neural plate. Thus we will determine directly whether or not the establishment of the normal sperm entry point-neural plate relations is a gravity- dependent process.

EXPECTED RESULTS

We expect that the embryos and tadpoles developing at microgravity will have essentially normal morphology. This expectation is based on the results of previous spaceflight, random motion, and clinostat experiments in which most embryos developed normally. However,no spaceflight experiment has exposed amphibian embryos to microgravity during the gravity-sensitive period between fertilization and second cleavage, so careful analysis of our specimens is necessary. With regard to the development of the vestibular system, abnormal swimming behavior and subtle alterations in vestibular system morphology have been observed in tadpoles that were exposed to microgravity after the gravity-sensitive period. Thus, we expect abnormal swimming behavior with associated small abnormalities of the vestibular system. Finally, we expect that the sperm entry point-neural plate topography will be normal, since it has recently been shown that this topography depends on a cytoplasmic rearrangement that can actually work against gravity in an experimental situation. However, other scientists predict a disruption of the normal cytoplasmic rearrangements, which might result in a randomization of the sperm entry point-neural plate relations; we will have to wait for the results of our spaceflight experiment to resolve this controversy. ■

RESULTS FROM THE SL-3 AMES RESEARCH CENTER LIFE SCIENCES PAYLOAD: A SPACEFLIGHT OF 24 RATS AND 2 MONKEYS

P.X. Callahan[1], R. Grindeland[1], G. Funk[2], and W. Lencki[2]
[1]*NASA/Ames Research Center, Moffett Field, California 94035* [2]*MATSCO/Ames Research Center, Moffett Field, California 94035*

Research Animal Holding Facilities (RAHFs), developed to support rodent and squirrel monkey animal husbandry in the Spacelab environment, have been flown on Spacelab 3 (April 29-May 6, 1985) together with a Biotelemetry System (BTS), a data processing Microcomputer and a Dynamic Environment Measurement System (DEMS) as an engineering evaluation of the hardware. The payload consisted of 2 squirrel monkeys and 24 rats.

The RAHFs performed very well, with the exception of an annoying and highly publicized particulate release which has resulted in the redesign of portions of the hardware to solve the problem. While all systems performed their required functions, temperature control and biotelemetry data were better than expected from results of ground control tests and activity monitoring deteriorated more rapidly than expected. Housekeeping data and biochemical/physiological measurements on the rats demonstrated that the RAHFs supported the flight animals very well. The animals were recovered clean and in excellent condition, and were microbiologically clean, as well. Food consumption and growth curves were normal for both large and small rats as compared to both ground and vivarium controls, as were adrenal and liver size and appearance and levels of liver tyrosine aminotransferase; all of which are indicative of an unstressed animal. While the squirrel monkeys were not examined biochemically, appearance, gross measurements and post-flight behavior indicate similar results with these animals. This information allows us to state that the RAHFs house animals in space in a manner equivalent (for biochemical and physiological investigations of the effects of weightlessness) to vivarium-housed animals in ground-based laboratories, and allows us to support future animal research in space in an experimentally valid manner.

A wealth of information was also obtained on the animals, themselves, as a result of testing to demonstrate that the RAHFs provided an adequate habitat in space, and as a result of a NASA Headquarters-sponsored program which insures that biological specimens which have flown in space will provide a maximum amount of information. In addition to the project scientists who examined the animals as part of the evaluation of the RAHFs, approximately 85 investigators took part in the study by examining those portions of the animal which were not required for the evaluation of the RAHFs. As much of this information has been, or is in the process of being, published elsewhere, this presentation serves the function of an overview.

Since one monkey experienced space adaptation syndrome while the other did not, these monkeys, as a pair, are valuable in evaluating models designed to diagnose, study and develop preventative measures for this syndrome. They are currently being used for this purpose in laboratories of other investigators.

The rats returned to earth different animals. They were flaccid, showing an almost total absence of muscle tone. They demonstrated a marked loss of mass in certain muscles (8 to 36%, primarily antigravity, but some voluntary), a loss in fiber diameter (50% in the soleus muscle), and an almost total absence of a Krebs cycle in muscles examined. This, coupled with a marked increase in stored glycogen, argues for the existence of an altered metabolism in weightlessness. That most rats showed a hemorrhaging in one muscle (*adductor longus*) is thought to be the result of readaptation to 1g rather than a reaction to launch or reentry loads, since controls exposed to higher g levels did not show a similar result.

While food consumption of the rats was normal, patterns of food and water consumption in flight were changed as compared to both control (both RAHF and RAHF-like housing) and vivarium-maintained animals. On the first day in orbit, food consumption decreased while water consumption increased and the water/food ratio increased markedly. After the second day, food consumption returned to vivarium levels, but water consumption continued to increase about linearly over the seven-day mission. In addition, the circadian food rhythm deteriorated markedly by the fourth day of the

mission. This information, coupled with reported delayed phase temperature rhythms, decreased body temperature during the active phase and decreased heart rate with a marked decreased in the difference in heart rate between active and resting phases indicates that the effect of weightlessness on circadian rhythms in the rat needs more intensive investigation.

These rats also showed bone changes, the most spectacular being a marked bone loss in the third lumbar vertebra, and a 25% decrease in elasticity and a 40% decrease in breaking strength as measured in the humerus. A decrease in prolactin producing cells, an increase in growth hormone producing cells, and an increase in stored growth hormone were found, but augmented production *and release* of growth hormone is unlikely since thymus gland size was found to be decreased. (Of interest here is the finding from an earlier flight that *in vitro* pituitary cells show a similar effect.

Other interesting, but as yet not understood, results obtained in this study demonstrate the need for further work on the physiology of spaceflight. ■

VALIDATION OF CLINOSTAT SIMULATIONS—A LONG STANDING PROBLEM

D. K. Chapman and A. H. Brown
Biology Department, University of Pennsylvania, Philadelphia, Pennsylvania 19104-6017

For higher plants, tissue cultures, microorganisms, and small animals, the horizontal clinostat, in use for more than a century especially for studies in plant gravitational physiology, has been employed with the usually tacit assumption that its simulation of hypogravity (most often 0 G) is at least an excellent approximation of the true environmental condition it putatively imitates. Obviously that assumption ought to be tested because, if it cannot be validated, an unfortunately large number of experimental findings based on tests with clinostatted biological material necessarily must be reevaluated.

Direct tests of the validity of clinostat simulations of course were impossible until scientists could attain experimental access to a (nearly) weightless environment achievable only in space. In recognition of the importance of knowing the validity of hypogravity simulations, NASA's first orbital mission designed exclusively for its effort in space-related gravitational biology (1) included two major experiments with a large number of functional objectives that would become biologists' first direct tests of clinostat simulation validity.

The experiments, flown on Biosatellites I and II, were designed to acquire quantitative data of known precision and, for each of the biological processes tested, results obtained from spaceflight were compared with appropriate ground controls. One growth process that has been studied extensively on earth and on earth bound clinostats was the epinastic response (altered position of lateral plant organs such as leaves and secondary roots). It provided the best data for the desired tests of agreement between results from the clinostat environment and from true microgravity.

It is in principle nearly impossible to "prove a negative" and if, for one or a few phenomena, results from spaceflight and results from clinostatting are in statistical agreement, we can only conclude tentatively that there may be no "real" difference—a conclusion strongly encouraged by our wishful thinking. But if the differences are large (unquestionably significant), that would be a serious blow to our tentative conclusion of equivalency and would demonstrate that clinostat simulation would not always be dependable without verification by spaceflight tests for each new phenomenon to be studied.

Epinastic responses of wheat roots and of pepper plant leaves were not the same on clinostats and in microgravity (2,3). Although the several differences were statistically significant at the 1% level, the results were qualitatively similar and some experimenters chose to discount the importance of statistical analyses of Biosatellite II results—presumably because the data showed that effects of clinostatting were less extreme that those of space flight; a possible consequence of an only small deficiency in the clinostat's ability to simulate true weightlessness.

Sixteen years after the flight of Biosatellite II, NASA's Spacelab-1 mission provided data that permitted definitive quantitative comparisons for parameters of sunflower circumnutation on earth based clinostats and in microgravity. When compared with plant behavior at 1 G circumnutation was

less vigorous on clinostats than during space flight. The changes were large, but especially significant was the difference between the effect of space flight and the effect of clinostatting; the clinostat environment suppressed circumnutation much *more* than did microgravity, a result that reasonably could not be attributed to clinostat imperfection. One could not criticize the microgravity condition as a poor simulation of the clinostat environment!

It seems evident that validation of clinostat simulations, especially for research in plant biology, has warranted a high scientific priority for about two of the "Three Decades of Life Science Research in Space", the theme of this symposium. However, the number of phenomena studied and the number of flights on which such tests were possible have been discouragingly few. We conclude that this important topic remains in the category of NASA science's unfinished business. ■

REFERENCES

(1) Saunders, J.F. (ed.) 1971. The Experiments of Biosatellite II. NASA SP-204, Sci. Tech. Info. Office, Washington, DC.

(2) Brown, A.H., Chapman, D.K., and Liu, S.W.W. 1974. A comparison of leaf epinasty induced by weightlessness or by clinostat rotation. Bioscience 24:518-520.

(3) Brown, A.H., Dahl, A.O., and Chapman, D.K. 1976. Limitation on the use of the horizontal clinostat as a gravity compensator. Plant Physiol. 58:127-130.

SLS-1, A DEDICATED LIFE SCIENCES PAYLOAD INCORPORATING RODENT, SPACE BIOLOGY, AND HABITAT STUDIES

B.P. Dalton[1], H. Leon[1], R. Hogan[1], B. Clarke[2], and E. Robinson[2]
[1]*NASA/Ames Research Center, Moffett Field, California 94035,* [2]*MATSCO/Ames Research Center, Moffett Field, California 94035*

Spacelab Life Sciences -1 (SLS-1), currently scheduled for launch in December, 1989, will be the first mission dedicated to life sciences. The Ames Research Center (ARC), as the developer of nonhuman life sciences experiments, will supply approximately 50% of the experiments for this mission. Several pieces of hardware are under development to support the ARC experiments. These include a Small Mass Measuring Unit (SMMI), a Refrigerator/Incubator Module (RIM), a General Purpose Workstation (GPSW) and General Purpose Transfer Unit (GPTU), two Animal Enclosure Modules (AEMs), and a rodent Research Animal Holding Facility (RAHF).

The SMMI will be functionally calibrated and operated in the zero-g environment as an engineering verification of its capabilities prior to use on future missions.

The RIM will support a general biology investigation of gravity sensitive structures in *Aurelia ephyrae* (jellyfish). The study will involve pre-flight and in-flight metamorphosis inducement of jellyfish polyps and subsequent inflight fixation of flight-developed *ephyrae* and photography of newly-developed *ephyrae* to provide information of graviceptor function in microgravity.

An engineering verification test of the GPWS will be performed during SLS-1. A Particulate Containment Demonstration Test (PCDT) will be carried out utilizing the GPWS, the GPTU, and the RAHF. RAHF cages will be transferred from the RAHF to the GPWS to verify particulate containment at the cage, RAHF, GPTU, and GPWS interfaces. Particulates and fluids will also be released within the GPWS to verify containment capabilities of that unit under the functional and operational constraints to be implemented in the SLS-2 and Spacelab J missions.

The two AEMs will house a total of nine rodents; four will be surgically implanted for cardiovascular studies. Data obtained from the five animals flown in the second AEM will be compared with that obtained from animals housed in the RAHF. THe AEMs allow safe flight of research animals in middeck lockers, but do not have the capability for inflight animal manipulation or data collection.

The SLS-1 RAHF is a modified version of the unit flown on Spacelab-3. The unit has been modified to contain particulates, primarily at the cage level. A high energy fan has been installed in the unit to facilitate particulate containment during activities requiring opening of the RAHF module, *i.e.*, cage removal, food changeout, waste tray changeout. In contrast to the AEMs, the RAHF does accommodate manipulation of animals in flight. The RAHF is a self-contained unit providing food, water, waste, temperature, and air flow control. Temperatures, humidity, activity, and water consumption are monitored on the ground during flight as well as in the Spacelab. During the SLS-1 mission, animals will be housed in 20 cage compartments; 4 empty cage compartments will be used for engineering tests. In addition to providing engineering data on particulate containment, use of the RAHF for animal maintenance will provide data for investigators in the following disciplines: cardiovascular, muscle, hematology/immunology, vestibular, and bone.

Two experiments have been designed to study cardiovascular changes. The objective of these studies is to elucidate the basic causal mechanism responsible for the loss of microvascular tone and orthostatic intolerance following the elimination of gravitational influences, its attendant hypodynamia, and subsequent readaptation. Implanted animals will be maintained in an AEM throughout the flight. Rodent microcirculatory bed preparations will be examined post-flight to determine the accumulative effects of weightlessness on microvascular dimensions, vasomotion, and tone. Animals will be subject to cardiovascular testing both pre- and post-flight.

Three experiments are designed to study the effects of zero-g on muscle. The objective of the first is to measure the oxidative capacity of the muscle homogenates from zero-g exposed rats using 14C-palmitate and 14C-pyruvate as substrates. Alterations in mitochondrial and glycogenolytic enzymes due to zero-g will be assessed by quantitative enzymological methods. The second study will investigate the "slow twitch" versus "fast twitch" phenomena of skeletal muscles through isoenzyme alteration. The third study also examines the "slow/fast twitch" phenomena. The investigator will determine anatomical changes of muscles via electron microscopy and biochemical changes via proteolytic enzymes of the soleus, gastrocnemius, and EDL muscles.

One of two of the hematology studies is intended to determine if the effect of the spaceflight environment on the regulation of blood volume in the rat is comparable to that in man. The red cell mass, plasma volume and related hematologic parameters will be measured pre- and post- flight. The second experiment will examine red cell production and associated parameters, *i.e.*, erythropoietin levels, cell sensitivity to erythropoietin, and the functional state of circulating red blood cells. All data will be compared to and be used as an expansion of the limited flight crew data currently available.

The vestibular study is designed to determine the extent to which deleterious changes occur in gravity receptors over the duration of an entire spaceflight and the degree to which any changes noted remain static, progress, or recover over a one-week period following recovery. The study will utilize electron microscopy to evaluate otolith organ changes and the implication to vestibular function.

The remaining study, on calcium, is intended to clarify results observed in Cosmos flights. These include reports of negative calcium balance, decreased bone density, and inhibition of bone formation. The study will incorporate tetracycline derivative labeling of bone to determine bone turnover. Pulse labels will also be used to assess periosteal formation.

The nine rodent studies will share animals in a complex and coordinated manner which will be diagramatically illustrated as part of the presentation. Processing of specimens post- flight will be coordinated between the Dryden landing site and the Kennedy Space Center facilities housing the ground controls. ■

NEW EXPERIMENTAL HARDWARE FOR SHUTTLE MIDDECK BIOLOGICAL CULTURE EXPERIMENTS

C. Dant
MATSCO/Ames Research Center, Life Sciences Project Office, Mail Stop 240A-4, Moffett Field, California 94035

Through newly developed hardware and existing space-flown hardware, new research opportunities for many biological culture experiments are available for Shuttle Middeck or SpaceHab. The Cell Culture Unit (CCU) recently built by the NASA-Ames Life Sciences Project Office (LSPO) was developed for experiments for the European Space Agency (ESA) Biorack Facility; the CCU was designed as 8 (4 double) separate culture chambers to be held within the Biorack Type I container. Each 1.6-cc chamber is a closed, sealed sterile unit that can contain a variety of organisms with media or gases; each has a piston that raises or lowers for addition or removal of liquids or gases. The ESA Passive Thermal Conditioning Units (PTCU's) can hold the containers at 11°C, 5°C, or -10°C for preflight, inflight, or postflight operations. Containers can be loaded at ambient temperatures. The LSLE Refrigerator/ Incubator Module fits in place of a middeck locker and can hold experiment containers at either 37° C or 4° C; a variable-temperature carry-on container can allow experiments to be on- or off-loaded at virtually any temperature from 0-37° C. Therefore, animal, human and plant cells, yeast, bacteria, fungi, and certain ova can be grown at these temperatures during pre- and inflight periods, and fixed or frozen inflight; media or gases can be removed and stored in any of the specified temperatures inflight. Zero-gravity and radiation studies can include developmental processes, secretory studies, cell-cell communication, immunology, hematology, regeneration/aging, and plant physiology. ■

ISOZYME ANALYSES OF REGENERANT WHEAT

Z. N. Hashim, W. F. Campbell and J. G. Carman
Plant Science Department, Utah State University, Logan, Utah 84322-4820

It is now possible to produce shoots and plantlets of wheat, *Triticum aestivum* L., by using immature wheat embryos as explants in selective media. Research, however, has shown relatively high frequencies of genetic variability and morphological abnormality in plants regenerated from wheat tissue culture. Allozyme techniques have been useful in analyzing the genetic variation in cultivated plant populations, and considerable information is now available on the genetic control of wheat isozymes. The chromosomal locations of genes that encode the multiple molecular forms of more than 20 wheat enzymes have been identified. Comparison of the banding patterns from parental wheat plants and those produced from *in-vitro*-grown plants should provide clues to the type of variant induced in the tissue culture grown wheat. For example, if certain banding patterns are missing in variant plants, it might suggest that point mutations, deletions or certain types of chromosomal aberrations have occurred. If, however, the banding patterns in the variants from the *in-vitro*-grown wheat plants have shifted to different locations from what was observed in the parental lines, then perhaps only point mutations have occurred. Examination of zymogram phenotypes of parental lines and tissue culture regenerated plants should confirm this hypothesis. To explore this possibility, spring wheat, *Triticum aestivum* L. cv PCYT-10 (CIMMYT Ciano X Gallo, EBWN 7582) plants were regenerated from immature embryos. Parental plants and three consecutive generations of regenerants were analyzed for leaf isozymes: glutamate oxaloacetate transminase (GOT) (E.C. 2.6.1.1), endopeptidase (EP) (E.C. 3.4.99), and leucine aminopeptidase (LAP) (E.C. 3.411.1). None of the regenerants exhibited any

variation with GOT or LAP. However, one generation of regenerants showed a mutation for EP. The fast-moving EP band was missing in forty-four percent of the plants from SC_2 regenerants. Of the remaining plants, 28% of them showed a light band in that EP region, while the rest showed normal EP bands. However, approximately 30% of these plants did not set seeds, thus, the variants did not survive. ■

THE LSPO FLIGHT PRIMATE PROJECT

K. L. Hinds, W. E. Hinds, C. D. Tollinger and G. A. Funk
MATSCO/Ames Research Center, Life Sciences Project Office, Mail Stop 240A-4, Moffett Field, California 94035

The Life Sciences Project Office (LSPO) Flight Primate Project was developed to support life sciences research in microgravity using the nonhuman primate as a model for humans in space. The successful execution of the program requires the coordination and completion of several different elements for each flight experiment. Project design involves the consideration of numerous factors, including the monkey model(s) to be used, the source and number of animals needed, animal training regimen and hardware requirements, experimental and microbiological requirements and constraints, and the parameters of the flight environment itself. Flight animal housing must be developed and tested; at a minimum, this should provide safe housing with automatic feeding and watering, and animal restraint where needed. It may also be desirable to incorporate a means for clinical specimen or data collection within the housing envelope. A thorough system of flight and control animal support must be established, including a method for acquiring and maintaining flight-candidate animals in the microbiologically acceptable condition known as "NASA Flight Quality." Planning of the various operational aspects of the proposed mission must be initiated early in the development cycle to allow for accurate translation of the Principal Investigator's (PI's) one-g experiments to a set of zero-g operational instructions that will permit execution of the experiment on-orbit. Clearly, the extensive training of crewmembers and their incorporation into the research team is of increasing importance as the mission matures. With the support of other NASA Centers, the payload hardware is integrated into the flight vehicle and the entire flight operations team is trained as an integrated system. Finally, the actual mission is flown and experimental flight and ground control data is collected. PIs and Development Center personnel again work as a team to analyze the data and issue the reports. Information gathered during each flight experiment is ultimately used to enhance the science return of subsequent Primate Flight Project missions, to contribute to the development of technology to benefit earthbound mankind, and to promote the long-term presence of humans in space. ■

MAGNETIC RESONANCE IMAGING OF RAT HINDLIMB MUSCLES

J. A. Hodgson[1], P. L. Lee[2] and P. Barker[3]
[1]*Department of Kinesiology and Brain Research Institute, University of California, Los Angeles, California 90024,* [2]*Jet Propulsion Laboratory, California Institute of Technology, Pasadena, California, and* [3]*Huntington Memorial Research Institute, Pasadena, California*

Studies of hindlimb suspension in rats have demonstrated substantial atrophy of skeletal muscle over a short period of time. Similar effects in spaceflight provide a major incentive to study the probable causes of atrophy and develop procedures to minimize the extreme loss of mass observed in some muscles. Research into the timecourse of atrophy and procedures or exercises which may prevent or reverse atrophy require measurements of muscle mass to be made over a range of time periods and following specific manipulations. Usually this has been achieved by sacrificing individual animals over the requisite time periods and estimating trends from the combined results. Recent developments in noninvasive imaging now provide an opportunity to follow the course of internal changes in individual animals over unlimited periods of time. Such procedures eliminate inaccuracies introduced into experimental results due to variability between animals and minimize the number of experimental subjects.

We are therefore developing a Magnetic Resonance Imaging protocol to obtain serial sections of a rat hindlimb and computational techniques to reconstruct 3-dimensional images of specific muscles. Rats are anesthetized with Pentobarbital Sodium and a small custom-built Helmholtz coil (25-30mm diameter, 30-50mm long) is fitted over the rat hindlimb. The rat is then placed in a General Electric Chemical Shift Imaging unit having a 4.7 Tesla magnet and a bore diameter of 33cm. Imaging is performed at 200 MHz for protons over a 20mm-square area with a resolution of 256 points over each dimension. Serial images of 2mm slices at 5mm intervals are collected for 3D reconstruction.

Initial results indicate that resolution down to 0.1mm is possible in the cross sections and that such resolution provides considerable structural detail of the internal organization of the limb. Outlines of some muscles, blood vessels and tendons are clearly discernible and provide images from which 3D reconstruction of individual muscles and groups of muscles will be possible.

Muscle volume is not a direct measure of a muscle's potential for generating force. Many short fibers in parallel develop more force and shorten more slowly than a similar muscle volume made up of fewer longer fibers (Wickiewitz *et al.*, 1983, 1984). It is a further aim of this project to validate estimates of muscle force derived from measures of muscle volume and known muscle anatomy. The rat provides a model where estimates of muscle force may be compared directly with forces measured directly in a terminal experiment before the imaging techniques are used to estimate muscle force in human subjects. ■

REFERENCES

1. T.L. Wickiewitz, R.R. Roy, P.L. Powell and v.R. Edgerton: Muscle architecture of the human lower limb. J. App. Physiol. 52, 435-443, 1983.
2. T.L. Wickiewitz, R.R. Roy, P. L. Powell, J.J. Perrine and V.R. Edgerton: Muscle architecture and force-velocity relationships in human. J. App. Physiol. 52, 435-443, 1984.

EFFECTS OF HYPERGRAVITY ON CRANIOFACIAL MORPHOLOGY IN MICE

J. Moore, W. S. Leifeste, N. P. Leifeste, and J. Duke
University of Texas Dental Branch, Dental Science Institute, P. O. Box 20068, Houston, Texas 77225

INTRODUCTION

The first non-weightbearing bones found to be affected by gravitational changes were humeri of centrifuged chickens, which were longer and wider than those of controls (1). Changes in humeri were also noted in rats flown on Cosmos 1129 (2). Mandibles of these rats, and of rats from Spacelab 3, were found to have changes in matrix maturation (3,4). In the studies described here, skulls of mice that had been centrifuged for a year were subjected to cephalometric analyses, and found to be longer and flatter than skulls of control rats.

MATERIALS AND METHODS

The small animal centrifuge used in this study was based on the design of Walters, Wunder and Smith (5), carries eight cages at four g levels (only six were used for this study), and at the 45 rpm used in this experiment, has a maximum swing-out radius of 155 cm. Sixty ICR female mice (Harlan-Sprague-Dawley, Indianapolis) were placed on the centrifuge when four weeks old and centrifuged for over a year. Mice were housed in groups of ten, and centrifuged at 2.3g (one cage), 2.6g (one cage), 2.9g (two cages), and 3.5g (two cages). Sixty control female mice, also in groups of ten, were housed in the same room. Centrifuge operation was interrupted twice weekly for cleaning and feeding (average stop: 45 minutes) and three times weekly for procedures in a mating study (average stop: 24 minutes).

After 55 weeks of centrifugation, one-half of the mice were sacrificed by cervical dislocation; the remainder were sacrificed a week later. The heads were removed, cleaned of soft tissues and fixed in 10% buffered neutral formalin, or in 2% paraformaldehyde in 0.1M cacodylate plus 0.5% glutaraldehyde.

Skulls were positioned by the external auditory meati in a specially constructed cephalostat, and a standard dental X- ray machine (Gendex-GX-1000) and Kodak ultra-speed periapical film were used to take lateral radiographs. After developing, the radiographs were used to make prints with a final enlargement of 8.78. Measurements of craniofacial reference points were made directly on the prints using a ZIDAS digitizing tablet (6; Fig. 1). Significance was determined by Student's t test.

RESULTS

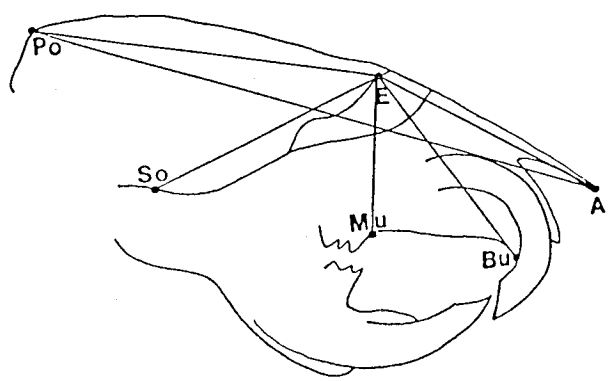

Figure 1. Reference Points on the Skull (from Engstrom et al., 1985).

The portion of the skull most affected in centrifugation was the viscerocranium. Viscerocranial height (E-Mu) was significantly decreased in all centrifuged animals (Fig. 2). Viscerocranial length (E-Bu) was also less in centrifuged animals, significantly so at 2.9 and 3.5 g (Fig. 3). Nasal bone length (E-A) decreased as the g level increased, but these differences were not significant. Significant *increases* occurred in neurocranial length (E- Po) at 2.6 and 3.5 g, and in total skull length (Po-A) at 3.5 g.

DISCUSSION

Figure 2.

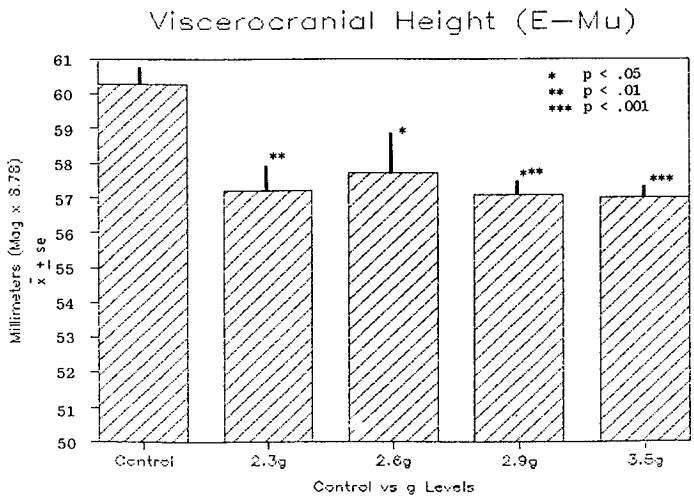

Figure 3.

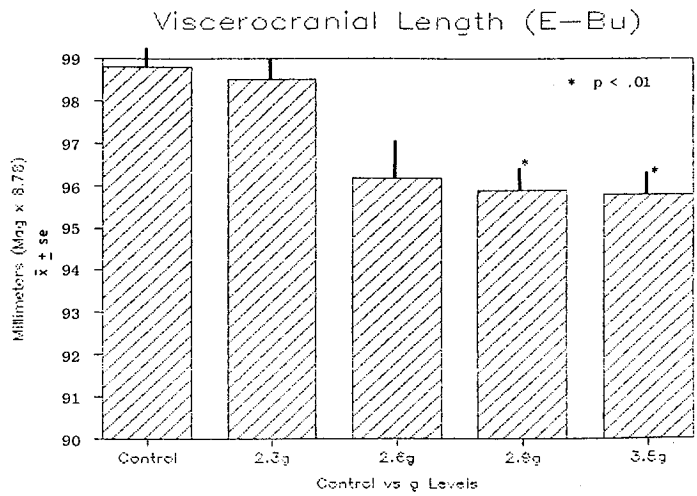

Previous studies have shown that non-weightbearing bones (*i.e.*, humeri and mandibles) are affected by gravitational changes (1,2,3,4). In this study, skulls of female mice centrifuged for over a year were found to be elongated and compressed, changes that could be attributed to increased activities of the antigravity muscles of the trunk and neck which attach in the posterior/dorsal region of the skull. These muscles must exert more pull in excess gravity in order to fulfill their functions of holding erect and/or raising the head. This increased pull could produce skull elongation and contribute to flattening. The masseter, also, must work harder in excess g, and may have played a role in the decrease in skull height. Studies of muscle attachment sites are now in progress, as are studies of the thickness of the cranial vault. These will be followed by histological and electron microscopy analyses of decalcified specimens.

Other explanations for the decreased skull heights are possible. When first placed on the centrifuge, animals undergo an adaptation period during which they lose weight, or at least, do not gain weight (7). Since these mice were still in a growing phase when the study began, the changes seen in skull dimension may have been due to nutritional deficiencies during this adaptation period. Skulls of mice sacrificed immediately after the adaptation period will be analyzed to determine if the changes seen after a year are already present after two-three weeks of centrifugation. Decreased hydrostatic pressure in the brain may also have played a role in smaller skull size.

This important aspect of skeletal morphology has not previously been addressed in gravitational studies. Continuation of this investigation should provide valuable information on the effects of gravitational changes on non- weightbearing bones.

ACKNOWLEDGMENTS

J. Cham, E. Yu, C. Williams, E. Puente, A. Kilpatrick. Supported by NASA Grant NAG2-332. ■

REFERENCES

1. Smith, A.H. and Kelly, C.F. 1961 Ann. N.Y. Acad. Sci. *110*: 410-413.
2. Wronski, T.J., *et al.* 1981. In: NASA Technical Memorandum 81289, pp. 101-126.
3. Simmons, D.J., *et al.* 1981. In: NASA Technical Memorandum 81289, pp. 279-306.
4. Russell, J.E. and Simmons, D.J. 1985. The Physiologist: *28*: s235-s236.
5. Walters, G.R., *et al.*, 1960. J. Appl. Physiol. *15*: 307-308.
6. Engstrom, H. *et al.* 1985. In: Normal and Abnormal Bone Growth: Basic and Clinical Research. Liss: pp 109-124.
7. Janer, L. and Duke, J. 1984. The Physiologist *27*: s75- s76.

EFFECTS OF MICROGRAVITY ON RAT PITUITARY GROWTH HORMONE (GH) CELL FUNCTION: COMPARISON OF RESULTS OF THE SL-3 MISSION WITH RAT "UNLOADING" ON EARTH

K. Motter[1], M. Vasques[2], C. Hayes[1], M. Kendall[1], G. Tietjen[2], W. C. Hymer[1], and R. Grindeland[2]
[1]*Department of Molecular and Cellular Biology, The Pennsylvania State University, University Park, Pennsylvania 16802* [2]*NASA/Ames Research Center, Moffett Field, California 94035*

RATIONALE

We recently reported that anterior pituitary GH cells prepared from glands of rats flown for 7 days on the SL-3 mission (April, 1985) showed changes compared to cells prepared from ground based controls (Grindeland *et al.*, Am. J. Physiol. 252:R209-R215, 1987). Specifically, flight cells had *more* GH/cell, but released *less* GH into culture media during a subsequent 6 day test period *in vitro*. Since release of prolactin from another cell type in these suspensions was unaffected by flight, we concluded that the "secretory defect" might be specific for GH. When other aliquots of the flight cells were encapsulated into XM-50 Amicon hollow fibers and implanted into the cerebral ventricles of hypophysectomized rats (Hymer *et al.*, Neuroendocrinology, 1981), the tibial line plates of animals implanted with flight cells were about 1/2 the width of epiphyseal plates of animals implanted with control cells. Thus, both *in vitro* and *in vivo* tests of the flight cells supported the secretory lesion hypothesis. Finally, we tested for the presence of multiple molecular forms of secreted GH into the serum free culture medium. After HPLC fractionation, testing for the immunological (RIA) and biological (3T3 mouse fibroblast adipogenic assay) activities revealed that the flight cells were apparently unable to release a high MW (~ 100 kD) form that was rich in biological activity. A flight-induced lesion of secretion of bioactive GH of the type described here could account for the muscle and bone changes observed in the SL-3 rats.

During the hiatus in microgravity research, we recently sought to determine if we could mimic the SL-3 pituitary experiment on earth using the rat hindlimb suspension model. Although the analyses are as yet incomplete, we compare, in this poster, the results of our two experiments obtained to date.

METHODS

Rats were housed in the same cages as those used on board the SL-3 mission. They were maintained either in hindlimb suspension (experimental) or freely moving (control) for 7 days. Pituitary glands from 8 animals were dissociated into single cells by trypsinization, counted by hemocytometry, analyzed by flow cytometry to determine the percentage of GH cells, cultured in serum-containing or serum-free media for 6 days to determine GH release *in vitro*, implanted into hypophysectomized rates to determine GH release *in vivo*, and finally analyzed for different secreted GH molecular forms by HPLC/3T3 assay/RIA. (See Grindeland *et al.*, Am. J. Physiol. 252:R209-R215, 1987 for methodological details).

RESULTS

- The % of GH cells in glands of the "unloaded" animals (37%) was not different from that of the controls (39%)—based on counts of 80,000 cells by laser flow cytometry. This negative result basically agrees with our SL-3 data.
- The concentration of GH within the pituitary cells of the "unloaded" rats was 77 ng/1000 GH cells, while that in the controls was 48 ng/1000 GH cells. In the SL-3 experiment, these levels were 33 ng/1000 GH cells for flight and 20 ng/1000 GH cells for control.
- In serum containing medium, cells from "unloaded" rats secreted GH at 145±6 ng/1000 GH cells while those from the controls secreted 188±10 ng/1000 GH cells. In the SL-3 experiment, GH release prepared from cells of the rats flown in space was 60±2 ng/1000 GH cells, while that of the controls kept at Cape Kennedy was 105±4 ng/1000 GH cells.
- In chemically defined (serum-free) medium, release of GH from cells of "unloaded" rats was 52±10 ng/1000 GH cells vs 128±12 ng/1000 GH cells from controls.
- HPLC fractionation of GH variant forms released into the defined culture medium is not yet complete.
- Application of our newly developed cell blot assay for the determination of GH secretion by single cells revealed interesting GH subpopulation heterogeneity. The data suggest that the GH cells belonging to the "high secretor" population are most affected by unloading.

SUMMARY

These preliminary results document that a majority of the changes in GH cell function observed thus far in "unloaded" rats are in the same direction and of similar order to those found in the actual microgravity experiment. These results are particularly encouraging in that they argue for continued use of the "unloaded" rat to seek answers to such basic questions as the time course of recovery after exposure to microgravity simulation. Further, they will encourage study relating to mechanism(s) of the secretory defect as well as testing for *in vivo* countermeasures.

Supported in part by NASA NCC 2-370 to WCH. ■

HEAVY ION RADIATION EFFECTS IN *C. ELEGANS*

G. A. Nelson[1], T. P. Coohill[1], T. Marshall[1], W. W. Schubert[1], E. V. Benton[2]
[1]*Applied Sciences and Microgravity Experiments (125-112), Jet Propulsion Laboratory, California Institute of Technology, Pasadena, California 91109 and* [2]*Department of Physics, University of San Francisco, San Francisco, California 94117*

The nematode, *Caenorhabditis elegans*, is being used as a model system for the evaluation of high and low LET radiation effects on cell reproduction, differentiation and mutation *in vivo*. *C. elegans* is a small, simple nematode with a variety of tissues and organs including digestive system, nervous system, muscles, and reproductive system providing a variety of target cells for radiation studies. The anatomy is invariant from individual to individual with fixed numbers of cells and fixed patterns of cell division. Organs and tissues develop from single cell primordia and the developmental timing is fixed so that whole populations of animals can be age-synchronized to produce animals with anatomical targets of precisely controlled cell number and function. Sophisticated genetic methods are available for the production and analysis of mutations, chromosomal aberrations and chromosome loss. Finally, short generation times (3-4 days) and high reproductive rates (282 progeny per worm) provide a means of collecting data on large populations in a relatively short period of time.

Gamma rays from Cobalt 60 sources and accelerated particles produced at the Lawrence Berkeley Laboratory BEVALAC accelerator have been used in studies aimed at providing risk assessment data for spaceflight crews encountering cosmic rays in earth orbit.

CELL INACTIVATION STUDIES

Fertility analysis. This assay quantifies damage to 4 primordial gonad cells which interferes with the developmental program resulting in an adult gonad whose normal function is to produce 282 progeny.

This test is a type of *in vivo* colony forming assay. Figure 1 shows a series of inactivation curves as functions of particle fluence for ions of widely varying LET. An RBE vs LET curve normalized to gamma rays has been constructed. It shows a sharp RBE peak of about 2 at an LET of about 120 KeV/um. The production of males has also been quantified during brood analysis. This is a direct measure of the rate of X- chromosome loss or inactivation which produces XO males from XX mothers.

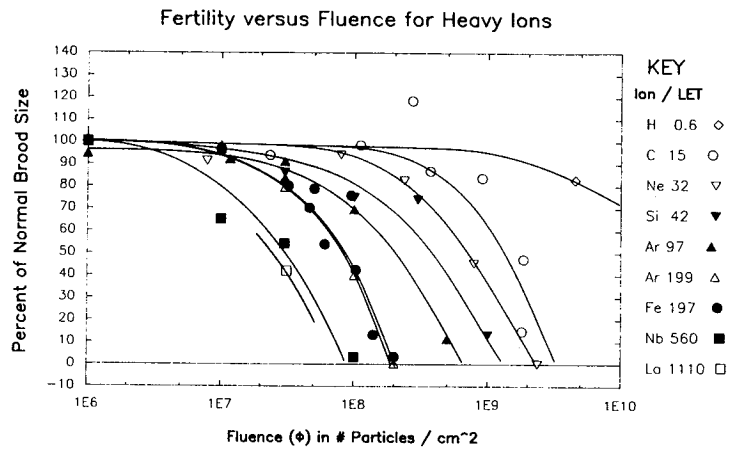

Figure 1. Brood size as a function of ion fluence for a variety of ion species. Note the strong LET dependence for gonad cell inactivation as seen in the fluence required to produce D10 and D37 levels of "survival." The extent of the shoulder and slope of the linear portions of the curves is also LET dependent. Each point represents the mean of a population of hermaphrodites.

Embryo inactivation. The inactivation of young embryos has been investigated in conjunction with radiation hypersensitive mutations (putative DNA repair genes) rad-1 I, rad-3 I, rad-4 V, and rad-7 IV to determine whether high LET radiation damage is repaired by mechanisms which are the same as or different from those used for UV and gamma/X-ray damage. eT1 strains bearing these rad-# mutations have been constructed for use in similar experiments with mutation (see below).

GENETIC STUDIES

Recessive lethal mutation. A sensitive assay for the detection of recessive lethal mutations in a large genetically defined region corresponding to 15% of the nematode's genome is being used. The principle of the assay is to isolate recessive lethals in a strain balanced by the reciprocal translocation eT1(III;V) so that new mutations are located in recombinationally suppressed chromosomes where they can be maintained in the heterozygous state for testing. Mutation rate versus fluence relationships have been established for ions of LET from 1 to 1110 KeV/um. An RBE versus LET curve has been constructed and shows a broad peak of RBE = 6-7 over an LET range of 50 to 250 KeV/um. The probability of converting a single ion hit into a lethal mutation in the eT1 region of 1.2x107 base pairs has been calculated to 0.054 for iron ions of LET 190 KeV/um. A set of 60 mutants generated by C, Ne, Si, Ar, Fe and La ions is being characterized to determine the relative abundances of point mutations, deletions and chromosomal rearrangements.

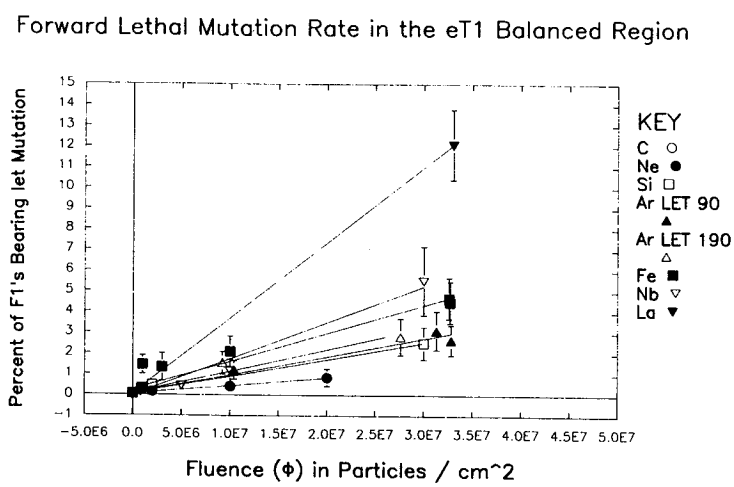

Figure 2. Mutation rate (linear regression lines) versus fluence for ions of various LET. Mutation rate is the percentage of lethal-bearing offspring that are derived from irradiated parents. The target is a mature sperm plus an average meiotic oocyte located in a parent JP10 hermaphrodite which fertilize each other to produce one of the scored F1 animals. In other words, this mutation rate is the percent of diploid JP10 genomes which sustained a lethal mutation in the 40 map unit or 1.2×10^7 base pair eT1 balanced region. Note the strong LET dependence of mutation.

Nucleoplasmic bridge formation. When newly-hatched larvae are irradiated, defects in karyokinesis of intestinal cells arise which we propose are derived from radiation- induced mitotic crossover or breakage and reannealing of chromosomes at random. Some of these events may lead to stable dicentric chromosomes which prevent completion of nuclear division and are seen in adult worms as nucleoplasmic bridges. Fluence vs response relationships for nucleoplasmic bridge formation have been constructed. The response saturates at high fluence and exhibits a strong LET dependence.

Other studies. Several other endpoints are being investigated. The production of duplications of the right arm of the X-chromosome has been quantified with interesting kinetics suggesting that particles are very efficient in producing chromosome breaks, but also are likely to produce second site lethals. Developmental delay and dominant lethality in sperm are being studied as are sex-linked lethals and mutations in the unc-22 gene for which molecular probes are available. ■

GRAVITY DEPENDENT BEHAVIOR OF *AURELIA AURITA* EPHYRAE

C. M. Oman[1] and D. B. Spangenberg[2]
[1]*Center for Space Research, Massachusetts Institute of Technology, Cambridge, Massachusetts 02139 and*
[2]*Department of Pathology, Eastern Virginia Medical School, Norfolk, Virginia 23501*

Gravity dependent behavior of young ephyrae of the common jellyfish *Aurelia aurita* (Norfolk), was studied in parabolic flight on the NASA KC-135 aircraft. Ephyrae were strobilated from laboratory polyps in iodinated seawater (Spangenberg, 1967). Active animals were selected, and transported to the test site, where they were kept for up to 5 days near 70 deg. F. in containers. 6-20 ephyrae were transferred into each of several observation chambers several hours prior to flight each day. The chambers were filled with seawater and capped. Polyps were also flown in a separate chamber on two occasions. Each day, the KC-135 flew up to 40 successive parabolas in rollercoaster fashion, providing periods of weightlessness (typically 18 sec. duration) preceded and followed by longer intervals of hypergravity (typically 1.5 - 1.8 g). Occasionally the hypergravic period was followed by a 1-2 min. period of normal gravity. Informal observations were made on 3 flights under both hand held and free floating conditions. G dependent behavior of ephyrae was then recorded during 6 parabolas on each of 3 subsequent flights using a single video camera (Panasonic Newvicon, 105 mm macro lens, 1 in. sq. field of view at 18 inches) and 3/4 inch U-Matic recorder. The camera, chamber, and an aircraft Z axis accelerometer were mounted near the c.g. of the airplane, with the optic axis parallel to the aircraft X axis.

Behavior of ephyrae was clearly gravity dependent: With the onset of hypergravity, many animals swam more vigorously "upward" for at least half a dozen strokes. The swimming path usually deviated less than 20-30 degrees from the apparent vertical. Animals oriented in inverted attitudes at the end of the 0-g phase typically performed a looping maneuver (radius several body diameters) in hypergravity until reoriented mouth "downwards". When not actively stroking in hypergravity, animals would sink passively, mouth downwards, more rapidly than in 1-g, and the lappets of the animals' arms usually deflected aborally, above the animals. When the subsequent interval of weightlessness began, active animals consistently stopped stroking for several seconds. Thereafter, most animals would start to swim again, but usually more slowly than in normal or hypergravity, and in directions dictated by their initial orientation. Orienting behavior was not apparent in 0-g. Animals occasionally turned randomly and some swam towards the "bottom" of the container. When gravity reappeared, most of the ephyrae would immediately start swimming vigorously again for at least several strokes. The threshold for this effect was estimated to be less than 0.2 g. Several animals were observed to respond to g onset at or below the 0.05 - 0.1 g level. If the g level then increased to normal 1.0 g levels, animals typically stopped swimming momentarily, in a manner similar to the pause seen upon entry into weightlessness. The sessile polyps flown exhibited no obvious 0-g change in active behavior.

The small (1-2 mm dia.), eight armed, free swimming ephyrae we used in the present experiments metamorphose from small bottom dwelling polyps. Ephyrae subsequently mature into larger

medusaeform adults. *Aurelia aurita* medusae are believed to normally orient to gravity using tilt information sensed by 8 rhopalial organs located at the outer edge of the bell of the medusa (Frankel, 1925; Bozler, 1926, cited by Hyman, 1940; Hundgen and Biela, 1982). The individual rhopalium is a small, clublike, appendage containing gypsum crystals at the distal end (Spangenberg and Beck, 1968). The position of this weighted, pendulous structure is believed transduced by mechanoreceptive ciliated cells located at the base of the rhopalium. Activity of rhopalial mechanosensory cells is thought to modulate pacemaker cells in the giant fiber nerve net which in turn controls adjacent radially oriented muscles and the coronal muscles used in swimming. An active orienting reflex in scyphozoan medusae has been demonstrated by Frankel (1925) and Bozler (1926), who showed that the righting reflex was absent when rhopalia on the upturned side were extirpated. Whether or when this righting reflex becomes expressed in ephyrae is not yet known. Ephyrae have less mesoglea than the nearly neutrally buoyant medusae, and swimming behavior typically consists of several swimming strokes, followed by a passive sinking phase. If ephyrae are to remain in their normal environment near the surface of the water column, they must functionally be able to localize the direction of gravity and swim "up". Since ephyrae typically encounter prey while passively sinking between swimming stroke phases, the maintenance of a mouth down orientation prior to the onset of each "sink" phase is likely also important for normal feeding.

We believe G-orienting behavior we observed in our ephyrae takes place by at least one of several possible mechanisms: a) "Shuttlecock" passive orienting: When an ephyra stops swimming, and sinks under the influence of gravity, the lappets of the arms flow back well above the center of gravity of the animal, and flow drag on the lappets exerts a turning moment until the animal is oriented upright. This mechanism reorients the possibly falling ephyrae mouth down in a manner reminiscent of a falling badminton shuttlecock, or a parachutist beneath his canopy. b) Rhopalial modulation of stroke frequency: In 0-g or when inverted in 1-g, rhopalia may assume anatomical positions which functionally inhibit activity simultaneously in all the radial swimming muscles. In 1-g, an inhibition of stroking would in turn lead to sinking, and subsequent passive orientation to the upright via the shuttlecock mechanism. c) Hydrostatic buoyancy effects: Turning moments likely arise during some phases of stroke due to separation of center of gravity and the hydrostatic center of buoyancy. d) Active rhopalial reflex steering may exist when the animal tilts, due to differential contraction of swimming muscles, caused by asymmetrical stimulation of rhopalial mechanoreceptors, as is believed to occur in adult medusae.

Our videotape documented the existence of the passive shuttlecock mechanism. The rhopalial stroke frequency modulation hypothesis is supported by our observations of momentarily decreased stroke frequency during g offset, and increased frequency during onset. That inhibition was observed with any decrease in g level (*e.g.* when going from 1.8 to 1.0 g conditions), and that excitation was seen with g increase is also consistent with this hypothesis, but suggests that the sensory/motor reflex arc also exhibits stimulus adaptation. We believe the hydrostatic buoyancy effect—although arguably physically present during some phases of stroke—is likely physically negligible. The existence of active rhopalial reflex steering in ephyrae as well as adult jellyfish is clearly suggested—but not proved—by the "looping towards g" behavior seen in some stroking animals during hypergravity. More conclusive evidence may come from behavioral experimentation with animals raised in a low sulfate medium (Spangenberg, 1968) and which lack rhopalial statolithic crystals.

Supported in part by NASA Contracts A42390C (CPL) and NAG 2-343. We thank D. M. LaFrance, S. Davis, L. R. Young, R. L. Renshaw, M. A. Shelhamer, and R. Williams. ■

REFERENCES

Bozler, E (1926) Z vergl Physiol 4:797-817.
Frankel, G (1925) Z verg Physiol 2:658-690.
Hyman, L (1940) The Invertebrates: Protozoa through Ctenophora, McGraw Hill.
Hundgen, M and Biela, C (1982) J Ultra Res 80:178-184.
Spangenberg, D (1967) J Expt. Zool 165:441-450.
Spangenberg, D (1967) J Exptl Zool 169:487-500.
Spangenberg, D and Beck (1968) Trans Am Microscopical Soc 87:329-335. ■

A SELF-CONTAINED INDUCEMENT/FIXATION SYSTEM FOR SMALL AQUATIC ORGANISMS

K. Rossberg and D. Spangenberg
MATSCO/Ames Research Center, Life Sciences Project Office, Mail Stop 240A-4, Moffett Field, California 94035

A system was developed for inducing and fixing live jellyfish easily and quickly in zero gravity. Several key features make it ideal for use in small payload, middeck experiments. It is small, compact, lightweight, self- contained and reliable. It requires minimal crew time to operate and completely isolates toxic substances and gases from live test animals until the desired introduction time. The system consists of a series of plastic syringes each containing an inner, sealed, burstable bag filled with the desired solution. The syringe is secured to an aluminum cylindrical guide which slides into a plastic housing. The housing connects the syringes to the specimen bag and provides an injection path through a rubber septum. To operate, the cylinder is slid into the housing, forcing penetration of the syringe needle through the septum, and locked into place. The plunger is depressed until the inner bag bursts and contents are fully injected into the specimen compartment. The system was designed for and ground tested on an extremely fragile and sensitive developing organism (*Aurelia* jellyfish) and proved highly successful. The entire operation can be completed within 15 seconds. ■

TIME COURSE OF SOLEUS MUSCLE MYOSIN EXPRESSION DURING HINDLIMB SUSPENSION AND RECOVERY

D. B. Thomason, R. E. Herrick, D. Surdyka, and K. M. Baldwin
Department of Physiology and Biophysics, University of California, Irvine, Irvine, California 92717

The purpose of this study was to utilize a rodent hindlimb suspension model in which to examine the time-course of adult rodent soleus muscle myofibril and myosin isoform expression following 4, 8, 16, 28, and 56 days of suspension. The time course of soleus muscle recovery was also examined after 28 days of unweighting followed by an additional provision of 4, 8, 18, and 28 days of unrestricted cage activity.

During suspension, the hindlimb unweighting produced a dramatic, though relatively selective atrophy of the hindlimb musculature. The greatest degree of atrophy was observed in muscles with a predominance of histochemically classified slow-twitch-oxidative fibers (soleus, adductor longus, vastus intermedius) and containing a predominance of the slow-myosin isoform (SM). Selective fast-twitch muscles, acting synergistically to the above described slow-twitch muscles, responded with remarkably lower degrees of atrophy. The recovery of muscle weight resulting from subsequent unrestricted cage activity following termination of suspension was similarly rapid, with nearly complete recovery of both slow- and fast-twitch muscle weight after 28 days.

During suspension, soleus muscle myofibril protein (mg per muscle pair) decreased from 34.1 ± 1.5 in the control group to 6.9 ± 0.7 in the suspended group (t=56 days of suspension). The calculated half life for this loss was 4.1 days. The estimated slow-myosin isoform content (mg per muscle pair) decreased from 13.4 ± 1 in the control group to 2.1 ± 0.1 in the suspended group, reflecting a half-life of 3.6 days. The relative proportion of the other myosin isoforms (collectively designated as fast-myosins (FM) was increased after 28 and 56 days of suspension, reflecting an apparent *de novo* synthesis of FM and the loss of SM.

Recovery of contractile protein following 28 days of suspension was slower for both the myofibril protein and the SM isoform (half-life of 10 days). These data suggest that loss of weight bearing specifically affected the mechanisms of contractile protein expression reflected in soleus muscle protein degradation processes. In addition, the SM and FM isoforms appear to be differentially affected by the loss of weight bearing activity. ■

POSTFLIGHT ANALYSES OF FUNGI EXPOSED TO THE ENVIRONMENT OF DEEP SPACE ON APOLLO

P. A. Volz[1] and M. J. Kennedy[2]
[1]*Mycology Laboratory, Eastern Michigan University, Ypsilanti, Michigan 48197,* [2] *The Upjohn Company, Kalamazoo, Michigan 49001*

Fungal species serve as excellent test organisms when studying environmental systems and the influences of environmental parameters on cells, cell organelles, and cell structure. Many studies have been conducted with fungi and other microorganisms aboard balloons, earth satellites and high-altitude sounding rockets for evaluations of environmental conditions in space. No spaceflight mission before the Apollo program gave opportunity to qualitatively and quantitatively examine cellular systems in space after exposure to space parameters.

Selected fungal species were placed in the Microbial Ecology Evaluation Device (MEED) of Apollo and were exposed to various qualitative and quantitative spaceflight parameters according to the designs and construction of the flight hardware. Two yeast fungi, *Rhodotorula rubra* and *Saccharomyces cerevisiae*, and two filamentous fungi, *Trichophyton terrestre* and *Chaetomium globosum*, were the four species selected from two years of preflight studies that examined all classes of fungi in order to gain maximum postflight data and information on the effects of space on living cellular systems.

Upon retrieval of the organisms at splashdown, the flight hardware was immediately air-transported to the Lunar Receiving Laboratory at NASA/JSC for unloading and for initial studies on each species. The first group of studies on the four unrelated fungi concerned survival rates at each of several spaceflight parameters examined. Postflight studies followed on the retrieved organisms for 10 years after Apollo, examining gross changes at the macroscopic level. Several additional studies identified tissue variation, cellular changes, subcellular variation, and changes in the physiology of the organisms according to the selected exposure parameters examined in space. The designed studies on space-flown fungal phenotypes were made in comparison to various spaceflight controls, solar simulation, launch and ground controls. ■

BENDING OF OAT SHOOTS TOWARD LIGHT IN MICROGRAVITY

M. R. Williams
MATSCO/Ames Research Center, Life Sciences Project Office, Mail Stop 240A-4, Moffett Field, California 94035

Two chambers of oat seedlings were flown in th Plant Growth Units aboard Spacelab Mission 2. The Plant Growth Units, designed by NASA-Ames Research Center, are self-contained units holding six individual closed chambers for small seedlings. Photographs taken of the seedlings during spaceflight showed that the shoots responded phototropically by growing toward the light. Seedlings growing at the ends of the chambers were bent towards the center of the chambers where the light is most intense. Control experiments using the Plant Growth Units were performed at NASA's Kennedy Space Center after the flight. The bending of the oat shoots grown in microgravity was greater than the bending of the shoots grown on Earth due to the gravitropic response of plants on Earth. ■

REVIEW OF SPACE CABIN AND EVA SUIT ENVIRONMENTAL RESEARCH AT THE SCHOOL OF AEROSPACE MEDICINE: THREE DECADES

J. D. Adams
Space Science Application Laboratory, La Vernia, Texas 78121

From the inception of the manned space program, the protection of man in the space flight environment was the main research thrust of the School of Aerospace Medicine. This paper reviews the highlights of the environmental research with regard to space cabin and suit atmosphere, pressure, gas mixture, etc., from the Mercury through the Shuttle programs. Through space cabin simulation, basic questions such as, "What pressure range can man tolerate breathing 100% O_2 or O_2/N_2 mixtures with regard to hypoxia, oxygen toxicity, decompression sickness, etc.?" to "Can man live without nitrogen in his environment? How much inspired CO_2 can man tolerate?" as well as man's thermal regulation and tolerance at reduced pressure.

Denitrogenation and staged pressure reduction were used early on to prevent decompression sickness during exposure to EVA suit pressure of 3.5psia. Many pressure reduction profiles were evaluated for a myriad of scheduled exposures from hours to months. Decompression sickness prevention studies centered on suit pressure selection and capability, with varying denitrogenation times; stage decompression including studies in portable chambers at different mountain levels, both in the U.S., as well as the Peruvian terrain.

More recent developments have been the capability to detect decompression-induced gas emboli in the bloodstream using Doppler bubble detector and two-dimensional ultrasonic echo's gas emboli prior to the onset of clinical bends. This provides a greater insight into this difficult malady. Recent studies centered on the threshold of clinical symptoms and the bubble threshold pressure reduction. These and other aspects of this research area will be discussed.

Where does the past thirty years of research lead to? How far have we come, and where are we going? ■

EXERCISE COUNTERMEASURES FOR BED REST DECONDITIONING

S. Arnaud[1], P. Berry[1], M. Cohen[1], J. Danellis[1], C. DeRoshia[1], J. Greenleaf[1], B. Harris[1], L. Keil[1], E. Bernauer[2], M. Bond[3], S. Ellis[4], P. Lee[5], R. Selzer[5], and C. Wade[6]
[1]*Nasa/Ames Research Center, Moffett Field, California 94035,* [2]*University of California, Davis, California,* [3]*Loredan Biomedical, Davis, California,* [4]*San Jose State University, San Jose, California,* [5]*Jet Propulsion Laboratory, Pasadena, California, and* [6]*Letterman Institute of Research, San Francisco, California*

The purpose of this 30-day bed rest study was to investigate the effect of short-term high intensity isotonic and isokinetic exercise training on maintenance of working capacity (peak oxygen uptake), muscular strength and endurance, and on orthostatic tolerance, posture and gait. Other data were collected on muscle atrophy, bone mineralization and density, endocrine analyses concerning vasoactivity and fluid-electrolyte balance, muscle intermediary metabolism, and on performance and mood of the subjects.

Nineteen men (32-42 yr) were divided into 3 groups: no exercise control (peak V_{O2} once/wk, N=5), isotonic exercise (electronic ergometer, supine, N=7), and isokinetic exercise (electronic lido, supine, N=7). The exercise regimens were conducted near peak levels for 30 min. in the morning and 30 min. in

the afternoon 5 days/wk. The protocol consisted of a 7-day ambulatory control period where the subjects equilibriated on the standardized diet, 30 days of -6° head-down bed rest, and a final 5 days of ambulatory recovery.

The diet consisted of normal fresh and frozen foods; mean caloric consumption of 2,678 hcal/day (control), 2,833 hcal/day (isotonic), and 2,890 hcal/day (isokinetic) resulted in mean weight losses during bed rest of 1.01 kg, 0.85 kg, and 0.0 kg, respectively.

Results from the various investigations will be presented and discussed.

TESTS CONDUCTED:

- Isotonic Exercise (Bernauer)
- Isokinetic Exercise (Bond)
- Orthostatic Tolerance (Greenleaf)
- Posture-Equilibrium-Gait (Cohen)
- Exercise Hormonal Responses (Wade, Keil)
- Fluid Balance Hormones (Danellis)
- Bone Anatomy-Physiology (Arnaud)
- Cellular Calcium (Harris)
- Performance-Mood (DeRoshia)
- Muscle Ultrasound (Ellis)
- Muscle Magnetic Imaging (Lee, Selzer)
- Muscle Spectroscopic Biochemistry (Berry) ■

A NEW DEVICE FOR AMBULATORY CENTRAL VENOUS PRESSURE MEASUREMENT

J. C. Buckey, R. L. Goble, D. E. Watenpaugh, L. D. Lane, J. B. Charles, W. T. Harvey, C. G. Blomqvist
Departments of Internal Medicine and Physiology, University of Texas Health Science Center, Dallas, Texas 75235

We have developed a device for continuous measurement of human central venous pressure (CVP) during space flight. Normal resting CVP typically ranges from 5 to 10 mmHg. The expected changes at zero gravity are ± 5 mmHg or less. A 1 mmHg CVP change can represent a substantial intravascular fluid shift. Thus, the requirements for resolution and absence of baseline drift are stringent.

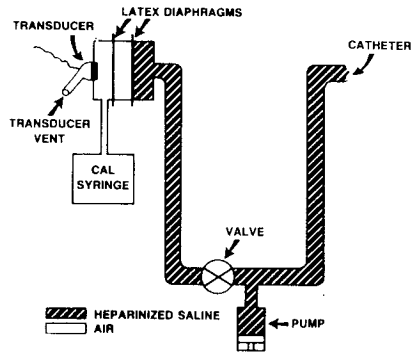

Figure 1. A schematic diagram of the CVP fluid paths.

The unit is small (weight 0.63 kg, length 16.9 cm, width 6.8 cm, height 3.2 cm), battery powered and designed to run for approximately 30 hours. Pressure is measured in a saline filled catheter inserted into a central vein. The transducer is placed in the axilla at the level of the catheter tip to offset hydrostatic gradients. A pump and electronics assembly mounts on the leg. This assembly provides a slow continuous heparinized saline infusion to maintain catheter patency; the electronics provides a readout

in mmHg and a visual and audible alarm for excessive pressure. An air-filled syringe allows for a two-point calibration (zero from ambient atmospheric pressure and a positive pressure generated by a measured compression of a known gas volume). Shock hazards are minimized by a two-failure tolerant system. Two latex diaphragms separate the saline from the transducer surface; the electronics and pump chamber are in separate enclosures. The case is clear polycarbonate so that bubbles can be seen.

To evaluate the unit a series of tests were performed. The pump was run on battery power until empty to give the total continuous run time (28 hrs) and average flow rate (1.47 ml/hr, total volume delivered=41.1 ml). The unit was then run continuously on external power while connected to a fluid filled catheter in a reservoir at 37.9 mmHg for evaluation of drift and leakage. The displayed reading dropped 0.2 mmHg over 63 hours. Temperature sensitivity was evaluated by transient heating of the transducer block and associated tubing. The indicated pressure rose 0.4 mmHg as temperature increased by 28 to 65° C. Accuracy of the electronics was evaluated by connecting the transducer to a manometer and increasing pressure from 0 to 40 mmHg in 2 mmHg steps; these data were analyzed using linear regression. The regression equation was: Display pressure = 1.01 × Manometer pressure - 0.29; SEE=0.095 mmHg.

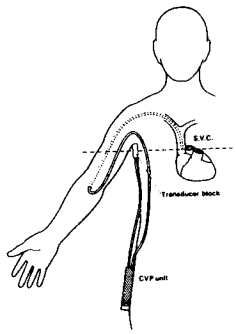

Figure 2. The CVP unit mounted on the body. The catheter tip and transducer block are at the same level to balance hydrostatic gradients at 1 g.

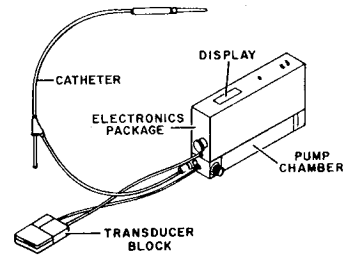

Figure 3. An isometric drawing of the unit.

An initial in-vivo test was performed to examine the relationship between G_x forces and central venous pressure (CVP) during a simulated Space Shuttle launch. Three male subjects had saline filled CVP catheters inserted through an antebrachial vein. The subjects were placed in a replica of a mid-deck seat mounted in the human centrifuge at Brooks AFB, TX. The centrifuge was then run through a typical launch profile. The simulation was repeated twice in each subject. In all subjects the CVP increased in concert with the G forces. The mean peak CVP data were:

	Before Launch	SRB Sep	MECO
G_x	1.0	2.3	2.9
CVP Increase, mmHg	—	2.7	3.1

SRB Sep denotes the time of Solid Rocket Booster Separation and MECO Main Engine Cut-Off. The results show that CVP is likely to increase significantly during launch. This increase is preceded by a prolonged period with the astronauts in a head down-tilt position before launch. This posture is usually also associated with an elevated CVP. A substantial central fluid shift probably takes place well before entering zero-G.

We conclude that the unit has sufficient stability, accuracy and temperature insensitivity for measuring CVP during launch and the initial stages of space flight. The unit allows for accurate ambulatory measurement for up to 28 hours and may with minor modifications also be suitable for the ambulatory measurement of other intravascular and intracardiac pressures. ■

EFFECT OF PHYSICAL FITNESS ON THE CARDIOVASCULAR RESPONSES TO ADRENERGIC AGONISTS

J. C. Buckey, D. E. Watenpaugh, L. D. Lane, W. E. Moore, F. A. Gaffney, C. G. Blomqvist
Departments of Internal Medicine and Physiology, University of Texas Health Science Center, Dallas, Texas

The effects of physical training on neurohumoral cardiovascular control mechanisms are still poorly understood. Potential links between physical fitness and autonomic function are particularly important in aerospace medicine. It has been suggested that high levels of fitness are associated with decreased ability to tolerate both hypo- and hypergravic environments. However, the mechanisms that may be responsible have not been defined. We examined the hypothesis that physical fitness alters adrenergic responsiveness, expressed as the cardiovascular effects of graded exogenous alpha- and beta-adrenergic stimulation.

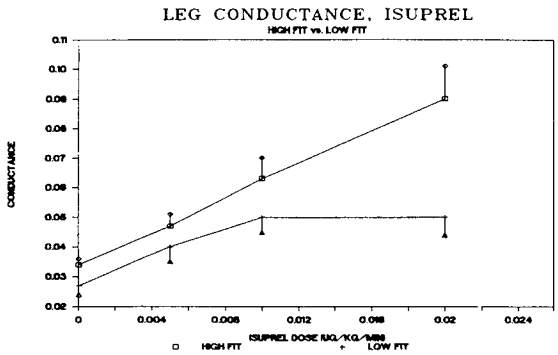

Figure 1. Leg conductance in ml/100 ml/min/mmHg with increasing isuprel dose. The means at the 0.02 level are significantly different ($p<0.002$). Triangles indicate the standard error of the mean.

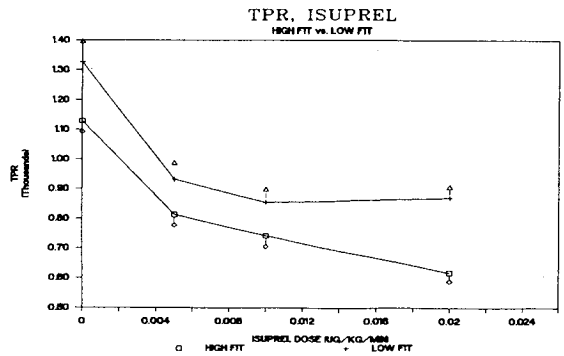

Figure 2. Total peripheral resistance in dynes·sec/cm^5 with increasing isuprel dose. The higher fitness level was associated with significantly lower resistance at all levels of beta-adrenergic stimulation.

Twenty-four normal subjects, 17 men and 7 women, mean age 32.9 years, had graded isoproterenol infusions to raise heart rate 30 beats/min, followed after a rest period by phenylephrine infusion to raise systolic pressure 20 mmHg. Cardiac output (acetylene rebreathing technique), heart rate (ECG), blood pressure (indirect, semi-automatic system), calf conductance (occlusion plethysmography), left ventricular echocardiographic dynamic dimensions and plasma catecholamines were measured at rest

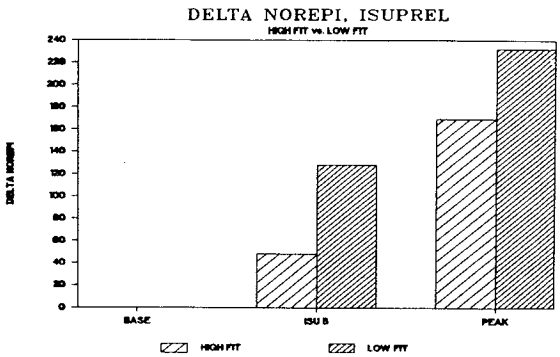

Figure 3. Norepinephrine changes from baseline in pg/ml, at level 2 and at the subject's peak isuprel level. The changes, which presumably reflect baroreflex-mediated intrinsic alpha-adrenergic vasoconstrictor activity in response to exogenous beta-adrenergic vasodilator stimulation, show a tendency to be greater in the less fit individuals.

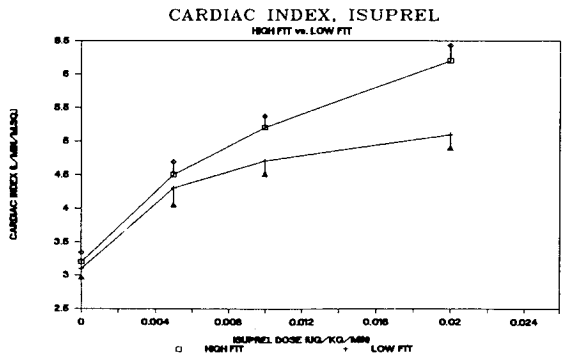

Figure 4. Cardiac index increases at a greater rate in the more fit subjects. The differences between the groups at the 0.01 and 0.02 infusion levels are significant ($p<0.005$).

at each of four infusion levels. Isoproterenol infusion rates progressed from 0.005 to 0.04 $ug \cdot kg^{-1} \cdot min^{-1}$ Corresponding levels for phenylephrine were 0.25 to 2.0. Maximal oxygen uptake (VO_2 max) was measured at a separate session during upright bicycle exercise. The subjects were divided on the basis of the median VO_2 max into two equally large groups: More Fit (MF) with a mean VO_2 max of 40.2 $ml \cdot kg^{-1} \cdot min^{-1}$ and a Less Fit (LF) group below the median with a mean VO_2 max of 27.2 ($p<0.001$). The total group range of VO_2 was 19.3 to 54.4 ml/kg/min.

The fitness levels had no apparent effect on the responses to *alpha-adrenergic* stimulation. The MF subjects had higher mean leg and systemic conductance at rest, but vascular responses expressed as change in per cent of control levels were equally large in both groups as were the changes in mean arterial pressure, +17 (LF) and +13 (MF) mmHg from control to infusion level 3. Reflex adjustments to the alpha-adrenergic stimulation also appeared to be the same magnitude in both groups with heart rate decreases of 16 (MF) and 15 (LF) beats/min combined with a gradual reduction in plasma norepinephrine levels.

Systemic and leg hemodynamic responses to *beta-adrenergic* stimulation were also similar in the two groups at levels 1 and 2. However, the MF group showed a further significant increase in leg and systemic vascular conductance from level 2 to level 3 whereas there was no significant change in the LF group. Mean arterial pressures were equally well maintained in both groups and heart rate also increased similarly in both groups. However, cardiac output increased more rapidly in the MF group. The intergroup difference at level 3, 5.2 $l/min/m^2$ compared to 4.5 $l/min/m^2$ was significant. On the other hand, the LF group had a larger increase in plasma norepinephrine levels at the peak infusion level, +232.1 compared to +169.3 above control levels.

Together these data indicate that moderate interindividual differences with respect to physical fitness have no effects on the vasoconstrictor responses to alpha-adrenergic stimulation. However, MF subjects tend to have higher leg and systemic conductance at rest and an enhanced vasodilator response to exogenous beta-adrenergic stimulation. The increased response does not appear to be caused by an increased vascular sensitivity. Rather, a progressive increase in systemic cardiac output probably enabled the MF group to respond to the progressive exogenous vasodilator drive while maintaining arterial pressure without activating intrinsic vasoconstrictor mechanisms. On the other hand, the limited cardiac output response in the LF group seems to have required intrinsic alpha-adrenergic activation (as reflected by the increased plasma norepinephrine levels) to maintain arterial pressure. ■

HUMAN-USE CENTRIFUGE FOR SPACE STATION OPERATIONS

R.R. Burton and L.J. Meeker
Crew Technology Division, USAF School of Aerospace Medicine, Brooks AFB, Texas 78235-5301

U.S. Air Force pilot-astronauts, while in space (weightless) for extended periods of time, may be required to fly spacecraft with maneuvering capability (*i.e.*, the development of accelerative $+G_z$ forces). It is well known that, upon exposure to a weightless environment, orthostatic tolerance — and, we must assume, tolerance to increased acceleration — begins to decrease at an unknown rate. Although methods are available to measure the rate of loss of orthostasis (*e.g.*, lower body negative pressure), these methods are not capable of determining tolerance to increased G, nor do they have the ability to prevent the development of these intolerances. The same statement applies to bone structure and calcium metabolism relationships. In order to determine these rates of decay and to limit (or even prevent) their occurrence, some means of generating acceleration forces (G) for use by humans must be made available for these specific activities. A short-arm centrifuge, with a radius of approximately 5 ft., for human use is proposed. By means of appropriate body positioning, increased G tolerance measurements can be made and accurately correlated with G tolerances determined on a 20-ft. radius centrifuge. Centrifuges of these short-arm dimensions are well tolerated for extended continuous durations of exposure (at least 2 hrs), and at high rotation rates (at least 67 rpm). A centrifuge of these

dimensions would require little electrical power, and only simple controls that would include some automation and a counter-rotating mechanism to eliminate the problem of torque. Such a centrifuge would be safe for human use, and could be provided at a moderate cost. ■

SKIN IN SPACE

V. H. Carter
1301 West Persimmon, Rogers, Arizona 72756

Space exploration and dermatology have both had their technical advances within each discipline, but they have not interacted. In the early days of spaceflight anticipation, there were those physicians and physiologists who predicted dire and tragic physical effects of weightlessness. A few of the minor predictions were true, but by and large new discoveries shaped the course of physiology in space. Physician-astronauts have been on several space flights and appreciate the short-term physiologic effects of microgravity. With the inevitable Space Stations and future human long-range deep probes, it is imperative that we develop a database on the skin.

The Union of Soviet Socialist Republic's Space Station "Mir" is now in place. The United States Space Station with Canada, the European Space Agency, and the Japan Experimental Module cooperating, will be in place in the early 1900's.

The loss of the Challenger has delayed the continuing accumulation of data in the United States space program. However, to the best of our knowledge, there has been scant specific evaluation of the skin as an organ during any space flights. A space dermatologic database must be accumulated and collated. The Shuttle flights will resume next year, but basic physiologic studies will initially be given a low priority. This must not diminish continued dermatologic involvement and awareness.

The Space Station will provide a permanent habitation for continuing long-term evaluation of microgravity and its effect on animal and plant physiology. In contrast to present experience, a round trip to Mars will take in excess of eighteen months. It becomes evident that severe physical changes will occur on trips of this magnitude. It is unclear to what extent this may proceed before physiologic stabilization occurs. To continue long-term space exploration, there are only two alternatives available with our present knowledge. The most logical approach to maintain physiologic balance would be to develop an earth environment in our vehicle-habitats. The size of a vehicle-habitat capable of creating gravity is beyond our capabilities at this time. The most bizarre alternative is to accept that we will have terrestrial and extraterrestrial beings. Certainly an individual born and matured in weightlessness will have altered anatomy and morphology. This neo-formation will be incompatible with survival in gravity. The skin will become a container for such an individual.

There have been several medical problems encountered by astronauts during spaceflight. The major problem that will invite dermatologic interaction is bone demineralization. It is progressive, and, unlike other changes noted, it does not tend to stabilize with increasing duration of flight. The findings are not only of increased bone resorption, but decreased bone formation has been documented. Since calcium metabolism is involved, the skin and ultraviolet light exposure must be included in studies related to this deficit. Unless measures are found to alter calcium loss this will be a major limiting factor to flight duration.

There are other physiologic findings with skin interaction. These include fluid shift, with the skin storing some of this shift; increased blood pressure, with increased peripheral vascular resistance; and altered lymphocytes, with the myriad of associated dermal disorders. Returning astronauts' lymphyocyte samples were subjected to mitogen challenge, and dormant T-cells were activated at only 3% of the rate of earthbound lymphocyte cultures.

The primary mission of the Space Station Health Maintenance Facility will be to avoid the necessity of a rescue in space. An illness has necessitated at least one Soviet early-return because of a cosmonaut medical emergency. Within these parameters we can predict certain incompatible skin disorders with

latency, such as psoriasis, dermatitis herpetiformis, lichen planus, keratosis follicularis. Other potentially complicating dermal disorders that on earth are considered somewhat mundane are seborrhea and acne from the lack of sebum removal; candidiasis, with its yeast forms being aspirated; and skin flora contamination of the habitat. On Skylab I, II, and III, skin bacterial cultures of the launching astronauts were compared with the cultures on return, and it revealed an accumulative contamination from previous missions.

With this background, a group of United States' dermatologists, with various interests and qualifications, an astronaut, and a principal of the dermatologic pharmaceutical industry have formed the Space Dermatology Foundation. Our first goal is to accumulate both direct and indirect data pertaining to dermatology and ultimately to use this data to improve the well-being of space-travelers and to promote research for both practical application and for basic physiology. We have defined several research projects for flight when the vehicle becomes available. There will be an international membership. ■

INFLIGHT SALIVARY PHARMACOKINETICS OF THERAPEUTIC AGENTS

N. M. Cintron[1], L. Putcha[2], J. M. Vanderploeg[1], and Y. M. Chen[1]
[1]NASA/Johnson Space Center, Biomedical Laboratories Branch, Houston, Texas 77058 and [2]KRUG International, Technological Life Sciences Division, Houston, Texas 77058

INTRODUCTION

The observation that a wide range of physiological and biochemical changes occur during spaceflight suggests that these changes alter the kinetics and dynamics of drugs administered to crewmembers during flight. While the need for elucidating such changes has been widely recognized, technical and operational constraints of multiple blood sampling required for these studies limit their implementation during spaceflight. The usefulness of salivary concentration profiles as an alternate noninvasive method for clinical monitoring of certain drugs has been established (1). The feasibility of such an application of saliva drug levels depends upon the distribution of detectable levels into saliva and establishment of a consistent saliva/plasma (S/P) ratio over the entire disposition profile of the drug (2). In an attempt to determine the applicability of noninvasive salivary drug monitoring for pharmacokinetic and pharmacodynamic evaluation of therapeutic agents during spaceflight, three drugs that are frequently used by crewmembers have been selected for inflight study - acetaminophen, a relatively innocuous, common pain relief medication whose disposition characteristics have been well established, and a scopolamine/dextroamphetamine combination, an operational medication for the treatment of space motion sickness during mission.

Ground-based, inhouse investigations to establish the S/P ratios of acetaminophen (Tylenol®) and scopolamine have been conducted in normal subjects. Following oral administration, both acetaminophen and scopolamine readily distribute into saliva with consistent S/P ratios over their entire disposition profiles. Therefore, in the present investigation, pharmacokinetics of acetaminophen and scopolamine/dextroamphetamine using salivary concentrations have been evaluated, following oral administration to crewmembers before and during spaceflight.

METHODS

Participating crewmembers received an oral dose of 650 mg of acetaminophen as two tablets or 0.4 mg of scopolamine and 5 mg of dextroamphetamine as a capsule (SMS medication) twice on separate occasions during ground-based studies and once during flight. Saliva samples were collected at designated time periods, 8 hours for acetaminophen and 36 hours for the scopolamine/dextroamphetamine combination using the saliva collection kit designed and developed at JSC. Acetaminophen samples were analyzed using an HPLC method (3) for determining drug concentrations. The scopolamine/dextroamphetamine samples were divided into two aliquots and scopolamine concentrations were determined using the RPLC-receptor binding assay (4) in one sample aliquot set

collected over the first 12 hours after dosing. The remaining sample aliquot set was frozen for future analysis of dextroamphetamine concentrations.

RESULTS

Acetaminophen Study: Representative saliva drug concentration-time profiles of a crewmember during preflight and inflight phases of the study are presented in Figure 1. Significant changes in the concentration profiles occur during spaceflight. These changes are more pronounced during the absorption phase of the profile than during the elimination phase. Rate of absorption and time to reach

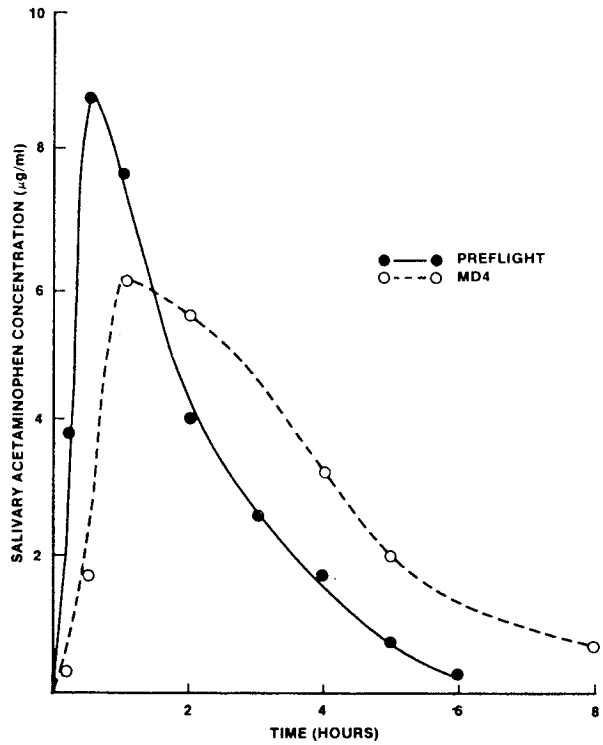

Figure 1. Salivary concentration—time profiles of acetaminophen oral administration of 650 mg dose to a crewmember.

peak saliva concentration calculated from preflight and inflight data are presented in Table 1. The data indicate that there is a significant decrease in the absorption rate of acetaminophen during flight when compared to the respective preflight value. There is a resultant twofold increase in the time to reach peak concentration during flight. Elimination rate of the drug, however, did not change significantly.

Scopolamine/Dextroamphetamine: Analysis of a limited number of samples from the ground-based and inflight study suggest that detectable changes in saliva concentration-time profiles occur with

Table 1. Absorption Parameters of Acetaminophen

Subject No.	Peak Concentration (mg/ml)		Time to reach peak (h)	
	Control	Inflight	Control	Inflight
1	9.6	6.4	0.5	1.1 (MD4)
2	8.9	6.1	0.5	1.0 (MD4)
3	9.8	14.1	0.5	1.0 (MD3)
4	12.6	14.8	0.5	≤0.25 (MD2)
5	13.0	15.6	0.5	≤0.25 (MD2)

scopolamine (Figure 2). Due to inadequate sample size and incomplete analyses, the results of the study are inconclusive at the present time.

DISCUSSION

The limited results of this investigation support the theoretical predictions that changes in drug dynamics would occur during flight as a result of the physiologic condition of crewmembers. For example, dehydration and reduction of gastrointestinal motility, both of which prevail in astronauts during missions, influence the absorption of acetaminophen (5). Similar changes in the pharmacokinetics of drugs administered to crewmembers during a mission may result in ineffective therapeutic response or unexpected side effects depending upon the degree and magnitude of these changes.

The present investigation constitutes the beginning of a comprehensive pharmacokinetic characterization of drugs administered to crewmembers during mission. Results of this study confirm that changes in the drug dynamics, especially during the absorption phase of the drug, occur during

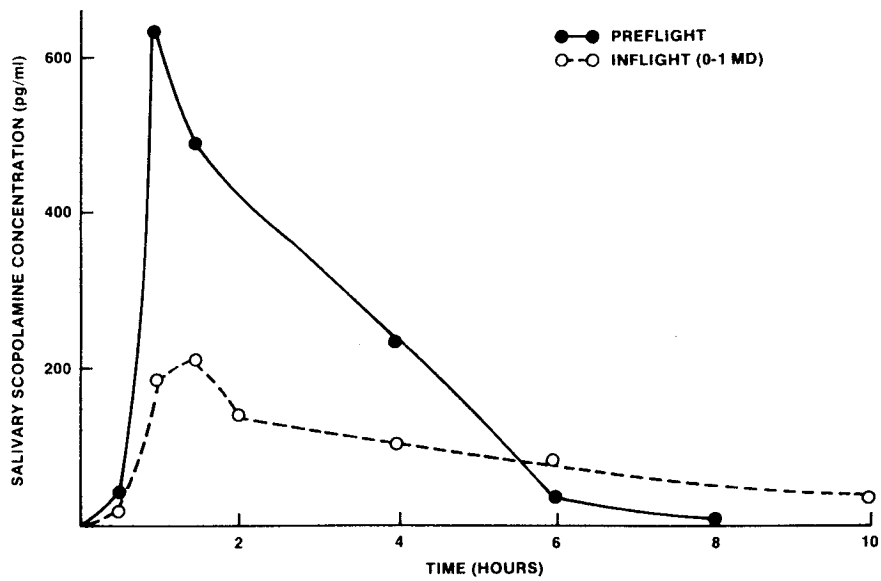

Figure 2. Salivary concentration—time profiles following oral administration of 0.4 mg scopolamine and 5 mg dextroamphetamine to a crewmember.

spaceflight. The degree and magnitude of these changes depend on a number of flight specific variables such as mission day, manifestation of space motion sickness, and the overall physiologic response to weightlessness of the participating crewmember. Therefore, a comprehensive pharmacokinetic characterization of therapeutic agents during spaceflight may be useful for identifying effective methods of pharmacologic intervention for spaceflight-induced pathophysiologic conditions in general, and space motion sickness in particular. ■

REFERENCES

1. Graham, G.C. Noninvasive clinical methods of estimating pharmacokinetic parameters. *Pharmac. Ther.* *18*:333-349, 1982.
2. Danoholf, M. and D.D. Breimer. Therapeutic drug monitoring in saliva. *Clin. Pharmacokinet.* *3*:39-57, 1978.
3. O'Connell, S.E. and F.J. Zurzola. A rapid quantitative determination of acetaminophen in plasma. *J. Pharm. Sci.* *71*:1291-1294, 1982.
4. Cintron, N.M. and Y. Chen. A sensitive radioreceptor assay for determining scopolamine concentrations in plasma and urine. *J. Pharm. Sci.* (in press).
5. Channer, K.S. and C.J. C. Roberts. Effect of delayed oesophageal transit on acetaminophen absorption. *Clin. Pharmacol. Ther.* *37*:72-76, 1985.

EMPIRICAL MODELS FOR USE IN DESIGNING DECOMPRESSION PROCEDURES FOR SPACE OPERATIONS

J. Conkin[1], B. F. Edwards[1], J. M. Waligora[2] and D. J. Horrigan, Jr.[2]
[1]*KRUG International, Technology Life Sciences Division, 17625 El Camino Real, Suite 311, Houston, Texas 77058 and* [2]*Environmental Physiology Laboratory, Medical Sciences Division, Code SD5, NASA/Johnson Space Center, Houston, Texas 77058*

Empirical models for predicting the incidence of Type I altitude decompression sickness (DCS) and venous gas emboli (VGE) during space extravehicular activity (EVA), and for use in designing safe denitrogenation-decompression procedures are developed. The models are parameterized using DCS and VGE incidence data from 26 NASA and USAF manned altitude chamber decompression tests involving 607 male and female subject tests.

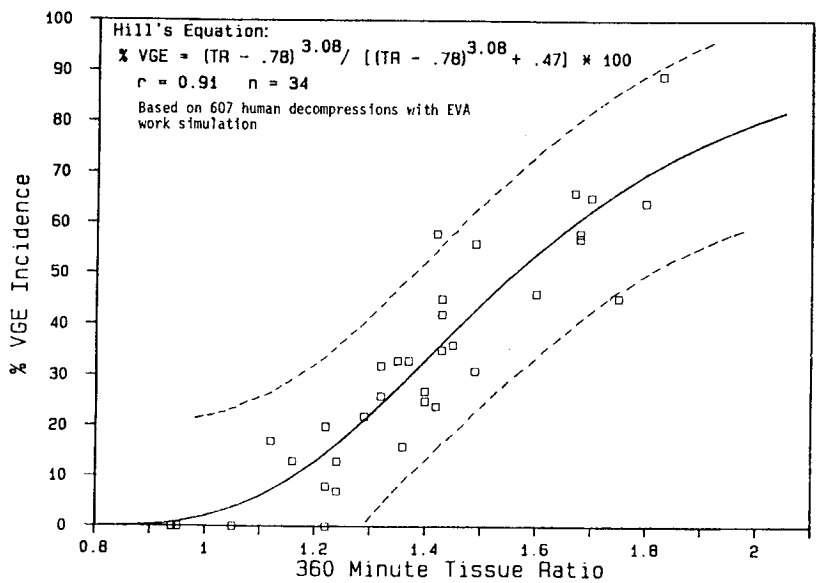

Figure 1. Hill plot of VGE incidence using 360 minute theoretical half-time tissue and its Tissue Ratios with the 95% confidence interval.

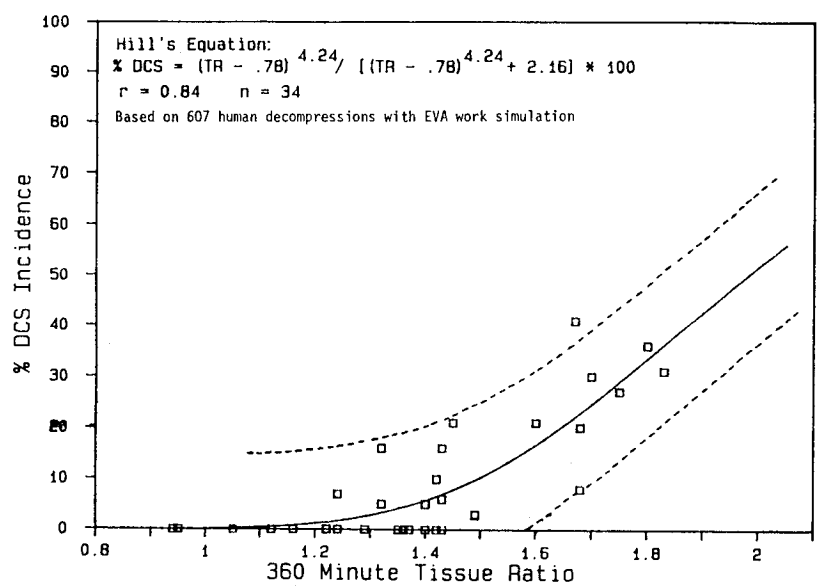

Figure 2. Hill plot of DCS incidence using 360 minute theoretical half-time tissue and its Tissue Ratios with the 95% confidence interval.

These models, and procedures for their use, consist of:

(1) an exponential relaxation model and procedure for computing tissue nitrogen partial pressure resulting from a specified prebreathing and stepped decompression sequence;

(2) a formula for calculating Tissue Ratio (TR), a tissue decompression stress index;

(3) linear and Hill equation models for predicting the total incidence of VGE and DCS attendant with a particular TR; and

(4) graphs of cumulative DCS and VGE incidence (risk) versus EVA exposure time at any specified TR. Several examples of realistic EVA preparations are provided to demonstrate the predictive models and interpretation of the results. ■

HUMAN ADAPTATION TO VISUAL-VESTIBULAR CONFLICT INDUCED BY TELESCOPIC SPECTACLES

J. L. Demer, J. Goldberg, F. I. Porter, H. A. Jenkins, and K. Schmidt
The Sensorimotor Visual Rehabilitation Project, Cullen Eye Institute, and Clayton Neurotology Laboratory, Baylor College of Medicine, Houston, Texas 77030

Experiments performed in space have demonstrated that microgravity induces significant reductions in the performance of the optokinetic and vestibulo-ocular reflexes (VOR) (5). While these perturbations become compensated after a period of several days in space (5), it is likely that the visual-vestibular conflict generated during the period of ocular motor dysmetria is a contributing factor in space motion sickness (4). Further, abnormal optokinetic and VOR gains permit retinal image slip to occur during head movements (2). The combined action of the VOR and visual tracking mechanisms is called the visual-vestibulo-ocular reflex (VVOR), which has a gain defined to be slow phase eye velocity divided by head velocity.

Telescopic spectacles provide a terrestrial means of simulating the visual-vestibular conflict induced by insufficient VVOR gain. These devices require that VVOR gain increase from its normal value of 1.0 to a value equal to the magnification factor of the telescopes. Preliminary studies using 2.2X telescopic spectacles have indicated that there are two types of adaptative processes acting to reduce the visual-vestibular conflict induced by these devices: an immediate increase in VVOR gain produced by visual tracking, and a long-term adaptive increase in VOR gain (2). The present report describes these adaptive responses to 4× telescopic spectacles in a large diverse subject population.

We studied 34 normally-sighted volunteers of both sexes, with an average age of 40 ± 17 years (mean ± standard deviation, SD, range 16-72). Eye movements were measured by DC-coupled, digitally sampled electro-oculography (EOG). Peripheral vestibular function was evaluated by caloric irrigations in 31 subjects, and was normally symmetric in 28 of these; the three others were without symptoms attributable to the vestibular system.

Vertical axis vestibular stimulation was provided by rotating subjects sinusoidally in a servo-motor driven chair. Subject's heads were comfortably fixed to a headrest on the chair. Except during EOG calibration, subjects wore 4× binocular telescopic spectacles having a field of view limited to the central 10°. Binocular visual acuity was measured using an automated projection system (3), with the head stationary (static visual acuity, SVA), and during rotation at 1.0 Hz, amplitude 20°/s, (dynamic visual acuity, CVA). VOR gain was measured in darkness during rotation at 0.1 Hz, amplitude 70°/s. VVOR gain was measured during wearing of telescopic spectacles in the light during rotation at 0.1 Hz, amplitude 30°/s. After initial measurements of SVA, DVA, VOR gain, and VVOR gain, subjects underwent a 15 min adaptation period of sinusoidal rotation at 0.2 Hz, amplitude 20°/s, while viewing a distant video display using telescopic spectacles. Measurements were then repeated to ascertain the extent of adaptation.

Three subjects withdrew from the protocol due to immediate motion sickness, a syndrome of diaphoresis, nausea, and deep visceral discomfort; quantitative measurements were impossible in these.

Three other subjects experienced moderate motion sickness during the adaptation period but elected to complete the protocol. Initial VOR gain was 0.67 ± 0.12 (mean ± SD, n = 31). Initial VVOR gain was 1.59 ± 0.39. Representative VOR and VVOR eye velocities for one subject prior to adaptation are shown in Fig. 1A. Initial SVA was -0.612 ± 0.157 logMinarc (~20/5 Snellen equivalent). Initial DVA was -0.110 ± 0.170 logMinarc (~20/16). Correlations among variables were examined by linear regression analysis. VVOR gain was found to be highly correlated with age, decreasing by 0.015 per year of age ($p < 0.001$), as seen in Fig. 2. The other measures were not significantly correlated.

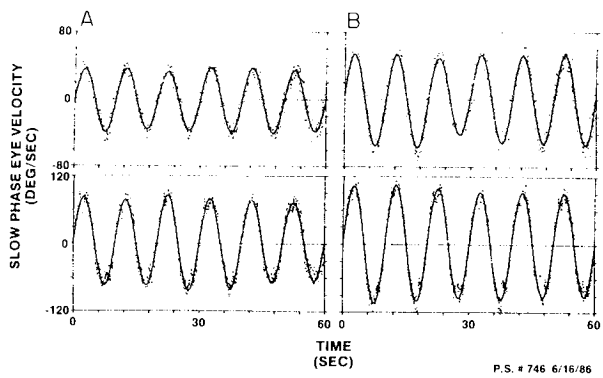

Figure 1.

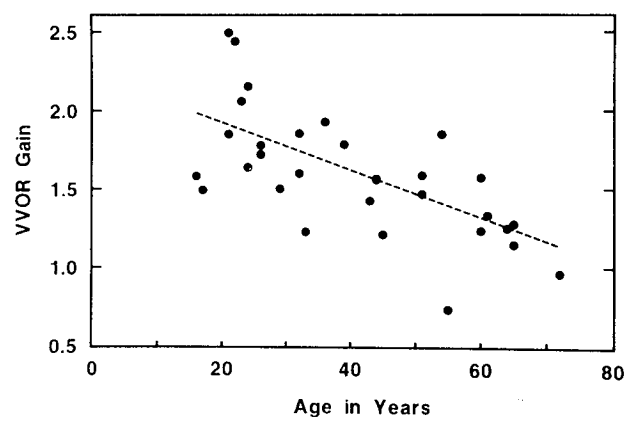

Figure 2.

Some subjects noted oscillopsia during the start of the adaptation period, but lost this sensation as adaptation progressed. Others developed mild motion discomfort as adaptation continued. Adapted VOR gain was 0.72 ± 0.16 (mean ± SD), increasing in 24 subjects by up to 46% (mean 13%). This increase was significant at $p < 0.05$ for 19 subjects. Adaptive increase in VOR gain was not correlated with age, SVA, or DVA. Adapted VVOR gain was 1.63 ± 0.47, increasing in 17 subjects by up to 82% (mean 19%). This increase was significant for 12 subjects. Representative adapted VOR and VVOR eye velocities are shown for one subject in Fig. 1B. Adapted DVA was -0.240 ± 0.180 logMinarc (~ 2-/12). This represented a mean improvement with adaptation of 0.130 logMinarc (30% of visual angle resolvable) for 31 subjects. None of the adaptive changes correlated with age, sex, or acuity.

These data indicate that the wearing of 4× telescopic spectacles induces measurable ocular motor adaptations in a brief time period. These adaptations reduce visual vestibular conflict and improve DVA. The capacity for adaptation varies widely from person to person, although VOR gain adaptation is not systematically related to age or sex. The ability to use vision to immediately increase VVOR gain in response to telescopic spectacles does decline significantly with age, possibly related to the known decline in visual pursuit performance (1). The relationship of immediate visual modification of eye movements to motion sickness remains to be elucidated.

Supported by EY-06394 and the Clayton Foundation for Research. ■

REFERENCES
1. Barin, KM, Barin KG, and Stockwell, CW. Normative values of velocity and acceleration limits of smooth pursuit eye movements. Abstracts of the Ninth Midwinter Research Meeting, Association for Research in Otolaryngology, 1986, pp. 125-6.
2. Demer, JL, Goldberg, J, Jenkins HA, and Porter, FI. Vestibulo-ocular reflex during magnified vision: adaptation to reduce visual-vestibular conflict. Aviat. Space Environ. Med., 1987 (in press).
3. Demer, JL, Porter, FI, Goldberg, J, Jenkins, HA, and Schmidt, K. Technical Digest: Topical meeting on noninvasive assessment of the visual system. Washington DC: Optical Society of America, 1987, pp. 104-7.
4. Money, KE, Oman, CM, Watt DG, and Cheung, R. Preflight and postflight motion testing of payload crew of Spacelab I, 41G, and D1. Aviat. Space Environ. Med., 1987 (in press).
5. Vieville, T., Clement, G., Lestienne, F., and Berthoz, A. Adaptive modifications of the optokinetic and vestibulo- ocular reflexes in microgravity. In Adaptive Processes in Visual and Oculomotor Systems. EL Keller and DS Zee (eds), Oxford: Pergamon Press, 1986, pp. 111-20.

PRIMATE PHYSIOLOGIC MONITORING AND TELEMETRY SYSTEM FOR SHUTTLE

P.N. Cutchis, R.C. Eberhart, S. Mantel, and K.H. Sanders
The Johns Hopkins University, Applied Physics Laboratory, Laurel, Maryland 20707

INTRODUCTION

This paper describes the development of the Physiologic Acquisition and Telemetry System (PATS), which is a multi-channel data acquisition, telemetry and storage system for large primates. The program effort at The Johns Hopkins University Applied Physics Laboratory (JHU/APL) is part of a joint US/French Large Primate Facility Program being supported by the National Aeronautic and Space Administration's Ames Research Center, Moffett Field, California.

The data are acquired via a multi-channel subsystem, the Data Acquisition and Telemetry Subsystem (DATS), that will be implanted within the abdominal cavity of each of two Rhesus monkeys which will be carried in separate enclosures in the Spacelab. The implanted DATS units will acquire data from transducers placed in the animal, condition and digitize the electronic signals, and transmit the data upon request to a Flight Support Station to be located within the Spacelab. Each implanted DATS unit will contain its own power source and will operate for at least two years *in vivo* to permit pre-launch and post-mission baselines to be established.

The design and prototypes resulting from the current program effort are expected to lead to the development of spaceflight hardware that will be flown on two International Microgravity Laboratory missions tentatively scheduled for 1992 and 1993. Future applications of PATS may also include the instrumenting of crew members on the Shuttle and/or on Space Station, in which case the data acquisition units and sensors would be attached externally.

SYSTEM DESCRIPTION

The PATS equipment consists of the implanted Data Acquisition and Telemetry Subsystem (DATS), and the Flight Support Station (FSS). Linking the DATS with the FSS is the command/telemetry link, called the APL Biomedical Inductive Link (ABIL). The FSS communicates with the Shuttle computer system via an interface with one of the Shuttle Remote Acquisition Units (RAU's). The overall system configuration is illustrated in Figure 1.

The current breadboard version of the DATS unit monitors up to eight single-ended channels simultaneously. In this configuration, the maximum sample rate per channel is 100 samples per second. It is anticipated that the flight version will have a capability of sampling up to 200 samples per second on each channel.

The DATS unit uses a single-chip microcomputer, the Hitachi 63701. The microcomputer runs at a relatively low clock frequency (approximately 200KHz) to conserve power. DATS includes 32K bytes of random access memory.

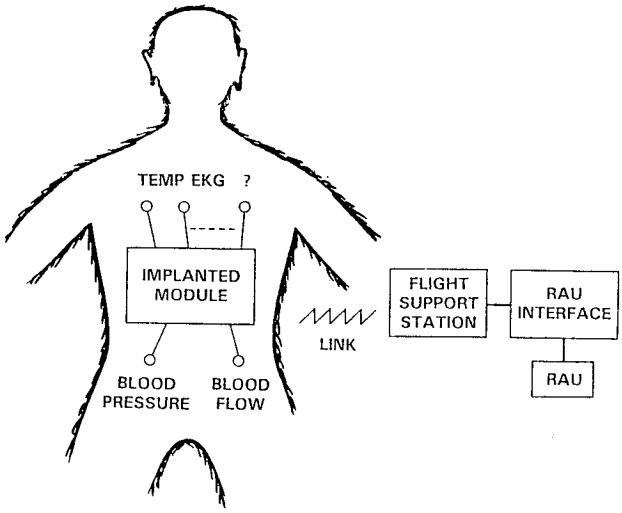

Figure 1. PATS System Configuration.

The command/telemetry link, ABIL, is an inductive link running at about 50 KHz. The command rate into the DATS unit is 200 BPS; telemetry out of DATS occurs at 1600 BPS. One command/telemetry coil is located inside the DATS unit, the other is in a jacket worn by the monkey. A block diagram of the DATS unit appears in Figure 2.

The Flight Support Station (FSS) design features an IBM PC 80286 machine as the central computer. An IBM PC AT is being used as the development system. It is anticipated that either the AT or an 80386 machine will be used in the Ground Support Equipment (GSE) version of the FSS, including being used for testing, training and post-flight evaluation by the Principal Investigators. Some form of flight-hardened 80286 (or 80C286, if feasible) machine will be used as the FSS aboard Shuttle. A block diagram of the FSS appears in Figure 3.

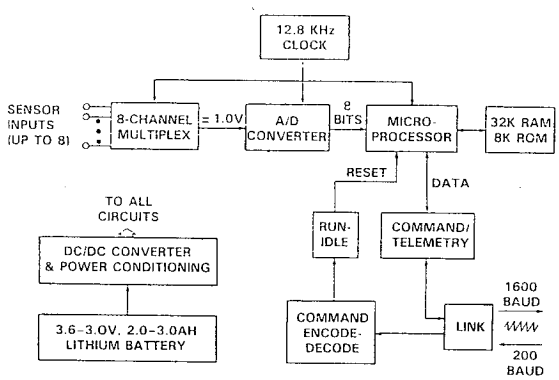

Figure 2. PATS Data Acquisition and Telemetry Subsystem Block Diagram.

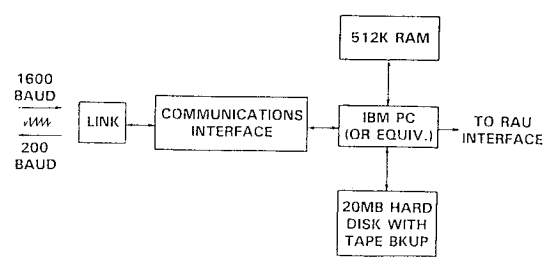

Figure 3. PATS Flight Support Station Block Diagram.

DATA ACQUISITION

Physiologic parameters to be measured will include temperature (one or two channels), ECG, EMG (one to three channels) and blood pressure. Heart rate and respiration rate will probably be derived from the ECG and/or blood pressure waveforms. Other parameters being considered for data acquisition include blood flow and cardiac dimensions.

The rate at which measurements are taken will be determined for each parameter independently, and may be varied from time to time before, during and after the flight. Three main constraints exist as limiting factors on data acquisition. First, and probably most important, is how much data are really useful to the PI. Second is the energy available from the battery, currently planned to have a rated

capacity of about 2.6 amp-hours. Third is the 1600 BPS telemetry link data rate with which data can be transmitted from the DATS to the FSS.

The accuracy and resolution associated with each parameter are a function of the sensor chosen for use, and the A/D converter design. The A/D converter has an eight-bit resolution (one part in 256, or about 0.4 percent). Signal conditioning on the inputs from the sensors will be used to ensure that the dynamic range of 256 steps is optimized for each parameter.

An overall systems design issue being addressed is the amount of "artificial intelligence" to incorporate into the DATS and the FSS. Should, for example, data acquisition protocol be changed automatically by the FSS and/or DATS based upon some pattern or trend in one or more of the measured parameters? A sudden increase in heartrate, or a slowly increasing temperature, for instance, could serve as a trigger for a revised data acquisition protocol.

CURRENT PROGRAM STATUS

A breadboard version of the complete PATS system (less sensors) has been designed and fabricated. It is currently being tested, and the DATS unit is being miniaturized to the size required for implantation. Work is beginning on the integration of temperature, ECG, EMG and blood pressure sensors with the DATS unit.

Meanwhile, a hardwired prototype version of PATS without the ABIL command/telemetry link has been designed and fabricated, using off-the-shelf hardware. The hardwired version is being used for software development, and will be made available to the PI's for testing and evaluation in late 1987. ■

EFFECT OF WEIGHTLESSNESS ON MORPHOLOGY OF RED CELL AGGREGATION IN DISEASE: EXPERIMENT ON "DISCOVERY" STS 51-C

L. Dintenfass
Clinical Haemorheology Dept., Rachel Forster Hospital, Redfern, and Department of Medicine, University of Sydney, Australia

---

Experiment on aggregation of red cells (coded "ARC") took place on the space shuttle 'Discovery' STS 51-C, on January 24-25, 1985. The aim of the experiment was to define changes in kinetics and morphology of aggregation of red cells in blood of patients suffering from heart disease, cancer, hyperlipidaemia, and insulin-dependent diabetes, mainly. This project, which had been approved by NASA in August, 1977, required development of new instrumentation (which also had to be space-rated) and new methodology to study qualitatively and quantitatively two-dimensional aggregation of red cells in a slit-capillary of 12.5 micrometer (micron) gap. Details on new instrumentation (slit-capillary photo-viscometer) have been published from 1979 on, and reports on methodology (carried out in the ground studies) were published over 1979-1984. A list of publications is included.

The slit-capillary photo-viscometer contains as the basic part two parallel plates made of "Crown" glass, and polished to one Sodium light wave-length accuracy. Blood flows like a sheet through the gap between plates, and macro-and micro- photography is carried out during flow and during stasis (no-flow) conditions. During the latter stage, aggregates of red cells are formed over a period up to and above 6 minutes. Blood samples, adjusted to cell mass of 0.30 using native plasma, and anticoagulated (EDTA), were contained in 8 syringes placed in an original infusion pump (a rotating drum, syringes along the periphery like a revolver). This infusion pump, and cameras and flush guns, are motorized and computerized. The whole series of experiments runs according to a computer program: that is, infusion of blood, photography of flowing blood, photography at stasis, washing out of blood with saline, infusion of new sample, etc. Actually, each sample was tested three times. Solid state memory recorded real time, temperature, pressure drop, etc. The temperature of the test was 25°C; the temperature during the waiting mode was 5°C. The total duration of the experimental series was 9 hours and 39 min. Initiation of the experiment was carried out by pushing an ON button on the middeck of the space shuttle by the astronaut (late) Onizuka. Instrumentation switched off itself automatically. Cameras and flushguns

operated on batteries; however, the infusion pump, operation of the mechanical assembly, and heating utilized current from the Orbiter.

The orbital flight took only three days, as against the usual NASA seven days. After return of the shuttle, instrumentation (contained in two canisters) was recovered and opened in the presence of the NASA Quality Control Officers.

The instrumentation worked, and we obtained 500 photographs from the experiments carried out under near-zero gravity (and, of course, 500 photographs from the analogous ground instrumentation using identical blood samples). Even preliminary evaluation of photographs indicated that: 1) aggregation of red cells did take place under conditions of weightlessness, although the size of aggregates was smaller; 2) the morphology of aggregates obtained in blood from patients with ischaemic heart disease, hyperlipidaemia, insulin-dependent diabetes, and silent colon cancer, was of the rouleaux type, that is, of the type corresponding to morphology of normal blood on the ground; the same blood showed compact aggregation and sludge formation in the ground experiment; 3) the morphology of normal blood, which did show (as expected) rouleaux formation in the analogous ground experiment, did show random swarm formation under near-zero gravity; 4) sporadic and incidental results on platelets appeared to indicate that there is no aggregation of platelets under near-zero gravity. These results must be confirmed before one is entitled to carry out deductions.

Nevertheless, due to great delays in our second space experiment, it is perhaps safer to indicate possibilities as they appear to us: namely that (subject to confirmation) near-zero gravity (or weightlessness) affects cell-cell interaction, and probably affects the microstructure of the cell membrane: it is likely that the nature of receptors on the membrane is modified. Such possibility is made more likely by the unexpected behavior of platelets. Furthermore, it is also made more likely by the fragmental data we obtained on behavior of IgG and IgM paraproteins which did not affect greatly aggregation of red cells under near-zero gravity, while they caused occlusion of the ground apparatus.

ACKNOWLEDGMENT

Crucial help in the critical design of the space rated unit was given by Hawker de Havilland (Mr. John Raju, and his Special Projects Group), by the CSIRO Division of Applied Physics (in electronics and optics), by B.M.&B.Maguire Co (Heathcote NSW) in construction of the ground and space instruments, and W.F. Chew Enterprises (Los Angeles) in construction of titanium skeleton and internal subsections. Preliminary vibration tests were carried out at the St. Mary's Royal Australian Navy Guided Missiles Establishment, and final tests at the Marshall Spaceflight Center. We are indebted to NASA officers at the Marshall Spaceflight Center and at the Kennedy Space Center for their supervision, help, and assistance.

THE TEAM

Members of the team at Cape Canaveral included: Dr. L. Dintenfass (Principal Investigator); Peter Osman (electronics and data acquisition); Brian Maguire (mechanics and optics); Henry Jedrzejczyk (research assistant); and Barbara Jedrzejczyk (nursing sister). Dr. K.D.G. Edwards supervised patients during two days of blood collection. Patients participated at their own expense (three from New York, N.Y., and three from Sydney, NSW, Australia). During the years of preparation of the experiment, two other participants were Donna Francis (nursing sister cum photographer cum organizer) and Alan Willard (stereology). ■

REFERENCES

A. Preparation of instrumentation and development of methodology. (incomplete).

Dintenfass, L. Aggregation of red cells and blood viscosity under near-zero gravity. Biorheology 16, 29-36, 1979.

Dintenfass, L., and Jedrzejczyk, H. Morphology and kinetics of aggregation of red cells in 12.5 micrometer slits: A micro- and macro-photographic study. In: Haemorheology and Disease. J.F. Stoltz and P. Drouin (Eds.) Paris: Doin Editeurs 1980, pp 87092.

Dintenfass, L. Blood viscosity in Outer Space - a project for the NASA Space Shuttle. In: Blood Viscosity in Heart Disease and Cancer. L. Dintenfass and G.V.F. Seaman (Eds.). Oxford: Pergamon Press 1981, pp. 128-137.

Dintenfass, L., Jedrzejczyk, H. and Willard, A. Application of stereological methods to evaluation of aggregation of red cells in 12.5 um slit: a photographic and statistical study. Biorheology 18, 387-404, 1981.

Dintenfass, L., Osman, P., and Maguire, B. Measurement of aggregation of red cells in Space - a project for the NASA Space Shuttle. J. Electrical & Electronic Engineering, Australia 4(2), 118-125, 1984.

B. Preliminary results of the ARC experiment on STS 51-C (incomplete).

Dintenfass, L. Red cells under zero gravity. Lancet 1, 747-748, 1985.

Dintenfass, L. Mystery of red cell aggregation under zero gravity on STS 51-C. Med. J. Aust. 143: 281-283, 1985.

Dintenfass, L., Osman, P., and Jedrzejczyk, H. First haemorheological experiment on NASA Space Shuttle 'Discovery' STS 51-C: Aggregation of red cells. Clinical Hemorheology 5: 917-936, 1985.

Dintenfass, L., Osman, P., Maguire, B., Jedrzejczyk, H., Jedrzejczyk, B., and Edwards, D.K.G. Results of 'aggregation of red cells' (ARC) experiment on Space Shuttle 'Discovery' STS 51-C on January 24/25, 1985. Proceedings of the Second National Space Symposium, Sydney, Feb. 1986. Canberra: Institution of Engineers, Australia, 1986, pp 5A1-5A12.

EXECUTION OF "ARC" EXPERIMENT ON SPACE SHUTTLE "DISCOVERY" STS 51-C: SOME RESULTS ON AGGREGATION OF RED BLOOD CELLS UNDER ZERO GRAVITY

L. Dintenfass
Department of Medicine, University of Sydney, NSW 2006, Australia

---

A project on "Aggregation of Red Cells" has been accepted by NASA in 1977. An automated slit-capillary photo-viscometer has been designed during 1979-1984, and its last version met NASA's space hazards requirements. The "heart" of the instrument is a set of two highly polished glass plates, spaced by a gap of 12.5 micrometers. An original drum-like infusion pump allows utilization of up to eight blood samples. During a sequential process, blood flows through the slit, and then stops to allow formation of aggregates. Micro- and macro-photography is carried out, and 500 photographs are obtained. Blood from normal donors and patients with history of ischaemic heart disease, colon cancer, juvenile-onset diabetes, hyperlipidaemia, etc., is anticoagulated and adjusted to haematocrit of 0.30 using native plasma. Samples are divided and infused into the "flight" and "ground"' instruments. Prior to experiment temperature is 5°C; temperature during experiment is 25°C. Experiments took place on 24-25 January 1985, on the middeck of space shuttle "Discovery". Subsequent results showed that red blood cells do not change shape under zero gravity, while identical blood shows clumps of red cells on the ground. The latter observation suggests that zero gravity might affect cell-to-cell interaction, and perhaps microstructure of the cell membrane. These aspects must remain, however, tentative till a confirmation by subsequent experiments can be obtained. ■

A FACTORIAL INVESTIGATION OF THE EFFECTS OF DESENSITIZATION AND COGNITIVE COUNSELING ON TOLERANCE TO VISUALLY-INDUCED MOTION SICKNESS

T. G. Dobie[1], J. G. May[2], W. Fisher[2], and N. Bologna[2]
[1]*Naval Biodynamics Laboratory, P. O. Box 29407, Michoud Station, New Orleans, Louisiana 70189-0407 and*
[2] *Department of Psychology, University of New Orleans, New Orleans, Louisiana 70148*

Previous investigations of visually-induced motion sickness (VMS) have indicated that a cognitive-behavioral approach combining counseling and desensitization training was extremely effective in increasing tolerance to such stimulation.

The present experiment was undertaken to determine the degree to which each component in the treatment resulted in increased tolerance. A factorial design was employed in which four groups, each receiving a different treatment, were compared on a measure of tolerance to visually induced motion. All subjects were selected on the basis of a pre- test (1) which indicated that all were highly susceptible to VMS. The first group received 10 sessions of combined cognitive-behavioral treatment (counseling and desensitization); the second received 10 sessions of counseling only; the third received 10 sessions of desensitization only and the fourth served as a control group and received neither counseling nor desensitization. Each group was tested before and after treatment to determine the amount of visual stimulation that they could tolerate.

The visual stimulation was provided by a large rotating drum (5' in diameter) the inside of which was covered with vertical black and white stripes (6" wide). Subjects sat inside the drum while it rotated at 10 rpm. Under these conditions, all subjects reported the perception of vection (that they were rotating and the drum was stationary). The two pre-tests (1 and 2) and post-test (3) were identical. Subjects were told to keep their eyes open and to signal when they felt they could no longer tolerate the stimulation.

The counseling condition involved confidence building and assurances that the subjects' reaction to motion was normal. They were told that apparent resistance to disorienting stimuli exhibited was actually the capability to tolerate the autonomic responses elicited in such situations.

The desensitization condition involved repeated responses to visual stimulation in the drum used for testing, with the stipulation that any subject could terminate the stimulus if he felt he could no longer tolerate it.

The results are summarized in Figure 1 and indicate that the combined treatment yielded significant increases in tolerance to VMS. Tolerance in the cognitive (counseling) only group also increased

Figure 1.

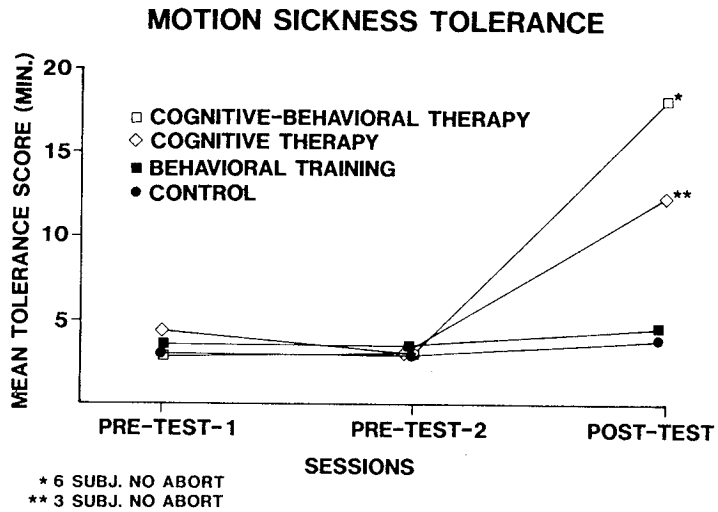

significantly over control, but this mean tolerance was significantly lower than the combined group. There was no significant difference between the behavioral (desensitization only) group and control. Desensitization did not succeed alone, but was helpful in the reinforcement of cognitive counseling.

These findings support the contention that there is a significant cognitive component in motion sickness induced by disorientation. In addition, it is quite apparent that the combined treatment employed holds promise for training individuals who are prone to motion-sickness to tolerate the stimuli that give rise to disorientation. ■

PHYSIOLOGICAL CONCERNS FOR PROTECTIVE APPARATUS

D. F. Doerr
Biomedical Operations and Research Office, J. F. Kennedy Space Center, Florida 32899

INTRODUCTION

The Kennedy Space Center is the focal point of most of this nation's space launch activity. Preparation of spacecraft and launch vehicles involves the handling of rocket propellants, many of which are extremely toxic to humans. These materials, such as nitrogen tetroxide and monomethyl hydrazine are damaging to the respiratory system and the skin. Threshold limit values are as low as 0.1 ppm. Despite considerable effort to institute engineering controls, there are certain operations where workers must be involved in hands-on activities during propellant servicing and transfer operations. Protection during these operations may necessitate the use of complete body enclosures or whole body suits. The size, weight, and encumbrance of these suits imposes significant physiological stress even before actual productive work is initiated. Limitations to mobility vision, and dexterity can result and adversely affect the safety of the worker.

In addition to scheduled operations, there is a need to plan for emergencies occurring during launch, landing, or ground operations. Emergency response crews must also be protected, not only from toxins, but physical hazards such as flame and explosion. Protective apparatus must allow relatively free movement, yet support high respiratory demands during rescue activities.

The marketplace can provide a wide variety of protective apparatus. However, unique requirements for protection make much of the off-the-shelf equipment unsuitable in the KSC setting. It has therefore been necessary to perform testing of selected protective apparatus to assure adequate protection and safety of workers.

METHODS

Testing was accomplished on two primary types of protective apparatus: whole body suits and supplied air respirators. The most recent suit to undergo testing was the new Propellant Handler's Ensemble (PHE). A work-rest protocol, performed in cold (-7° C), ambient lab (23° C), and hot (43° C) conditions, was developed to represent the worst case scenario in the field. Volunteer subjects were instrumented for recording ECG, skin temperatures, and rectal temperature while the suit was instrumented to measure oxygen, carbon dioxide and temperature in the helmet area. All parameters were continuously monitored while the subjects performed tests in each of the three environmental conditions.

The supplied air respirators, also referred to as self contained breathing apparatus (SCBA), were tested to assure that the respiratory needs of the user were satisfied while the mask pressure was maintained positive with respect to the ambient. Volunteer subjects exercised at workloads selected to elicit respiratory responses of either 30% or 60% of measured VO_2 maximum while in the unencumbered state. Once again, ECG was monitored while oxygen, carbon dioxide, and pressure from the mask were gathered. Subjects exercised continuously at the preselected levels on a treadmill until the unit's air supply was exhausted.

RESULTS

The physiologic response to work while wearing the autonomous backpack version of the PHE may easily be summarized as stressful. The work involved with wearing a 65 pound suit and walking at 2.5

mph up a 12% grade (Bruce II) elevated subject's heart rate nearly to maximum. Some of the smaller subjects were unable to complete the tests, especially those carried out in the 43° C chamber. Carbon dioxide concentrations rose to 4.5% during this same work period and oxygen concentrations decreased by a similar percentage. The cryogenic air-supplied environmental control unit provided some temperature relief during lab and hot tests, but contributed unfavorably during the cold tests. Subjects' skin temperatures dropped to less than 70° F (82° F normal) with some subjects reaching the onset of uncontrollable shivering.

Many types of SCBA were tested, but most attention was focused on those to be used by the fire-rescuemen performing the physically demanding crew rescue activities. Only the more recent designs incorporating very responsive and high flow regulators (> 450 liters/minutes) could maintain positive pressure within the mask during heavy work. NIOSH approved units certified for 30 minutes lasted an average of 17 minutes during the 60% tests. These same units, however, would last an average of 42 minutes during the much easier 30% tests. Mask concentrations of oxygen and carbon dioxide differed little among the units.

CONCLUSION

We conclude that the imposition of these two forms of personnel protective apparatus can have adverse functional and physiological effects on the user. Seemingly easy tasks in normal street attire can become monumental while wearing a whole body suit. Small individuals may be incapable of safely wearing the suit or may not be strong enough to assist an injured companion during a hazardous operation. Consequently, managers must carefully plan operations not to exceed the capabilities of the suit or user. Medical and physical standards should also be imposed.

SCBA does not exact the physical toll of a suit; however, one must remember that these devices are frequently employed with some sort of garment, such as the turnout coat that firefighters wear. Even though the SCBA may weigh between 23 and 35 pounds, it does not seriously affect the physiology of the user. Gas concentrations are satisfactory and heart rates are elevated over unencumbered rates, but the most important finding is that users must be aware that a demand type apparatus is not likely to last as long as the certified duration when used for heavy labor. Therefore, long entry and exit paths may allow very short working times at the destination. These apparatuses must also be employed carefully to assure the safety of the user. ■

LOW FREQUENCY HEART RATE OSCILLATIONS IN SHUTTLE ASTRONAUTS: A POTENTIAL NEW MARKER OF SUSCEPTIBILITY TO SPACE MOTION SICKNESS

A. L. Goldberger[1], W. Thornton[2], W. R. Jarisch[1], W. J. Manning[1], J. Mietus[1], D. R. Rigney[1], and A. J. Mandell[3]
[1]Department of Medicine, Harvard Medical School and Cardiovascular Division, Beth Israel Hospital, Boston, Massachusetts 02215, [2]NASA/Johnson Space Center, Houston, Texas 77058 and [3]Laboratory of Biological Dynamics and Theoretical Medicine, University of California at San Diego, La Jolla, California 92093

Space Shuttle astronauts often suffer Space Motion Sickness (SMS), a syndrome that limits their productivity and potentially alters their cognitive and physical responsiveness. Investigations of SMS have been hampered by a lack of objective physiological criteria that may be used to quantify the syndrome's presence and severity. We report here that heart rate data might be used for this purpose. The availability of such criteria for SMS might be useful in evaluating the efficacy of therapy during flights, in attempting to simulate SMS on the ground, and in understanding the physiology of the syndrome.

We postulated that dysfunction in neuro-autonomic control, possibly initiated by sensory mismatch, is important in the pathophysiology of SMS. Work in our laboratory has suggested that neuro-autonomic dysfunction during a variety of illnesses may produce changes in the normal pattern of heart rate variability, often involving low frequency oscillations (~0.02 Hz). We suspected that spaceflight might also be associated with abnormal low frequency heart rate oscillations and that these oscillations

could be related to susceptibility to the SMS syndrome. Accordingly, we analyzed electrocardiographic (ECG) data obtained from two Space Shuttle crewmembers who developed symptoms of SMS. Cardiac interbeat (R-R) intervals from analog ECG data recorded on Holter monitor tapes were digitized and subjected to time series and spectral (Fourier) analysis.

Both astronauts showed distinctive low frequency heart rate oscillations (≤ 0.01 Hz) that were present, at least intermittently, during periods of severe SMS characterized by marked sensitivity to rotational movement, malaise, and anorexia. Figure 1 (upper panel) from Astronaut A shows a time plot of heart rate over about 15 minutes. Visually apparent, large-amplitude oscillations are present. The frequency spectrum (lower panel) shows a prominent low frequency band (arrow). Figure 2 from

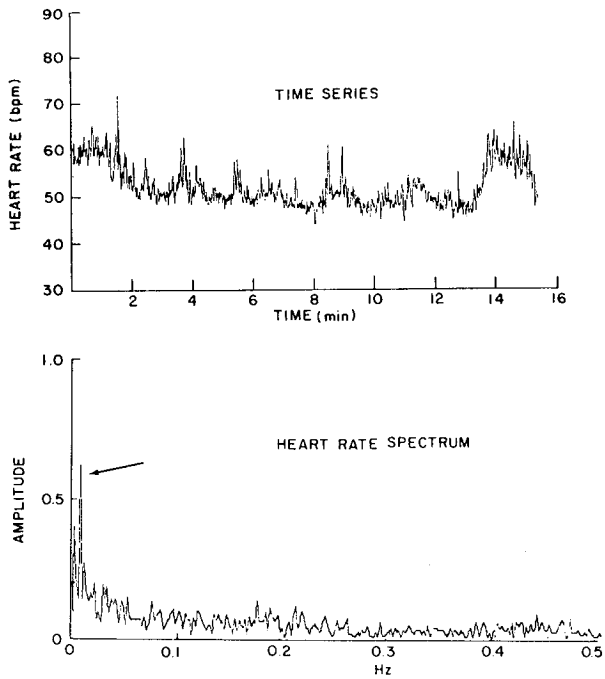

Figure 1. Heart rate time series and corresponding frequency spectrum from an astronaut with SMS. Upper panel: during SMS, heart rate exhibits a series of large amplitude oscillations that might be used as a marker of the syndrome's presence. Lower panel: Fourier spectrum of the heart rate series, showing range of frequencies over which the oscillations occur, in the band centered around 0.01 Hz, indicated by arrow.

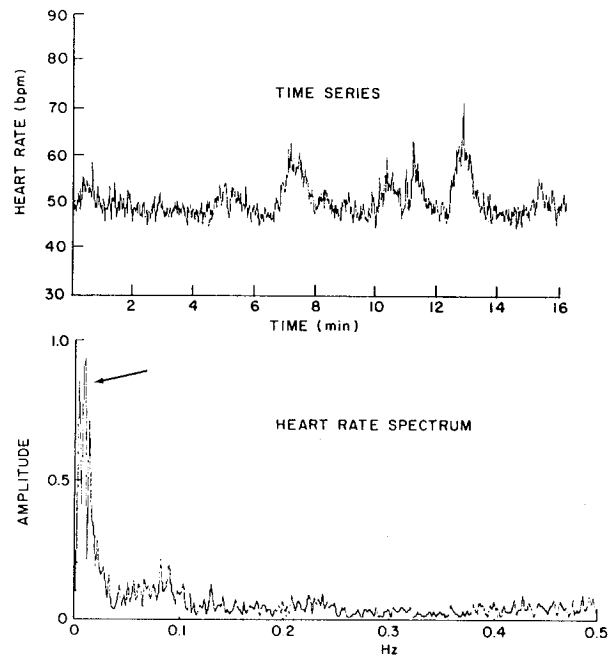

Figure 2. Heart rate time series and corresponding frequency spectrum from an astronaut during recovery from SMS. Same subject as Figure 1, later in flight when he reported he was still sick but felt better. Low frequency oscillations are still present in heart rate time series (upper panel) as seen in spectrum of time series (lower panel, arrow).

Astronaut A shows similar findings when the SMS symptoms were still present, but abating. Figure 3 is from the same subject after recovery from space sickness was reported, and does not contain the unusual low frequency oscillations. However, in this astronaut, prominent oscillations were also noted intermittently in the apparent absence of overt symptoms of SMS. Figure 4, from Astronaut B during SMS shows findings similar to those observed in Astronaut A.

These findings are of potential importance for a number of reasons:

(1) Heart rate oscillations that are observed in the ECG data may provide a sensitive, objective diagnostic marker of the SMS syndrome and therefore might be used both for detection of the syndrome and for monitoring response to therapy. Further studies (preflight, inflight, and postflight) are needed to correlate the onset and cessation of these oscillations with SMS, to determine their sensitivity and specificity in predicting SMS symptoms, to discover their possible association with other periodic phenomena during SMS (*e.g.*, oscillations in gastrointestinal motility or respiration), and to establish their relation to particular activities and to diurnal variations. The presence of intermittent oscillations in Astronaut A after apparent recovery could be interpreted either to indicate that the periodic heart rate is necessary but not sufficient to demonstrate the presence of SMS, or that SMS is in fact present, but below the threshold needed to produce overt symptoms.

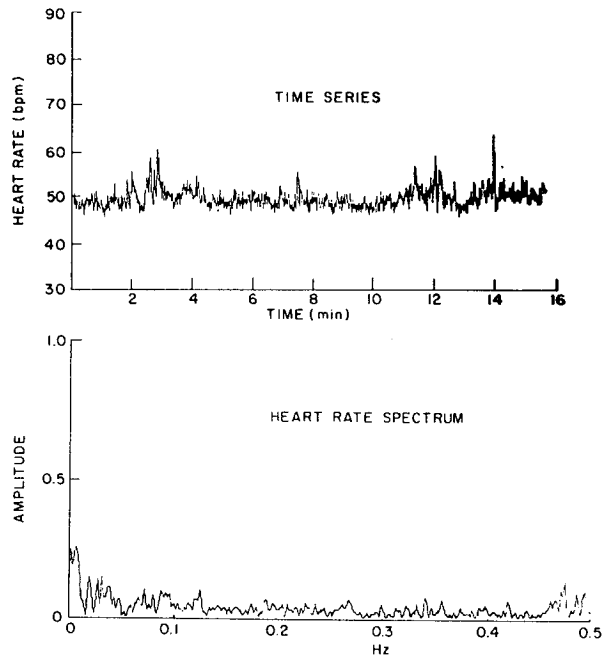

Figure 3. Heart rate time series and corresponding frequency spectrum from same astronaut (Figures 1, 2) on recovery from SMS when symptoms had largely disappeared. Low frequency oscillations are no longer apparent (upper panel) as confirmed by decreased amplitude of low frequency band in spectrum (lower panel). However, the subject showed intermittent, prominent heart rate oscillations after apparent recovery from SMS.

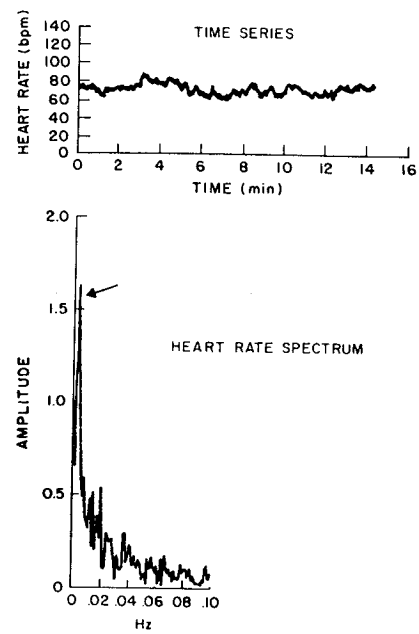

Figure 4. Heart rate time series and corresponding frequency spectrum from another astronaut with SMS. As in Figure 1, heart rate shows low frequency oscillations (upper panel). Spectrum shows that oscillations occurred over the same range of frequencies as Figure 1 (lower panel, arrow).

(2) The presence of low frequency heart rate oscillations in spaceflight suggests an abnormality in neuro-autonomic control. Oscillatory behavior of this kind is seen in a variety of complex nonlinear systems, associated with alterations in one or more control parameters. Realistic physiological models of cardiac dynamics in space will have to account for the oscillations.

(3) These oscillations, if shown to be related to SMS, may also provide a way of comparing SMS with conventional motion sickness syndromes. It is not known whether terrestrial motion sickness is associated with cardiovascular oscillations and if so whether they occur at the frequencies characteristic of SMS. Studies of heart rate dynamics during attempts to simulate SMS on earth should prove helpful in assessing whether these simulations adequately reproduce the physiological alterations seen in spaceflight.

In summary, we report the first evidence of unusual low frequency heart rate oscillations during spaceflight, suggesting an alteration in neuro-autonomic control during flight. These oscillations were observed in astronauts when they were sick from SMS. They also occurred intermittently when symptoms were no longer pronounced, suggesting that (1) the syndrome was still present but subthreshold or (2) the oscillations indicate susceptibility to SMS, rather than SMS itself. To clarify the relation of the oscillations to SMS, it will be necessary to compare longer ECG time series with detailed logs of activities and symptoms obtained from astronauts who did and did not exhibit SMS during spaceflight. ■

HEALTHCARE DECISION SUPPORT AND DIAGNOSTIC AIDS FOR ASTRONAUTS

R. R. Grams, Z. M. Jin, Y. Z. Shen, J. Fisher, F. S. Yu, G. Peck and the NASA Technical Advisor Dr. P. Buchanan
Medical Systems Group, Department of Pathology, College of Medicine, University of Florida, Box J-356, Gainesville, Florida 32610

INTRODUCTION

Since 1979, the focus of our project has been to design, test, and implement a portable, stand-alone, medical decision support system that allows a medical as well as nonmedical personnel to access problem-oriented expert information for life support activities in remote areas or facilities such as the Space Shuttle, Space Station, or manned deep space probe. Over the past seven years, we have had an opportunity to redesign and rebuild the system on several occasions because of a total inability to accomplish our original objectives. Today, we can demonstrate the viability of a microcomputer-based medical decision support system that can present the world's knowledge of medicine and make this instantly available to those who have need for such information.

DESIGN SPECIFICATIONS

A decision support system and diagnostic aid package for astronauts must encompass the world's knowledge of medicine, must be as current as possible within the framework of established editing procedures, and must allow an online access to this wealth of information using both technical and nontechnical terminology. The system must be designed as a stand-alone, self-contained unit presenting color pictures of high quality as well as voice and motion pictures. The system must ultimately include a linguistic processing module that can directly interact with speech and verbal commands.

PROGRESS TO DATE

The current implementation of a stand- alone medical decision support system and diagnostic aid has made great strides in the last several years, allowing us to demonstrate the feasibility of maintaining multiple medical texts simultaneously and accessing these through keywords, synonyms, and a combination of Boolean constructs put together in medical phraseology. The system is now being linked with a color picture archives which will allow us to store high-quality test illustrations which directly amplify and extend the knowledge base. The data that is currently resident in the system includes material from the following texts: (1.) *The Merck Manual*, (2.) *Control of Communicable Diseases in Man*, (3.) *A Manual of Laboratory Diagnostic Tests*, (4.) *Color Atlas and Synopsis of Clinical Dermatology*, (5.) *USSR Space Life Sciences Digest*, and (6.) *Differential Diagnostic Database* (special hybrid text).

CURRENT EFFORTS

In the 1987-1988 development cycle, our staff will complete the final editing of all of these texts with a seven-stage verification process. This includes the archiving of all pictures, graphs, and illustrations. The combined text and graphics database will permit the retrieval of all of this information using an internally developed Pascal DBMS specifically designed for this task. Pictures, data, and index will be archived on a laser disk using the write once, read many (WORM) technology. The text and pictures will be displayed on a high resolution screen using a PA/AT-type machine for processing and text manipulation.

The text-processing software and editorial package designed for this system allows us to create a dictionary and a thesaurus for each text which highlight the unique features of that database.

SYSTEM OPERATION

The system is presented to the user as a library bookshelf so that he/she may select from that shelf the text which is most appropriate for their particular need. This "virtual library" can be used as a bookshelf, and the books can be digitally extracted from the shelf and viewed as their paper equivalents. In this format, the system shows the title page, table of contents, and then the reader can go to any of the chapters and pages throughout the text looking at pictures and material as they choose. One can move among a number of texts just as you would in a library and save or store certain elements of any text for printout or secondary review.

Also contained on the virtual library shelf is a diagnostic text which is a special hybrid of the materials that are currently resident in the database. This diagnostic text is disease-oriented. When this document is selected, the diagnostic aid allows the use of individual signs, symptoms, and problems to reference the full array of all medical knowledge maintained on diseases. The database is designed to retrieve an exhaustive list of possible disease entities or problems that could cause such a combination of signs and symptoms.

SUMMARY

The ability to move from text to query to decision support in a matter of seconds has never been possible prior to the advent of this microcomputer-based decision support tool. It now will be augmented in the coming months and years with artificial intelligence to take the database and extract optimal information for the user. Several projects are contemplated that will allow us to summarize free text and manipulate this wealth of knowledge in such a way that it can aid in the decision support process. For the future, we are looking at an active system versus a passive approach in areas where we are dealing with individuals who may not have extensive experience with the system and may not know how to proceed to a logical or reasonable conclusion.

Future research will involve the ability to verbally interact with the system and to conversationally query the database for either a voice or display-driven response which could then be incorporated into the basic communication system of any space vehicle or extraterrestrial habitat. The technology that has been assembled for medicine can obviously be transposed to other areas such as engineering or biology with similar types of potential. The fact that we can now make laser disks which encompass thousands of pages of expert information makes it possible to package this system and transport it economically into the space environment. ■

DOES ALTERED GROWTH HORMONE PHYSIOLOGY PLAY A ROLE IN MUSCLE ATROPHY OF SIMULATED WEIGHTLESSNESS?

R. E. Grindeland[1], T. N. Fast[2], M. Vasques[2], T. Satyanaranyana[2], and M. Ruder[2]
[1]Life Science Division, NASA/Ames Research Center, Moffett Field, California 94035 and [2]Santa Clara University, Santa Clara, California

INTRODUCTION

An abundance of evidence, direct or indirect, indicates that human beings and animals sustain atrophy of their antigravity muscles during spaceflight. It is not known if the atrophy is entirely attributable to the decreased force exerted by the muscles in weightlessness or if systemic factors also contribute to the atrophy. A number of systemic factors, such as decreased secretion of growth hormone or insulin, or increased adrenal steroid secretion could affect the rates of muscle protein synthesis or catabolism. In support of the possible role of altered hormone concentrations in spaceflight muscle atrophy was the observation that pituitary glands of Space Laboratory 3 rats secreted about one-half as much growth hormone as control glands. Further, secretion of a large molecular weight form of growth hormone was decreased about 90% in flight rat pituitary cells. Ablation of the pituitary gland decreases muscle protein synthesis about 70%, a deficit almost identical to that observed in muscles of limb-casted rats. It is also possible that muscles of weightless animals are resistant to the circulating hormones; a recent report has shown that exogenous insulin is less effective in inhibiting protein catabolism in muscles of suspended rats than of control rats.

OBJECTIVES

The overall aim of this study was to clarify the role of altered growth hormone (GH) physiology in muscle atrophy of weightlessness. Using hindlimb suspension as a simulation of weightlessness, the specific questions addressed were:

(1) Do pituitary and plasma concentrations of GH decrease?

(2) What are the time courses of changes in GH concentrations and muscle atrophy?

(3) Do hypophysectomized rats, with their reduced muscle protein synthesis, show atrophy in response to simulated weightlessness?

(4) Does exogenous GH alleviate the muscle atrophy of suspended rats?

RESULTS

Experiment 1: Intact male rats (Simonsen Albinos, 200 g) were suspended for periods of 1, 2, 5, and 7 days (6 rats/group). At the end of suspension hindlimb muscles, blood, and pituitary glands were collected and the tissues weighted. Statistically significant differences ($p<0.05$) in weights occurred for the six muscles after varying periods of suspension: 1 day: SOL (12%), GAST (6%); 2 days: AL (- 21%), PLANT (16%); 5 days: TIB ANT (9%); and 7 days: EDL (10%). At 7 days all muscles were significantly smaller than controls; the differences varied from 8% (TIB ANT) to 39% (AL). Pituitary GH and plasma GH, measured by bioassay, were decreased 35% after 1 day and 50% on all successive days ($p<0.05$ in all cases). Plasma GH measured by RIA did not differ from control at any time. Plasma corticosterone was moderately elevated on day 1 but similar to control rat values at all other times.

Experiment 2: Male rats (Zivic-Miller, 200 g) were hypophysectomized (hypox), kept for two weeks, and then suspended for 7 days. In interval between surgery and suspension the rats lost 17-20% of their body weight in two studies. During this period the two slow muscles (SOL, AL) lost 0.5 and 16% of their mass, and the other muscles lost from 7% (PLANT) to 17% (TIB ANT). During suspension, results differed slightly in the two experiments. The reason for this difference is unknown. Body weights of suspended and control hypox rats did not differ from their weights at the beginning of suspension. In the first experiment the SOL, GAST, PLANT, TIB ANT, and EDL showed statistically similar changes (0-9%) in weight in hypox control and suspended rats; only the AL lost significantly more mass (15%) during suspension. In the second experiment the SOL, GAST, PLANT, and AL all showed somewhat greater losses of mass in hypox suspended than in hypox controls (8-13%). For both experiments, however the losses of mass during suspension were significantly less than in intact suspended rats. When compared to controls sacrificed at the beginning of suspension the two slow muscles (SOL, AL), which show net loss of mass in weightlessness, atrophied 1/3-1/2 as much as muscles of intact, suspended rats. The other four muscles, which grow at a reduced rate in weightlessness, showed either no (EDL, TIB ANT) or slight (GAST, PLANT) atrophy in the hypox, suspended rats.

Experiment 3: Growth hormone (bovine GH 2-100 ug injections/day) did not alleviate muscle atrophy in intact, suspended rats. Data from other studies suggest that secretion of endogenous GH was inhibited in these rats. When GH was given to hypox suspended rats (2-100 ug injections, human GH) the atrophy due to hypophysectomy and/or suspension was significantly attenuated (SOL, AL, PLANT) or a net growth of muscle occurred (GAST, TIB ANT, EDL). For four muscles the increase in muscle mass was less than the increase in body weight (13%), equal to body weight increase for the EDL, or greater for the TIB ANT. Suspended rat muscles showed some refractoriness to the exogenous GH. The EDL showed comparable responses in suspended and control hypox rats, whereas the other five muscles showed 2-6 times greater weight increments in hypox control than in hypox suspended rats.

SUMMARY AND CONCLUSION

(1) Pituitary and plasma GH (bioassay) decrease the first day of simulated weightlessness and remain depressed for 7 days.

(2) Decreased GH concentrations parallel or precede significant muscle atrophy.

(3) Hypophysectomy attenuated muscle atrophy of simulated weightlessness.

(4) Muscles of hypox suspended rats are significantly less sensitive to exogenous GH than those of control rats.

(5) Collectively these data indicate that altered GH physiology contributes to the muscle atrophy of simulated weightlessness.

These studies were performed in conformity with "Guiding Principles in Animal Care and Use of Animals" approved by the Council of the American Physiological Society. ■

SPACELAB LUNG FUNCTION TEST SYSTEM

H. J. B. Guy, G. K. Prisk and J. B. West
Department of Medicine, M-023A, University of California, San Diego, La Jolla, California 92093

We have developed a lung function package for Spacelab Life Sciences Mission 1 (SLS-1), designed to allow efficient data collection in the face of major crew time constraints. The hardware comprises four investigator-designed modules closely coupled with NASA furnished Life Sciences Laboratory Equipment (LSLE). The automatic experiment sequence enables the following studies to be performed:

- Resting ventilation and gas exchange
- Single Breath Nitrogen washouts
- Topographic distribution of perfusion (cardiogenic O_2 and CO_2 oscillation technique)
- Carbon monoxide diffusing capacity and volume of pulmonary blood
- Multibreath nitrogen washout
- Distribution of ventilation-perfusion ratios (from intrabreath gradients in gas exchange)
- Rebreathing estimation of cardiac output
- Ensemble averaged maximal expiratory flow - volume curves

Some of these tests have revealed major changes in lung function during short periods of microgravity in ballistic flight, and during ground-based simulations such as tilting and immersion. The test package is now mature, ready for the SLS-1 mission, and applicable to an ongoing series of ground based and flight studies. ■

TRANSCUTANEOUS OXYGEN CHANGES DURING THE PROGRESSION OF MOTION SICKNESS

D. L. Harm, M. F. Reschke
Space Biomedical Research Institute, NASA/Johnson Space Center, Houston, Texas 77058

INTRODUCTION

Facial pallor is widely accepted as one of the cardinal signs of motion sickness, and is usually observed in close conjunction with the first subjective reports of epigastric awareness. Changes in skin color (pallor/blush) reflect changes in the volume of blood in the skin microcirculation. Peripheral blood flow is regulated primarily by the sympathetic division of the autonomic nervous system. Increased sympathetic activity produces vasoconstriction, whereas inhibition or withdrawal of sympathetic activity results in vasodilation. It follows that oxygen delivery to the skin will vary directly with blood volume/flow in the skin.

A relatively simple method for continuous monitoring of transcutaneous oxygen ($P_{tc}O_2$) was developed 20 years ago and has been used primarily in clinical settings. The sensor used to monitor $P_{tc}O_2$ is a Clark-type polarographic electrode consisting of a platinum cathode and a silver anode covered by an electrolyte and an oxygen-permeable membrane. Oxygen diffuses across the membrane to the cathode initiating an electro-chemical reaction that produces in an electrical current (proportional to the reduction in oxygen at the cathode) which is first converted to a voltage and then to PO_2 in mmHg.

The purpose of the present study was to evaluate the potential utility of $P_{tc}O_2$ as a quantitative measure of pallor/blush responses associated with motion sickness, and to examine differences in response patterns of susceptible and insusceptible subjects.

METHODS

Twelve subjects participated in the experimental protocol which consisted of three phases: (1) pretest baseline (30m), (2) motion test (CSSI) at 15 rpm with a Nausea I endpoint, and (3) recovery (20m).

Oxygen values were recorded continuously from one sensor positioned on the side of the face; recordings from a second sensor were obtained from either the forehead (6 subjects), or the sternum (6 subjects). Transcutaneous oxygen was monitored on four of these subjects on a second occasion (same stimulus conditions), and again during parabolic flight.

RESULTS

Observations from preliminary inspection of the data are as follows: (1) Moderate differences in absolute O_2 values between sites, with facial values generally being higher than forehead, but lower than sternum values. (2) Time and direction of changes in O_2 were virtually identical between the two sites within individuals. (3) Large increases and decreases in O_2 values were observed in some subjects. (4) Susceptible and insusceptible subjects showed distinctly different response patterns. In general, changes in $P_{tc}O_2$ from baseline values in the two groups began to diverge early in the test, with susceptible subjects exhibiting increases in $P_{tc}O_2$ and insusceptible subjects showing decreases in $P_{tc}O_2$. These response patterns emerged earlier (just prior to epigastric awareness) in susceptible than insusceptible subjects (whose $P_{tc}O_2$ began to decline after epigastric distress was reported). Finally, recovery of $P_{tc}O_2$ to baseline values occurred more quickly and was characterized by greater linearity in insusceptible than susceptible subjects. These observations are depicted in Figure 1 by sample tracings of a susceptible and an insusceptible subject. (5) With only a few exceptions, subjective observations of pallor/blush were consistent in time and direction with $P_{tc}O_2$. (6) Similar response patterns are expected to emerge during repeated testing and during parabolic flight conditions.

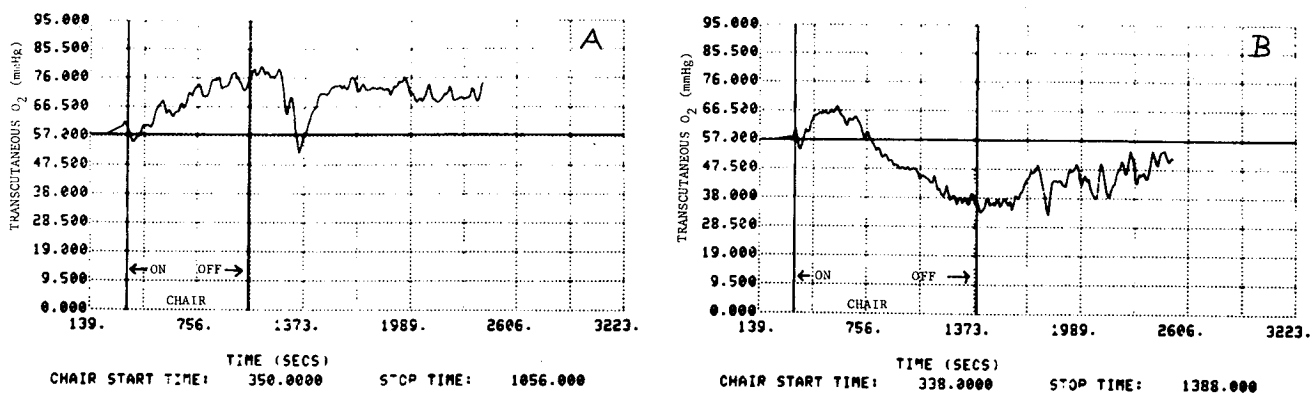

Figure 1. Sample tracings from 2 subjects that best exemplify the transcutaneous oxygen response pattern of susceptible (A), andd insusceptible (B) individuals exposed to a CSSI test with a nausea I endpoint.

Further analyses are expected to yield information concerning changes in the characteristics of the underlying frequency components of cutaneous O_2 perfusion.

In conclusion, this preliminary evaluation supports the potential utility of $P_{tc}O_2$ as a quantitative measure of pallor/blush responses to motion stimuli. In addition, the data indicate decreased sympathetic activity in susceptible subjects, and increased sympathetic activity in insusceptible subjects. These findings are consistent with reports of other investigations concerned with autonomic manifestations of motion sickness symptoms. ■

TACHYGASTRIA DURING PARABOLIC FLIGHT

D. L. Harm, R. S. Stern and K. L. Koch
Space Biomedical Research Institute, NASA/Johnson Space Center, Houston, Texas 77058

Epigastric discomfort and nausea are pathognomonic symptoms of motion sickness, and are associated with changes in the basic electrical rhythm (BER) for the gastrointestinal tract. The normal gastric BER is approximately 3 cpm. Tachygastria (5-9 cpm) has been observed in patients with ideopathic nausea and in subjects experiencing vection-induced motion sickness. Increases in the frequency of the gastric BER appear just prior to, or concomintantly with subjective reports of nausea. Electrogastrography (EGG) is a noninvasive technique used for measuring electromechanical gastric activity, and estimating the BER. The present study employed EGG to examine the relationships between gastric rhythm and motion sickness symptoms induced by parabolic flight aboard the KC- 135.

METHODS

Sixteen subjects (2 per flight) participated in the experiment, 10 susceptible and 6 insusceptible to motion sickness during parabolic flight. Subjects were considered susceptible if they reached a Nausea I level (Pensacola Scale) of sickness. Immediately prior to leaving home for the flight, subjects were instructed to eat a substantial breakfast to maximize the normal 3 cpm gastric rhythm. Upon arrival at Ellington Field, prepasted disposable electrodes were position on the subject's abdomen as shown in Figure 1. Once the subject was seated on the plane, the electrodes were connected to an AC coupled amplifier with a bandpass of .05-.30H_z, and a time constant of 10 sec. A mercury strain gauge was positioned around the chest to monitor respiratory rate. Respiratory and EGG signals were displayed on an oscilloscope, digitized, and stored by an LSI-11 computer. Continuous recording of stomach symptoms was accomplished using an electronic dial scale from 0 to 7 (0 = no symptoms and 7 = vomiting), with an incremental output of .5V for each dial setting.

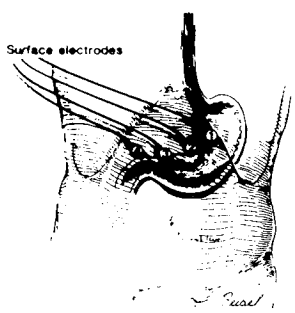

Figure 1. Illustration of electrode placement for EGG recording.

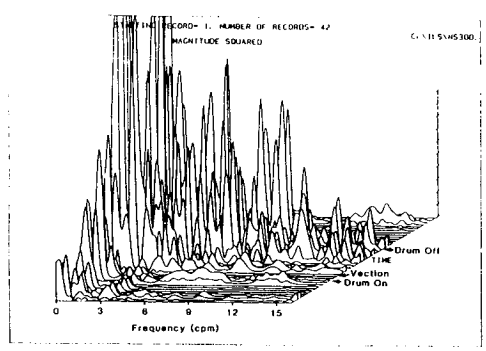

Figure 2. Example of running spectrum analysis (RSA) of EGG signals from a subject with vection-induced nausea.

Data were digitized continuously beginning 30 min before take-off and ending 30 min after landing, with the exception of short periods when electrical power was from the ground to plane generator and back again. All flights consisted of 40 parabolas flown in rollercoaster fashion in either 5 sets of 8 or 4 sets of 10 parabolas.

RESULTS

Based on visual observations of the EGG signal displayed on the oscilloscope, the normal 3 cpm gastric rhythm was present during gastric symptom-free periods, and shifted to tachygastria around the time subjects reported epigastric symptoms. The data are currently being analyzed by means of fast Fourier transformations and running spectrum analysis (RSA). An example of a pseudo 3-dimensional plot produced from a RSA is provided in Figure 2. Spectral density estimates derived from these analyses will be entered into analysis of variance for group comparisons and examination of temporal relationships between gastric BER frequency and stomach symptoms accompanying motion sickness. We expect our statistical results will support our visual observations of the EGG signal. ■

PERSONALITY-PERFORMANCE RELATIONSHIPS IN DEMANDING ENVIRONMENTS

R. L Helmreich and J. A. Wilhelm
Department of Psychology, The University of Texas at Austin, Austin, Texas 78712

A critical concern in demanding work environments such as manned spacecraft is to achieve the highest possible levels of crew performance. Failure to optimize performance can be extremely costly both in financial terms and in terms of risk to participants. The goals of the present research are (1) to isolate those measurable aspects of personality that act to influence both individual and group performance, (2) to develop valid measures of individual and group performance on complex tasks, (3) to determine and measure environmental and organizational factors that influence the performance and adjustment of groups in isolated environments; and (4) to evaluate the effectiveness of strategies for selecting crewmembers for complex missions and the utility of training attempting to improve the *quality* of group interaction and performance.[1] The present report addresses the first two of these goals and will concentrate on work accomplished with multiperson aircraft crews.

ISSUES AND PERFORMANCE

While the measurement of performance on routine, production-type tasks has been accomplished with high reliability for many decades, accurately assessing the quality of output in complex, intellectual pursuits such as scientific research has proved to be a much more elusive goal. In aviation, for example, measurement of technical aspects of flight (such as proper manipulation of controls) is easily accomplished while evaluating the quality of decisions made regarding proper action in urgent, nonstandard situations has been less successful. When the performance in question is that of groups rather than individuals, the question is even more complex and less well defined. There is little solid evidence relating group processes to performance outcomes and few guidelines for partitioning performance variance among group members.

MEASURING CREW PERFORMANCE

The assessment of flightcrew performance used two approaches. The first involves the development of rating instruments for use by expert observers in evaluating the coordination and individual and team performance of multiperson crews. Evaluations of this form have been validated and demonstrate that the technical and interpersonal/managerial aspects of flight can be differentiated and related significantly to crew attitudes and personality (Helmreich, Foushee, Benson, & Russini, 1986; Helmreich, in press). The second methodology involves the decomposition and coding of behavior across time to capture central elements in interpersonal communication and group process that can be related to performance outcomes. The primary means of data reduction consists of coding videotapes of actual flight segments conducted in simulators under controlled conditions. Work is in progress on both code development and data analytic techniques.

PERSONALITY-PERFORMANCE RELATIONSHIPS

Although the conceptual relationship between personality and performance has long been recognized by psychology, empirical validation of this linkage has been scanty. In aviation, few reliable relationships between personality and performance have emerged from forty years of research. Part of the problem may rest in the choice of criteria of performance: aviation researchers have relied exclusively on performance in training (or the binary Pass-Fail measure of training success) as the indicator of attainment while overlooking the operational performance. A recent study (Helmreich, Sawin, & Carsrud, 1986) clarifies this situation. In a longitudinal study of work performance, no relationships between personality and performance were found at the end of job training. However, by the end of three- and six-month periods, significant and theoretically meaningful correlations between personality and performance were found. The results were interpreted as a "honeymoon effect" -initial motivation for a new position masks underlying personality determinants of behavior which emerge only over time.

PERSONALITY CONSTELLATIONS

A group of personality constructs has been isolated which relate conceptually and empirically to performance. These fall into two general categories: instrumental, achievement-related factors and factors reflecting interpersonal, expressive concerns (Spence & Helmreich, 1983; Helmreich, in press).

Within these broad domains, particular constellations of traits reflecting more focused positive and negative aspects of the self have been specified. These include such characteristics as a need for mastery of challenging tasks, orientation towards work, verbal aggression, impatience and irritability, and submissiveness. A series of studies has found significant, predictive validity for these measures as determinants of a wide variety of performance outcomes including scientific attainment, academic performance, susceptibility to illness, white-collar performance, and both technical and managerial aspects of flying. Current research focuses on isolating the constellations of these trait dimensions in various populations using cluster analytic techniques and on relating these constellations to both individual and group performance.

[1]The research falls under the purview of both the Aeronautics and Space components of NASA in recognition of the numerous similarities in the two endeavors. The program of research is a *group* endeavor with a number of close collaborators. These include, at the University of Texas, Professor Janet T. Spence and Doctoral students Valerie Edwards, Robert Gibson, Steven Gregorich, and Robert Fred, and at NASA Ames, H. Clayton Foushee and Thomas R. Chidester. ■

REFERENCES

Helmreich, R.L., Foushee, H.C., Benson, R., & Russini, W. (1986) Cockpit management attitudes: Exploring the attitude-behavior linkage. Aviat. space environ. med. 57:1198-1200.

Helmreich, R.L. (in press) Exploring flight crew behaviour. Social Behaviour.

Helmreich, R.L., Sawin, L.L., & Carsrud, A.L. (1986) The honeymoon effect in job performance: Delayed predictive power of achievement motivation. J. Appl. Psyc. 71:185-188.

Spence, J.T. & Helmreich, R.L. (1983) Achievement-related motives and behavior. In J.T. Spence (ed.) Achievement and achievement motives: Psychological and sociological approaches. San Francisco: W.H. Freeman.

IN VIVO BIOCOMPATIBLE IMPLANT SYSTEMS FOR STUDIES OF BONE PATHOPHYSIOLOGY UNDER EARTH GRAVITY AND MICROGRAVITY CONDITIONS

G. R. Holt[1], T. B. Aufdemorte[2], P. J. Sheridan[3], R. G. Triplett[4], B. F. Boyce[5], and G. R. Mundy[5]
[1]Department of Surgery, The University of Texas Health Science Center, 12709 Toepperwien Road, San Antonio, Texas 78233, [2]Department of Pathology and Department of Surgery, [3]Department of Cellular and Structural Biology, [4]Department of Oral and Maxillofacial Surgery, and [5]Division of Endocrinology, The University of Texas Health Science Center, 7703 Floyd Curl Drive, San Antonio, Texas 78284

Abnormalities of the musculoskeletal system are problems of enormous magnitude in both the earth-bound population as well as astronauts, who must function in microgravity environments for prolonged periods. In astronauts, the inexorable loss of bone mineral appears to be one of the most significant problems of long-term spaceflight. Thus, the primary objective of this research is to study musculoskeletal pathophysiology, developing methods to prevent and treat osteoporosis and musculoskeletal atrophy suffered by astronauts under weightless conditions. The first step in achieving these objectives will be the development of an animal model which mimics this musculoskeletal deconditioning as well as to produce *in vivo* experimental methodologies to study metabolic bone disease.

At present, tissue for support of such *in vitro* or *in vivo* studies of bone pathophysiology must be obtained by trephination techniques or other surgical methods. These procedures are relatively invasive, time-intensive, and have other constraints relative to the number of biopsies which may be performed in a given site as well as time intervals which must separate each biopsy. Further complications arise from variation in sample quality and/or quantity as a consequence of technical variability. In addition, most studies of local factors in the pathobiology of osteoporosis have been limited to *in vitro* techniques

as a result of these well-known constraints, which are of even greater significance when attempting to study the pathophysiology of osteoporosis of spaceflight. Thus, the specific aims of this study are to further develop and test an implantable biocompatible bone harvest chamber in an effort to facilitate *in vivo* research and complement *in vitro* studies currently in progress.

For this study, a bone harvest chamber machined from implant-grade pure titanium and passivated to obtain a TiO_2 external host implant interface was placed (under appropriate anesthesia) in the tibeal plateau of the baboon (*Papillo cynocephalus*). The implant was positioned to allow pores and internal aspects to communicate with trabecular bone. Once inserted in place, the implant was covered with periosteum and the incision closed. Following a six-week interval for healing, tissue was removed from the implant core under general anesthesia. Additional samples may be obtained in like fashion as suited to the protocol of a particular complementary *in vitro* investigation.

Preliminary data indicate this implant may be rapidly and atraumatically placed with negligible morbidity, that it is completely biocompatible, becoming intimately incorporated within the implanted bone in less than six weeks. Ingrowth of new bone readily occurs into the implant chamber and this bone is rich in osteocytes, osteoblasts and osteoclasts, varying quantitatively and qualitatively with time and subject. Bone samples may be harvested for detailed biochemical, histomorphometric or other analyses for purposes of diagnosis or to support other studies of local factors important in the pathobiology of osteoporosis such as Lymphotoxin, Interleukin-1, Tumor Necrosis Factor, Transforming Growth Factor-β, and others. This specimen also has other attributes as a consequence of its standardization with respect to volume, time, site and means for atraumatic harvesting.

Results of this study will be presented to support the value of the implant in studies of pathophysiology of bone demineralization under earth gravity and conditions of space weightlessness. Information gained should assist in establishing an integrated approach to studies of the pathophysiology of osteoporosis and in developing the most effective diagnostic, preventative or therapeutic countermeasures. ■

DEVELOPMENT OF CAPABILITY TO PERFORM EMERGENCY SURGICAL PROCEDURES IN THE REMOTE, SELF-CONTAINED, MICROGRAVITY ENVIRONMENT OF SPACE STATION

B. A. Houtchens
Department of Surgery, The University of Texas Health Science Center at Houston, 6431 Fannin, Houston, Texas 77030

BACKGROUND

It is intended that clinical medical care for Space Station crew be provided within the context of a dedicated health maintenance facility (HMF). Among intended HMF capabilities at "permanent manned presence" are initial evaluation and management of trauma, and performance of emergency (minor) surgical and dental procedures. Included in this last category are the following: intubation of the airway (endotracheal or tracheostomy); establishment of vascular access (percutaneous or cutdown); evacuation of the pleural space (thoracentesis of tube thoracostomy); evacuation of the stomach; evacuation of the bladder (transurethral or suprapubic); incision and drainage of (relatively superficial) abscess; suture closure of a laceration; reduction and stabilization of a fracture.

In the remote, self-contained environment of Space Station, ability to perform emergency surgical procedures implies the ability to manage administration of anesthetic, and to provide critical care. To support that level of care, the following are intended: mechanical ventilator, and pulmonary care system; postitive pressure volumetric intravenous fluid infusion system; critical care and anesthetic (local/intravenous) drug formulary; diagnostic imaging system; complement of surgical and dental instruments; medical suction and fluid collection/containment system; patient care area with

appropriate surfaces, configuration, lighting; self-contained critical care transport (evacuation) support system; protocols for equipment use.

SPECIFIC PROBLEMS

With exception of the last 4 items above, it is anticipated that most of the support requirements can be satisfied by modification of existing, clinically-proven hardware and supplies. It is anticipated that many of the management problems and decisions to be faced will be those common to delivery of medical care in remote, self-contained environments on earth. However, with regard to development of apparatus and techniques for the performance of surgical procedures in microgravity, novel approaches are needed to provide the following: the ability to maintain desired relative positions of patient, anatomic components of interest, surgeon(s), and instruments, without interfering with visibility and access, and with ability to conveniently and rapidly reposition without contamination; the ability to contain and collect biologic and other medical fluids, from the surface of or from within a patient's body, with separation of fluids from (aspirated) air proximal to a source of suction; and the ability to test and verify proposed solutions in both one-G and micro-G.

METHODS, RESULTS

1. A modular micro-G surgical workstation has been designed, and a prototype has been fabricated of aluminum, magnesium, and (radiolucent) carbon fiber composite. A deck grid with a pattern of open circles facilitates foot restraint by engagement (or release) of a toe catch mounted on a lightweight shoe, using leg muscle action. An adjustable vertical support column is attached to (and detached from) the deck grid by dentent pins or bolts. A three-axis angle-adjustable "cradle" is attached to (and detached from) the vertical column by detent pins or bolts. A patient restraint/support surface, articulated at hips and knees, weighing less than 30 pounds, is attached to (and detached from) the support cradle by spring-loaded pins. To the patient-support surface can be attached fittings which mate to the seat leg-locking lugs in the Shuttle orbiter middeck, thus allowing the surface to function as a transport litter. At all edges of the patient restraint surface there is incorporated a rail to which clamps with an over-center cam lock can be attached. Medial to the rail is a pattern of vertical slots in which posts may be positioned. By attachment to clamps or posts, support equipment, instrument trays, and surgeon waist restraint belts may be attached at a variety of locations, depending upon optimum configuration relative to a particular clinical problem being addressed. A magnetic catch surface is used to retain (series 400 stainless steel) surgical instruments.

2. A centrifugally based micro-G air-fluid separator unit has been designed and several prototype variations on the theme have been fabricated of plexiglass, aluminum, and stainless steel. The shaft of the same diaphragm pump which provides negative pressure for suction is used to turn the rotating air-fluid separator chamber at about 3000 RPM. Under negative pressure, air and entrained fluid enter the chamber centrally where the fluid comes in contact with blades protruding from a disk. Centrifugal force moves fluid to exit ports at the circumference where it is collected in collapsible plastic bags; air exits centrally to be cycled through the suction pump.

3. The prototype surgical workstation and fluid containment system have been tested during repeated 25-second intervals of micro-G generated by parabolic arc flying in the NASA KC-135 aircraft. Restraint of the operator at the workstation appears to be more than adequate using belt and toe catch together, or either one separately. It is not difficult to accomplish tasks representative of surgical procedures, such as making and suturing an incision in synthetic skin. It is easy to access instruments, and an adjacent "operative field" of interest, and to reposition. Using the suction system, it has been possible to transfer several liters of fluid, over a few minutes, from a fluid source bag to fluid collection bags, without overloading the chamber so that fluid is aspirated through the pump, and with minimum accumulation of air in the collection bags.

DISCUSSION, SIGNIFICANCE

The establishment of a permanently manned space station and, beyond that, the probability of undertaking a manned mission to Mars and establishing a lunar base, represent the first plans for "permanent" presence of humans off the surface of the earth. Historically, where man has ventured as explorer, solider, entrepreneur, or settler, clinical medical care capability has accompanied. Historically, also, trauma and emergency surgical problems have been among those most likely to afflict relatively young otherwise healthy individuals, and most rapidly to result in morbidity or mortality if not appropriately managed. Fortunately, work to date suggests that it should be possible to accomplish

surgical procedures and provide emergency clinical care in the micro-G environment with minimum departure from equipment and techniques used in one-G. This is important because it is in one-G that most of the preparation and training for clinical medical care will occur. ■

INFLUENCE OF BRIEF ISOMETRIC TRAINING ON ISOMETRIC AND ISOKINETIC STRENGTH OF THE HUMAN QUADRICEPS MUSCLE

M. M. Jaweed, G. J. Herbison, and J. F. Ditunno, Jr.
Dept. of Rehabilitation Medicine, Jefferson Medicinal College, Thomas Jefferson University, Philadelphia, Pennsylvania 19107

INTRODUCTION

Isometric exercises are routinely employed in clinics to prevent muscle atrophy and increase muscle strength of the patients afflicted with neuromuscular diseases. Short-term (one to six weeks) six-second isometric contractions have been reported to produce 20-30% increase in isometric muscle strength of the subjects (Liberson and Asa, 1959; Stillwell *et al*, 1966; Moritani *et al*, 1982). Muller (1970) demonstrated that isometric exercise performed for only one second, once daily at 65% MVC was sufficient to increase the maximum force as much as the force generated at 100% MVC carried out 6 seconds, 5 times per day. This suggests that neither the number of seconds for sustained contraction or the number of repetitions influences the improvement of muscle strength due to isometric exercise. However, it is not established whether these brief isometric contractions are able to increase the isokinetic strength of the muscle, as well.

The objective of this study was to examine the influence of a single maximum isometric contraction performed daily for 2 weeks on isometric and isokinetic strength of the quadriceps muscles in healthy female human subjects.

METHODS

Eleven adult female volunteers (between the ages of 24 and 35 years and 120-150 lbs in weight) were familiarized with the exercise and methods of testing for 2 days and their initial maximum isometric (100% MVC) and isokinetic strength (at speeds of 300°/sec, prior to exercise, the subjects "warmed up" by performing 3 isokinetic contractions at a speed of 300°/sec, on a Cybex dynanometer. For exercise, the subjects performed one maximum isometric contraction of the quadriceps bilaterally at 60 degrees of knee extension and at a dynanometer speed of 0/sec. The exercise was performed on alternate days, 3 days per week, for 2 weeks. At the end of two weeks, the subjects' final isometric (in lbs) and isokinetic (in ft lbs) torque of the right and left quadriceps was evaluated. The isometric evaluations were based on recording the force growth by a single maximum isometric contraction of each leg. The isokinetic evaluations were based on selecting the maximum from 5 isokinetic contractions each at a speed of 300°/sec, 150°/sec and 60°/sec. An interval of 2 minutes was allowed between two speeds of the dynanometer. The postexercise muscle force values were compared with the preexercise values by paired student "t" tests.

RESULTS AND DISCUSSION

The salient feature of this study is that a single maximum (100% MVC) isometric contraction performed once every alternate day for a period of 2 weeks is sufficient to significantly increase (14-16%, $P<0.01$) the isometric but not isokinetic strength of the quadriceps muscles in female subjects (Fig. 1). These data therefore suggest that the adaptations of the muscle to isometric exercise are specific to the type of the stress. The isometric force of all subjects showed improvement (Fig. 2) during the 2 weeks with a similar mean percent coefficient of variance for the right (strength = 118.1 ± 11.5 lbs, % CV = 9.7) and left (strength = 119.0 ± 10.7, % CV = 9.0) quadriceps. This improvement in muscle strength was independent of the age, height, weight or muscle size of the subjects. Although an improvement in isometric muscle strength also can be brought about by tetanic electrical stimulation (ES) at a frequency of 50 or 100 Hz (Edwards *et al*, 1977; Currier *et al*, 1979; Kramer, 1987), it is

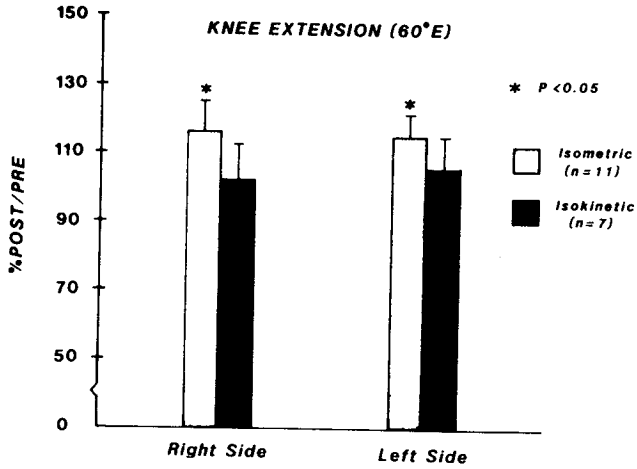

Figure 1. Changes in isometric (light bar) and isokinetic (shaded bar) strength of the quadriceps in female subjects after 2 weeks of isometric exercise. Compared to the pre-exercise, the post-exercise isometric strength of the subjects was increased (14-16%, P<0.05) significantly.

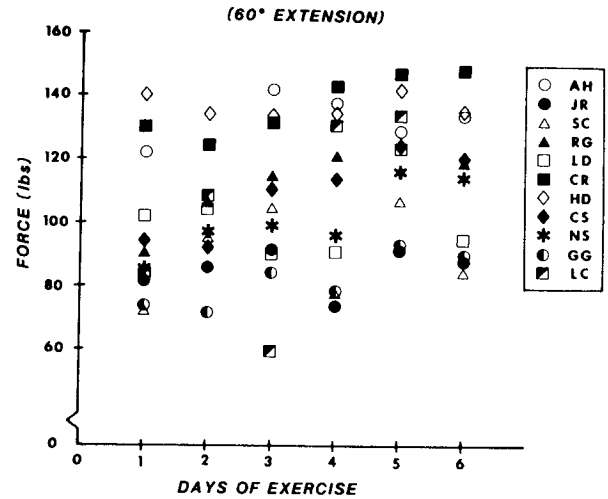

Figure 2. Scattergram showing changes in isometric quadriceps strength of the subjects. All subjects appeared to improve in muscle strength. The % CV of the subjects was 9-10%.

uncomfortable. In addition, the maximum isometric force or torque generation due to ES alone has been reported to be no more than 77%-84% of the MVC (Kramer, 1987).

In conclusion, it is proposed that since brief maximum isometric exercises increase muscle strength of the normal subjects they may be therapeutically employed in preventing muscle strength loss due to hypokinesia. ■

REFERENCES

1. Currier, D.P., Lehman, J. and Lightfoot, P. (1979) Electrical Stimulation in exercise of the Quadriceps Femoris Muscle. Phys. Ther. 59:1508-1512.
2. Edwards, R.H.T., Young, A., Hosking, G.P. et al (1977) Human Skeletal Muscle Function: Description of Tests and Normal Values. Clin. Sci.Mol. Med. 52:283-290.
3. Kramer, J.F. (1987) Effect of Electrical Stimulation Current Frequencies on Isometric Knee extension Torque. Phys. Ther. 67:31-38.
4. Liberson, W.T. and Asa, M.M. (1959) Further Studies of Brief Isometric Exercises. Arch. Phys. Med. 40:330-336.
5. Moritani, T. Nagata, A. and Muro, M. (1982) Electromyographic Manifestations of Muscular Fatigue. Med. Sci. Sports Exer. 14:198-202.
6. Muller, E.A. (1970). Influence of Training and of Inactivity on Muscle Strength. Arch. Phys. Med. Rehabil. 51;449-462.
7. Stillwell, D.M., McLarren, C.L., and Gersten, G.W. (1966). Atrophy of Quadriceps Muscle Due to Immobilization of the Lower Extremity. Arch. Phys. Med. Rehabil. 32:142-145.

EVALUATION OF AUTONOMIC REFLEXES BY ISOMETRIC HANDGRIP EXERCISE AND VALSALVA MANEUVER

D. Katz[1], D. Propert[1], P. Williams[2] and C. Philput[2]
[1]*Department of Internal Medicine, Eastern Virginia Medical School and* [2]*Department of Parmacology, Eastern Virginia Medical School, Norfolk, Virginia 23501*

DESCRIPTION OF RESEARCH, SIGNIFICANCE

It is well known from many of the NASA space missions that prolonged exposure to microgravity precipitates significant changes in blood volume, blood distribution, and blood pressure. These changes contribute to the development of Space Adaptation Syndrome (SAS), a condition which produces orthostatic intolerance upon return to earth and may impair the ability to work at optimal levels during spaceflight.

During spaceflight, blood volume is shifted from the lower extremities to central (thoracic) portions of the circulation, indicating possible changes in relative vascular resistance between these areas under microgravitational conditions. Vascular resistance is known to be mediated by the sympathetic nervous system under peripheral, central, and humoral control. Weightlessness may cause alterations in sympathetic nervous system activity with respect to cardiovascular (CV) function, thereby contributing to the development of SAS. While these changes in CV function have been observed, the physiological basis underlying their production remains uncertain.

The goal of this study was to develop a simple, reproducible, noninvasive technique that could be used to evaluate the effects of autonomic reflexes on CV functions in space. To this end, isometric handgrip exercises (IHE) and the Valsalva maneuver were chosen as methods of initiating the sympathetic reflexes.

The specific aims of the study were to:

(1) Determine the optimum pressure for the Valsalva maneuver to maximize Phase II blood pressure response.

(2) Determine the optimum duration of the Valsalva and the points at which to record maximum blood pressure changes.

(3) Determine optimum percent of maximum voluntary contraction (MVC) and duration of handgrip.

(4) Determine time for measurements to return to baseline after each intervention which influences the interval required between performing the Valsalva and the handgrip maneuvers.

(5) Investigate whether there are differences in the response depending on the order in which the maneuvers were performed.

(6) Estimate the magnitude of both intra- and intersubject variation.

(7) Determine the influence of body position on CV response to induced autonomic reflexes.

METHODS

Blood pressure and heart rate were recorded during control and rest periods and during the Valsalva and sustained IHE. Blood pressure and heart rate were measured by an automated-cuff blood pressure monitoring system. The length of time from the inflation of the cuff to deflation signifying the conclusion of the measurement was approximately 40 sec. Pulse pressure was derived from the systolic and diastolic blood pressure readings.

A handgrip dynamometer was used for the IHE. The MVC for each subject was determined by the subject's maximally squeezing the dynamometer with one hand. Ten percent, 15%, and 20% of the MVC were tested to determine the appropriate percent of MVC that would give maximal increases in blood pressure. Sustained period of IHE of 1.0, 2.0, and 2.5 minutes were also examined for maximal effect.

A manometer for the Valsalva maneuver was constructed in our laboratories of a glass U-tube (2 mm diameter) containing mercury. One end of the tube was attached to a rubber disposable mouthpiece; the other end of the tube to insulated copper wires immersed in the mercury and connected to a DC power source. When the subject, exhaling through the mouthpiece, reached the appropriate pressure for the Valsalva, a white light would illuminate. A red lamp would light when the required pressure was exceeded. The red light was a sign for the subject to reduce the pressure of exhalation so that only the

white light remained lit. Valsalva pressures of 10, 20, and 30 mm of Hg held for approximately 35-40 seconds (time required for complete BP/HR measurement) were tested to determine peak phase II response.

RESULTS

Based on the responses of 2 normal, male volunteers, the following parameters were chosen for further study:

(1) 20 mm of Hg sustained for approximately 40 seconds provided optimal Valsalva response. The BP and HR measurements were taken approximately midway through the maneuver.

(2) 20% MVC sustained for 2.5 minutes produced optimal IHE response.

(3) These measurements returned to normal approximately 5 minutes after completion of the intervention.

Table 1: Effect of Intervention on Cardiovascular Response

	Systolic	Diastolic	HR	Pulse Pressure	
Baseline	0	0	0	0	"0" = No significant difference
20% MVC IHE for 1.0 min	+	+	0	0	"+" = Significant increase $p < 0.05$
20% MVC IHE for 2.5 min	++	++	0	0	"-" = Significant Decrease $p < 0.05$
Rest	I	0	0	0	0
20 mm Valsalva	0	+++	+++	---	

Based on responses of six normal male volunteers, it was determined that:

(4) Systolic values in IHE, diastolic values in IHE and Valsalva, HR values in Valsalva, and PP values in Valsalva were significantly different from baseline and rest readings ($p<0.05$ by ANOVA and Duncan Multiple Range Test).

(5) The order of intervention did not significantly affect the CV response to the intervention.

(6) Differences observed inter-/intrasubject were not of significant magnitude to mask physiological changes.

(7) The initial test of positional effects using one subject with seven repetitions showed no significant difference in response to intervention during positional changes.

CONCLUSIONS

The results indicate that a noninvasive method for measuring BP and HR is feasible to evaluate cardiovascular responses to stress produced by Valsalva and Isometric Handgrip Exercises. This method may be useful in following autonomic reflexes in microgravity as well as responses to interventions to prevent SAS. (Supported in part by an EVMS Student Research Fellowship.) ■

OCULAR TORSION IN RESPONSE TO CHANGING FORCE MAGNITUDES ACTING ALONG THE Z-AXIS OF THE HEAD

N. M. Kirienko, K. E. Money, D. G. D. Watt, W. H. Johnson, C. H. Markham, S. G. Diamond
St. Michael's Hospital, Toronto, Canada, National Research Council, Ottawa, Canada, Defence and Civil Institute of Environmental Medicine Toronto, Canada, Aerospace Medical Research Unit, McGill University, Montreal, Canada, and UCLA School of Medicine, Los Angeles, California

OBJECTIVE

To determine whether the eye's normal torsional position in 1-G is altered during parabolic flight in NASA's KC-135 aircraft when the transient forces are applied along the z-axis of the head of a subject seated normally upright in the aircraft.

HYPOTHESIS

If, in response to the force changes of parabolic flight, the eyes of experimental subjects undergo a torsional displacement in a systematic fashion, it could be hypothesized that: (1) the same peripheral and central vestibular mechanisms which produce this torsional displacement in experimental subjects could be involved in the appearance of, and in the resolution of, Space Motion Sickness in Shuttle crewmembers; or, (2) the torsional displacement which could occur in Shuttle crewmembers on entry into orbit may contribute to a visual provocation of Space Motion Sickness; or, (3) some crewmembers may experience a combined effect of (1) and (2).

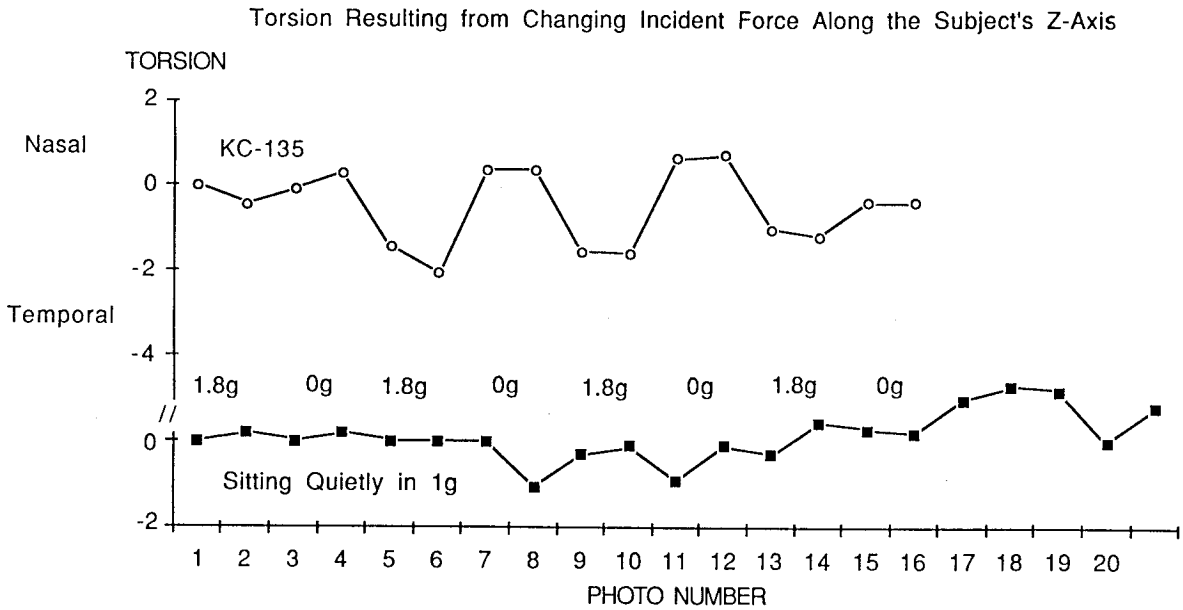

Figure 1. Results for one subject tested in a preliminary experiment completed in November 1985.

METHOD

The data was collected in February 1987. One eye of each of 6 subjects was photographed using a head-mounted camera system. This system included a head strap, dental bite and chest support. Penlights provided constant illumination of the eye. The subject was seated upright aboard the KC-135 aircraft while it flew continuous parabolas producing approx. 25 sec. of hypogravity (near zero G) and hypergravity (varying between 1.4 and 2 G). Baseline (1-G) data was collected during the straight and level portion of flight. Test data was collected near the end of each period of hypogravity and hypergravity. The subject's head was maintained in a level position during the hypergravity periods by referring to a carpenter's level. Data was gathered from a minimum of 5 parabolas for each subject on each of 2 flights. Information collected on slide film was processed using the superimposition technique developed at UCLA.

RESULTS

Torsional eye displacements did occur in response to the changes of G forces along the z-axis. Three of the 6 subjects responded with mostly small and inconsistent torsional displacements; the other 3 subjects responded with consistent displacements, and in 2 of these, the displacements were systematically in one direction with hypogravity and in the opposite direction with hypergravity. ■

RELATIONSHIPS BETWEEN THE ONSET OF GASTRIC DYSRHYTHMIAS AND MOTION SICKNESS IN MAN

K. L. Koch, R. M. Stern, A. Dwyer, and M. Vasey
Departments of Medicine and Psychology, Pennsylvania State University, Hershey and University Park, Pennsylvania 17033

Symptoms of motion sickness include various degrees of epigastric distress and nausea. The relationship between symptoms of motion sickness and gastric responses evoked by motion stimuli has been neglected since the 1940's. The present investigators have recently reported that healthy subjects who experience symptoms of motion sickness during illusory self-motion develop abnormal gastric myoelectric activity; that is, during motion sickness symptoms the normal 3-cycle-per-minute (cpm) gastric "pacemaker" rhythm shifted to abnormally fast frequencies (4-9 cpm) termed tachygastrias (Aviat Space Environ Med 1985; 56:1074-7; Gastroenterology 1987;92: 92-7). Tachygastrias had been considered abnormal gastric myoelectric events and were described previously only in patients with chronic and unexplained nausea and vomiting.

The aim of the current study was: (1) to determine the specific motion sickness symptoms reported during the illusory self-motion (vection) and (2) to determine the temporal relationships between the onset of reported motion sickness symptoms and the onset of gastric dysrhythmias such as tachygastrias.

Electrogastrography was the method used to record gastric myoelectric activity. Four Ag-AgCl electrodes were positioned on the abdomen over the region of the stomach to record gastric myoelecyric activity or electrogastrograms (EGGs). The cutaneous electrodes were connected to a rectilinear recorder through direct nystagmus couplers. High and low pass filters were set at 0.016 Hz and 0.3 Hz to obtain the range of relevant gastric frequencies and to reduce cardiac and respiratory interference. Respiratory rate was measured with a belt pneumograph. Vection was induced by rotating a drum around the stationary and seated subject. The inner surface of the drum was painted with alternating black and white vertical stripes. The drum was rotated at a rate of 10 revolutions per minute. The protocol included a 15-minute baseline period with the subject seated in the drum, a 15-minute period of drum rotation, and a 15-30-minute recovery period after drum rotation. Approximately every 2 minutes during drum rotation, the subjects described any symptoms if present. The EGGs were recorded continuously during the protocol on chart paper and on magnetic tape for subsequent computer analysis of EGG frequency changes during the protocol. Thirty-three healthy subjects were studied. The results are presented below.

Of the 33 healthy subjects studied, 22 developed nausea during vection and were considered to have motion sickness (MS); 11 did not have nausea and were considered to have no MS. Tachygastrias (tachy) were observed in 19 of the 22 subjects with nausea. Other symptoms reported during vection were sweating (Sweat), dizziness (Diz), and headache (HA). THe number of subjects with these symptoms is shown in the table.

In addition to nausea, sweating occurred significantly more frequently in the subjects with motion sickness. As shown above, the typical symptom chronology during vection was dizziness, sweating, headache and nausea, as measured by the time from onset of vection to onset of symptom, *i.e.*, mean latencies.

TABLE 1

	Tachy	Diz	Sweat	HA	Naus
MS (n=22)	19*	9	15	6	22*
No MS (n=11)	1	2	3	1	0
Mean latency from vection (min)	2.4	3.9	5.1	5.7	6.2

*P<0.01, MS vs No MS

Incidence of tachygastria in subjects reporting nausea (19 of 22) was significantly greater than in subjects with no nausea during vection (1 of 11). Tachygastria preceded the subject's report of nausea in 15 of 19 subjects, preceded sweating in 12 of 15, dizziness in 6 of 9 and headache in 4 of 6 subjects. Mean latency from vection to tachygastria was 2.4 minutes, whereas mean latencies from vection to reported symptoms were 3.9 minutes or longer.

In summary: The central nervous system visual stimuli producing vection, and the accompanying visual-vestibular sensory mismatch, evoked nausea in 22 of 33 healthy subjects, and 19 of the 22 subjects developed gastric responses, *i.e.*, tachygastrias. Gastric dysrhythmias frequently preceded symptoms such as dizziness, sweating, headache and nausea. Ten of 11 subjects without nausea did not develop tachygastrias.

In conclusion: Vection-induced gastric dysrhythmias are objective physiologic antecedents of impending motion sickness symptoms, particularly sweating and nausea. This work was supported in part by NASA grant NAG 9-118. ■

DOXEPIN, DEXAMETHASONE, AND SCOPOLAMINE PLUS AMPHETAMINE FACILITATE ADAPTATION TO CHRONIC STRESSFUL MOTION

R. L. Kohl
Division of Space Biomedicine, Universities Space Research Association, 2525 Bay Area Blvd., Suite 530, Houston, Texas 77058

INTRODUCTION

Daily exposure to stressful angular acceleration may model adaptive processes occurring during orbital flight. The present data indicate that certain antimotion sickness drugs facilitate the adaptive process.

METHODS

Male subjects received scopolamine plus amphetamine (n=10), doxepin (n=4), dexamethasone (n=8), or thyrotrophic releasing hormone (TRH, n=4) in a placebo-balanced, crossover study design. Drug or placebo was administered prior to each of five consecutive daily Staircase Profile Tests (Homick *et al.*, 1983). Some of the drugs were also loaded over several days prior to the test sequence. A three-day preloading period was employed for placebo, dexamethasone (3 mg) and TRH (0.5 mg); a 21-day preloading period was used for doxepin (70 mg). Scopolamine (0.4 mg) plus amphetamine (5 mg) was administered 1.5 hours prior to each test only (Mon-Fri). Individuals undergoing a week of experimental tests after either placebo or drug returned three months later to receive the opposite treatment and the final week of tests to complete the crossover design. The Nausea II level of sickness was the endpoint used. Total number of head movements were converted to Coriolis Sickness Susceptibility Index (CSSI) for comparison (Kohl, 1987).

RESULTS

Dexamethasone, scopolamine plus amphetamine, and doxepin promoted a more rapid adaptation than placebo. When individual groups were matched according to adaptability, such that performance after placebo showed a 3-fold increase in CSSI from Monday through Friday, we found an 8- and 14-fold rise in resistance after scopolamine plus amphetamine (n=4), and doxepin (n=4), respectively. These are the first data to indicate the acute and chronic efficacy of doxepin following 21-day loading. The other agents tested have already been shown to possess antimotion sickness properties.

CONCLUSIONS

Doxepin, dexamethasone, and scopolamine plus amphetamine can facilitate adaptation to stressful angular acceleration and may therefore shorten the 3-4 day period of impairment observed during spaceflight. ■

REFERENCES

Homick, JL, RL Kohl, MF Reschke, J Degioanni, NM Cintron-Trevino. Transdermal scopolamine in the prevention of motion sickness: Evaluation of the time course of efficacy. Aviat. Space Environ. Med. 54:994-1000, 1983.

Kohl, RL. Failure of metoclopramide to control emesis or nausea due to stressful angular or linear acceleration. Aviat. Space Environ. Med. 58:125-31, 1987.

THE SEA SNAIL *HERMISSENDA CRASSICORNIS*: A MODEL SYSTEM TO STUDY THE CELLULAR NEUROPHYSIOLOGY OF LEARNED ADAPTATIONS TO GRAVICEPTIVE INPUT

I. I. Lederhendler, B. Bank, J. LoTurco, and D. L. Alkon

Section on Neural Systems, NINCDS, IRP, NIH, Bethesda, Maryland at the Marine Biological Laboratory, Woods Hole, Massachusetts 02543

Classical Pavlovian conditioning has been demonstrated for responses of *Hermissenda* to pairings of light and rotation. Individuals learn that light, the conditioned stimulus (CS), predicts the onset of rotation, the unconditioned stimulus (US). These important predictive features of conditioning in *Hermissenda* are therefore held in common with vertebrates at the level of behavioral psychology. Recent studies, however, have also demonstrated certain impressive similarities between *Hermissenda* and rabbit conditioning at the level of cellular neurophysiology.

Hermissenda has proved a good model for the study of learning and memory in higher vertebrates. Many of the essential and defining features of vertebrate learning behavior have been demonstrated: stimulus and pairing specificity, extinction, savings, retention, contingency sensitivity, and optimal interstimulus interval. In addition, the cellular mechanisms which are readily studied in its relatively simple nervous system, and which have been correlated and causally related to the learning, appear to be a foundation for studies of the neurophysiology and biophysics of learning and memory in the rabbit. Such results are cause for optimism that some of what we learn from *Hermissenda* will lead to additional insights about the cellular mechanisms that underlie modification of vestibular-ocular reflexes. Understanding of these mechanisms may contribute to cellular models of the adjustments of individuals to the environments of space and spaceflight.

Classical conditioning of *Hermissenda* consists of a modification of responses to a light stimulus as a result of repeated pairings of light and rotation stimuli. Randomly associated presentations of the same light and rotation stimuli do not significantly change the response to light. Normally, within seconds of presenting a light of moderate intensity we can measure a lengthening of the foot muscle (the single organ of locomotion). On the other hand, within seconds of the onset of a rotational stimulus, the animal contracts this muscle and reduces the length of the foot. Following repeated pairings of light and rotation, the animals are tested again for their response to the light stimulus. This time, however, a new

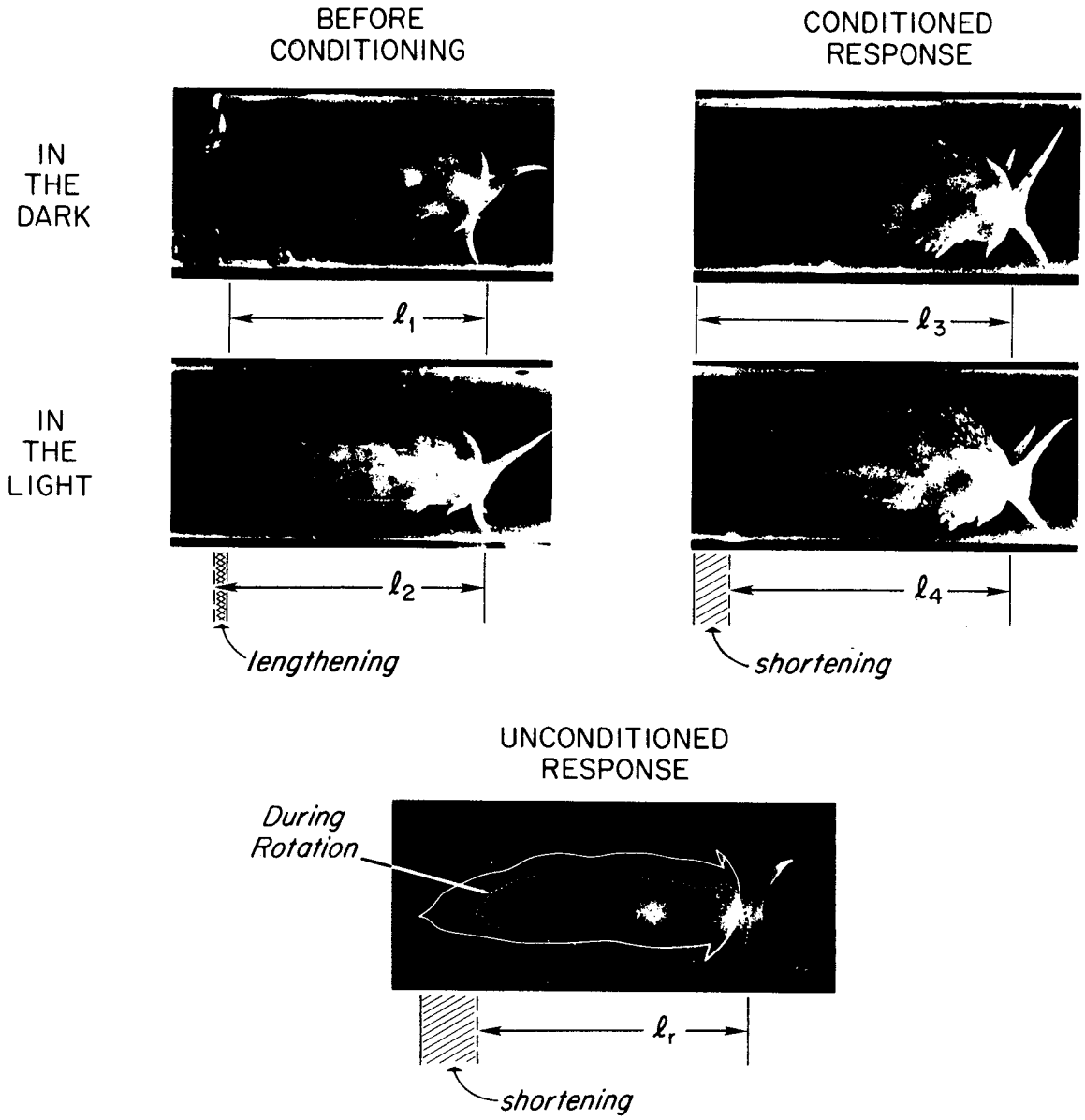

Figure 1. Photographic representation of classically conditioned responses of *Hermissenda* foot. *Bottom panel,* An overlay of two photographs taken in the dark; *solid white line,* the outline of the foot 1 sec before rotation; *dashed line,* outline of the foot after 3 sec of rotation at 97 rpm. *Upper panels,* Comparisons of lengths in the light to lengths in the dark before and after conditioning with paired light and rotation stimuli. ℓ_1, Length in the dark before training. ℓ_2, Length in the light before training ($\ell_2 > \ell_1$ = lengthening). ℓ_3, Length in the dark during retention of learned behavior. ℓ_4, Length in the light during retention ($\ell_3 > \ell_4$ = shortening). ℓ_r, Length during rotation was always smaller than before rotation began.

response is observed. That is, the foot becomes shorter rather than longer in response to light. Light has taken on some of the features of rotation.

The nictitating membrane response (NMR) in the rabbit eye has served as an exemplary instance of classical conditioning. In this case, a behaviorally neutral conditioned stimulus (CS), say light or tone, is repeatedly paired with an unconditioned stimulus (US), say air puff or shock, which reliably elicits a response. After sufficient CS-US pairings, the CS alone will evoke a conditioned response (CR) which resembles the response to the US. One of the hallmarks of rabbit NMR conditioning is the temporal specificity which characterizes the functional relationship between the CS and US. In general, the association is learned best when the CS and US are separated by an interval of 200-400 msec.

Recently we have shown that conditioning in *Hermissenda* shows a similar ISI function with an optimal CS-US interval at 1.0 sec. *Hermissenda* not only shows Pavlovian conditioning, but the temporal

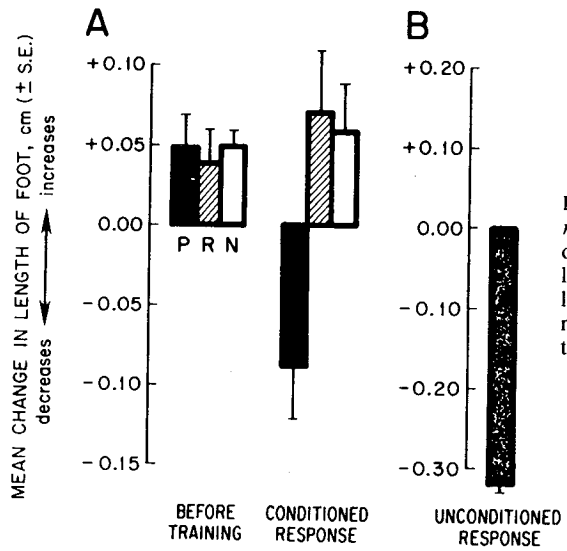

Figure 2. Classical conditioning of a new response to light in *Hermissenda*. *A*, Before training, foot length increased in response to light onset. Random (▨) and Naive (□) groups continue to show light-elicited lengthening, but Paired (■) animals became conditioned to shorten the length of the foot in response to a light stimulus. *B*, Unconditioned response after 6 sec of rotation. The CR is about 28% of the UCR. Note the difference in scale between *A* and *B*.

specificity of the conditioning is exquisitely tuned. In the case of *Hermissenda*, we have been able to make considerable progress in uncovering the cellular mechanisms that may cause learning and persistence of the memory. This can be attributed to success with (1) cellular identification of the neuronal circuitry mediating visual and graviceptive stimulation, and (2) localization of specific cellular sites where the visual and graviceptive stimuli converge.

This level of specific localization has been more difficult to achieve in the rabbit. However, in one brain region which is significantly involved in the learning—the hippocampus—it has been possible to demonstrate persistent intracellular changes which are correlates of the conditioning. The most exciting aspect of these recent findings is the degree of similarity (at the cellular level) between the rabbit and *Hermissenda* in the mechanisms used for storing the learned information.

Figure 3.

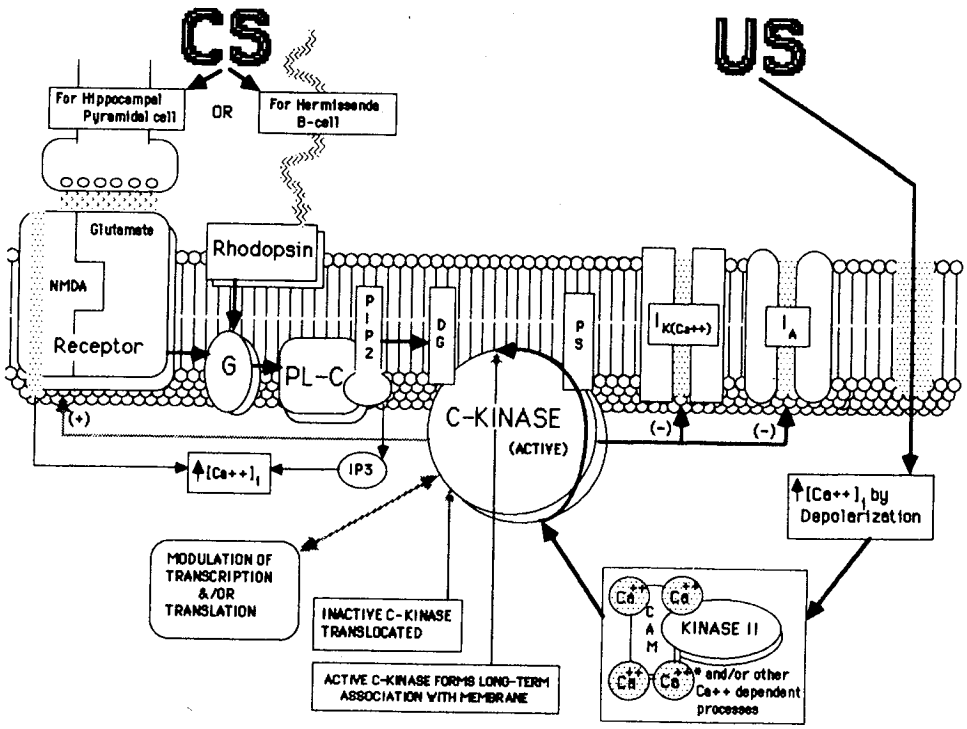

In both species, a biophysical record of classical conditioning involves a persistent reduction of calcium-dependent potassium currents $I_{K(Ca^{++})}$ at least 24 hours after training. In *Hermissenda* this change has been measured in the medial type-B photoreceptor, a cellular site of CS(light) and US (rotation) convergence. In rabbits, this change was measured in hippocampal CAI cells. In both species, these changes in conductance give rise to conditioning-specific changes in synaptic excitability. At a more molecular level these changes seem to depend on the formation, during conditioning, of stable associations of protein Kinase C with the plasma membrane of the critical cells.

These common biophysical and biochemical steps in the photo-receptors of *Hermissenda* and hippocampal CAI cells of rabbits leads to the interesting proposal that critical cellular convergence points in the CS-US pathways will acquire persistent biophysical representations of classical conditioning where a calcium-mediated process (US-dependent) works synergistically with activators of Kinase C (CS-dependent) to promote stable associations of Kinase C with the plasma membrane. These changes, we expect, will lead to alterations of the excitable and signalling properties of the critical neuron or groups of neurons.

This hypothesis has important implications for the learned modification of behaviors that depend on the interactions of two or more sensory inputs. We are particularly hopeful, for example, that *Hermissenda* may prove a useful model for studies of the cellular mechanisms that subserve modifications of vestibular-ocular reflexes in rabbits. ■

MECHANISMS OF RESPIRATORY MUSCLE CONTROL DURING MOTION-INDUCED VOMITING

A. D. Miller
The Rockefeller University, 1230 York Avenue,New York, New York 10021

Space motion sickness affects about one-half of astronauts and cosmonauts, yet knowledge of its basic mechanisms and development of effective treatments remain limited. During the last five years, our conception of the role of various central nervous system structures in the production of motion-induced vomiting has undergone major revisions and thus necessitated new approaches to understanding the underlying neural mechanisms.

In contrast to earlier models (9), we demonstrated that the nodulus and uvula of the vestibulo-cerebellum are not essential for vestibular-induced vomiting (8). Other investigators have shown that lesions of the area postrema (the chemoceptive emetic trigger zone) do not prevent vomiting during motion sickness (1,10). Moreover, we have been unable to confirm the existence of an anatomically discretely localized "vomiting center" (7).

In view of the above findings, we have undertaken a new approach of studying how the muscles that produce vomiting are controlled, with the aim of determining how this control system is engaged during motion sickness. The pressure changes responsible for vomiting are generated by the coordinated action of the major respiratory muscles (3). We sought to determine whether the same brain stem premotor neurons that are responsible for activating these muscles during respiration are also responsible for their control during vomiting. We have recorded from spinal-projecting brain stem respiratory neurons during "fictive vomiting" in decerebrate, paralyzed cats, that is, during a characteristic pattern of coactivation of phrenic and abdominal muscle nerves that would be expected to produce vomiting in unparalyzed animals (6). We first studied expiratory neurons, located in the ventral respiratory group between the obex and C1, which are known to be of primary importance for expiratory modulation of abdominal muscle activity (4,5). About two-thirds (17/27) of these neurons had the appropriate firing pattern to contribute to internal intercostal muscle activity during vomiting while another one-third (9/27) could contribute to abdominal muscle control. However, since abdominal muscle EMG activity during vomiting can be largely unaffected by sectioning the axons of these neurons, other as yet unidentified inputs can also be important for abdominal muscle control during vomiting (6).

We have recently begun to record from inspiratory neurons in both the dorsal (N=9) and ventral (N=7) respiratory groups (2). In contrast to expiratory muscle control, most (15/16) of these inspiratory neurons do not have the appropriate response pattern to initiate phrenic discharge during vomiting since the neurons are either silent when the phrenic nerve is active during fictive vomiting, or else fire only at the end of phrenic discharge. Therefore, it would appear from these data that other descending inputs must be important for the control of the diaphragm during vomiting.

The continued elucidation of the underlying neural mechanisms that produce vomiting may provide new insights into ways of preventing or treating motion sickness in space. For example, better knowledge of the pathways involved and of their neurotransmitters may lead to more effective drug treatments.

Parts of study were supported by grants from NASA (NAG2164, NSG2380), NIH (NS20585), and NSF (BNS8317651). ■

REFERENCES

1. Borison HL, Borison, R. Motion sickness reflex arc bypasses the area postrema in cats. Exp. Neurol. 92: 723-737, 1986.
2. Feldman JL. Neurophysiology of breathing in mammals. In: Handbook of Physiology, The Nervous System IV, Intrinsic Regulatory Systems of the Brain, Bloom FE (ed), 1986, pp 463-524.
3. McCarthy LE, Borison HL. Respiratory mechanics of vomiting in decerebrate cats. Am. J. Physiol. 226: 738-743, 1974.
4. Merrill EG. Finding a respiratory function for the medullary respiratory neurons. In: Essays on th Nervous System, Bellairs R, Gray EG (eds). Oxford, Clarendon, 1974, pp 451-486.
5. Miller AD, Ezure K, Suzuki I. Control of abdominal muscles by brain stem respiratory neurons in the cat. J. Neurophysiol. 54: 155-167, 1985.
6. Miller AD, Tan LK, Suzuki I. Control of abdominal and expiratory intercostal muscle activity during vomiting: role of ventral respiratory group expiratory neurons. J. Neurophysiol., in press.
7. Miller AD, Wilson VJ. "Vomiting center" reanalyzed: an electrical stimulation study. Brain Res. 270: 154-158, 1983.
8. Miller AD, Wilson VJ. Vestibular-induced vomiting after vestibulo-cerebellar lesions. Brain Behav. Evol. 23: 26-31, 1983.
9. Wang, SC, Chinn HI. Experimental motion sickness in dogs. Importance of labyrinth and vestibular cerebellum. Am. J. Physiol. 185: 617-623, 1956.
10. Wilpizeski, CR, Lowry LD, Goldman WS. Motion-induced sickness following bilateral ablation of area postrema in squirrel monkeys. Laryngoscope 96: 1221-1225, 1986.

ACUTE CHANGES IN LUNG FUNCTION CAUSED BY HEAD-OUT WATER IMMERSION

G. K. Prisk, H. J. B. Guy and J. B. West
Department of Medicine, M-023A, University of California, San Diego, La Jolla, California 92093

Head out immersion in thermoneutral (35 degrees C) water has been used to simulate some of the effects of microgravity on man. It is known to increase pulmonary capillary blood volume (Vc), and is therefore a tool for testing Vc measurement techniques that will be used in microgravity.

The calculation of pulmonary capillary blood volume is made from measurements of diffusing capacity for carbon monoxide, under normoxic and hyperoxic conditions. The standard single breath measurement for diffusing capacity involves a breathhold at total lung capacity, often against a closed shutter. If, during this breathhold, the subject does not actively inspire, mouth, and hence alveolar pressures, may be raised, and this may decrease the trans-vascular pressure gradients that determine Vc.

We investigated this potential problem, by measuring Vc in normal seated subjects, both dry, and immediately following immersion, at three different mouth pressures during the breathhold phase of the

measurement. In the control studies (dry) pulmonary capillary blood volume was unrelated to mouth pressure. In contrast however, during immersion, increased mouth pressure resulted in significant decreases in the measured pulmonary capillary blood volume despite other indications of large cephalad shifts in fluid (increased cardiac output, decreased vital capacity, decreased size of cardiogenic oscillations in O_2 and CO_2).

The results suggest that standardization of measurement techniques may be necessary if adequate interstudy comparisons of changes in pulmonary capillary blood volume are to be made.

We have also used immersion to investigate a non-invasive method of defining topographic gradients in ventilation/perfusion ratios (V_A/Q_c).

V_A/Q_c ratios determine the local P_{O_2}, P_{CO_2}, and respiratory exchange ratio (R) in the lung. In normal seated subjects, during vital capacity exhalations, there is a terminal rise in R. This is associated with preferential emptying from the top of the lung, which is underperfused with blood and thus has a high V_A/Q_c ratio. We have found that immersion causes this terminal rise in R to disappear, despite persistence of the characteristic pattern in the single breath nitrogen test, that shows that there is persisting terminal preferential emptying from the top of the lung. We therefore have evidence of a decrease in the normal gravitational V_A/Q_c gradients during immersion, almost certainly because of greater distension (less collapse) of apical pulmonary vessels.

Interestingly, we found striking gradients in expired R in the first deep breath after prolonged quiet breathing during immersion. This effect disappeared after the first deep breath.

Immersion causes a decrease in lung volumes, which favors the development of gas trapping, absorbtion, and atelectasis. We found that previous oxygen breathing increased the "first deep breath" effect dramatically. We suspect that it is caused by transient inhomogeniety of ventilation in the lung as atelectatic areas re-expand. It may be that microgravity is associated with a reduction in lung volumes, and an increased chance of atelectasis, especially during and after oxygen breathing to prepare for EVAs. The R gradient test may be useful in investigating this possibility. ■

DETECTION OF MOTION SICKNESS ONSET USING ABDOMINAL BIOPOTENTIALS

B. W. Rague and C. M. Oman
Man Vehicle Laboratory, Massachusetts Institute of Technology, Cambridge, Massachusetts

BACKGROUND

Electrogastrography is a method of recording stomach electrical activity from electrodes placed on the abdominal surface. The electrogastrogram (EGG) signal is small in amplitude (typically 100-500 uv), roughly sinusoidal, and has a dominant frequency component often referred to as the Basic Electrical Rhythm (BER), which predominantly reflects the myoelectrical activity of the stomach's smooth muscle (Smout, 1980). The BER is generated on the greater curvature of the stomach where a group of longitudinal smooth muscle fibers originates. The signal sweeps distally along the curvature to the pylorus, where gastric emptying occurs. The BER frequency has been measured at 0.05 hz (3 cpm) in man and is believed present even during quiescent periods when smooth muscle contractions are absent. When gastric smooth muscle contractions occur, they are phaselocked to the BER. Increases in BER frequency ("tachygastria") occur in gastric pathologies, (*e.g.* Geldof, et al, 1986). BER amplitude varies with subject, electrode position with respect to the gastric antrum, gastric contractile activity, extent of fasting, and other factors.

Subjects experiencing motion sickness symptoms are believed to exhibit decreased gastric contractions (Wolf, 1943; McDonough and Schneider, 1944), and anecdotally, absence of abdominal sounds. More recently, Stern *et al.* (1985; 1987) have presented evidence of a disappearance of the 3 cmp BER, and increased tachygastric activity in the 4-9 cpm frequency range, using running spectral analysis in 15 subjects (single trials). We attempted to confirm these findings and to establish the consistency of the EGG changes seen during motion sickness onset.

METHODS

To record EGG, disposable cutaneous electrodes (Hewlett-Packard 14445A) were applied to the abdomen. To enhance signal stability, the skin beneath the electrode was lightly scratched with the tip of a sterile hypodermic needle. A point half the distance along the vertical midline from the umbilicus to the xiphoid was located. From this location, the first electrode was placed 1 cm. caudad and 6 cm. to the subject's left, and the second electrode was placed 2 cm. cephalad and 5 cm. to the subject's right. Electrodes were connected to a computer data acquisition system through a DC amplifier (Denver Research Institute NASA/LSLE EOG preamp; 0-30 hz; input imped. 50 megohm). No high-pass filtering was required because the amplifier contained step autobalancing circuitry. Resets were compensated in software before signal analysis. Aliasing of the amplifier output was suppressed by filtering above 0.35 hz (8-pole Butterworth low pass). Respiration was monitored using a nostril thermistor. EGG and thermistor signals were sampled at 1 Hz using a computer (PC Limited AT) equipped with Metrabyte Dash 16 data acquisition board. Running power spectrum analysis software was written to process and display the EGG input. The spectra consisted of time windows of length 512 samples (512 seconds) with an overlap of 87.5% (448 secs.). A Hamming window was used to suppress leakage. Using this method, independent frequency samples exhibit a resolution of .0039 hz. Since the magnitude of the EGG signal varied between subjects and between runs, we defined a dimensionless index of the relative height of the most prominent spectral peaks: the magnitude of the highest peak (usually the BER) within the frequency range from 2.5 to 9.0 cpm was divided by the geometric mean of the three next highest peaks (which usually occurred at frequencies above the BER). Frequencies above 9 cmp were excluded to avoid any possible influence of respiration artifacts.

Six subjects (3M, 3F; ages 21-27) participated in a pilot session and four test sessions each. All subjects fasted at least 6 hours before the session. The time of day of the session was kept constant for each subject. The subjects were seated in a rotating chair, and baseline EEG spectra were monitored for at least 15 mins prior to chair rotation. One test session was repeated because the subject did not exhibit a prominent resting BER. To induce motion sickness, a modification of the Coriolis Velocity Staircase method (Kohl, 1987) was used: the subject was rotated about an earth vertical axis while executing head movements in pitch and roll. The subject made head movements in five specific directions (front, up, right, up, back, up, left, up, front, up) to a 1 hz candece for ten seconds. The subject was allowed 20 seconds to report symptoms, and then began the next set of head movements. Chair rotation typically began at 7 RPM and was incremented by 2 RPM after every 4 minutes (80 movements). Once a moderate sickness level was achieved, chair RPM was maintained constant. If symptoms thereafter moderated, the 2 RPM staircase was resumed. When the subject reached his symptom endpoint (see below), chair rotation was gradually stopped over a 180 sec period.

The pilot session was performed to familiarize the subject with his own range of symptoms, and to establish a "halfway to vomiting" subjective sickness endpoint for subsequent experiments using the overall discomfort magnitude estimation method of Bock and Oman (1982). The subject's symptoms were simultaneously scored according to the Pensacola Diagnostic method (Graybiel, et al, 1968).

RESULTS

The staircase stimulus successfully elicited moderate to severe symptoms in all sessions. (Two subjects experienced brief vomiting or retching in individual sessions). Prior to chair rotation, the EGG spectrum peak index was typically 15, but in all sessions dropped below 3 by the time the endpoint was reached (see Fig 1 example), reflecting a loss in amplitude of the 3 cpm BER component by an average of 80%. During this period, spectral amplitudes increased slightly in the range of frequencies from just above the BER through the respiration range, but quantitatively not to the extent recently described by Stern *et al.* (1987). Examination of our time domain EGG records showed very few distinct "tachygastric" events. Based on our data, it appeared that the dominant change during motion sickness onset is the reduction of the BER component, and tachygastrias in motion sickness onset is the reduction of the BER component, and tachygastrias in motion sickness are better described as low level broadband noise rather than a specific shift in the BER fundamental frequency. Our study differed from that of Stern, et al in numbers of subjects and repeat trials. Also, our recording system frequency response was less narrowly tuned to the putative tachygastric range, our spectra were not smoothed in the frequency domain, our electrodes were centered closer to the abdominal midline, and a somewhat

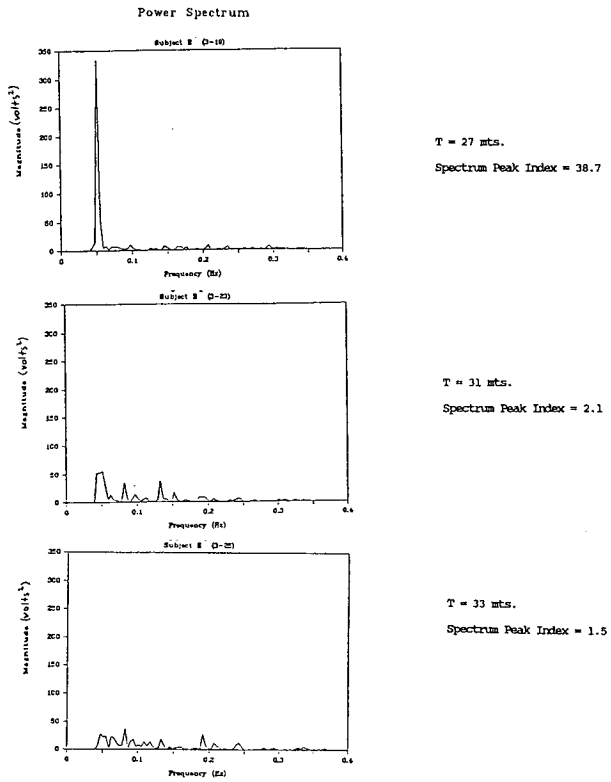

Figure 1. Change in EGG Power Spectrum during motion sickness.

more provocative Coriolis staircase stimulus was employed. We looked for but could not find consistent evidence of respiration or head movement related artifacts in our own records.

Supported by NASA Contract NAS9-17371. ■

REFERENCES

Bock, O and Oman, C (1982) Aviat Space Environ Med 53:773-77.
Geldof, H, et al. (1986) Gut 27:799-808.
Graybiel, A (1968) Aerosp Med 33:453-55.
Kohl, RL (1987) Aviat Space Environ Med 58:125-31.
McDonough, FE, Schneider, M (1944) Gastro 2:32-45.
Smout, AJPM, et al. (1980) Dig Dis Sci 25:179-87.
Stern, RM, et al. (1985) Aviat Space Environ Med 56:1074-77.
Stern, RM et al (1987) Gastro 92:92-97.
Wolf, S (1943) J Clin Invest 22:877-82.

SEGMENTAL NECROSIS OF MUSCLE FIBERS IN THE SOLEUS MUSCLES OF NORMAL, IMMUNIZED, AND SPACELAB-3 RATS

D. A. Riley[1], S. Ellis[2], G. R. Slocum[1], and F.R. Sedlak[1]
[1]*Department of Anatomy & Cellular Biology, Medical College of Wisconsin, Milwaukee, Wisconsin 53226* and [2]*Department of Chemistry, San Jose State University, San Jose, California 95192*

The vast majority of the soleus muscle fibers in the SPF rats orbited 7 days aboard Spacelab 3 (SL3) exhibited simple fiber atrophy, a 30% reduction in mean fiber area. Other fibers appeared necrotic; either the plasma membrane was violated and the cell was invaded by macrophages and eosinophils or the fiber had snapped and formed contraction clots (Riley *et. al.*, Muscle & Nerve, 1987, in press). If fiber necrosis is progressive and cumulative, long term exposure to microgravity could produce severe muscle deficits.

For the present study, necrotic fibers were examined in the existing SL3 light and electron microscopic material and in soleus muscles of SPF Sprague-Dawley rats (319 ± 11 g, n+10) used for experiment verification testing (EVT) of SLS-1 Animal Enclosure Modules. Segmental fiber necrosis, similar in appearance to that observed in SL3 flight rats, was detected in the EVT animals. The characteristics of these disrupted fibers were analyzed to gain insights into possible causes of muscle fiber necrosis during spaceflight.

Soleus muscles were harvested from nontreated control rats and rats injected intravenously by the SLS-1 Hematology investigators 1, 7, and 17 days before sacrifice with ^{125}I human serum albumin (HSA, 1 mg/rat/day, 1 uCi/mg HSA). The muscles were quick frozen in a liquid nitrogen-cooled freon slurry, and cross (10 um) and longitudinal (20 um) sections were cut with a cryostat microtome. Sections were stained with hematoxylin and eosin and examined for disrupted fibers showing segmental necrosis or contraction clots.

Using a light microscope, the occurrence of segmental lesions was determined, and the mean length of the lesions was measured in longitudinal sections with a calibrated ocular reticule. A single cross section through the midbelly of the muscle included all fibers (2,848 ± 77). Also counted were normal fibers, angular fibers with central nuclei, and regenerating fibers.

The muscles of the EVT animals did not have fibers with contraction clots. They did have fibers with segmental lesions invaded by macrophages, eosinophils and neutrophils. Calculations based on the rates of occurrence of lesions in 10 um sections, mean lesion length (683 ± 194 um), and total fiber length (around 1,875 um) indicated that, on average, the lesions occurred in 0.04% of the fibers in the control group and 0.20% of the HSA immunized animals. Similar calculations for the SL3 muscles revealed that in control muscles, 0.21% of the fibers had segmental necrotic lesions and 0.20% showed contraction clots whereas 0.23% of the flight fibers possessed segmental necrosis and 0.33% exhibited contraction clots. While the percentages of fibers affected are small, these values indicate that 10% of the SL3 control muscle was lesioned and 14% of the flight muscle was disrupted.

Ultrastructural examination showed that segmental necrotic areas represented weak portions of fibers across which only the basal lamina was continuous. During strong muscle contractions, these defects probably broke generating contraction clots. For the SL3 flight animals, the stresses of increased workload during reentry and the 12-16 hour postflight exposure to terrestrial gravity may have generated contraction clots in the soleus muscles. Snapped fibers in the ground control muscles may have resulted from animals kicking during handling or during the 15 to 30 minute post mortum period when the excised muscles were being manipulated during weighing and freezing.

In the EVT and SL3 material, around 90% of the fibers with segmental necrosis were at the periphery of fascicles and abutted the perimysium. They occurred equally throughout the muscles showing no superficial or deep preferential disposition. The HSA injected animals exhibited many regenerating muscle fibers which were also most common at the periphery of fascicles. The myotube stage of regeneration observed in these muscles indicated that injury had occurred around 7 days earlier (Riley, Exp Neurol 41:690, 1973). This coincided with the time of the second HSA injection which was expected to generate a significant antibody response. HSA probably leaked into the perimysium of the muscles

and bound to IgE antibodies on mast cell surface receptors causing mast cell degranulation which, in turn, precipitated eosinophil infiltration and secretion. This inflammatory process could have generated cytotoxic substances that focally damaged cell membranes leading to segmental disruption and subsequent repair. In support of this hypothesis was the finding that mast cells, most numerous in the periomysial connective tissue, were reduced in number by 67% within 70 um of disrupted fibers compared to normal. In this zone, eosinophil number was 22.5 times greater than around normal fibers. Furthermore, neutrophils, very rare in normal muscles, were common around disrupted fibers in the HSA injected animals. Neutrophil infiltration indicated attraction by antibody-antigen complexes; this was consistent with HSA injected 1 day before sacrifice. Neutrophils were not detected in SL3 muscles. If the SL3 rats had been exposed to immunogens inflight, the transient 24 hour influx of neutrophils would have been over by the postflight sacrifice.

The causes of fiber necrosis in SL3 flight rats remain unknown, but the present findings suggest a number of testable hypotheses. The macrophage infiltration and segmental necrosis of fibers in SL3 rats were similar to that in EVT rats reacting subclinically to HSA antigen. While neither the EVT nor the SL3 rats showed changes in white blood cell counts reflecting significant challenges to their immune systems, circulating neutrophils were significantly elevated in both cases (Lange *et.al.*, Physiologist 28:S195, 1985; Hematology EVT Report, 1987). Immune reactions resulting in muscle inflammation and disruption may have been generated during spaceflight. Stress may have encouraged endemic organisms to flourish and evoke a subclinical immune response. In addition, nonfiltered Spacelab air could have entered the RAHF during cage maintenance operations and infected the rats with human pathogenic organisms.

Other factors capable of producing discrete muscle lesions are vascular reperfusion injury and high energy radiation damage (Granger *et. al.*, Gastroent 81:22, 1981; Khan, J. Neuropath Esp Neurol 23:43, 1974). Reduced gravity and decreased muscle contractions during spaceflight may have lessened blood flow through the lower limbs. Periods of ischemia and anoxia followed by reperfusion may have generated free radicals that lysed the plasma membranes of muscle and nonmuscle cells. Radiation could also have produced free radicals that damaged membrane phospholipids.

Skeletal muscle fibers are long multinucleated cells that can survive membrane disruption of a magnitude that would kill most small mononucleated cells (Riley, Exp Neurol 41:690, 1973). Therefore, it was not surprising to find fibers with segmental lesions that were apparently cleared of cellular debris by macrophages and repaired by satellite cell regeneration. The absence of regenerating fibers in the flight muscles suggests that either injury happened late inflight and regeneration was minimal at sacrifice, or if the flight fibers were injured early, then regeneration was inhibited during the spaceflight.

When muscle weakness, induced by microgravity, results from simple fiber shrinkage, recovery depends on regrowth of the atrophic fibers. However, recovery of fibers partially or totally destroyed by lesions is less certain, subject to the success of regeneration. The present findings suggest that intramuscular inflammatory immune reactions, altered blood flow, and radiation damage may have contributed to the segmental necrosis of SL3 muscle fibers.

Supported by NASA grant NAS 2-11305. ■

CHANGES IN SKELETAL MUSCLE MASS AN UNAVOIDABLE CONCERN FOR FUTURE LONG-TERM SPACE FLIGHTS

O. Sampson
Department of Biology, USAF Academy, Colorado Springs, Colorado

DESCRIPTION

Skeletal muscle is the voluntary force-producing tissue within the body. Its ability to generate tension is governed by several factors: its mass in terms of functional cross-sectional area or "number of sarcomeres in parallel" (Wickiewicz *et al.*, 1983); pinnation angle, fiber type, and leverage characteristics. These factors vary between individuals (Powell *et al.*, 1984; Buskirk and Mendez, 1985). However, within individuals, pinnation angle and leverage are fixed and fiber type can change only to a limited extent, depending on the circumstances. By far, the muscle factor that is capable of the greatest intraindividual variability is mass.

MASS

Skeletal muscle represents approximately 40 to 50 percent of the average adult weight (Tortora, 1986). Following birth, the number of muscle cells, called myofibers, appears to be capped; *i.e.*, they do not increase. Although they can decrease in number, this usually takes considerable time and/or trauma. Consequently, transient changes in muscle mass generally reflect changes in the size of individual fibers. Muscles can decrease in size (atrophy) or increase in size (hypertrophy) in response to various factors. They have been shown to atrophy under conditions that include: disease (O'Doherty *et al.*, 1977; Bulcke *et al.*, 1979; Brenton *et al.*, 1981); immobilization (Jaffe *et al.*, 1978; Ingemann-Hansen and Halkjaer-Kristensen, 1980), paralysis (Whedon and Shorr, 1957a,b), reduced activity as in sedentary jobs (Wilmore and Davis, 1979), and aging (Frantzell and Ingelmark, 1951; Skerlj, 1959; Inokuchi *et al.*, 1975; Forbes, 1976; Rossman, 1977; Borkan *et al.*, 1983). Added to this list is the phenomenon known as weightlessness or zero-G (Morey-Holton and Wronski, 1981; Oganov *et al.*, 1982; Grigor'yeva and Kozlovskaya, 1983; Leonard *et al.*, 1983).

In contrast to the general observation that muscle mass varies between individuals is the finding that apparent muscle size and strength are not perfectly correlated. It has been found that increases in limb girth appear not to be a predominant consequence of exercise-induced strength gains. Wilmore (1974) obtained correlations between girth and strength ranging from 0.63 to 0.77 for men, and from 0.09 to 0.42 for women. He cites similar values obtained by other investigators (range = 0.06 to 0.69). In another study, the relationship between strength and muscle cross-sectional area as measured by computed tomagraphy (CT) was found to be only moderate, $r = 0.58$ (Maughan *et al.*, 1983). Furthermore, this relationship appeared not to be significantly different between trained and untrained subjects.

REGULATION

The actual mechanism responsible for muscle atrophy has not yet been discovered and, indeed, some of the data are contradictory (*e.g.*, compare Almon and DuBois, 1983, Riley and Ellis, 1983, with Almon and Ellis, 1985, and Max and Ellis, 1985). Nevertheless, it appears clear that inactivity somehow affects the endocrine system and alters the production of specific anabolic and catabolic hormones which, in turn, produce the atrophy (Edgerton, 1985; Ellis, 1985).

When atrophy from disuse first occurs, it involves the loss, not of muscle cells (myofibers), but of specialized structures within each fiber called myofilaments (Ellis *et al.*, 1985). In addition, the loss is not uniform, but occurs most in slow-twitch muscle fibers; *i.e.*, those responsible for chronic force production, as in overcoming the force of gravity or in prolonged physical activity (Chui *et al.*, 1981; Templeton and Sutko, 1982; Almon and DuBois, 1983; Dettbarn and Misulis, 1984). This leads to a change in the relative mass of slow- vs. fast-twitch fibers. Long-term increases in g-loading, as seen in centrifuge studies, produce the opposite effect; *i.e.*, a relative increase in the mass of slow-twitch fibers compared to fast-twitch fibers (Martin and Romond, 1975).

Recovery from atrophy takes a long time (Almon and Ellis, 1985). Exercise can hasten the recovery process (Ingemann-Hansen and Halkjaer-Kristensen, 1980; Wilmore *et al.*, 1980; Caiozzo *et al.*, 1981).

Passive movement may offer some benefit (Whedon *et al.*, 1949), although this is debated (Wyse and Pattee, 1954). Stretching retards atrophy and even adds sarcomeres at the ends of the muscle (Spector *et al.*, 1982; Goldspink and Ellis, 1985). And, electrical stimulation can counter the atrophic process (Van Der Meulen *et al.*, 1974).

IMPLICATIONS

These findings may lead to an improper conclusion: namely, that muscle mass is not the principal element in governing strength. Indeed, as reflected above, girth and even cross-sectional area measurements are not highly correlated with muscle strength. It must be remembered, however, that these measurements assume a uniformity of muscle tissue which, when examined closely, is difficult to substantiate; *e.g.*, they give no information about the packing density of myofilaments within individual fibers or the amount of extracellular substances or nonmuscle space present (Close, 1972). In light of this, it is obvious that the actual mass of muscle, particularly in these studies, really has not been measured very precisely after all. In other words, changes in girth could easily be independent of true muscle hypertrophy, especially when changes in the fat compartment are not accounted for. Indeed, this may explain why the correlations between girth and strength are so much less for women than for men. Moreover, when studies have been designed to examine this relationship more rigorously, as Wickiewicz and his colleagues have done using human cadavers (1983) and living subjects (1984) and as Powell *et al.* have done on guinea pigs (1984), a much closer correspondence between actual muscle mass and force-production is evident. In fact, Powell's group, comparing dissected and live guinea pig muscles, obtained a correlation of 0.99 between estimated and measured maximum tension values.

The implications arising from this review of muscle highlight the necessity for improved measuring techniques. More specifically, there is need to: specify the relationships between mass, strength, fiber number, and size; specify changes in fiber number and size during atrophy and hypertrophy and characterize the differences between the various causes; discriminate between fiber number, size, and nonfiber substances; identify the mechanism of atrophy and hypertrophy; compare fiber types during atrophy and hypertrophy; and devise and assess countermeasures to atrophy. ■

REFERENCES

Almon, R.R. and D. C. Dubois. Glucocorticoid Sensitivity, Disuse, and the Regulation of Muscle Mass. The Physiologist, 26(6):S92-93, 1983.

Almon, R.R. and S. Ellis. Immobilization/Re-immobilization and the Regulation of Muscle Mass. NASA Technical Memorandum 86692:75-77, 1985.

Borkan, G.A. and D.E. Hults. Change in Body Fat Content and Distribution During Aging. American Journal of Physical Anthropology, 60:175, 1983.

Brenton, D.P., R.H.T. Edwards, S.R. Grindod, P.S. Tofts. Computerized X-Ray Tomography to determine Human Skeletal Muscle Size and Composition in Health and Disease. Journal of Physiology, 317:3P, 1981.

Bulcke, J.A., J.-L. Termont, Y. Palmers, D. Crolla. Computed Tomograph of the Human Skeletal Muscular System. Neuroradiology, 17:127-136, 1979.

Buskirk, E.R. and J. Mendez. Sports science and Body Composition Analysis: Emphasis on Cell and Muscle Mass. Medicine and Science in Sports and Exercise, 16(6):584-593, 1984.

Caiozzo, V.J., J.J. Perrine, V.R. Edgerton. Training-Induced Alterations of the In Vivo Force-Velocity Relationship of Human Muscle. Journal of Applied Physiology, 51 (3):750-754, 1981.

Chui, L.A., K.R. Castleman, J.P. Van Der Meulen. Morphometric Analysis of Rat Muscle Fibers Following Space Flight. Advanced Physiological Science, 19:113-119, 1981.

Close: Physiological Reviews, 52(1):129-197, 1972.

Dettbarn, W.-D. and K.E. Misulis. Physiological Changes in Fast and Slow Muscle with Simulated Weightlessness. NASA Space Biology Program, Washington D.C., pp 35-36, 1984.

Edgerton, V.R. Methods for Long-Term Electromyographic Recordings from Suspended Animals. Workshop on Advances in NASA-Relevant, Minimally Invasive Instrumentation, JPL D-1942, pp. 2/3-2/10, 1985. (JPL internal document)

Ellis, S. Muscle Atrophy. Biomedical Research Division Significant Accomplishments for FY 1984, NASA Technical Memorandum86692, Ames, pp. 66067, 1985.

Ellis, S., D.A. Riley, J.L.W. Bain, J.G. Barnett. Proteolysis in Muscle Atrophy. Biomedical Research Division Significant Accomplishments for FY 1984, NASA Technical Memorandum 86692, Ames, pp. 68-69, 1985.

Forbes, G.B. The Adult Decline in Lean Body Mass. Human Biology, 48(1):161-173, 1976.

Frantzell, A. and B.E. Ingelmark. Occurrence and Distribution of Fat in Human Muscles at Various Age Levels. Acta Societatis Medicorum Upsaliensis, 56:59-87, 1951.

Goldspink, G. and S. Ellis. The Combined Influence of Stretch and Mobility on Muscle Atrophy Caused by Immobilization. Biomedical Research Division Significant Accomplishments for FY 1984, NASA Technical Memorandum 86692, Ames, p. 78, 1985.

Grigor'yeva, L.S. and I.B. Kozlovskaya. Effect of Seven Days Without Gravity Load on Velocity and Strength of Human Skeletal Muscles. Kosmicheskaya Biologiya I Aviakosmicheskaya Meditsina, 17(4):29-35, 1983.

Ingemann-Hansen, T. and J. Halkjaer-Kristensen. Computerized Tomographic Determination of Human Thigh Components. Scandinavian Journal of Rehabilitative Medicine, 12:27-31, 1980.

Inokuchi, S., H. Ishikawa, S. Iwamoto, T. Kimura. Age-Related Changes in the Histological Composition of the Rectus Abdominis Muscle of the Adult Human. Human Biology, 47(2):231-249, 1975.

Jaffe, D.M. R.D. Terry, A.J. Spiro. Disuse Atrophy of Skeletal Muscle. Journal of the Neurological Sciences, 35:189-200, 1978.

Leonard, J.I., C.S. Leach, P.C. Rambaut. Quantitation of Tissue Loss During Prolonged Space Flight. American Journal of Clinical Nutrition, 38:667-679, 1983.

Martin, W.D. and E.H. Romond. Effects of chronic rotation and Hypergravity on Muscle Fibers of Soleus and Plantaris Muscles of the Rat. Experimental Neurology, 49:758-771, 1975.

Maughan, R.J., J.W. Watson, J. Weir. Relationships between Muscle strength and Muscle Cross-Sectional Area in Male Sprinters and Endurance Runners. European Journal of Applied Physiology, 50:309-318, 1983.

Max, S. R. and S. Ellis. Gonadal Steroids and Muscle Atrophy. Biomedical Research Division Significant Accomplishments for FY 1984, NASA Technical Memorandum 86692, pp. 72-73, 1985.

Morey-Holton, E. and T. J. Wronski. Animal Models for Simulating Weightlessness. The Physiologist, 24(6):S/45-S/48, 1981.

O'Doherty, D.S., D. Schellinger, V. Raptopoulos. Computed Tomographic Patterns of Pseudohypertrophic Muscular Dystrophy: Preliminary Results. Journal of Computer Assisted Tomography, 1(4):482-486, 1977.

Oganov, V.S., S.A. Skuratova, L.M. Murashko, M.A. Shirvinskaya, T. Szilagyi, A. Szoor, M. Rapcsak, O. Takacs, S.S. Oganesyan, Z.S. Davtyan. Change in Composition and Properties of Contractile Proteins After Spaceflight. Biofizika, 27(1):41-46, 1982.

Powell, P.L., R.R. Roy, P. Kanim, M.A. Bello, V.R. Edgerton. Predictability of Skeletal Muscle Tension from Architectural Determinations in Guinea Pig Hindlimbs. Journal of Applied Physiology, 57(6):1715-1721, 1984.

Riley, D.A. and S. Ellis. Research on the Adaptation of Skeletal Muscle to Hypogravity: Past and Future Directions. Advanced Space Research, 3(9):191-197, 1983.

Rossman, I. Anatomic and Body Composition Changes with Aging. Handbook of the Biology of Aging, edited by C.F. Finch, Van Nostrand Reinhold Co., New York, pp. 189-221, 1977.

Skerlj, B. Age Changes in Fat Distribution in the Female Body. Acta Anatomica, 38:56-63, 1959.

Spector, S.A., C.P. Simard, M. Fournier, E. Sternlicht, V.R. Edgerton. Architectural Alterations of Rat Hind-Limb Skeletal Muscles Immobilized at Different Lengths. Experimental Neurology, 76:94-110, 1982.

Templeton, G.H. and J.L. Sutko. Influence of Suspension-Hypokinesis on Skeletal Muscle. 1982 NASA Space Biology Accomplishments, NASA Technical Memorandum 86244, pp 61-62, 1982.

Tortora, G.J. Principles of Human Anatomy Harper and Row, New York, 713 pp., 1986.

Van Der Meulen, J.P., P.H. Peckham, J.T. Mortimer. Use and Disuse of Muscle. Annals New York Academy of Sciences, 228:177-189, 1974.

Whedon, G.D., J.E. Deitrick, E. Shorr. Modification of the Effects of Immobilization upon Metabolic and Physiologic Functions of Normal Men by the Use of an Oscillating Bed. American Journal of Medicine, 6:684-711, 1949.

Whedon, G.D. and E. Shorr. Metabolic studies in Paralytic Acute Interior Poliomyelitis. II.Alterations in Calcium and Phosphorus Metabolism. Journal of Clinical Investigation, 36:966-981, 1957b.
Wickiewicz, T.L., R.R. Roy, P.L. Powell, V.R. Edgerton. Muscle Architecture of the Human Lower Limb. Clinical Orthopaedics and Related Research, 179:275-283, 1983.
Wilmore, J.H. and J.A. Davis. Validation of a Physical Abilities Field Test for the Selection of State Traffic Officers. Journal of Occupational Medicine, 21(1):33-40, 1979.
Wilmore, J.H., J.A. Davis, R.S. O'Brien, P.A. Vodak, G.R. Walder, E.A. Amsterdam. Physiological Alterations Consequent to 20-Week Conditioning Programs of Bicycling, Tennis, and Jogging. Medicine and Science in Sports and Exercise, 12(1):1-8, 1980.
Wyse, D.M. and C.J. Pattee. Effect of the Oscillating Bed and Tilt Table on Calcium, Phosphorus and Nitrogen Metabolism in Paraplegia. American Journal of Medicine, 17:645-661, 1954.

EFFECTS OF LOWER BODY NEGATIVE PRESSURE ON PLASMA ATRIOPEPTINS AND EVOKED ELECTROENCEPHALOGRAPHIC POTENTIALS

J. F. Schmedtje, Jr.[1], A. A. Taylor[1], J. Chelly[1], J. E. Skinner[1] and J. Gutkowska[2]
[1]Baylor College of Medicine, Houston, Texas 77030 and [2]Clinical Research Institute of Montreal, Montreal, Quebec, Canada H2W 1R7

INTRODUCTION

Lower body negative pressure (LBNP) increases plasma norepinephrine (NE) concentrations when applied at levels that model gravitational stress. LBNP unloads thoracic baroreceptors resulting in an increase in adrenergic tone peripherally (3). The changes in hemodynamic parameters that occur during LBNP are similar to those associated with intravascular volume loss, including decreased preload, increased heart rate, and decreased stroke volume (9).

It has been suggested that the atriopeptins represent one of the missing links in our understanding of the baroreceptor control of blood pressure. It is known that atrial stretch leads to degranulation of atriopeptin-secreting myocytes. Atriopeptins are also known to relax isolated strips of blood vessel, suggesting that they have a direct vasodilatory action *in vivo*. (4). It is possible that atriopeptins are tonically released by the heart to maintain preload at optimal levels. Neurons which are immunoreactive for atriopeptins are known to be present in the anteroventral periventricular nucleus of the rat hypothalamus (6). Atriopeptin injection into the third ventricle of the rat brain leads to decreased vasopressin release (5). Given the identification of atriopeptins near the vasoregulatory centers of the rat brain, it is reasonable to suggest that baroreceptor signals are sent via both circulating peptide and direct CNS afferent pathways, and that the integration of this dual feedback loop occurs in the hypothalamic regions.

The stretching of atrial myocytes which occurs during volume expansion is associated with the release of atriopeptins. We are proposing that the decrease in preload associated with LBNP causes a decrease in atrial myocyte stretch and therefore a tonic decrease in the release of atriopeptins.

Certain frontocortical-brainstem pathways are known to mediate the transfer of sensor information to higher cerebral centers via thalamic gating mechanisms. These thalamic centers are in close proximity to centers regulating autonomic tone. Electroencephalographic measurement of event-related slow potential (ERSP) production is thought to reflect the activity of these frontocortical-brainstem pathways associated with the regulation of autonomic tone (1,7,8).

The ERSP can be elicited by multiple types of stimuli, including auditory attention stimuli and exposure to novel situations. In animal studies, ERSP-producing stimuli have been shown to increase frontal lobe norepinephrine release.

We believe that if the frontocortical-brainstem pathway does mediate changes in autonomic tone we should be able to demonstrate a change in the amplitude of the ERSP when afferent signals from baroreceptor sites are modulated by LBNP.

METHODS

In this study four normal individuals were exposed to lower body negative pressure (LBNP) at -55 mmHg (to unload thoracic and carotid baroreceptors) and neck negative pressure (NNP) at -80 mmHg (to load carotid baroreceptors). Plasma samples were drawn from subjects in an initial control period, at the end of 5 minutes of LBNP at -55 mmHg and at the end of a subsequent 5 minute exposure to neck negative pressure (NNP) at -80 mmHg. NE was measured by HPLC-ECD and atriopeptin determinations (only performed in three of these subjects) were made by RIA.

The ERSP responses to a repetitive four-beep auditory stimulus were recorded during an initial control period and then during LBNP exposure and NNP exposure. Recordings were performed at the Cz and Pz sites (10-20 system) with simultaneous monitoring of the electrooculogram for oculomotor interference. The three environmental conditions were repeated and the average sizes of the ERSP voltage time integral (VTI) over repeated periods were used for comparison between environments.

RESULTS

The results are summarized in Figures 1-4. The effectiveness of LBNP was documented by an increase in NE in each of the subjects: 264 ± 48 pg/ml (mean ± SEM) control vs. 399 ± 22 pg/ml during LBNP. NE during NNP was 265 ± 59 pg/ml. Atriopeptin values decreased in each subject during LBNP. The control average was 28.9 ± 4.6 pg/ml, the LBNP average was 22.3 ± 4.5 pg/ml and the NNP average was 21.4 ± 3.1 pg/ml.

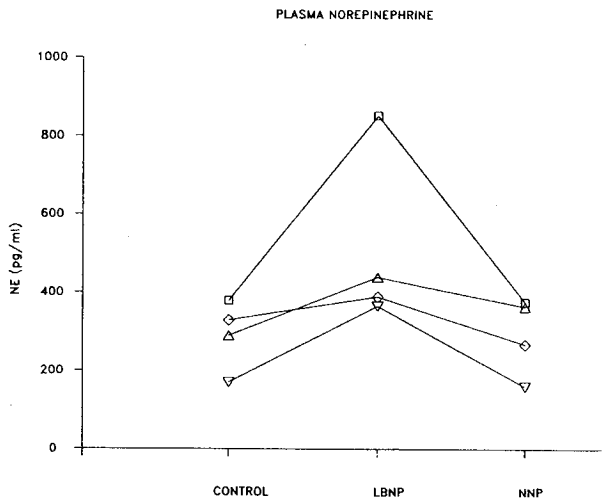

Figure 1.

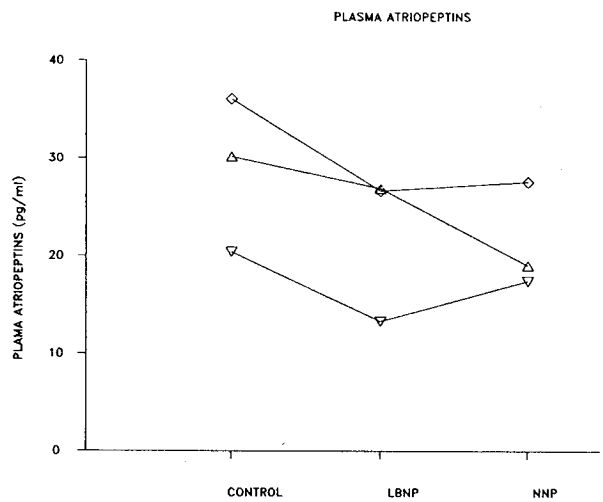

Figure 2.

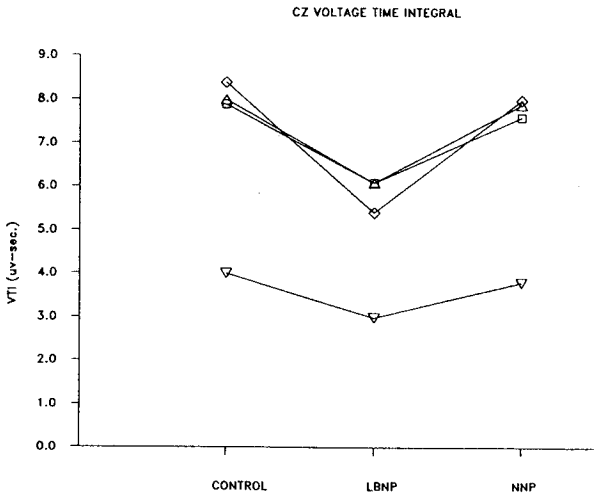

Figure 3.

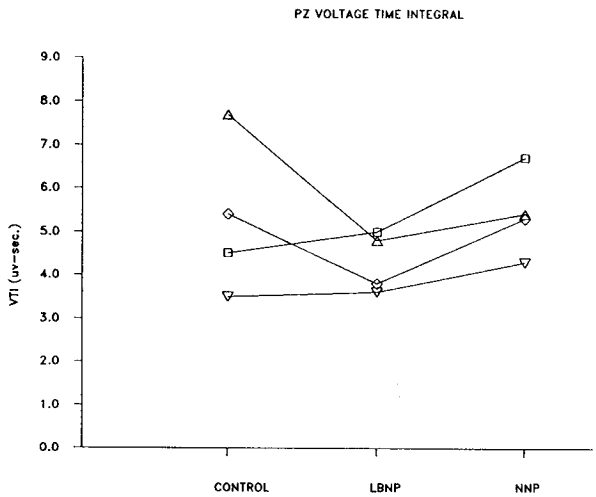

Figure 4.

ERSP measurement at Cz revealed a consistent decrease in the voltage time integral (VTI) during LBNP when compared to control in all four subjects. Friedman's non-parametric test demonstrated a statistically significant difference among the three environments; $p=0.005$. However, the number of subjects is too small to reach conclusions about the differences between specific interventions. The control average was 7.05 ± 1.04 uv*sec (mean $\pm$ SEM), with a LBNP average of 5.15 ± 0.75 uv*sec and a NNP average of 6.83 ± 1.01 uv*sec. Measurement of the VTI at Pz did not reveal a significant trend.

NNP did not appear to have a large effect on NE, CzVTI or PzVTI since values appeared to return to baseline levels after prior LBNP. However, atriopeptins were observed to remain depressed in two out of our three subjects during NNP.

CONCLUSION

In this preliminary study LBNP was found to be associated with the expected increase in NE and the anticipated decrease in atriopeptins, demonstrating the relevance of further study of the role of atriopeptins in human adaptation to changes in gravity. In addition, this data supports the hypothesis that the functions of frontocortical pathways responsible for cerebral acquisition of data, as reflected in the ERSP, are modulated by changes in autonomic tone. These findings suggest a neuroanatomical association between atriopeptins and baroreceptor signal phenomena that may represent the crossroads between the neuroendocrine and the neurological arms of the baroreflex feedback loop in adaptation to gravitational stress. ■

REFERENCES

1. Elbert, T., Rockstroh, B., Lutzenberger, W. and Birmbaumer, N., eds., Self-Regulation of the Brain and Behavior. Springer-Verlag, 1984. 42-58, 128-169.
2. Gutkowska, J., Bourassa, M., Roy., R., Thibault, G., Garcia, R., Cantin, M., Genest, J. "Immunoreactive atrial natriuretic factor (IR-ANF) in human plasma." Biochemical and Biophysical Research communications 1985, 128(3) P 1350-57.
3. Hilton, S.M. "Inhibition of the baroreceptor reflex by the brainstem defense centre." In P. Sleight, ed. Arterial Baroreceptors and Hypertension.Oxford, 1980. 318-323.
4. Needleman, P. and Greenwald, J.G. "Atriopeptin: a cardiac hormone intimately involved in fluid, electrolyte and blood-pressure homeostasis." New England Journal of Medicine, 1986, 314:828-834
5. Samson, W.K., "Atrial natriuretic factor inhibits dehydration and hemorrhage-induced vasopressin release." Neuroendocrinology 1985 40:277-9.
6. Saper, C.B. et al. "Atriopeptin-immunoreactive neurons in the brain: presence in cardiovascular regulatory areas." science 1985 227:1047-49.
7. Skinner, J.E. "The regulation of cardiac vulnerability by the cerebral defense system." J.Amer. Col. Cardiol., 1985. 5:88B-94B
8. Skinner, J.E., and Yingling, C.D. "Central Gating mechanisms that regulate event-related potentials and behavior: a neural model for attention." In: J.E. Desmedt, ed. Progress in Clinical Neurophysiology, V.1., Karger-Basel, 1977
9. Wolthus, R.A., Bergman, S.A., Nicogossian, A.E. "Physiological effects of locally applied reduced pressure in man." Physiological Reviews 1974, July Vol. 54(3) p. 566-95

A SENSITIVE TECHNIQUE FOR MONITORING INTRACELLULAR CALCIUM AND ELECTROLYTES

B. B. Silver[1], B. A. Harris[2] and S. B. Arnaud[2]
[1]*Spectro-Scan, Inc., San Bruno, California 94066 and* [2]*NASA/Ames Research Center, Moffett Field, California 94035*

INTRODUCTION

Until recently, methods for quantifying intracellular ions have been limited and required invasive techniques such as venipuncture or biopsy for cell analysis. The preparation procedures required by the methods, the insensitivity of the measurements and the uncertainty of the meaning of the results, are major deterrents to the use of intracellular ion measurements in clinical settings.

A novel technique was developed to accurately measure the ion concentration in sublingual cells. These cells satisfy the criteria needed for analysis and can be removed noninvasively. Sublingual cells are obtained and fixed to low-background carbon slides, and analyzed by energy dispersive X-ray analysis. This method provides sufficient sensitivity to detect changes in the range of 10 to 30 percent, according to the specification.

We applied this technique to two physiologic studies to determine its value in the assessment of calcium metabolism.

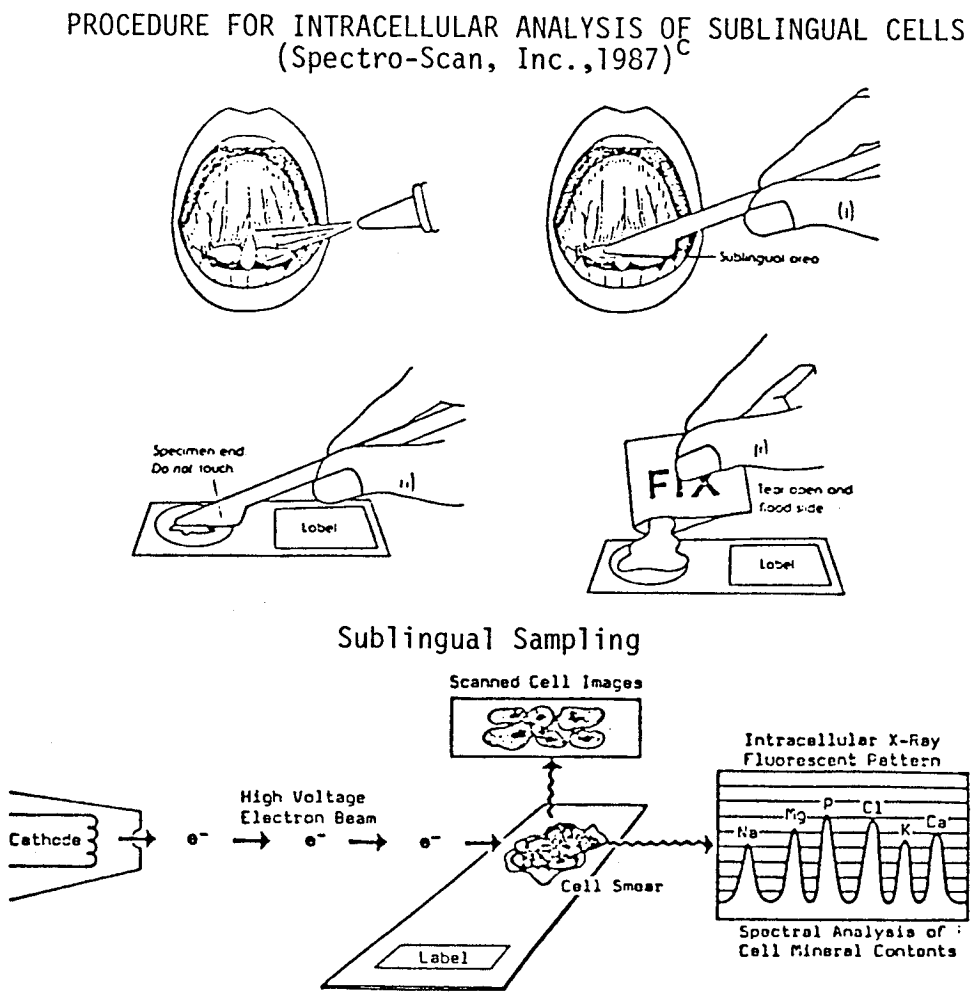

Figure 1. Procedure for Intracellular Analysis of Sublingual Cells.

METHOD

Sublingual cells are obtained from cleansed sublingual areas of the buccal cavity with an applicator stick, and spread on a low-background carbon slide. These cells are ideal because they are non-cornified, polarized, protected from trauma, and easily obtained. The smears are immediately preserved with cytology fixative, and allowed to dry. This preparation requires no further manipulation and can be transported and stored at room temperature, with no loss of ions. The cells are visualized in a scanning electron microprobe and analyzed with energy X-ray dispersion. Single cells are selected for analysis if they are well-nucleated and have intact membranes with normal ultrastructure. Each cell is scanned at a magnification of 2500X for 100 seconds. A minimum of three cells on each smear are examined to obtain reproducible values. The intracellular ion concentration is quantitated by the spectra generated from energy dispersive X-rays and expressed in EXA units, defined as the X-ray intensity, peak to background per unit cell volume (800u3), (patent pending for Elemental X-Ray Analysis or EXA).

STUDY 1: Young adult male monkeys (*M. mulatta*) were fed synthetic diets containing no vitamin D, 0.05% calcium and 0.5% phosphorus. After 1, 3, and 6 months the ion concentration of calcium (ICCA) and phosphorus (ICPi) was determined in sublingual cells, obtained from anesthetized animals. The results of these analyses were compared to data from 12 adult monkeys (control) fed standard diets containing vitamin D, 1.6 IU/Kg, 0.9% calcium and 0.5% phosphorus.

ANIMAL	MONTHS OF DIET	ICCA, EXA units	ICPi, EXA units
A	1	371	2126
B	3	147	2227
C	6	255	1840
D	6	227	1645
CONTROLS (±SD)		95±28	1210±118
NORMAL RANGE (Monkey)		39-151	1081-1446

Increases in intracellular calcium and phosphorus concentrations in sublingual cells of the experimental animals are consistent with the recognized disturbance of impaired efflux of calcium from intestinal cells in vitamin D deficiency.

STUDY 2: Sublingual cells from 5 healthy adult male volunteers were obtained before and 27 days after bedrest in a -6 degree head-down position. Changes in intracellular ion concentrations were as follows:

	ICCA	ICPi	ICMg	ICK	ICNa
CONTROL	81 ±14	1180 ±109	775 ±18	92 ±29	13 ±0.43
DAY 27	109* ±15	1577 ±209	811 ±16	207* ±60	14 ±1.2
NORMAL RANGE	56-102	1027-1365	726-852	59-144	12-16

*$p < .05$, †$p < .01$

These data suggested disturbances in the two ions, calcium and potassium, whose metabolism is known to be vulnerable to both the effects of prolonged bedrest and spaceflight.

SUMMARY AND CONCLUSION

The first study shows the effects of low-calcium, vitamin D-deficient diets on the intracellular ion concentrations of calcium and phosphorus in the nonhuman primate. The second study illustrates the value of this test in monitoring physiologic changes during bedrest. Preliminary results in both of these studies indicate that the method using sublingual cells, is a reliable, sensitive and practical means of detecting changes in the distribution of calcium secondary to nutritional or metabolic alterations and potentially, spaceflight. ■

EFFECTS OF ANTIORTHOSTATIC SUSPENSION AND SPACEFLIGHT ON INTERFERON PRODUCTION AND IMMUNITY TO VIRUSES

G. Sonnenfeld[1], J. Williams[2] and A. D. Mandel[2]
[1]*Department of Microbiology and Immunology, School of Medicine, University of Louisville, Louisville Kentucky 40292,* [2]*NASA/Ames Research Center, Moffett Field, California 94035*

Over the past several years, there have been several reports of alterations in immunological responses after spaceflight. Included among those was a report of inhibited interferon production by blood cells from two Soviet cosmonauts after spaceflight. The inhibited interferon production appeared to be a transient effect, and not all cosmonauts were affected in the same manner. In view of this report and others suggesting alterations in respiratory tract infections in astronauts after spaceflight, we have, for the past several years, been engaged in a study of the effects of suspension and spaceflight on immune responses, and, in particular, on immune responses to viruses. The results of those studies are reviewed below.

Interferons make up a family of proteins produced by the body. They were originally described as antiviral substances, but now it has become clear that interferons have several additional important bioregulatory functions, including a general regulatory role for immune responses. There are three major types of interferon: interferon-α is produced primarily by leukocytes, interferon-β by fibroblasts, and interferon-γ is the product of T-lymphocytes as part of any immune response. Interferons -α and -β are often referred to in a combined fashion as interferon-α/β.

Our original studies have used antiorthostatic, hypokinetic, hypodynamic suspension to simulate some aspects of weightlessness. The model we have used is the well-described rat model as well as a newly designed mouse model. This model has its limitations, but has allowed us to carry out studies that have been useful in planning spaceflight studies.

The first model studies that we carried out were done with the rat. In these studies, Sprague/Dawley rats were antiorthostatically suspended for one to two weeks. Immediately after the end of suspension, the rats were challenged with polyriboinosinic-polyribocytidylic acid interferon-α/β. The rats were bled six hours after challenge, and the sera were assayed for interferon antiviral activity. To carry out this assay, a known number of plaque-forming units of the Indiana strain of vesicular stomatitis virus was placed on L-929 cells that had previously been treated with serial dilutions of the serum sample. The titer of interferon was equivalent to the reciprocal of the greatest dilution of serum sample that decreased virus plaques by 50%. Rats that had been suspended in an antiorthostatic fashion showed severely inhibited production of interferon-α/β.

Our next study was carried out using Swiss/Webster mice. In this case mice were either orthostatically or antiorthostatically suspended for a one-week period. Some mice were challenged with polyriboinosinic-polyribocytidylic acid immediately after removal from suspension. Others were allowed to rest in normal caging for one additional week prior to challenge. In this experiment, the mice that had been antiorthostatically suspended showed greatly inhibited interferon-α/β production. Mice that were orthostatically suspended showed no effect on interferon-α/β production, suggesting that the special antiorthostatic orientation which resulted in simulation of some aspects of weightlessness was required to affect interferon production. The effects of suspension were transient, as mice that were allowed to recover in normal caging were able to produce interferon-α/β and, in fact, produced greater than normal levels of interferon.

This study was next extended to determine the effects of suspension on the resistance of mice to the diabetogenic strain of encephelomyocarditis virus (EMC-D). Female Swiss/Webster mice are normally resistant to infection with this virus. The virus is sensitive to inhibition by interferon. The majority of antiorthostatically suspended female mice that were challenged with EMC-D virus developed diabetes, indicating successful infection. Orthostatically suspended mice remained resistant to EMC-D virus infection. Susceptibility to EMC-D virus infection correlated with the loss of production of interferon-α/β in the antiorthostatically suspended mice.

The latest study we have carried out was performed on rats that were flown in Space Shuttle mission SL-3. In this case, rats were flown for 7 days, and the spleens were removed from them. The spleens

were challenged with concanavalin-A, a mitogen, to induce both interferon-γ and interleukin-3. Interleukin-3 is another important immunoregulatory substance. The great majority of cells from flown rats could not produce interferon-γ in response to mitogen challenge; however, interleukin-3 production by these cells did not display a different pattern from that by spleen cells from ground control rats. These data indicated that spaceflight did appear to result in inhibited production of interferon, supporting our earlier results using the antiorthostatic model. The lack of effect of spaceflight on interleukin-3 production suggests that there may be some special sensitivity of the interferon system to the effects of spaceflight.

The results of the studies described above indicate that immune responses, and particularly those directed against viruses, can be affected by antiorthostatic suspension and by spaceflight. The full range of the effects of spaceflight on the immune system, the duration of those effects, and the significance of those effects to resistance to infection should be the basis for extensive future studies. ■

ENFORCED BEDREST IN MAN RESULTS IN DECREASED ACTION OF INSULIN ON GLUCOSE METABOLISM PRIMARILY IN MUSCLE

C. A. Stuart[1], R. E. Shangraw[2], E.J. Peters[1], M. J. Prince[1], and R. R. Wolfe[2,3]
Departments of Medicine[1], Anesthesia[2], and Surgery[3], University of Texas Medical Branch at Galveston and the Shriners Burn Institute, Galveston, Texas 77550

Absolute bedrest is a land-based model of the muscular inactivity which occurs in the weightlessness of prolonged spaceflight. We sought to determine what effect enforced bedrest of 7 days duration might have on insulin regulation of glucose and protein metabolism using basal and post-bedrest sequential multidose euglycemic clamp studies with infusions of the stable isotope-labeled amino acid 1-^{13}C-leucine. Six normal young adult males were each subjected to 7 days complete bedrest on a waterbed. Nitrogen balance was negative by 24 hours in each subject with an average cumulative loss of 6.3 g nitrogen after 6 days. On a totally defined liquid diet containing 30 kcal/kg/day with a protein content of 15 g/kg/day our subjects had a 5-8% loss of muscle volume in the lumbar paraspinal muscles and a 3-5% decrease in thigh muscle volume accompanied by a 3-5% increase in thigh fat content as quantitated by magnetic resonance imaging (MRI). The euglycemic clamp studies demonstrated that insulin suppressed in a dose-dependent manner plasma leucine concentrations, plasma leucine rate of appearance (Ra), plasma alpha-ketoisocaproic acid (KICA) Ra, and leucine oxidation. Plasma leucine was 93 ± 2 um in the basal period and fell to 38 ± 2 at maximally effective plasma insulin levels. Plasma leucine rate of appearance was decreased from a basal value of 1.41 ± 0.07 umol/kg min to 1.04 ± 0.07 (mean ± SEM). Plasma KICA Ra fell from a basal value of 2.10 ± 0.07 umol/kg min to 1.31 ± 0.04 at maximal insulin doses. Leucine oxidation was determined by quantitating the ^{13}C enrichment of exhaled CO_2 during ^{13}C-leucine infusions. Insulin suppressed leucine oxidation from 0.60 ± 0.09 umol/

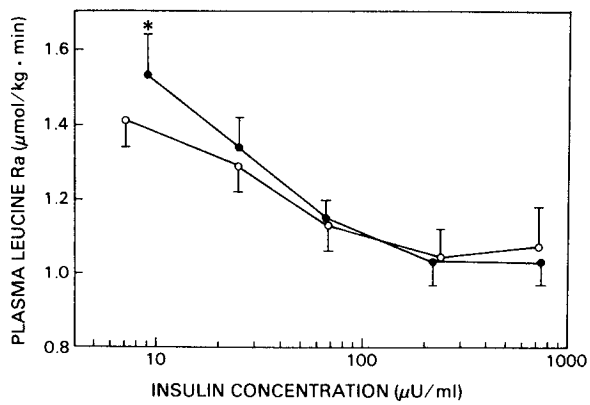

Figure 1. Insulin regulation of the rate of appearance of plasma leucine. The insulin dose response curve of leucine Ra from multidose euglycemic insulin clamps in 6 normal subjects is shown. Open circles: control studies; solid circles: bedrest clamp data. The basal leucine Ra was increased 10% by bedrest ($p<0.05$).

kg min to 0.33 ± 0.04. Bedrest resulted in an increase in the basal plasma leucine Ra from 1.41 ±0.07 to 1.53 ± 0.11 ($p<0.05$, paired t test), but insulin suppression of leucine Ra was not affected by bedrest (Figure 1). The maximal suppression of leucine Ra achieved was 1.04 ± 0.07 umol/kg min pre-bedrest and post-bedrest was 1.03 ± 0.06. The concentration of insulin achieving 50% of the maximal effect (ED50) was 38 uU/ml pre-bedrest and 36 uU/ml post-bedrest.

The absence of a defect in insulin action on protein breakdown and oxidation was in contrast to our findings from investigation of insulin action on glucose metabolism. Before and at the end of the bedrest period, each subject underwent a multidose euglycemic insulin clamp study, a glucose tolerance test, and assessment of insulin binding to blood mononuclear cells. The results of these studies are shown in Table 1. We found that bedrest resulted in a deterioration of glucose tolerance, an increase in fasting insulin, and increase in insulin secretion following a glucose challenge. These data document the appearance of resistance to endogenous insulin.

TABLE 1. GLUCOSE TOLERANCE AND INSULIN BINDING STUDIES

	Fasting Glucose mg/dl	Fasting Insulin uU/ml	Glucose Area mg/dl.hr	Insulin Area uU/ml.hr	Insulin Binding $\%10^6$ monos
Pre-Bedrest	74±3	6.7±0.6	305±27	119±21	0.517±0.096
Post-Bedrest	74±2	9.5±1.6*	354±27*	145±28*	0.473±0.076

*Significantly different from pre-bedrest value, $p<.05$

The euglycemic clamp data shown in Figure 2 revealed a shift to the right of the plot of whole-body glucose utilization vs insulin concentration (ED_{50} 78±8 uU/ml post-bedrest vs 45 ±3 pre-bedrest) with little change in the maximal glucose utilization (14.0 ± 1.3 mg/kg/min post-bedrest vs 15.4 ± 1.4 pre-bedrest). In contrast, the hepatic glucose output insulin dose-response curve (Figure 3) did not shift after bedrest (ED_{50} 20 ± 3 uU/ml post-bedrest vs 19 ± 3 pre-bedrest). These data suggest that the insulin resistance induced by bedrest occurs primarily in muscle with little effect on liver insulin sensitivity.

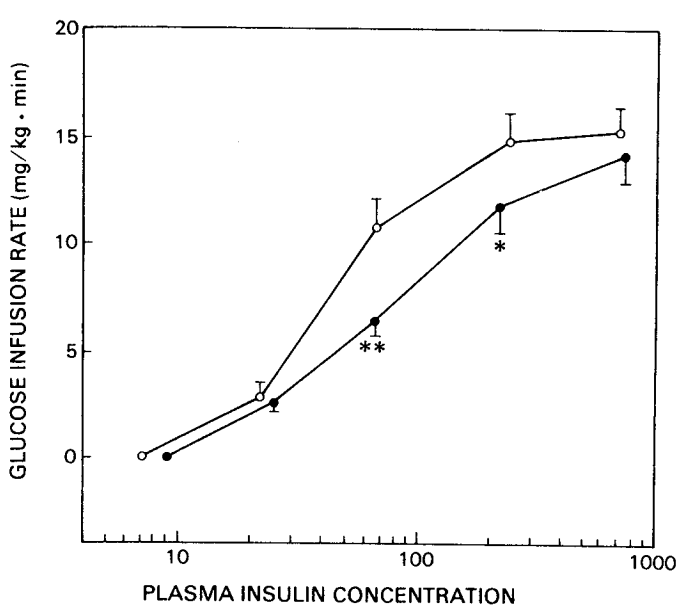

Figure 2. Whole body glucose utilization. Plotted are the data from multidose euglycemic clamp studies in 6 normal males who underwent 7 days of absolute bedrest. Open circles: control data; solid circles: bedrest data. Single asterisk represents a decrease significant at $p<0.05$; double asterisk at $p<0.01$ by ANOVA repeated measures.

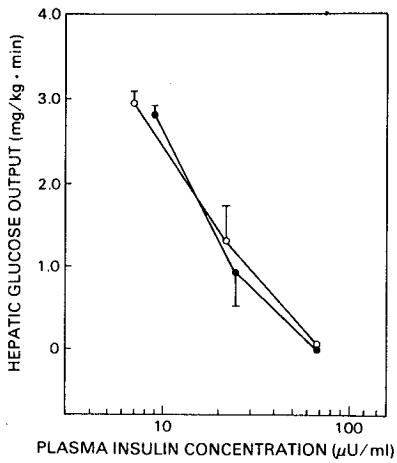

Figure 3. Hepatic glucose output. Endogenous glucose production suppression during insulin infusions before (open circles) and after (solid circles) bedrest.

We conclude that (1) insulin suppresses protein breakdown and leucine oxidation in a dose-dependent manner; (2) bedrest results in negative nitrogen balance associated with enhanced basal net proteolysis; (3) bedrest does not alter insulin suppression of net protein degradation; and (4) the bedrest-induced glucose metabolism insulin resistance is confined primarily to muscle. ■

THE ADAPTATION OF CPR TECHNIQUES FOR USE IN THE WEIGHTLESS ENVIRONMENT

D. A. Tipton, K. J. Myers, O. H. Loyd
NASA/KSC Biomedical Operations and Research Office, Kennedy Space Center, Florida 32899

INTRODUCTION

Many Advanced Cardiac Life Support (ACLS) techniques, including standard Cardiopulmonary Resuscitation (CPR) as currently performed on earth, cannot be successfully executed in the weightlessness of space. In fact, recent studies have cast doubt on the effectiveness of standard CPR even on earth. Therefore, in order to effectively deal with the eventuality of cardiac arrest in space and to determine the optimum resuscitation techniques for both the earth and space environments, we have proceeded with an assessment of the state-of-the-art and made suggestions for further work.

BACKGROUND

There is a need for developing the capability to perform effective and efficient CPR for use in space. The hazards of electrocution, hypoxia, decompression, trauma, and toxic exposure are present as potential sources of injury from which a healthy astronaut might recover if properly resuscitated and supported. There is the eventuality of a cardiac arrest in space as horizons expand and more and more people of all ages and physical conditions arrive. Finally, it is important to plan now for a future in space which will allow the propagation of standards of medical care and lifestyles equivalent to those we now enjoy on earth.

A number of factors render conventional CPR useless in the space environment: a lack of smooth hard surfaces to stabilize the victim against; the absence of rescuer weight to convert into driving force in the administration of CPR; the need for immediate attention to, and correction of, any possible spacecraft malfunction which may have caused the arrest; and the lack of large numbers of bystanders to carry out CPR.

The technique for CPR in space will have the following requirements: provision of adequate perfusion/oxygenation during resuscitation; compact size and minimum mass for associated materials or constructions; easy application and use by nonmedical personnel; some degree of automation to allow crewmembers to attend to other immediately pressing duties during prolonged periods of

support; the integration of ventilation, perfusion, monitoring, IV therapy, and other resuscitative modalities into one intact unit.

The current standard of CPR employs closed chest massage, a technique first described by Boehm in 1878 but not widely used until 1960 when Kouwenhoven, Knickerbocker, and Jude presented their landmark study in JAMA, demonstrating its utility[4]. This is combined with any of several forms of direct airway ventilation, the efficacy of which was shown in the 1950's[9].

Original conjecture has been that CPR "works" by compression of the heart between the sternum and the vertebral column. A variety of studies[3] have now shown that increases in intrathoracic pressure are responsible for perfusion during CPR, and perfusion can be maintained with very little direct compression of the sternum. It appears that the increased pressure is transmitted out the aorta but collapses the great veins resulting in forward flow. These studies are corroborated by the following findings: the valves of the heart are incompetent and the volume of the left ventricle does not change significantly during standard CPR as measured by 2-D echocardiogram[8]. Further indication that intrathoracic pressure fluctuations are the mechanism of perfusion is the fact that consciousness has been maintained in cardiac arrest patients (induced inadvertently during cardiac catheterization) for up to one minute by coughing. The intrathoracic pressure increases are directly related to each cough[2].

Studies recently in animal subjects using standard CPR found that the blood flow to the coronary arteries during resuscitation was poor due to inadequate perfusion pressure (12 mmHg vs. a requirement of 28 mmHg for significant flow to occur)[7]. Obviously, the standard method of resuscitation is in need of some refinement. Some work has been done along these lines. Researchers have demonstrated that simultaneous ventilation and chest compression along with abdominal binding provides a useful modification[6]. In addition, the use of pneumatic vest CPR to create fluctuations in intrathoracic pressure was found to produce improved survival in an animal model compared to conventional CPR (7 of 9 vs. 1 of 9). It is of import that the pneumatic vest causes virtually no rib fractures and their accompanying complications. The vest technique requires an automated inflation mechanism for the proper timing of all events. Another automated device, the Thumper, is available but it functions in the same inefficient manner as conventional CPR, directly displacing the sternum and thereby creating a risk of rib fracture complications.

A NEW STUDY

Initial trials of a chest enclosure using pneumatic bladders by Drs. Loyd, Rosborough, and Tipton are showing promise. While previous dog studies have demonstrated the superiority of pneumatic vest CPR to thumper or conventional CPR, the results could not be directly extrapolated to humans because of the much lower chest compliance in man. Therefore, the animal model selected was swine due to similarities between swine and human chest compliance[5]. Ten swine subjects were fibrillated and randomized into control (no pumping) and experimental (pumping) groups. The initial studies have demonstrated systolic pressures of up to 170 mmHg., as well as significant blood flows indicated by dye injection.

DISCUSSION

The current technique for CPR in space involves placing the victim in the Shuttle seat and strapping the rescuer on top; compression is then achieved by the rescuer forcing his body against the victim's chest. It is unknown what perfusion pressures this produces but assumed to be similar to conventional CPR, since it relies on sternal compression[1]. The current information suggests that a device or technique should be developed which can maximize intrathoracic pressure fluctuations to produce adequate perfusion of vital organs and allow venous return for continued perfusion, while not increasing but perhaps even lessening the risk of injury. In this regard an enclosed pneumatic compression device would be superior to any form of direct compression. It is also true that such a device can be adapted to fulfill the requirements of: prolonged or intermediate duration life support independent of other personnel, ease of application and use, and integration into a single intact total life support/ICU type unit.

SUMMARY

(1) If people are to live and work permanently in space as on earth, the standards of earth medical care, such as CPR, need to be adapted for use in space.

(2) The development of an automated, integrated, pneumatic CPR device could fill this need.

(3) This technology may result in improved CPR techniques here on earth which could save many lives, further demonstrating the benefits of space exploration. ■

REFERENCES
[1]Adams, P.; Shuttle crew prepared for medical emergencies; Aviat Space Environ Med, V. 82, p. 96, January 1982.
[2]Criley, J.M., et. al.; Cough-induced cardiac compression; JAMA, V. 236, pp. 1246-1250, September 13, 1976.
[3]Halperin, H.R., et. al.; Determinants of blood flow to vital organs during cardiopulmonary resuscitation in dogs; Circulation, V. 73, pp. 539-550, March 1986.
[4]Jude, J.R., et. al.; Cardiac Arrest: Report of application of external cardiac massage on 118 patients; JAMA, V. 178, pp. 1063-1067, December 16,1961.
[5]Loyd, O.H.; A proposal for automation of basic life support/cardiopulmonary resuscitation and advanced life support in space; unpublished, May 9, 1984.
[6]Niemann, J.T., et. al.; Circulatory support during cardiac arrest using a pneumatic vest and abdominal binder with simultaneous high-pressure airway inflation; Ann Emerg Med, V. 13, pp. 18-24, September 1984.
[7]Niemann, J.T., et. al.; Coronary perfusion pressure during experimental cardiopulmonary resuscitation; Ann Emerg Med, V. 11, pp. 23-27, March 1982.
[8]Rich, S., et. al.; Clinical assessment of heart chamber size and valve motion during cardiopulmonary resuscitation by two-dimensional echocardiography; Am Heart J, V 102, pp. 368-373, September 1981.
[9]Safar, P., et. al.; A comparison of the mouth-to-mouth and mouth-to-airway methods of artificial respiration with the chest-pressure arm-lift methods; NEJM, V. 258, pp. 671-677, April 3, 1958.

STUDIES OF HZE PARTICLE INTERACTIONS AND TRANSPORT FOR SPACE RADIATION PROTECTION PURPOSES

L. W. Townsend[1], J. W. Wilson[1], W. Schimmerling[2], M. Wong[2]
[1]NASA Langley Research Center, Hampton, Virginia 23665-5225; [2]Lawrence Berkeley Laboratory, Berkeley, California 94720

As the era of Space Station, lunar bases, and manned Mars missions approaches, cumulative radiation exposures of career astronauts to biologically significant levels of the high-energy heavy ion (HZE) component of solar and galactic cosmic rays will occur for the first time in the history of manned spaceflight. Since these HZE particles include nearly all nuclear species, and possess a very broad range of incident energies, considerable attention must be devoted to developing accurate methods of describing their physical interactions and transport through bulk matter in order to properly assess spacecraft shielding effectiveness, and to evaluate the self-shielding factors of the astronauts' bodies themselves. As these extremely energetic cosmic rays traverse bulk matter, their radiation fields change composition through interactions with any target materials encountered. Aside from continuously losing energy through collisions with atomic orbital electrons, the incident ions collide with target nuclei within the shield and experience nuclear attenuation (absorption) and breakup (fragmentation) reactions. The struck target nuclei also recoil leaving highly ionized tracks in their wakes. These interactions remove particles from the incident field while concomitantly producing secondary and subsequent generation reaction products. The altered composition of the transported field then results in an internal radiation field within some critical organ of the astronauts body which differs appreciably from that incident upon the external spacecraft structure. Proper evaluation of the biological damage to this critical organ requires an adequate knowledge of the physical characterizations (energies and composition) of the complex radiation fields incident upon that organ. Studies of the physical transport and interactions of these space radiation fields are presently hampered by a paucity of experimental HZE interaction and transport data. Consequently, an experimental apparatus has been built to study the composition and spectra of heavy ion beams of different types as they pass through various materials of variable thickness. Sufficient measurements will be made to fully specify biologically

interesting dosimetric quantities as a function of shield type and depth for each beam type. Because of the large numbers of projectile/target combinations and their nuclear fragmentation products, it is unreasonable to expect that experimental measurements alone will ever provide the necessary interaction and transport data. Therefore, experimentally-validated calculational methods are needed to accurately describe them. To this end a NASA-supported collaborative research effort involving theoreticians at Langley Research Center (LaRC) and experimentalists at Lawrence Berkeley Laboratory (LBL) has been established to develop the necessary radiation physics methodologies for properly evaluating future HZE particle shielding and dosimetry requirements for manned spaceflight. In this presentation current and planned research efforts for the LaRC-LBL collaboration will be described.

The main emphasis in the theoretical research program at Langley is to develop general methods for accurately predicting HZE particle interactions and transport for use by researchers at Langley, Johnson Space Center, and elsewhere, in mission planning studies, in evaluating astronaut self-shielding factors, and in spacecraft shield design and optimization studies. To accomplish these goals, research efforts are focussed upon two interrelated tasks: (1) to develop computationally fast and accurate solutions to the Boltzmann (transport) equation, and (2) to develop accurate HZE interaction models, from fundamental physical consideration, for use as inputs into these transport codes. We have formulated accurate solutions to the HZE transport problem through a combination of analytical and numerical techniques. Representative results for the absorbed dose due to a 670 MeV/amu neon beam incident upon a thick water target are displayed in figure 1 and compared to experimental data from the LBL experimental effort. In figure 2 we display calculated LET (Linear Energy Transfer) spectra in aluminum

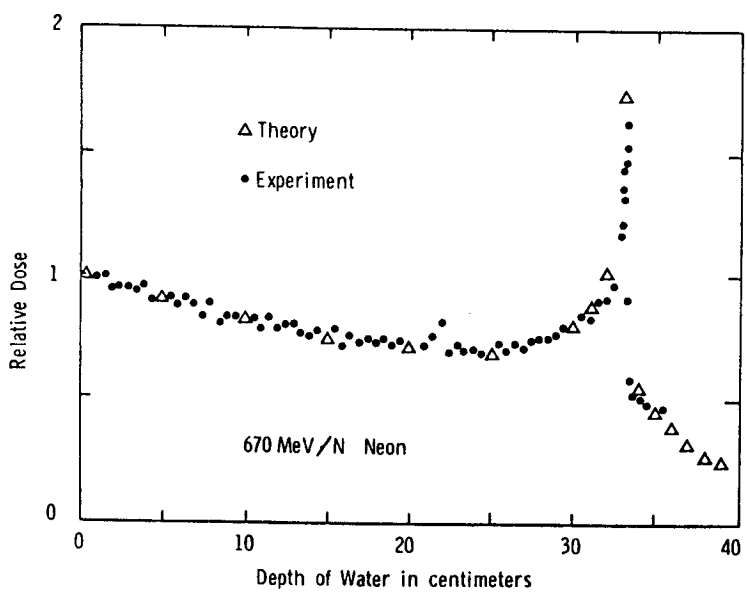

Figure 1. Dose versus depth in a thick water target for 670 MeV/amu neon beams.

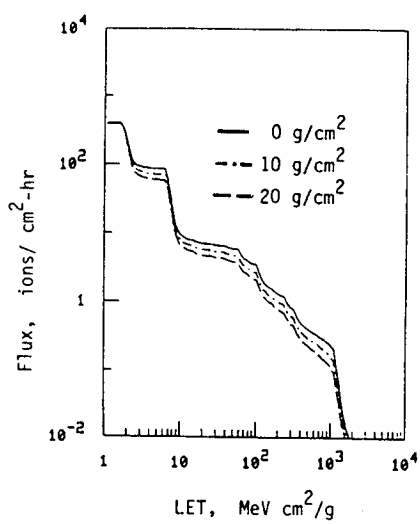

Figure 2. GCR integral LET spectra in aluminum for a 30° orbit at 400 km altitude

for a typical LEO (Low Earth Orbit) mission using the GCR transport code. Validation of these solution methods has been established to within one percent by direct comparison to a realistic, nontrivial, analytic benchmark solution to the Boltzmann equation. Therefore, the main sources of uncertainty in HZE transport are the input interaction parameters, and the physical assumption used to simplify the Boltzmann equation from its original six-dimensional integro-differential form. Testing of these simplifying assumptions is a major goal of the thick target transport experiments at Lawrence Berkeley Laboratory.

In addition to the development of HZE transport codes, extensive efforts are underway at Langley to develop accurate theoretical models for the input interaction parameters: stopping powers, nuclear absorption cross sections, and fragmentation parameters. Methods for estimating stopping powers are reasonably well-developed; therefore, the main focus is upon modelling the nuclear absorption cross sections and fragmentation parameters. Because the transmitted flux in a thick target transport calculation possesses an exponential functional dependence upon the absorption cross sections,

accuracy is crucial since even small cross section inaccuracies can result in large calculated flux errors. We have formulated, from first principles, a fully energy-dependent quantum-mechanical theory for nuclear absorption cross sections which is applicable to any projectile nucleus-target nucleus combination at any energy above 25 MeV/amu. Typical accuracies, when compared with available experimental data, are within three percent for energies greater than 80 MeV/amu and within ten percent for energies as low as 25 MeV/amu. For illustration purposes, sample calculations will be presented and compared with available experimental data.

Unlike absorptive processes, the physics underlying nuclear fragmentation is not well understood and the scope of the experimental data base is inadequate. The lack of a suitably-accurate nuclear fragmentation theory is a major hindrance to present HZE transport modelling. Although some progress has been made in developing fundamental fragmentation models, current efforts are hampered by the paucity of relevant experimental data. Hence, existing quantum-mechanical models are typically cumbersome to use and limited in scope. To correct this situation, theoretical models at both the fundamental and semiempirical levels are being developed at LaRC for further experimental validation at LBL. Aside from expanding the data base of experimental fragmentation measurements, the recently initiated LBL experiments will emphasize measurements of elemental and isotopic production cross sections for iron beams onto various targets over a broad range of incident ion energies. Iron was chosen because it is a major cosmic ray ion of radiobiological interest. This experimental approach will also systematically evaluate the fragmentation cross section energy dependence, if any, for a given projectile-target combination over a range of incident energies. Knowledge of any possible energy dependence is critical because major reductions in computational times for HZE transport calculations are attainable if the fragmentation cross sections are essentially independent of the incident projectile's energy. We have recently developed a semiempirical fragmentation model for use in HZE transport calculations. Unlike alternative formulations from astrophysical studies which have numerous arbitrarily-adjusted parameters, the LaRC semiempirical model has only a single adjustable parameter. This fragmentation model, which is independent of the incident ion's energy, predicts fragment elemental cross sections which agree with the limited experimental data base to the extent that these data agree among themselves. Representative comparisons between theoretical predictions and experimental data will be presented. ■

VISUAL FINDINGS OF ASTRONAUTS

Col. T. J. Tredici, Col. B. G. Martin, Lt. Col. E. E. Kirby
Ophthalmology Branch, USAF School of Aerospace Medicine, Brooks Air Force Base, Texas 78235-5301

INTRODUCTION

In the past NASA astronaut candidates were given complete physical examinations at the USAF School of Aerospace Medicine. Visual standards were formulated from our findings.

METHODS

Our past experience with NASA astronaut candidates has been our best source of data. From 1962 to 1966, 117 carefully screened astronaut candidates were evaluated at the USAF School of Aerospace Medicine for the National Aeronautics and Space Administration (NASA). Of these candidates, 48 were chosen for astronaut duties. Complete ophthalmologic evaluations were done. This gave us the unique opportunity to examine the visual and ocular findings of a select and superior group of individuals.

RESULTS

As a result of this study, data produced can be used as a standard of comparison of usually accepted "normal adult values" in such areas as visual acuity, accommodation, horizontal and vertical phorias, amplitudes, refraction, nigh vision, intraocular pressure, tonography, etc.

CONCLUSION

Graphs and charts illustrating and comparing the maximum, minimum, and mean ocular findings will be displayed. ■

HISTO- AND ORGANOGENESIS OF THE CHICK EMBRYO IN HYPOGRAVITY

J.C. Vellinger[1], R.L. Hullinger[2] and M.F. Hollick[3]
[1]*NASA Shuttle Student Involvement Program Participant, Purdue University, West Lafayette, Indiana 47907,* [2]*Department Veterinary Anatomy, Purdue University, West Lafayette, Indiana 49707 and* [3]*Vitamin D and Bone Metabolism Laboratory, Tufts University, Boston, Massachusetts 02111*

BACKGROUND AND GENERAL OBJECTIVE

This is a study of early chick development related to the environment of space and, as such, it is a ground-based control in support of the NASA Student Involvement project of John Vellinger. The goal of the larger project is to provide a model system for the study of vertebrate development in hypogravity. It should provide a pilot for subsequent diverse investigations of development, the results of which are essentially unpredictable, and the potential of which is unlimited. As noted by Santy (1984), it is just not known if embryos will grow properly or at all when in the space environment.

A forthcoming shuttle mission will carry three sets of fertilized chicken eggs. One set will incubate in orbit for days 1-4 of embryonic life; another will incubate for days 4-7; and the third will incubate days 14-18. These eggs will be in an incubator, the design of which was proposed by Vellinger, a Purdue mechanical engineering student. It was constructed with financial and engineering support from Kentucky Fried Chicken, Inc., Louisville, KY. The project has been developed from a competitive proposal submitted to NASA by Vellinger in 1983.

Two basic scientists of biomedicine will assist Vellinger in the design and analysis of this Phase I Study: Hullinger, veterinary embryologist, Purdue, will measure embryonic development at the conclusion of the flight and until hatch; Hollick of the Human Nutrition Research Laboratory, Tufts, will measure the musculoskeletal loss of mass, especially its potential demineralization.

This is the first attempt to investigate vertebrate development in the "real space environment." It will allow measurement of the effects of hypogravity (zero gravity) on a relatively large vertebrate embryo system. The early development period (1-4 days) is one of formation of the base for organs and organ systems. These organs include face and neck, limbs, ventricles in brain along with pineal and pituitary glands, pancreas and liver, subdivision of heart, and the definitive kidney. In the second period (4-7 days) the pattern is one of differential growth and maturation of the organ systems established in the earlier period. In the third period (16-19 days) osteogenesis is begun, including some mineralization. In these periods selective (programmed) cell death will be monitored for any variation from the normal pattern in skeletal muscle, nervous system, thymus, cartilage, the reproductive ducts, and germ cells of the testes and ovaries.

The chick embryo lies upon a great volume of yolk during its early development. During the second day the heart is displaced to the right and soon shifts to the left side of the thorax. On the 4th day the entire embryo completes a rotation and "fall" onto its left side. This is the pattern in nearly all eggs. Its cause is unknown. If this were a random phenomenon, there should be a ratio of falls to left and right approaching 1; the observed ratio favors left side rotation, more than 99/1. It is tempting to implicate gravity in this process, although a satisfactory explanation of the mechanism for this action of gravity remains unknown.

Other examples are known. Only one half of the reproductive system of hens is functional. In the female embryo of 13 days only the left gonad is "selected" for continued development to an ovary with it duct system; the right side does not develop. In males both gonads develop as testes. If the left gonad (presumptive ovary) is removed at day 13 from a female chick embryo, the right gonad resumes development, not as one might intuitively predict, but as a testis. The influence of the left side rotation is again raised. If both the left and right gonads could be developed as normal ovaries with ducts, the impact upon the production of eggs might be quite significant. There has long been interest in the role that movement against a mechanical resistance plays in the normal development of the synovial joints of limbs. Embryos do push against the interior of the shell, but the much earlier movement may be influenced by gravity. It is this movement which may play the determining role in the early "fracturing" of the cartilage model of limb buds, in turn forming joints. This in part can be measured from this study.

In modern investigative embryology, it is axiomatic that all "daughter" cells of the embryo contain all the genetic information as passed to them from the single fertilized egg. The processes of development, resulting in these cells becoming different from others of "their own kind," are under control of the microenvironment of each cell. Gravity is an ubiquitous influence in that microenvironment, and is surely the same for all cells. An effect of gravity on the details of structure and function of tissues has been demonstrated and measured in shuttle crew members, especially as affecting the myocardium, bones, and erythrocytes.

The following observations have been reported from one or more earlier bioscience experiments. Erythrocytes show major changes in shape (Dentenfass, 1985); there is a significant mineral loss from bone (Globus *et al.*, 1985); Steffen and Musacchia (1984) demonstrated a loss of muscle protein from limbs not bearing weight. Experiments aboard Spacelab I demonstrated that microgravity depressed the rate of proliferation of cells grown in culture (Cogoli *et al.*, 1984), a finding of special import as relating to embryonic growth, which is essentially a form of "culture." A gravitational influence (exogenous) upon the indigenous cellular "timing mechanism (clock)" has been proposed by Sulzman *et al.* (1984).

Earlier "Biostack" experiments have shown *Artemia* eggs to have lower hatch rates and presumed radiation-induced alterations in mortality rate, growth pattern, and sexual maturation. These experiments are of special interest because of their relation to an exposure of human tissues (*e.g.*, brain and heart muscle) to potentially lethal radiation. These tissues, after their definitive differentiation, do not generate new replacement cells (Goode, 1980). In the embryo, replacement cells may be formed from the neuroblasts or myoblasts, but altered sequencing (timing) of this histogenesis may mean a loss of key relationships, *e.g.*, the neurotrophism effects.

TO BE PRESENTED

The Phase I investigation is now under way and uses the methods of light, electron, and scanning microscopy, and cytogenetics. Morphometric analysis follows the principles of stereology. Eggs from SPF laying flocks are to be incubated for their entire developmental period, with some collections at the appropriate (Shuttle flight duration) times in order to master appropriate collection and fixation procedures and the proper pre-flight controls. Some eggs are exposed to near-zero in a clinostat apparatus and others to 3g conditions. Others are exposed to both hyper- and hypogravity to mimic Shuttle flight conditions. The data presented in this Poster will illustrate the macroscopic and microscopic findings and summarize our morphometric findings.

This Phase I of a Space Bioscience Project, NASA Shuttle Student Involvement Program, is funded by a grant from Kentucky Fried Chicken and USDA Hatch Fund #US84-158, Purdue University. ■

REFERENCES

1. Cogoli, A., *et al.* Science 225;228-230, 1984.
2. Dentenfass, L. Lancet (1):747-748, 1985.
3. Globus, R.K., *et al.* Endocrinology 114;2264-2270, 1984.
4. Goode, A. Lancet (1):767-769, 1981.
5. Goode, A. Nature 283:525-526, 1980.
6. Santy, P.A., J. A. Med. Wom. Assoc. 39:13-17, 1984.,
7. Sulzman, F.M., *et al.* Science 225:232-234, 1985.

DESIGN PRINCIPLES FOR A SPACE-BASED FITNESS MANAGER SYSTEM

T. D. Wade
Medical Computing Center Artificial Intelligence Lab, University of Colorado Health Sciences Center, Denver, Colorado

Physiological adaptation to spaceflight can potentially compromise mission objectives and personal safety, both inflight and on return to earth. The fact that physical fitness training on earth is more art than science suggests, by analogy, that prescribing countermeasures for each astronaut must be approximate and refined by experience.

There will probably be no simple, easy remedy, free of side effects, for each of the several risks to fitness (Table 1) posed by life in space. Instead we can expect to discover a set of countermeasure techniques, each of which has (a) its own costs, such as other risks, consumption of time and living space, disruption of mission objectives, and personal discomforts, and (b) its own levels of benefits against possibly more than one kind of deconditioning risk.

Table 1: Fitness modalities having space deconditioning risks

Modalities Affected	Some Possible Risks
anaerobic muscular	Impaired extravehicular activity; less emergency strength; weakness on earth
aerobic muscular	postural muscle wasting; inability to stand and walk on earth
aerobic cardio-respiratory	Shortened EVA; fatigue; less vigor; less endurance on earth
cardiovascular	Blackout on deceleration; fluid redistribution and discomfort; orthostatic intolerance on earth
hard tissue	Osteoporosis; bone fractures; dental problems
neurovestibular	Space adaptation syndrome; sensorimotor discoordination on earth

The mix of costs and benefits should be weighed individually, considering each astronaut's mission role, health needs, and personal goals, all of which can change over time. Countermeasures, costs and benefits will be related in ways that our knowledge of underlying physiology may not be adequate to predict. Empirical study of these relationships will take a long time, and some will only be observable in space.

One solution (currently in use) would be to teach astronauts all that we know, and let them figure out how they want to maintain their fitness. A better solution would be to supply to them a convenient, dedicated, intelligent system which will optimize countermeasure regimes as well as possible and also use its own "experience" as a guide for future improvements, i.e., be able to learn.

This approach differs from many previous attempts to have knowledge-based systems function with incomplete knowledge. For example, there are techniques to "reason with uncertainty", using probabilities, certainty factors, fuzzy logic, and the like (5). However, we may lack estimates of the probabilities, or not even know the statements whose uncertainty needs estimating.

Another touted solution is "deep reasoning"—that is, reasoning from underlying principles, as opposed to surface correlations or heuristics. This approach is being tried in ONYX, a program which attempts a complex, dynamic cost/benefit calculation in treatment of unusual cancer cases (2). This approach might help for space fitness management if adequate physiological models can be found.

There have been recent suggestions that research in machine learning, especially work on inductive reasoning from data, will help to solve the "bottleneck" of acquiring knowledge for expert systems (1). We suggest that the use of induction be extended through the lifetime of a system, so it may always attempt to improve its performance. We shall describe several techniques that differ in sophistication and potential.

The simplest technique would be used in reasoning from research results. When the current consultation situation doesn't match any one known result, the system could interpolate desired values between the "nearest" ones. Since this approach assumes very simple additive models of effects, it can only be used as a first approximation. However, the underlying ability of a program to recognize a gap in its knowledge will also be useful for other techniques.

The program should keep a database of previous consultations and their results that can be used in "course corrections" of a person's fitness, and in searching for situations similar to the current consultation. It is surprisingly rare for an expert system to have historical (long-term) memory of this type, even though there is much database technology that is relevant.

A more sophisticated kind of learning would be for the program to detect, as in the two cases above, that it had a gap in its knowledge, and then attempt to induce from its database a rule that covered the current situation but would also be useful in similar situations in the future. There are various techniques for rule induction (called *symbolic concept acquisition* in artificial intelligence) which are starting to become practical (3). A program which used them to fill its own needs for knowledge would be very powerful.

Given that there is no way to prove an inductive assertion, a program which relied on it would be prone to error. It would not be prudent to let the program extend its knowledge base without human supervision. Still, automated induction has been known to discover useful knowledge (3).

The system proposed above would have a different kind of knowledge base from that found in conventional expert systems, whose knowledge consists of system goals and the "given" (by the expert) knowledge necessary to pursue the goals. Figure 1 shows a *Knowledge Memory* in the form of a

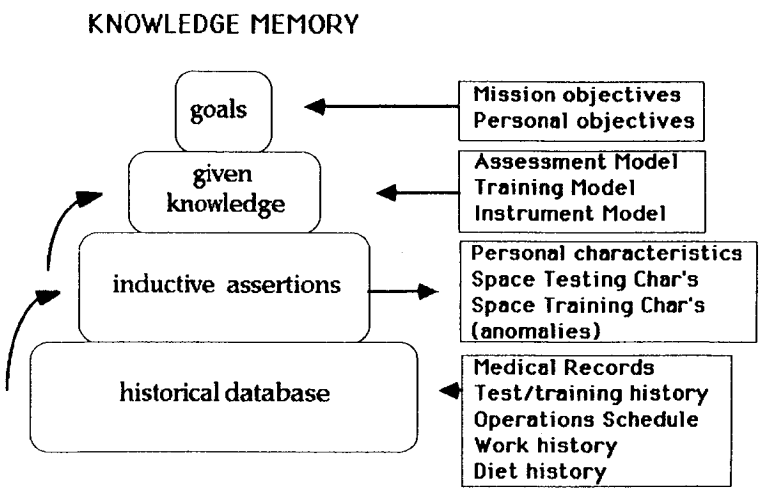

Figure 1. Form and content of the knowledge base for a space-based fitness manager system.

pyramid. As one goes from the top to the bottom, knowledge becomes less general, and more particular. Historical data can be generalized into (tentative) inductive assertions. Assertions that have been tested for validity can either be "promoted" to the level of given knowledge, revised, or discarded. A system using such a knowledge memory would require an induction engine as well as the typical (deductive) inference engine. ■

REFERENCES

(1) Forsyth R, Rada R (1986) Machine learning: applications in expert systems and information retrieval. Wiley, NY, 277 pp.
(2) Langlotz C, Fagan L, Tu S, Williams J, Sikic B (1985) An architecture for planning in uncertain environments. Proc. Int. Joint Conf. Artificial Intelligence, IJCAI-85, Los Angeles.
(3) Michalski RS, Carbonell JG, Mitchell TM (1986) Machine learning: an artificial intelligence approach, Vol. II, Morgan Kaufman Publ., Los Altos, Ca., 738 pp.
(4) National Aeronautics and Space Administration (1986) Life Sciences Accomplishments Report.
(5) Spiegelhalter DJ (1986) A statistical view of uncertainty in expert systems. In: Artificial Intelligence and Statistics (WA Gale, ed.) Addison-Wesley, Reading, MA, pp. 17-55.

DYNAMIC OTOLITH EYE MOVEMENT RESPONSES IN NORMALS: BIAS AND MODULATION COMPONENTS

C. Wall III[1] and J.M.R. Furman[2]
[1]*Massachusetts Eye and Ear Infirmary, Boston Massachusetts and* [2]*Eye & Ear Hospital of Pittsburgh, Pittsburgh, Pennsylvania*

The eye movement responses of subjects rotated about their rostral-caudal (Z) axis depends upon the orientation of the Z axis with respect to the vertical. During constant angular velocity and when the axis of rotation is coincident with the earth gravity vector, the slow phase velocity (SPV) of nystagmus quickly builds up in a direction compensatory to the direction of rotation and then dies out with a decay time corresponding to the 'long vestibular time constant.'

During off-axis rotation the rotation axis of the subject is not colinear with the earth's gravitational force vector. Off-axis rotation produces two eye movement response components due to dynamic otolith stimulation termed "modulation" and "bias." These can be observed in addition to the normal compensatory nystagmus resulting from stimulation of the semicircular canals during earth vertical axis orientation:

1. Modulation: There is a periodic waxing and waning of the slow-phase velocity (SPV) of nystagmus during constant-velocity off-axis rotation. The modulation component has a period inversely related to the rotational speed of the subject.
2. Bias: The compensatory nystagmus during off-axis rotation does not "die off" as it does during prolonged, constant-velocity vertical-axis rotation, but remains long after the response normally attributed to the semicircular-canal stimulus has subsided.

The relative magnitude of these two components vary with species. Cats and squirrel monkeys tend to have large bias components and small modulation components, but with humans the situation is reversed. The objective of this study was to determine how the modulation and bias components varied within a group of 50 normal humans. Our hypothesis was that individuals having small bias components would have large modulation components. We also wished to determine how these two parameters were affected by the age and gender of the subjects.

RESULTS

Our preliminary analysis of these data indicates that bias and modulation components are not highly correlated. The modulation component increases monotonically with subject age, but the bias component shows no such monotonic trend. Female subjects tend to have smaller values of both bias and modulation components compared with males.

DISCUSSION

The fact that the modulation and bias components are not correlated in a group of individuals suggests that the pathways through which these signals that originate from dynamic otolith stimulation are separate and independent. ■

SUSCEPTIBILITY TO DECOMPRESSION-INDUCED VENOUS GAS EMBOLI: HEMATOLOGY AND BIOCHEMISTRY

J. T. Webb[1], K. W. Smead[2], J. R. Jauchem[2], and P. T. Barnicott[2]
[1]*KRUG International, Technology Services Division, San Antonio, Texas 78216,* [2]*USAF School of Aerospace Medicine, Crew Technology Division, Brooks Air Force Base, Texas 78235*

Extravehicular activity (EVA) of Shuttle astronauts currently requires decompression from a cabin pressure of 760 mmHg to the suit pressure of 222 mmHg. This degree of decompression carries a potential for altitude decompression sickness (DCS) even with six hours of prebreathing. A study to determine the effects of decompression from cabin pressure to 429 mmHg (8.3 psi) has been completed. This pressure was selected to correlate with a bends incidence of no more than 5% based on several studies by NASA and the Air Force (Krutz *et al.*, 1985; Mason and Johnson, 1984; Waligora and Horrigan, 1984).

The many attempts to quantify hematologic/biochemical changes that occur during onset of decompression sickness have resulted in conflicting reports of significance (Philp, 1974; Philp *et al*, 1967, 1972; Anderson *et al.*, 1981; Dembert *et al*, 1984; and Jauchem *et al*, 1986). Comparison of parameters in the blood of humans resistant to venous gas emboli (VGE) formation versus those prone to bubble formation during decompression has been limited (Philp *et al*, 1972a; Dembert *et al*, Jauchem *et al*, 1986).

We examined 43 parameters in blood before and after a six-hour chamber flight. Data were obtained from thirty volunteer subjects (20 males and 10 females) representative of the Air Force population. They had passed a USAF Flying Class II physical examination and were certified in accordance with applicable USAF regulations to participate in research altitude chamber flights.

The subjects were exposed, in groups of three or less, to decompression from 745 mmHg (ground level pressure at Brooks AFB, TX) to 429 mmHg (15,000 ft; 8.3 psi). The study pressure and workloads simulated expected extravehicular activity (EVA) conditions. The breathing gas mixture of 50% O_2 and 50% N_2 at altitude was chosen to ensure at least normoxic conditions. Bubble sounds during the chamber exposures were monitored by precordial Doppler, recorded, and graded on the Neuman scale. Two 40cc blood samples were drawn from the subjects on the day of exposure; one immediately before entering the chamber and one postaltitude exposure.

Eight subjects (5 male and 3 female) were bubble-prone (bubble grades = 3 or 4), and 22 (15 male and 7 female) were resistant (bubble grade = 0) to forming bubbles as detected with precordial Doppler. One (male) subject who was bubble-prone exhibited symptoms of DCS.

In this study, significantly higher levels of cholesterol were observed in the bubble-prone males and combined subjects (males and females) than in their resistant counterparts. Jauchem *et al.* (1986) also reported that VGE-susceptible subjects had significantly higher cholesterol than VGE-resistant subjects. Increasing age and cholesterol/HDL ratio may alter vessel wall geometry/flexibility and increase the level of cavitation pressure, favoring formation of bubbles. Reduction in cholesterol could therefore affect the susceptibility to VGE and ensuing bends.

The cholesterol/HDL ratio in our female subjects was significantly correlated with age. The levels of derived factors, cholesterol/HDL and cholesterol minus HDL, showed significant differences between resistant (low values) and susceptible (high values) female subjects. Cholesterol minus HDL levels in the combined subjects were higher in the susceptible group. These findings tend to support an ameliorative role of high HDL levels which may relate to cardiovascular risk indices and the hemodynamics of bubble formation.

VGE-susceptible males exhibited higher pre-exposure magnesium levels than VGE-resistant males in a study by Jauchem *et al.* (1986). In the present study, magnesium was also found to be significantly higher in the VGE-susceptible males.

Anderson *et al.* (1981) found significantly decreased prothrombin time when Doppler Grade 3 or 4 bubbles were detected or bends occurred. In this study, pre-exposure prothrombin time was shorter in bubble-prone males and combined subjects versus bubble-resistant subjects. Bubble-prone females

also exhibited shorter, albeit not significant, prothrombin times. Additionally, the VGE-susceptible females showed an increase in partial thromboplastin time (PTT) which was significantly different from the resistant females who had a decrease in PTT.

Anderson *et al.* (1981) found increased hematocrit when Doppler Grade 3 bubbles were detected or bends occurred. Loss of plasma and associated increases in hematocrit have been associated with the onset of DCS as noted by Bove *et al.* (1974) and Cockett *et al.* (1965). Our study showed a significantly higher pre-exposure hemoglobin, hematocrit, and red blood cell count in the susceptible female group. The susceptible females had a significant reduction in hemoglobin, red blood cell count, and serum osmolality during the exposure relative to an increase in these values in the resistant females. A relatively large but not significant reduction in the hematocrit of susceptible vs resistant females was also evident. These data seem to indicate that the females who exhibited VGE entered the chamber more hemoconcentrated than their resistant counterparts, but underwent hemodilution prior to the postexposure sampling. ■

SPACE STATION HEALTH MAINTENANCE FACILITY (HMF) KNOWLEDGE BASED SYSTEM FOR ANALYZING NONINVASIVE MEASUREMENTS OF DECONDITIONING ONBOARD AND ADVISING EXERCISE COUNTERMEASURES

L. Webster
NASA/Johnson Space Center, Systems Development and Simulation Division, Intelligent Systems Branch, Mail Stop EF5, Houston, Texas, 77058.

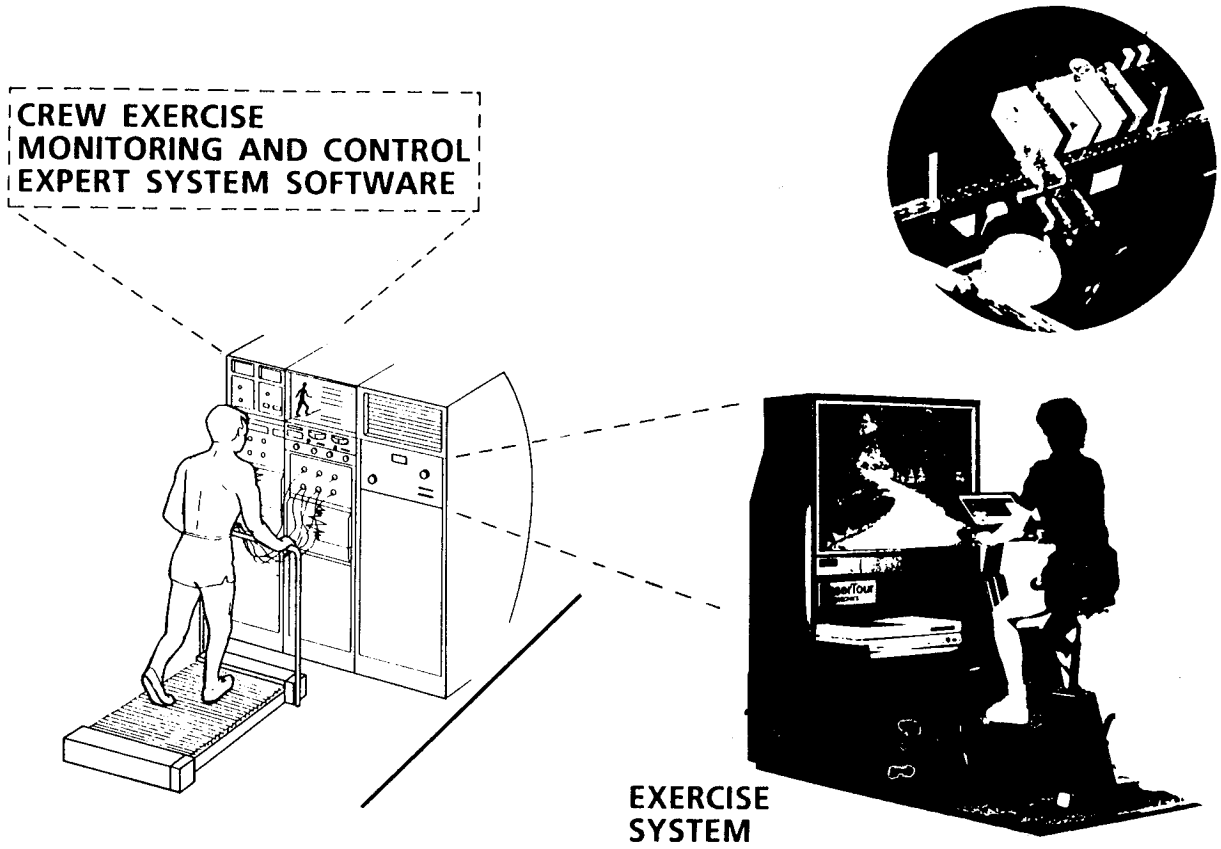

Figure 1. HMF Exercise Monitoring and Control Knowledge-Base System

NASA

This paper will discuss the ongoing work at Johnson Space Center in support of NASA's Space Medicine Data Analysis component of its Life Sciences Program (Special Data Analysis—Artificial Intelligence). This research explores the use of Artificial Intelligence (AI) techniques on a Space Station-related knowledge-based health maintenance system for analyzing noninvasive physiological measurements of deconditioning onboard and advising exercise countermeasures with display, text, and voice synthesis.

The well-being of Space Station personnel requires giving attention to their physiological and psychological adjustments to life on Earth after their return. One of the primary concerns is the physiological adaptation to zero-gravity, in terms of its effects both inflight and afterwards. This adaptation includes the loss of skeletal calcium, of muscle mass and nitrogen stores, and of red cell mass and blood volume. Also decrements in exercise capacity and orthostatic tolerance are seen after extended periods of weightlessness. Each of these changes is a predictable physiological response to the reduced physical stress of life without gravity and is also a serious impediment to the resumption of regular activities on Earth.

Research concerned with the physiological adaptation of man to the weightlessness environment of space is a challenge. To add to this challenge is the fact that the proposed Space Station is envisioned as a highly automated vehicle integrating expert systems into normal operations, making it capable of more autonomous operations than any previous space platform. The HMF Exercise Monitoring and Control System (HEMACS) (Fig.2) is a prototype designed utilizing AI techniques to aid in meeting this challenge in two significant ways: (1) provide an environment in which to evaluate exercise protocol countermeasures, and develop hardware and software specifications for an "intelligent" onboard monitoring of Space Station crew exercise regimen supporting medical operations, and (2) using AI techniques composed of inductive inference and time series relational databases for management and analysis of physiological data supporting the achievement of improved understanding of the physiological effects of long-term exposure to microgravity.

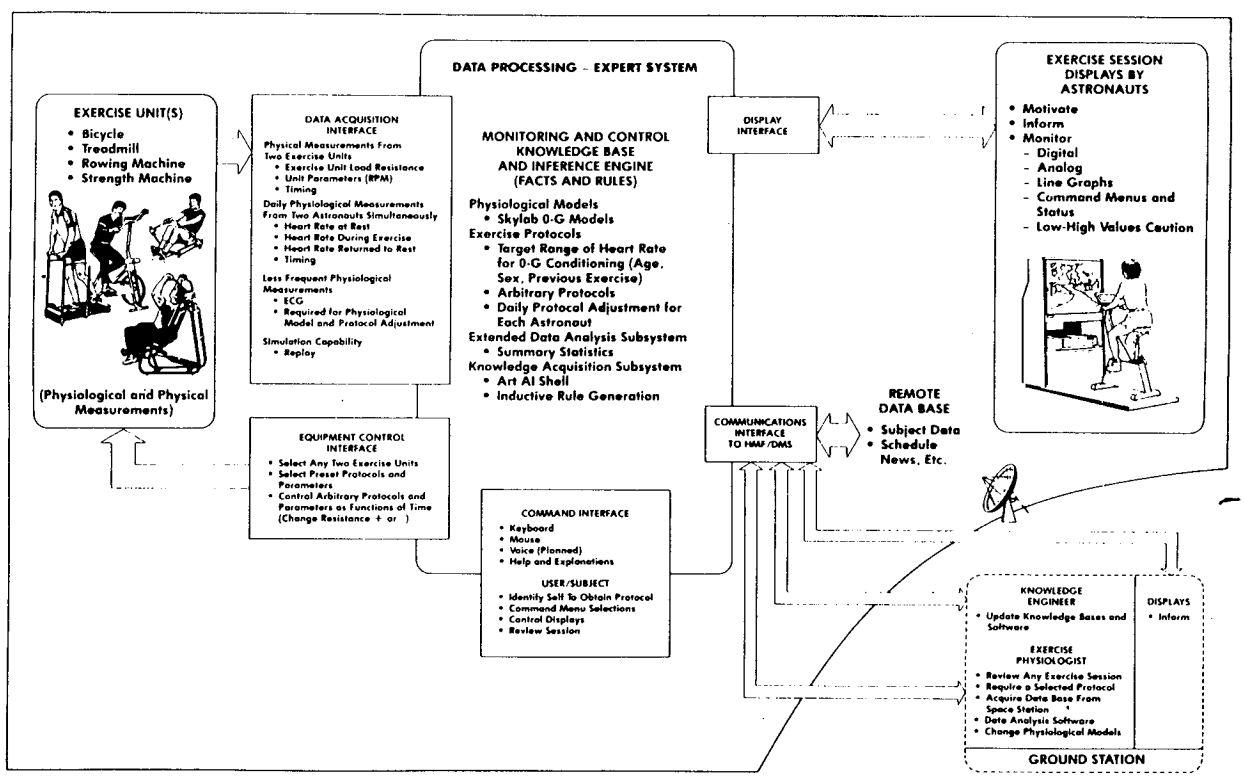

Figure 2. Prototype Concept

NASA
Lyndon B. Johnson Space Center

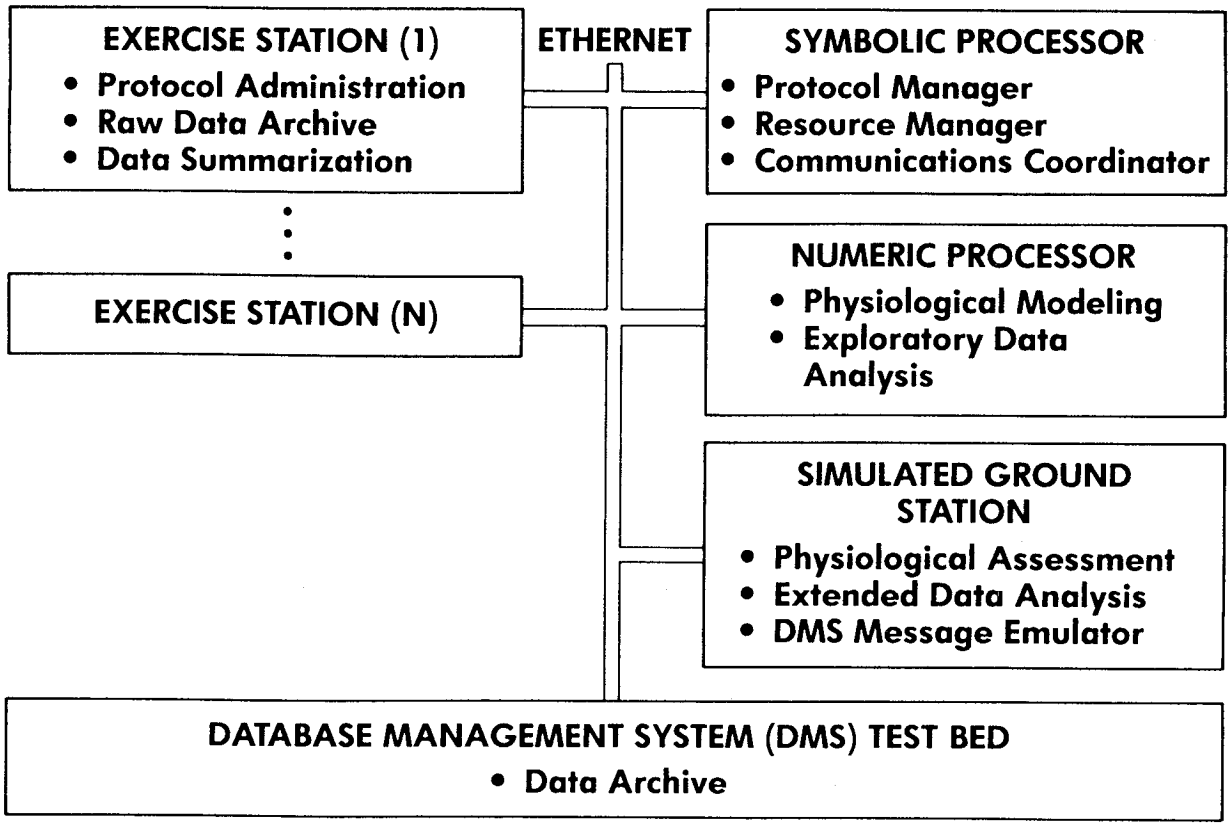

Figure 3. HEMACS-II Functional Overview.

The current design concept for HEMACS includes three elements (Fig.3): (1) physiological and exercise device workload measurements, (2) symbolic processing for monitoring and control, and, (3) numerical processing for simulation and data analysis. HEMACS has a distributed processing (problem solving) architecture. Distributed problem solving is the cooperative solution of problems by a decentralized and loosely coupled collection of knowledge sources (KS's) (procedures, sets of expert rules, etc.) located in a number of distinct processor nodes. The KS's cooperate in the sense that no one of them has sufficient information to solve the entire problem; mutual sharing of information is necessary to allow the group as a whole to produce a solution.

Expert System for Monitoring and Control of Exercise Sessions

The core expert system incorporates the capability to reason about the effectiveness of prescribed protocols by comparing the results of the protocols to model predicted values, and to revise a given crewmember's exercise countermeasure protocol as required. The protocol management function is designed to adjust the protocol for each crew-member from day to day based on rules provided by the exercise physiologist that include heuristics for incorporating trends found in the history of the exercise performance for a given crewmember and condition indices based on the results obtained from simplified cardiovascular microgravity response models, bone demineralization models, etc.

HEMACS contains inference programs to perform conceptual data analysis, finding patterns in data, and providing conceptual or logical descriptions of such patterns. Describing data in terms of logical, functional, and causal relationships is the goal of such analysis. Automated generalizations of many examples is used to find common features of similar objects and distinct features of disimilar objects. An extension of conceptual data analysis includes use of a program called ASTRA (Automated Structural Rule Acquisition) to evaluate the feasibility of partially automating the knowledge acquisition process. ASTRA is an inductive learning program that discovers rules for classifying objects or events

from examples of classification. The input to the program consists of structural descriptions of objects associated with correct a decision or class. This information is provided by an exercise physiologist along with problem background knowledge. This inductive rule acquisition program operates on symbolic descriptions expressing variable-value logic calculus. This feature of HEMACS will provide a tremendous tool for gaining a better understanding of the physiological effects of microgravity. ■

DOSAGE ROUTES FOR ANTIMOTION SICKNESS DRUGS

C. D. Wood, M. J. Wood, J. E. Manno, B. R. Manno, and H. M. Redetzki
Louisiana State University Medical Center, P. O. Box 33932, Shreveport, Louisiana 71130

A large number of antimotion sickness drugs have been evaluated for effectiveness in preventing motion sickness. The oral route of administration has been used for these medications, and we have long known that they are more effective if taken long enough before exposure to motion to permit complete absorption into the blood stream. Dr. Thornton reported that during his Shuttle flights there was a lack of bowel sounds in crewmembers with symptoms of motion sickness. This lack of gastrointestinal motility could have been due to the effect of antimotion sickness drugs, motion sickness, or the effect of microgravity on the gastrointestinal contents. This laboratory investigated the effects of scopolamine 0.6 with d-amphetamine 5 mg on gastric emptying using nuclear medicine techniques. Two hours after taking the drug the subjects ingested 10 oz. of isotonic saline containing 1mCi of technitium 99m D.P.T.A. The medication produced a slight slowing of gastric emptying, which was relieved by a minimum oral dose of neostigmine (15 mg). Rotation to the M-III endpoint of motion sickness produced a profound inhibition of gastric activity, with 90% of count still in the stomach at 30 minutes, and 47% remaining at the end of the one-hour counting period.

The results of this study demonstrate that motion sickness to the M-III level inhibits gastric motility and thereby the absorption of any oral medications ingested after symptoms of motion sickness are established. Oral medications must be given long enough before exposure to motion to permit absorption into the blood stream. Alternate routes of administration must be used after symptoms appear.

The transdermal (Td.) application of scopolamine 1.5 mg and intramuscular injection of scopolamine 0.2 mg was compared for efficacy with an oral dose of scopolamine 0.6 mg. Time of application prior to testing was 24 hrs for transdermal, 2 hr for oral and 1 hr for intramuscular doses. The transdermal scopolamine produced an increase of 88 head movements above the placebo level (0 line on Fig. I) of 302 head movements. The oral scopolamine 0.6 mg increased tolerated head movements to 120 while the I.M. scopolamine produced an increase of 278. The I.M. route increased the efficacy of scopolamine

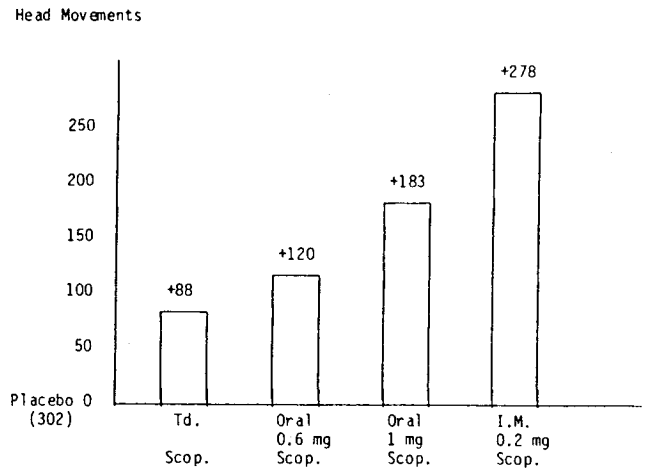

Figure 1. Dosage routes of antimotion sickness drugs.

by a factor of at least 5 over that of the oral route. Therefore the 0.2 mg I.M. dose of scopolamine was equivalent to an oral dose of 1 mg or greater (Fig. I).

The principal side effects reported by the subjects with the various doses and routes of administration are compared in the following table.

TABLE I (eight subjects)

DOSE AND ROUTE	Placebo	Oral 0.6 mg	I.M. 0.2 mg	Transdermal
SIDE EFFECTS:				
Dry Mouth	1	2	5	3
Dizzy	1	3	6	1
Blurred Vision	0	2	3	1
Drowsy	1	2	5	4
Anxiety	1	0	0	1

The side effects of the I.M. dose may be diminished by a concomitant I.M. dose of 25 mg ephedrine. Ephedrine 25 mg I.M. has been shown to be effective in counteracting drowsiness produced by scopolamine and also to prevent slowing of brain waves and loss of performance proficiency in the period following rotation to the M-III endpoint of motion sickness. Further investigations are planned to evaluate the 0.1 mg I.M. dose of scopolamine for efficacy with and without an I.M. dose of ephedrine.

The effectiveness of I.M. doses of 0.2 mg scopolamine given at 1 hr, 2 hrs, 4 hrs, and 6 hrs prior to rotation was tested. The chair was rotated at 7 rpm and the enclosure was rotated at 12 rpm during these tests. These speeds of rotation were most effective in previous studies. The limit of rotation was one hour, which produced 480 head movements unless the M-III endpoint was reached in a shorter time.

In this study the peak effectiveness was found to be at 1 hr as expected. The average number of head movements tolerated declined over the next five hours until it reached a level at six hours that was not significantly above the placebo level. Therefore a second injection would be required between five and six hours after the first injection. This would be indicated by reappearance of symptoms of motion sickness. The I.M. injection is effective even after symptoms appear and therefore can be used therapeutically.

RECOMMENDATIONS

1. The I.M. dose of scopolamine should be used therapeutically, that is, only after symptoms of motion sickness indicate that it is needed.
2. The dose should be reduced to 0.1 mg I.M. This dose should be highly effective with fewer side effects. It also can be repeated if required.
3. An I.M. dose of 25 mg of ephedrine should be given concomitantly with the scopolamine to reduce the side effects and increase the efficacy.

Research supported by NASA Grant NAG-167. ■

CLENBUTEROL, A β_2-RECEPTOR AGONIST, RETARDS DENERVATION ATROPHY OF SLOW SKELETAL MUSCLE

R.J. Zeman, R. Ludemann, G. Silver and J.D. Etlinger
State University of New York Health Science Center at Brooklyn, Department of Anatomy and Cell Biology, Brooklyn, New York 11203

INTRODUCTION

β-adrenergic receptor function is involved in the regulation of numerous metabolic functions including glycogenolysis, Na±K+ transport and adenylate cyclase activity (1). In addition, β_2-agonists can promote skeletal muscle growth and mediate certain training effects (2,3,4). We are exploring the applications of β_2-agonists for conditions that cause muscle wasting, such as weightlessness. Since disuse atrophy is most extensive in slow antigravity muscles, we compared the influence of the β_2-agonist, clenbuterol, on slow and fast muscles deprived of neural input, by denervation, as well as in innervated controls. Our results demonstrate that the β_2-agonist, clenbuterol, is particularly effective in retarding atrophy in chronically denervated slow muscles, since two fold differences were observed in muscle protein and contractile strength. Analysis of muscle fiber populations showed that the atrophy of both slow and fast fibers was reduced by β-agonist treatment, while in innervated muscles, stimulation of muscle growth occurred mostly in fast fibers (2,3).

MATERIALS AND METHODS

Muscle Weight and Protein. Clenbuterol (Boehringer Ingleheim) was administered to female Wistar rats (Charles River, 50-70 gms) at a dose of 1-2 mg/kg/day via the drinking water. At the beginning of the treatment period, unilateral denervation of the hindlimb muscles was performed by sectioning the sciatic nerve at midthigh level in groups of clenbuterol-treated and control rats. After 2-3 weeks, soleus, extensor digitorum longus, anterior tibialis, and gastrocnemius muscles were freshly dissected from both hindlimbs of control and clenbuterol-treated Wistar rats and weighed. Muscles from control and clenbuterol-treated unoperated rats were obtained after 2-12 weeks. Muscles from denervated rats were dissolved in 1 M NaOh at 100°C and assayed for protein with Bradford reagent (Biorad), using bovine serum albumin (Sigma) as a standard. In innervated solei, rates of synthesis of the myosin light chains were measured according to the methods of Silver and Etlinger (5) after incubating the muscles for two hours at 37°C in Krebs-Ringer bicarbonate solution containing 833 uCi/ml ^{35}F-methionine. Under these conditions, rates of incorporation of methionine into total protein of muscles from control and clenbuterol treated rats were equal.

Muscle Contractility. Soleus and extensor digitorum longus muscles from rats treated as above were placed in a temperature-regulated (25°C) chamber containing Krebs-Ringer bicarbonate solution gassed with 95% O_2/5%CO_2. Isometric twitch and tetanic tensions were recorded as previously described (2).

Cross-sectional Area of Muscle Fibers. Soleus muscles from control and clenbuterol-treated rats were sectioned and stained for myosin ATPase according to the methods of Brooke and Kaiser (6). Type I and II fiber cross-sectional areas were measured planimetrically in 100-300 fibers in each section.

RESULTS AND DISCUSSION

Denervation, itself, produced marked decreases in the weight (41-67%) and protein content (38-82%) of the four muscles sampled, relative to the muscles in the contralateral mobile limbs. Clenbuterol reduced the loss in wet weight due to denervation to 16-37% and reduced the loss in protein content to 21-63%. When the clenbuterol-treated denervated soleus, anterior tibialis and gastrocnemius muscles were compared directly to the untreated denervated muscles, approximately twice the protein content was found. The denervated extensor digitorum longus was exceptional in that protein content was not altered by clenbuterol treatment, while approximately two-fold increases were observed with the other muscles. The extensor digitorum longus also exhibited the smallest decreases in weight and protein content in response to denervation. In general, the extent of the sparing effect of β-agonist treatment on denervated hindlimb muscles increased with the degree of atrophy caused by denervation. In contrast, in the innervated limbs, clenbuterol caused only small increases (20-32%) in muscle weights and

protein content was elevated significantly only in extensor digitorum longus (32%) and the anterior tibialis (19%).

To determine whether clenbuterol caused increases in functional muscle mass, the isometric contractions of denervated and innervated muscles were measured. Clenbuterol treatment increased the maximal tetanic tension of denervated solei 129%, but had no significant effect on the innervated solei or the the extensor digitorum longus muscles, whether denervated or innervated. Although clenbuterol also increased the cross-sectional area of denervated solei 24%, this increase was insufficient to account for the much larger increase in contractile tension. Thus, when the maximal isometric tensions of denervated solei were normalized to the muscle cross-sectional area, this specific tension was still increased substantially (91%) while little or no change was observed in the other muscles.

Since denervation can markedly alter muscle histology resulting in altered proportions of non-contractile elements, we examined the profiles of individual fibers. Measurements of fiber cross-sectional areas in cryostat sections showed that denervated soleus fibers are approximately twice as large after clenbuterol treatment (Figure 1). In addition, these treated fibers were surrounded by less extracellular space. These results suggest that the increased contractile strength of these muscles is due, in large part, to a decline in muscle fiber atrophy. Examination of histochemically identified slow and fast fibers showed that the effects of β-agonist treatment were nonselective since atrophy was reduced equally in both fiber types.

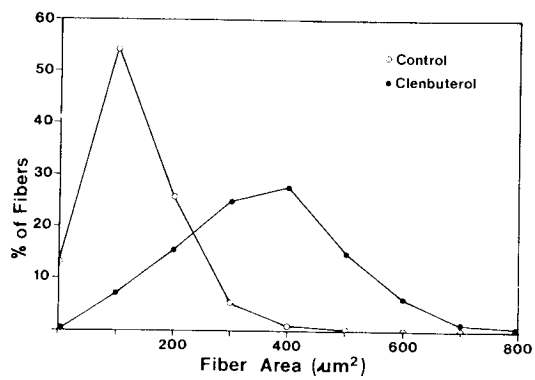

Figure 1. Frequency distributions of muscle fiber cross-sectional areas of denervated soleus muscles from control and clenbuterol treated rats at two weeks. For comparison, the mean soleus fiber area of unoperated control rat was 1006 μm^2. Figure from reference 2.

In contrast, treatment of unoperated rats with clenbuterol for two weeks resulted in a 10% increase in the cross-sectional areas of slow and fast fibers within the soleus. However, after 8-12 weeks of treatment, fast fibers were 17-40% larger while no difference was observed in the slow fibers. Figure 2 shows the effects of clenbuterol on the size distribution of fast fibers expressed as a percent of total fibers after 8 weeks of treatment. Clenbuterol increased the proportion and mean size of the fast fibers without affecting the range of fiber sizes. Increases in maximal tetanus tension of 26-31% were observed in both solei and extensor digitorum longus muscles during 2-12 weeks of treatment with

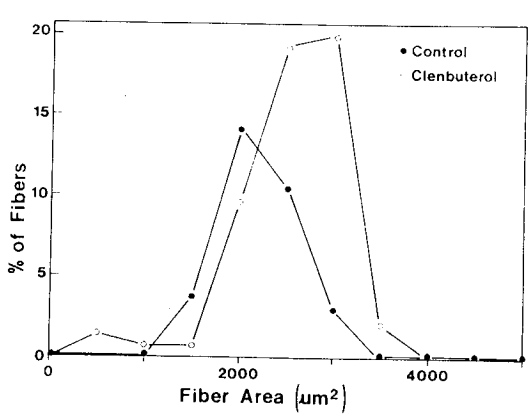

Figure 2. Frequency distributions of type II muscle fiber cross-sectional areas of denervated soleus muscles from control and clenbuterol treated rats at eight weeks. The frequencies of type II fibers at each size interval are expressed as a percentage of total fibers examined in the muscle.

clenbuterol. However, the greater tension was paralleled by 22-35% increases in muscle cross-sectional area in the EDLs, while cross-sectional area was not significantly increased in the soleus until 12 weeks (29%). After 2 and 4 weeks of treatment the solei exhibited increases in tetanus tension toward values characteristic of fast muscle, which is consistent with slow to fast fiber conversion.

During the treatment period, contractile speed progressively increased in the solei, since twitch contraction and half-relaxation times were reduced 15% and 16%, respectively, at 4 weeks and 34% and 47% at 12 weeks while no differences were observed at 2 weeks. In addition, in the solei, rates of synthesis and the content of fast myosin light chains, LC1f, LC2f and LC3f were increased 42-244% after 8 weeks of treatment. This was accompanied by a 21-23% decrease in the synthesis of the slow myosin light chains LC1s and LC2s. Our results suggest that in the innervated soleus, the muscle hypertrophy is mostly due to selective growth in fast fibers that occurs progressively with clenbuterol treatment.

A prominent result of our study is that clenbuterol treatment spares muscle mass and contractile function in an antigravity muscle undergoing denervation atrophy. The muscle wasting that occurs subsequent to denervation is thought to be largely due to inactivity since electrical stimulation greatly retards the atrophy (7). We are currently examining hindlimb-suspended rats in order to determine whether the disuse atrophy of slow muscle that occurs with this model can also be retarded by clenbuterol. ■

REFERENCES

1. Bowman, W.C. Effects of adrenergic activators and inhibitors on the skeletal muscles. In Handbook of Experimental Pharmacology, Vol. 54/II. Szekeres, L. editor. Springer Verlag, Berlin, Heidelberg, 47-128, 1980.
2. Zeman, R.J., R. Ludemann, and J.D. Etlinger. Clenbuterol, a β_2-agonist, retards atrophy in denervated muscles. Am. J. Physiol. 252 (Endocrinol. Metab. 15): E152- E155, 1987.
3. Zeman,R.J., R. Ludemann, G. Silver, and J.D. Etlinger. Slow to fast alterations in skeletal muscle fibers caused by clenbuterol, a β_2-receptor agonist. (submitted for publication).
4. Ji, L.L., D.L.F. Lennon, R.G. Kochan, F.J. Nagle, and H.A. Lardy. Enzymatic adaptation to physical training under β-blockade in the rat. J. Clin. Invest. 78:771-778m 1986.
5. Silver, G. and J.D. Etlinger. Regulation of myofibrillar accumulation in chick muscle cultures: evidence for the involvement of calcium and lysosomes in non-uniform turnover of contractile proteins. J. Cell Biol. 101:2383- 2391, 1985.
6. Brooke, M.H. and K.K. Kaiser. Muscle fiber types - how many and what kind? Arch. Neurol. 23:369-379, 1970.
7. Lomo, T., R.H. Westgaard and L. Engebretsen. Different stimulation patterns affect contractile properties of denervated rat soleus muscles. In Plasticity of Muscle. D. Pette, editor. Walter de Gruyter. Berlin, New York. 297-309, 1980.

PRECEDING PAGE BLANK NOT FILMED

Parallel Sessions

PAGE 138 INTENTIONALLY BLANK

MODELS OF BONE HYPERTROPHY DUE TO INTENSE PHYSICAL FITNESS AND BONE ATROPHY DUE TO IMMOBILIZATION

J. E. Block, H. K. Genant, G. Brooks, C. Wilmont and P. Steiger
University of California, San Francisco, California

To assess the validity of previous research on the effects of exercise on bone mass, cross-sectional and longitudinal studies were evaluated for adherence to several methodologic criteria. In general, good methodologic rigor was not used in these studies, making the interpretation of their results difficult and potentially rendering their conclusions invalid. Common flaws included inadequate description of subjects and fitness regimens, failure to utilize blind outcome assessment, lack of discussion of exercise compliance, substantial subject attrition and inadequate statistical adjustment for drop-outs, no estimations of the necessary sample size, and uniform absence of randomization in longitudinal trials.

To address the inherent problems identified in previous studies of exercise and bone mass, we initiated a broad-based, three-phase research effort. The first phase of this series is complete; specifically, a pilot cross-sectional investigation aimed at evaluating the possible role of different and distinct fitness regimens on vertebral bone density. Briefly, young males engaged in both weight-training and aerobic forms of exercise had significantly greater bone density than individuals engaged in either regimen alone or relatively sedentary individuals.

Phase II of our research effort will commence during the second quarter of 1987. Our aim is to elucidate the factors associated with increased bone mass among different types of exercisers and decreased bone mass following immobilization. Correlations of spine and hip bone density under investigation include associated muscle mass, associated muscular strength, and overall aerobic fitness (VO2max). Exercising subjects include college varsity swimmers and weight-lifters; while immobilization subjects will include post-trauma para- and quadraplegic students. The identification of models or mechanisms of bone hypertrophy and atrophy will aid in the characterization of effective interventions for building bone mass among healthy adults and retarding bone loss during immobilization.

Based upon the results of our second phase, we will conduct a randomized well-defined study of the effects of the most potentially beneficial exercise programs on bone mass at multiple skeletal sites (Phase III). Rates of change in bone mass between exercisers and non-exercisers will be compared after a two year trial. Subjects will include young males at the time of peak bone mass development, with initial study recruitment slated for 1988. ■

QUANTITATIVE IMAGE EVALUATION TECHNIQUES FOR QUANTITATIVE COMPUTED TOMOGRAPHY IN LONGITUDINAL STUDIES

P. Steiger, H. K. Genant, S. Steiger, J. E. Block, and R. Smith
Department of Radiology, University of California at San Francisco, San Francisco, California

Bone mass measurements are important tools in assessing bone loss in all forms of osteoporosis. Modalities widely in use today include: Quantitative Computed Tomography (QCT), Single Photon Absorptiometry (SPA), Dual Photon Absorptiometry (DPA) and various X-ray techniques for assessing vertebral fractures and cortical thickness. The strength of QCT lies in its unique capability to accurately locate a sample of purely trabecular bone in the axial skeleton.

We developed a software system called QUIET (Quantitative Image Evaluation Technique) that performs quantitative image evaluation (QIE) on either single (2-d) or stacked (3-d) images by evaluating calibration phantoms, automatically determining regions of interest, and logging all evaluation data in a patient data base for statistical analysis and future reference during follow-up visits of the same patient. QUIET contains a module (called VB) developed specifically for vertebral body analysis. Apart from doing automated image evaluation for different regions of interest of the vertebral body, VB supports a number of automatic quality control functions. Other elements of QUIET allow the contour finding of other objects of potential interest such as muscles.

We will present the techniques we use for image evaluation and quality control and illustrate each step between measurement and statistical evaluation ■

EFFECTS OF WEIGHTLESSNESS ON THE HUMAN MUSCULOSKELETAL SYSTEM: RESULTS OF SKYLAB SPACEFLIGHT STUDIES

G. D. Whedon
Consultant, Medical Research Programs, Shriners Hospitals for Crippled Children, Tampa, Florida 33622

The idea that the weightlessness of space flight might have deleterious effects on the musculoskeletal system arose from observations in normal human beings that restricted bed rest resulted in significant losses of calcium and nitrogen. The longest observation showed that urinary calcium remained significantly higher than control levels for as long as bed rest was continued (7 months); calcium balance remained on the average at -200 mg/day during bed rest.

The first opportunity to study comprehensively the possible effects of weightlessness on calcium metabolism came in the U.S. Skylab program of 1973-1974. The mineral and nitrogen metabolic balance study required of the three astronauts on each flight nearly constant dietary intake, continuous 24h urine collections, and total fecal collections. In flight calcium excretion in the urine increased in a pattern of gradual rise over the first 2.4 weeks to a plateau level varying in different astronauts from 60% to more than 100% greater than the control level, which persisted throughout the flights. Fecal calcium excretion showed an unusual but fairly consistent pattern of a decrease during the first few weeks in flight, followed by a gradual rise to levels greater that in the preflight control phase, presumably reflecting decreasing intestinal absorption of calcium. Calcium balance shifted from positive during preflight to negative inflight, with much interindividual variation. Bone mineral content measurements by photon absorptiometry showed significant losses in the os calcis in the 3 astronauts who had the greatest increase in urinary calcium and greatest negative shifts in calcium balance.

Nitrogen balance data revealed during flight an increase in urinary nitrogen excretion of 20%. The average daily negative nitrogen balance in weightlessness was 0.9 g, equivalent to a loss per month of a little less than 2 pounds of muscle protoplasm, despite muscular exercise.

The increases in urinary calcium of astronauts in space flight were strikingly similar in pattern to those observed in immobile bed rest and nearly as great in degree. The total calcium loss rate generated by the second month in space amounted to approximately 5.5 g/month or about 0.4% of total body calcium per month. If mineral loss continued at this rate in very long flights, as is expected, in one year to total loss would be 5%. However, since in this situation losses are differentially greater in the lower extremities, decreases in bone content there could be as much as 25%, clearly putting such bones at risk for fracture. Development of effective countermeasures is indicated. ■

IMPEDANCE CARDIOGRAPHY FOR SPACE PHYSIOLOGY

M.A.B. Frey
Biomedical Operations and Research Office and The Bionetics Corporation, John F. Kennedy Space Center, Florida 32899

Cardiovascular disease is a major health risk for the American population and, thus, is potentially a risk for our astronauts whose ages range from 30 to 60 years. Furthermore, some aspects of spaceflight are known to affect cardiovascular function. Therefore, monitoring and evaluating cardiac function is essential in the care of our astronauts. NASA needs the capability to measure stroke volume and cardiac output inflight—both at rest and during work—and on the ground for monitoring crewmembers pre- and postflight and for research with human volunteer subjects and animals models.

Impedance cardiography (IC) is one technique which potentially provides this capability for NASA. It is a noninvasive method for determining stroke volume, which is based on the theory of conduction of electricity and on empirical data. This paper will discuss theory and application of the technique, shortcomings, advantages, and validity, and some data obtained by biomedical researchers at the Kennedy Space Center (KSC).

IC considers the thorax to be a volume conductor of electricity with a relatively constant component of impedance plus a changing component which is a function of the movement of blood into the aorta. Electrical current is transmitted between electrodes across the thorax, and constant monitoring of the resultant potential difference (PD) with surface electrodes allows calculation of the impedance (Z) from Ohm's equation, Z = PD/current.

This technique, as most commonly used today, was developed by Kubicek (5). Four band electrodes are placed circumferentially around the body: bands 1 and 2 are located at the neck; bands 3 and 4 are located at the upper abdomen. A physiologically-safe, 4-mA r.m.s., 100-kHz alternating current is passed between outer electrodes 1 and 4. PD is monitored between inner electrodes 2 and 3. Stroke volume is calculated as $SV = \Delta V = \rho \cdot L^2/Z_o^2 \cdot T \cdot (dZ/dt)_{min}$ where: ρ (ohm.cm) is resistivity of blood; L (cm) is distance between electrodes 2 and 3; Z_o (ohm) is basal impedance; T (sec) is ejection time from the dZ/dT trace; and $(dZ/dt)_{min}$ (ohm.sec-1) is peak amplitude of dZ/dt.

This technique is based on many assumptions, including: (1) the thorax is a cylinder; (2) Interelectrode tissue is homogeneous conducting material; (3) Reactive component is negligible: $\Delta Z = \Delta$Resistance; (4) dZ/dt reflects cardiac events. (5) ΔV is a function of the resistivity of blood; (6) L and cross-sectional area are not changed by ΔV; (7) Max dZ/dt applies over entire ejection time, *i.e.*, runoff during ejection can be ignored.

Comparison with other, invasive techniques shows IC to be valid in many circumstances which are summarized and discussed by Mohapatra (6). Absolute values for stroke volume by IC have correlated well with values from electromagnetic flow probes in humans and animal models. IC appears to be reproducible, more so than dye dilution. And IC is especially well correlated with other techniques when looking at relative changes after intervention, as opposed to absolute values. In many tests, however, IC has failed to correlate well with other techniques when comparing absolute values, and the correlations are especially poor when monitoring critically ill patients (4). Modifications of Kubicek's equation based on more sophisticated theory and experimental data reportedly improve its accuracy (1,2,3).

The shortcomings of IC include lack of standardization of procedures among users and lack of certainty in the theoretical bases for the technique. Individual variations in Z_o and L produce inaccuracies and poor interindividual comparisons for stroke volume. Furthermore, the technique is of no use in situations, such as severe cardiovascular abnormalities, where a decipherable dZ/dt waveform cannot be obtained.

Nevertheless, the technique has many advantages which make it potentially valuable to NASA. It is noninvasive, except for the introduction of electrical current, and is safe even for continuous monitoring.

It is simple to perform and requires no active participation by the subject. It is reliable and is especially good for serial intrasubject measurements and comparisons. In addition to a beat-by-beat measure of stroke volume, IC provides other information relative to cardiac function, such as systolic time intervals, and thoracic fluid volume. And, the equipment is convenient for laboratory or flight use.

At KSC, we have used IC to study responses to lower body negative pressure (LBNP) and head-down tilt (HDT), to postural changes, and to hyperhydration and dehydration. We are currently analyzing impedance (dZ/dt) waveforms as a function of body habitus to increase our understanding of the technique and its possible drawbacks.

In conclusion, IC is a potentially valuable technique for NASA's use inflight and on the ground. It offers many advantages. Additional research is needed, however, to refine the technique to accurately monitor absolute values for stroke volume and cardiac output.

ACKNOWLEDGMENTS

The author acknowledges the significant contributions of the following individuals at the Kennedy Space Center; G.H. Hoffler and C.M. Tomaselli who were Principal Investigators of studies referenced herein; D.S. Doerr and H. Reed for getting the IC technique operational at KSC; K.L. Mathes and M.L. Lasley for extensive activity in using the technique; and P. Buchanan for his support of the laboratory and research. She also thanks Dr. D.S. Miles of Wright State University for sharing his library on impedance cardiography. ■

REFERENCES

1. Appel, P.L., H.B. Kram, J. Mackabee, A.W. Fleming, W.C. Shoemaker. Comparison of measurements of cardiac output by bioimpedance and thermodilution in severely ill surgical patients. Critical Care Medicine. 14:9333-5, 1986.
2. Bernstein, D.P. Continuous noninvasive real-time monitoring of stroke volume and cardiac output by thoracic electrical bioimpedance. Critical Care Medicine. 14:898-901, 1986.
3. Bernstein, D.P. A new stroke volume equation for thoracic electrical bioimpedance: Theory and rationale. Critical Care Medicine. 14:904-9, 1986.
4. Donovan, K.D., G.J. Dobb, W.P.D. Woods, B.E.Hockings. Comparison of transthoracic electrical impedance and thermodilution methods for measuring cardiac output. Critical Care Medicine. 14:1038-44, 1986.
5. Kubicek, W.G., F.J. Kottke, M.U. Ramos, R.P. Patterson, D.A. Witsoe, J.W. Labree, W. Remole, T.E. Layman, H. Schoening, J.T. Garamella. The Minnesota impedance cardiograph - theory and applications. Biomedical Engineering. 9:410-6, 1974.
6. Mohapatra, S.N. Noninvasive Cardiovascular Monitoring by Electrical Impedance Technique, Pitman Medical.

CARDIOVASCULAR RESPONSES TO SIX HOURS OF HEAD DOWN TILT

D. R. Pendergast, D. Bascom and L. E. Farhi
Department of Physiology, State University of New York at Buffalo, Buffalo, New York 14214

INTRODUCTION

Previous investigators have studied the cardiovascular and renal responses to simulated zero gravity utilizing head down tilt, focusing on daily responses of the renal system over several days of HDT or shuttle flights. More recent work in our laboratory (utilizing head out water immersion, WI, in thermal neutral water to simulate weightlessness) has shown that cardiac output, $\dot{Q}$, increases initially (~40%); however, it is modulated over the first 3-4 hrs of WI and remains at pre-immersion levels from this time until 6 hrs. Mean arterial blood pressure ($\bar{P}a$) is not significantly affected by the increase in $\dot{Q}$ as muscle blood flow (qm) is increased, and as $\dot{Q}$ returns to pre-WI levels, qm decreases to pre-WI levels. Although there is a diuresis during WI, plasma volume increases initially, ~8% during the first 30 min, and returns to pre-WI levels after 1 hr, where it remains for the next 5 hrs of WI.

METHODS

We conducted the present study to examine the cardiovascular responses to 6 hrs of HDT (6°) as a model of weightlessness. The subjects (n = 7) completed two protocols: the first (control) was 8 hrs of sitting; and the second, 1 hr of sitting, 6 hr in the 6o HDT position, followed by 1 hr sitting. Measurement of $\dot{V}O_2$ (open-circuit), $\dot{Q}$ (CO_2 rebreathing), heart rate (HR, ECG), blood pressure (ausculation), urine volume (UV), plasma hematocrit, hemoglobin, protein, sodium (Na), potassium (K), creatine (Cr), urinary Na, K, and Cr and forearm and calf blood flow (plethysmograph q_A, q_L) were measured hourly throughout the experiments. From the measured data, stroke volume and plasma volume were calculated. All data were analyzed by a multivariate analysis of variance for repeated measures ($P<.05$).

RESULTS

Oxygen consumption decreased significantly from .280 ± .16 SEM to significantly from 6.70 ± .38 l·min to 7.56 ± .67 and 7.41 ± .33 $l \cdot min^{-1}$ at .5 and 1.0 hrs of HDT and subsequently dropped to 6.85 ± .22 $l \cdot min^{-1}$ over the first 2.5 hrs of HDT after which it was constant and not significantly different from pre-HDT or recovery. Heart rate decreased significantly from 71 ± 3 during pre-HDT to 66 ± 4 and 59 ±1 $b \cdot min^{-1}$ at .5 and 1 hr, respectively, after which it remained constant until the recovery period where it increased to the pre-HDT level (69 ± 2 $b \cdot min^{-1}$). Stroke volume increased significantly from 95 ± 6 to 125 ± 11 ml, where it remained throughout the 6 hr of HDT, returning to pre-HDT levels during recovery (97 ± 3 ml).

In spite of the initial increase in $\dot{Q}$, and its subsequent decrease, systolic (118 ± 3), diastolic (66 ± 2) and mean (88 ± 2) blood pressure (mmHg) did not change significantly during HDT (6 hrs) or recovery. The total peripheral resistance decreased from 13.13 to 11.64 $mmHg \cdot l/min^{-1}$ during the first hr of immersion, after which it returned to 12.90 $mmHg \cdot l/min^{-1}$ during HDT and recovery. Calf blood flow (1.25 ± .11 ml/cm) did not change during the first 4 hrs of HDT; however, it decreased significantly during recovery (0.7 ± .08 ml/cm). Forearm blood flow decreased significantly from 1.45 ± .25 ml/cm during pre-HDT to 0.9 ± .12 ml/cm after 1 hr of HDT, where the level of A remained for the remainder of the experiment.

Plasma hemoglobin did not change significantly during HDT or recovery when compared to pre-HDT (14.5 ± .2 cm/dl). Hematocrit (45.3 ± .6%) and plasma protein (71.4 ± 1.4 mg/ml) decreased significantly from pre-HDT by 5% the .5 hr of HDT after which time they returned and remained at pre-HDT levels. Calculated plasma volume increased significantly (from 100 to 104.5+%) with increase up to 106% after 5 hr HDT. Urine flow increased from 3.4 ± 0.9 to 5.0 ± 0.6 $ml \cdot min^{-1}$ for the first 2 hr and then decreased to 2.0 ± 0.4 ml·min over the remaining 3 hr and recovery. Plasma osmolality (286 ± 1.4 m Osmos/kg) remained unchanged during HDT and recovery; however, plasma sodium and chloride increased and plasma potassium and creatine decreased significantly during HDT. The diuresis and plasma volume changes were accompanied by a natriuresis and kaliuresis as well as increased creatine clearance.

DISCUSSION

Initial responses: The results from the present study confirm the results of previous investigations using HDT and WI, indicating that HDT results in an initial ~15% increase in $\dot{Q}$ and SV. These changes are accompanied by a hemodilution of blood (5% after ~.5 hrs) and increases in plasma sodium, potassium, and chloride which are followed by a potent diuresis (170% increases in UV). In spite of the increased $\dot{Q}$, the mean arterial blood pressure appears to be tightly regulated as it does not increase. The vascular resistance of calf and arm blood flow does not decrease, and therefore the decreased TPR was a result of vasodilation of other vascular beds. From these data it would appear that there is a translocation of blood to the chest, causing an increase in SV and $\dot{Q}$. In addition, there is a movement of fluid and ions into the plasma, presumably from cells that subsequently result in a diuresis, natriuresis, and kaliuresis.

Sustained Responses: After the initial increase in $\dot{Q}$, this variable returns to pre-HDT levels within the first 2.5 hrs of HDT, where the value remains throughout the remaining 2.5 hrs of HDT. It is most important that $\dot{Q}$ does not decrease significantly when the subjects are seated after the 6 hrs of HDT. The decrease in $\dot{Q}$ over the 2.5 hrs of HDT is independent of plasma volume, as it is not depressed, and is most likely due to a decrease in SV, which is offset by the significant decrease in HR. These findings are consistent with a decreased sympathetic tone over the entire period of HDT. Other than a transient

(~1-2 min) very mild lightheadedness, the $\dot{Q}$ and $\bar{P}a$ does not decrease upon standing and sitting after the HDT. This ability to control $\bar{P}a$ was most likely due to the normal plasma volume and vasoconstriction of leg and arm blood flow during recovery. It would appear from these data that if orthostatic intolerance (cardiovascular deconditioning) was present, as was the case in one subject, it would be due to the absences of vasoconstriction of leg blood vessels. ■

CARDIOVASCULAR RESPONSES TO A SIMULATED SHUTTLE LAUNCH PROFILE

D. R. Pendergast and L. E. Farhi
Hermann Rahn Laboratory of Environmental Physiology, Department of Physiology, State University of New York at Buffalo, Buffalo, New York 14214

INTRODUCTION

Previous studies have investigated the cardiovascular responses to simulated weightlessness. Other studies have examined the cardiovascular responses of astronauts in spaceflight. Little data are available for the first hours of spaceflights; likewise, we are not aware of any data obtained just prior to or during launch. To this end, we have investigated the cardiovascular responses to a simulated prelaunch and postlaunch profile.

METHODS

Specifically, subjects (n = 7) reclined in a flight chair with 6° tilt for both legs and torso. Prior to assuming the HDT position, 1-hr sitting control measures were made. The subject then reclined in the flight chair for 3 hrs (preflight). After this preflight period, a simulated launch was performed (1 to 2 to 1 Gz over an 8-min period). In the postlaunch period, the subjects remained in the HDT position to simulate weightlessness. During the prelaunch and postlaunch periods subjects were not given fluid. Thirty minutes prior to the sitting recovery period of 1 hr, the subjects were given 1 liter of water as a "countermeasure."

Measurements of oxygen consumption ($\dot{V}O_2$), cardiac output ($\dot{Q}$), heart rate (ECG), mean arterial blood pressure ($\bar{P}a$), plasma hematocrit, hemoglobin and proteins and urine volume were determined hourly throughout the protocol. Q and HR were measured during the 2 G portion of the launch profile. From the data collected, stroke volume and plasma volume were calculated. All data were analyzed by a multivariate analysis of variance for repeated measures ($P<.05$).

RESULTS

Oxygen consumption (.28> ± .049 SEM $l \cdot min^{-1}$) did not change significantly over the entire 8 hr of the protocol. Cardiac output (6.49 ± 0.5 sitting SEM $l \cdot min^{-1}$) increased during the first hour of HDT (7.29 ± 0.3 l•min) and decreased to 6.98 ± 0.2 l•min after 3 hr. During the launch, $\dot{Q}$ increased significantly (7.64 ± 0.2 1 min); however, it decreased to pre-"launch" levels (7.28 ± 0.3 l•min) immediately after the launch and then decreased to 6.82 ± l•min after 6 hr of HDT. Cardiac output decreased to 6.48 ± .3 l•min during recovery; however, this decrease was not significant from pre-HDT sitting or the values of the last hour of HDT. Heart rate decreased from pre-HDT (68 ± 3 b•min) to 56 ± 3 $b \cdot min^{-1}$ within the first hour of HDT, after which time it did not change significantly during HDT. Heart rate increased significantly during the launch (70 ± 3 b•min) when compared to pre- and postlaunch. Heart rate also increased dramatically. Calculated SV increased from 102 ± 10 ml to 130 ± 11 ml initially during HDT and then decreased progressively to 120 ± 12 ml over the 6 hr of HDT; however, its values were still significantly greater than the values for pre-HDT. During recovery the SV was 99 ± 6 ml, the level of which was not significantly different from the pre-HDT values. Mean arterial blood pressure increased from 92.4 ± 6 mmHg during the pre-HDT to 94 ± mmHg after 1 hr of HDT and then continued to increase up to a value of 98 ± 7 mmHg after 4 hr, after which time it remained elevated, even during recovery. The $\bar{P}a$ during the launch was 99.8 ± 5 mmHg.

In spite of a diuresis (3.0 ± 0.6 to 6.0 ± 1.2 ml•min for sitting and HDT, respectively) and natriuresis (68 ± 12 to 116 ± 13 meq/l for sitting and HDT, respectively) plasma volume did not change

significantly for the first hour. During the second to fourth hour PV increased significantly (3.3 ± 3.0%) after which it returned to pre-HDT levels. As a result of the administration of 1 liter of water as a countermeasure prior to the sitting recovery, there was an increase in PV (5 ± 3.0%) and a marked diuresis (8.3 ± 1.0 ml min).

DISCUSSION

The purpose of the present study was to examine the cardiovascular responses to a simulated launch. As a result of 6° HDT in a flight chair, there was a significant increase in SV and $\dot{Q}$, with a mild increase in Pa. Over the 3 hr period prelaunch, $\dot{Q}$ decreased in spite of the sustained elevation in SV. This was most likely a trend to decrease SV; however, the dramatic increase in HR appears to offset this tendency for SV to decrease, and it remained constant. During the simulated launch, $\dot{Q}$ increased as venous return was increased, but because it was coupled with a dramatic increase in HR the SV decreased. In spite of these increases during increased G, $\dot{Q}$ and SV continued to decrease over the remaining period of simulated weightlessness, and after 6 hr $\dot{Q}$ was not increased when compared to pre-HDT. In spite of the dramatic diuresis PV actually increased over the first 4 hr of HDT, indicating a movement of fluid from the tissues into the plasma. The decrease in SV, $\dot{Q}$ and HR are not a result of decreased venous return secondary to a sympathetic tone. Mean arterial blood pressure increased throughout HDT and recovery, while $\dot{Q}$ was increased and then decreased. This increased Pa pressure suggests a marked and sustained vasoconstriction during the last 4-6 hrs of HDT, which is most likely a result of the feet being elevated above the heart in the HDT position in the flight chair.

We did not observe any orthostatic intolerances during the recovery period following 6 hrs of HDT. $\dot{Q}$ and Pa did not decrease during the recovery period when compared to pre-HDT; in fact, Pa was significantly elevated. In addition, while administration of a 1 liter water countermeasure did increase PV and urine flow, it did not affect $\dot{Q}$ and apparently SV and HR.

It appears the $\dot{Q}$ returns to sitting levels over 6 hrs of simulated weightlessness and that this decrease is independent of plasma volume. Under the conditions of this experiment, there was not orthostatic intolerance, and $\dot{Q}$ and Pa were maintained within normal 1 Gz limits. The administration of a countermeasure altered the renal responses during recovery but had no effect on the cardiovascular variables. ■

DOPPLER ECHOCARDIOGRAPHIC DETERMINATION OF CARDIAC OUTPUT

K. L. Richards, S. R. Cannon and M. S. Lujan
University of Texas Health Science Center and V. A. Hospital, San Antonio, Texas

---

Cardiac output (CO) is the product of cross sectional area of flow (A) times velocity of that cross section of flow (V): (CO) = (A) (V). Combined imaging and Doppler echo allow noninvasive determination of both (A) & (V) at aortic, pulmonic, mitral and tricuspid valves. In adults aortic and mitral valve sites are utilized.

The most accurate method of calculating Doppler cardiac output (1) is to determine aortic diameter (Da) immediately downstream from the Sinuses of Valsalva with A- or M-mode imaging. Because aortic cross section is circular and relatively constant throughout systole, mean (Aa) = $3.14\ (Da/2)^2$. Stroke volume is the product of ascending aortic systolic velocity-time integral (VTa), determined by Doppler, and (Aa). (COa) is the product of stroke volume and heart rate (HR): (COa) = $3.14\ (Da/2)^2$ (VTa) (HR).

Doppler CO (1) correlates well with thermodilution CO (r=.94; SEE = .58L/MIN). The "aortic anulus" is an alternative site (2).

At the mitral valve orifice (VTm) is determined by integrating the diastolic mitral velocity tracing. Mean diastolic mitral cross sectional area (Am) is more difficult to measure because instantaneous mitral area varies greatly in diastole. Methods of estimating mean (Am) include: M-mode echo to determine mean/maximum mitral leaflet separation (3), multiple 2-D echo images, and a constant correction factor (4). (COm) = (CF)(Am-max) (VTm) (HR).

Correlation coefficients & standard errors vary with the method used to determine area (4): r=.78-.94; SEE=.41-.83 L/MIN).

The advantages of using 2 sites for CO include: 1) in normals, accuracy at one site is suggested by similar results at a second site; 2) in patients, valve regurgitation or stenosis, or shunt size, are quantified by comparing CO at different sites. ■

REFERNCES

1. Huntsman LL, Stewart DK, Barnes SR, Franklin S, et al: Noninvasive Doppler determination of cardiac output in man. Circulation 67:593, 1983.
2. Lewis JF, Kuo LC, Nelson JG, Limacher MC, Quinines AM: Pulsed Doppler echocardiographic determination of stroke volume and cardiac output: Clinical validation of two new methods using the apical window. Circulation 70:425, 1984.
3. Fisher DC, Sahn DJ, Friedman MJ, Larson D, et al: The mitral valve orifice method for noninvasive 2-D echo Doppler determination of cardiac output. Circulation 67:872, 1983.
4. Miller WE, Richards KL, Miller JF, Crawford MH: Comparison of Doppler echo methods for measuring cardiac output at the mitral valve. J Am CO11 Cardiol, in press, 1978.

NON-INVASIVE ESTIMATION OF EFFECTIVE PULMONARY BLOOD FLOW DURING EXERCISE STRESS TESTING

G. D. Swanson and D. L. Sherrill
Department of Anesthesiology, University of Colorado Medical Center, Denver, Colorado 80262

Breath-to-breath (B-B) measurements during exercise stress testing yield an estimate of alveolar CO_2 production ($\dot{V}_ACO_2$) via an algorithm that compensates for variation in pulmonary stores (Swanson and Sherrill, *J. of Appl. Physiol.* 55:1936, 1983). The algorithm involves the concept of *effective* lung volume (V'_L); that volume that is effective for pulmonary gas exchange on a B-B basis.

In this paper, these concepts are extended to the estimation of an *effective* pulmonary blood flow. After compensation for pulmonary stores, the remaining $\Delta\dot{V}_ACO_2$ can be related to a variation in arterial CO_2 (ΔP_aCO_2) on a B-B basis via the linear equation $\Delta\dot{V}_ACO_2 = \alpha Q \Delta P_aCO_2$. An estimate of *effective* pulmonary blood flow (Q'_L) is determined by a scatter diagram between $\Delta\dot{V}_ACO_2$ and $\Delta P_{A-}CO_2$ via a linear regression line where $\Delta P_{A-}CO_2$ is an estimate of ΔP_aCO_2. A number of techniques are available for determining $P_{A-}CO_2$ on a B-B basis. These techniques have been evaluated using a computer simulation of pulmonary gas exchange and an appropriate technique has been developed.

These concepts have been applied to the estimation of *effective* pulmonary blood flow during exercise ramp stress testing. This approach yields an estimate of a nominal Q'_L and a rate of change for Q'_L during the ramp test. The results are reported and interpreted in five subjects. They demonstrate the utility of estimating an *effective* pulmonary blood flow from a subject's natural breathing pattern during exercise without artificial maneuvers. ■

VENOUS GAS EMBOLISM

B. D. Butler and J. Katz
Department of Anesthesiology, University of Texas Medical School, Houston, Texas 77030

Studies simulating decompression associated with extravehicular activity (EVA) by astronauts have demonstrated venous gas emboli (VGE) using a precordial Doppler. Oxygen prebreathing regimens have been devised to minimize the development of VGE; however, their success at preventing decompression sickness remains unresolved. We have proposed the examination of several factors associated with VGE and, in particular, the ability of the lungs to protect the systemic circulation from the more serious consequences of arterial air emboli. Our first report concerns the length of time VGE remain as bubbles in the pulmonary circulation. This may become a risk factor when considering multiple episodes of VGE resulting from repetitive EVAs.

To study the residence time of VGE in the pulmonary circulation, air was infused into the right atrium of dogs anesthetized with thiopental and maintained with halothane (0.8–1.5%). Ventilation consisted of oxygen (30%) in air at a rate and volume to maintain $PaCO_2$ (control) at 35–40 mmHg. Three doses of VGE were studied (0.10 and 0.25 $ml.kg^{-1}.min^{-1}$ for 15 mins and 2 ml/kg bolus at 2 ml/sec). Following the VGE, pulmonary artery pressure (PAP), end-tidal CO_2 (ET-CO_2), arterial CO_2 ($PaCO_2$), and pulmonary vascular resistance (PVR) were recorded. After 10 mins recovery, the 70% air was switched to 70% N_2O for 5 mins to amplify the volume of the bubbles. This is possible owing to the relative differences in solubility of N_2O and nitrogen in blood (0.46 and 0.013 blood gas partition coefficients, respectively). Nitrous oxide is quickly taken up by the bubbles causing them to increase in volume and hence elicit hemodynamic responses consistent with VGE. The subsequent rise in PAP (>2 mmHg), $PaCO_2$ (>2%) and PVR (>10%), and fall in ET-CO_2 (<1%) associated with the expanded bubbles were interpreted to reflect the presence of residual intravascular pulmonary gas. This procedure was repeated until no further response was elicited. Control animals were ventilated with 70% N_2O, 30% oxygen without VGE. The mean residual times for the pulmonary vascular bubbles were 33±10 mins (0.10 $ml.kg^{-1}.min^{-1}$), 35 ±10 mins (0.25 $ml.kg^{-1}.min^{-1}$) and 30±10 mins (bolus). VGE produced by decompression for EVA may continue to shower the lungs for prolonged periods of time, partially depending upon the degree of denitrogenation, exercise, and pressure reduction. However long the tissue source for VGE, the results of this study suggest that up to 35 mins may be necessary for excretion of the gas phase once the bubbles reach the lungs.

In a second project, we are examining the pressure gradient across the pulmonary vasculature following VGE and at the instant that the bubbles are observed to spill over into the arterial circulation. Dogs are anesthetized with halothane and ventilated with oxygen (30%) in air. Blood pressure is measured with a catheter placed into the abdominal aorta via the femoral artery. A left lateral thoracotomy is performed between the 5th and 6th ribs and the 6th rib removed to gain clear access to the pulmonary left lower lobe (LLL) vein. A pressure-monitoring catheter is placed in the left atrium and a pulmonary artery catheter is placed directly into the LLL artery via the jugular vein. Cardiac output is measured using thermodilution. VGE are infused into the proximal lumen of the pulmonary artery catheter at 0.35 $ml.kg^{-1}.min^{-1}$. This air infusion dose has been previously studied to ensure that spillover of VGE into the arteries occurs in a large percentage of the animals. Venous bubbles that escape filtration by the lungs and spill over into the arteries are detected by a Doppler ultrasonic probe (Parks 912) located directly over the descending aorta.

The mean time to spillover of the VGE into the arteries was 8.8±4.1 mins following the infusion of 64.9±33.8 ml of air. PAP rose from 16±1.4 to 40±4.5 mmHg and pulmonary venous pressure decreased from 9.4±1.1 to 5.7±1.1 mmHg. PVR increased from 252±136 to 1343±673 $dynes.s.cm^{-5}$. The pressure gradient across the lungs (PAP-PV) increased from baseline 6.6±0.7 mmHg to 34.3±4.9 mmHg ($p<0.05$) at the instant that VGE spillover occurred.

The results of this study suggest that a greater than 5-fold increase in the driving pressure (PAP-PVP) is required to push VGE through the pulmonary circulation into the arteries. The results do not delineate the type of vessel involved however.

Supported in part by NASA Grant NAG9-215. ■

DYSBARIC DISORDERS INDUCED BY ALTITUDE DECOMPRESSION

C. P. Chryssanthou, G. Goldstein, T. Palaia, and R. J. Stenger
Department of Pathology, Beth Israel Medical Center and Mount Sinai School of Medicine of the City University of New York, New York, New York 10003

Astronauts and persons operating at high altitudes or in space environments may be subjected to critical reductions in atmospheric pressure and thus expose themselves to the potential dangers of dysbaric disorders. The most common of these disorders is decompression sickness, which produced immediate and overt symptoms and signs. Pressure changes, however, can cause other potentially serious disorders which exhibit no obvious clinical manifestations (e.g., blood-brain barrier alterations) or develop after long latent periods (osteonecrosis).

The objectives of our investigations are to (a) develop animal models for such altitude-induced dysbaric disorders, (b) study their pathogenesis and manifestations, (c) determine possible sex differences in their incidence, and, (d) explore means for their prevention of amelioration. Specific attention is given to (1) decompression sickness (DS), (2) blood-brain barrier alterations (BBB), and, (3) effects on the renin-angiotensin-aldosterone axis.

Animal Models for Altitude-Induced DS and Other Dysbaric Disorders

Dysbaric disorders were produced in albino rabbits, genetically obese mice, and, to a lesser degree, in their thin siblings by subjecting the animals to a simulated altitude of 30,000 feet (4.3 psi) for 45 minutes. The chamber contained a mixture of air and O_2 that at 4.3 psi provided a partial pO_2 equal to that in air at sea level (158.8 mmHg).

Development of DS was evidenced by clinical signs (respiratory distress, pruritus, paralysis, convulsions, and death) and by gross and microscopic findings (intravascular and tissue gas bubbles, perivascular edema, increased BBB permeability). Manifestations of DS were particularly observed in obese mice which exhibited scratching, hiccup, chokes, convulsions and a mortality rate of about 20%. Thin mice developed DS to a much lesser degree. In rabbits, DS was manifested by respiratory distress (17.2%), paralysis (3.4%), convulsions (3.4%), and death (6.9%). Autopsies and histologic examination revealed intravascular gas bubbles in many animals (44.8%), even in those that did not exhibit clinical signs of DS ("silent bubbles"). Some of these "asymptomatic" rabbits, however, developed other dysbaric disorders such as alterations of the BBB and changes in plasma renin activity.

Blood-Brain Barrier (BBB) Alterations Induced by Altitude Decompression

Modification of the BBB by physical, chemical and biological means has long been established. Our previous studies on rabbits and mice, which were subsequently confirmed by other investigators working with guinea pigs and rats, indicate that BBB permeability to vital dyes and antibiotics is altered by exposure to compression-decompression. We have recently observed that changes in the BBB can also be induced by altitude decompression. This conclusion is based on multidimensional studies including gross observations, light and electron microscopy and chemical determination of tracers.

Exposure of rabbits to 30,000 feet for 45 min significantly ($p<0.001$) increased the penetration of an intravenously injected tracer (4 ml/kg of 2% trypan blue) into the cerebrum. Mean due concentration was 27.06 ± 4.42 $\mu g/g$ of brain tissue in experimental animals, while only 4.52 ± 1.52 $\mu g/g$ in controls. Ultrastructural studies suggest that the increased BBB permeability is due to transendothelial vesicular transport, and, occasionally, to penetration through transendothelial junctions. It is important to underscore that BBB changes were observed even in the absence of overt manifestations of DS.

The pathogenesis of BBB alterations is still obscure. It could involve direct mechanical injury of blood vessels by bubbles, ischemic changes, or permeability alterations induced by chemical factors activated by blood-bubble interface reactions. In several animals with BBB changes, however, there was no evidence of gas bubbles. Altitude-induced changes of the BBB are relevant to the pharmacotherapy of astronauts and high altitude fliers. A variety of drugs, particularly those with low lipid solubility or high degree of ionization, which do not readily penetrate the BBB, may do so under conditions of reduced pressure and produce undesirable and even toxic effects.

Effect of Altitude Decompression on Plasma Renin Activity (PRA)

Hypovolemia and hemoconcentration have long been observed in DS. It is conceivable that reduction of the intravascular fluid in DS may stimulate renin elaboration and release. We have previously reported an increase in PRA in animals subjected to compression-decompression. Recently we studied possible implication of the renin-angiotensin-aldosterone system in hemodynamic changes produced by altitude decompression.

Following exposure to 4.3 psi for 45 min, PRA increased in 19 out of 20 rabbits. The mean PRA value was 1.48±0.13 ng AngI/ml/hr prior to exposure and 5.88±0.61 after altitude decompression ($P<0.001$). The hypothesis that altitude-induced increase in PRA may be triggered by reduction of plasma volume is not supported by our findings since there were no significant changes in hematocrit. There are additional pathogenetic possibilities including stimulation of renin production by bradykinin and prostaglandin, both of which have been implicated in dysbaric disorders.

Influence of Sex on the Incidence of Dysbaric Disorders

With the anticipated greater role of women in aerospace activities, determination of the relative susceptibility of females to DS and other dysbaric disorders becomes important in dysbaric medicine and relevant to NASA programs. So far, reports on this question have been contradictory. Some studies suggest higher incidence of DS in women; others indicate no differences in predisposition to DS between males and females. Our studies on mice and rabbits revealed no significant sex differences in susceptibility to altitude-induced DS and to other dysbaric effects such as changes in BBB and PRA.

Prevention of Altitude-Induced Decompression Sickness (DS)

The pathogenesis of DS and other dysbaric disorders has not yet been elucidated. The bubble theory is not all-inclusive and leaves an appreciable deficit in our understanding of these disorders. On the basis of recent evidence it seems plausible that gas bubbles initiate a complex self-propagating disease process, the development and severity of which depend more on secondary factors than on the bubble itself. Bubble-induced platelet aggregation, coalescence of plasma lipids, activation of factor XII, and the subsequent activation of the kinin and coagulation systems may play important pathogenetic roles. Vasoactive agents may be released or activated by various conceivable mechanisms involving cell and tissue disruption by bubbles, anoxia, and blood-bubble interface activity. Our investigations yielded data strongly suggesting that smooth muscle stimulating factors such as bradykinin (BK), histamine (H), and serotonin (5-HT), are implicated in the mechanism of DS. We have been able to prevent DS in animals subjected to compression-decompression with drugs which combine activities against BD, H, and 5-HT. We are currently studying the effect of these drugs on altitude DS. Because antihistiminic drugs produce sedation, which is an undesirable side effect, we are investigating the possible DS preventing effect of H_2-antihistamines (cimetidine) and selected H_1-antagonists (terfanadine), which produce minimal or no impairment of central nervous functions and are considered safe drugs for individuals involved in skilled activities. Since platelets are implicated in DS, we are also exploring the effect of inhibitors of thromboxane production. Preliminary ongoing experiments with aspirin produced encouraging results. Low doses of the drug (2 mg/kg) administered intraperitoneally for several days prior to exposure appear to reduce morbidity and mortality in mice subjected to altitude decompression. (Supported by NASA Grant #NAG-9-86.) ■

A THEORETICAL MODEL OF EXTRAVASCULAR BUBBLE GROWTH DURING EVA

M. Gernhardt
Ocean Systems Engineering, Inc., Visiting Scientist, USRA, Johnson Space Center, Houston, Texas 77058

It is widely accepted that bubbles through some mechanism are the cause of marginal symptoms of decompression sickness. For this reason a theoretical model of extravascular gas bubble dynamics has been derived to aid in developing and evaluating decompression procedures. The model assumes that gas nuclei exist or, through one or more processes, form in extravascular tissues during decompression. The model then describes the subsequent growth and resolution dynamics of a gas bubble during the course of decompression. The model accounts for the diffusion of inert gas across the tissue/bubble interface, gas solubility and diffusivity, surface tension, tissue elasticity and a perfusion limited inert gas exchange with the tissues. The model can account for various breathing gas mixtures, pressurization and depressurization rates.

The model confirms empirical data indicating that without oxygen prebreathing to lower tissue nitrogen tensions, a suit pressure of between 8 and 9.5 psi should protect against DCS when depressurization from 14.7 psi.

The model also displays the expected bubble growth and resolution during the course of an EVA. Through a comparison of maximum bubble size and growth rate, when correlated with empirical data, it is generally able to distinguish the relative DCS likelihood for a variety of complex hypobaric exposures including simulated repetitive EVA's.

The model does not account for the statistical nature of decompression sickness and therefore there is no critical bubble size that would always result in DCS, or conversely, always prevent DCS. Instead, it is thought that the theoretical bubble size could be used as a tool which can be cross referenced to R-values and empirical decompression data. In this manner, patterns of bubble growth and resolution can be used as one index to compare a wide range of aerospace and diving empirical decompression data.

Work is now on-going with the NASA Space Biomedical Institute to correlate the model with empirical aerospace data to further refine the predictive capabilities.

Similar studies are on-going at the University of Pennsylvania and Oceaneering International with empirical diving decompression data. ■

THE RELATION OF WHOLE-BODY NITROGEN ELIMINATION DURING OXYGEN BREATHING TO THE ACQUISITION OF DECOMPRESSION SICKNESS PROTECTION

W. A. Gerth, R. D. Vann and N. E. Leatherman
F. G. Hall Laboratory for Environmental Research, Departments of Physiology, Anesthesiology and Medicine, Box 3823, Duke University Medical Center, Durham, North Carolina 27710

INTRODUCTION

The prevention of astronaut Decompression Sickness (DCS) during Extravehicular Activity (EVA) from the Shuttle Orbiter requires pre-EVA astronaut denitrogenation, which is usually achieved by breathing 100% oxygen for a period preceding decompression. Earlier evidence suggests that the efficacies of such denitrogenations should be improved by factors which enhance whole-body N_2 washout during the oxygen breathing period. In our present work, we are seeking to verify this suggestion and establish a quantitative predictive relationship between the whole-body N_2 elimination profile measured during oxygen breathing and the acquired level of DCS protection.

METHODS

In each experiment, the whole-body N_2 elimination profile is measured from a human subject breathing 100% O_2 for 3.0 hr under each of three different conditions which effect different "whole-body

tissue perfusion states" and different corresponding N_2 elimination profiles. The three conditions are: 1) seated, feet on floor rest [SR]; 2) supine, 6° head-down rest [HDR]; and 3) seated, light bicycle exercise (upper and lower body) [SE]. The N_2 elimination profiles are measured using an open-circuit breath-by-breath method which was developed earlier in this program. After each denitrogenation, the subject walks to an altitude chamber, still breathing 100% O_2, and 3.5 hr after commencing 100% O_2 breathing, is decompressed to the Shuttle EMU pressure of 4.3 psia where an EVA exercise simulation protocol is performed during the ensuing 4.0 hr or until DCS develops. While at altitude, the subject is periodically monitored for bubbles in the central venous circulation using a precordial Doppler ultrasonic technique. A minimum of 6 days elapses between successive runs by a given subject.

Each N_2 elimination profile begins at the first inspiration of 100% O_2 and consequently includes N_2 washed from the pulmonary residual volume to which the subject expires immediately before run start. Accordingly, each profile is adjusted in post-run analysis by subtracting the pulmonary N_2 washout from the whole-body profile. Parameters describing the kinetics of pulmonary washout are found by fitting a series of semi-exponential decay equations to the data using an iterative nonlinear last squares parameter optimization algorithm. The pulmonary compartment is taken as that which emerges from the analysis with the shortest half-time (usually approximately 0.8 min).

Twenty-one man-flights with 10 different subjects have been completed under this experimental protocol and 5 subjects have completed the present three-run experimental series.

RESULTS

A continuing series of control runs show that a given subject produces closely similar N_2 elimination profiles on different days under otherwise practically identical conditions. Figure 1 shows three separate N_2 elimination profiles taken from the same subject while seated at rest. Profiles 2 and 3 were taken three weeks apart in late spring and profile 1 was taken about seven months earlier. The "surge" in profile 3 at the 1 hr mark is attributable to the subject uncrossing his legs at that time.

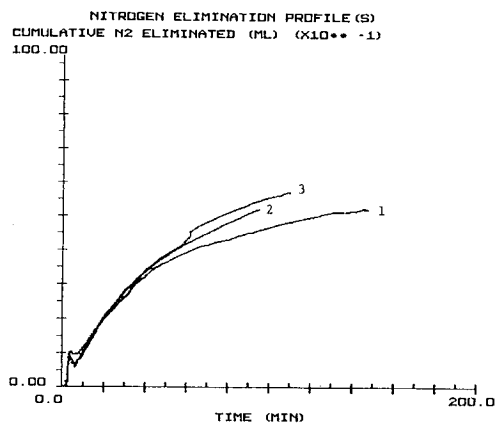

Figure 1.

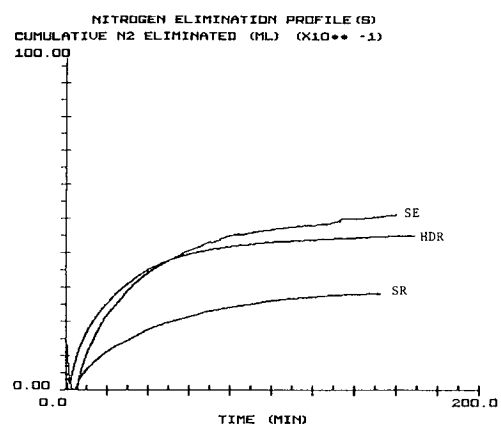

Figure 2.

Each subject acts as his own control when different profiles from that subject are compared and differences are related to corresponding changes in subject response during subsequent hypobaric exposures. Figure 2 shows results for one subject who performed the EVA simulation after each denitrogenation shown. Typically, more N_2 is eliminated at any given time during HDR denitrogenation than at corresponding times during SR denitrogenation. Accordingly, this subject developed central venous gas emboli (VGE) and DCS symptoms during simulated EVA after both the SR and HDR denitrogenations, but onset times for VGE and DCS were increased after performance of the HDR denitrogenation. Another subject who developed VGE and DCS after SR denitrogenation showed markedly increased N_2 elimination during HDR denitrogenation and completed the latter post-denitrogenation EVA simulation DCS free. As exemplified in the Figure, denitrogenation while seated and exercising (SE) tends to cause the largest whole-body N_2 elimination enhancement of the 3 conditions tested. No VGE or DCS symptoms developed during simulated EVA after this or any other subject SE denitrogenation.

CONCLUSIONS

Although results do not yet warrant firm conclusions, they support earlier indications that higher levels of DCS protection are acquired as whole-body N_2 washout during oxygen breathing is enhanced. However, cardiovascular responses during HDR may cause N_2 elimination enhancements in some subjects that improve the level of acquired DCS protection to an extent smaller than improvements achieved with similar or even smaller N_2 elimination enhancements caused by exercise. Increased N_2 elimination during HDR may therefore reflect perfusion increases and enhanced N_2 washout from body tissues that are not involved in DCS, such as splanchnic and adipose tissue, to a greater extent than similar washout enhancements caused by exercise. ■

PATHOPHYSIOLOGY OF SPONTANEOUS VENUOUS GAS EMBOLISM: RELATION TO PULMONARY OXYGEN POISONING

C. J. Lambertsen, K. H. Albertine, D. Flores, and J. Pisarello
Institute for Environmental Medicine, University of Pennsylvania Medical Center, Philadelphia, Pennsylvania 19104-6068

Reduction of ambient pressure from the normal air breathing state of one ATA (as for EVA) can produce venous gas embolism of the lungs even in the absence of symptomatic decompression sickness. Prolonged breathing of oxygen to accomplish partial denitrogenation prior to ambient pressure reduction reduces both venuous gas embolism and likelihood of overt decompression sickness. However, prolonged oxygen breathing at one atmosphere induces progresive pulmonary effects of oxygen poisoning.

This project concerns the effects of venous gas embolism upon blood and lung vasculature, and the interaction of such effects with those induced in the pulmonary airwarys by local effects of oxygen poisoning.

Since the gas lesions and the venous gas embolism of altitude decompression sickness originate in peripheral tissues, the process may introduce chemical products related to local tissue damage into the venous circulation, along with gas emboli. Such chemical factors could add to effects of the gas emboli upon lung or other functions.

To provide reproducible conditions of experimental gas embolism, this investigation in Yorkshire piglets utilizes the spontaneous, steady-state venous gas embolism induced at one ATA by "Isobaric Inert Gas Counterdiffusion" (1,2) without exposure to compression or decompression. The continuing uniform rate of spontaneous, peripherally-generated venous gas embolization is produced by respiration of a normoxic nitrous oxide mixture with the animal surrounded by helium. The different diffusion rates of the two counterdiffusing gases leads to supersaturation of superficial tissues, leading to growth of gas nuclei.

Measurements of hemodynamic changes, and sampling of blood and lung tissue are performed in relation to different durations of gas embolism. The present stage of investigation concerns effects of embolism without prior exposure to pulmonary oxygen poisoning. Investigation of gas embolism in the presence of pulmonary oxygen poisoning will follow. Extensive initial investigations utilized prominent (fatal) degrees of venous gas embolism, in order to identify the nature of effects. The present series seeks to define effects of nonlethal degrees of embolism.

GENERAL SUMMARY

Selected initial observations in more than 12 piglets indicate that (1) the degree of change in hemodynamic functions and survival duration are related to degree of venous gas embolism, (2) lag in appearance of venous gas emboli is not related to surface area of counterdiffusion, and (3) full body (except head and neck) counterdiffusion induces progressive pulmonary hypertension; arterial hypoxia, hypercapnia and acidosis; tachycardia and late arterial hypotension; progressive hemoconcentration and late thrombocytopenia. Coagulation system factors are not activated even after 4 to 6 hours of continuous venous gas embolism.

Following initial experiments, seven full experiments were performed involving physiologic measurements and pathologic examinations in animals exposed to less than full body counterdiffusion (inferior to xiphoid). A unique component of this series was performance of serial biopsy of lung tissue during venous gas embolism, for light and electron micrographic study. These direct pulmonary histopathologic examinations are in progress. Other concurrent measurements have included: pulmonary artery blood pressure, systemic arterial blood pressure, cardiac output, systemic vascular resistance, cardiac frequency and electrical activity, blood cellular (formed element) composition, arterial blood gas tensions and pH.

Detailed findings based upon these multiple pathophysiologic and histopathologic measures, at different degrees of gas embolism, will be presented. ■

REFERENCES

1. Lambertsen, C.J., and J. Idicula. A new gas lesion syndrome in man induced by "isobaric gas counterdiffusion." J. Appl. Physiol. 39:434-443, 1975.
2. Graves, D.J., J. Idicula, C.J. Lambertsen and J.A. Quinn. Bubble formation resulting from counterdiffusion supersaturation. A possible explanation for isobaric inert gas 'urticaria' and vertigo. Phys. Med. Biol. 18:356-364, 1973.

THE EFFECTS OF EXERCISE AND BODY POSITION DURING PRE-FLIGHT OXYGEN BREATHING ON DECOMPRESSION SICKNESS AT 4.3 PSIA

R. D. Vann, W. A. Gerth, and N. E. Leatherman
F. G. Hall Laboratory and Department of Anesthesiology, Box 3823, Duke University Medical Center, Durham, North Carolina 27710

INTRODUCTION

The risk of decompression sickness, be it during altitude exposure or after diving, depends to a large extent upon the dissolved gas content in an astronaut or diver's body. The most common method of reducing the nitrogen content prior to altitude exposure is to breathe 100% oxygen. Our hypothesis is that any procedure which changes the rate of nitrogen elimination will also affect decompression risk. We are presently studying nitrogen elimination and the responses to subsequent decompression under three conditions during oxygen breathing: seated rest, supine rest, and seated exercise. This report summarizes the results of the altitude decompression exposures. The nitrogen elimination measurements are described separately.

METHODS

Each experiment begins with a a 3.5 hour oxygen-breathing period, during which the subject inspires ultrapure oxygen by mouthpiece while wearing nose clips. To eliminate nitrogen leaks, the subject's head is immersed in an oxygen-filled headtent. This period is followed by an 8-minute ascent to an altitude of 30,300 feet (4.3 psia) and 4 hours of standard NASA EVA exercise simulation. The subject wears a full headtent through which respiratory gases are recirculated to remove carbon dioxide. Headtent oxygen and carbon dioxide percentages are measured every 15 minutes and determinations of pre-cordial Doppler bubble grades are made every 16 minutes. Doppler bubble grades are recorded with the subject supine after movement of each limb.

During seated rest, subjects sit an an armchair with feet on the floor. During supine rest, they recline on a bed with a 6 degree head-down tilt. During seated exercise, they ride a Schwinn Air-Dyne ergometer which allows both upper and lower body exercise. Exercise begins after a 10-minute rest period and continues for 2 hrs, 50 min at a precalibrated level of 50 Kcal/hr (equivalent to 24.5 watts, an oxygen consumption of 0.6 lpm, or a walking speed of 2 mph. Upon completion of the exercise, the subjects walk to the altitude chamber while breathing from a portable oxygen supply.

RESULTS

Table 1 summarizes the Doppler bubble incidence and decompression sickness incidence under the 3 experimental conditions. Of 10 subjects tested, 5 have completed all 3 conditions. A total of 21 experiments have been conducted with a 52% bubble incidence and a 38% bends incidence. The bubble and bends incidences were 75% and 63% for seated rest, 67% and 50% for supine rest, and 14% and 0% for seated exercise.

Table 1. Incidences of Bubbles and DCS Condition During 3.5 hrs of Oxygen Breathing

	Seated Rest	Supine Rest	Seated Exercise	Totals
Bubbles	6	4	1	11
DCS	5	3	0	8
Total exposures	8	6	7	21
% Bubbles	75%	67%	14%	52%
% DCS	63%	50%	0%	38%

Table 2 summarizes the maximum precordial Doppler bubble grades recorded for all conditions. Decompression sickness generally occurred at high bubble grades and did not occur when bubbles were absent. In all cases of symptoms at altitude, symptoms occurred in the knees or ankles, and the limb affected with decompression sickness had the maximum bubble grade. In one unusual case, a subject developed shoulder pain (Grade 2 on a 0 to 10 scale) 18 hours after returning to sea level. The pain was relieved by recompression on a U. S. Navy oxygen treatment Table 6.

Table 2. Maximum Doppler Bubble Grades

Bubble Grade	0	1	2	3	4	Total
DCS	0	0	2	1	5	8
No-DCS	10	2	0	1	0	13
Total	10	2	2	2	5	21

CONCLUSIONS

Initial results suggest that of the 3 conditions tested, seated exercise is the most effective method of eliminating nitrogen and preventing bubbles, while seated rest is least effective. ■

RED BLOOD CELL DECREASES OF MICROGRAVITY

P. C. Johnson
NASA/Johnson Space Center, Houston, Texas 77058

Postflight decreases in circulating red blood cell mass have regularly been recorded after exposure to microgravity during missions as short as 4 days and as long as 175 days. These 5-25% decreases are accompanied by similar decreases in plasma volume producing no significant change in peripheral hematocrit early after landing. However, plasma volume is reconstituted in the first postflight day producing a lowered peripheral hematocrit until the bone marrow can reconstitute the red blood cell mass over the first few postlanding weeks. Decreased red blood cell masses are seemingly not related to mission duration, intramission workload, caloric intake, or the type of spacecraft used. The decreases are accompanied by normal red blood survivals, increased serum ferritin levels, normal radioactive iron erythokinetic studies and increases in calculated mean red blood cell volumes. Comparable decreases in red blood cell mass are not found after bedrest, a commonly used simulation of the microgravity state. After bedrest, the plasma volume decreases are similar or greater than those found after spaceflight. Inhibited bone marrow erythropoiesis has not been proven to date although reticulocyte numbers in the peripheral circulation are decreased about 50%. The causes of the microgravity induced decreases in red blood cell mass are unknown. Increased splenic trapping of circulating red blood cells seems the most logical way to explain the results since the decrease is too rapid to be explained only by a decrease in bone marrow production of red cells as a result of decreased erythropoietin release. ■

HEMATOLOGICAL STUDIES OF ANIMALS FLOWN IN MICROGRAVITY AND OF THE SUSPENDED RAT MODEL

J. B. Jones[1], R. D. Lange[2], L. A. Gibson[2], and P. C. Johnson, Jr.[3]
[1]*College of Veterinary Medicine, University of Tennessee, Knoxville, Tennessee 37920,* [2]*Memorial Research Center and Hospital, University of Tennessee, Knoxville, Tennessee 37920, and* [3]*NASA/Johnson Space Center, Houston, Texas 77058*

INTRODUCTION

Astronauts and cosmonauts have had a reduced red cell mass (RCM) following spaceflight. The reduction in RCM is accompanied by a reduction in plasma volume. Erythrocyte life-span studies have indicated there may be a mildly reduced life-span of erythrocytes, and reticulocyte studies indicate erythropoiesis is reduced.

Animal studies to define the cause of the anemia have been carried out in rats flown in microgravity and in simulated weightlessness. These studies have been hampered by the design restrictions of flight and by the inadequacy of the animal model to study spaceflight anemia. The strain, age and size of the rats, as well as the differences in flight and postflight conditions of the various flights, have created inadequate and sometime conflicting data. It is now apparent that in order to adequately understand erythropoiesis in microgravity further studies of cellular life span, plasma volume, erythropoietin production and marrow erythropoiesis studies must be carried out.

The literature relative to the hematology of animals flown in microgravity and to simulated flight is reviewed and hematologic data collected from rats flown on Space Lab 3 are presented.

ANIMAL MODELING

Bed rested humans have RCM changes similar to space travelers. In one attempt to develop an animal model to study hematologic effects of microgravity, rats were suspended in a jacket and harness device with the head tilted downward at a 30° angle. The forepaws contacted a surface and provided a means for the rats to move in a complete circle. When compared to controls, the suspended rats had a reduced RCM and a more greatly reduced plasma volume resulting in a transient increase in hematocrit. The suspended rats lost weight and consumed less food and water than did the control rats. The oxyhemoglobin disassociation curve was shifted to the right and erythropoiesis was suppressed. Dietary inadequacies produce nearly identical results. A summary of these results is shown in Table 1.

Table 1

Parameter	% of Controls (Suspended vs. nonsuspended)
Body weight	71.2 ± 6.9
RCM (M)	81.8 ± 11.5
Reticulocyte %	50.0 ± 20.9
^{59}FE%	75.7 ± 17.7
^{51}CrRBC	101.5 ± 3.1

Erythropoietin values for the suspended rats fluctuated considerably from significantly below controls on the 4th day of suspension to well above controls on the first day of recovery from suspension. These data seem compatible with responses found in "starved rats" and may be of little value in understanding erythropoietic changes resulting from microgravity.

STUDIES OF RATS FLOWN IN MICROGRAVITY

The U.S.S.R. investigators have flown rats on several Cosmos missions. Six rats were flown on NASA flight STS-8 and 24 rats on Spacelab-3 (SL-3). Differences in strain of rats, age, flight duration and type of studies completed have produced data that is not directly comparable, but is of interest on a case by case basis.

The animals flown on the Cosmos flights were found to have a leukocytosis, a neutrophilia and a lymphopenia. One study reported decreased marrow and spleen erythropoiesis, decreased RBC survival, and increased hemolysis. Reticulocyte values were reported by Gazenko as unchanged and by Ilyin as decreased.

On the American flight, STS-8, postflight animals had a leukocytosis and an increase in RBC counts, hemoglobin, hematocrit and platelet counts. RCM, plasma volume and life-span studies were not carried out, but it is apparent that these isotope studies would have been extremely valuable in interpreting the increased values.

Our studies on SL-3 revealed a number of similarities to those of the U.S.S.R. and the STS-8 studies. Our animals were of two sizes. Both groups had increased red cell parameters as did the STS-8 animals. A neutrophilia and lymphopenia occurred in the SL-3 animals as had been reported in the U.S.S.R. studies.

The bone marrow differential studies of Cosmos flight 605 showed a depressed erythropoiesis, but our studies of rats flown on SL-3 showed no differences between flight animals and ground controls.

An erythropoietin (Epo) study was carried out on the SL-3 animal subjects and was the first study of Epo in animals subjected to actual microgravity flight. Epo values for flight and ground control animals were not significantly different. In two studies of humans, Cosmonauts have been found to have Epo blood levels 3-5 times above normal 5-18 hours after landing, while astronauts from the STS-9 flight had statistically non-significant decreases in EPO.

The post-SL-3 studies of clonal *in vitro* erythropoiesis in rats were the first to be reported. At Epo doses of 0.02 units and 1.0 units, flight animal cells formed significantly more erythroid colonies than did ground control animals. At a dose of 0.2 units the two groups showed similar growth. It is possible

Table 2. Baseline data for analysis of erythrokinetics of spaceflights*

Parameter	Settings and Subjects			
	Ground-Based†		Inflight‡	
	Animal	Human	Animal	Human
Red cell count	+	+	+	+
Hemoglobin	+	+	+	+
Hematocrit	+	+	+	+
Red cell mass	+	+	+	+
Blood volume	+	+	+	+
Plasma volume	+	+	+	+
Reticulocyte count	+	+	+	+
Erythropoietin	+	+	+	+
Plasma or serum haptoglobin	+	+	+	+
Platelets	+	+	+	+
Red cell shape	+	+	+	+
Red cell size	+	+	+	+
Blood P_{50}	+	+	+	+
Blood PCO_2	+	+	+	+
Red cell 2,3-DPG	+	+	+	+
Red cell sodium	+	+	+	+
Skin petechiae	—	—	+	+
Subcutaneous, subserosal oozing of RBC	—	—	+	+
Bone marrow smear	+	—	+	—

*When feasible, measure sequentially for temporal aspects.

†Examples: Biological laboratories, hospitals, space simulation facilities (bed rest, water immersion, etc.), spacecraft simulators.

‡Include pre-, in-, and postflight phases.

Talbot, J.M. and K.M. Fisher, LSRO, Fed. Am. Soc. for Exp. Biol. 1985.

that the marrow of flight animals is more sensitive to EPO than is that of nonflight animals, but the studies must be repeated.

The true state of erythropoiesis in animals and people subjected to microgravity flights is unknown. Several carefully controlled studies of RBC life span, plasma volume, *in vitro* growth of marrow cells and EPO are needed to understand this new environment of hematopoiesis. The need to perform isotope studies of red cell mass and plasma volume to determine if these values decrease as do those of human astronauts is inferred from the animal studies. The needs for future studies were pointed out by a working group of the life sciences research office of the Federation of American Societies of Experimental Biology and are given in Table 2. ■

PAGE 159 INTENTIONALLY BLANK

PRECEDING PAGE BLANK NOT FILMED

SKELETAL MUSCLE GENE EXPRESSION IN EITHER SUSPENDED OR IMMOBILIZED RAT HINDLIMBS

F. W. Booth, P. Babij, G. Muller, and P. R. Morrison
Department of Physiology and Cell Biology, The University of Texas Medical School, Houston, Texas 77225

Wasting of skeletal muscle in man can occur as a consequence of prolonged spaceflight. It is our long-term aim to investigate the mechanisms through which a decrease in muscle loading alters the normal phenotypic expression of contractile proteins in skeletal muscle. We have employed two animal models which partially mimic the hypogravity of space, in order to study the molecular control of muscle protein synthesis. Previously, we used the immobilized rat hindlimb to reduce both muscle loading and contraction. Our recent work utilizes the tail-suspended rat hindlimb which in contrast to the former model, permits contraction of the unloaded muscle.

When fast-twitch adult rat skeletal muscle is immobilized at less than its resting length, muscle size and protein content decrease by 30% after the first 7 days. The synthesis rate of mixed proteins decreases 35% during the first 6 ours of immobilization and remains depressed throughout the next 7 days. Under these circumstances, the total RNA concentration remained unchanged, indicating that a loss of RNA capacity to support synthesis was not the reason for the observed decrease in mixed muscle protein synthesis during immobilization. It is possible that a decrease in the population abundance of poly A+ mRNA species accounts for the reduced synthesis rate of mixed proteins. The purpose of the next series of experiments was to measure the level of specific mRNAs in atrophied skeletal muscle as a result of decreased loading.

After 7 days of limb immobilization, a-actin mRNA and cytochrome c mRNA decreased by 30% and 25% respectively in fast-twitch muscle. We also observed a reduced abundance of the largest two (1400 and 1050 bases) of four mature cytochrome c mRNA species in fast-twitch muscle. These results indicate that the failure of protein synthesis may occur as a result of pre-translational modifications in immobilized skeletal muscle. Since the synthesis rates of a- actin and cytochrome c proteins decreased prior (6 hr) to measurable decreases in the levels of their respective mRNAs, an early defect in the translational control of protein synthesis may also occur in immobilization induced atrophy.

We have recently repeated some of the above measurements in the slow-twitch soleus muscle of hindlimb suspended adult rats because this muscle fibre atrophies the most in this type of model. After 7 days of suspension, there was a 5% decrease in body weight and no significant enlargement of the adrenal glands. Soleus muscle wet weight and protein content decreased by 30%, RNA concentration decreased 18% and DNA concentration increased 26%. The preliminary data from this model indicates that after 7 days of hindlimb suspension both a-actin mRNA and cytochrome c mRNA levels decrease by approximately 30% in the soleus muscle. Further experiments are now in progress to characterize changes in the synthetic rate of specific proteins in the soleus muscle of hindlimb suspended rats. (Sponsored by NAG 2-239). ■

ELECTRICAL STIMULATION TO LEG MUSCLES IN AMBULATORY AND LEG CASTED SUBJECTS

P. Buchanan[1], V. Convertino[2], G. Dudley[2], J. F. Flores[1], M. A. B. Frey[2], and M. Duviosin[1]
[1]*Biomedical Operations and Research Office, Kennedy Space Center, Florida 32899,* [2]*The Bionetics Corporation*

INTRODUCTION

To diminish muscle wasting during long duration space missions, crews have used 2+ hours nonproductive time daily doing relatively conventional exercise. We conducted a pilot study of electrical stimulation of muscle (EMS) on ambulatory subjects to test its potential as a countermeasure to muscle atrophy using intensities that permit reading, computer operation, or sleep. This was followed by a 16-day study of the effect of EMS on casted lower extremities.

METHODS

In both studies eight men 25-55 years of age participated: 4 test subjects (TS), 4 age-matched controls. Quadriceps, hamstrings, gastrocnemius/soleus, and anterior tibialis muscles of one leg were sequentially stimulated (3.5 sec on, 0.5 sec off) one hour/day, 4 times/week, for 8 weeks. Voltage-controlled EMS (biphasic, 30 Hz, 150 usec pulses) was performed in a fixture with leg brace-force transducers. In the casted study, 8 subjects wore a bivalved cast on the dominant lower extremity for 16 days. During that period, 4 subjects received EMS to the casted leg as described for the pilot study, and 4 acted as controls. The vastus lateralis and soleus muscles were biopsied on both the stimulated and unstimulated extremities and in both extremities of the controls before and after the test period.

RESULTS

In pre-testing vs. week 8 testing: knee flexion strength and prone plantar flexion strength, total work, and power (Cybex) increased more in TS; calf muscle area (computed tomography) increased for TS only; and percent body fat (hydrostatic weighing) was unchanged. TS were comfortable during EMS and performance on computer-presented mental tasks during EMS did not differ from performance without EMS. Results from the casted study will be available at presentation.

CONCLUSION

EMS shows potential for sparing muscle in space with minimal overhead in productive time. It deserves further testing for possible use in long duration space missions. ■

SOME FACTORS THAT INFLUENCE THE NEUROMUSCULAR RESPONSE TO SPACEFLIGHT AND SIMULATION MODELS OF SPACEFLIGHT

V. R. Edgerton, R. R. Roy, T. P. Martin, M. Herbert, E. O. Hauschka
Department of Kinesiology and Brain Research Institute, University of California, Los Angeles, California 90024

The adaptive capacity of the neuromuscular system is remarkable. It can adapt to chronically imposed high mechanical forces by enlarging its cross-sectional area by as much as twofold. On the other hand, when these chronic loads are reduced to some threshold level the cross-sectional area (CSA) can be reduced markedly in a matter of days in some muscles. Resistance to fatigue and the speed of shortening of the muscle fibers are other physiological properties shown to be adaptive under a variety of use-related conditions.

Spaceflight certainly provides a unique set of functional circumstances for the neuromuscular system. For example, the load imposed on the extensor musculature is undoubtedly reduced in microgravity and the quantity of activity that normally occurs during spaceflight is virtually unknown. Although there is only limited data on the muscle forces, length changes and electrical activities during everyday

movements even at 1-G, it is clear that the magnitude and the quantity of neuromuscular activity can influence the force, endurance and speed capacities of a muscle. With respect to the biomedical issues related to neuromuscular function during spaceflight, it is imperative to define the typical load and activity levels that occur at 1-G and 0-G if an effective and efficient training program is to be developed to prepare humans for prolonged spaceflight.

To begin to address some of these issues a series of experiments have been conducted using the hindlimb suspension model to simulate 0-G. Also, some tissue samples have been obtained from rats after a 7-day Shuttle flight, SLS-3. In addition, other investigators (Chui and Castleman, Physiologist 23:576, 1980) have reported data from rats and monkeys that have flown for 18-22 days on Cosmos Biosatellites.

It appears that the strength of some muscles as indicated by muscle weight and muscle fiber CSA is reduced markedly within one week of spaceflight (SLS-3). The soleus wet weight was 36% less than control and CSA of both low and high ATPase fibers was about 30% less than for simulated ground control rats (Martin and Edgerton, Physiologist 28:379, 1985). Similar amounts of atrophy for comparable muscles have been observed in rats flown on Cosmos for 18-22 days.

The strength-related data from rats that have had their hindlimbs suspended, (no weight support for 1-4 weeks) suggests similar effects in magnitude and kind as seen with spaceflight. For example, wet muscle weights of the soleus after 1 and 4 weeks of hindlimb suspension were 36 and 49% less than control. CSA was reduced by 67 and 50% after 4 weeks in light and dark ATPase fibers, respectively (Hauschka *et al.*, Physiologist 28:315, 1985). After 1 week the CSA were reduced by 36% and 34% in light and dark ATPase fiber. Maximum tetanic tension of the soleus was reduced by 69% after 4 weeks of suspension. Based on a combination of these results as well as those from other studies, it appears that (1) CSA and, therefore, the force potential of a muscle is reduced markedly within 7 days of flight; (2) the rate of atrophy differs among muscles and muscle fiber types; and (3) the rate of atrophy is rapid within the first 7 days of flight, but is much less thereafter.

There are some indications that the soleus muscle develops properties that are more fast-like after spaceflight and hindlimb suspension. For example, 50% of the soleus fibers in SLS-3 rats had high ATPase staining properties (alkaline preincubation) compared to 39% in ground based control rats. (Thomasson *et al.*, Med. Sci. Sports Exer. 18:55, 1986) have found an elevated proportion of the fast myosin isozymes and reduced proportions of slow myosin in the soleus muscle after hindlimb suspension. We have reported shorter contraction times and half-relaxation times after 4 weeks of hindlimb suspension whereas the maximum velocity of shortening was unchanged in the soleus (Winiarski *et al.*, Physiologist 28:316, 1985). However, Fitts *et al.* (J. Appl. Physiol. 60:1946, 1986) have reported an elevated Vmax following 7 and 14 days of suspension. It appears that there are minimal or no speed-related adaptations in muscles that are fast normally. In summary, the soleus, a normally slow extensor muscle tends to become more fast-like after hindlimb suspension, although not as fast as fast muscles of the hindlimb are normally. This response is similar to observations following several months of paralysis by spinalization (Roy *et al.*, Applied Physiol. 56, 1594, 1984) hindlimb immobilization and 4 weeks of paralysis by tetrodotoxin applied to the sciatic nerve (Spector, J. Neurosci 5:2177, 1985).

Resistance to fatigue is affected little or none following hindlimb suspension (Winiarski *et al.*, Physiologist 28:316, 1985). The soleus muscle is as resistant to fatigue after 4 weeks of hindlimb suspension as it is normally (fatigue index of .94 in control vs. .97 in suspended rats). The medial gastrocnemius fatigue index decreased from .49 to .36 following suspension whereas the fatigability of the tibialis anterior was unchanged (fatigue indexes of .38 and .41 for control and suspended rats). Some enzyme markers of important metabolic pathways have been studied as well. Interestingly, when the enzyme activities are measured per muscle fiber, the succinate dehydrogenase (SDH) activity is higher in the soleus after 1 and 4 weeks of hindlimb than in control rats (Hauschka *et al.*, Physiologist 28:315, 1985). SDH decreased from 8.37% in the MG and from 38 to 43% in the TA in light and dark ATPase fibers (Bello *et al.*, Physiologist 28:315, 1985 and Boissou *et al.*, Physiologist 28:315, 1985). Alpha glycerophosphatedehydrogenase activity increased in the high ATPase but did not change in the dark ATPase fibers after 4 weeks of suspension. These results are similar to observation in the soleus fibers of SLS-3 rats (Martin and Edgerton, Physiologist 28:379, 1985).

Another point addressed in recent studies has been the means necessary to prevent hindlimb muscles from atrophying when the hindlimbs are prevented from supporting the body weight or by

spaceflight. The efficacy of different kinds and amount of overload as well as the temporal distribution of these activities during hindlimb suspension have been studied. The exercise training regimes tested have been: (1) controlled dropping of suspended rats on their hindlimbs from a moderate height 10 times/day, (2) very slow walking at a 19° positive or (3) negative slope on a treadmill belt 10 min every six hours, and (4) climbing up a vertical grid with weights up to 75% of body weight attached to their tails for 2 or 4 series of climbs (5 climbs/series) within each 12-hour active period. Based on wet muscle weights (and dry weights on occasions) the most efficacious exercise was grid climbing. For example, 2 series of climbing sessions per day, requiring a total of about 4 min to complete, had an ameliorating effect on atrophy of the soleus that was equivalent to 40 min of negative or positive treadmill walking. Endurance training on a treadmill for 1.5 hours per day (20 m/min at a 30% grade) has been reported to reduce the atrophy by about half that which occurs in continuously suspended rats. Although these training procedures reduced the atrophy in the soleus that typically occurs after 7 days of continuous suspension by half, 4 climbing series per each 12-hour active period (total of about 8 min per day) almost completely eliminated atrophy in the soleus and maintained the medial gastrocnemius to within 4% of its normal weight. ■

CONSIDERATION OF PROTEOLYTIC MECHANISMS OF MYOFILAMENT DELETION OBSERVED IN RAT SOLEUS MUSCLE AFTER REAL AND SIMULATED MICROGRAVITY

S. Ellis[1], D. A. Riley[2], J. L. W. Bain[2], and J. G. Barnett[3]
[1]Department of Chemistry, San Jose State University, San Jose, California 95192, [2]Department of Anatomy and Cellular Biology, Medical College of Wisconsin, Milwaukee, Wisconsin 53226, [3]Department of Biological Sciences, Saint Vincent College, Latrobe, Pennsylvania 15650

A pronounced loss of mass and myofibrillar cross-sectional area of the soleus muscle is a characteristic result of exposing rats to microgravity or suspension hypokinesia and hypodynamia (1). Hindlimb immobilization and hindquarter suspension studies by several investigators have revealed that these procedures reduce the rate of protein synthesis and increase the rate of protein degradation. As a consequence, atrophy ensues and the muscle incurs a demonstrable reduction in total and contractile protein content. The process of partial disassembly of the atrophying myofiber and degradation of its protein constituents is poorly understood. Our quantitative morphometric analyses by electron microscopy revealed random areas of myofilament deletion from the interior and margins of myofibrils that appear as focal areas of electron lucency in both the A and I bands. The mean area of the focal lesions was twice as great in the soleus muscles of the SL-3 rats after seven days flight than in the controls (2). The deletion of myofilaments from these regions of the myofibril presents a promising approach for elucidating the ultrastructural changes with immunochemical probes for native and fragmented myofibrillar proteins as well as identifying the specific proteases involved.

Immunological evidence was obtained for the presence of the ubiquitin-mediated and ATP-mediated pathway of protein degradation in slow, and to a lesser extent, in fast fibers of rat skeletal muscle where the concentrations of total ubiquitin (free plus conjugated) were higher than in the EDL. Soleus atrophy induced by suspension of rat hindquarters or from rats from the 7-day SL-3 flight showed substantially increased concentrations of ubiquitin conjugates. This result suggests an increased activity of the ubiquitin-ATP pathway in slow twitch fibers which parallels the increased myofilament deletions.

The calcium-activated protease is known to degrade certain regulatory myofibrillar and cytoskeletal proteins (desmin, connectin) and to release α-actinin from the Z-lines of sarcomeres. We have found that the calcium-activated protease increased in the atrophied soleus muscles of rats from the SL-3 flight to an extent similar to that previously observed after five days of hindquarter suspension (3). The rise in the activity of the calcium-activated protease has a significance probably greater than that for the dissolution of intermediate filaments of the myofibrillar cytoskeleton which are degraded at high rates with K_m values of 10^{-7} to 10^{-8}M (4). The rapid degradation of steroid and EGF receptors is a case in point.

Another proteolytic enzyme, tripeptidyl aminopeptidase, which we have shown by electron microscopy to be localized in lysosomes and also in the sarcoplasmic reticulum was also elevated. Since other lysosomal proteases were not elevated and lysosomes were largely absent from the focal lesions of missing myofilaments, the increase in tripeptidyl aminopeptidase appears to be due to a relatively higher proportion of sarcoplasmic reticulum, as occurs in immobilization atrophy (5). The role of this peptidase in the sarcoplasmic reticulum remains to be established. Thus, at least three degradative systems are activated in the atrophic response of muscles to real and simulated microgravity.

Microgravity-induced atrophy of the soleus displays a Z-line misalignment across myofibers which occurs at the focal lesions and beyond (Riley, D.A., in preparation). It has been proposed that Z-lines are held in lateral register by desmin and vimentin filaments in association with α-actinin (6). In order to determine if Z-line and thick filament misalignment presents a deficit of intermediate filament proteins, the soleus muscles from control and 10-day suspended rat limbs were extracted with urea-detergent and submitted to 2-dimensional electrophoresis (isoelectric point and molecular weight). The desmin, vimentin, and α-actinin concentrations were found not to be detectably different, although the concentration of several as yet unidentified proteins in the M_r range of 18,000 to 32,000 were markedly altered by atrophy (7).

The macroproteins connectin/nebulin form elastic filaments that are believed to link the ends of thick filaments to the nearest Z-disks and also provide a mechanical basis for passive elasticity (8). A quantitative electrophoretic evaluation of these large proteins is underway, although data on passive tension changes in single fibers from atrophying muscle are lacking at present. Incipient myofibrillar atrophy may be signalled by a reduction in connectin/nebulin content concurrently with the appearance of Z-line and thick filament misalignment.

If myofilaments are in equilibrium with a small pool of soluble myosin molecules (9) as recent studies suggest, a reduction of the rate of myosin synthesis with either maintenance of the rate of dissociation from the myofilament and proteolysis of the myosin, or an increase in these rates, may be viewed as an essential feature of myofilament deletion and formation of focal lesions. On the other hand, fragments have been reported to form *in vivo* by proteolytic cleavage of peptides from the amino terminal (S1) end of the myosin heavy chain while still imbedded in the thick filament (10). In either case, an inhibitor-protease complex of calpain or high molecular weight endopeptidases (11) may be closely associated with myofilaments and activated through a phosphorylation mechanism triggered by muscle hypokinesia and hypodynamia. Prostaglandin E_2 has been proposed as initiating accelerated proteolysis (12). We have tested the influence of PGE_2 on protein degradation in isolated rat and mouse muscles. PGE_2 over a wide range of doses had no influence on protein degradation rate in mouse muscles under several different incubation conditions, and neither PGE_2 nor arachidonic acid influenced protein degradation in rat muscles as well (13). Hence the role of prostaglandin E_2 as a mediator of protein degradation appears highly unlikely. Similarly, glucocorticoids do not accelerate the degradative phase of protein turnover in the soleus muscle (maintained at resting length) as measured by tyrosine release *in vitro*, since neither injected dexamethasone or adrenalectomy affected the response of the soleus, plantaris, or gastrocnemius muscles to 7 days of cast immobilization (14). In this regard, limb muscle mass is maintained for at least 4 weeks following hypophysectomy in the rat, although the growth of skeletal muscle is suppressed. Thus, circulating levels of pituitary hormones or their receptors in muscle would not appear to be regulators of protein degradation; however, insulin-like growth factors and their receptors which are largely, but not completely, pituitary-dependent, as well as other local polypeptide growth factors need to be investigated.

The mitogenic activities of atrophying rat soleus muscles were no different from controls as measured by the proliferative response of L_8 myoblast cultures, although elevated levels were detected in stretch-induced growth of chicken wing muscles.

The recent discovery of tension dependent Ca^{2+}- channels in the membranes of tissue cultured chick pectoral muscle may be the major intrinsic signal for the cascade of processes which maintain normal protein mass (16). ■

REFERENCES
(1) Goldspink, D.F., Morton, A.J., Loughna, P. & Goldspink, G. Pflugers Archiv. 407: 333-340. (1986)
(2)Riley, D.A., Ellis, S., Slocum, G.R. et al., (1987) Muscle and Nerve (in press).
(3) Ellis, S. and Nagainis, P.A., The Physiologist (Suppl) 27: S-72 (1984).
(4) Traub, P. Intermediate Filaments: A Review. Springer- Verlag, Berlin 1985.
(5) Guba, F., Magda, M.G., and Takacs, O., Acta Biol. Med. Germ. 36: 1605-1619 (1977).
(6) Lazarides, E. Nature 283: 249-256 (1980).
(7) Ellis, S., giometti, C.S., and Riley, D.A. The Physiologist (Suppl.) 28:S-159 (1985).
(8) Horowits, R., Kemper, E.S., Bisher, M.E., and Podolsky, R.J. Nature 323: 160-164 (1986).
(9) Saad, A.D., Hamilton, K.A., and Fishman, D.A., J. Cell. Biol. 103: 117a (1986).
(10) Ball, R.D., Krus, D.L. and Alizadeh, B., J. Mol. Biol. 193, 47-56. (1987).
(11) Murakami, K. and Etlinger, J.D., Proc. Natl. Acad. Sci. 83: 7588-7592 (1986).
(12) Rodemann, H.P. and Goldberg, A.L., J. Biol. Chem. 257: 1632-1638 (1982).
(13) Barnett, J.G., and Ellis, S., Muscle and Nerve, in press (1987).
(14) Barnett, J.G., and Ellis, S., in preparation (1987).

WHOLE BODY SUSPENSION IN THE RAT: MUSCLE, FLUID AND CARDIOVASCULAR EFFECTS

R. D. Fell[1], J. M. Steffen[2] and X. J. Musacchia[3]
[1]Exercise Physiology Laboratory, [2]Department of Biology and [3]Department of Physiology and Biophysics, University of Louisville, Louisville, Kentucky 40292

The primary research thrust of the laboratory has been the development of a ground based model for simulations of and comparisons with responses from exposure to weightlessness. Experiments with hypokinesia and hypodynamia were initiated with the development of a whole body suspension (WBS) model in which the hindlimbs were unloaded (1). Since that time several variations of suspension model systems have been developed, including: 1) WBS with either denim suit or plexiglass cradle harness, 2) dorsal subcutaneous steel rod, 3) tail suspension, and 4) lumbar vertebrae fixation with rigid pin system. All of these models accomplish the primary goal of eliminating weight bearing function from the hindlimbs, i.e., hypodynamia, and subsequent reduction of contractile activity, i.e., hypokinesia. There may be some subtle differences between the various models when assessing the levels of stress on the animal and the degree of versatility each model provides. The WBS system provides a head down or a horizontal positioning that allows additional fluid shifts or fluid redistributions studies. In contrast, tail cast suspension is often limited to a head down tilted position.

Our initial investigations with the WBS model examined both muscle atrophy and recovery, and the fluid and ionic changes imposed by hypokinesia/hypodynamia (H/H) on the rat (2,3). With H/H there was a rapid loss in muscle mass and a similar rapid recovery following removal from suspension unloading. Diuresis accompanied by naturesis and kaliuresis was observed during seven days of H/H in young, rapidly growing, 180-200 g male rats. In these animals an increase in urinary excretion of nitrogenous end products such as was observed in urine such as urea, ammonia, and 3-methylhistidine.

Studies of one and two week H/H clearly established the presence of differential muscle atrophy (soleus>gastrocnemius=plantaris>extensor digitorum longus). Muscle atrophy was paralleled and substantiated by of increased 3-methylhistidine excretion (Table 1) and total protein loss.

The decreased total protein content was associated with reduced protein/DNA ratios (4) which suggested a reduction in muscle cell size. This hypothesis has recently been supported through histochemical studies showing a 15 to 20% decrease in fiber size (5). Since the majority of muscle RNA is ribosomal, our measurement of decreased muscle RNA content during H/H indicates that reduction in protein content reflects decreased protein synthesis. Furthermore, recent studies showing significant

TABLE 1. Excretion of 3-methylhistidine during WBS

	Week 1	Week 2	Recovery
Controls	2.01 ± 0.10	1.98 ± 0.18	—
H/H	2.86 ± 0.18*	3.33 ± 0.42*	2.11 ± 0.19

Values are mean + sem. N = 10-17 samples per group.
*Significantly different from control values at P<0.001

reductions of specific mRNA levels supports the hypothesis that H/H impairs protein synthetic capacity. While the mechanism underlying these effects has not been elucidated, our measurements of increased plasma corticosterone and elevated muscle glucocorticoid receptor levels suggest the potential for an endocrine influence (6). The results of these investigations are consistent with observations of SL-3 flight animals exposed to 7 days of weightlessness. In both SL-3 and WBS rats there is a differential atrophy with slow twitch muscles showing the greatest level of tissue wasting (7).

The earlier noted losses in 3-methylhistidine and protein content suggested a change in muscle fiber composition. This led us to explore potential alterations in muscle functional capacity. To test this possibility, *in situ* measurements of speed related muscle properties, strength, and fatigability were determined in 7 day WBS rats (8). No changes were observed in contractile properties. Despite a decrease in absolute muscle strength, strength per unit muscle mass was unaltered (Table 2). An

TABLE 2. Absolute and relative soleus muscle strengths following 7 days of WBS

	Muscle Mass, mg	Absolute Tension, (g)	Relative Tension, (g/g mus)
Control	65 ± 3	72 ± 9.3	1079 ± 123
H/H	48 ± 1*	46 ± 10.1*	1028 ± 228

Values are mean + sem for 6-8 muscles per group.
*Significantly different from control at P<0.001.

increased rate of fatigue was observed in muscles from rats exposed to 7 days WBS, despite unaltered contractile and strength properties. This loss of work capacity may in part be explained by alterations in the metabolic profile of the tissue. We have noted significant decreases in oxidative capacity in atrophied muscle in response to H/H (9). Additional studies have shown a loss in insulin sensitivity suggesting a lessened carbohydrate utilization by disused muscles. This correlates with observations of increased glycogen storage in H/H atrophied muscles (9).

One of the advantages of the WBS model is the ability to alter the angle of suspension. Early studies compared blood pressure responses in the head down tilt, i.e. antiorthostatic (AO) position to orthostatic (O) horizontal position. There was an early elevation (3 days) in blood pressures (mean arterial, systolic and diastolic) in AO tilted subjects compared to 0 positioned subjects (10). In concert with our earlier observation of diuresis in AO subjects, these blood pressure data are consistent with the Gauer Henry reflex, indicative of a cephalad fluid shift.

Increased blood pressures may be a reflection of changes in peripheral vascularity. In recent studies, significant changes in capillarity have been observed in disused muscle (5). With a shrinkage of muscle cells there is a concomitant increase in capillary density, which in turn may contribute to increased blood pressures during AO suspension. Clearly the relationship between cardiovascular parameters and fluid redistribution in both ground based simulations and space flight subjects require much additional study.

Using these previous studies as a base, we have initiated a series of experiments investigating the potential preventive and rehabilitative aspects of exercise before and after WBS. In addition, since most of the previous use of suspension models has centered on rapidly growing juvenile subjects, studies of

adult responses to H/H have been initiated. Our approach will to compare treadmill endurance exercise, strength training, and electrical stimulation as countermeasures to H/H effects. (Supported by NASA NAG2- 386). ■

REFERENCES
(1) Musacchia XJ, Deavers DR and Meininger GA. Physiologist 20:67, 1977.
(2) Musacchia XJ, Deavers DR, Meininger GA and Davis JP. JAP 48(3):479, 1980.
(3) Deavers DR, Musacchia XJ, and Meininger GA. JAP 49:576, 1980.
(4) Steffen JM and Musacchia XJ. AJP 247:R728, 1984.
(5) Musacchia XJ, Steffen JM, Fell RD and Dombrowski J. Physiologist, 30(1):S-102, 1987.
(6) Steffen JM and Musacchia XJ. Aviat Space Environ Med (in press) 1987.
(7) Steffen JM and Musacchia XJ. AJP 251:R1059, 1986.
(8) Fell RD, Gladden LB, Steffen JM and Musacchia XJ. AJP 249:R308, 1985.
(9) Fell RD, Steffen JM and Musacchia XJ. AJP. (10) Musacchia XJ and Steffen JM. Physiologist, 27:S-41, 1986.

FUNCTIONAL CHANGES IN SINGLE MUSCLE FIBERS WITH DISUSE ATROPHY

R. H. Fitts, P. R. Gardetto, A. L. Heywood-Cooksey, and B. R. Unsworth
Department of Biology, Marquette University, Milwaukee, Wisconsin 53233

Muscle atrophy is a direct consequence of weightlessness (1), and the experimental models' hindlimb casting and suspension (2). Additionally, important functional changes have been associated with muscle atrophy including: 1) a drop in peak tetanic tension (P_0); 2) a shortened isometric twitch duration; and 3) an elevated maximal shortening velocity (V_{max}) (2). Two weeks of hindlimb suspension (HS), but not hindlimb casting, caused a major increase in the V_{max} of the slow-twitch soleus (6.83±0.74 vs. 3.05±0.08 fiber lengths/s). The increased V_{max} was associated with, and perhaps caused by, the increased expression of a second faster migrating isozyme of myosin. The new native isozyme comigrated with fast myosin, but its light chain subunits contained only LC_{1s} and LC_{2s} (2). Presently, the fiber type specific effects of disuse atrophy mediated by either HS or weightlessness are unknown. Recently, we began experiments designed to address this question. This work has utilized the single skinned fiber and freeze-dried preparations to study cell physiology and metabolism, respectively. Preliminary results from these studies are presented here.

Following 2 wks of HS, male rats (~200 g) were anesthetized with the Na^+ pentobarbital, 50 mg/kg body wt. and the soleus muscle surgically removed. The muscle was divided into small bundles (~50 fibers each), some of which were freeze-dried while the others were stored at -20°/C in relaxing solution containing 50% (v/v) glycerol for a period of 3 to 21 days before use (3). Single skinned fibers were prepared from the bundles and P_0, V_{max}, and pCa-force relationships determined (3). Type I fibers from control soleus muscles were found to have a mean P_0 of 1.42± 0.09 $kg.cm^{-2}$ and a V_{max} of 1.68±0.11 fiber $lengths.s^{-1}$. The pCa required to obtain 50% of P_0 was 6.08. The analysis of single fibers from the HS rats are not yet complete, but preliminary results show a significant increase in V_{max}. Additionally, the fibers from the HS rats showed a second myosin heavy chain (MHC) following one dimensional polyacrylamide gel electrophoresis (SDS-PAGE). The new MHC species has a mobility indistinguishable from the heavy chain species present in fast-twitch fibers.

Confirmation that the newly synthesized minor species represents fast myosin heavy chains (MHC), associated with slow myosin light chains, was undertaken by electroeluting the myosin isoenzyme species from the non-dissociating pyrophosphate gels, digesting with proteolytic enzymes and peptide mapping. It is our aim to eliminate possible ambiguity, by generating two dimensional peptide maps of the MHC digests.

We have reported earlier (4) that atrophied muscles appeared to have an increased dependence on anaerobic metabolism, as reflected by the greater depletion of glycogen and enhanced lactate formation during contractile activity. Our working hypothesis is that the increased glycolytic rate compared to control muscles is due to an elevated enzymatic activity of specific enzymes and/or to substrate level activation. In support of the former, we have found 2 wks of HS to significantly increase ($p<0.05$) lactate dehydrogenase [15.25=-1.15 vs. 10.10±1.2 $mM.kg^{-1}$ (dry wt).hr^{-1}] and phosphofructokinase [1.03±0.19 vs. 0.60±0.05 $mM.kg^{-1}$ (dry wt).hr^{-1}] activity in the slow type I fiber of the soleus. No significant alterations were observed in the fast type II muscle fibers.

In conclusion, HS selectively alters the slow type I fibers, yielding hybrid fibers containing fast and slow myosin heavy chains, elevated maximal shortening velocities, and enhanced glycolytic enzyme content. ■

REFERENCES

1. West, J.B. Spacelab—the coming of age of space physiology research. *J. Appl. Physiol.* 57:1625-1631, 1984.
2. Fitts, R.H., J.M. Metzger, D.A. Riley, and B.R. Unsworth. Models of disuse: a comparison of hindlimb suspension and immobilization. *J. Appl. Physiol.* 60:1946-1953, 1986.
3. Moss, R.L., G.G. Giulian, and M.L. Greaser. Physiological effects accompanying the removal of myosin LC_2 from skinned skeletal muscle fibers. *J. Biol. Chem.* 257:8588- 8591, 1982.
4. Witzmann, F.A., D.H. Kim, and R.H. Fitts. Effect of hindlimb immobilization on the fatigability of skeletal muscle. *J. Appl. Physiol.* 54:1242-1248, 1983.

DETERMINATION OF LEG MUSCLE VOLUME BY MAGNETIC RESONANCE IMAGING

P. L. Lee, R. H. Selzer, and S. Ellis
[1]*Jet Propulsion Laboratory, Pasadena, California,* [2]*San Jose State University, San Jose, California*

INTRODUCTION

A computer technique to measure lower leg muscle volume from magnetic resonance (MR) images is under development and has been partially tested with 19 subjects in a bed rest study at the Ames Research Center. For each subject, 60 cross-sectional MR images of one leg were obtained at one centimeter intervals beginning at the ankle. Imaging was carried out before and after the four-week bed rest. Computer programs were developed to find the borders of individual muscles or groups of muscles in each cross-section and to compute the entire muscle volume. Muscle volume five days following bed rest was found to be 94% of that measured three days prior to the start of the bed rest. A description of the technique is given in this paper.

IMAGING PROTOCOL

Magnetic resonance images of the 19 subjects were obtained at the University of California San Francisco Radiology Imaging Laboratory with a Diasonics MT/S MRI system operating at a field strength of 0.35 Tesla. All imaging was done in a quadrature detection head coil, which gave a inplane resolution of 0.95 x 0.95 mm. The maximum axial field of view of this system is 20 centimeters. As a result, in order to cover the entire lower leg, it was necessary to image the leg in three sections, 20 cm. long, with the leg translated 18 cm each time. The standard protocol was a spin echo image with TR = 1 sec. and TE = 30 ms. In addition, TR = 0.5 images were taken at the middle position to provide for T1 information. For each subject the same protocol was used for the pre- and post-bed-rest study.

A lucite leg rest was made to facilitate the 18 cm translation of the subjects. The foot of the subject is held by Velcro straps against the leg rest and three fiducial marks on the leg rest provide for proper registration for the pre- and post-bed-rest imaging. To monitor possible geometric changes in the MR imaging system over time, the cross sectional images of four oil-filled lucite tubes built into the base of the footrest were tracked in each image.

IMAGE ANALYSIS

The original image processing objective was to compute the volume of individual muscles but the image resolution was not sufficient to consistently visualize the boundaries between muscles. Thus, tracking was applied to a posterior group of muscles which included the following: soleus, lateral gastrocnemius, medial gastrocnemius, flex. digitorum longus, tibialis post, and flex. hallucis longus. The computer edge detection proceeded automatically to find the boundary of this group in each cross-section but operator intervention was allowed to correct tracking errors.

The soleus and gastrocnemius muscles for one of the 19 subjects was separately traced. When the boundary between the two could not be detected by the edge tracking program, the operator used a cursor to supply a "best guess" of the boundary. An example showing the determined edges in the middle region of the lower leg is shown in Figure 1. After a sequence of outlines were found, they were combined in a three dimensional shaded surface display as shown in Figure 2. This type of display may be useful for determining if disuse atrophy occurs uniformly or selectively along the muscle length.

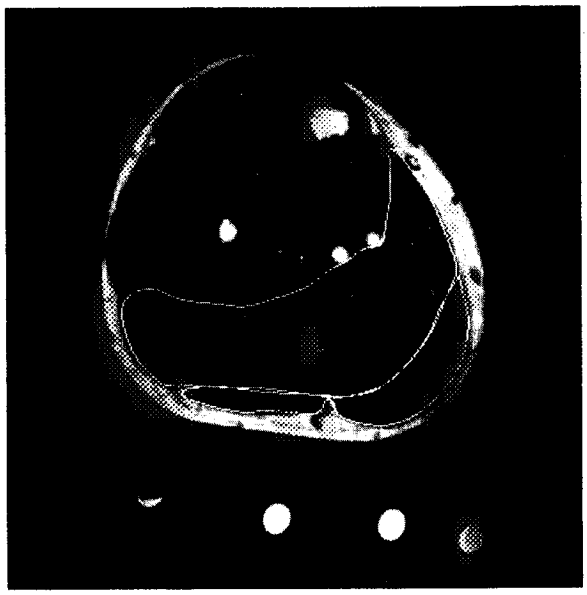

Figure 1. MR Image of a cross section of the leg taken about 20 cm above the ankle. The Soleus and the two parts of the gastrocnemius are outlined.

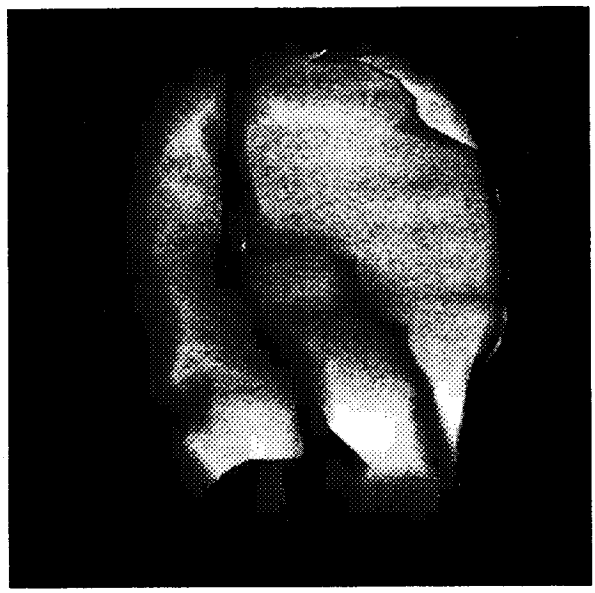

Figure 2. 3D shaded surface reconstruction of the middle leg showing the Lat. and Med. gastrocnemius. The Soleus muscle is hidden in this view.

RESULTS

Measurement of the posterior group of muscles as described above in approximately 2000 cross sectional images for the 19 subjects indicates an overall 6% decrease in muscle volume during the bed rest period as measured 5 days following the end of the bed rest period. The accuracy and precision of this method has not yet been determined so that no indication of significance can be assigned to this result.

CONCLUSIONS

We have measured, quantitatively, atrophy of a group of muscles. The edge detection program can be used automatically on well-defined muscle groups. Otherwise, operator modifications are required. The 3-D displays gives a visual image of the muscle. In order to measure individual muscles unambiguously, improvement of image quality is needed. One way of achieving this is to reduce the slice thickness from the present 1 cm. An imager with the zoom capability would increase the inplane resolution. Registration between pre- and post-bed-rest images will improve if the whole leg can be imaged at once. With the improvements in resolution, magnetic resonance imaging and the computer analysis will be a noninvasive tool to estimate volumes of individual muscles. ■

MUSCLE ATROPHY AND DECREASED SENSITIVITY TO INSULIN DURING HINDLIMB SUSPENSION

C. E. Mondon, K. Rodnick, C. Dolkas, and G. Reaven
Veterans Administration Medical Center, Palo Alto, California and NASA/Ames Research Center, Moffett Field, California 94035

Suspension of laboratory rats so that the hindlimbs are not load bearing has been used for study of the causes of muscle atrophy. In our laboratory, we have demonstrated that head down suspension of hindlimbs from six week old laboratory rats for two weeks results in a marked atrophy of soleus muscle, despite a substantial gain in body weight. Male Sprague Dawley rats fed Purina laboratory chow (#5012) *ad libitum* gained 83g during two weeks of hindlimb suspension (averaging 5.9g/day) and soleus muscle averaged 42.3mg/100g body weight. In contrast, nonsuspended control animals on a similar diet gained 126g (9.0g/day) and soleus muscle weighed 79.9 mg/100g body weight. Although the weight of soleus muscle in suspended rats is almost one half that of control rats, this muscle atrophy was not due to the diminished body weight gain. Control animals fed a calorically reduced diet (consisting of equal parts chow and cellulose) for two weeks show a body weight gain comparable to suspended rats (6.2g/day) and a normal soleus weight (80.4mg/100g body weight). Conversely, forelimb movement of suspended rats is visually increased over control rats and weight of the epitrochlearis muscle in the forearm of suspended rats is greater (32.8±.8mg/100g rat) than that in control rats (27.6±8mg/100g body weight). The reduced body weight gain by suspended rats might be due to a voluntary decrease in food intake resulting from hypokinesia associated with unloading the hindlimbs. However, subsequent studies indicated that food consumption by suspended rats averaged 11.0±SE .3g/day/100g rat measured 11 to 13 days after suspension and was comparable to chow fed control rats (11.4±.3g/day/100g rat). Since food intake was equal between groups, the 2/3 reduction in body weight gain by suspended rats must be attributable to an increased caloric expenditure associated in part with increased movement of the forelimbs. Control rats fed the cellulose-chow diet consumed 18.9±.7g food/day/100g rat indicating that the decreased body weight gain in these animals was due in part to ingesting less calories as well as an increased caloric expenditure from eating a large quantity of cellulose containing food.

The concern for matching body weight gain of control and suspended animals is important for assessing responsiveness to insulin. Preliminary studies have indicated that the difference in body weight gain between control and suspended rats has a major impact on the animals' sensitivity to insulin. We found that administration of an insulin suppression test elicits differences in insulin-induced glucose uptake by control and suspended rats. In this test, rats are anesthetized and receive a continuous infusion of glucose, insulin, epinephrine and propranolol. Under these conditions, endogenous insulin is suppressed and addition of glucose and insulin provides a steady-state serum glucose and insulin concentrations after 120 minute infusion. Serum insulin levels are comparable in all groups (60uU/ml) and serum glucose levels are higher or lower depending on the animal's sensitivity to insulin. Thus, we noted that steady- state serum glucose levels during the insulin suppression test were significantly higher in the suspended rats than in chow fed control animals (95±11 vs 145±9mg/dl). However, when suspended rats were compared with control rats fed a cellulose-chow diet and showing similar rates of body weight gain, serum glucose levels during the insulin suppression test were significantly higher in the suspended rats than control rats (95±11 vs 64±7). These results indicate that hindlimb suspension for 14 days resulted in a major 50% reduction in soleus muscle weight when animals were matched for body weight gain and these animals exhibited an increased resistance to insulin-induced glucose uptake. Furthermore, these findings suggest that decreased body weight gain by suspended rats resulting from an increased caloric expenditure enhances insulin sensitivity which compensates in part for the deleterious effects of hindlimb suspension on inducing muscle atrophy and decreasing insulin sensitivity.

To determine whether atrophy of soleus muscle arising from suspension disuse of the hindlimbs is due to a decreased response to insulin action on protein metabolism, we conducted a series of studies

on perfused hindlimbs from control rats and rats suspended for 14 days to assess net protein breakdown in the absence and presence of varying concentrations of insulin. Rats were anesthetized and killed prior to isolation and perfusion of the hindlimbs with a blood buffer media containing glucose and amino acids at physiological concentrations. The accumulation of tyrosine in the perfusing medium was used as an index of net protein breakdown by hindlimb muscle since this amino acid is not catabolized by peripheral tissues. Hindlimbs from suspended rats perfused in the absence of insulin release amounts of tyrosine (540±47 pmol/min/g muscle) comparable to chow-fed control rats (558±28 pmol/min/g muscle) and control rats fed the cellulose-chow diet (490±33 pmol/min/g muscle). Insulin was infused at rates to stabilize perfusate insulin at low and high physiological levels, 75 and 175uU/ml, as well at rates to evoke a maximal response (>6000uU/ml). The extent to which insulin suppressed tyrosine outflow (Δ) at maximal concentrations was again comparable in suspended (550±35 pmol/min/100g rat) and chow fed control rats (545± 42 pmol/min/100g rat) and slightly greater in control rats fed the cellulose-chow diet (603±45 pmol/min/100g rat). However, a major difference was noted in suspended rats perfused at physiological insulin levels. Specifically, insulin at 75uU/ml decreased tyrosine outflow 155 pmol/min/100g rat (28% of the maximal response) in suspended rats and 255 pmol/min/100g rat (42% of maximum) in control rats fed the cellulose-chow diet. At 175uU/ml insulin concentration, tyrosine outflow was reduced 279 pmol/min/100g rat (51% of maximum) in suspended rats and 404 pmol/min/100g rat (67% of maximum) in control rats fed the cellulose-chow diet. The response to physiological insulin levels in chow-fed control rats was similar to suspended rats. Thus, suspended rats show a decreased sensitivity to the effect of insulin on suppressing net proteolysis when compared with control rats fed cellulose-chow showing the same rate of body weight gain as suspended rats.

In conclusion, hindlimb suspension of laboratory rats has been employed as a model for inducing atrophy common to hypokinesia during bed rest and exposure to weightlessness. However, from body weight gain, food intake data and hypertrophy of epitrochlearis muscle in forelimbs, suspended animals show an increased energy expenditure and atrophy of the soleus muscle must be ascribed to unloading of hindlimb muscles rather than hypokinesia. When compared with control rats showing a similar reduced body weight gain, suspended rats show a resistance to insulin-induced suppression of net protein breakdown suggesting that atrophy of skeletal muscle may be due in part to a decreased action of insulin on enhancing protein synthesis and/or suppressing protein catabolism. ■

FIBER SIZE AND SUCCINATE DEHYDROGENASE ACTIVITY IN THE RAT SOLEUS FOLLOWING HINDLIMB SUSPENSION AND PERIODIC MECHANICAL LOADING

R. R. Roy, E. O. Hauschka and V. R. Edgerton
Brain Research Institute and Neuromuscular Research, Laboratory, University of California at Los Angeles, Los Angeles, California 90024

An important stimulus for the maintenance of skeletal muscle structure and function appears to be the presence of normal forces counteracting gravity. In a weightless environment and under conditions of chronic "unloading" such as that found in the hindlimb suspension model, the affective musculature responds by atrophying and/or demonstrating metabolic and structural changes. the extent of these adaptations appears to be muscle-specific, *i.e.*, extensors and muscles composed primarily of slow-twitch fibers are more affected than flexors and muscles that have a high proportion of fast-twitch fibers. An important challenge for space biologists, therefore, is to prevent this attrition of muscle mass and associated metabolic and structural adaptations during prolonged spaceflight. The present study was an initial attempt to determine the quantity of "weight-supporting" activity that is necessary to maintain the functional and structural integrity of the slow twitch soleus muscle in hindlimb suspended rats.

Male rats (Sprague Dawley, 230-250 grams body weight) were assigned to one of the following groups: control (CON, n=10), hindlimb-suspended (HS, n=11) or hindlimb-suspended plus daily treadmill exercise ((HS-EX, n=12). All rats were housed individually in 36x36x36 cm cages, provided food and water *ad libitum* and maintained on a 12:12 hour light- dark cycle. HS rats were suspended by their tails (Roy *et al.*, J. Appl. Physiol., In Press) for seven days. A cast was molded around the proximal half of the tail and the rats were suspended at a height that allowed complete mobility of the forelimbs and 360° rotation. The HS-EX rats were walked slowly on a treadmill (5 meters/min at a 19° grade) for ten minutes every six hours, *i.e.*, a total of 49 minutes per day. These studies were approved by the Animal Use Committee at UCLA and followed the American Physiological Society Animal Care Guidelines.

Immediately following cervical dislocation, the soleus was excised, trimmed of excess fat and connective tissue, blotted dry and weighed (wet weight). The midbelly of the soleus was then quick-frozen and prepared for histochemical analysis. Serial 10 μm thick sections were stained for succinate dehydrogenase (SDH) quantitatively (Martin *et al.*, J. Histochem. Cytochem. 10:1053, 1985) and for myosin ATPase, alkaline preincubation, qualitatively (Nwoye *et al.*, Am J. Physiol.242:R401, 1982). Fibers were classified as light or dark staining for myosin Atpase.

Approximately 60 fibers (one half being of each fiber type) per muscle were analyzed for fiber cross sectional area and SDH activity using an image processing system. A larger sample of 600 to 2300 fibers per muscle was examined to determine fiber type composition. All statistical comparisons were made at the .05 level of confidence.

Body weights of both suspended groups were approximately 10% less than that of the CON. The difference could be attributed mainly to a loss in weight at the initiation of the suspension. Adrenal wet weights were similar in the three groups indicating that the suspension was not overly stressful to the rats.

Soleus absolute wet weights in the HS and HS-EX rats were 35 and 19% less than that of the CON rats. This effect was even more impressive when the difference in body weights were 28 and 8% lower in the HS and HS-EX groups, respectively. Fiber size adaptations paralleled the decrease in muscle mass. Fibers staining lightly and darkly for myosin ATPase were 36 and 34% smaller in HS than in CON. In HS-EX rats the light and dark ATPase fibers were 20 and 12% smaller than control. Fiber type distributions were unchanged following seven days of suspension.

Following seven days of suspension, SDH activities were 10 and 26% higher in the light and dark ATPase fibers in comparison to control rats. HS-EX rats had SDH activities similar to control. In contrast, the number of enzyme units per fiber (SDH activity x cross sectional area) was decreased in

both fiber types of the HS rats, whereas the low intensity exercise program prevented this loss in enzyme units in the dark but not the light ATPase fibers.

These results indicate that short periods of low intensity exercise can significantly ameliorate the atrophy in the soleus muscle associated with hindlimb suspension. Further, the effect is greater for the dark than the light ATPase fibers. In conjunction with the observation that the number of SDH units is maintained in the dark but not the light ATPase fibers of the soleus of the exercised rats, these data suggest that the dark ATPase fibers may have a lower activity threshold for maintaining their size and enzyme content. Future work in this area should concentrate on determining more precisely the amount and the type of exercise that would maximize these effects. ■

BIOCHEMICAL, MORPHOLOGICAL AND MECHANICAL CHARACTERISTICS OF CORTICAL BONE IN YOUNG GROWING RATS EXPOSED TO 7 DAYS OF SPACEFLIGHT: RESULTS FROM THE SL-3 FLIGHT MISSION

A.C. Vailas[1], D. Martinez[1], S. Shaw[1], R.F. Zernicke[1], and R.E. Grindeland[2]
[1]University of California, Department of Kinesiology, Connective Tissue Research Laboratory, Los Angeles, California 90024 [2]NASA/Ames Research Center, Biomedical Research Division, Moffett Field, California 94035

INTRODUCTION

There is considerable interest in studying the adaptation of bones to weightlessness. It has been reported that astronauts in spaceflight progressively show an increase in the excretion of calcium indicating a loss of mineral from bone (1). This decline of bone mineral may result in alteration of the mechanical properties and become an important factor to consider during recovery upon entering earth's gravity. Soviet and U.S. scientists have initiated animal flight missions to better understand the etiology of mineral loss and changes in calcium homeostasis during exposure to weightlessness (1). The primary purpose of our involvement with the recent SL-3 mission was to evaluate specific mechanical properties of selected long bones (humerus and tibia) of rats exposed to 7 days of weightlessness and determine whether these properties reflect alterations in cortical bone structure and composition.

METHODS

Young pathogen-free male rats were randomly assigned to three experimental groups: (1) pre-flight (Pre-Flt), (2) simulated (Sim) and (3) flight (Flt). Pre-flight animals (48d old) were anesthetized and sacrificed, whereas the remaining groups were terminated at 58d (sim) and 56d (Flt). Flight animals were exposed to zero gravity for a period of 7 days and control flight rats (Sim) remained in simulated cages for the same duration of time as the flight group. All groups had free access to food and water. Temperature and light cycle for Sim and Flt groups were also adjusted to conditions on board the shuttle. Humeri and tibial bones were obtained from each group of animals (6 bones per group) and frozen in hermetically sealed containers and stored at - 70°C. Limbs were thawed and prepared for mechanical testing, morphology and biochemical analysis (2,3). Univariate analysis of variance with *post hoc* comparisons were used to detect differences among group means. A significance level of $p=0.05$ was accepted for all statistical tests.

RESULTS AND DISCUSSION

The results in Figure 1 showed that short term spaceflight induced a suppression of longitudinal bone growth. Corrected growths for Sim animals revealed significant differences of humeri lengths as compared to Pre-Flt and Flt rats. However, tibial lengths of Flt animals were lower that Sim, but not statistically significant. These data suggest that spaceflight may affect growth plate maturation by suppressing age dependent chondrogenesis and/or bone formation thereby minimizing the longitudinal growth of the long bones.

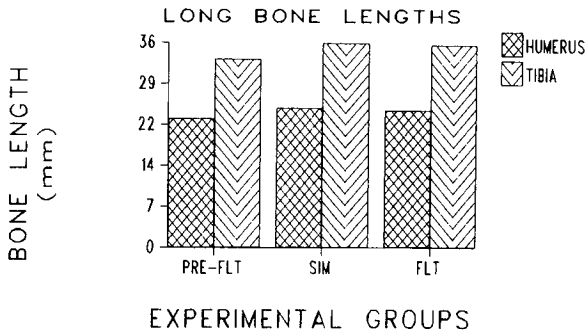

Figure 1.

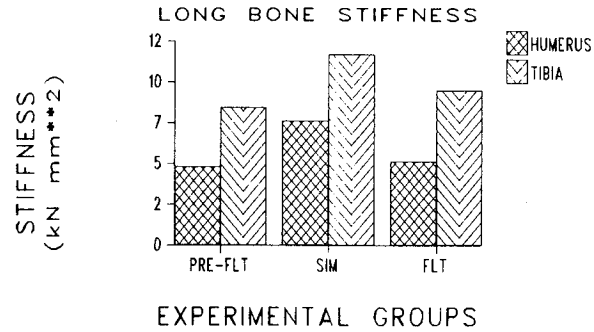

Figure 2.

Short term spaceflight induced cortical bone changes that resulted in more compliant bones (Figure 2). The humerus and tibia of Flt rats were significantly more compliant than Sim animals. A variety of factors are associated with bone stiffness (4). Some are age dependent and to some extent associated with the degree of mineralization (4). Our results would suggest that stiffness characteristics of bones from Flt rats further support the hypothesis of suppressed maturation. However, the underlying factors still remain unclear. For example, the diaphyseal cortical density of the humerus was unchanged, whereas the tibial density was significantly lower in Flt animals (Figure 3). Similar trends were evident when evaluating the calcium to collagen ratio in the same region of diaphyseal bone (Figure 4). Furthermore, the ultimate load was also significantly lower in Flt rats (Figure 5) for both bones. The

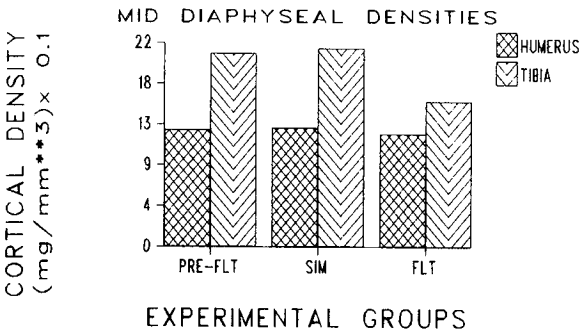

Figure 3.

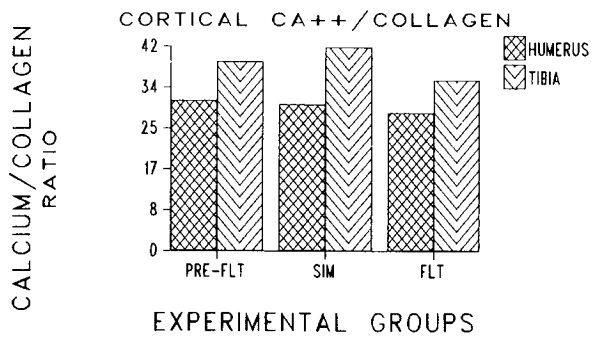

Figure 4.

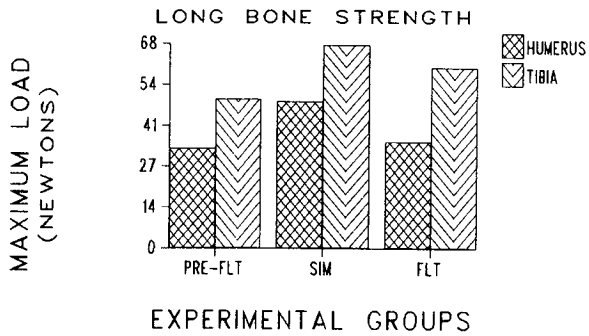

Figure 5.

combined results of tibial density and mineral to collagen ratio suggest spaceflight may affect mineralization in some bones, therefore altering the material properties of long bones. However, not all bones are equally affected by acute exposure to spaceflight. This may be due to differences in load history for each bone that could alter regional microstructure, macromolecular organization and composition. This research is supported by NASA grants NCA2-1R390-501 and NCA2-156. ■

REFERENCES
1. Wronsky, T.J. *et al.* Med. Sci. Sports and Exercise. 15:410-414, 1983.
2. Shaw, S.R. *et al.* J. of Biomech. (In Press), 1987.
3. Vailas, A.C. *et al.* Comp. Biochem. and Physiol. 82B:283-285, 1985.
4. Torzilli, P.A. *Mechanical Properties of Bone*, ASME. 45:145-162, 1981.

SIMULATING EXERCISE IN A TISSUE CULTURE MODEL SYSTEM: STUDIES ON HOW TENSION ALTERS SKELETAL MUSCLE GROWTH

H. H. Vandenburgh
Department of Pathology, Brown University Program in Medicine, Providence, Rhode Island 02906 and Department of Laboratory Medicine, The Miriam Hospital, Providence, Rhode Island 02906

Long-term manned space travel will require a better understanding of skeletal muscle atrophy which results from the microgravity found in space. Astronaut strength and dexterity must be maintained for normal mission operations, for emergency situations, and for the rigors of reentry into the earth's atmosphere. A biochemical understanding of how gravity, by increasing the tension on muscle cells, helps to maintain muscle size and strength, should ultimately allow pharmacological intervention to prevent muscle atrophy in microgravity. Because of the limited availability of performing experiments in space, a number of earth-based model systems have been designed to study the relationship of muscle tension to muscle growth (1). These models include the casting of an animal's limbs so that the limb muscles are held under increased (stretched) or decreased (shortened) tension; placing weights on limb muscles to increase their load; cutting the tendons of synergistic muscles to increase the workload on the remaining intact muscles; and suspending an animal's hindquarters above the ground in order to reduce muscle use.

The field of cellular engineering (*i.e.* designing *in vivo*-like environments for tissue culture cells) is becoming increasingly popular as a method for examining physiological processes which normally do not exist in the artificial environment of tissue culture. These systems have been extensively used for studying basic biochemical growth processes in many cell types and allow easier manipulation of experimental conditions than whole animals. They have been especially helpful in studying the role of growth factors in normal and pathological cell growth.

Our laboratory has developed several tissue culture model systems for studying the relationship of tension to skeletal muscle growth under more *in vivo*-like growth conditions (2,3). We isolate skeletal muscle cells from 12 day old chick embryos and grow them on a highly elastic substratum material in a humidified CO_2 incubator at 37°C (3). The muscle cells, growing in a complex medium, initially proliferate, and then fuse to form multinucleated, spontaneously contractile myotubes in a manner very similar to growth and differentiation *in vivo* (5). These cells actively synthesize actin and myosin and incorporate them into cross-striated myofibrillar material. These *in vitro* differentiated myofibers can be subjected to different patterns of mechanical activity with a "Mechanical Cell Stimulator" which simulates *in vivo* muscle activity. The activity patterns are generated by an Apple IIe computer. In effect, we can subject muscle fibers in a defined *in vitro* environment to different types of "exercise" programs, and study their growth response on a molecular level. Under appropriate growth conditions, the cells can be maintained in tissue culture for 3 to 4 weeks (8,9).

We are utilizing this *in vivo*-like environment to determine the role played by exogenous and endogenous growth factors in tension-induced skeletal muscle growth. We have found that increased tension on these culture cells in a complex culture medium stimulates their growth rate (2). The culture medium contains growth factors from the serum and embryo extract supplements that the cells are grown in, and endogenous growth factors produced by the muscle cells (6,7). To date, our studies indicate that the presence of some as yet undefined growth factor or factors is essential for tension-induced muscle growth to occur. By understanding the interactions between these growth factors and

mechanically-stimulated muscle growth, the mechanisms by which gravity-induced tension are transduced into the biochemical alterations leading to muscle growth will be more clearly defined, and methods for prevention of protein loss from disused muscles in microgravity can be developed. (Research supported by NIH Grant AM36266 and NASA Grant NAG2-414) ■

REFERENCES

1. Vandenburgh, H.H. Motion into Mass: How does tension stimulate muscle growth? *Med. Sci. Sports Exercise*, In Press.
2. Vandenburgh, H.H.; Kaufman, S. An *in vitro* model for stretch-induced hypertrophy of skeletal muscle. *Science* 203: 265-268, 1979.
3. Vandenburgh, H.H. A computerized model system for studying the effects of mechanical activity on cell growth *in vitro*. *In vitro* abstract, in press (copy in Appendix).
4. Rozengurt, E. Early signals in the mitogenic response. *Science 234*: 161-166, 1986.
5. Coleman, J.R.; Coleman, W.W. Muscle differentiation and macromolecular synthesis. *J. Cell. Physiol. 72*: 19-34, 1968.
6. Vandenburgh, H.H. Cell shape and growth regulation in skeletal muscle: exogenous versus endogenous factors. *J. Cell. Physiol. 116*: 363-371, 1983.
7. Summers, P.J.; Ashmore, C.R.; Less, Y.B.; Ellis, S. Stretch-induced growth in chicken wing muscles: Role of soluble growth-promoting factors. *J. Cell. Physiol. 125*: 288-294, 1985.
8. Vandenburgh, H.H.; Karlisch, P.; Farr, L. Maintenance of highly contractile tissue-cultured avian skeletal myotubes in collagen gel. *In vitro* abstract, 1987.
9. Vandenburgh, H.H.; Karlisch, P.; Farr, L. Maintenance of highly contractile tissue-cultured avian skeletal myotubes in collagen gel. *In Vitro*, in revision, 1987.

PAGE 177 INTENTIONALLY BLANK

POTENTIAL HEALTH HAZARDS ASSOCIATED WITH WATER RECYCLING IN SPACE

R. J. Bull
College of Pharmacy, Washington State University, Pullman, Washington 99164-6510

Health hazards that might arise from the recycling of wastewaters are of two types: infectious disease and chemical toxicity. To consider one of these problems without the other can lead to potentially dangerous conclusions. Toxic chemicals will arise in the water system of the Space Station from several sources including human wastes, hygiene water, outgassing of chemicals from materials of construction, experimental studies, synthesis of commercial products, the water storage and distribution system and the treatment processes that are applied to renovating the water. Experience in water treatment systems has shown that the interaction between the latter two variables with the preceding variables is often the major determinant of the hazardous chemicals that will be present in the treated water. A major case in point is the use of disinfectants to prevent waterborne infectious disease, a traditional goal of water treatment. Disinfection processes are receiving considerable attention as major sources of toxicologically important chemicals in water systems. Toxic, carcinogenic, mutagenic and teratogenic chemicals are created in the water by reactions between disinfectants and otherwise innocuous organic material such as that found in human wastes. In addition, chemicals produced by such a process may have completely different tendencies to accumulate in the water system than chemicals that are introduced through the use of the water. Simple judgments based upon the contaminants that might be introduced without consideration of the introduction of new compounds by treatment processes, may in fact be dangerous. The reverse situation can also be hazardous. There might be a temptation to utilize a less effective disinfectant because of very small or even abstract increase in cancer risk due to a by-product of the disinfectant. If this problem is analyzed objectively, the risk attributable to by-product may be very small in comparison to the increased risk of an infectious disease outbreak in space. The obvious goal of research in this area is a program that moves systematically towards a treatment train that minimizes overall risk. This requires close coordination of research efforts in toxicology, analytical chemistry, microbiology and engineering design.

Full evaluation of a water recycling system must consider the human input into the system. Human wastes are likely to be a major source of substrates for interactions with the treatment processes. As a consequence, determination of whether the water is free of hazardous chemicals cannot be done without this input. The input of particulate matter into the cabin condensate on the Space Station is a second major input of substrates for the production of potentially toxic by-products. Therefore, the health hazards that might be associated with recycled water on the Space Station cannot be fully evaluated until it has been placed in space with a crew. Preliminary ground testing of potential treatment systems should be conducted under conditions that simulate conditions in space as closely as possible. The Space Station should be equipped to confirm that the system performs in a manner that is consistent with ground tests. Sufficient analytical capability must be available to ensure that unexpected reaction products do not arise in flight.

In conclusion, it is essential that standards for recycled water on the Space Station be developed in conjunction with the treatment system. It does not make sense to develop a treatment system based upon standards. Standards need to be based upon the actual occurrence of chemicals in the finished water, a variable that is strongly dependent upon the treatment system. On the Space Station, the nature of the chemicals of concern cannot be determined without including man in the overall evaluation of the system. ■

MICROBIOLOGY OF A CLOSED ENVIRONMENT (AS VIEWED BY A CLINICAL MICROBIOLOGIST)

D. H. M. Gröschel
Department of Pathology, University of Virginia School of Medicine, Charlottesville, Virginia 22908

Early studies in the space program have shown that people living in a closed environment for several weeks exchange normal flora, and that eventually the normal flora is quite similar among study participants. With the lack of gravitational force, particles generated either by equipment or by a human body will stay suspended indefinitely, unless removed by artificial means. Thus, the problem posed by the closed environment to the clinical microbiologist is the evaluation of potential exogenous and endogenous sources of microbe-containing particles or nuclei. Such particles may be generated exogenously during biological space experiments or by the mechanical systems of a space station due to contamination before or during the spaceflight. Endogenous flora organisms are generated by the crew during normal breathing, sneezing, or coughing, voiding of urine and feces, and from the skin. Air flow, temperature, and humidity will influence the removal of suspended particles, but an exchange of microorganisms between environment and crew and among crewmembers is unavoidable. Whether microorganisms generated by one crewmember will colonize another member will depend on the type of microorganism and the crewmember's receptors on mucosal surfaces. Special attention must be paid to the role of environmental contamination during body cleansing and waste voiding.

The control of these problems requires both engineering and environmental considerations and personal hygiene. Air handling systems need to be designed so that no primary or secondary contamination of the system can occur and that suspended particles are efficiently removed without altering air speed, temperature, and humidity, because such changes could cause alterations in the crew's physiologic responses to the environment. The normal flora of the crewmembers should not be interfered with by frequent changes in the environment, by special diets or supplements or any other means to change its composition. Whereas broad spectrum *antiseptics* may be useful for the care of mucosa and skin, *antibiotics* should be avoided since the normal flora could be altered and antibiotic-resistant, potentially pathogenic microorganisms could be selected. These could colonize susceptible crewmembers and cause disease. Provisions must be made to recognize health problems due to infection early, and to respond rapidly. Reasonable infection control measures should be designed for the Space Station if an unexpected infection should occur. ■

SPECIAL CONSIDERATION IN EVALUATING THE TOXICITY OF AIRBORNE POLLUTANTS IN A MICRO-GRAVITY ENVIRONMENT

R. O. McClellan, H.-C. Yeh, and R. F. Henderson
Lovelace Inhalation Toxicology Research Institute, P.O. Box 5890, Albuquerque, New Mexico 87185

A considerable body of information exists on the toxicity of airborne material in the earth's environment. This body of information has been developed from opportunistic epidemiology studies on occupationally and environmentally exposed people, from clinical studies in man and from studies in laboratory animals. The key aspects of this body of knowledge will be reviewed with regard to their utility in estimating the toxicity of airborne materials in the space environment. In earth's environment, the normal gravitational force influences the dynamic behavior of the airborne particles and their deposition within the respiratory tract upon inhalation. Normally, inhaled particles are deposited by inertial impaction, gravitational sedimentation, direct interception and Brownian diffusion, with different processes assuming the major role dependent on the size of the particles. In the micro-gravity

environment of space, the sedimentation forces will be substantially reduced. The potential effects of this change on the deposition and the toxicity of particles inhaled in space will be discussed.

Research sponsored by the U.S. Department of Energy's Office of Health and Environmental Research under Contract No. DE-AC04-76EV01013. ■

BACTERIAL RESISTANCE TO DISINFECTION BY IODINE IN WATER SYSTEMS ON SPACECRAFT

G. A. McFeters and B. H. Pyle
Microbiology Department, Montana State University, Bozeman, Montana 59717

This study was done to investigate the adaptation of bacteria to iodine resistance in water systems treated with iodine. Iodine resins have been used in the microbial check valve (MCV) on the Shuttle Orbiters, and it has been proposed to use similar treatment on the Space Station. The Space Station environment will also necessitate reclamation of used water which may lead to colonization of the system by resistant bacteria.

Cultures of bacteria isolated from water on Shuttle Orbiters and a prototype recycled body shower system have been tested for sensitivity to iodine under controlled conditions in the laboratory. These include members of the genera *Pseudomonas, Staphylococcus,* and *Bacillus.* All of these species include opportunistic pathogens which may cause infections. These isolates were 1-4 logs more resistant to iodine (1 mg/l for 2 min) than a culture of *P. aeruginosa* obtained from the Centers for Disease Control, Atlanta (GA). The *P. aeruginosa* had been isolated from a hospital povidine-iodine solution and was considered by CDC to be iodine-resistant.

It was found that the resistance of *P. cepacia* and *P. aeruginosa* was 3-4 logs greater when the cultures had been grown under nutrient-limited conditions (phosphate buffered water, pH 7.2 [PBW], or reverse osmosis water) than when they had been grown in rich medium (brain heart infusion [BHI] or mineral salts medium enriched with glutamate and glucose) before iodination. Cultures grown as biofilms on stainless steel were 2-3 logs more resistant than controls grown in PBW.

Iodinated cultures of *P. cepacia* and *P. aeruginosa* grown in BHI or PBW were centrifuged and resuspended in fresh PBW after iodination. The *P. cepacia* increased from 10^2 to 10^6 CFU/ml within 3-5 days, the uniodinated controls increasing at similar rates to iodinated cell suspensions. Cultures originally grown in BHI recovered in PBW more rapidly than those grown in PBW before iodination. Iodinated *P. aeruginosa* originally grown in BHI increased from 10^2 to 10^5 CFU/ml in PBW within 5 days after iodination; uniodinated controls did not increase from 10^2 CFU/ml or became undetectable after 2-7 days. Both iodinated and uniodinated *P. aeruginosa* grown in PBW increased from 10^1 to 10^5 CFU/ml within 4-6 days. These results indicated that although there may be a low or undetectable number of bacteria surviving disinfection with iodine, this recalcitrant population may grow to significant numbers within a few days if water is stored after treatment.

The observed differences in sensitivity to disinfection after growth under high- and low-nutrient conditions are similar to those reported for pseudomonads and other bacteria including mycobacteria and legionellae disinfected with chlorine. Recovery of disinfected bacteria has been observed after water and waste treatment. In this study, iodinated cell suspensions generally recovered faster and attained higher numbers of viable colony-forming units in PBW than uniodinated controls. It is thus possible that iodination (or other forms of disinfection) may stimulate some bacteria to grow better in low-nutrient environments, such as potable water systems. This sensitivity to disinfection and subsequent recovery depend not only on the antecedent growth conditions, but also on the characteristics of the bacteria present. Isolates from low-nutrient environments may respond differently than those isolated from nutrient-rich situations.

The increased resistance of bacteria grown in biofilms may be significant in spacecraft water systems because colonization of such a system may lead to large numbers of bacteria sloughing off surfaces and

becoming suspended in the water. If these bacteria are highly resistant to the disinfectant used, they may pose a potential health risk to users of the water. Further, growth of bacteria in biofilms may lead to corrosion and clogging of system components.

The finding that all isolates from the Shuttle Orbiters or shower system were more resistant to iodine than the CDC isolate suggests that treatment of water in these systems with iodine selects bacteria with increased iodine tolerance or resistance. It may thus be necessary to select alternative disinfectants for use instead of or as well as iodine.

We consider that disinfection studies should include examination of bacteria freshly isolated from low-nutrient environments, if possible those for which the study is being done. They should be grown and maintained in low-nutrient media, and their ability to recover after disinfection should be tested. Their potential for biofilm development and subsequent resistance should also be examined. Systems for potable water treatment and reclamation in confined environments such as the Space Station should be designed taking into consideration the sensitivity of bacteria growing in low-nutrient environments, possible development of biofilms, and consequent disinfection and corrosion problems. ■

ENVIRONMENTAL HEALTH MONITORING ONBOARD SPACE STATION

D. L. Pierson and D. M. Russo
Biomedical Laboratories Branch, NASA/Johnson Space Center Houston, Texas 77058

The Space Station is the most ambitious and complex program in NASA's history. It will establish a permanent manned presence in space and provide an essential base camp for future manned explorations of earth's solar system. The planned orbital life of the Space Station together with its man-tended laboratory capabilities and long tours of crew duty will provide unparalleled opportunities for basic and applied research in a microgravity environment. However, many of the Space Station features which afford these unique research opportunities also necessitate that a comprehensive environmental health monitoring program be developed and implemented for the health and safety of the Space Station crew. During the afternoon parallel session on Environmental Factors, Space Station operational and design features which create the special need for environmental monitoring will be outlined and the current plans for the Environmental Health Monitoring subsystem (EHMS) described. An overview of the approach taken in developing the EHMS together with a summary of currently baselined monitoring requirements will be provided. In addition, this session will provide a special focus on some of the major toxicological, microbiological, and water quality issues which must be addressed in order to ensure the continuous habitability of the Space Station. ■

THE SPACE STATION ENVIRONMENTAL HEALTH SUBSYSTEM

R. L. Sauer[1], D. L. Pierson[1], N. M. Cintron[1], D. Russo[2]
[1]Biomedical Laboratories Branch, Johnson Space Center, Houston, TX and [2]KRUG International, Technology Life Sciences Division, Houston, Texas

---

Many of the unique features of the Space Station present inflight environmental maintenance and monitoring requirements not previously encountered in US manned space programs. These features include a closed loop water recycling system, 90-day duty tours, and a 20-30 year orbital life. A major effort associated with the successful development, deployment, and operation of the Space Station will be the provision of the Environmental Health Subsystem (EHS). The EHS is being developed to address crew health and safety issues related to the special operational characteristics of the Space Station and to help ensure its continuous habitability. The EHS includes subsystem components which focus on prevention of environmental contamination, inflight environmental monitoring, contamination countermeasure, and information management. The functions and development needs of the EHS monitoring component are highlighted in the presentation. ■

PAGE 183 INTENTIONALLY BLANK

PRECEDING PAGE BLANK NOT FILMED

OVERVIEW OF CELL BIOLOGY—Panel Discussion

Studies from early space flights have demonstrated that there are basic physiological changes in microgravity. These include loss of electrolytes, loss of lean muscle mass, reduced immune activation response and loss of calcium and mineralized bone. The cause of most of these clinical manifestations is not known. Until recently these changes were thought to be systemic. However, data from many of the scientific investigations from Biosatellite, Skylab, and shuttle flight would support a more basic biological response to microgravity that might occur at the tissue and cellular level. These investigations demonstrated a change in growth and differentiation in insects, eukaryotic and prokaryotic cells, and in simple organisms that were exposed to microgravity.

This minisymposium will bring together scientists from Biosatellite, STS-8 and D-1 for an indepth discussion of their results describing basic changes of cell function in microgravity. The cell systems to be discussed include plants, simple single cell organisms and human cells.

The presenters will include Dr. Abraham D. Krikorian who will discuss growth and differentiation of plant cells in microgravity. He will give special emphasis on his experiments on competent carrot cells as they underwent somatic embryogenesis. The implications of chromosomal data from flight experiments will be integrated. He will attempt to correlate circumstantial evidence as well as the limited space flight data on gravity and plant development. The second speaker, Dr. R. R. Theimer will discuss his results from D-1 on anise (*Pimpinella antisurum L.*) plant cells grown in microgravity. His presentation will include his observations of increased callus cell growth and accelerated rate of somatic embryogenesis in flight specimens.

Changes in function and growth of simple life forms will be addressed by Dr. H. Planel. He will discuss his paramecium experiment from D-1, where he observed that *Paramecium tetraurelia* grew at four times the rate of ground and 1-g controls. Dr. von Borstel will discuss results on genetic experiments conducted at Biosatellite II using *Habrobracon juglandis* wasps. He will also discuss the implications of the genetic changes to space flight.

Human lymphocyte cell function will be discussed by Dr. A. Cogoli. Dr. Cogoli's presentation will include his results showing a 90% decrease in cell proliferation in flight. He will also discuss the interaction of basic research to biotechnology.

The final speaker Dr. Marian Lewis will discuss results of the STS-8 flight electrophoretic separation as well as the progress of the new NASA bioreactor.

These presentations promise to present new insights and lively discussions on the effects of microgravity on basic cell function. ■

CELL CULTURES IN SPACE: FROM BASIC RESEARCH TO BIOTECHNOLOGY

A. Cogoli
Laboratorium fur Biochemie, Eidgenossische Technische Hochschule, Zurich, Switzerland

Investigations performed by us and several other laboratories on recent space missions clearly show that single cells in culture are sensitive to gravity. Important cellular functions like proliferation rate, biosynthesis, membrane permeability, and cytoplasmic streaming are altered under microgravity conditions.

The extent of the alteration and the appearance of an inhibiting or promoting effect depend on the type and properties of the cells. This means that one must distinguish between differentiating/

nondifferentiating cells, adhering/nonadhering cells, cells moving on a substrate/cells capable of active swimming in a medium. In addition, other important aspects must be considered: sedimentation/distribution of cellular organelles, cytoplasmic streaming/distribution of metabolites, cell shape/membrane properties, cell movements/cell-cell interactions. Although much progress has been achieved in the knowledge of the adaptation processes of the cell to altered gravity conditions, many important investigations are required on future missions in order to understand the phenomena observed.

Nevertheless, some of the effects detected in microgravity might be exploited for biotechnological endeavors. Cell cultivation together with electrophoresis and cell fusion are the most promising technologies for bioprocessing in space. Biorack, the multipurpose facility provided by ESA and flown for the first time on Spacelab D-1, has proven to be an excellent instrument for biological research in space.

Future experiments on Spacelab missions like SLS-1, IML-1 and D-2 shall provide further important information on the behavior of cells in microgravity.

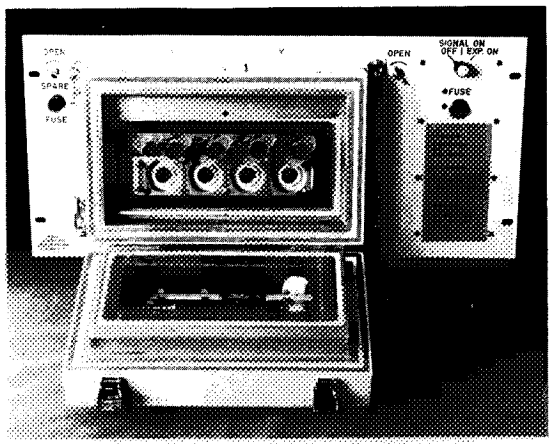

Figure 1. Cell culture incubator flown on STS-8 (Challenger), Spacelab-1 and to be used on SLS-1 in 1989. The incubator, developed and manufactured in our laboratory, consists of a carry-on box in which the temperature can be kept at 37°C, with battery or Spacelab power.

Figure 2. Prototype of a cell culture chamber, developed in our laboratory, with automatic medium replacement based on an osmotic pump. To be flown in Biorack/IML-1 in 1990.

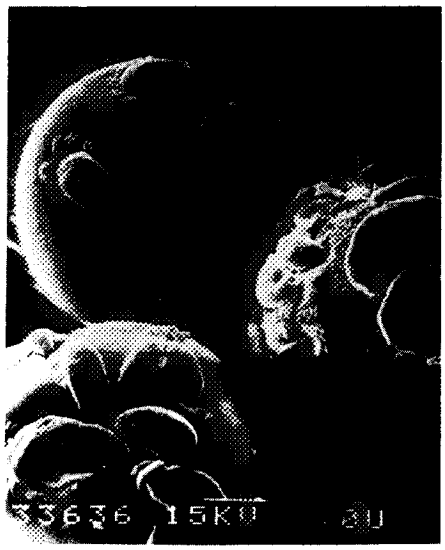

Figure 3. Biotechnology in space. Human Embryonic Kidney cells adhered normally to microcarrier beads in microgravity. Cells are fixed with glutaraldehyde after 24 hours incubation time (see reference 1).

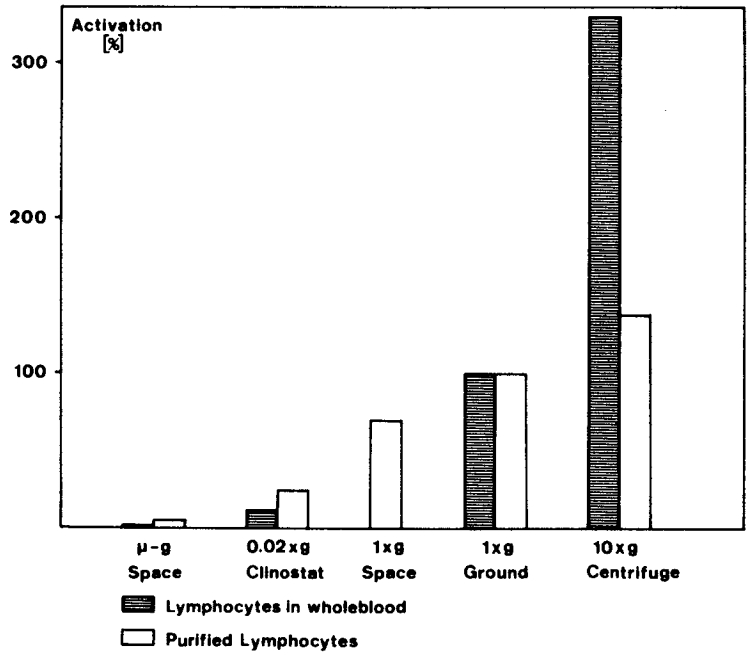

Figure 4. Correlation between g-level and human lymphocyte activation by concanavalin A, from data in references 2,3,4,5. Cultures of lymphocytes, either purified or in blood diluted with medium, were exposed to concanavalin A for 3 days at different g-levels in space and on the ground. The activation at 1-g on the ground is taken as 100%.

Most of the flight hardware used in our experiments in space was developed and manufactured in our laboratory: a tissue culture incubator and flasks flown on STS-8 and Spacelab-1, a blood kit for inflight blood draws, syringe containers and cell culture flasks flown with Biorack on Spacelab D-1. Figures 1-4 give a pictorial representation of our activities in space biology and biotechnology. A selection of references concerning our work is given below. ■

REFERENCES
1. A. Tschopp, A. Cogoli, M.L. Lewis and D.R. Morrison, J. Biotechnology 1: 287-293 (1984).
2. A. Cogoli and A. Tschopp, Adv. Biochem. Eng. 22: 1-50 (1982).
3. A. Cogoli, A. Tschopp and P. Fuchs-Bislin, Science 225: 228-230 (1985).
4. B. Bechler, A. Cogoli and D. Mesland, Naturwissenschaften 73: 400-403 (1986).
5. G. Lorenzi, P. Fuchs-Bislin and A. Cogoli, Aviat. Space Environ. Med. 57: 1131-1135 (1986).

CELL ELECTROPHORESIS AND PRELIMINARY CELL ATTACHMENT INVESTIGATIONS ON STS-8

M. L. Lewis[1], D. R. Morrison[2], G. H. Barlow[3], P. Todd[4], A. Cogoli[5] and A. Tschopp[5]
[1]KRUG International, Technology Life Sciences Division, Houston, Texas 77058, [2]NASA/Johnson Space Center, Houston, Texas 77058, [3]The Bioprocessing Research Center at Houston, Houston, Texas, [4]Bioprocessing and Pharmaceutical Research Center, Philadelphia, Pennsylvania, and [5]ETH Zentrum, Zurich, Switzerland

During the last decade, the Cell Biology Research Laboratory of the Medical Sciences Division, NASA/Johnson Space Center, has conducted cell biology space research in two general areas. The first area, whole-cell electrophoresis, had as its objective the exploitation of microgravity to enhance the separation of specific populations of cells in heterogenous suspensions. The second research area, cell attachment and growth on microcarrier beads in microgravity, demonstrated the capability of initiating cell cultures in space and provided the background for more sophisticated future cell biology experimentation such as high density culture of anchorage-dependent cells and effects of microgravity

on metabolic and structural macromolecules and on secretory processes. This presentation summarizes both of these research areas and describes microgravity compared to ground-based results.

Electrophoresis, movement of charged particles through a medium by application of an electrical field, is one method of cell purification. On earth, this method is severely limited by sedimentation and gravity-driven convective mixing. In microgravity, these factors may be negated. Production of desirable natural products from cells in culture may be enhanced if the producer cells can be separated from nonproducers. The earliest space-based cell electrophoresis occurred on the Apollo Soyuz Test Project (ASTP) mission in the summer of 1975. A small-volume, static-column electrophoresis device was used to separate human kidney cells. One fraction produced much higher levels of urokinase than other fractions (1) and thus, demonstrated the potential of the microgravity environment for separation of functionally discrete cells.

On STS-8, human kidney cells were separated in duplicate runs on the continuous flow electrophoresis system (CFES) developed by the McDonnell Douglas Aeronautics and Astronautics Company in St. Louis. Postflight, the subpopulations were cultured and assayed for urokinase (u-PA) and tissue plasminogen activator (t-PA) as markers for separation of functionally discrete populations. The cells separated into 34 and 37 subpopulations respectively in runs designated 3 and 4 (Fig. 1A). The resolution of separation of cells inflight appeared to be superior to that of earth-based separations. Substantial cell numbers were found over most of the range, 28-32 fractions from flight, compared to only 16 or 17 midrange fractions in the ground-based separations. For each subpopulation, two to ten replicate cultures were set up and medium was tested for plasminogen activators by a battery of fibrinolytic and chromogenic assays. Good reproducibility of separation of functionally similar cells was apparent as exemplified by t-PA. Spread over the whole range of mobilities, cells in the same general mobility locations produced highest levels of t-PA in both flight separations (Figs. 1B and 1C, dark hatch bars). In the ground-based separations, the t-PA producers were concentrated mainly over several fractions in the mid-mobility range. Although the cells were successfully separated inflight, the experiment was compromised in several ways including reduced viability due to suspension of the cells for long periods of time in the CFES buffer, microbial contamination of several of the collected fractions, and possible failure to collect very low mobility cells due to the collection tray configuration. One of the advantages in space-based CFES separations is that much higher concentrations of materials may be input into the device. During the STS-8 tests, this advantage was not realized because many of the cells did not exit into the CFES chamber from the CFES syringe in which they were suspended prelaunch for

Figure 1.

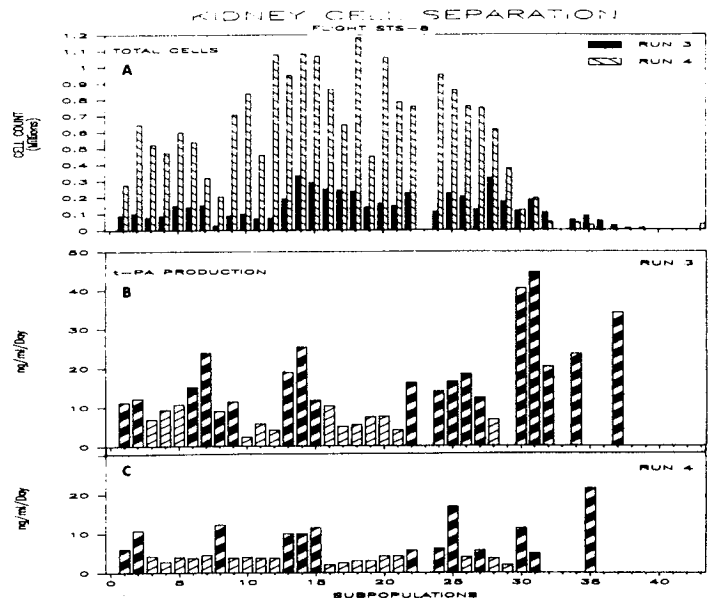

transport into space. A future experiment should include input of high cell numbers as an objective to demonstrate this as an advantage for microgravity CFES cell separations.

The second research area, attachment and growth of anchorage-dependent cells in space was investigated by use of human kidney cells and dextran polymer beads coated with collagen. The attachment of cells to growth surfaces in 1g is normally affected by the settling of the cells onto the surface of flasks or other culture vessels. On STS-7, at ambient temperature and on STS-8 in a 37°C cell culture incubator, cells were mixed with microcarrier beads on orbit and fixed by injecting glutaraldehyde at selected times. After return to earth, cell-to-bead attachment was evaluated by counting beads with cells attached, numbers of cells per bead and the numbers of unattached cells. To determine numbers of beads with cells attached, a total of 300 beads were scanned per each of four slide preparations. Each bead was classified as having no cells, one to five cells, or ten or more cells. A plot of the means and standard deviations for the categories of beads with no cells (A) and beads with one to five cells (B) attached is shown in Fig. 2. Although no apparent differences were seen by electron

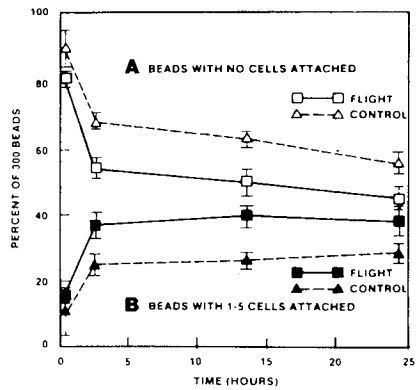

Figure 2. Kidney cell attachment to microcarrier beads on STS-8.

microscopy in the manner in which cells attached in microgravity compared to the ground control, the attachment efficiency in microgravity appeared to be superior to that in the earth-based control. These findings clearly showed that cell cultures may be initiated on microcarrier beads in the environment of space.

This cell attachment data is vital to the development of a bioreactor for the mass culture of anchorage-dependent cells in microgravity. The Space Bioreactor being developed in our laboratories at JSC will be capable of supporting growth and maintenance of many cell types under a wide shear range in a zero headspace vessel under process control. Looking forward into the next decades of Life Sciences research in space, such a bioreactor will be capable of providing cell cultures for basic microgravity research on cellular functions at the molecular level. Such functions may induce secretory processes, cell cycle control, expression of latent viruses, cytoskeletal arrangement and production of specific proteins. ■

REFERENCES

1. R.E. Allen, P.H. Rhodes, R.S. Snyder, G.H. Barlow, M. Bier, P.E. Bigazzi, C.J. Van Oss, R.J. Knox, G.V.F. Seaman, F.J. Micale and J.W. Vanderhoff. Column electrophoresis on the Apollo-Soyuz Test Project, Separation and Purification Methods 6:1-59, 1977.

EFFECTS OF MICROGRAVITY ON A SINGLE-CELL ORGANISM, *PARAMECIUM TETRAURELIA*

H. Planel, G. Richoilley, J. Templier, R. Tixador, and G. Gasset
Laboratoire de Biologie Médicale, Faculté de Médecine, 37 allées Jules Guesde, 31073 Toulouse Cedex, France

The problem of a possible effect of microgravity on cells is still unsolved in spite of several theoretical works and results of some space experiments. However, no effects were noted on human embryonic lung ficroblasts (Montgomery et al. 1978), hamster epithelial cells (Souchkov and Roudneva 1979) and carrot cells (Steward and Krikorian 1978). Microgravity effects were investigated in our laboratory in *Paramecium tetraurelia,* i.e., in a biological object we have been working on for many years in the field of radiobiology.

A new technique for cell culturing and fixation was developed.

Ten-day post-autogamous cells in division were isolated by cloning. Sister cells were picked and each cell was introduced in a small plastic (polyethylene) bag with 1.3 ml in Cytos experiments or 0.65 ml of medium in Paramec experiment (straw medium bacterized with Aerobacter aerogenes) (fig. 1). Each plastic bag included one or two small glass ampullae filled with a fixative (formaline 85%, acetic acid 5% and sulfuric ether 10% or glutaraldehyde 35% in cacodylate buffer 0.2M). Plastic bags were placed in trays which were housed in a culture box. Metallic spindles were laid above the cultures; their rotation made by crew induced glass ampulla breaking. Fixative could spread out resulting in whole culture fixation within one or two minutes.

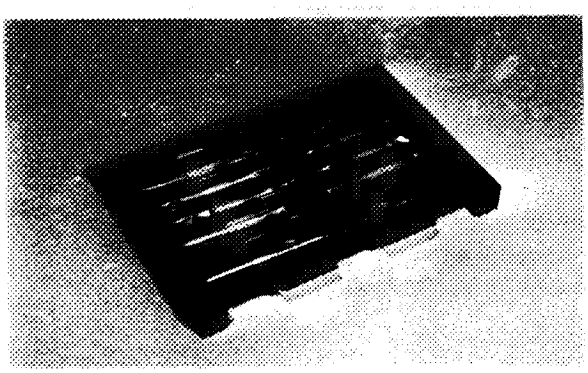

Figure 1a. Culture chambers (plastic bags, before and after soldering, including glass ampullae filled with a fixative under pressure and held in small plastic pieces).

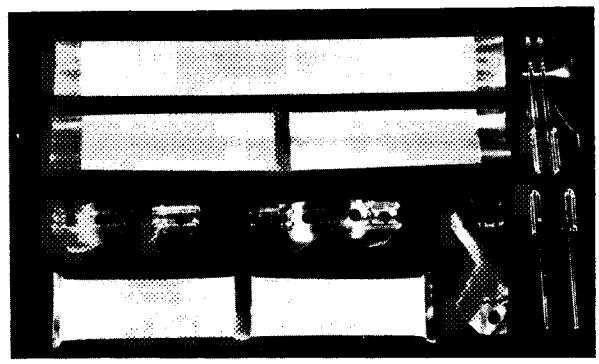

Figure 1b. Flight package: culture chambers and metallic rotating spindles.

Just after cloning, cultures were kept at a low temperature (8 or 9°C) in order to avoid cell division during launch, when cultures were exposed to the space flight dynamic factors. In orbit cultures were transferred into an incubator at a temperature of 25°C ± 0.1 (Cytos experiment) or 22°C ± 0.5 (Paramec experiment). Sequential fixations were made simultaneously for inflight and control cultures.

The two Cytos experiments, carried out aboard the Soviet Space Station Salyut 6, have shown that the spaceflight resulted in a stimulatory effect on cell growth rate (fig. 2), higher cell volume, decrease in cell dry weight, cell total protein content and changes in intracellular electrolytes (fig. 3).

Several experiments were carried out later in order to understand the origin of these responses:

—First, the assumption of a possible indirect microgravity effect has been rejected: cell growth rate was unchanged when paramecia were cultivated in a low clinostat, ie, when the distribution gradient of nutrients and waste was disturbed as in space;

—On the other hand, Cytos experiment responses could be ascribed to cosmic rays. On earth previous experiments have shown that background or very low doses can stimulate the proliferation of

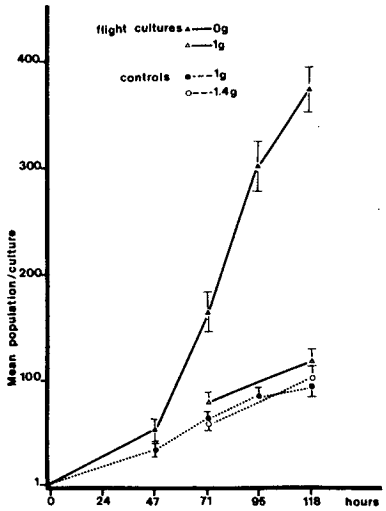

Figure 2. Experiment Cytos, flown aboard the orbital Saliut station. Growth curves of in-flight and control cultures.

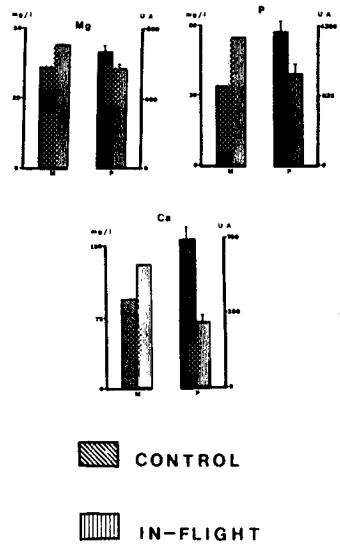

Figure 3. Experiment Cytos. Changes in extracellular (M) and intracellular (P) electrolytes (UA: arbitrary units).

paramecia (Planel et al. 1976-1987). Using the same techniques as in space, experiments were carried out in airborn balloon flights. Under these conditions, gravity was normal but cells were exposed to a radiation level closer to that of orbital flights. A higher cell growth rate was noted but other parameters remained unchanged (Planel et al. 1985). It can be concluded it was likely that changes in the cultures flown aboard Salyut could be also related to a direct effect of microgravity.

This assumption was confirmed by the "Paramec experiment" performed in the Spacelab, aboard Challenger in October 1985. In this case, static cultures and cultures placed in a 1-g centrifuge were investigated. Fig. 4 shows that the spaceflight resulted in a strong stimulatory effect on cell growth rate, but this effect disappeared in the centrifuged cultures. The small differences between these cultures and earth-based controls could be due to cosmic rays (Richoilley et al. 1986).

This microgravity effect on the proliferative activity of paramecia is in good agreement with experiments on earth which have shown that growth rate was reduced after exposure to different levels of hypergravity. Furthermore, the discrepancy between experiments conducted with paramecia and

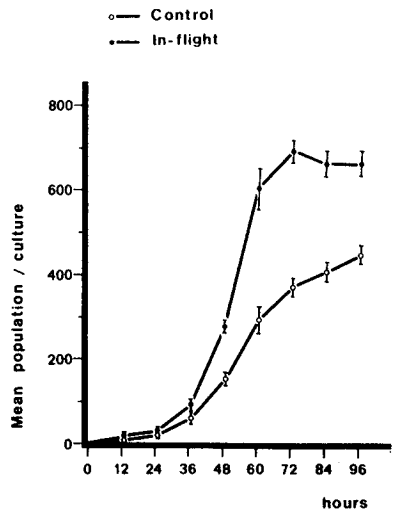

Figure 4. Experiment Paramec carried out in Spacelab (D-1 Mission of Challenger). Growth curves of static and centrifuged in-flight cultures, of static and centrifuged cultures on earth.

other space experiments can be related to the nature of the biological objects: indeed, gravity and microgravity effects must be different in adherent cells, fixed on solid supports (Montgomery, Souchkov and Foudneva experiments), in lymphocytes (Cogoli et al. 1984), free cells devoided of active motility or in a free swimming cell, such as paramecium, which exhibits a negative geotactism on earth. In microgravity, we can assume that cell moving was facilitated: ATP could be saved and used for cell metabolism and cell division. ■

REFERENCES

Cogoli A, Tschopp A, and Fuchs-Bislin P. Cell sensitivity to gravity. Science 1984, 225:228-30.

Montgomery P. O'B, Cook JE, Reynolds RC, Paul JS, et al. The response of single cells to zero-gravity. In vitro 1978, 14:165-73.

Planel H, Soleilhavoup JP, Tixador R, Croute F and Richoilley G. Demonstration of a stimulating effect of natural ionizing radiation and of very low radiation doses on cell multiplication. In: Biological and Environmental Effects of Low-Level Radiation. International Atomic Energy Agency, Vienna, 1976, 1:127-40.

Planel H, Tixador R, Nefedov Y, Gretchko G, Richoilley G, Bassler R and Monrozies E. Space flight effects on Paramecium tetraurelia flown aboard Salyut 6 in the Cytos I and Cytos M experiments. Adv. Space Research, 1981, 1:95- 100.

Planel H, Soleilhavoup JP, Tixador R, Richoilley G, Conter A, Croute F, Caratero C, Gaubin Y. Influence on cell proliferation of background radiation or exposure to very low chronic gamma radiation. Health Physics, 1987, 52 (in press).

Richoilley G, Tixador R, Gasset, G, Templier J and Planel H. Preliminary results of the "Paramecium experiment." Naturwissenschaften 73, 1986, 404-6.

Souchkov FV and Roudneva SV. Experiments performed on Mammalian cells cultivated in vitro. In: Biological Research in "Cosmos" Biosatellites, ed. Science Moscow, 1979, 199- 213.

Steward FC and Krikorian AD. The morphogenetic responses of cultured totipotent cells of carrot (Daneus carota L) at zero gravity. Final reports of US experiments flown on the soviet satellite Cosmos 782. NASA 1978, TM 78525, 71- 159.

MICROGRAVITY: UNDERSTANDING INFORMATION PROCESSING IN GRAVITY RECEPTORS—Panel Discussion

Gravity receptors (statocysts in invertebrates and otolith organs (maculas) in vertebrates) are the only organs that evolved in animals for the sole purpose of measuring linear accelerations, both gravitational and translational. Information from these biological accelerometers is used to orient the organism in earth's gravitational field, and to guide its motion while maintaining balance relative to the gravitational vector. Fundamental biological questions concern the activity of gravity receptors in an environment in which the gravitational vector is essentially absent, and the resulting physiological and behavioral consequences to the animal. Particularly, adaptive mechanisms inherent in this neural tissue cannot be understood except by study of specimens exposed to microgravity. While it might be expected that a system as sophisticated functionally as a gravity receptor would be a complex processor of incoming signals, such an interpretation has not been readily apparent from past experimental results. Traditional views of these accelerometers held that the neural snesing cells were essentially passive conduits standing between the inertial test mass (otoliths, otoconia) and the nerves leading to the central nervous system. The receptor/nerve combination functioned in most cases as a sequential (or digit digital) computer. Now, however, reconstructions of nerve terminals and their hair cells in rat maculas are revealing that these gravity receptors are morphologically organized for parallel processing of information. Study of other available species (gerbil, monkey) shows that they are similarly organized. These results bring the gravity receptors into line with other complex neural tissues, such as retina and brain, that are known to be organized into networks for parallel processing and transmission of information. The findings also open the possibility for cross-fertilization between computer and vestibular researchers. Theoreticians working with computers have developed methods for analyzing models of neural networks which, they hope, will lead to greater understanding of processes involved in learning. Maculas provide the most simple, biological neural network yet observed. Research on them as parallel processors would appear to be useful both to computer-based neural network theoreticians and to vestibular researchers. This workshop, then, begins the exploration of mammalian gravity receptors as neural networks which process information in parallel, and as end products of an evolutionary history that has seen them progress from units that are both the sensors and the responders to linear acceleratory vectors, through a stage of sequential (digital) computing, to the end product in which maculas became parallel processors. It is the first attempt to ask investigators in the field, whether they work on invertebrate or on vertebrate gravity receptors, to examine their data not as isolated bits of information, but in the context of what the findings contribute to our understanding of how the receptors analyze information. The interpretations will be important in efforts to model the neural network in a dynamic way, to better understand how it works. Such a model will also be important to help us determine the most important gaps in knowledge which experiments on the ground or in space can address most profitably. It can also be used to predict adaptive mechanisms to novel gravitational environments, such as microgravity; and the predictive model can be tested and sharpened through spaceflight. The expected outcome in years ahead is a greater understanding not only of how gravity receptors function on earth and adapt to microgravity, but of how brain functions. An ultimate issue, which is of potential usefulness to many fields, is whether unravelling the functional organization of gravity receptors will yield a return in terms of the future design of "smart" computers. ■

PHYSIOLOGICAL STUDIES ON SEMICIRCULAR CANAL AND OTOLITH AFFERENTS IN RAT

R. H. I. Blanks
Department of Anatomy and Neurobiology and Department of Surgery University of California Irvine, Irvine, California 92717

The rat is an extremely valuable, low-payload mammalian model for studies on the developing and mature vestibular system. Unfortunately, neither the orientation of the semicircular canal planes nor the response dynamics of primary otolith afferents are known for this species. Accordingly, recordings were obtained: 1) from primary semicircular canal afferents during "null-point" testing *i.e.*, during rotation of the animal about different axes to define mathematically the canal planes in relation to stereotaxic coordinates, and 2) from primary otolith afferents to examine response characteristics during lateral (roll) head tilts. Both the superior and inferior division of the eighth nerve were sampled in anesthetized rats so as to observe the behavior of each semicircular canal (horizontal, anterior and posterior) and otolith receptor (uricle, sacculus).

Preliminary data using "null-point" technique indicates that the three canals are approximately orthogonal, and that the horizontal semicircular canals in rats are inclined 35 ° relative to the horizontal stereotaxic plane. Thus, the optimal position for maximally stimulating the horizontal canal during horizontal rotation and for minimally stimulating the vertical canals is with the animal pitched 35 ° (nose-down) re. Horsley-Clarke horizontal.

In response to ramp changes in head position, the response of many otolith afferents showed a phasic-tonic response pattern with an overshoot (or undershoot) followed by a return to a new steady state level of activity within 4-12 sec. The remaining units showed predominantly tonic responses in which the rate was proportional to head position and was independent of the velocity of transition. During sinusoidal roll accelerations, the tonic units showed small phase leads (0-20 ° re. angular displacement) and approximately flat gain curves over the frequency range examined (0.025 to 0.5 Hz.). In contrast, phasic-tonic units showed large phase leads (20-55 ° phase leads) and 2-5 fold gain increases over the same frequency range.

Such quantitative data from semicircular canal and otolith afferents will permit quantitative studies on the physiology of central canal-otolith convergence in rat. Such information from ground-based experiments will eventually permit an analysis on the effects of microgravity on the developing and mature mammalian gravity receptor system. ■

MECHANOSENSORY-ACTIVATED AND VOLTAGE-DEPENDENT ION CHANNELS IN STATOCYST HAIR CELLS OF *HERMISSENDA CRASSICORNIS*

J. Farley and L. M. Grover
Program in Neuroscience and Behavior, Department of Psychology, Princeton University, Princeton, New Jersey 08544

We have studied mechanosensory-activated and voltage-dependent ion channels in statocyst hair cells of the nudibranch mollusc *Hermissenda* with the aim of understanding how these currents shape the generator potential and the patterning of action potentials in response to gravitational stimulation. In these experiments,the hair cell soma was isolated from active and synaptic membrane areas by lesioning the static nerve (which carries hair cell axons) at the point where the nerve enters the cerebropleural ganglion. Following treatment with a nonspecific protease solution (Sigma type XXIV or XXV, 1 mg/ml, 10-11 min), a hair cell was impaled with two microelectrodes (35-50 MΩ, 3M KCl) connected to a conventional 2 micro-electrode voltage-clamp system.

Previous intracellular recording studies of *Hermissenda* hair cells under current-clamp conditions (Alkon & Bak, 1973; DeFelice & Alkon, 1977; Grossman & Alkon, 1982; Stommel *et al.*, 1980) have presented evidence that the increased voltage-noise and depolarizing generator potential produced by mechanical- or gravitational-induced interaction between hair cell cilia and statoconia reflects mechanosensory-activation of a Na^+-selective channel in the receptor membrane. We have studied these channels by means of fluctuation analysis of ionic current-noise, under voltage-clamp control. Current noise amplitude is typically 1-2 orders of magnitude greater for hair cells exposed to 1 g force by tilting ("loaded" condition, Figure 1) than in the non-stimulated ("unloaded") case. Current noise

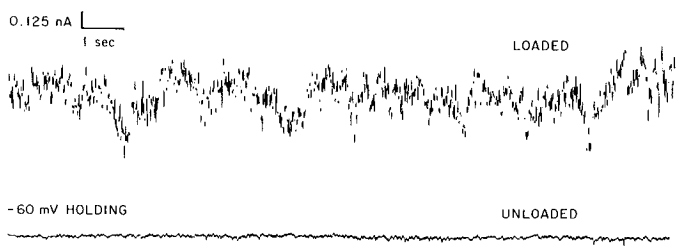

Figure 1. Current-noise from *Hermissenda* statocyst hair cell in loaded vs. unloaded conditions. Cell was voltage-clamped at -60 mV in a standard ASW solution, using conventional two microelectrode voltage-clamp techniques. Current signal was amplified 200 times, filtered at 300 Hz (high-frequency cutoff) and stored on an HP instrumentation recorder for later off-on line analysis. Tilting of preparation resulted in the mass of statoconia coming to rest on or near the caudal portion of the statocyst (loaded condition). Tilting 90° in the opposite direction resulted in the statoconia moving toward the opposite pole of the cyst, away from the caudal hair cells (unloaded condition). Note the two conspicuously large bursts of inward (down) current in the loaded condition. These are likely to reflect the simultaneous interaction of a statoconia with one or more motile cilia.

amplitude increases in an approximately linear fashion as the steady stateholding potential of the hair cell is made more negative than -40mV (Figure 2). Removal of extracellular sodium results in a reversible decrease in noise (Figure 2) amplitude, though it does not completely abolish it. In addition, the power spectra for many (~50%) cells was decidedly non-regular (see Figure 3) with a peak in the 7-12 Hz range. This coincides with the mean frequency of the inherent motions of statocyst hair cells. Individual records of current noise (Figure 2) revealed that the 7-10 Hz peak in the power spectra corresponded to the presence of large, discrete, inward currents, with an extrapolated reversal potential $> +10$ mV. Collectively, these results indicate that Na^+ ions make a significant contribution to the ionic current through the mechanosensory-activated channels.

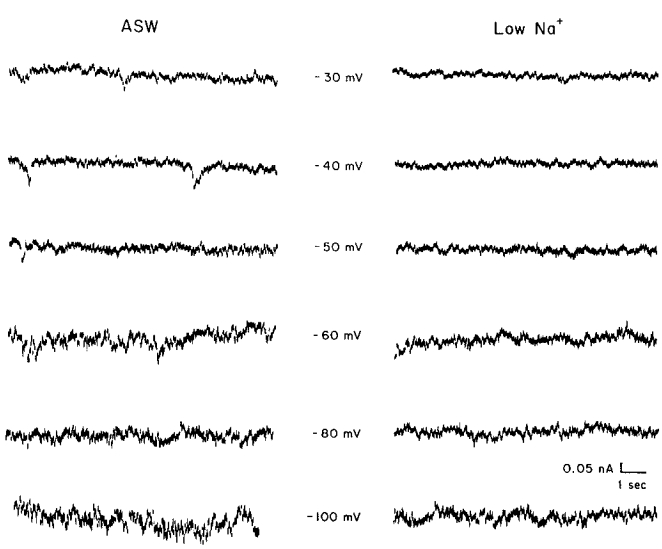

Figure 2. Effects of Na^+ ions and holding potential level on current-noise amplitude of a partially loaded caudal hair cell. All records obtained from same cell. In normal Na (430 mM) ASW (left half) increases in holding potential result in progressively larger current noise variance (~2-3 times as large as when Na^+ ions are not present; (right half).

C-3

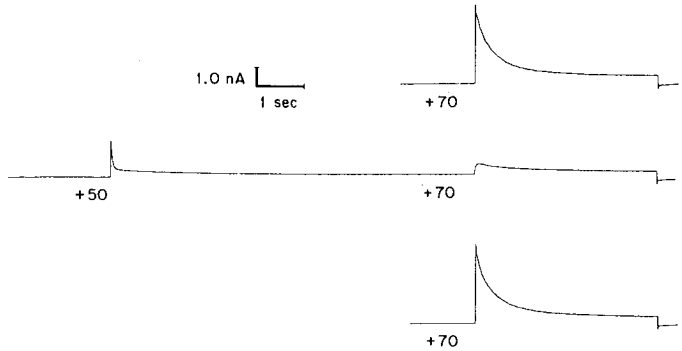

Figure 3. Transient outward K^+ current (I_A), recorded from statocyst hair cell under voltage-clamp. Top: Cell stepped from V_H = -60 mV to +10 mV; middle: 5 sec pre-pulse depolarization to -10 mV (+50 command step) inactivates early transient current without effect upon the slower delayed K^+ current; bottom:~2 min later, transient current has returned to full amplitude. Transient current is abolished by 4-AP (2-3 mM) but not TEA (50 mM, not shown).

Three distinct components of outward (K^+) current was observed under voltage-clamp during command steps to depolarized potentials, two of which appear to be identical to K^+ currents previously described in detail in a variety of central neurons in other molluscs. When depolarized from a holding potential of -60mV to potentials more positive than -40 mV, a rapid (~10 ms to peak at 0 mV), transient, 4- AP sensitive, outward current was observed (I_A). The voltage-dependent inactivation of I_A was studied using a twin-pulse protocol in which the cell was first held at -60 mV, then stepped to a variable potential (from -100 to 0 mV), before being stepped to a final potential of 0 mV. I_A was half-inactivated at ~-45 mv, which is considerably more positive than values typically reported in other cells and implies that I_A can contribute to the resting membrane conductance of the hair cell. Activation of I_A was also studied with a twin-pulse protocol. The cell was first stepped to -100mV, to remove testing inactivation, and then to a variable potential from -60 mV to 0 mV. Activation was steeply voltage-dependent at potentials positive to -40 mV.

A second slower component of outward current, which showed a moderate rate of inactivation, was observed when hair cells were depolarized to 0 mV. At + 20 mV, time to peak for this current was ~40-60 ms. This current was blocked by 100 mM TEA, and appears to be similar to the "delayed rectifier" current (I_K) seen in other molluscs (Thompson, 1977) and *Hermissenda* Type B photoreceptors (Shoukimas & Alkon, 1980).

With I_A and K_K blocked by 5 mM 4-AP and 100 mM TEA, an extremely slow outward current was elicited by depolarization to potentials > -30 mV. This current, which showed little inactivation during depolarizing steps as long as 15 sec, increased in amplitude during a sustained depolarization, reaching its steady-state value after ~5 sec. Although the kinetics of activation appear similar to those of a

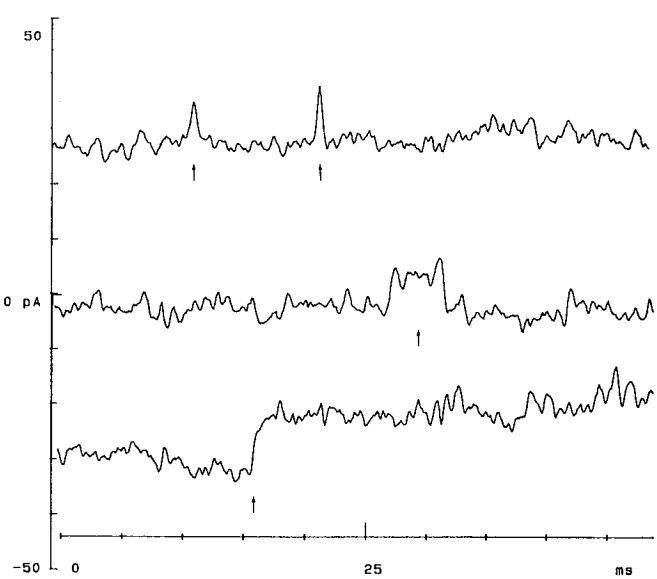

Figure 4. Examples (arrows) of channel currents recorded from *Hermissenda* statocyst hair cells using cell-attached patch-clamp recording techniques. Depicted here are three successive 50 mS samples of channel activity. Channel openings appear as upward deflections, closings appear as downward deflections. The channel opens twice in trace 1, and once in traces 2 and 3. All recordings obtained at the resting potential of the cell (~-50 mV). Slope conductance of the channel was ~35 pS. Records filtered at 3 KHz.

calcium-activated potassium current (I_{K-Ca}) in *Hermissenda* Type B cells, this current proved to be insensitive to: (1) changes in extracellular Ca^{2+} concentration over the range of 0-100 mM, (2) addition of calcium channel blockers to the bath (Cd^{2+}, 5 mM), and (3) intracellular injections of EGTA, a calcium chelator. However, each of these manipulations produced the expected changes in the magnitude of a transient, inward, voltage- dependent (calcium) current. We conclude that the delayed outward current is *not* a calcium-activated current, although it is most likely a potassium current, since: (1) both peak (I_A) and steady-state (measured 500 ms following depolarization) outward current components show the same reversal potential in elevated K^+ solutions (-12 mV in 300 mM K^+). I_A is extremely K^+ selective, and the similar reversal potential for I_A and the delayed component implies a similar K^+ selectivity. (2) An outward tail current was observed in 4-AP and TEA when the cell was stepped back to -60 mV from command steps more positive than -30 mV, consistent with our estimate of E_K in 10 mM K^+ ASW (approx. -100mV).

Single-channel K^+ currents were recorded from *Hermissenda* hair cells, using the cell-attached recording configuration (Hamill *et al.*, 1981). Figure 4 depicts several examples of the ~ 35 pS channel we have seen. Open time distributions indicate that no single exponential decay function will suffice as a fit of the data. This implies the presence of multiple open states. The channel is clearly voltage-dependent and is open a large fraction of the time at potentials more positive than rest (~ -50 mV). This channel may underlie one of the slower components of macroscopic K^+ current seen in the previous voltage clamp studies. ■

REFERENCES:

Aldrich, R.W., Getting, P.A.,Thompson, S.H. 1979. *J. Physiol. (Lond.) 291*: 507-530.
Alkon, D.L., Farley, J., Sakakibara, M., Hay, B. 1984. *Biophys. J. 46*: 605-614.
Alkon, D.L., Bak, A.J. 1973. *J. Gen. Physiol., 61*: 619- 637.
Connor, J.A., Stevens, C.F. 1971a. *J. Physiol. (Lond.) 213*: 1-20.
Connor, J.A., Stevens, C.F. 1971b. *J. Physiol. (Lond.) 213*: 21-30.
DeFelice, L., Alkon, D.L. 1977. *Nature, 269*: 613-615.
Grossman, Y., Alkon, D.L. 1982. *Neurosci. Lettr.*
Hamill, O.P., Marty, A., Neher, E., Sakmann, B., & Sigworth, F.J. 1981. *Pflugers Arch., 391*: 85-100.
Shoukimas, J.J., Alkon, D.L. 1980. *Soc. Neurosci. Abstr. 6*: 17.
Stommel, E.W., Stephens, R.W., Alkon,D.L. 1980. *J. Cell Biol., 87*: 652-662.
Thompson, S. 1977. *J. Physiol., 265*: 465-488.

PAGE 197 INTENTIONALLY BLANK

PRECEDING PAGE BLANK NOT FILMED

NONINVASIVE ASSESSMENT OF CARDIORESPIRATORY FUNCTION AND REGULATION BY MATHEMATICAL ANALYSIS OF PERIODIC WAVEFORMS

R. J. Cohen
Harvard-MIT Division of Health Sciences and Technology, Massachusetts Institute of Technology, Cambridge, Massachusetts 02139

Over the past several years a large number of investigators in our laboratory have been pursuing a new approach to the characterization of the regulation and stability of cardiopulmonary function. The hypothesis being tested under this research effort, is that a wealth of information regarding regulation and stability of cardiovascular, respiratory and autonomic nervous system function may be obtained by applying signal processing techniques to the analysis of conventionally recorded physiologic signals such as the ECG, respiratory activity and arterial blood pressure. This signal processing involves both averaging of waveforms to detect low amplitude features of the waveform normally buried in the noise, and analysis of subtle beat-to-beat variability in waveform morphology and timing. Analysis of variability in physiologic signals provides a means of assessing the ongoing perturbations to the physiologic system in question, and the dynamics and integrity of the closed-loop feedback and control systems involved in maintaining homeostasis.

This nonperturbative approach provides a means for studying hemodynamic control and electrical stability during physiologic stresses such as those encountered during space flight. Furthermore, this approach promises to provide a practical, noninvasive means of evaluating "physiologic fitness" of space flight personnel before and after missions, as well as providing a means for real-time physiologic monitoring during space flight. In the latter mode, this approach may provide a means of predicting physiologic dysfunction in flight which may lead to an inability to complete tasks and/or life threatening cardiovascular or respiratory failure. This approach may lead to important advances in understanding: (1) mechanisms of cardiovascular deconditioning during weightlessness, (2) syncope and near syncope following reentry and during high G acceleration and (3) the role of the autonomic nervous system in motion sickness, (4) the affect of space flight on cardiac electrical stability and myocardial perfusion. ■

QUANTIFICATION OF HUMAN CAROTID BARORECEPTOR-CARDIAC REFLEX RESPONSES IN SPACE

J. M. Fritsch, G. A. Kasting, and D. L. Eckberg
Departments of Medicine and Physiology and Biophysics, Medical College of Virginia and Hunter Holmes McGuire Veterans Administration Medical Center, Richmond, Virginia 23249

Arterial pressure is monitored continuously by carotid, aortic, and cardiopulmonary baroreceptors. Neural input from baroreceptors modulates, on a second-by-second basis, neural output to the heart and vasculature, carried over sympathetic and vagus nerves. Vagal nerve traffic to the heart is translated linearly into changes of the interval between heartbeats, which can be measured accurately from surface electrocardiograms. The arterial pressure-heart period relation is used widely as a measure of baroreflex control of the heart; it is described by a sigmoid function with threshold, linear, and saturation pressure ranges.

Two principal techniques have been used experimentally to study baroreceptor-cardiac reflex responses in humans. In one, arterial pressure is lowered or raised by intravenous injections of

vasoactive drugs. In the other, arterial pressure is not changed appreciably, but carotid baroreceptor activity is reduced or increased by applications of positive or negative pressure delivered to a chamber worn over the anterior aspect of the neck. With both techniques, changes of afferent baroreceptor activity are gauged by changes of electrocardiographic heart period. We have used the neck chamber approach to delineate the entire carotid baroreceptor-cardiac reflex response relation.

Circumstantial evidence suggests that normal autonomic reflex mechanisms are impaired during and following space travel. Astronauts and cosmonauts experience greater-than- usual liability of arterial pressure and heart rate during spaceflight, and orthostatic hypotension, tachycardia, and syncope or presyncope upon return to earth. We speculate that hemodynamic changes occurring during exposure to microgravity lead to altered autonomic responsiveness after return to earth. Within this context, headward shifts of blood volume that are believed to occur early after exposure to microgravity alter usual patterns of barosensory input and thereby alter usual patterns of autonomic output. Definition of the carotid baroreceptor-cardiac reflex relation before, during, and after spaceflight may provide insights into possible changes occurring in autonomic reflex control.

We have developed new equipment to quantify human carotid baroreceptor-cardiac reflex responses in space. The centerpiece of this new system is a unique neck chamber made of silicone rubber. This chamber has a latex diaphragm that forms a seal against the neck when positive pressure is applied, and a gel edge that forms a seal when negative pressure is applied. The chamber is connected by flexible tubing to a stepping-motor-driven bellows pressure system that delivers sequential, R-wave-triggered neck chamber pressure changes between +40 and -65 mmHg.

The pressure system is controlled by a microprocessor that also collects and averages data. The electronics system includes a digital oscilloscope that displays respiratory activity, the electrocardiogram and neck pressure in real time, and operator instructions before, and experimental results after pressure sequences. Experimental sequences are initiated by the subjects themselves. During held expiration, neck chamber pressure increases to about 40 mmHg to reduce carotid sinus diameter and thereby reduce afferent baroreceptor activity to levels below those necessary to trigger reflex responses. Then, a series of R-wave-triggered pressure reductions is delivered in 15 mmHg decrements to - 65 mmHg. Pressure then returns to ambient levels.

For each subject, the stimulus train is delivered seven times and neck pressures and R-R intervals are averaged. Arterial pressure is measured manually. Neck chamber pressures are subtracted from systolic pressure to derive estimates of carotid distending pressures, and these are plotted against corresponding R-R intervals. The resulting sigmoid function is analyzed mathematically. Our data suggest that curves obtained from individual subjects are highly reproducible (if these subjects have not changed their level of physical fitness).

We have completed one study, which was conceived to define possible circadian variability of human carotid baroreceptor-cardiac reflex responses. We measure carotid baroreceptor-cardiac reflex responses every three hours during a 24-hour period in 11 normotensive volunteers. Subjects maintained their usual sleep-wake cycles, but were awake and cooperative during all testing. We found no systematic change of baroreflex slope during the 24-hour periods. There were, however, parallel shifts of the entire baroreceptor-cardiac reflex relation along R-R interval and arterial pressure axes, which were associated with small but significant circadian changes of baseline R-R intervals and arterial pressures. Our data suggest that baroreflex responses are superimposed upon existing levels of vagal- cardiac activity and arterial pressure; circadian changes of arterial pressure involve mechanisms that are independent of the baroreflex; and the baroreflex acts to limit the variability of arterial pressure rather than to establish its absolute level. ■

HYDRATION EFFECTS ON THE CARDIOVASCULAR SYSTEM

G. W. Hoffler[1], M. A. Frey[2], and V. A. Convertino[2]
[1]*Biomedical Operations and Research Office, Kennedy Space Center, Florida 32899,* [2]*The Bionetics Corporation*

INTRODUCTION

Mammalian homeostatic mechanisms maintain tight control of volume or osmolality of major body fluid compartments. By processes not yet fully understood, but most certainly related to the headward shift of fluids, a new equilibrium with reduced intravascular volume (and probably other compartments) begins to occur in human beings exposed to weightlessness for even a few days of continuous exposure and remains relatively stable thereafter. However, consequences of this new fluid state manifest as reduced orthostatic tolerance and diminished upright exercise capacity upon return to earth's gravity. Soon after this phenomenon became appreciated, investigators began to search for means to prevent or mitigate the condition or its adverse effects. Among countermeasures studied were augmenting body fluid volume, particularly the vascular compartment, by timely and selective oral intake. In several bedrest studies, and in actual space flights (pre-deorbit) consumption of electrolyte-containing fluids has proven in a qualitative fashion the short-term efficacy of this technique.

This study was designed to quantify effects of acute manipulations of intravascular volume on cardiovascular, and particularly orthostatic, responses. Further, by selecting two distinctly different groups of subjects based on maximal oxygen capacity, the relative effects of fluid status and aerobic fitness could be determined; this latter factor has been the subject of much scientific controversy.

METHODS

Sixteen healthy men (32-47 years) underwent lower body negative pressure (LBNP) stress tests (Skylab stages) in each of two induced-fluid states and a baseline or control state (protocols): (1.) 4+ hours after oral administration of furosemide 40 mg (dehydration=DE), (2.) in an overnight, 12±hour fasting state of hydration (no oral intake), and (3.) within 3 hours after oral intake of isotonic saline (flavored for palatability) equal to 2.0% of lean body mass (hyperdydration = HY).

The sixteen men were selected from two otherwise matched subsets according to maximal oxygen consumption (fitness) as measured by the Bruce protocol, with separations being low fit (LO $\leq$ 42 ml O_2/kg/min) and high fit (HI$\geq$ 50 ml O_2/kg/min).

Discrete measurements included body weight, plasma osmolality (OSMO), plasma renin activity (PRA), hemoglobin (HGB), and hematocrit (HCT), before and after each LBNP test. Aldosterone (ALDO), total protein and plasma volume (PV, by the Evans blue dye dilution method) were obtained 1/2 hour before each LBNP test, timed to occur approximately at the estimated maximal effect of each fluid manipulation.

During the last (fifth) minute of each major stage of LBNP, heart rate (HR—from the electrocardiogram); systolic (SBP) and diastolic (DBP) blood pressures (by automatically inflated arm cuff); thoracic impedance (ZO) and stroke volume (SV) from an impedance cardiogram; systolic time intervals from simultaneous recordings of the electrocardiogram, the carotid pulse, and the phonocardiogram; and change in calf circumference using a Whitney strain gauge were recorded.

All data were processed by the SAS statistical package using a three-factor analysis of variance with repeated measures on two factors and the Newman-Keuls multiple comparison procedure. Alpha was set at 0.05.

RESULTS

Mean values for age (38.4 and 36.4 years for HI and LO fitness, respectively) and height (178.9 and 178.7 cm) were the same for the two subject subsets, otherwise clearly separated by oxygen consumption (56.5 and 36.8 ml 02/Kg/min). Weights (72.2 and 82.5 Kg) differed primarily due to body fat content (13.1 and 27.0%). Weights also varied significantly across all three fluid states.

The two fluid manipulations produced significant differences in PV (3151, 3609, and 4031 ml for DE, control, and HY, respectively) across all three fluid-state protocols. Total protein, HCT, and HGB were evaluated by DE; only total protein decreased with HY. Plasma OSMO unexpectedly was lowest in the

control state. None of these potential measures of fluid effects showed differences according to fitness, except that plasma osmolality was higher before, but not after, LBNP in the LO fitness group.

Only DE caused significant variation (elevation) in PRA (3.76, 1.73, and 1.05 ng/ml/hr) and ALDO (151.4, 105.1, and 86.8 pg/dl). LBNP evoked further elevations in PRA in both DE (3.76 and 7.99 ng/ml/hr, pre- versus post-LBNP, respectively) and control state (1.73 and 3.24 ng/ml/hr), but not in HY (1.05 and 1.38 ng/ml/hr); there was no difference in this response with LBNP between HI and LO fitness.

During LBNP, HR and ZO increased in DE; SV differed only between the extreme states of hydration. These variables also differed between the two fitness groups, with HR and ZO lower and SV higher in the HI fitness group. Maximal calf circumference and percent change in calf volume during LBNP differed only between the two extreme states of hydration (DE versus HY); no effect was seen between the two fitness groups. The preejection period/left ventricular ejection time ratio demonstrated categoric differences across all three hydration states and all stages of LBNP, but no distinction between fitness groups. Blood pressure remained unchanged by hydration or fitness; SBP fell slightly at the highest level of LBNP.

CONCLUSIONS

These results with discrete manipulations of body fluids have shown quantitative orthostatic benefit from short term augmentation of plasma volume and concomitant adverse effects from acute fluid loss. Nearly complete dissociation of these orthostatic relationships is observed from level of fitness in this cross-sectional study. Besides the obvious assistance in delineating aspects of cardiovascular function relevant to spaceflight, this technique may have applicability to study of other body systems.

ACKNOWLEDGEMENT

The authors thank the following for their assistance in conducting this tedious study: D. Doerr, S. Reed, M. Duvoisin, A. Maples, L. Crane, R. Triandafils, C. Tomaselli, Ph.D., K. Mathes, R.N., M. Lasley, R.N., M. Merz, V. Hall, D. Holley, S. Loffek, and M. Antiel. The contribution of the subjects is also gratefully acknowledged. ■

SERUM LIPOPROTEIN CONCENTRATIONS AFTER SPACEFLIGHT

J. M. Krauhs[1], C. S. Leach[2], P. C. Johnson[2], N. M. Cintron[2]
[1]*NASA/Johnson Space Center, SD4/KRUG International, Houston, TX 77058;* [2]*Johnson Space Center, SD4/ Biomedical Laboratories, Houston, Texas 77058*

INTRODUCTION

Blood levels of cholesterol in Apollo and Skylab astronauts were significantly lower when the crewmembers returned from space than during the preflight period (1,7). It has recently been established that low levels of the high density lipoprotein (HDL-C) fraction of cholesterol are associated with increased risk of cardiovascular disease (5,8). The lipoprotein fractions of cholesterol were measured in space shuttle crewmembers, and the effects of flight on these lipoproteins are reported here.

METHODS

Cholesterol, triglycerides, very low density lipoprotein cholesterol (VLDL-C), low density lipoprotein cholesterol (LDL-C), and HDL-C were measured in 125 crewmembers (116 males, ages 29-59 years, and 9 females, ages 32-42 years) on the first 24 Space Shuttle flights. Flight length varied from 2 to 10 days.

Venous blood was drawn before each mission. After landing, blood was drawn as soon as possible (L+O) and/or 3-23 days later. All blood samples except the ones at L+O were collected after 14 hours of fasting and abstention from alcoholic beverages, as early in the morning as possible. The L+O samples were obtained 3-6 hours after crewmembers ate breakfast.

Cholesterol was measured in serum by the enzymatic method using cholesterol esterase and cholesterol oxidase (2), and lipoproteins were measured or calculated by the method of Friedewald *et al.* (4).

The paired t test was used to test for significant differences between preflight and postflight measurements.

RESULTS

On landing day total cholesterol, triglycerides, LDL-C and VLDL-C were not significantly different from their preflight levels (Table 1). Mean HDL-C was 12.8% lower at landing, and this difference was statistically significant.

Measurements from blood samples taken 3-23 days after landing (Table 1) showed that mean levels of all variables had decreased compared to the preflight levels for that group of crewmembers. Total cholesterol and LDL-C as well as HDL-C had decreased significantly. (Because percent change was calculated for each individual, the mean percent change was not always consistent with the difference between the pre- and postflight means.)

DISCUSSION

The decrease in blood cholesterol of Skylab astronauts ($n = 9$) immediately after landing (7) was not confirmed by this study of Space Shuttle astronauts, but the longest Shuttle flight was only 10 days, whereas the Skylab missions lasted from 28 to 84 days. Except for HDL-C, which was significantly decreased in Space Shuttle astronauts at landing, lipoproteins showed more changes several days after landing.

The reason for the significant postflight decrease in HDL-C is unclear. Possible explanations include differences in diet before and during flight and the fact that preflight samples were taken after fasting whereas L+O samples were not, failure to control at L+O for possible circadian changes in blood lipoprotein levels, effects of physical and nonphysical stresses on crewmembers during flight, inactivity relative to preflight activity, and effects of weightlessness itself.

The persistence of a significant decrease in HDL-C levels during the postflight period argues against the first three possibilities, since blood samples were taken under preflight conditions on all days except L+O.

TABLE 1. EFFECTS OF SPACEFLIGHT ON BLOOD CHOLESTEROL, TRIGLYCERIDES, AND LIPOPROTEINS

	Cholesterol, total	Triglycerides	VLDL-C	LDL-C	HDL-C
Population normal range, mg/dl	140-330[1]	10-190[1]	0-55[2]	44-330[2]	30-70
PREFLIGHT VS. LANDING					
n	47	47	47	47	47
Preflight mean, mg/dl	210	87	17.4	149.4	45.7
SEM	5.3	6.1	1.2	5.3	1.4
Postflight mean, mg/dl	214	87	17.2	156.7	39.9*
SEM	7.0	5.8	1.2	6.6	1.6
Percent change, mean	1.6	4.5	4.7	5.7	-12.8
SEM	2.2	6.2	6.3	3.1	2.2
PREFLIGHT VS RECOVERY (3-23 DAYS)					
n	127	127	127	127	127
Preflight mean, mg/dl	204	88	17.6	146.5	39.7
SEM	3.6	3.6	0.7	3.3	0.9
Postflight mean, mg/dl	187*	86	17.2	132.9*	37.8*
SEM	3.6	3.7	0.7	3.3	1.0
Percent change, mean	-7.9	4.4	3.9	-8.7	-4.2
SEM	1/0	3/8	3/7	1/3	1/6

[1] Ages 30-59.
[2] Range given applies to males only.
* Significantly ($p < .05$) different from preflight mean.

Although plasma and urinary levels of the "stress hormones" such as aldosterone, cortisol, and catecholamines are increased after Shuttle flights (6), results of regression analyses (data not shown) indicated that levels of these hormones were not related statistically to those of HDL-C at L+O. This piece of evidence argues against the possibility that stress was responsible for the change in HDL-C.

The postflight decrease in HDL-C may be related to physiological effects of space flight that are similar to those of inactivity. Soviet investigators found that in subjects confined in sealed chambers, a decrease in alpha lipoprotein, the blood protein fraction containing HDL-C, occurred between 6 and 18 days after the beginning of confinement (3).

Effects of weightlessness might include an increased metabolic rate, which could cause a decrease in blood lipoproteins levels. At L+O, HDL-C was negatively correlated with insulin ($r = -.13$, not significant) and thyroxine ($r = -.38$, $p < .05$). The significant negative correlation of HDL- C with thyroxine provides evidence that metabolic changes in spaceflight may be related to the postflight reduction in serum HDL-C.

The decrease in serum HDL-C in space shuttle crewmembers immediately after flight is not of clinical significance, but HDL-C should be measured after long space flights in view of its importance as a "negative risk factor" for heart disease.

Acknowledgements We thank the Space Shuttle crewmembers for providing blood samples, the Clinical Laboratories staff of the Biomedical Laboratories for collecting and analyzing the samples, and Mrs. Sharon Jackson for typing the manuscript. ■

PRELIMINARY FINDINGS IN THE NEUROMUSCULAR JUNCTIONS OF THE SOLEUS MUSCLE OF ADULT RATS SUBJECTED TO SIMULATED WEIGHTLESSNESS. LIGHT AND ELECTRON MICROSCOPY

F. D'Amelio, N. G. Daunton, T. Fast and R. Grindeland
NASA/Ames Research Center, Life Science Division, Moffett Field, California 94035

The interdependence of motoneurons and skeletal muscle, both in health and disease, has been extensively documented in the literature. However, very little is known with respect to the effects of long-term muscle inactivity upon the neuromuscular unit.

It is possible that the clinical condition known as "disuse" muscle atrophy observed in astronauts and cosmonauts upon return to earth gravity, might in part be explained by an inadequate interaction between neural and muscle components. To investigate this possibility, a research program has been initiated to: 1) Determine the effects of muscle "disuse" atrophy induced by simulated weightlessness, on the structure and metabolic activity of the neuromuscular units (motor end plate, peripheral nerve and motoneuron); 2) Assess the time course and extent of recovery of neuromuscular units following exposure to simulated weightlessness. This study is performed in rats using hind leg suspension, which has been shown to be an appropriate model for the investigation of the effects of weightlessness on muscle.

The preliminary results reported here indicate that, after seven-day suspension, the motor end plates undergo pathological changes recognizable both with light and electron microscopy.

Light microscopic studies were performed using a combination of histochemical (acetylcholinesterase) and silver impregnation methods (Namba's procedure). The low power images show that the spacing between subneural structures appears to be decreased with respect to the control animals (Fig. 1A and B). In addition, a longitudinal expansion of the end plates in relation to the perpendicular axis, is also observed. Both changes might be attributed to the decrease in the mean

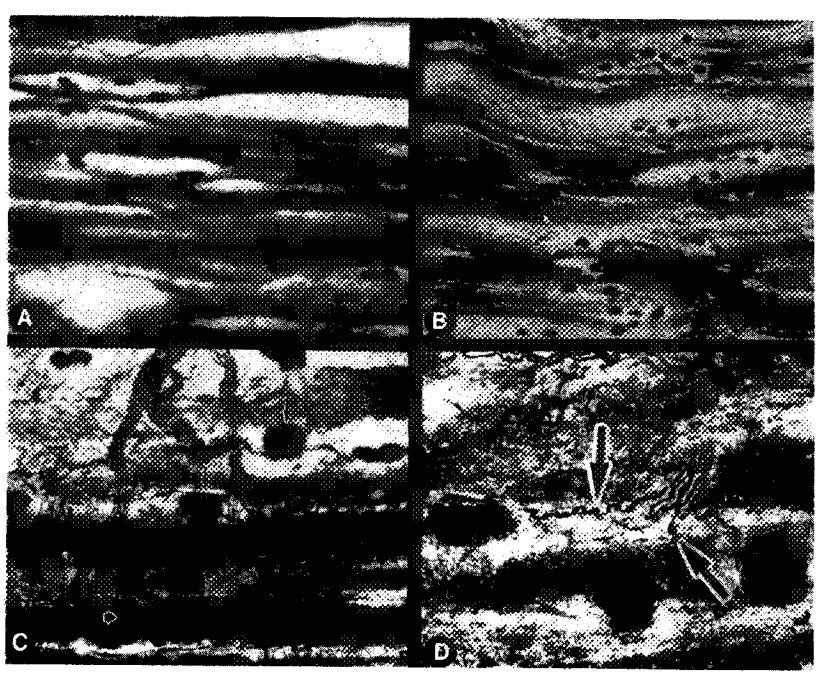

Fig. 1. Rat soleus. (A) Control. Normal distribution of end plates. (B) Seven-day suspension. Notice the decrease in spacing between the end plates, the irregular arrangement, and also the difference in size and shape, with respect to the control. (C) Control. Normal innervation pattern. Nerves, axon terminals (thick arrow) and end plates (thin arrows) are shown. (D) Seven-day suspension. Rounded end plates with irregular borders. Distorted pattern of terminal innervation with localized spherical enlargements along the course of the axons (arrows). Combined silver-thiocholine method of Namba. Original magnification: A and B: ×30; C: ×150; D: ×200.

diameter of the muscle fibers. When seen with high power, the subneural apparatus of the suspended animals appears rounded or markedly decreased in size, with irregular borders. The terminal innervation is frequently distorted, with thickenings, swellings or spherical enlargements along the preterminal segments. Each end plate seems to be innervated by a single axon (Fig. 1C and D).

The main changes observed in the electron microscopic images consist of abnormal, vacuolated mitochondria, within the axonal profiles. In some cases, large translucent membrane-bound cavities fill a considerable portion of the terminal. Myelin figures, probably the product of mitochondrial degeneration, are also discernible (Fig. 2A, B and C).

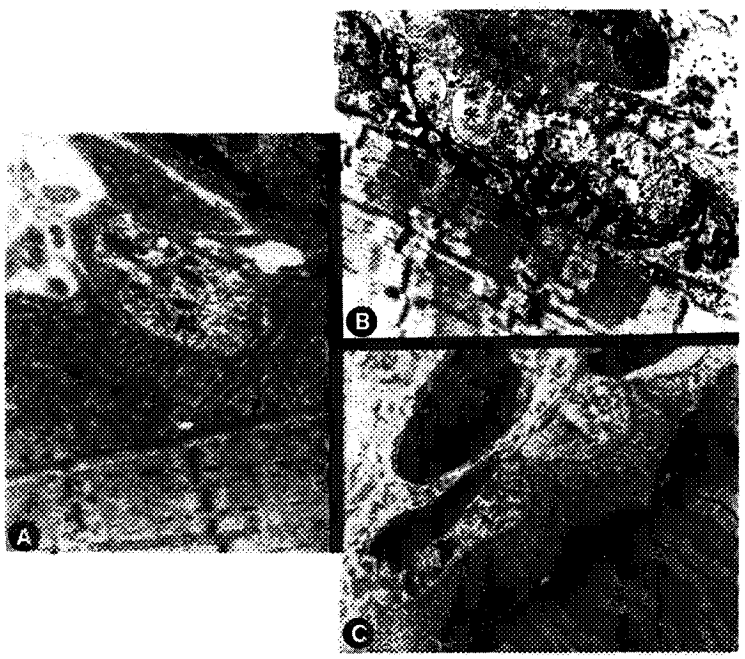

Fig. 2. Rat soleus. (A) Control. Normal neuromuscular junction. The axon terminal (At) lies in the sarcoplasmic groove. Primary and secondary synaptic clefts are of normal appearance. (B) Seven-day suspension. Abnormal terminal showing large, translucent membrane-bound cavities (asterisk) (mitochondrial degeneration?). (C) Seven-day suspension. Abnormal, vacuolated mitochondria (asterisks) and myelin figures (arrows) within the axonal profile. Original magnification: A: ×12,000; B: ×8,100; C: ×4,550.

The relevance of the modifications summarized in the foregoing should be assessed in the light of previous studies conducted mainly to explore changes in the muscle mass itself. These studies demonstrated that rats suspended for periods of 1–28 days begin to show significant losses of muscle mass after only 3 days, with progressively greater losses up to seven days. At three days, a significant decrease of electrical activity is also observed. A further, slow loss of mass and qualitative deterioration of the muscle, continues for at least 28 days. Either one week of spaceflight or one week of suspension results in more than a 20% decrease in soleus muscle mass, as compared with the controls. Cross sectional areas of individual soleus muscle fibers show a decrease of approximately 40% during spaceflight or suspension. Moreover, flight rat muscles show decrease of ribonucleic acid content, amino acid pools and malate (suggesting a blockade in the Kreb's cycle).

If, as has been shown in various experimental situations, the functional properties of the spinal motoneurons depend upon the trophic influences of the innervated target muscles, it is critically important to pursue a thorough study of the neuromuscular unit with the methodology at our disposal. ■

AN INVESTIGATION INTO THE CELLULAR MECHANISMS UNDERLYING SPACE MOTION SICKNESS USING INTRACELLULAR ELECTROPHYSIOLOGICAL RECORDINGS FROM THE RAT MEDIAL VESTIBULAR NUCLEUS, *IN VITRO*

J. P. Gallagher; M. R. Lewis, K. D. Phelan and P. Shinnick-Gallagher
Department of Pharmacology, University of Texas Medical Branch, Galveston, Texas 77550

Space Motion Sickness (SMS) affects at least 60% of crewmembers during the first few days in a micro-g environment. SMS can affect mission timelines and operational objectives by significantly decreasing crew productivity and performance. One hypothesis as to the mechanism(s) underlying SMS suggests that a malfunction in the normal processing of information within the vestibular system is a key contributory factor to its etiology. We undertook these studies to determine the identity of the neurotransmitters within the central component of the vestibular system, since these had not been defined critically at the cellular level. Once knowing the neurotransmitter responsible for primary afferent transmission in the mammalian vestibular system, we would then determine other transmitters and/or modulators that may be responsible for modifying information transfer within the central vestibular nuclei. Without this basic information as to how the normal circuitry within the vestibular complex transfers information under normal conditions, it would be impossible to suggest countermeasures to prevent or treat SMS.

We have developed an *in vitro* brain slice preparation from rats containing the medial and lateral vestibular nuclei along with the axons and terminals of the eighth cranial nerve (N.VIII). A typical slice preparation is depicted in Fig. 1, which indicates sites for recording and stimulating. We have recorded intracellularly from over 200 MVN neurons. Second order MVN neurons display a mean resting potential of -55 ± 8 mV (n=47) with a range of -40 to -80 mV. Eighty-nine percent of the neurons tested received a synaptic input via N. VIII. The top of Fig. 2 depicts a synaptic response with an action potential, while the bottom demonstrates the underlying synaptic response.

Fig. 1. Drawing of the anatomy of the rat brainstem at the level of a typical slice. 1: Fourth ventricle. 2: Medial vestibular nucleus (MVN). 3: Spinal tract of cranial nerve five. 4: Dorsal cochlear nucleus. 5: Cerebellum.

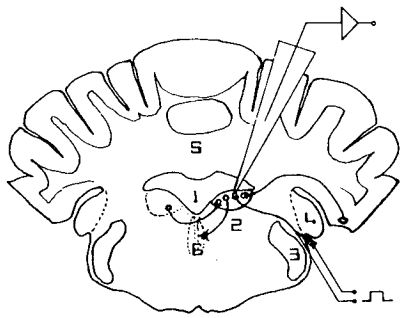

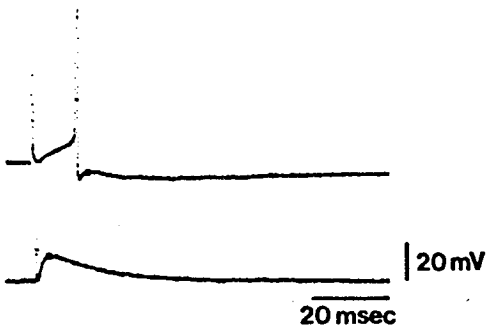

Fig. 2. Orthodromically induced (N. VIII Stimulation) responses from MVN. TOP: Synaptically mediated action potential. BOTTOM: Excitatory postsynaptic potential (EPSP) from same neuron.

Since atropine has been used with some success in the treatment of SMS, we applied 1 micromolar atropine and observed its action on either spontaneous or synaptically evoked action potentials. Fig. 3 demonstrates that atropine has no effect on action potential frequency or amplitude, or EPSP amplitudes. This data suggests that when atropine is effective in ameliorating the symptoms of SMS, it is probably acting somewhere else in the nervous system other than at the primary afferent to second order vestibular synapse. Since we had also demonstrated that the synaptic response was not affected by treatment with nicotinic cholinergic antagonists, histamine antagonists or adenosine antagonists, we

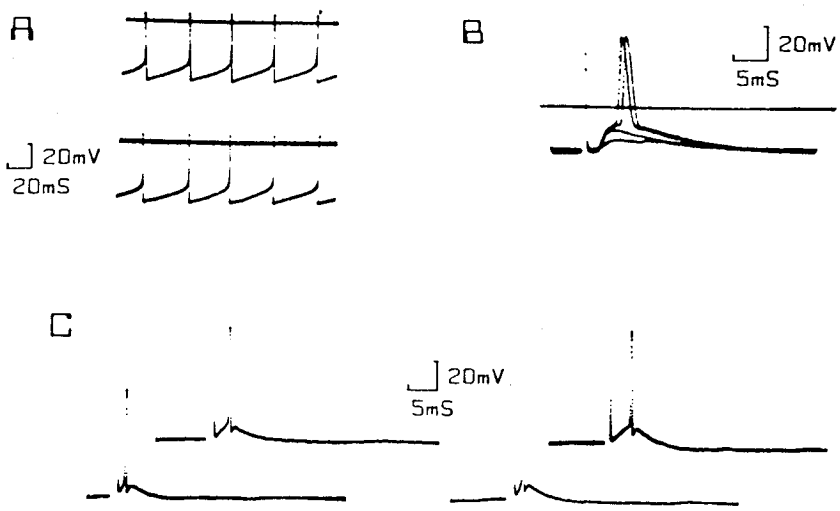

Fig. 3. Atropine (A drug that shares the same biological activity as scopolamine) does not affect information transfer (monitored as spontaneous spiking activity or synaptic activity) in medial vestibular neurons. A. Spontaneous spiking before (on top) and after atropine (bottom). B. Orthodromically induced (N. VIII stimulation) synaptic potentials and action potentials are unaffected by atropine. C. Orthodromically induced (N. VIII stimulations) action potentials with their afterpotentials before (on the left) and after (on the right) atropine.

began to apply various excitatory amino acid antagonists to test if these agents affected transmission.

Fig. 4 depicts a series of such experiments, wherein we were able to block the synaptic response with kynurenic acid and aminophosphonobutyric acid. On the other hand, aminophosnovaleric acid, a "selective NMDA" receptor antagonist, was without effect, while D-aminoadipic acid was only partially successful. Based on these and other results with putative excitatory amino acid transmitter candidates, we have come to the conclusion that excitatory transmission at the primary afferent to second order

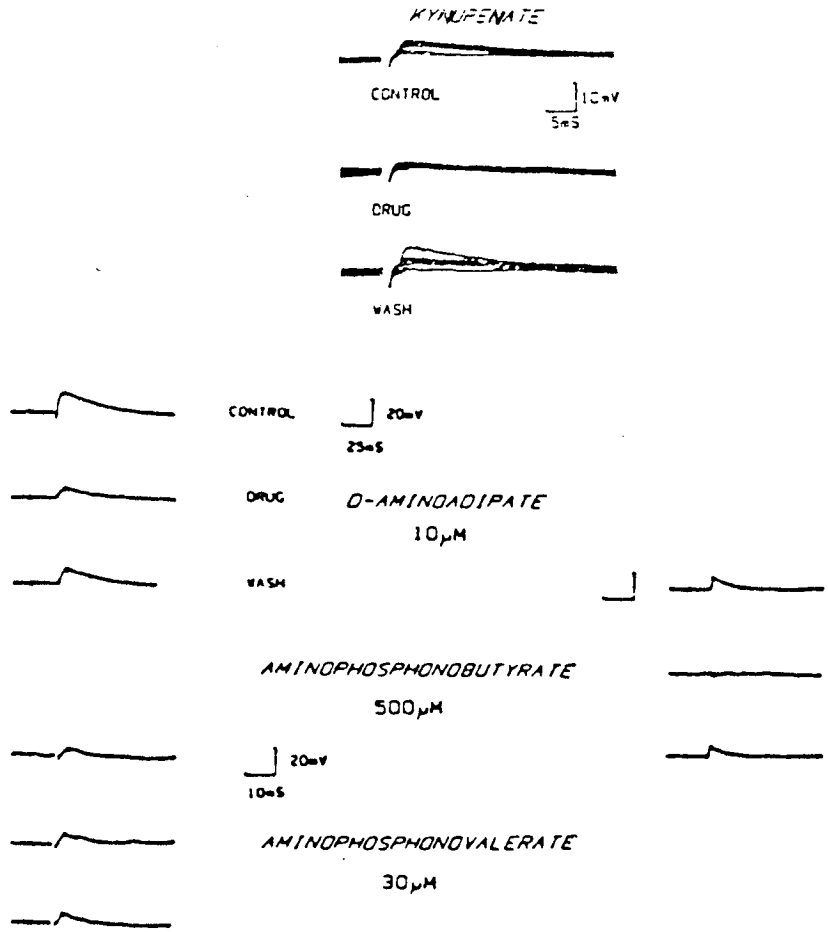

Fig. 4. Examples of drugs which affect excitatory amino acid transmission at the N. VIII to MVN synapse. Both Kynurenic acid and aminophosphonobutyric acid are able to block synaptic response. D-amino-adipic acid depresses synaptic transmission, while aminophosphonobutyric acid does not affect transmission.

medial vestibular nucleus of rats is mediated by an excitatory amino acid. We are not able presently to specify which amino acid is the endogenous transmitter, but would speculate that aspartic acid or similar substance acting on a receptor-type most resembling that activated by homocysteicptic acid would be a likely candidate. This conclusion is supported by neurochemical experiments described by Godfrey *et al.*, 1984, but is opposed in the recent review by Matsuoka *et al.*, 1985, who still promotes the concept that excitatory primary afferent transmission is mediated by acetylcholine.

Based on our results, we have begun to examine other transmitters and drugs which may be able to modulate normal excitatory transmission in the medial vestibular nucleus. Briefly, we have demonstrated that both γ-aminobutyric acid (GABA), probably via cerebellar input, is able to both hyperpolarize (inhibit) or depolarize (excite) second order MVN neurons directly when applied exogenously. Similarly, histamine acting by two different receptors, namely, H_1 and H_2, is able (like GABA) to depolarize and hyperpolarize second order MVN neurons. On the other hand, the antianxiety/skeletal muscle relaxant diazepam (Valium) acts to hyperpolarize (inhibit) these same vestibular neurons.

Thus, our approach will continue to examine the normal circuitry within the vestibular nuclei, in an effort to discover the transmitters responsible for information transfer and integration of information within this central relay system position to make recommendations concerning prevention and/or treatment of malfunctions that may occur within the central vestibular system. (Supported by NAG2-260 to JPG). ■

THE CHANGE IN COEFFICIENT OF VARIANCE OF R-R INTERVAL AND THE SUSCEPTIBILITY OF SENSORY-CONFLICT SICKNESS (SUBHUMAN PRIMATE EXPERIMENT)

M. Igarashi, T. Himi, M. Ishii, S. Patel, and W. B. Kulecz
Department of Otorhinolaryngology and Communicative Sciences, Baylor College of Medicine, One Baylor Plaza, Houston, Texas 77030

It has been reported that the cardiac irregularities were associated with nausea and vomiting in dogs (1) and subsequently Graybiel and Lackner (2) reported that a close relationship existed between motion sickness symptomatology and heart rate. Moreover, there are reports to describe that the R-R interval variation is regulated by the vagus nerve (5). In order to gain an objective measurement of experimentally induced sensory-conflict sickness, we analyzed R-R interval variations in squirrel monkeys.

A total of 17 young adult squirrel monkeys (*Saimiri sciureus*) of both genders, weighing an average of 780 g were used in this experiment. All animals were "naive" and had not been used previously in any other experimentation.

Pitch conflict situation was produced by microprocessor-controlled turntable and optokinetic drum, which were rotated about the earth's horizontal axis. The black-and- white-striped pattern was used in the drum. The restrained animal was placed in the center of the turntable, with its head positioned at the center of the vertical optokinetic drum. At 15 min before the trial, an injection of amphetamine sulfate (0.25 mg/kg I.M.) was given in order to maintain the animal's alertness. At 10 min before the trial, the animals were given 20 g of banana and 5cc of fruit juice to control the condition of stomach loading. A daily session of exposure to conflict consisted of the following: 15 min exposure; 5 min rest (in the apparatus without stimulation); 15 min exposure; 5 min rest; and 15 min exposure.

Conflict stimulation (in pitch) was provided by sinusoidal rotation of the turntable and optokinetic drum. Both the turntable and the drum were driven at a frequency of 0.25 Hz, and amplitide of 90°. The conflict was created by delaying the turntable for 0.5 sec, resulting in a 45° phase lag as compared with the optokinetic drum.

To obtain sickness scores, monkeys were observed through a closed-circuit TV throughout the conflict exposure. The scale of scoring was as follows:

1 point = minimal salivation, drowsiness
2 points = moderate salivation, vocalization
4 points = severe salivation, usually with foam, urination, defecation
8 points = retching
16 points = emetic expulsion

Points were accumulated for each 15-min exposure and the three scores were summated to provide an overall score for the daily sessions.

In order to quantify R-R interval variation, a computer system which recorded and calculated the mean value and standard deviation of 200 R-R intervals (in msec) used. The electrocardiogram was analyzed each 3-5 min during rest and with conflict exposure. The mean value and standard deviation were calculated for the first 200 intervals, and then the coefficient of variation (CV = SD/mean value × 100%) was calculated (4).

Animals were classified based on conflict sickness scoring and salivation measurement (Table 1), which showed a good cross correlation (Table 2).

Table 1.

Group A:	susceptible with emesis
Group B:	no emesis salivation more than mean +1SD
Group C:	non-susceptible salivation equal to or less than mean +1SD

Mean ±1SD = 379.8 ± 185.6 mg

Table 2

	n	Conflict Sickness Scores (mean ± SD)	Salivation (in mg) (mean ± SD)	% Emesis
Group A	4	22.75 ± 2.06	*ND	100
Group B	5	14.40 ± 2.30	598.0 ± 23.9	0
Group C	8	12.50 ± 2.33	234.4 ± 58.8	0

A:B and A:C $p < 0.001$
*No data due to emesis

Table 3

	A	B	C
Increase of CV (mean ± SEM)	2.54 ± 0.77	1.48 ± 0.89	-0.42 ± 0.82

A:C $p < 0.05$

When the increase in CV of R-R interval was compared between the group A and group C, there was a significant difference ($p<0.05$). But the comparisons between group A and group B, and also between group B and group C, did not depict any significant difference. Indeed, the mean value of group B was exactly at the median of those of group A and group C (Table 3).

In summary, the difference in CV increase of R-R interval at the first time exposure to vestibular-visual conflict clearly parallels the difference in sickness scores between the groups; the more increase, the more susceptible. The finding strongly suggests that this autonomic nervous system output is useful to monitor the severity and build-up pattern of induced sickness, with some predictability reaching the endpoint emesis. ■

REFERENCES

1. Crittenden PJ, Ivy AC: A study of viscerocardiac reflexes; the experimental production of cardiac irregularities in icteric dogs with an analysis of the role played by nausea and vomiting. Am Heart J 8:P 507-518, 1933.
2. Graybiel A, Lackner JR: Evaluation of the relationship between motion sickness symptomatology and blood pressure, heart rate, and body temperature. Aviat Space Environ Med 51: 211-214, 1980.
3. Igarashi M, Kobayashi K, Kulecz WB, Isago H: Vestibular- visual conflict in pitch and yaw planes in the squirrel monkey. Aviat Space Environ Med 57: 1071-1074, 1986.
4. Ishii M, Igarashi M, Patel S, Himi T, Kulecz WB: Autonomic effects on R-R variations of the heart rate in the squirrel monkey: An indicator of autonomic imbalance in conflict sickness. Am J Otolaryngol, 1987.
5. Perrson A, Solders G; R-R variations, a test of autonomic dysfunction. Acta Neurol Scand 67: 285-293, 1983.

PHARMACOLOGY AND NEUROCHEMISTRY OF MOTION SICKNESS

J. B. Lucot and G. H. Crampton
Department of Pharmacology, Wright State University, 060 FAWC, Dayton, Ohio 45435

This laboratory is using an animal model for space/motion sickness to investigate the neural basis of the disorder. The motion stimulus is provided by a device resembling a Ferris wheel. An acrylic box 0.51 m × 0.25 m × 0.33 m is suspended from each end of a 0.89 m beam which rotates about a central axle. The boxes are counter-rotated so that they remain vertical. A motion challenge consists of 30 min of motion followed by one minute of observation. Parametric studies have determined that the most provocative stimulus is a rotation rate of 0.28 Hz (17 rpm). We have also determined that tests must be separated by at least two weeks to prevent habituation to the motion stimulus. Cats are screened on five tests to determine their susceptibility to motion sickness, and only cats with some probability of becoming motion sick are used for motion testing.

The cerebrospinal fluid from the fourth ventricle was analyzed for a broad spectrum of constituents. Samples were taken before, during and after motion tests which produced emesis in half of the subjects. The significant differences found were between subjects likely to become motion sick and subjects not likely to become motion sick. No differences were found between samples differing in their relationship with the motion challenge or with emetic events. High susceptibility cats had lower levels of serotonin metabolites, dopamine metabolites, uric acid, MHMG sulfate and vasopressin. These results were interpreted as establishing fundamental neurochemical differences between individuals which lead to a variety of functional differences, one of which is susceptibility to motion sickness.

Subjects were ranked by susceptibility to motion sickness and tested for their response to the emetic drug, xylazine, which acts by stimulating α-2 noradrenergic receptors. A significant correlation was found between susceptibility to the two emetic stimuli. This suggests that the fundamental differences between individuals found neurochemically applies to their sensitivity to emetic stimuli in general.

Further, the α-2 noradrenergic blocker yohimbine blocked xylazine-induced emesis, but not motion sickness. This not only verified the site of emetic action of xylazine, but also verified research by others suggesting that the two stimuli used different neural pathways to activate the brainstem region that organizes the emetic reflex.

The area where antiemetic drugs act can be localized by testing its effectiveness against motion sickness and xylazine-induced emesis. Drugs blocking emesis elicited by only one stimulus act on the neural pathway specific for that stimulus, while drugs blocking both probably act on the region organizing the emetic reflex. In the case of yohimbine, it blocked the receptors activated by xylazine, but was not effective on the motion sickness pathway or on the region organizing emesis.

The results from the analysis of the cerebrospinal fluid were pursued by manipulation of the serotonin system with the partial agonist at serotonin-1A receptors, buspirone. Buspirone blocked both motion sickness and xylazine-induced emesis, leading to the conclusion that it acts on the neural network organizing the emetic reflex. This conclusion was verified by further work demonstrating that buspirone also blocked cisplatin-induced emesis.

Studies also provided the first evidence that the standard antimotion sickness drug, scopolamine, works in animals as well as man. Interestingly, the other therapy commonly used, amphetamine, was not effective over a wide range of doses. This could be either a species difference or a difference in the measure used, as we use vomiting as an endpoint, while the researchers testing humans use nausea. ■

EFFECTS OF GRAVITY ON THE PRINCIPAL AXES OF VELOCITY STORAGE IN THREE DIMENSIONS

T. Raphan[1] and B. Cohen[2]
[1]*Dept. of Computer and Information Science, Brooklyn College of CUNY, Brooklyn, New York, and* [2]*Depts. of Neurology and Physiology, Mount Sinai School of Medicine, New York, New York*

Rotation of the visual surround that induces horizontal optokinetic nystagmus (OKN) excites the velocity storage integrator and induces horizontal optokinetic after-nystagmus (OKAN). If horizontal OKN is induced while monkeys are tilted with regard to gravity, then the OKAN which follows has a vertical component; if monkeys are supine or prone then the OKAN has a roll component (Raphan and Cohen, 1987). The cross-coupled components of the nystagmus do not appear immediately but build up and decay slowly with dynamics consistent with those associated with velocity storage. This indicates that the principal axes of the velocity storage integrator in three dimensions, *i.e.*, those axes along which velocity storage is maximal are dependent on the orientation of the head with regard to gravity. The purpose of this study was to determine the orientation of these axes as a function of angle of head tilt in response to optokinetic stimulation. To this end, oblique optokinetic stimuli were given with monkeys upright as well as on their sides. If monkeys were upright when they received an oblique stimulus at any angle, the direction of the OKN was oblique and followed the stimulus, but only horizontal OKAN was induced and the vertical component was essentially absent. This is consistent with the fact that pure vertical OKN with subjects upright is associated with little vertical OKAN (Matsuo and Cohen, 1974). It indicates that the animal's vertical is the principal axis for storage in the upright position. When animals are on their sides, vertical OKAN tends to be stronger and is asymmetrical, being weaker for downward than for upward nystagmus (Matsuo and Cohen, 1974). If subjects were given an oblique optokinetic stimulus such that the cross-coupling would tend to produce a vertical component in the same direction as that of the stimulus, the vertical component of both upward and downward OKN and OKAN were stronger. If the oblique stimulus was such that the cross-coupling would tend to produce a vertical component opposite to the direction of that component induced by the stimulus, then the vertical component of the OKAN was canceled. The vertical cross-coupling was stronger with greater angles of tilt. Consequently, the angle of the stimulus relative to the animal that augmented or canceled

the vertical component increased, becoming more oblique. This tended to maintain the principal oblique axes for velocity storage constant in space. The data suggest that gravity orients the principal axes of the velocity storage integrator toward the space vertical and attempts to maintain them spatially invariant regardless of head orientation.

Supported by EY 04148, NS 00294, and NASA NAG 2-336. ■

INTERACTION BETWEEN OTOLITHIC AND SEMICIRCULAR CANAL RESPONSES DURING LINEAR ACCELERATION

S. Watanabe[1], S. Nagaoka[2], M. Hashiba[3], A. Takabayashi[1], M. Tanaka[1] and S. Takagi[1]
[1]*Department of Aerospace Physiology, Research Institute of Environmental Medicine, Nagoya University, Furo-cho, Chikusa-ku, 464 Nagoya, Japan,* [2]*Space Experiment Group, NASDA, Tokyo, Japan,* [3]*Nagoya City University School of Medicine, Nagoya, Japan*

Caloric nystagmus is modified by head position; especially the reverse phase which is caused by changing head position from faceup to facedown. This phenomenon is explained by a hypothesis of mutual interaction between semicircular canal and otolith responses (1,2,3), which is supported by some animal experiments such as canal plugging (4) and canal destruction (5). The detail of the investigation with respect to otolith and canal interaction on ground-based experiments can provide a possible explanation about the influence of functional privation of the otolith upon canal response in space.

METHOD

Subjects were 12 volunteer health students. Linear acceleration was applied to the subjects in either sitting position or supine position. Changing the direction of the sled chair caused the subjects to accelerate in a transverse or lateral direction. Supine position was added to raise the head 30° upward. The head was fixed on a backboard of the sled chair by goggles fastened by belts. A sinusoidal acceleration mode was achieved on the movement span of 512 cm or 256 cm with 8 sec interval, resulting in peak acceleration of 0.16 g or 0.08 g, respectively. Recording of the eye movement was conducted by an electro-oculogramme (EOG) and an eye movement recorder (EMR). The EMR is constructed mainly with a infra-red illumination device, two infra-red video cameras and goggles, and is allowed to provide positional signals (X, Y) of the target illumination spot on the right eye and also to picture the iris of the left eye. All signals were transmitted through a UHF telemeter and recorded on a PCM and a video tape recorder separately. The positional signal of spot illumination and movement of the iris were used for analysis of the rotation of the eye ball. The EMR is advantageous especially for recording the vertical eye movement, for which the EOG includes more artifacts than the EMR.

Acceleration imposed on the head was picked up by a three dimensional accelerometer, and analyzed in comparison with the movement of the sled.

RESULTS AND DISCUSSION

In the sitting position, subjects did not reveal nystagmus from transverse acceleration even at 0.16 g, while small deviating movement of the eye balls was observed in vertical EMR during acceleration, which showed an eye ball movement upwardly during the positive phase of acceleration and downward during the negative phase. During lateral acceleration, horizontal nystagmus was observed parallel to the acceleration profile. Movement of the sled from right to left produced the leftward nystagmus and *vice versa* (Fig. 1). In the subject shown in Fig. 1, slight rotation of the eye balls was observed in a clockwise direction during the positive phase of acceleration and counterclockwise during the negative phase. In order to analyze the horizontal nystagmus caused during lateral acceleration, the slow phase was extracted from the nystagmogramme, as shown in Fig. 2-B. The reconstructed slow phase nystagmus (Fig. 2-C) revealed the inphase response with the sinusoidal acceleration. This fact implies that the load of acceleration to the otolith organs induces the eye movement in the opposite direction to the acceleration. This is the same phenomenon as the eye movement response caused by excitation

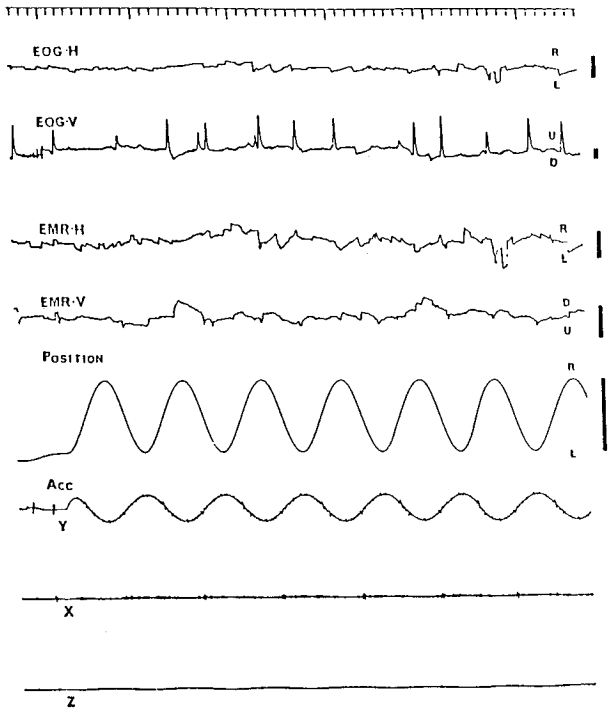

Fig. 1. Eye movement during lateral acceleration. Vertical bars indicate 10° in EOG and EMR, and 512 cm in position.

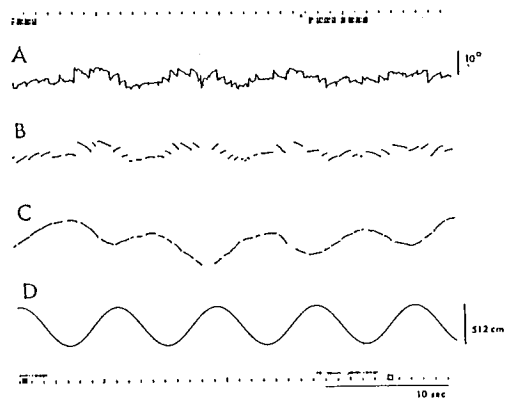

Fig. 2. Horizontal nystagmus during lateral acceleration. A: original EOG. B: slow phase of nystagmus extracted. C: reconstruction of slow phase of nystagmus. D: movement of sled.

of the hair cells in the semicircular canals to head rotation, which is of an advantage to visual stabilization during head movement. The otolith organs also play the same role as the semicircular canal organs as to visual stabilization during head movement.

An effect of linear acceleration to caloric nystagmus was examined. The caloric nystagmus was elicited by 24°C cold water into the right ear, resulting in leftward nystagmus. Linear acceleration was applied immediately after the water injection. As shown in Fig. 3-C, the amplitude of the caloric nystagmus, especially rapid phase, was modified markedly by lateral acceleration. The amplitude of

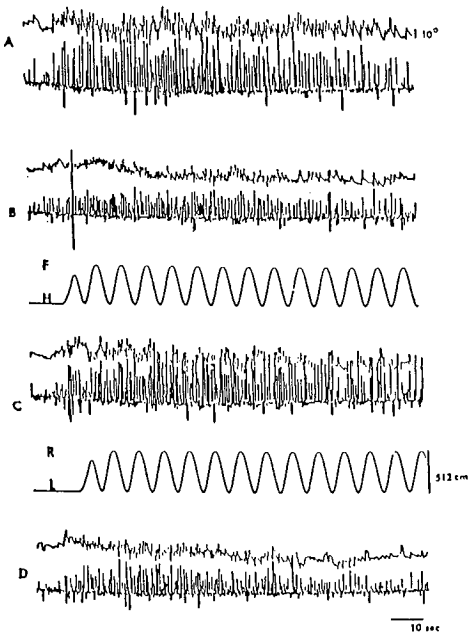

Fig 3. Effects of linear acceleration on caloric nystagmus induced by 24°C cold water pouring in right ear. A: initial control. B: transverse acceleration. C: lateral acceleration. D: last control.

nystagmus increased with leftward movement of the sled and decreased with the opposite movement. On the other hand, transverse acceleration merely influenced the caloric nystagmus (Fig. 3-B). The order of A to D in Fig. 3 represents the sequence of experiments, so that the decrease of responses in A to D (except C) implies that the caloric nystagmus habituates by repetition of tests. Accordingly, Fig. 3-C shows that the lateral acceleration mutually affects the caloric nystagmus. This experiment may be a plausible example for a survey of the otolith organs. ■

REFERENCES

1. A.J. Benson (1974) Modification of the response to angular acceleration by linear acceleration. In: H.H. Kornhuber (ed) Handbook of sensory physiology. Vol VI/2. Springer, pp 281-320.
2. E. Fluur and J. Siegborn (1973) Interaction between the utricles and the horizontal semicircular canals. Acta Otolaryng. 75. 17-20.
3. R. Mayne (1980) A systems concept of the vestibular organs. In: H.H. Kornhuber (ed) Handbook of sensory physiology. VI/2. Springer, pp 493-580.
4. K.E. Money and J.W. Scott (1962) Functions of separate sensory receptors of nonauditory labyrinth of the cat. Amer. J. Physiol. 202, 1211-1221.
5. J. Tail and W.J. MacNally (1934) Some features of the action of the utricular maculae (and of the associated action of semicircular canals) of the frog. Phil. Trans. Roy. soc. 241-286.

VISUAL-VESTIBULAR INTERACTION AS A TOOL FOR INVESTIGATING GRAVITY EFFECTS ON SPATIAL ORIENTATION

L. R. Young
Man-Vehicle Laboratory, Department of Aeronautics and Astronautics, Massachusetts Institute of Technology, Cambridge, Massachusetts 02139

Moving visual fields, along with other sensory cues, can produce a sensation of self-motion and concomitant eye, head and trunk postural stabilization. It has been hypothesized that the vestibular influence upon this visually induced "vection" is largely inhibitory to sudden changes in orientation. For example, the delay in onset of vection for a large acceleration of the visual field, is attributable to semicircular inhibition, and the limit to induced tilt is attributable to gravity influences sensed by the otolith organs. If this theory is correct, then visually induced tilt, if not the reflex level oculomotor, cervical and trunk stabilization responses, should be strengthened when and if otolith orientation cues are removed in weightlessness. This paper reviews the supporting evidence behind this hypothesis, from supine and head tilt vection studies. The perception results from two "rotating dome" experiments on the Spacelab-1 and D-1 orbital missions are examined in the light of this hypothesis. They demonstrate both the immediate effect of removing the inhibitory gravity cues to orientation, and the growing dependence on visual cues during adaptation to weightlessness. ■

PAGE 215 INTENTIONALLY BLANK

PRECEDING PAGE BLANK NOT FILMED

NEUROSCIENCE II OVERVIEW: THE ROLE OF NEUROVESTIBULAR RESEARCH IN SPACE STATION AND BEYOND—Panel Discussion

Vestibular and related sensory responses to space flight have been considered to be of rapid onset and of relatively short duration. However, recent findings from Spacelab flights and Shuttle middeck experiments suggest that neurovestibular changes are a continuous process. These have stimulated a revision of the theoretical models concerned with adaptation to the flight environment. The new direction of thought has implications for living aboard Space Station, on the lunar surface, and an extended mission to Mars. This panel will review the findings from the current ground and flight programs and propose requirements for neurosensory research in support of future missions. ■

ADAPTIVE MODIFICATIONS OF POSTURE AND OCULOMOTOR REFLEXES IN MICROGRAVITY

G. Clement, T. Vieville, F. Lestienne, and A. Berthoz
Laboratoire de Physiologie Neurosensorielle du CNRS, 15 Rue de l'Ecole de Medecine, F-75270 Paris Cedex 06 - France

A series of experiments on postural and oculomotor systems was performed on the crews of the flight of Salyut-7 in 1982 and STS 51-G in 1985. Our laboratory also participated within a group of European investigators in vestibular experiments during the flight of Spacelab-1 in 1983. One important aspect of our experiments concerned the time course of the adaptation of postural and oculomotor function to orbital weightlessness during a 7-day space flight. For this reason not only inflight, but also extensive pre- and postflight tests were conducted repeatedly with the crews. These tests were conducted in our laboratory and in the training center of the astronauts. During the preflight tests at 30, 10 and 5 days (coded F-30, F-10, F-5) before the mission, the crews were given ample theoretical and practical training in motor and vestibular physiology and practiced the experiments. The same tests were repeated again after the return on ground till the third postflight day (coded R, R+1, R+3).

We studied standing posture control with a subject at rest, and during body disturbances provoked by voluntary movements or by unexpected movement of the foot support in the microgravity condition. The question raised concerned the persistence of the terrestrial postural programs in weightlessness. The results have shown that the postural perturbations subsequent to the movement of a part of the body in microgravity were similar to those observed on the ground. However, in microgravity, in contrast with the Earth's gravity condition, the standing posture was ensured by a tonic contraction of the ankle flexors. The activation sequences of the postural muscles associated with the elevation of the arm were very structured and varied appreciably during the space flight. These data seem to highlight a short-term and a long-term adaptation of postural control to microgravity.

During the standing position in microgravity, the afferent signals of the otolithic, tactile and proprioceptive receptors are different from those which the central nervous system received under the Earth's gravity condition. We assumed that the contribution of vision to postural control would increase in order to serve as a substitute for the sources of information the detection conditions of which have changed as a result in microgravity. The study of the subject's capability to reproduce postures acquired on Earth was compared during three visual situations: normal vision, without vision, and stabilized vision (fixed visual environment with respect to the subject). Results have shown that the subject's body axis in the standing position was exaggeratedly tilted forward with respect to the support to which his

feet were attached, especially in darkness and in stabilized vision. This fact gives evidence of the prevailing nature of visual cues with respect to the other sensory information.

It is currently thought that the otoliths of the vestibular organs exert an influence on visuo-motor function and particularly on vestibulo-ocular reflex (VOR) and optokinetic nystagmus (OKN). On Earth, it is difficult to evaluate exactly the role played by the otoliths in the vertical planes since the gravity vector cannot be suppressed. Weightlessness situation offers a unique opportunity to test the influence of the otoliths in the vertical VOR gain and in the OKN. Analysis of eye movements during active head oscillations in darkness performed by the astronauts revealed a strong decrease of VOR gain both during horizontal and vertical head movements. This suggests an important contribution of the otoliths, such as absence of phase shift between head and eye movements, could be attributed to the fact that trained subjects could suppress the vestibular input in order to prevent any conflict which may cause space motion sickness, or that they could not in space maintain fixation on an imagined target related to the spaceship.

Evidence of the role of the otoliths on OKN stems from lesion experiments in monkeys, and from strong effects of dynamic otolithic stimulation by linear acceleration on OKN. Furthermore, the asymmetry of upward and downward OKN has been attributed to a potential action of gravity. Orbital weightlessness, which suppresses the gravity vector selectively, was used to study the influence of gravity on OKN. Inflight measurements of eye movements during monocular horizontal and vertical optokinetic stimulation at constant velocities have shown a reversal of the vertical asymmetry of OKN and a downward shift of the beating field on the first three days in microgravity. On return to Earth's gravity, there was a general drift of the eye in the upward direction. This suggests that the sacculus normally influences mean vertical eye position and the perception of the subjective horizontal direction, both of which are gravity dependent.

The process of adaptation of sensori-motor systems to orbital weightlessness is complex and its nature is not yet understood. However, the comparison between the adaptation process of postural, perceptual and oculomotor systems to a 7 day spaceflight gives evidence of synchronization. Indeed, as shown in Figure 1, the increase of a postural visual dependence (A), the improved capability for body

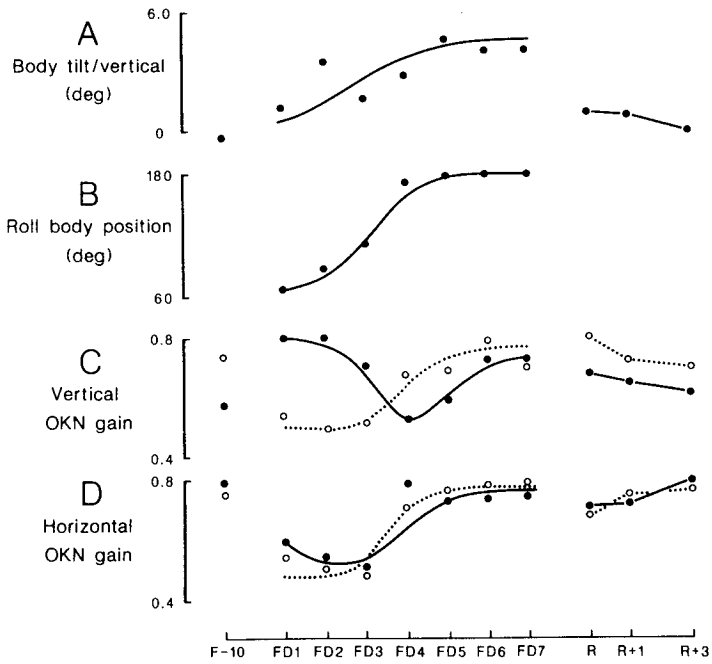

Figure 1.

orientation (B) and the modification of the OKN gain in both vertical (C) and horizontal planes (D) have similar time courses, especially during transition from the early exposure to the fifth day in a microgravity. This would suggest that space adaptation is a partially learned process, the brain having to reinterpret the new pattern of multisensory informations. ■

SIMULATION OF THE STIMULUS REARRANGEMENT PRODUCED BY WEIGHTLESS SPACE FLIGHT

D. E. Parker, A. P. Arrott, and M. F. Reschke
Space Biomedical Research Institute, NASA/Johnson Space Center, Houston, Texas 77058

Preflight exposure to an apparatus that simulates the stimulus rearrangement of weightless spaceflight could benefit astronaut training by demonstrating basic sensory phenomena, altering sensory-motor reflexes, and alleviating or reducing space motion sickness symptoms. Based on theoretical analysis and data recorded during and after spaceflight, we have proposed four design concepts for simulating the stimulus rearrangement of weightlessness. All of these alter relationships between signals received by the eyes and those received by graviceptor systems.

The proposed trainers derive from the following postulates. First, weightlessness is a form of stimulus rearrangement to which people adapt. Secondly, because of the fundamental equivalence between linear acceleration and gravity, graviceptors signal both orientation with respect to gravity and linear acceleration. Thirdly, gravity does not affect these receptors during orbital flight; consequently, graviceptors do not respond to static pitch or roll in weightlessness. However, linear acceleration during orbital flight does affect these receptors. Finally, the spatial orientation control system is activated by visual and somatic receptors as well as by the vestibular apparatus. In the absence of appropriate signals from one receptor, another receptor can provide substitute information.

The proposed design concepts will be implemented with a set of four "part-task" preflight adaptation trainers (PATs). As illustrated in Fig. 1, three trainers are designed to stabilize the otolith graviceptors with respect to gravity, and one uses passive pitch or roll movement to simulate translation in weightlessness.

In the Mode A apparatus, the trainee's head is held in the upright position. A visual scene representing the Shuttle middeck or Spacelab is presented to him via projectors and a screen or a helmet-mounted display. Scene motion results from attempted head movements by the trainee and/or from inputs to hand controllers. The attempted head movements are detected by force transducers in the head restraint. Signals from the force transducers or hand controllers activate a robot arm which carries an array of video cameras, and the visual scene recorded by the cameras is seen by the trainee. In this apparatus, visual feedback is appropriate for the commands from the hand controllers and the attempted head motions. However, gravity information transduced by the otolith and somatosensory receptors does not change. This mode was developed following suggestions from A. P. Arrott and J. Kerwin.

The Mode B apparatus employs a two degree-of-freedom moving base to stabilize the otolith receptors with respect to gravity during active head/body movement by the trainee. Both the trainee and the visual scene are located on the moving base. The trainee's movements are detected by a head tracker which provides the input signals to the hydraulic actuators. Visual and neck receptor feedback is appropriate for the trainee's head and body motions; however, the signals from the otolith graviceptors remain constant. This mode was developed following suggestions from D. Anderson and W. L. Eisenhart.

In the Mode C apparatus, the trainee is restrained on a one degree-of-freedom moving base. Roll or pitch motion is used to simulate an otolith receptor signal that would be elicited by translation in weightlessness, and the visual scene translates with respect to the trainee. This trainer, which is intended to recorrelate otolith and visual scene motion signals, derives from the otolith tilt-translation reinterpretation model of sensory-motor adaptation to weightlessness that was described initially in Aviat. Space Environ. Med. 1985; 56, 601-606.

In the Mode D PAT trainer, the trainee is permitted to move his head in a plane orthogonal to gravity. The visual scene is fixed with respect to the subject; consequently, the visual feedback is appropriate to the attempted head motion, as is the neck receptor and semicircular canal feedback. As with Modes A and B, the otolith signals remain constant.

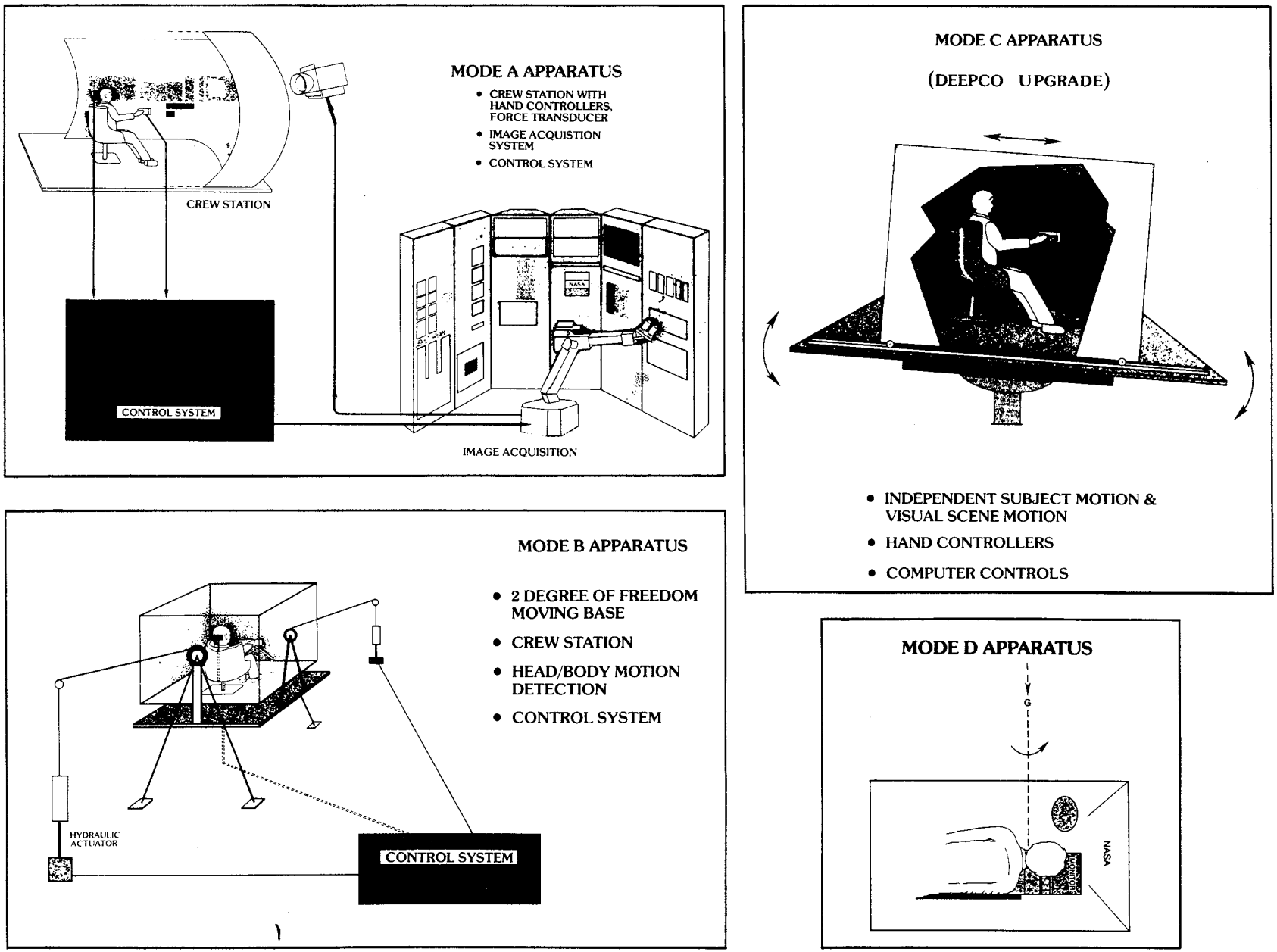

Figure 1. Four Preflight Adaptation Trainer Modes.

In summary, we hypothesize that preflight adaptation training in apparatus that simulates the stimulus rearrangement of weightlessness will enhance comfort and performance during the initial days of orbital flight.

Acknowledgement. The apparatus described in this paper was developed following consultation with a Preflight Adaptation Trainer Advisory Committee including D. Anderson, M. Cohen, W. Eisenhart, J. Evans, R. Held, J. Hoffman, J. Homick, R. Kennedy, F. Kutyna, J. Lackner, R. Seddon, H. von Gierke and R. Welch. ■

THE INVESTIGATION OF OCULAR COUNTERROLLING DURING ORBITAL FLIGHT

M. F. Reschke, D. E. Parker, J. M Vanderploeg
Space Biomedical Research Institute, NASA/Johnson Space Center, Houston, Texas 77058

Maintenance of an "Earth vertical" reference seems to be important for many crewmembers during orbital flight to reduce symptoms associated with space motion sickness, and increase efficiency. Missing gravity cues from otolith stimulation may be compensated by increased contributions of neck (and perhaps spinal) receptor input. This increased input would help maintain torsional eye movements and the stable perception of an Earth vertical reference.

METHODS:

Ten subjects participated in ground-based laboratory studies, and two astronaut subjects completed the protocol during orbital flight. The apparatus developed to obtain ocular torsion was a goggle arrangement housing a template of an inverted "T" that could be rotated in the frontal plane. An electronic flash unit was placed behind the template to provide a patterned retinal after-image. Target fixation was provided by the flash-ready light also positioned behind the template. A digital readout indicating target position was viewed with the left eye; the right eye saw the inverted "T". Rotation of the thumbwheel allowed the subject to match the retinal after-image with the target. The after-image was refreshed by a low intensity strobe (2 Hz). The goggles were held in place with a set of flexible rubber eye pieces fixed to the main body of the goggles and a wide Velcro strap. The goggles could be fixed to any smooth surface in either a horizontal or vertical position using a set of large suction cups. The interface between the suction cups and the main body of the goggles was fitted with a tilt assembly allowing the subject's head to be tilted with respect to the body in 15 deg increments. For whole body/head tilts on Earth, a servo-controlled device capable of rolling the subject was used. The subject's task was to report to a test operator or read into a voice- activated tape recorder the value indicated on the digital display.

Four experiments were conducted. In Experiment I, torsional eye movements were measured as a function of whole body tilt. In Experiment II the subject was supine, and counterrolling was measured when the head was rolled with respect to the body. For Experiment III, the relative contributions of vestibular and neck inputs to torsional eye movements were measured using two different conditions: 1) with the subjects standing and the head rolled with respect to the body, and 2) with the subjects lying on their right or left sides and the head rolled with respect to the body. In Experiment IV the effects of microgravity were examined when the head was: 1) rolled with respect to the body, and 2) held in line with the body (neck brace) and the whole subject rolled.

RESULTS.

The results indicate that the after-image method of measuring ocular counterrolling is reliable in trained subjects. Figure 1a shows the magnitude of torsion recorded in three conditions: 1) when the body and head were tilted together, 2) with the subjects standing and the head tilted with respect to the body, and 3) with the subjects supine and the head tilted with respect to the body. Our model assumed that the difference between conditions 1 and 2 above would equal the neck effect (condition 3). Note, however, that responses in the supine position do not follow this model, indicating instead that counterrolling in the supine condition begins to increase rapidly at ±30 deg. Reasons for this difference

FIGURE 1a

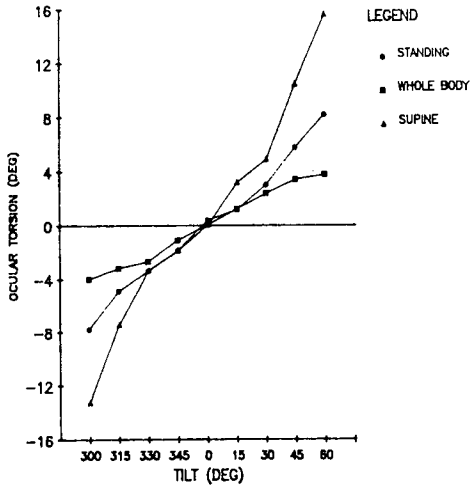

FIGURE 1b-1
RIGHT SIDE DOWN

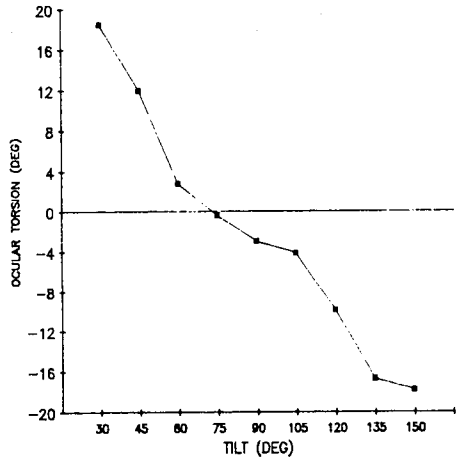

FIGURE 1b-2
LEFT SIDE DOWN

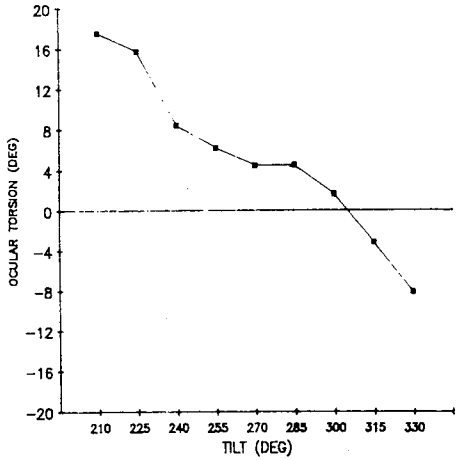

FIGURE 1c
PREFLIGHT

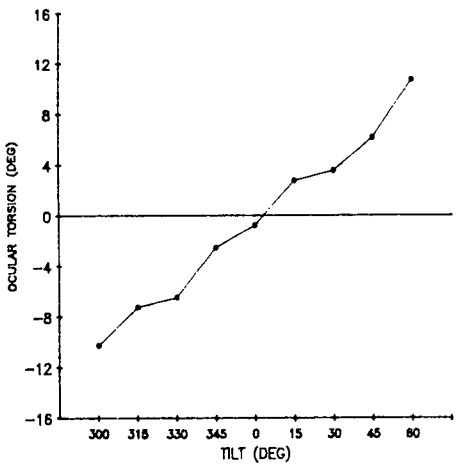

FIGURE 1d
FLIGHT

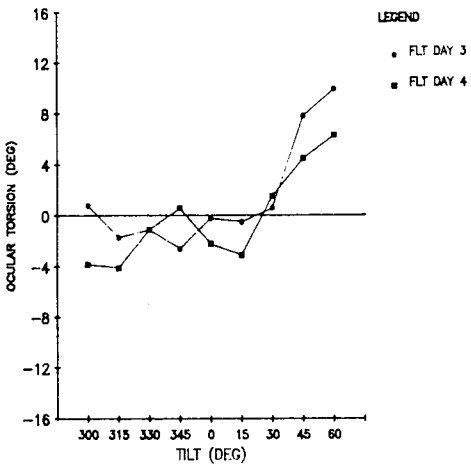

FIGURE 1e
POSTFLIGHT

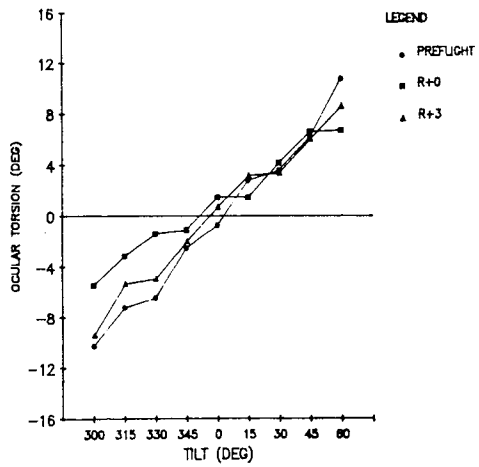

are not clearly understood, but may indicate differences in spinal and skin pressure receptor activity across conditions. Figure 1b shows the magnitude of torsion recorded with the subjects lying on their right side (Fig 1b1) or left side (Fig 1b2) and rolling the head with respect to their body. Two findings are clearly noticeable. First, counterrolling in the direction opposite neck flexure continues to increase even though otolith input decreases (head approaches the upright), suggesting that neck modulated torsion is apparently not driven by vestibular input when the utricular maculae are moved from a position of minimum sensitivity (±90 deg). Second, there is an off-set indicating that torsion is biased by the requirement for the subject to partially bear the weight of the head in this condition. Figure 1c shows the preflight data obtained from 2 astronauts in the standing condition (see Experiment III); Figure 1d shows the data obtained inflight. Note that counterrolling does occur inflight as a function of head roll relative to the body, and decreases in magnitude (but more symmetrical) as the flight progresses. Immediately postflight (within 1 hr following landing, R+O) there was a tendency for the magnitude of the counterrolling to be of lower magnitude (again directional) relative to preflight, with a return to baseline by the fourth day (R+3) postflight (Figure 1e). ■

ALTERATIONS OF PROPRIOCEPTIVE FUNCTION IN A WEIGHTLESS ENVIRONMENT

D. Watt and K. E. Money
Aerospace Medical Research Unit, Department of Physiology, McGill University, 3655 Drummond Street, Montreal, PQ Canada H3G 1Y6 and National Research Council of Canada, Ottawa, Canada

---

Anecdotal evidence from previous spaceflights has suggested that astronauts quickly lose track of limb position in the absence of vision. Money (1984) has confirmed this phenomenon during the flight of Spacelab-1, as has Veringa (1986) during Spacelab D-1. Brenske (1986) has also reported apparent alterations in neck proprioception during spaceflight. Postural experiments performed inflight on French and Russian subjects (1984) have demonstrated difficulty in maintaining a body position perpendicular to the vehicle floor in the absence of vision and when held by the feet only, a phenomenon which may also be the result of abnormal proprioceptive feedback.

During experiments carried out on Shuttle flight 41-G, 2 subjects were required to estimate joint angles after passive limb movement. Tests were conducted at the elbow, knee, and at the distal joint of one toe and finger. Other experiments measured accuracy during an active pointing task, in which the subjects attempted to shine a light pointer at memorized targets. All testing was performed in the absence of vision, and was carried out repeatedly before, during, and after the mission.

The subjects, both of whom were normal preflight, demonstrated degraded proprioceptive function in weightlessness in both passive and active tests. Estimates of joint angles were often grossly in error, especially at the elbow and knee. The ability to point at unseen targets was very poor, particularly in the "vertical" direction. These results did not change during the flight. Postflight, there was rapid recovery of normal function.

Besides emphasizing the importance of gravity in normal proprioceptive function, these findings suggest a possible source of error during manual control tasks in space when vision is directed away from the hands. Because of the known role of proprioceptive inputs in gaze control, and the fact that gaze instability on the ground often leads to motion sickness, these proprioceptive abnormalities may even contribute to the generation of space motion sickness. (Supported by Medical Research Council of Canada, National Research Council of Canada, and National Aeronautics and Space Administration). ■

PAGE 223 INTENTIONALLY BLANK

PRECEDING PAGE BLANK NOT FILMED

OVERVIEW OF PLANTS AND GRAVITY—Panel Discussion

The goal of the symposium and the workshop which is to follow is twofold: first, to elucidate the state of knowledge regarding the relationship of gravity to plant development, physiology, and behavior and second, to define future directions to take to build on that which is known. Broad areas of research to be discussed are gravity perception, gravity and development, gravity and cellular and molecular functions, and gravity and biological adaptation. Examples of topics to be covered are cell wall changes in gravistimulated plant shoots, the involvement of plant hormones and calcium in plant gravity responses, characteristics of root growth in a microgravity environment, sensitivity of metabolism to gravity, and requirements of a seed-to-seed space experiment. Practical considerations such as the design and utilization of microgravity facilities in space will also be discussed. ■

PLANT BIOLOGY AND SPACE SCIENCE IN CSIRO, AUSTRALIA

R. M. Gifford
CSIRO, Division of Plant Industry, GPO Box 1600, Canberra, A.C.T. 2601, Australia

Australia has had an exceedingly low per capita level of expenditure on space R and D compared with other countries like Canada. This short-coming was recognized by the CSIRO Executive when, in December 1984, it formed COSSA - the Office of Space Science and Applications. COSSA, Directed by Dr. Ken McCracken, supports research throughout Australia which is seen to have a prospect of contributing significantly to space-related technologies and applications. Emphasis is on collaborative efforts with existing space agencies such as NASA, and on research which will lead to manufacturing and export opportunities for Australian industry.

The CSIRO Division of Plant Industry has a wide range of plant physiological research potentially relevant to developing methods for growing plants in space facilities. Notably there is work on controlled-environment plant growth in CERES the Canberra Phytotron, regulation of flowering, impact of gaseous composition of the air (CO_2, O_2) on plant growth and yield, circadian and other rhythms, and plant growth regulators that alter tropic responses of plants.

So far COSSA has no biological component to its efforts, other than aspects relating to remote sensing. My participation in this conference is to evaluate the scope of space plant science to see whether there are areas which we could effectively contribute to. ■

PAGE 225 INTENTIONALLY BLANK

PRECEDING PAGE BLANK NOT FILMED

EARLY EFFECTS OF WEIGHTLESSNESS ON GROWING BONE

S. B. Arnaud[1], E. M. Holton[2], P. P. Buckendahl[3] and G. Tietjen[1]
[1]*Space Physiology Branch, SLP 239-17, NASA/Ames Research Center, Moffett Field, California 94035,* [2]*Space Biology Branch, SLB 236-7, NASA/Ames Research Center, Moffett Field, California 94035, and* [3]*Biology Board, Thimann Laboratories, University of California, Santa Cruz, California 95064*

The changes reported in growing rat bone after only 7 days in space are impressive evidence of how rapidly growing bone adapts to a stimulus. Martin (1) and Shaw (2) were unable to show increases in the strength of the humerous and tibia, respectively, in spite of some increase in bone mass and volume. Alterations in the chemical composition of these young bones in 7 days are nearly the same as reported in animals after 3 weeks in space, who also show deficits in bone strength (1,3). It is not known if these changes represent the temporary reaction of the bone, responding directly, (as an organ system) to microgravity, (a biochemical effect); or responding indirectly, through vascular, endocrine, or neuromuscular systems.

The interdependence of multiple systems in the normal functioning of any one organ system makes it difficult to establish the principle cause of the early changes which occur during spaceflight. While it may be unrealistic to separate the effects of systemic and local factors which contribute to the changes which we have observed, the understanding of the problem, and the different disciplines which are involved, all favor dissecting the problem in order to solve it and then select appropriate preventive measures.

The underlying rate of metabolic activity in a growing bone can be shown to be a major factor in the response to spaceflight. Chemical changes in the third lumbar vertebrae, a more rapidly growing bone than humerus in 2-month-old animals, were more pronounced in the Spacelab 3 experiments and less pronounced in the 3.5-month-old animals in the Cosmos 1667 7-day flight (4). How the endocrinology of normal growth or of stress responses at different ages determines metabolic activity in the skeleton is uncertain. Added to these systemic influences on skeletal metabolism is the response of each bone to

EARLY EFFECTS OF WEIGHTLESSNESS ON BONE
FEATURES IN GROWING BONE OF YOUNG RATS

FUNCTIONAL DEFECT
- ↓ BONE STRENGTH (NO CHANGE FROM PREFLIGHT)

QUANTITATIVE
- ↓ PERIOSTEAL BONE FORMATION
- ↓ OSTEOBLAST AND PREOSTEOBLAST NUMBER
- ↓ CA, MG, Pi, CONTENT (CONCENTRATION NORMAL)
- ↓ CA/COLLAGEN RATIO
- ↓ NONCOLLAGENOUS PROTEIN, OSTEOCALCIN, IN BONE AND BLOOD
- OSTEOCLASTS AND RESORPTION PARAMETERS NORMAL

QUALITATIVE
- DENSITY PROFILE SHIFTS TO HIGH & LOW FRACTIONS
- HYPOMINERALIZED GROWTH ARREST LINE
- ↓ HYDROXYAPATITE CRYSTAL SIZE BY X-RAY DIFFRACTION
- MINERALIZED AND NON-MINERALIZED COLLAGEN NORMAL
- ALK PTASE AND DIPEPTIDASE IN OSTEOBLAST NORMAL

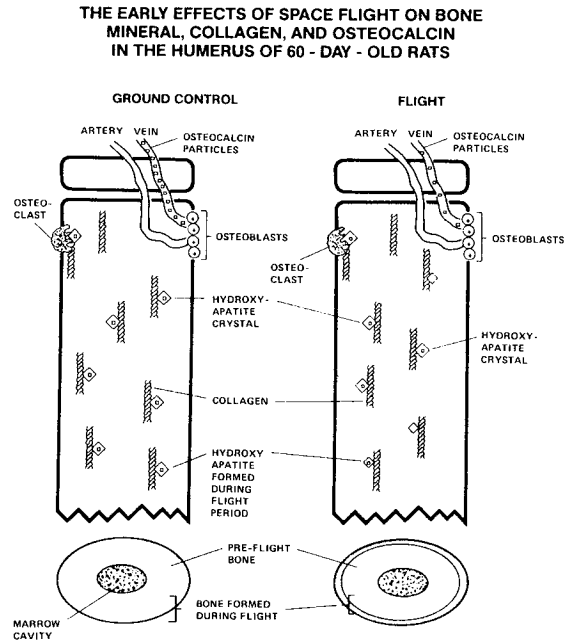

Figure 1.

the withdrawal of the weight imposed by 1 G. There is currently no data relating the load imposed on each bone at 1 G to the metabolic and cellular changes in microgravity. The dramatic fluid shifts which occur in space, our awareness of the buffering capacity of bone salts, and the very short time in space preceding the chemical changes in bone, all place the vascular and fluid compartments of bone as a strong candidate for initiating the cellular or tissue events at 0 G.

Table I summarizes the qualitative and quantitative features observed in a variety of individual bones from growing rats after one and three weeks in space. Whether these findings are part of the adaptation process or will persist in long duration flights to modify the architecture of bone for a space environment is not known.

The figure is a computer-generated theoretical representation of the structural and chemical changes in a long bone of a growing animal. These is a barely perceptible decrease in the volume or cross section of the whole bone. Collagen content is the same in both flight and control bones, as is the percent mineralized and unmineralized collagen. Hydroxyapatite crystals are represented as the same size in the control, and of variable size (5) in the flight bone. Osteocalcin, a noncollagenous protein, synthesized by the osteoblast, is shown as reduced in bone and blood. Whether this reflects reduced synthesis, and/or excretion or distribution is not yet known. Osteoclasts are shown as unchanged, which may be related to the existing high activity of these cells in growing animals. The cross sections show primarily the area of reduced bone formation at the periosteal surface of bone. ■

REFERENCES

1. Patterson-Buckendahl PE, Arnaud SB, Mechanic GE et al. Am J Physiol 252:R240, 1987.
2. Shaw S, Zernicke R, Vailas A, et al. North American Congress on Biomechanics. Montreal, August, 1986.
3. Spengler DM, Morey ER, Carter DR et al. Proc Soc Exp Biol and Med 174:224, 1983.
4. Vico L, Chappard D, Bakulin AV. The Physiologist 30:S-45, 1987.
5. Simmons DJ, Russell JE, Grynpas MD. Bone & Mineral 1:485, 1986.

FLUID DYNAMICS IN BONE

R. M. Dillaman[1], R. D. Roer[1], E. Rutherford[2]
[1]*Institute for Marine Biomedical Research, University of North Carolina at Wilmington, Wilmington, North Carolina;* [2]*New Hanover Memorial Hospital, Wilmington, North Carolina*

Bone is comprised of three general anatomical compartments: the mineralized matrix, the cellular components and the fluid compartment consisting of blood and plasma. While it is widely recognized that exposure to microgravity has a pronounced effect on the mineralized matrix of bone, it is unclear whether the other two components of bone are likewise perturbed. Moreover, it is equally unclear whether the effects of weightlessness on the mineralized portion of bone are the consequence of effects on the cellular and/or fluid compartments. We are investigating the relationship between gravity and the fluid dynamics of blood and plasma in bone and its influence on bone physiology.

In order to understand the fluid dynamics of bone, it is first necessary to identify and describe the anatomy of the fluid compartments of bone. In the long bone of the rat, we are employing a four compartment model of bone fluid, the anatomical correlates of which are: the vascular space, the extravascular space between the vessels and the osteogenic layer, the extravascular space between the osteogenic layer and the mineralized matrix, and the extravascular space within the mineralized matrix itself. These anatomical compartments are not randomly distributed, but form a regular three-dimensional array within the bounds of the organ. The gross morphology of the vascular compartment has been described by Brooks (1971) and others, but the detailed microanatomy has been restricted to isolated portions of the canine tibia (Lopez-Curto et. al., 1980). Physiological evidence has

demonstrated a difference in the perfusion of the different regions of the bone. In order to understand the mechanisms underlying this variation, it is necessary to examine, in detail, the microvasculature anatomy throughout the entire length of the bone. We are employing both vascular casting and three-dimensional reconstruction of serial sections of bone to describe the pattern of the vascular array and to describe the fine structure of the vascular elements.

To investigate the movement of fluid among the various compartments in bone, and to elucidate possible effects of microgravity on those movements, we have initiated anatomical studies employing extravascular markers. As a landbased model of hypogravity, we are using the antiorthostatic hypokinetic (tail-suspended) rat (Morey- Holten and Wronski, 1981). Horseradish peroxidase was injected into female Wistar Furth rats and animals were sacrificed at various intervals thereafter. Precise dosage of markers, timing of injections and the ability to deliver the marker while maintaining posture were made possible by the use of a small vascular access port. The ports were implanted subcutaneously on the hip of the rat and the catheter passed ventrally and ligated in femoral vein.

Histochemical localization of the peroxidase in the contralateral femur five minutes after injection showed it to be well into the canalicular system of selected vessels and evident in the osteocytic lacunae, suggesting an extravascular pathway into the mineral. By four hours post- injection, peroxidase was present throughout the bone and dense staining was seen in virtually all the osteocytic lacunae. At 24 hours after injection, peroxidase had all but disappeared from the endosteal portion of the bone, while periosteal staining, although diminished, was still evident. These observations suggest that there is rapid movement of large molecular weight substances from the vascular to the extravascular compartment between the vessels and the osteogenic layer, and from the latter to the extravascular compartment between the osteogenic layer and the mineralized matrix. The disappearance of the marker, albeit over a prolonged period, from the endosteal toward the periosteal surfaces suggests a unidirectional, centrifugal perfusion of the bone matrix by plasma.

This use of morphological markers can give a sense of the path of fluid movements within the bone compartments as well as the permeability of the compartments to molecules of various sizes. These studies do not, however, provide a quantitative measure of fluid flow rates in bone. Toward this end, investigators have employed multiple indicator dilution techniques (Morris et. al., 1982). Limitations to this technique are the absence of a defined afferent and efferent blood supply to cortical bone. These limitations necessitate the use of marker entrapment in bone and destructive sampling. We are initiating studies of trapped radioactive tracers in rats to determine whether differences in posture affect bone flow rates, again employing the antiorthostatic rat model. Indications that such difference are likely to occur are found in the studies of Morris and Kelly (1980) in which differences in blood flow were detected between the limbs of anesthetized, supine dogs. Our marker and anatomical studies will provide the bases for the formulation of a computer simulation of fluid movement through the bone vasculature and extravascular spaces. These approaches will feedback to one another to allow a continual refinement of our modeling of fluid dynamics in bone. Furthermore, our approaches will allow an integration the effects of spaceflight on bone physiology with the wider range of cardiovascular changes already so clearly demonstrated. ■

REFERENCES

Brooks, M. 1971. *The Blood Supply of Bone.* Butterworths, London.
Lopez-Curto, J. et. al. 1980. J. Bone Joint Surg. *62A:* 1362-1369
Morey-Holton, E. & T. Wronski. 1981. Physiol. *24:* S45.
Morris, M. et. al. 1982. Microvasc. Res. *23:* 188-200
Morris, M. & P. Kelly. 1980. Calcif. Tiss. Int. *32:* 69- 76.

THE DYNAMIC NATURE OF THE WEIGHT-BEARING FUNCTION OF THE SKELETON

W. S. S. Jee
Division of Radiobiology, University of Utah School of Medicine, Salt Lake City, Utah

It has been shown that the bone mineral mass of the body is directly proportional to gravitational loading over the range of 0 g to 2.0 g, emphasizing the dynamic nature of the weight-bearing function of the skeletal system. Our experiences with the growing skeleton in spaceflight, ground-based simulated weightlessness and immobilization further showed that skeletal unloading reduces the accumulation of bone by depressing bone formation, but consequently regains much of the skeleton on the reimposition of customary load. Unfortunately, nothing is known about the behavior of the adult skeleton in space, but there is plenty of experience of disuse osteoporosis on earth that can be extrapolated to disuse in weightlessness.

Sudden withdrawal of mechanical loading, i.e., of weight bearing and physical exertion against gravity, initiates a rapid bone loss that will abate even during continued immobilization. This phenomenon indicates an adjustment of bone mass to reduced mechanical demands. It appears that skeletal unloading (disuse or sudden immobilization) accelerates the excess of endosteal and paramedullary envelope expansion over the periosteal one until the bone volume matches the new reduced mechanical demands. Thus, the disuse osteoporosis is self-limiting; bone loss does not continue indefinitely. The bone loss is due to increased activation of osteoclast populations and a suppression of osteoblast recruitment (uncoupling).

There is significant recovery of bone on remobilization. This is most likely achieved by the increased rate of osteoblast recruitment where the quiescent resorption surfaces were converted to bone-forming ones. Usually, the recovery after remobilization is not complete and is less in old than in young individuals, suggesting an irreversible component to loss.

To date, astronauts have not remained in space long enough to reveal whether the bone loss due to weightlessness is self-limiting. They may be regaining much of the loss incurred in space, especially younger individuals. This may not be true after longer periods in space.

Since a complete recovery of bone loss may not be possible after remobilization, prevention of bone loss, stimulation of complete recovery during remobilization and addition of new bone mass, *de novo*, become the avenues available. It remains uncertain whether disuse osteoporosis can be prevented by other than biomechanical means, by drugs or hormones blocking the initial burst of resorption activity. Studies to stimulate osteoblastic activity during the recovery phase do not exist, but should be pursued. Efforts to increase bone volume, *de novo*, and by manipulating the bone remodeling cycle show promise. The problem of increasing bone mass applies to the treatment of any type of established osteoporosis of any etiology in clinical medicine. The spin-off of this type of research to mankind is great. ■

WEIGHT-BEARING EXERCISE AND REGULATION OF BONE MASS

R. Marcus
Stanford University, Aging Study Unit, VA Medical Center, Palo Alto, California 94304

It is an article of faith to state that weight- bearing exercise promotes skeletal health. This axiom finds support from several lines of evidence. These include extensive documentation of rapid and devastating bone loss with immobilization, studies in which bone density of athletes is compared to that of sedentary controls, and a few studies in which sequential bone density measurements have been made in subjects on whom an exercise program is imposed. I wish to summarize the conclusions which one can draw from the published exercise literature, point out some problematic aspects of this information, suggest goals for future research, and touch on challenges posed for the health

professional who hopes to transform this body of research into realistic programs for the American public.

Most studies of exercise and bone mass in man have been cross-sectional comparisons of active and sedentary people. These studies consistently support the view that an active lifestyle is associated with a bone mass which may be as much as 30% greater than that of sedentary controls. In addition, some data suggest that physical activity can attenuate age-related bone loss and even protect the skeleton from menopausal estrogen withdrawal. However, one must interpret this literature cautiously in view of several potential confounding factors. Most important is the possibility that the decision to enter into exercise training and the ability to endure long enough to be categorized as "athletic" may not be independent of initial bone density. For example, the use in one study of an "athletic" group which had accumulated an average individual running experience of 12,000 miles preselects those individuals whose musculoskeletal systems could tolerate such long-term wear.

Relatively few exercise intervention trials have been directed at changes in bone mass. The following observations have been made: (1.) Increases in bone mineral density have been observed in some, *but not all* studies. (2.) These increases are relatively small compared to those suggested by the cross-sectional literature.

These studies must also be interpreted with caution. In some, the degree of exercise loading or its duration may have been inadequate. Sites of bone density measurement did not always correspond to the region which received loading. Assignment of subjects to exercise groups has generally not been random, and assessments have never been blinded.

Nevertheless, one takes from this literature reasonable optimism that weight-bearing exercise may increase peak bone mass and protect against subsequent loss. Understanding of *how* weight-bearing promotes bone mass is sketchy. Bone is a material with its own fatigue characteristics, and accumulates fatigue damage with repetitive strain. Construction of a suitable exercise program requires attention to several factors. These include the type of activity, its intensity, duration and frequency. To date, virtually *no* published information in man permits selection of an exercise regimen on a rational basis.

Dennis Carter and his colleagues at Stanford University have developed a mathematical approach to understanding the distribution of density within a bone and between bones. By their formulations, bone density reflects a customary daily loading history that can be expressed in terms of the number of cycles and the stress magnitudes of each individual activity. This is shown in the following equation, $S = \Sigma(n_i \times S_i^m)$ in which for each ith activity, "n" is the number of cycles and S_i is its stress magnitude. "m" is a constant which gives weight to the relative dependence of the density-determining stimulus on stress intensity versus number of repetitions. If m=1, intensity and repetitions are of the same order. Increasing values of m indicate increasing dependence on activities with high stress magnitude. Additional studies by this group suggests that "m" lies between 2.5 and 4.5, leaving the inference that bone density will be far more responsive to exercise at high load intensity, such as weight-lifting, than to low- intensity, repetitive activity, such as walking or jogging. If this is correct, important issues of clinical relevance are raised. It is clear that serious weight loading of frail individuals with established osteopenia could not safely be done. In this group there is no other choice but to continue to prescribe exercise of lesser intensity, and therefore lesser effect. It follows that the primary beneficiaries of high-intensity exercise would be teen-age and young adult men and women, whose growth is still active, who are still acquiring peak bone mass, and whose skeletons can tolerate increased loading with a low risk of fracture.

However these issues resolve, it will be important to assess them systematically. The time has come to move from descriptive cross-sectional comparisons to randomized prospective intervention trials to determine the parameters of an optimal exercise prescription. As a closely related issue, the field to date has not come to grips with quantitation of activity. Although maintenance of exercise records is relatively simple, it will not be trivial to construct accurate summaries of routine daily physical activity. ■

THE EFFECT OF MECHANICAL STIMULI ON BONE

E. L. Radin
Department of Orthopedic Surgery, West Virginia University Medical School, Morgantown, West Virginia

The musculoskeletal tissues, unlike those of other organ systems, respond to mechanical stimuli by altering their cellular metabolism and organization. Although the basic form of bones is predetermined and will even emerge in tissue culture, the presence of some features is dependent upon mechanical function. In some bones, such as the ethmoid bones of the skull, where mechanical stress is low, this dependence is small. In the long bones and appendicular skeleton, it is much higher. An example is failure of angulation of the neck of the proximal femur in the presence of paralysis of the lateral muscles of the hip joint. Full expression of bone's genetic potential will only occur under suitable conditions.

The relationship of bone formation to mechanical forces was first established by Julius Wolff in 1892 (11). Pauwels later related increasing stress to bone formation (5). Osteoblastic activity only occurs within a "window" of stress. Too much stress results in bone resorption (10). This is the basis for orthodontia. It is also well known that too little stress causes bone resorption. This will be a major problem in spaceflight (1).

Frost has enunciated the principle that strain, rather than stress, is the key factor in physically caused bone remodeling. The concept of Minimal Effective Strain (MES) (2), the minimum strain required to maintain skeletal mass, is attractive.

It is not only how much strain a bone is subjected to, but the way strain is delivered, that is critical to whether a bone mass will be maintained or not. It must be delivered sharply, as a peak dynamic load to effect bone formation (4).

Abundant circumstantial evidence indicates the major biomechanical factor maintaining skeletal mass is repetitive large loads. Weight lifters have massive bones; marathon runners do not. Exercise bike riding is unlikely to build or maintain skeletal mass. The major force on bone is muscle contraction. Because most muscles work against a poor mechanical advantage and the major effect of gravity on bone loads is to provide the resistance muscles must overcome, the peak muscle forces on bone required to push off from the floor with one leg with the force of 1.2 or 1.3 g's is several times body weight. Accordingly, applications of impulsive loads of .8 or 1.2 g's on the heel of a man at bed rest or a monkey or rabbit in a cast does not come close to duplicating the magnitude of loads on bone when an individual is actually walking. Adequately high repetitive peak loading has been shown to have an ameliorating effect on postmenopausal osteoporosis (7,9) and may well have a similar effect on the osteopenic of disuse or in circumstances of diminished gravity.

The number of repetitions of the strain cycle has also been recently investigated (6). It would appear as if 36 cycles of peak of stress are necessary to maintain skeletal mass.

It is unclear how strain acts at the cellular level. Simple deformation of cell membranes provokes considerable activity among intermediate mediators (3). Electrical factors have been suggested as a mechanism as well (8).

In summary, appropriate physical stimuli can provoke bone formation. ■

REFERENCES

1. Arnard, S., Personal communication.
2. Frost, H.M., Intermediary Organization of the Skeleton, Vol. I & II, CRC Press, Inc., Boca Raton, Florida, 1986.
3. Harrel, A., Dekel, S., and Bindermann, I., Biochemical effect of mechanical stress on cultured bone cells. Calcif. Tiss. Res., Suppl. 22, 202-207, 1977.
4. O'Connor, J.A., Lanyon, L.E., and MacFie, H., The influence of strain rate on adaptive bone remodeling. J. Biomech. 15:767-81, 1982.
5. Pauwels, F., Biomechanics of the Locomotion Apparatus: Contributions of the Functional Anatomy of the Locomotor Apparatus. Translated by P. Maquet and R. Furlong, Springer- Verlag, Berlin, Heidelberg, New York, 1980.

6. Rubin, C.T., and Lanyon, L.E., Regulation of bone formation by applied dynamic loads. J. Bone Joint Surg., 66- A:397-402, 1984.
7. Smith, E.L., Jr., Redden, W., Physical activity and calcium modalities for bone mineral increase in aged women. Med. Sci. Sports Exerc. 13:60-4, 1981.
8. Thompson, R.C., Jr., and Basset, C.A., Histological observations on experimentally induced degeneration of articular cartilage. J. Bone Joint Surg., 52-A:435-43, 1970.
9. White, M.K., Martin, R.B., Yeater, R.A., Butcher, R.L., Radin E.L., The effects of exercise on the bones of postmenopausal women. Intern. Orthop. 7:209-14, 1984.
10. Weinmann, J.P., and Sicher, H., Bones and Bones, Fundamentals of Bone Biology, St. Louis, C.V. Mosby Co., 1955.
11. Wolff, J., The Law of Bone Remodeling, Translated by P. Maquet and R. Furlong, Springer Verlag, Berlin, Heidelberg, New York, 1986.

PAGE 233 INTENTIONALLY BLANK

PRECEDING PAGE BLANK NOT FILMED

SELECTION FOR OPTIMAL CREW PERFORMANCE IN AEROSPACE ENVIRONMENTS

T.R. Chidester and H.C. Foushee
NASA/Ames Research Center, Moffett Field, California 94035

The U.S. Space Station will be a highly structured small-group environment, where sustained productivity and safety, over long periods of isolation, will be dependent upon a number of socio-psychological, personality, task, and environmental variables. NASA has spent a considerable amount of effort on the identification of individual skills and training methods to produce high levels of individual technical competence. As we move toward expecting humans to perform effectively in isolated and potentially dangerous environments for extended periods of time, we cannot assume that technically competent individuals will necessarily perform effectively as a team. In fact, a considerable amount of research in various group performance situations has demonstrated that such an assumption is untenable: In the context of transport aircraft operations, a number of incidents have underscored the need to consider crew communication and coordination in order to understand the process by which individual skills and characteristics are translated into group outcomes. Foushee (1984) and Helmreich (1986) have noted that while operation of modern multi-pilot aircraft is obviously a team task, the whole of performance evaluation and pilot selection has been focused on the individual technical proficiency of pilots to the neglect of skills associated with crew coordination. Transport aircraft accidents and incidents due to a lack of knowledge or technical skill of pilots are extremely rare. However, accidents and incidents due to failures of crew coordination have continued to occur (Cooper, White, and Lauber, 1979).

Having identified crew coordination as a problem in aircraft operations and suggested possible implications for space operations, we recognize that there are several strategies available for developing countermeasures. Classical approaches from industrial-organizational psychology include training, task design, and selection. Each of these approaches offers promise for optimizing crew function, and the best strategy would incorporate aspects of each. For example, training approaches are most likely to affect skills and attitudes (defined as learned patterns of responding). Selection is a means of appropriately utilizing the effects of personality (defined as stable, deep-seated predispositions to respond in particular ways), which are much more resistant to change. The two approaches are complementary, and each will have unique, but additive effects on crew coordination. This presentation focuses on selection for personality characteristics in order to study variables which cannot be manipulated through training or task design. A number of studies have already shown some of the promise of those approaches, but little or no systematic research on selection has been completed. High fidelity selection research seeks to fill this gap and round-out our knowledge about the crew performance process.

Several recently validated dimensions of personality may be expected to predict crew performance. Personality research in the multi-pilot aviation arena is focusing upon instrumentality, expressivity, and a number of multi-dimensional achievement criteria as reliable predictors of effective leadership and crew coordination. There is a developing perception in aviation that relatively high levels of both instrumentality and expressivity in the crew-member population are desirable characteristics. NASA research on cockpit communication patterns (*e.g.*, Foushee and Manos, 1981; Foushee, Lauber, Baetge, and Acomb, 1986) has shown that performance tends to be poorer in crews that communicate less. Overbearing interpersonal styles are repeatedly shown to be disruptive to the communications process in incident reports. These interpersonal styles may be effectively captured by the personality dimensions discussed in this presentation.

The interaction of cockpit role-structure characteristics with the predominantly instrumental pilot population is drawing considerable scrutiny as a problem area. High levels of expressivity may be functional in this environment, and Helmreich (1982) and Chidester (1986) have presented evidence

that bolsters this prediction. This shift in thinking about desirable psychological selection criteria is interesting in light of past emphases weighted heavily in favor of instrumental traits. Some airlines are now considering both instrumental and expressive traits in their selection criteria.

As an example of high-fidelity selection research in this area, a description of a full-mission simulation currently in progress is discussed. Four types of crews are being examined.

The first type of crew consists of a Captain, First Officer, and Flight Engineer randomly selected to participate together without regard to personality profiles. The second and third types involve selection for crew composition. That is, each crew consists of three crewmembers, all selected on the basis of their personality characteristics. The second type is composed of a Captain, First Officer and Flight Engineer, all selected for a cluster of positive personality characteristics identified in a previous study (Chidester, Helmreich, and Geis, in preparation). These positive characteristics (referred to as a Positive Instrumental/Interpersonal cluster) include goal orientation, independence, and interpersonal warmth and sensitivity. The third type is composed of a Captain selected for a set of negative characteristics including interpersonal competitiveness, arrogance, and emotional invulnerability; and a First Officer and Flight Engineer selected for unassertiveness. This combination, of a leader characterized by insensitivity and subordinates with a lack of assertiveness, is expected to exacerbate problems of crew coordination in response to the high workload demands of the emergency segments in the simulation scenarios. The fourth and final type of crew involves selection for leadership only; that is, only the Captain is selected for the Positive Instrumental/Interpersonal cluster. The First Officer and Flight Engineer are randomly selected.

This design allows us to address several of the issues discussed above. First, having a control group composed of randomly assigned crewmembers allows us to estimate what contribution selection could offer over and above the current operational practice. Second, by contrasting crews selected for leadership with crews selected for all crewmembers' personality characteristics, we may determine which is the maximally effective strategy. Finally, by having crews fly the simulator for an extended period we may determine how selection for leadership and crew personality interact with crew familiarity and experience in influencing the crew performance process. ■

IS "THE RIGHT STUFF" RIGHT?: THE LEADER'S ROLE IN CREW FORMATION AND DEVELOPMENT

R. C. Ginnett
United States Air Force Academy, Department of Behavioral Science and Leadership, United States Air Force Academy, Colorado 80840

Groups are sent into space. We have not put a lone individual into space since the Mercury projects. Yet there is little evidence that we have really considered the fact that a group in space (or anywhere else, for that matter) differs greatly from a mere collection of individuals. Because of the proliferation of groups as the means to accomplish work in organizational settings, we are paying more attention to them on earth, at least in organizational behavior classrooms. But we have not been able to study groups in space for a variety of reasons. Therefore, some of us (*e.g.* Foushee, Helmreich, Ginnett) have been using aeronautical crews as an analog. While we have no doubt surrendered some desired experimental control, these groups have given us some particular advantages. They are real groups in real organizations performing real tasks requiring interdependent work. And while not all pilots become astronauts, historically, most astronauts have been pilots. Of particular importance to me, cockpit crews form frequently, often are working together as a group for the first time, and have a designated leader. If you happen to be interested (as I happen to be) in understanding what a leader can do to form a crew into a coordinated team, then cockpit crews are especially useful groups for study.

Unfortunately, not all cockpit crews perform equally well. The impact of ineffective crew performance was demonstrated in a comprehensive review of jet transport accidents worldwide between 1968 and

1976 by Cooper, White, and Lauber (1979). They found that breakdowns in the performance of the crew as a whole played a significant causative role in more than 60 of the losses studied. We are still learning about the causes of crew effectiveness (or lack thereof), but there is a clear belief among pilots that whether a crew will perform well or not is a function of the captain.

Within a given company, pilots: (1) *can* reliably identify those captains who are effective at forming and developing a crew (Helmreich, Foushee, Benson & Russini, in press); (2) *cannot* articulate *what* the effective captains do to be seen as effective; and (3) claim that they can identify an effective captain in "just a few minutes" after meeting him or her. What happens in the crew formation process, what the leader does, and how this process carries over to crew performance during line operations were the questions addressed by this research.

The nature of this research was qualitative, both by design and by circumstance. First, there was virtually no literature on the formation process of flight crews. Second, as noted above, the pilots were unable to offer much help in identifying specific behaviors that might serve as experimental variables. And finally, the reasonably extensive social science literature on group formation and development did not seem to match the processes observed in preliminary research with cockpit crews.[1] Therefore, intensive observations of the formation process by a trained behavioral observer was selected as the most efficacious research method.

Based upon the nominations of check airmen (pilots responsible for evaluation of their fellow pilots), captains were selected for their relative ability to lead and manage crews (as opposed to their ability to fly the airplane—a skill in which all were presumed to be proficient by virtue of their rating and certification). The final group included six "highly effective" captains and four captains rated as "relatively less effective" at this leadership function. Each captain (and the crew assigned to him) was observed on two separate occasions. During the crew formation process, detailed data were recorded and analyzed using the normative model for group effectiveness (Hackman, 1986) as a framework. Subsequent critical events during line operations were also recorded. In all, over 300 hours of crew performance were observed.

In the company studied, the formation process formally began when the captain initiated the "crew briefing". Although this briefing was actually directed to the "cabin crew," the first officer and the flight engineer observed the captain's behavior and thus learned about the way he worked with people. Across crews and times, captains maintained their own individual style for the briefings (regardless of their relative ability to build and manage crews).

The effective captains as a whole displayed reasonably similar behaviors in their briefings, and, with only a few minor exceptions, behaved in accordance with the predictions of the normative model (*i.e.*, they discussed tasks, boundaries, and norms).[2] While they did not talk about the general task to be performed (a superfluous action), they did mention some task which required interrelated actions and coordination between the cabin and cockpit crews. Each captain also dealt with group boundary issues in several ways. First, they all entered the proxemic boundary established by the flight attendants in the briefing room. They also acknowledged the physical boundary that would separate them in the airplane — the cockpit door. They typically would establish a "linking pin" relationship between the engineer and the lead flight attendant, and all of them introduced the researcher as a part of the crew. Each of these captains explicitly described performance norms, stressing safety, communications or cooperation. Lastly, and critically for pilots, each of the effective captains managed the horns-of-the-authority dilemma. They did this not by trying to find some moderate point between the extremes, but rather by demonstrating both extremes. On the one hand, they demonstrated their competence by presenting an ordered briefing in which they displayed both their technical and social competence. But they also would disavow perfection by admitting lack of knowledge on some perfectly "knowable" item (such as, at which gate the airplane was parked). This tended to engage the crew in team performance, a tendency also clearly noted in the amount of time during the briefing in which the crewmembers spoke.

These early behaviors exhibited in the briefings were maintained and reinforced in subsequent line operations. The effective captains gave crew briefings in the cockpit on expected team performance following the same pattern established earlier. Other consistent behaviors included calmness in unusual circumstances, talking through their mistakes, coaching, and the relinquishing of responsibility for the

group's social behavior in the evening. Finally, the concept of "shells" is developed to explain the group formation process in organizational settings.

Let me conclude by extrapolating from the aeronautical leader to the space leader. When we sent a lone human into space, he needed to have the "Right Stuff." From liftoff to splashdown, he had the "Only Stuff" in the capsule, so it had better be "Right." But in the recent past and certainly in the future, there will be groups in space and we are now seeing evidence that an effective group leader displays different behaviors than the typical "right stuff" image might conjure up. Maybe it is time we followed Harold Leavitt's (1975) advice and started to take groups seriously. If we do, then the leaders of groups in space should not be selected merely because they are the best test pilots. If we are sending groups because we believe that groups can perform better than individuals, then what the group leader really needs to know is how to create and manage the conditions that will allow the crew to do its best work.

The research reported here was supported by Cooperative Agreement NCC 2-324 between NASA and Yale University. ■

NOTES

[1]Nor should it have been expected to. The majority of the research that produced that literature was conducted with either learning groups (which by definition do not know the task) or therapy groups (which, very often, are having trouble with daily life). In both cases, a relevant organizational context was lacking as well as a designated task leader.

[2]In contrast, the less effective captains deviated from the pattern of the effective captains in an apparent variety of ways. The only pattern that linked them was their inappropriate mastery of control—of either the group or of themselves. One of these captains overcontrolled the group while another provided insufficient group control. The remaining two each demonstrated an inability to appropriately control their own behavior in the group setting.

REFERENCES

Cooper, G.E., White, M.D., and Lauber, J.K. (Eds.). (1979). Resource management on the flight deck (NASA CP-2120). Moffett Field, CA: NASA Ames Research Center, (NTIS N80- 22283).

Hackman, J.R. (1986). The design of work teams. In J.W. Lorsch (Ed.). Handbook of organizational behavior. Englewood Cliffs, NJ: Prentice-Hall.

Helmreich, R.L., Foushee, H.C., Benson, R., and Russini, R. (in press). Cockpit management attitudes: Exploring the attitude-performance linkage. Aviation, Space and Environmental Medicine.

Leavitt, H.J. (1975). Suppose we took groups seriously. . . In E.L. Cass & F.G. Zimmer (Eds.). Man and work in society. New York: Van Nostrand Reinhold.

GROUP AND ORGANIZATIONAL INFLUENCES ON CREW EFFECTIVENESS

J. R. Hackman
Department of Psychology, Harvard University, William James Hall, 33 Kirkland Street, Cambridge, Massachusetts 12138

Teams are a prominent device for accomplishing work in space and aeronautical settings. Virtually all air transport operations and space missions require coordinated behavior by two or more crewmembers. Yet when performance problems involving cockpit or spacecraft crews have occurred, analysis traditionally has focused on the qualifications and behavior of individual crewmembers. In recent years, however, researchers have begun to recognize the critical role that *team* dynamics play in influencing mission effectiveness in air transport and space operations. In reviewing this evidence, numerous researchers have pointed out that it is incorrect to assume that crews will be effective merely because they are composed of technically proficient individuals. Indeed, analyses of aviation accidents and incidents indicate that approximately two thirds of them result from crew coordination failures. And, on the space side of the house, the need for knowledge about crew function is sure to increase as

we move toward missions (such as the Space Station) that require large and diverse crews to live and work together for extended periods of time in a remote and unforgiving environment. Clearly, there are good practical reasons for learning more about factors that influence the performance effectiveness of air and space crews. Such crews also have a number of features that make them uniquely valuable for generating basic knowledge and theory about team behavior and performance. These features include: (1) air and space crews must operate cooperatively within an aerospace culture that has a decidedly individualistic orientation; (2) such crews are *de facto* self-managing teams, operating remote from organizational authorities, but with a tight link to those authorities; (3) such crews operate within large and complex social systems whose overall effectiveness requires close coordination among diverse, interdependent subsystems; (4) most such crews (especially in aviation) have short lifespans and may be composed of people who initially are not known to one another, yet they must perform complex, challenging tasks and manage high variance workloads (*e.g.*, long periods of routine activity punctuated by demands for intense and highly interdependent work).

In sum, the special features of air and space crews provide opportunities for research that has both scholarly value and practical application. Existing research on team behavior and performance, unfortunately, turns out to be of limited use in guiding research on aerospace teams, for several reasons: (1) insufficient attention has been given to criterion issues; (2) group interaction process (*i.e.*, the transactions among crewmembers) has received disproportionate attention as a point of intervention for improving team performance; (3) the design of teams and their organizational contexts, on the other hand, often has been overlooked in group research, and these factors appear to be critical in creating conditions for team effectiveness; and (4) the influence of leader behavior on team performance has been viewed too narrowly.

To deal with these concerns and other gaps in the group behavior literature, a new conceptual model of team effectiveness has been constructed, and will be briefly described. The model specifies that crew performance will be enhanced when (a) the team is well-designed, (b) it is appropriately supported by the organization in which it operates, and (c) leaders and managers behave in ways that help members take advantage of the positive features of the team's performance situation and overcome the less supportive aspects of that situation. The factors that appear to have the greatest leverage in creating these three conditions for aerospace crews will be described and illustrated as they apply to four critical times in the lives of cockpit crews.

1. Pre-Arrival: The "Shell." Many features that significantly influence the life of a cockpit crew are already in place before crewmembers meet prior to their first leg. This preexisting shell is the overall structure within which the crew works, and it consists of things that are accepted as "givens" by crewmembers or that they assume to be true without questioning. Among the most significant features of a shell are (a) the basic flying task and cockpit technology, (b) the roles of crewmembers and the characteristics of the people who occupy those roles, and (c) the basic norms of conduct that regulate crewmember behavior. Shaped over time by technology, policy, and collective experience, the shell frames the crew's work and shapes how that work unfolds. Yet its impact often goes unnoticed—precisely because it is so generally accepted as "the way things are" in a given organization.

2. Team Creation. When people occupy a shell, they breathe life into it and become a *team*. Previously an abstraction, the shell now becomes a real working environment. This happens very quickly, and very early in a crew's life. Indeed, the team creation process begins the instant crewmembers first see one another—when they immediately and automatically begin to size one another up. The process continues at full tilt (even if subtly) as ground preparations for the flight are completed. By the time taxi begins, members have become a full-fledged team, and a great many things have been established that will shape behavior in the crew throughout its life.

3. Task Execution. The crew now proceeds to do its work: planning, solving problems, manipulating controls, communicating endlessly (with other team members, but also with passengers, ATC, and support staff from the organization), and so on. Most that has been written about the execution of the flying task focuses on how the crew functions during high workload times: the critical moments that surround takeoff and landing, plus other times when things are so busy and demanding that the safety of flight requires focused, competent team behavior. It also is true, however, that a great deal happens during those times when nothing seems to be happening—at 35,000 feet over Kansas, or at the hotel

over dinner. Such low-workload times are occasions for people to learn from one another, and for the team to evolve and mature as a performing unit. Things are *happening* during seemingly task-irrelevant times, and those things are worth attending to because they can powerfully shape subsequent team behavior and performance.

4. Team Termination. The aircraft has been shut down and the paperwork completed. The work has been performed, whether well or poorly, and individuals are preparing to go their separate ways, whether better or worse for their experience working together. The team ceases to exist. Whether or not crewmembers take some time to reflect on their collective experiences, people have learned and been changed by their experience in the team. There is, in effect, a residue, left behind each time a crew terminates— and that residue is one means by which the cockpit shell for a given organization evolves over time. The cumulative effect of thousands of such small episodes are powerful indeed in redefining the shell that will be occupied by crews in the future.

The presentation will end with a discussion of the implications of the material for the design and management of air and space crews, and for the future directions of scholarly research on team behavior and performance. ■

EXTENDED DURATION EXPOSURES FOR MAMMALIAN DEVELOPMENTAL BIOLOGY

J. A. Alberts
STAR Enterprises, Inc and Indiana University, Bloomington, Indiana 47405

The mammalian life cycle derives from at least 3.5 billion years of evolutionary shaping. Throughout the evolution of life on Earth, gravity has been constant, and omnipresent. Many life scientists believe that gravitational forces may be integrated into the expression of developmental programs, working at cellular levels during embryonic pattern specification, and later at physiological levels of organization.

Space biology research conducted on some previous shuttle flights and on numerous Soviet Cosmos satellites indicates that successful developmental biology will be a challenging but worthwhile pursuit. The U.S. Space Station will provide the necessary capability of maintaining animals in a microgravity environment for developmentally significant durations, and it will allow "hands-on" observations and experiments.

A complete view of mammalian developmental processes will involve studies beginning at fertilization and extending through the fertilization of subsequent generations. Research projects designed to provide the necessary foundation for long-duration maintenance of healthy, comfortable, space-adapted animals are now underway. Short-duration space flights can provide valuable confirmational and preliminary data for the more complete, long-term studies of mammalian growth, maturation and maintenance in space.

Developmental biological research will also be useful in providing the resources for maintaining a vivarium of space- adapted subjects for biomedical and other forms of basic research in space. As more humans spend more time in space, on our imminent Space Station and on future, long-duration missions, it will become increasingly important to understand the implications of such exposures on these people and their progeny. ■

APPLICATIONS FOR ARTIFICIAL GRAVITY IN BIOLOGY

C. A. Fuller
Department of Animal Physiology and California Primate Research Center, University of California, Davis, California 95616

Spaceflight and ground-based experiments have clearly demonstrated the importance of Earth gravity to normal hematologic, cardiovascular, musculoskeletal, vestibular and other functions in man and animals and to normal orientation and growth responses in plants. Many systems and functions are profoundly affected by exposure to microgravity. Understanding the mechanisms of these effects and the development of rational and effective countermeasures to astronaut deconditioning in space require the investigation of these gravity-dependent systems and functions under conditions of long-term weightlessness. Such opportunities will be available with the advent of the space station and free flying bioplatforms.

The principal physical change in orbiting vehicles is the removal of the effects of Earth gravity — weightlessness. However, the spaceflight environment also has other factors that modify biological function, such as solar and cosmic radiation, forces and materials produced in the spacecraft (noise, vibration, environmental contaminants, etc.), illumination schedule, etc. These secondary factors may produce separate biological effects, or modify the effects of weightlessness. An interaction of the effects of ionizing radiation and gravitational fields has been demonstrated in rats and also in plants and

microorganisms in orbiting satellites. In short term orbital experiments these extraneous factors may not significantly affect results, however, in the protracted exposure anticipated with future space missions, their cumulative effects may seriously interface with the research and eventually, habitation. It is of critical importance that any influence of these extraneous factors upon physiological responses to spaceflight be identified so they can be separated and not be confused with the effects of weightlessness. For this, provision must be made for a suitable control as a part of any research on gravitational biology, which can only be fulfilled by a variable gravity facility in space operating at 1 G. If the only biologically significant factor in the space station environment is weightlessness, the response of onboard 1 G controls should be the same as those exhibited by equivalent ground-based controls.

In order to fully understand the nature of the interaction of biological systems and gravity, it is also necessary to make repeated observations at several field strengths between 0 and 1 G. The difference between observations made at Earth gravity and in weightlessness will establish the weight-determined biological function, that which develops under a 1 G gravitational load. However, such information will be based on only two points of observation, and as such it cannot be generalized. Observations in at least three, and preferably more gravitational fields will be necessary for the development of any generalization, such as determining the kinetics of gravitational responses. A variable gravity facility, such as an inflight centrifuge, provides the only method for such studies of these gravity-dependent phenomena between a microgravity and Earth gravity. To perform such research, such a centrifuge must be capable of continuously accommodating experimental animals, plants and eventually humans.

Multi-field capability of a centrifuge is also essential in determining threshold fields for gravitational responses. It can be demonstrated that for some biological processes an acceleration field greater than weightlessness is required to elicit a gravitational response. Understanding such thresholds is essential to the development of a coherent science of gravitational biology. Knowledge of thresholds for adaptive responses will also provide information of biomedical concern. The "permanent presence of man" in space may be jeopardized by human inability to adapt to chronic weightlessness. Artificial inertial fields (artificial gravity) in future spacecraft or stations may provide the required countermeasure for our successful habitation of space. Understanding the threshold-G for various physiological processes will be an essential contribution in establishing the appropriate fraction of Earth's gravity required for such countermeasure. ■

LIFE SCIENCES SPACE STATION RESEARCH: A STATUS REPORT

J. R. Keefe
Life Sciences Space Station Program, NASA Headquarters, Washington, D.C. 20546

This paper is intended to present a status report of the Life Sciences Space Station Program and to reiterate the scientific premises that underlie the evolution of this flight program element.

A primary feature of the International Space Station is the capability for studying extended duration exposures of statistically significant numbers of diverse species of animals and plants to the full gravity continuum from station ambient into the hypergravity ranges that overlap earth-based research capability. Observations over lengthy periods of experimental exposure, matched populations established to control individual exposure variables and the capability to manipulate the primary variable over a broad range are experimental foundations upon which earth-based Life Sciences has evolved.

Based on our current knowledge, there is compelling justification for NASA to develop a sophisticated capability for Life Sciences research early on the Space Station. Space Station facilities will be a test bed to establish the basic research foundation for qualifying man for more complex missions of longer duration. Space Station requires exposure of human crews to increased radiation and extended stress, microgravity and isolation for lengthier periods of time in markedly enlarged facilities. Cycling crew members through repeated gravity transitions during regular duty cycles presents an additional

exposure variable not encountered previously. Future manned missions to Mars and establishment of a Lunar Base will extend the exposure time to these variables and add complications of intervening periods of fractional gravity and elevated radiation on lunar or Martian surfaces. Critical questions regarding the capability of human beings to undergo successful repeated physiological adaptation to long duration spaceflight exposures remain. The Space Station is the tool to utilize in studying these effects.

To enable man to fully "Pioneer the Space Frontier", the adaptive responses to varying gravity loads must be understood. Although there are many physiological, immunological, and psychological factors which impact the human presence in space, fundamental studies on the nature of gravity perception and the innate physiological responses to this omnipresent vector that have evolved in earth-based plants and animals are required to understand the complex adaptive mechanisms displayed by man upon entering spaceflight. Those species of microorganisms and plants which will provide necessary life support during prolonged Mars missions or lunar bases will require extensive baseline study. Complete life sciences basic research facilities with full variable-gravity exposure capability for plants and animals, from peppers to primates, must be an early objective of the Life Sciences Space Station Program.

A primary feature of Life Sciences Space Station research opportunities is the potential for long-duration exposure to varying controlled gravities required to perform suitable studies of reproduction, embryonic development, maturation, and aging. Such extended periods will permit multi- generational studies of plants and animals. This is a fundamental requirement for the development of a complete understanding of the role of gravity in shaping the entire range of morphogenetic processes. Additionally, the capability for "seed-to-seed-to-seed" studies is of prime significance to the development of bioregenerative (CELSS) life support capabilities which will require completely documented reproductive capability, along with the optimizing of plant species productivity at near-record levels.

Since individual biological variability is inherent in all life forms, primary requirements for biological research must include the capability of achieving experimental exposures of statistically significant numbers of experimental subjects, the ability to replicate experimental observations, and the provision of proper control populations. The Life Sciences Space Station Program must provide the resources required to meet these validation requirements. These resources include sufficient on-orbit pressurized volume, crew time and expertise, and logistics capabilities to provide adequate numbers of suitable experimental and control species. In addition, earth-based facilities must be provided for proper experiment integration, training, and synchronous controls.

Extended-duration, multiple-window fight opportunities require the development of new approaches to science management. Identification, selection, and integration of modern experimental approaches that optimize the use of the finite resources of the Space Station while complementing other ongoing flight opportunities must be evolved. They may involve international participation and require refinement of existing methods of science management. Primary foci of this management system must be the continuing role of the principal investigator in all aspects of the implementation of the research and the provision of suitable "Quick is Beautiful" experimental implementation.

The Life Sciences Space Station Program must define and establish a combination of facilities capable of supporting a complete range of experimental life sciences. These facilities include pressurized volumes with both man-tended and manned operational capability and attached unpressurized payloads for observational (Biospherics) and collecting (Exobiology) sciences. To study suitably the principal of gravity variation requires the provision of the full gravitational range. Such can only be provided by a rotating device on an orbiting space structure, capable of subjecting a statistically significant number and variety of cells, tissues, whole plants, and nonhuman animals to controlled alterations of the g-force. Ultimately, human-rated variable-gravity facilities, whether tethered or trussed, must be evolved. The Space Station will serve as a forerunner to such advanced facilities.

This paper will present the present status of the Life Sciences Division's planning efforts, illustrate the evolving concepts of science management under study and demonstrate the integration of the Life Sciences Space Station Program into the burgeoning flight program in support of the International Life Sciences community. ■

PLANTS AND EXTENDED DURATION SPACEFLIGHT

A. D. Krikorian
Department of Biochemistry, Division of Biological Sciences, State University of New York at Stony Brook, Stony Brook, New York 11794-5215

The space environment offers unique opportunities to erase and reapply gravitational signals in probing the relationship of gravity to development. Since all development has evolved in the presence of an Earth gravity vector, it seems likely that gravity can play a role in plant development. Edmund Sinnott even queried as far back as 1960 in his book *Plant Morphogenesis* whether the plant body as we know it could develop in the absence of specific gravitational stimuli or cues. The term gravimorphogenesis is increasingly being used to designate the emerging discipline of the relationship of gravity to development. Gravimorphogenesis studies require not only extended duration exposures but microgravity (10^{-4} g or under) environments. They require a "quiet" flight module or a free orbiting component that can be isolated from "noisy" flight environments.

In a microgravity environment where there is no gravity vector, no polarity, no buoyance, no convective current, no stratification of layers and where surface tension dominates, we can anticipate major impacts on metabolism and cell biological processes that may well be reflected in the morphogenesis of cells, tissues and organs. Since morphology is tightly linked to physiology, physiological perturbations of various sorts will have significance for distribution and partitioning of solutes and assimilates in cells, tissues, organs and ultimately the whole plant body, and may even be reflected in the further expression of diverse biosynthetic potentials. Much will be learned from examination of total plant development to see if a gravitational stimulus (?strength?, ?duration of exposure?, ?timing of exposure?) is required for continuous plant development - *e.g.*, can the entire life cycle be completed repetitively under microgravity conditions - but the use of aseptically cultures systems *in vitro* will provide even greater degrees of freedom and potential to release the full range of responsiveness and plasticity of the higher plant genome in the space environment.

Possibilities for releasing, capturing, constructing and/or fixing the differential expressions or response potentials of totipotent cells - both from the perspective of their nuclear and cytoplasmic components - exist using tissue culture technologies. One intuitively feels that the unique combination of untested environments and highly flexible, unrestrained biological systems will provide the right situation to disclose new capabilities. The disclosure of new facts from both broadly conceived and narrowly focused studies will go far in helping us understand what plant development is all about as well as have practical benefits for agriculture and other biology-based technologies. ■

NASA ASTRONAUT SELECTION

T. F. McGuire
Department of Psychiatry, University of Texas Health Science Center at San Antonio, San Antonio, Texas 78284- 7792

The author has been the psychiatric consultant to NASA/JSC for over two decades, with duties including the psychiatric element of astronaut selection.

Astronaut selection, as it has evolved over the years, is reviewed. The primary thrust of the paper is upon current selection and how it is done. An approach that utilizes a rich network of cross-correlations is described, and both the "real time" and prognostic value of this data is discussed. The data focus is upon tolerance for high-level stress/threat to life (both acute and extended in time), day-to-day effectiveness both in a professional and interpersonal sense, adaptability for close quarters confinement with others on both a short-term (Shuttle) and long-term (Space Station) basis, managerial and communication considerations, most prominent psychological needs, and most likely set-up to fail, including likely warning signs. The main body of this information is extractable on the basis of a highly structured two hour interview. Data extraction places greater emphasis upon process rather than content, though both are utilized. The implications of this kind of data in terms of crew selection and crew matching for space station are discussed. The advisability and methodology of teaching psychological self- defense to astronauts in the pre-station interval is also touched upon. Reflections about the personality construction of the prototypical astronaut are included. ■

ANALOGIES BETWEEN ANTARCTIC EXPEDITIONS AND SPACEFLIGHTS

C. M. Pierce
Graduate School of Education and Faculty of Public Health, Harvard University, Cambridge, Massachusetts 02138

For many years it has been theorized that experiences in Antarctica and in space travel might inform one another. At this time many more people have traveled to Antarctica than into space. Therefore, this presentation will review some findings relating to adaptation and adjustment in Antarctica. There will be emphasis on the concerns and management approaches during phases of pre- debarkation, expedition and reentry. Specific problems and how they were negotiated in Antarctica will be suggested for consideration by planners of long-duration spaceflight.

Both space and Antarctic literature indicate the importance of thermoregulation, group dynamics and immuno competence. The possible interrelationship in terms of individual performance will be discussed in terms of the need for focused research which would be of service in either environment. ■

HEALTH CONSIDERATIONS IN PLANNING LONG-DURATION SPACE MISSIONS

P. A. Santy
NASA/Johnson Space Center, Houston, Texas 77058

It is clear from the numerous studies of groups in isolated environments that planners will have to take into account the psychological sequelae of living for extended periods of time in space.

This paper reviews what we know about these psychological sequelae in other isolated environments analogous to the space environment (such as Antarctica, submarines, or artificially isolated groups), and then extrapolates these findings to the space environment. These data suggest that many potential psychological, psychosocial and psychophysiological problems which might interfere with accomplishment of mission goals, can be prevented by careful pre-mission planning and training. The paper will also discuss the identification and management of psychological problems in the hazardous space environment. ■

PHYSIOLOGICAL AND GENETIC STUDIES ON WHEAT FOR THE CONTROLLED ENVIRONMENTS OF SPACE

B. Bugbee and F. B. Salisbury
Plant Science Dept., Utah State University, Logan, Utah 84322-4820

Our studies on the physiological limits of plant productivity lead us to believe that the photosynthetic efficiency of a community of wheat plants can approach its theoretical potential (17% efficiency) when all environmental parameters are controlled at optimum levels. We have achieved high photosynthetic efficiencies by using appropriate combinations of environmental parameters, unusual cultural techniques, and genetic selection. This abstract summarizes our most significant findings in three categories: foliar environment, root-zone environment, and genetic alterations.

FOLIAR ENVIRONMENT

Shortening of the life cycle of wheat does not necessarily increase yield per unit time. Our initial studies used continuous light (24-hour photo period) and warm temperatures (27°C) to reduce the life cycle from 120 days (in the field) to 60 days. Recent studies have indicated that cooler temperatures (20°C light/15°C dark) and less than continuous light (20-h photoperiod) increase the life cycle by 32% (79 days), but increase yield by over 100% (from 1400 to 3000 g m^{-2}) at the same photosynthetic photon flux (PPF; 1000 μmol m^{-2} s^{-1}). The result has been an increase in yield per day of about 50%, due to better reproductive development (larger head size and increased seed set). We are now determining how a short (1 to 4 hours), daily, dark period affects growth and development, compared to continuous PPF.

Perhaps our most significant finding is that growth and yield of wheat appear to be limited by PPF even when integrated; daily PPF is well beyond terrestrial levels. Figure 1 shows the average growth rate

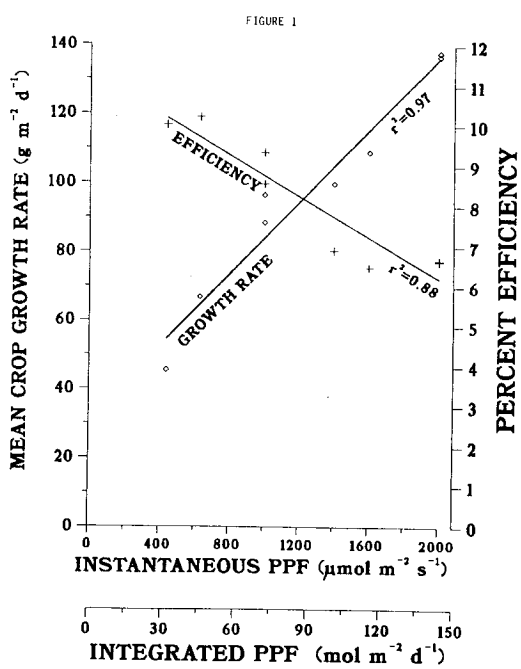

Figure 1.

TABLE 1. CULTIVAR EVALUATION IN AN OPTIMAL GREENHOUSE ENVIRONMENT

Cultivar	Height (cm)	Yield		Harvest
	$g\ m^{-2}\ d^{-1}$	$g\ m^{-2}\ s^{-1}$	Index %	
Veery 10	50	14.7	16.4	54
BB-8	52	10.1	11.0	42
Yecora Rojo	65	11.4	10.9	47
Olesen's Dwarf	35	8.0	10.6	44
BB-11	55	10.1	10.6	49
PCYT-20	75	11.7	10.2	45
Anza	108	14.7	9.9	43
Fremont	98	10.9	7.9	43
Duncan's L.S.D.	3	1.7	1.7	1.8

Yield per m^3 is calculated as yield per m^2 divided by the height plus 40 cm for the lighting system and the root-zone environment. A 60-cm-tall cultivar would thus have identical yields per m^2 and per m^3. In this particular study the volume measurement also compensates for the fact that taller cultivars grew into a higher PPF environment and would thus have a higher yield.

and photosynthetic efficiency from a trial in which PPF levels were as high as continuous midday summer sunlight (2000μmol m^{-2} s^{-1}) for 20 hours a day. The integrated daily PPF was thus 144 mol m^{-2} d^{-1}, more than twice that of any natural environment on earth. Yields in this study increased substantially over our previous best yields. In the highest PPF treatment, the average yield of dry, edible grain exceeded 60 g m^{-2} d^{-1} (707 bushel/acre in 79 days). Yield was a linear function of input PPF (r^2 = 0.97).

We are now studying different environmental conditions at each phase of the wheat life cycle, which we call phasic environmental control. The wheat life cycle can be separated into 5 stages: germination, reproductive initiation, stem elongation, anthesis, and grain fill. We hypothesize that a unique combination of environmental parameters at each life cycle stage will be necessary to optimize yield per unit time.

These studies involve many possible hypotheses. The testing of the hypotheses has been enhanced by sealing a growth chamber and using it to measure canopy gas-exchange (short- term, carbon and water-vapor fluxes). Results from these studies will be discussed.

ROOT-ZONE ENVIRONMENT

We have studied closure of recirculating, hydroponic root-zone environments for three reasons: (1.) they have direct application to the goals of a CELSS; (2.) we feel they can be effectively managed without extensive monitoring and control apparatus; and (3.) refilling all of our hydroponic systems every few days would be very expensive, even on our relatively small research scale.

Rapid flow rates (0.4 liters of m^{-2} of surface area s^{-1}) in our recirculating systems replenish and supply oxygen to the root surfaces and provide good uniformity in the root-zone environment. Inert construction materials have minimized the potentially toxic buildup of trace contaminants. We have not found it necessary to filter our solutions. Initial concerns about a buildup of organic compounds and microorganisms in solutions were unwarranted, total organic carbon has been less than 30 mg kg^{-1}, and almost half of this is contained in the iron chelating agent. Apparently there is a balance between root excretion of organic carbon into solution and microbial oxidation of these compounds to carbon

dioxide. Analysis of total organic carbon includes the carbon in microbial organisms. Altering the microbial composition in solutions might enhance growth, but we want to establish a solid baseline before altering microorganisms.

Control of the ionic composition of our solutions is based on mass balance. The ratio of nutrients in plant tissue resulting in good growth is the ratio of nutrients that we use in solution. This ratio of ions is kept constant, while the total ionic concentration of the solution is altered to match the ratio of transpiration to photosynthesis (g H_2O / g CH_2O). This ratio is about 400:1 with ambient CO_2 and 200:1 with high CO_2. Plant nutrient composition resulting from the use of this technique will be presented.

GENETIC SELECTION

Wheat is grown in thousands of different locations around the world, and an equal number of cultivars have been developed to match genetics with environment. Our first step in developing new cultivars for the space environment was the identification of desirable characteristics and the selection of wheat types with these characteristics. After several early studies, we selected Yecora Rojo for wider use; further tests, however, indicate that Veery 10, a newly discovered line from CIMMYT in Mexico, is superior to Yecora Rojo. The data in Table 1 show results from a replicated greenhouse trial. We have found that the yield of cultivars in controlled environments cannot be predicted from their yield in the field.

The cultivars BB-8 and BB-11 are our own breeding lines, which are the result of a cross between Olesen's Dwarf (from South Africa) and Fremont (a high yielding Utah cultivar). We have now made crosses among all the cultivars listed in Table 1 and are selecting desirable plants from their segregating progeny. All selection is being done in an optimal greenhouse environment. Our immediate goal is to develop an ultradwarf cultivar (30 to 40 cm tall) with a yield and harvest index better than Veery 10. ■

OPTIMIZING NUTRIENT, PHYTOHORMONE AND GAS CONCENTRATIONS FOR MASS PROPAGATION OF WHEAT THROUGH SOMATIC EMBRYOGENESIS

J. G. Carman, W. F. Campbell, N. E. Jefferson, S. K. Whitesides, B. Bugbee, and Z. N. Hashim
Plant Science Department, Utah State University, Logan, Utah 84332-4820

Research indicates that 12 m^2 $person^{-1}$ of surface area is required for wheat production in a closed, extraterrestrial environment. A high-yielding wheat to meet this small surface area requirement should be obtainable by plant breeding and by provision of optimal growing conditions. High planting densities of up to 4000 seeds m^{-2} will be required. This translates into about 220,000 seeds $person^{-1}$ $year^{-1}$, or about five percent of each grain harvest needed to seed the next crop. Artificial seed production using plant tissue culture is being investigated to circumvent the five percent yield loss and further reduce surface area requirements by permitting the use of hybrid wheat, which should raise grain yields by an additional 10 to 15 percent. Production of hybrid wheat seed by conventional procedures would be impractical in a permanently manned extraterrestrial station due to the added space and energy requirements to maintain parental nurseries.

Artificial wheat seed can be produced *in vitro* through somatic embryogenesis, where somatic cells are induced to respond as if they were fertilized zygotes. Normal plants can be produced when the resulting embryoids (asexual embryos) are provided with a proper balance of nutrients and phytohormones. In only a few crops, excluding wheat, is current technology adequate for large-scale artificial seed production. The major obstacles with regard to wheat include few embryoids produced per tissue culture, fusion of embryoids early in development into embryoidal clumps, precocious germination or other abnormal form of growth, poor germination percentages, and poor seedling vigor. Results of research that address these problems will be reported.

We have found several factors that affect numbers of embryoids produced per tissue culture. They include genotype (cultivar), types and concentrations of phytohormones, nutrient concentrations, and

Table 1. Media compared for induction of somatic embryogenesis

Medium[c]	MS[a] inorganics	MS[b] organics	Thiamine & asparagine	Sucrose	Coconut Water
				%	
A	2X	X		2	
B	X		X	2	
C	X	X		3	10

[a]Murashige T, Skoog F (1962). Physiol Plant 15:473
[b]MS growth regulators replaced with 1.0 mg/1 2,4-D.
[c]Medium A after Osias-Akins P, Vasil IK (1983) Protoplasma 117:40; Medium B after Sears R, Deckard EL (1982) Crop Sci 22:546; Medium C after Maddock SE, Lancaster VA, Risiott R, Franklin J (1983) J Exp Bot 34:915.

Table 2. Embryoids produced per explant at 28 and 56 days in culture, averaged over 10 genotypes

Medium	28 days		56 days	
	Mean	Genotype range	Mean	Genotype Range
A	19	3-61	15	3-93
B	8	2-27	6	1-32
C	7	2-26	2	0-22

Table 3. Nuclear DNA content at telophase of calli induced from immature wheat embryos at 2, 4, 6 and 8 weeks after culture initiation

Medium	Weeks after culture initiation			
	2	4	6	8
	pg			
A	11.1	9.9	10.5	12.2
B	32.3	37.6	17.1	13.8
C	15.6	24.7	16.7	13.2

[a]Mean telophase nuclear DNA content of wheat roots was 10.9 pg.

the O_2 and CO_2 concentrations that the tissue cultures are exposed to. Components of three media tested for their effects on embryoid formation are listed in Table 1. Significantly more embryoids formed per culture on medium A. Significant differences in numbers of embryoids produced were also detected among 10 different cultivars (Table 2). The significant improvements observed with medium A appear to be due to maintenance of genetic stability (Table 3). The observed "return" to the normal somatic DNA content (10.9 pg) in cultures incubated on media B and C by eight weeks (Table 3) was probably caused by the sampling of tissues that were undergoing organogenesis at these latter sampling dates, rather than sampling the less abundant highly aneuploid callus tissues.

Embryoid formation was significantly increased, from 20 to 39 embryoids per culture, by substituting in medium A (Table 1) 9.0 uM dicamba (3,6-dichloro-o-anisic acid) for 4.65 uM 2,4-D (2,4-

dichlorophenoxyacetic acid), which is generally used for wheat tissue culture, and by the addition of 4.65 uM kinetin (6-furfurylaminopurine). We have also significantly increased embryoid production by eliminating CO_2 from the environment in which callus cultures are growing and by reducing O_2 concentrations in this environment from 8.9 mol m^{-3} (approximately 21 percent) to 3.7 mol m^{-3} (approximately nine percent). High levels of respiratory CO_2, which normally accumulate in closed culture vessels, were shown to be deleterious to initiation of somatic embryogenesis and to the maturation and germination of embryoids. Likewise, ambient levels of O_2 induced rapid cell division that led to precocious germination of both cultured explants (immature sexual embryos) and young embryoids. Cytokinins (kinetin and coconut water) also significantly increased embryo and embryoid precocious germination, a negative phenomenon in producing vigorous plants.

Precocious germination of sexual embryo explants and somatic embryoids was delayed or stopped by reductions in culture vessel O_2 concentration. However, artificially reducing levels of O_2 in the callus culture environment did not cause normal maturation of embryoids. Embryoids in these experiments generally followed a normal pattern of development for about five to six days and occasionally up to nine days (based on morphology of sexual counterparts) whereupon normal maturation and development was interrupted by precocious germination (that occurred primarily under ambient O_2 conditions), callus formation, or other abnormal growth. We have found that additions of ABA (abscisic acid) at 0.38 or 1.89 uM not only reduce precocious germination of embryos and embryoids, but also extend the duration of normal embryoid development, regardless of O_2 concentration.

It is unlikely that complete normalcy in embryoid induction, maturation, dormancy and germination can be achieved by varying ABA levels alone. The effects of other hormonal, nutritional and environmental factors also need to be evaluated. We envision the development of a cell suspension culture system that will permit individual cells or small cell clumps to undergo embryogenesis in response to adjustments in medium composition. Such adjustments will mimic *in vivo* conditions. Currently we can produce about 150 embryoids per suspension culture in 30 days. It should be possible to repeat this process, with each of the 150 embryoids, such that numbers adequate for mass propagation in a CELSS could be generated. ■

CELSS BIOMASS PRODUCTION - THE PLANT SYSTEMS

J. C. Sager
Biomedical Operations and Research Office, John F. Kennedy Space Center, Florida

---

The concept of CELSS, a controlled ecological life support system of biologically and physically interactive components, includes as key components the production of food and oxygen for the human component, the crew. It has been shown that most of the critical nutritional components for human existence can be produced from plant products and the carbon-oxygen cycle is closed by plants. Productivity, specifically yield, of a plant growth system can be measured in several ways. For CELSS, yield can be quantified as edible biomass, and a measure of the ratio of edible biomass to total biomass is termed harvest index. Either yield or harvest index can then be optimized for a specific plant growth system. Plant growth systems have been commercially developed to optimize total yield and harvest index. However, these commercial systems are not directly transferable into a CELSS, because these systems have been designed to meet different criteria than those needed for a CELSS. For example, commercial systems are economically driven, have limited recycling capacity, and are not concerned with weight factors.

Plant growth and development can be divided into two categories: photosynthesis, the energy fixing process, and morphogenesis, the developmental control process. These processes in any plant growth system, as in any production system, are dependent on mass and energy inputs. They are controlled through variables in the environment or by biological regulation pathways internal to the plant. This concept was defined by Blackman in 1906 as the concept of "limiting variables." Any one of these

variables can limit the system if it lies on the critical path of the photosynthetic or morphogenic processes. The plant environment can be divided into the serial and root portions. Aerial variables include temperature; air composition - humidity, CO_2, nitrogen, oxygen, and other gases (contaminants); and irradiance and spectral quality. Root variables include temperature, water availability, nutrients, and the support media. Plants, unlike the human component, are sessile and therefore are often more susceptible to changes in their environment. Since they lack this ability to move, plants are often excellent transducers for quantitatively measuring changes in the environment. Their limitation lies in the relative slowness of their response, which requires a secondary transducer or monitor to interface with the "real time" physical subsystem in which they are growing.

The inductive morphogenic plant responses require an initiation signal from the environment which in turn, is transferred to a regulatory variable. These developmental responses include flowering leading to seed production, and tuberization of storage root formation. Some of the best known developmental responses are photomorphogenic and are dependent on irradiance, spectral quality, and/or photoperiod. Additional methods of control include stresses induced thermally, by water or nutrient deficiency, and by regulatory chemicals

Plants currently chosen for use in the CELSS project present species specific control requirements to reach the program goals of food and oxygen production with minimum energy and space requirements. These candidate plants are all dependent on high photosynthetic rates to provide the productivity levels necessary for the CELSS program. The energy delivery systems, radiation sources, and luminaries affect whether radiation is a limiting variable. The photoreceptors in the plants must be massed to provide high density or the sources must be concentrated on a receptor unit, a plant. Carbon dioxide, usually a limiting variable, may be a contaminant at the levels seen in today's spacecraft. Water exchange can be balanced, but timely delivery in a mode compatible between the plant and the contaminant requirements are species specific. Individual nutrients, on the other hand, may not be limiting, but must be controlled within a tolerance window for each plant species. The Biomass Production Chamber (BPC) and research program at the Kennedy Space Center was designed and is being used to determine these variable limits. The radiation sources, high pressure sodium lamps, are efficient in converting electrical energy to photosynthetically active radiation. The atmospheric control system provides a predetermined level of CO_2 and O_2 within a specified pressure range. The nutrient delivery system provides a continuous flow of a controlled water-based nutrient solution to the plant in a low volume root container. As the variable limits are further defined, the systems of the BPC will be refined to exploit these processes in plant growth technology.

The morphogenic responses necessary for food production are induced by a wide variety of environmental variables. Maximizing these responses is required to meet the energy and mass constraints. The candidate CELSS plants provide some examples: wheat can be induced to tiller or produce mono-culm to maximize yield and minimize area; potato can be induced to tuberize, or sweet potato to initiate a storage root to maximize productivity and reduce time to harvest; soybean can be induced to flower early and partition more photosynthate to edible biomass to maximize yield and minimize energy; and vegetative crops, such as lettuce, can be driven vegetatively without reproductive induction to maximize yield and reduce the time to harvest. The BPC and research program at Kennedy Space Center has integrated the photoperiod and thermoperiod controls currently used in inducing many morphogenic responses.

Development of plant systems for CELSS must meet several requirements. The plant growth systems must be designed to optimize the physical variables for maximal productivity within physical constraints imposed by the environment of space. The other requirement is to define and quantify these limiting variables to efficiently induce those developmental responses in the candidate plants. The latter requirement is not a trivial task. ■

UTILIZATION OF POTATOES IN CONTROLLED ECOLOGICAL LIFE SUPPORT SYSTEMS

T. W. Tibbitts and R. M. Wheeler
Department of Horticulture, University of Wisconsin, 1575 Linden Drive, Madison, Wisconsin 53706

The white potato (*Solanum tuberosum L.*) is being investigated for use in Controlled Ecological Life Support Systems (CELSS) because of its high productivity of both carbohydrate and protein, and low quantity of inedible plant biomass. Studies have been underway at Wisconsin for four years to determine the requirements for production of this species in controlled environments. These efforts have been directed toward selecting useful genetic lines, establishing the desirable ranges of environmental conditions for high productivity, and developing procedures for culture of the plants in controlled environments.

GENETIC LINES

The evaluation of diverse genetic material has led us to concentrate our efforts on two particular culivars, Norland and Denali. These cultivars have been selected because they have a high production of uniform, nearly round tubers under both 12-hr light periods and continuous light. The cv. Norland is a red-skinned cultivar with rapid maturity. The cv. Denali is a white-skinned cultivar that has a longer growing period and under continuous light has the best productivity. It was developed in Alaska under long light periods. A third cultivar, Russet Burbank has been studied intensively but tends to have a higher proportion of stems and develops a high number of irregularly shaped tubers.

ENVIRONMENTAL CONDITIONS

The major controlling factor for tuber production has been found to be temperature, with maximum production at cool temperatures, between 16 and 20°C. This research has been detailed in previous years' reports.

A level of 800 μmols s^{-1} m^{-2} of photosynthetic photon flux (PPF) has provided 45% greater tuber production than with 400μmol s^{-1} m^{-2} for the Denali cv., whereas this higher PPF level provided the same production as with the lower PPF for Norland and Russet Burbank, cvs.

Increasing the duration of light from 12 to 24 hr has also been shown to increase production when the level (400 μmol s^{-1} m^{-2}) is maintained for the entire light period. This also was reported previously.

Comparisons of different lamps have shown that high pressure sodium lamps and cool white fluorescent lamps (at the same PPF levels) provide similar growth of potatoes.

Studies with carbon dioxide supplementation of plants being grown under 400 μmol s^{-1} m^{-2} have documented some gains in tuber and total plant dry weight but not large gains (Table 1).

Table 1. Effect of carbon dioxide supplementation on tuber and total plant weight

Cultivar	Carbon Dioxide Level $\mu l\ l^{-1}$)*	Tuber Weight	Total Weight
		(g dry weight/plant)	
Norland	350	387	562
	1000	416	639
R. Burbank	350	228	546
	1000	265	612

*Continuous irradiance, 400 μmol s^{-1} m^{-2}, 16°C, 70% RH, harvested at 15 wks (NL) and 18 wks (RB).

Table 2. Effect of container size and shape on tuber and total plant weight

Containers*				
Volume (l)	Diameter (cm)	Height (cm)	Tuber weight (g/plant)	Total weight (g/plant)
17.8	29	27	94	198
11.2	29	17	86	171
5.3	29	8	80	152
5.6	18	20	79	159

*Continuous irradiance, 400 μmol s^{-1} m^{-2}, 16°C, 70% RH, harvested at 8 wks.

Fluorescent lamps have been added along the side between each row of plants to increase irradiation of lower leaves within the canopy. This has not produced any significant improvement in tuber yield but has reduced the height and spread of the plants.

Elevated levels of atmospheric humidity have increased tuber production significantly. A level of 85% relative humidity compared to 50% RH increased tuber production at an 8-week harvest date between 30-50% for three different cultivars. There were no apparent differences in leaf and plant morphology at the two humidity levels.

A plant growth model has been developed from a response surface design with three levels of irradiance, carbon dioxide, and temperature. This has provided the following response surface equations for the Norland cv. potato.

$$\text{Relative tuber weight} = 1 + .07 \times L - .13 \times L^2 + 0.6 \times C - .21 \times T - .27 \times T^2 - .10L \times C$$

$$\text{Relative total weight} = 1 + .04 \times T - .24 \times T^2$$

$$\text{Relative stem length} = 1 - .33 \times L - .33 \times L^2 - .12 \times C + .32 \times T + .11 \times L \times C$$

The values obtained are relative to the plant response at 20°C (T), 400μmol s^{-1} m^{-2} (L) for 24 hrs and at 1000 μl l^{-1} carbon dioxide (C). The unit values of each environmental factor have been coded from -1 to +1 with the unit values of -1 to +1 for T = 16-24°C, for L = 250 to 550 μmol s^{-1} m^{-2} and for C = 400 to 1600 μl l^{-1}.

The plant growth model obtained for R. Burbank cv. differed significantly, indicating that separate model equations will have to be developed for each cultivar.

Analysis of glycoalkaloids in tubers grown under the different environments have documented no toxic levels present (levels between 0.30 and 0.70 mg/g dry weight of total glycoalkaloids). However, this analysis has indicated that levels of glycoalkaloids increase as the plant is stressed with high temperatures, high irradiance, and high carbon dioxide levels.

CULTURAL PROCEDURES

Experimental studies most commonly have been undertaken in 19- and 38-liter containers using peat-vermiculite that is watered to excess four times each day with nutrient solution. However, effort has been directed toward growing plants in solution culture to permit recycling of nutrient and provide access to tubers as they develop. Successful tuber production has been obtained by placing 2 cm of calcined clay particles (arcillite) in the bottom of high-density polyethylene trays 90 cm long × 60 cm wide and 20 cm deep. The tray is slanted so that nutrient solution (at 300 ml min^{-1}) can be added along one end of the tray and drained out for recirculation through holes on the opposite end of the tray. The clay particle medium is covered with a black and then a white layer of polyethylene film. Potato plantlets are planted in slits in the plastic with approximately 5 cm of stem maintained horizontally in the medium. Tubers form under the plastic layers but extend above the medium so that they can be easily harvested.

Study has been made of the significance of plant spacing and container size on tuber production. The spacing studies indicate that highest production is obtained with closer spacing: spacing comparisons were made at 0.62, 0.31 and 0.15 m^2 per plant, and tuber production was 1.26, 1.42 and 1.79 kg/m^2 respectively at these spacings.

The container size studies indicated that both total growth and tuber production increased with increasing volume (Table 2). This study also indicated that surface area had little effect on plant growth if volume was held constant. The optimum spacing and container volume is dependent upon plant size and thus will vary with the length of the growing period and with environmental conditions, that affect plant size.

WHOLE PLANT REGULATION OF NITROGEN UPTAKE

L. Tolley-Henry and C. D. Raper, Jr.
Soil Science Department, Norht Carolina State University, Raleigh, North Carolina 27695

The stability of plant-growth systems in providing food and regenerating oxygen within CELSS is a function of plant response to limits and pertubations within aerial and root-zone environments. The efficiency of plant productivity is affected by irradiance, temperature, and carbon dioxide concentration in the aerial environment. It also is affected by the temperature, acidity, and nitrogen composition of the nutrient solution. However, the present knowledge of whole-plant regulation of nitrogen absorption and utilization from nitrate, ammonium, or mixed nitrate and ammonium sources during the growth cycle is inadequate to formulate decisions on the most effective nitrogen supply for efficiency of plant productivity. Experiments are being conducted with soybean to characterize changes in partitioning of dry matter and nitrogen among leaves, stems, roots, and reproductive growth and changes in rates of photosynthesis and expansion of leaves in response to nitrogen composition, acidity, and temperature of the nutrient solution and to changes in the aerial environment. ■

PAGE 255 INTENTIONALLY BLANK

PRECEDING PAGE BLANK NOT FILMED

ALGAL CULTURE STUDIES FOR A CELSS

P. Behrens, R. Radmer and K. Arnett
Martek Corporation, 9115 Guilford Road, Columbia, Maryland 21046

Microalgae are well-suited as a component of a Closed Environmental Life Support System (CELSS), since they can couple the closely related functions of food production and atmosphere regeneration. The objective of these studies was to provide a basis for predicting the response of CELSS algal cultures, and thus the food supply and air regeneration system, to changes in culture parameters (cell concentration, light intensity and temperature).

In an earlier communication (Biotechnology and Bioengineering, in press) we described experiments in which growth of the green alga *Scenedesmus obliquus* was measured as a function of light intensity, and the spectral dependence of light absorption by the algae and algal respiration in the light were determined as a function of cell concentration. These results were used to test and confirm a mathematical model that describes the productivity of an algal culture in terms of the competing

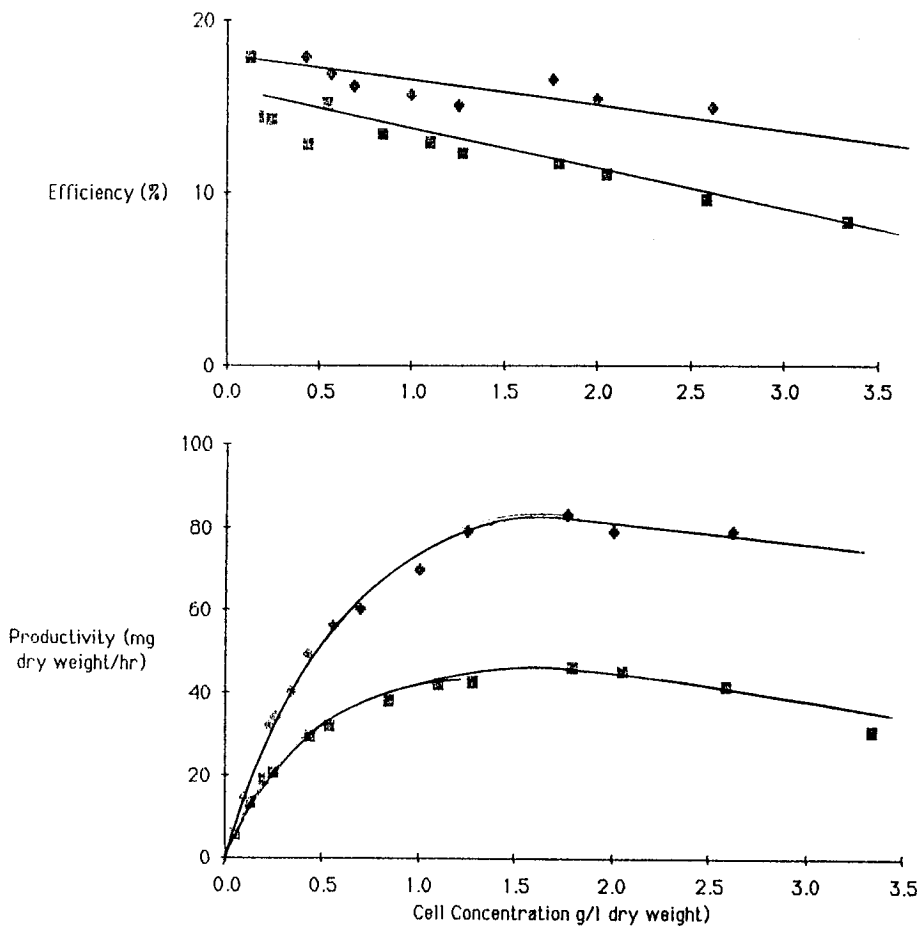

Fig. 1. Productivity and light efficiency as a function of cell concentration for a culture grown at either 12.9W/m^2 (squares) or 21 W/m^2 (diamonds).

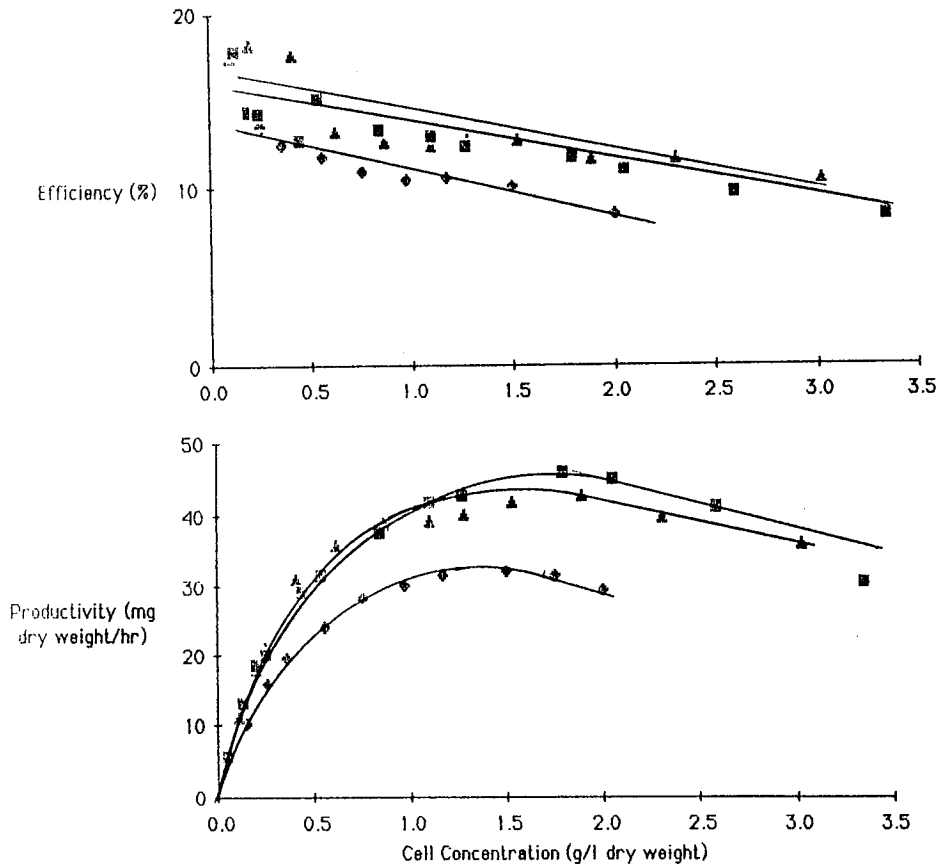

Fig 2. Productivity and light efficiency as a function of cell concentration for a culture grown at either 32°C (squares), 25°C (triangles), or 20°C (diamonds).

processes of photosynthesis and respiration. According to this model, the productivity of an algal culture is given by the relation $Y = EmI_0AK(1-e^{-\alpha cl})$ -GRcV, where Y = yield (g cells/hr), Em = the maximum attainable photosynthetic conversion on an energy basis (%), A = illuminated area (m^2), K = the energy equivalent of the algae (g cells/hr watt), I_0 = light intensity (watts/m^2), α = extinction coefficient (l/cm/g), c = cell concentration (g/l), l = light path length (cm), R= respiration rate (g carbon/g cells hr), V = culture volume (l), and G = cell/carbon mass ratio (g cells/g carbon.

In the present communication we describe experiments in which the relationship of algal productivity to cell concentration was determined at different light intensities and temperatures. The purpose of these experiments was to extend the applicability of the aforementioned model to other culture conditions of interest.

The approach for the first set of these experiments was to establish a continuous culture of *Scenedesmus* at a light intensity approximately 60% higher than that used in the "reference experiments" described earlier, an intensity that was still on the linear portion of the growth vs. photon flux curve. The cell concentration of the culture at this higher light intensity was varied, and the resulting biomass productivity and light efficiency determined.

The upper trace of Figure 1 (lower panel) shows the results of a continuous culture experiment conducted at a light intensity of approximately 21 W/m^2 and a temperature of 32°C. Note that the productivity at every cell concentration is greater than the productivity of a comparable culture maintained at a lower light intensity (c.f. lower trace), and that the cell concentration of maximum productivity is higher at the higher intensity (2.1 g/l compared to 1.7 g/l). The line through the points in Figure 1, calculated using the model described earlier, suggests that the model accurately describes these experimental data at both intensities.

The upper panel of Figure 1 shows the response of the light utilization efficiency to changes in cell concentration at the two different light intensities. Note that the efficiency of light utilization at the higher intensity is consistently equal to or higher than the comparable value obtained at the lower intensity. Also, as expected, the cell concentration of light compensation extrapolates to a higher value at the higher light intensity (13.8 g/l compared to 8.5 g/l). These results, like those shown in the lower panel, reflect instances in which biomass productivity and light utilization efficiency increase as the ratio of *usable* input energy to maintenance energy (*i.e.*, respiration) is increased.

The objective of the second series of experiments was to compare the response of culture productivity to changes in cell concentration at different temperatures in an attempt to ascertain the effect of temperature on biomass productivity light utilization efficiency. The results of these experiments are shown in Figure 2. At 25°C, the productivity curve at 2% CO_2 is very similar to that of the 32°C culture, suggesting that over the temperature range of 25 to 32°C the productivity of a continuous culture is relatively independent of temperature. However, as shown by the bottom trace, the productivity is lower at 20°C than for either the 25 or 32°C culture, indicating that 20°C is a less-than-optimum temperature for a *Scenedesmus* continuous culture. The solid line in Figure 2 was computed using the model described earlier. As in the earlier cases, the productivity vs. cell concentration profile computed with the aid of this model accurately describes the experimental data.

The upper panel of Figure 2 shows the efficiencies of light utilization for the cultures at the three temperatures. In the cases of the two higher temperatures, the efficiencies extrapolate to approximately 16-18% at very low cell concentrations, and the declines in efficiency with increasing cell concentration are similar. The 20°C culture, on the other hand shows a different efficiency vs. cell concentration profile, which is in keeping with the observed differences in productivity (c.f. Fig. 1).

In summary, the data and the accompanying computations presented herein indicate that the model proposed earlier to describe algal productivity in light limited systems can be directly applied to other related cases that fall within its proscribed limits. In the particular cases described in this communication, changes in algal productivity resulting from changes in temperature and light intensity could be accurately rationalized and predicted. ■

STRATEGIES FOR THE MANIPULATION OF FOOD QUALITY IN THE BLUE-GREEN ALGAE: APPLICATION TO CELSS

L. Packer, I. V. Fry, and J. Hrabeta
Membrane Bioenergetics Group, Bldg. 20 RM 2544 LSB, University of California, Lawrence Berkeley Laboratory, Berkeley, California 94720

The NASA-CELSS program is currently directed toward the use of biological components for the regeneration of consumables during prolonged spaceflight. Although such systems are under investigation for air revitalization and waste processing, it is in the area of food production and nitrogen recycling where biological systems show distinct advantages over physical/chemical methods. Photosynthetic organisms are of prime consideration due to their ability to grow with minimal nutrients and light, while consuming CO_2 and producing O_2. Classical crop plants (potato, wheat) are under consideration, and although sufficient in carbohydrate, they are lacking in required levels of protein and lipid. Algae in general, and Blue-Green Algae in particular, are versatile organisms which are capable of adjusting their cellular levels of carbohydrate, protein and lipid to survive changes in environmental conditions.

Our experiments with Blue-Green Algae have demonstrated that under "stress" conditions (*i.e.*, salinity, cold shock) there is an imbalance between nitrogen metabolism and carbohydrate/lipid synthesis, resulting in a decline in (excess) protein, and a marked increase in (required) carbohydrate and lipid. Under these "stress" conditions the relative ratios of carbohydrate and lipid are close to those

required in the human diet. It is our intention to use these "stress" regimes on several species of Blue-Green Algae to investigate the feasibility of employing a single, dietary compatible organism as a subsystem in CELSS. The productivity and chemical nature of the various food classes will be determined by the analysis procedures well established in our laboratory. In addition, the pathway of nitrogen, from N_2, NO_3^- or NH_4^+ to protein (useful), cell wall material and nucleic acid (recycled) under the "stress" conditions will be assessed to determine possible loss of biologically useful nitrogen projected in the waste recycling subsystems. Rates of N_2 reduction will be assessed to determine the feasibility of using nitrogen-fixing strains to counter this projected loss of biologically useful nitrogen. ■

INTERACTION OF HYDROUS MINERALS WITH BIOORGANIC PRECURSOR MOLECULES

G. Arrhenius
Scripps Institution of Oceanography, A-020, University of California San Diego, La Jolla, California 92093

Beginning with the work by Miller (1954) a number of processes have been indicated and experimentally or observationally tested, leading to the formation of organic molecules in interstellar space and under plausible early-Earth conditions (Arrhenius, 1987). Hydrophobic organic compounds, generated by such processes, would in an aqueous environment tend to accumulate as surface films, where they, on Earth, would be vulnerable to the solar UV flux, unimpeded by the ozone layer now present. Hydrophilic compounds on the other hand would suffer from dilution in comparatively large volumes of water, lowering the probability for selective reactions, which could lead to biomonomers and ordered biopolymers. Attempts to model early molecular evolution therefore need to show and experimentally prove mechanisms that cause selective concentration and reaction of bio-organic precursor compounds in aqueous solution.

Work in our laboratories addresses this problem by investigating to what extent minerals forming and dissolving in aqueous environments, including the Earth's ocean in an anoxic state, could provide effective means for selective concentration and oligomerization of organic reactants. Earlier speculation and experimental work in this field has, since the proposal of Bernal (1951), been focused on aluminosilicates, primarily clay minerals (for recent results see *e.g.* Ferris *et al.,* 1986). For reasons related to reactivity, solubility and dimensional structural properties our studies employ as potential templates common hydrous transition element minerals such as iron oxide hydroxides, manganates and iron manganese hydroxyphosphates and carbonates (Arrhenius and Tsai, 1981; Holm *et al.,* 1983; Arrhenius, 1984, 1986, 1987). In the current work phase we are pursuing two lines of investigation. One concerns the generation of organic compounds such as formate ion and formaldehyde at UV irradiation of iron (II) carbonate in solution (Åkermark *et al.,* 1980) or as a solid, the mineral siderite, common in marine anoxic environments including Archaean sediments (Joe *et al.,* 1986).

The other group of minerals of immediate interest comprises the mixed valence metal hydroxide hydrate anion sheet structures represented by minerals such as green rust, $[FE^{2+}_{3-x-2y}FE^{3+}_{x+2y}(OH)_6][xA^{-}yA^{2-}] \cdot 4H_2O$ where A^{-} is an exchangeable monovalent interlayer anion such as Cl^{-}, and A^{2-} a corresponding divalent anion such as CO_3^{-2}, HPO_4^{-2}, SO_4^{-2}, etc. Current experiments aim at controlled synthesis and structural characterization of this type of minerals, and determination of the intercalation isotherms for anionic compounds of probiotic interest such as formate and cyanide ion, sugar phosphates and nucleotides. At the present time the green rust-carbonate intercalation structure has been investigated, and the reaction with cyanide ion has been established. Attempts are being made to intercalate HCN and to achieve interlayer oligomerization of this molecule as a possible step toward purine-pyrimidine and nucleoside formation. ■

REFERENCES

Åkermark, B., Eklund-Westlin, U., Baeckström, P. and Löf, R., Photochemical, metal promoted reduction of carbon dioxide and formaldehyde in aqueous solution. Acta Chem. Scand., B34, 27, 1980.

Arrhenius, G., Minerals with channel structure as substrates for nucleotide and peptide synthesis. In: N.C. Wickramasinghe (ed.), Fundamental Studies of the Future of Science, Univ. of Cardiff Press, Cardiff, U.K., 1984.

Arrhenius, G., Dysoxic environments as models for primordial mineralization. In: A.G. CairnsSmith and H. Hartman (eds.), Clay Minerals and the Origin of Life, Cambridge Univ. Press, 1986.

Arrhenius, G., The first 800 million years—probiotic environmental models for early Earth. Earth, Moon and Planets, 37:187, 1987.

Arrhenius, G. and Tsai, A., Structure, phase transformation and probiotic catalysis in marine manganate minerals. SIO Ref. Ser. 81-28, 1-19, 1981.

Bernal, J.D., The Physical Basis of Life, Routledge and Kegan Paul, London, 1951.

Ferris, J.P., Huang, C.H. and Hagan, W.J., Clays as prototypical enzymes for the prebiological formation of phosphate esters. In: V. Buesch et al. (eds.), Abst. 8th International Conference on the Origin of Life, Univ. of Calif., Berkeley, CA, June 1986, p. 297.

Holm, N.G., Dowler, M.J., Wadsten, T. and Arrhenius, G., β- $FeOOH{\cdot}Cl_n$ (akaganeite) and $Fe_{1-x}O$ (wüstite) in hot brine from the Atlantis II Deep (Red Sea) and uptake of amino acids by synthetic β-$FeOOH{\cdot}Cl_n$. Geochim. Cosmochim. Acta 47:1465-70, 1983.

Joe, H., Kuma, K., Paplawsky, W., Rea, R. and Arrhenius, G., Abiotic photosynthesis from ferrous carbonate (siderite) and water. In: V. Buesch et al. (eds.), Abst. 8th International Conference on the Origin of Life, Univ. of Calif., Berkeley, CA, June 1986.

Miller, S.L., A production of amino acids under possible primitive Earth conditions. Science 117:528-9, 1954.

EFFECTS OF IRON AND STORED ENERGY ON THE KINETICS OF KAOLINITE SURFACE-CATALYZED OXIDATION OF HYDRAZINE

L. Coyne[1], R. Shipp[2], A. Rice[3]

[1]San Jose State University, San Jose, California 95192, [2]NASA/Ames Research Center, Moffett Field, California 94035 and [3]English China Clays International, Sandersville, Georgia 31082

With special acknowledgements to B.K.G. Theng and P. Isaacson

---

Prior work (Coyne *et al.*, 1984) has shown that ultraviolet light with peak emission intensity at 365 nm is released when kaolinite surfaces are wetted with hydrazine in air. The light emission intensity was also shown to be affected by clay pretreatments, heating and/or γ- irradiation, which affect the stored energy content and the energy-storing capacity of the kaolinites (Coyne *et al.*, 1984).

Chemical activity is indicated by bubble formation. Hydrazine is known to be readily air-oxidized on a variety of catalytic surfaces according to the equation: $N_2H_4 + O_2 \rightarrow 2\ H_2O + N_2$. The rate of oxidation of hydrazine hydrate is significantly slower than that of hydrazine (Schmidt, 1984).

That the intensity and the time-dependence of the light release is altered by properties intrinsic both to the clay and to the wetting agent, and that this agent appears to decompose during the interaction, leads us to speculate that: (a) the kinetics of light release and of chemical reaction are synchronous and in some manner related; (b) electronic energy, stored in the clay structure, may influence the rate of the reaction.

The trigger for the luminescence is, as yet, unknown. It has been variously hypothesized to be attributable to complex formation, intercalation, or hydrazine oxidation, all of which are known to occur during the clay/hydrazine interaction. It is also known that iron is a ubiquitous contaminant of kaolinites, occurring both as a lattice cation and as an admixed oxide impurity. Metal oxides are among the more effective catalysts of hydrazine oxidation (Schmidt, 1984). Our long-term objectives for these studies are to determine whether stored electronic energy or intercalation can serve as energy sources for surface reactions on clays. However, to demonstrate the possible roles of these novel energy sources in reaction mechanisms, it is requisite simultaneously to consider the role of iron. An interaction between hydrazine and iron might produce a chemiluminescent surface reaction, more or less independent of energy stored in the clay.

To control for the effects of iron in our investigations of the trigger for hydrazine-induced luminescence and the relationship between this luminescence and surface reactivity, we have measured electron-spin resonance (ESR) spectra of the clays and the kinetics of hydrazine oxidation on the surfaces of clays which have been selected and treated to provide a variety of surface and structural iron contents. The clays included: a Cornish kaolinite of low-surface, low-structural, ferric iron (by ESR)

ANALYSIS, CHEMICAL AND E.S.R. OF PARAMAGNETIC SPECIES IN CATALYTIC KAOLINITES

CLAY DESCRIPTION	CLAY TREATMENT	Fe(TOTAL) CHEMICAL ANALYSIS	Fe(TOTAL) ESR	Fe SURFACE ESR	Fe STRUCTURAL ESR	O^- ESR	Σ ESR
CORNISH RLO2101	NONE	0.408	7.6	2.4	5.2	230	240
GA 62-03 LOW IRON	MAG SEP AND CHEM BLEACH	0.30	26	7.6	18	359	395
GA 51-05 HIGH IRON	NONE	1.10	54	12	42	95	149
GA 6381 LOW IRON	MAGNET RESIDUE	0.47	80	62	18	324	404
RATIO HIGH/LOW		**3.7**	**10.5**	**26**	**8**	**3.8**	**2.7**

and an undetermined but, likely, a high content of structural ferrous iron (by the total iron analysis); a "low-iron" Georgia kaolinite (.3% total iron); and a "high-iron" Georgia kaolinite (1.1% total iron); all provided by E.C.C. International. The Georgia kaolinites were further treated by magnetic separation and/or chemical reduction (called bleaching) to diminish the concentration of surface iron. The total iron was determined by chemical analysis. The relative amounts of surface and structural ferric iron and O^--centers were determined by the intensities of the broad component at $g = 2$, the broad component at $g = 4$ and the narrow component at $g = 2$, respectively, of the ESR spectra. Total iron by ESR (not comparable to total iron by chemical analysis, because Fe^{+2} is ESR-silent) and "Σ", defined to be the total paramagnetism, were constructed appropriately from the sums of the individual measures. These values are shown in Table 1. ESR spectra of these various materials are shown in Figure 1.

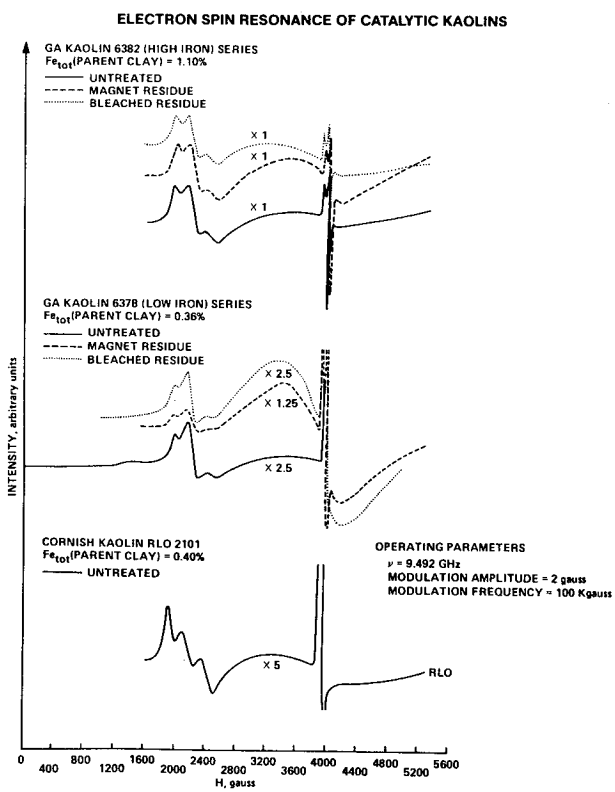

Figure 1.

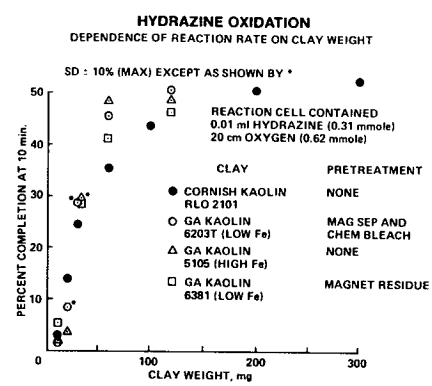

Figure 2.

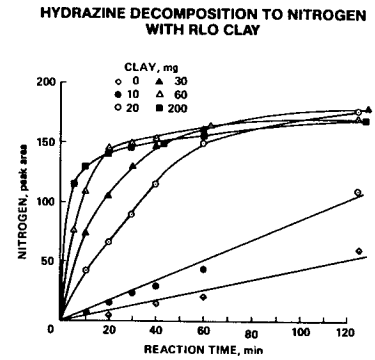

Figure 3.

The kinetics of hydrazine oxidation were monitored by gas chromatographic measurement of the time-dependence of N_2 release from a reaction mixture initially composed of 3×10^{-4} moles of N_2H^4 (10 microliters), from 0 - 10^{-3} moles of O_2 (O - 40 cm Hg) and 10^{-5} - 10^{-3} formula equivalent weights of kaolinite (3 - 300 mg). Degree of intercalation was controlled by equilibrating hydrazine with the clay for one hour in evacuated reaction vessels, before addition of oxygen. Direct decomposition of N_2H_4 in the absence of O_2 is negligible under our conditions.

A family of curves showing the time dependence of the oxidation process is shown for several weights of the Cornish kaolin in Figure 2. It should be noted that there is a strong weight dependence of the rate of the reaction throughout this range. Although the rate appears to plateau at the upper weights, this appearance is an artifact of the very high initial rate. The rate must plateau out at 50% completion, where the reactant becomes hydrazine hydrate, rather than hydrazine. This plateau is reached very early in our data-taking for the high weight samples. The weight dependence implies either that the reaction is strongly site-limited, or that the clay performs a stoichiometric, rather than purely catalytic, role in the reaction.

The weight dependence is also remarkable in that additional clay is effective in enhancing the rate well beyond a quantity of clay which can be wet by the 10 microliters of hydrazine. This fact suggests that the hydrazine is highly mobile,or that the reaction proceeds also at the vapor/solid interface.

Figure 3 is shows a family of curves indicating the weight dependence of the initial reaction rates (10 min) for the four clays whose iron and O^--center analysis data are shown in Table 1. Within the accuracy of our measurements, we can discern no apparent differences between these curves, despite the diversity of the values for total, structural and surface iron and O^--center contents for these materials. Remarkably, for all the diversity in the concentrations of the individual moeities, values for the "total paramagnetism", as represented by the sum of the ESR intensities of these individual moeities are considerably less divergent. The implication of these results is that total paramagnetism, which includes stored energy, as well as iron centers, is a better predictor of reactivity than iron alone. These results are crude and require much improvement in our methods for preparation and analysis, chemically and by ESR, of the clays and in measuring the reaction rates. This verification is extremely important because, if correct, these results not only confirm the validity of the hypothesis that stored energy affects surface chemistry, but it also suggests a novel mechanism whereby asymmetric synthesis might be induced in natural systems. Kondeputi (1984) has shown that molecular paramagnetism is an intrinsically asymmetric entity. Thus, a paramagnetic surface possesses a fundamental asymmetry. This asymmetry, acting on an asymmetric center of a surface reactant, could produce asymmetric synthesis or decomposition of optically active reactants.

Our results, while preliminary and incomplete, demonstrate that clay-catalyzed hydrazine oxidation is a model reaction with many possible facets of relevance to prebiotic chemical evolution. ■

REFERENCES

1. L Coyne, G. Pollock and R. Kloepping, (1984) Clays and Clay Minerals 32, 58-67.
2. E.W. Schmidt (1984) Hydrazine and Its Derivatives, Wiley- Interscience, N.Y.
3. D.K.Kondeputi (1984) physica 125A, 465-496.

ORIGINS OF MEMBRANE STRUCTURE: PREBIOTIC AMPHIPHILES DERIVED FROM CARBONACEOUS CHONDRITES

D. W. Deamer
Department of Zoology, University of California, Davis, Davis, California 95616

The first cellular life presumably utilized membrane structures assembled from amphiphilic components in the prebiotic environment. What kinds of amphiphiles might have been available? Carbonaceous meteorites contain a few percent by weight of organic carbon in the form of polycyclic

aromatic hydrocarbon derivatives as well as smaller amounts of alkanes, alcohols, monocarboxylic acids and amino acids. These substances were synthesized abiotically in the early solar system, and are representative of compounds plausibly available on the prebiotic earth through meteoritic infall. We have investigated the possibility that one or more of the compounds is sufficiently amphiphilic to participate in membrane formation. Samples of the Murchison carbonaceous chondrite were extracted under conditions which solubilize lipid-like material, and about 1 mg per g meteoritic mass (about 10% of the total organic content) dissolved in organic solvents. This was analyzed by spectroscopic, surface chemical and microscopic methods. The material was highly fluorescent, suggesting the presence of polycyclic aromatic compounds. Infrared bands corresponded to C-H, C=O, -OH, and C-O groups, and titrations gave pK values around 6.5 and 9.3, consistent with carboxylate and phenolic groups attached to aromatic hydrocarbons. If the extracted material was dried on microscope slides and examined by phase microscopy after rehydration in alkaline buffers, droplets containing numerous interior phase separations could be visualized. Polarized light microscopy showed birefringent patterns in the droplets typical of multilamellar organization in liquid crystals. Transmission electron microscopy also revealed lamellar structures within the droplets, and freeze-fracture microscopy confirmed that membranous compartments were present. The extracted material was surface active, spreading to form films at air-water interfaces (0.18 m^2/mg at 10 dynes/cm surface pressure). The mixture was separated by two-dimensional thin layer chromatography into at least 6 polarity groups, each of which was also fluorescent and surface active. We conclude that several of the organic components of the Murchison meteorite are amphiphilic and have the capacity to self-assemble into lamellar structures resembling membranes. Such components represent plausible candidates for self-assembling molecules involved in the origin of membrane structures required by the earliest cellular life forms. The fluorescent chromophores are also of interest, in that they represent a primitive pigment system with potential photochemical properties related to photosynthetic light transduction. ■

MONTMORILLONITE: A MULTIFUNCTIONAL MINERAL CATALYST FOR THE PREBIOLOGICAL FORMATION OF PHOSPHATE ESTERS

J. P. Ferris, C. H. Huang and W. J. Hagan, Jr.
Department of Chemistry, Rensselaer Polytechnic Institute, Troy, New York 12180-3590

The laboratory demonstration of the oligomerization of unblocked monomers to oligomers in aqueous solution using prebiological reaction conditions is both a fundamental and recalcitrant problem in the field of chemical evolution. The formation of the phosphate ester bond in aqueous solution by the reaction of prebiological molecule diaminomaleonitrile (DAMN) with 3'-AMP in the presence of montmorillonite clay is described herein. The montmorillonite has four different functions in its role as a catalyst: (1.) binding one of the substrate molecules (3'-AMP), (2.) activating the second substrate (DAMN), (3.) catalyzing the formation of product (2', 3'-cAMP) (4.) desorbing the product (Figure 1). The montmorillonite exhibits many of the characteristics of an enzyme; such characteristics have been postulated for clays on the primitive earth but have not been observed experimentally (1,2,3).

The condensing agent utilized in this study is diiminosuccinonitrile (DISN), a compound formed by the oxidation of DAMN (7,8). DAMN, a key intermediate in the proposed prebiological synthesis of purines, some pyrimidines and some amino acids, forms spontaneously by the self-condensation of aqueous HCN (9). DISN (0.1 M) effects the cyclization 3'-nucleotides to the corresponding 2',3'- cyclic phosphates in aqueous solution (10).

The catalytic role of montmorillonite clays in the formation of the phosphodiester link was demonstrated in the conversion of 3'-AMP to 2',3'-cAMP using dilute (0.005M) aqueous DISN. The highest yield of product was obtained using homoionic Na^+-montmorillonite. Catalysis by the montmorillonite was demonstrated by the observation that no 2',3'-cAMP was detected in a solution-phase reaction performed under identical conditions in which the clay was omitted, but with a

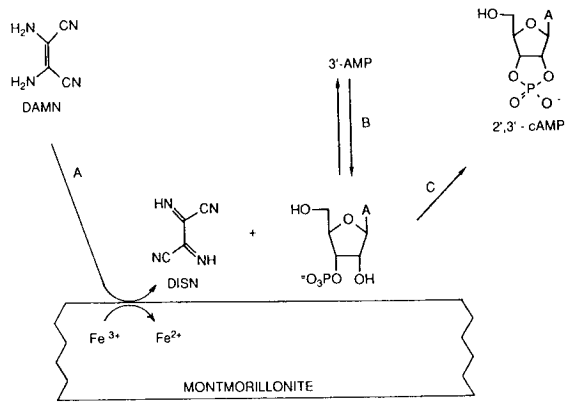

Figure 1.

A. OXIDATION BY THE Fe^{3+} IN THE MONTMORILLONITE LATTICE

B. EQUILIBRIUM BINDING OF 3'-AMP TO MONTMORILLONITE

C. MONTMORILLONITE-CATALYZED REACTION OF DISN AND 3'-AMP AND THE RELEASE OF THE 2',3' - cAMP

concentration of Na^+ equivalent to that associated with Na^+-montmorillonite. The Na^+-montmorillonite-catalyzed formation of 2',3'-cAMP was also observed when the concentration of 3'-AMP was reduced to 0.0125 M and 0.0025 M.

The natural clay (native montmorillonite 22A)(11) from which the homoionic montmorillonites were prepared also gave a significant yield of 2',3'-cAMP. This finding demonstrates that the procedures used to prepare the homoionic montmorillonites did not artificially induce the observed catalytic properties (11,12,13). Furthermore, it establishes that naturally-formed clays may have catalyzed the formation of the phosphodiester bond on the primitive earth.

DISN undergoes rapid hydrolysis, and so is unlikely to have served as a prebiotic nucleotide condensing agent unless it was generated in the presence of a nucleotide (7). We have found that the montmorillonite clay will oxidatively convert DAMN, a masked form of the condensing agent DISN, to the active condensing agent (8). The 5.5% Fe^{3+} present in the aluminosilicate clay lattice (11) oxidizes DAMN to DISN, which in turn affects the conversion of the 3'-AMP bound to the clay to 2',3'-cAMP.

Binding studies established that 2',3'-cAMP is not significantly adsorbed onto the montmorillonite under these conditions, although this study is complicated by the montmorillonite-catalyzed hydrolysis of the 2',3'-cAMP.

These findings provide direct experimental support for the postulate that clays may have served as prototypical enzymes on the primitive earth. DISN, a compound generated from HCN via DAMN, is a plausible prebiotic condensing agent.(9) The thermal reaction of 2',3'-cAMP on montmorillonite completes the prebiotic synthesis of oligonucleotides (14). It might be argued that the formation of 2',3'-cAMP is not a true enzyme-like system because the Fe^{2+} in the clay is not converted back to Fe^{3+} during the course of these transformations. However, this conversion is likely to have occurred on the primitive earth by the photochemical expulsion of an electron from the Fe^{2+} (15) or by the oxidation of Fe^{2+} to Fe^{3+} by photochemically-generated radicals (16), thereby completing the reaction cycle.

This work was supported by NSF Grant CHE 83-04466 and NASA Grant NGR 33-018-148. ■

REFERENCES

1. Bernal, J.D. Proc. Phys. Soc. London, 1949, 62A, 537.
2. Cairns-Smith, A.G. Genetic Takeover and the Mineral Origins of Life, Cambridge University Press, 1982.
3. The polymerization of alanine adenylate on sodium montmorillonite has been reported (4) but it was not possible to reproduce these experiments (5). The prebiotic relevance of this postulate is further diminished by the absence of a plausible prebiotic route to alanine adenylate (6).
4. Paecht-Horowitz, M. Origins of Life 1976, 7, 369 and references therein.
5. Brack, A. Clay minerals 1976, 11, 117.
6. Warden, J.T.; McCullough, J.J.; Lemmon, R.M.; Calvin, M.J. Mol. Evol. 1974, 4, 189.
7. Webster, O. W.; Hartter, D.R.; Begland, R.W.; Sheppard, W.A.; Cairncross, A.J. Org. Chem. 1972, 37, 4133.

8. Ferris, J.P.; Hagan, W.J., Jr.; Alwis, K.W.; McCrea, J.J. Mol. Evol. 1982, 18, 304.
9. Ferris, J.P.; Hagan, W.J., Jr. Tetrahedron 1984, 40, 1093 and references therein.
10. Ferris, J.P. Yanagawa, J.; Dudgeon, P.A.; Hagan, W.J., Jr.; Mallare, T.E. Origins of Life 1984, 15, 29.
11. Ferris, J.P.; Edelson, E.H.; Mount, N.M.; Sullivan, A.E. J. Mol. Evol. 1979, 13, 317.
12. Lawless, J.G.; Banin, A.; Church, F.M.; Mazzurco, J.; Church, F.M.; Margulies, L.; Orenberg, J.B. Origins of Life 1985, 15, 77.
13. Banin, A.; Lawless, J.G.; Mazzurco, J.; Church, F.M.; Margulies, L.; Orenberg, J.B. Origins of Life 1985, 15, 78.
14. Verlander, M.S.; Lohrmann, R.; Orgel, L.E. J. Mol. Evol. 1973, 2, 303; Verlander,M.S.; Orgel, L.E. J. Mol. Evol. 1974, 3, 115.
15. Braterman, P.S.; Cairns-Smith, A.G.; Sloper, R.W. Nature 1983, 303, 163.
16. The very highly oxidized character of the Martian surface is attributed to ultraviolet radiation: Banin, A.; Rishpon, J.J. Mol. Evol. 1979, 14, 133.

PROPERTIES OF IONOPHORE ASSISTED ION TRANSPORT ACROSS MEMBRANES

B. Owenson, R. D. MacElroy and A. Pohorille
NASA/Ames Research Center, Moffett Field, California 94035

One of the essential steps in protobiotic evolution was the formation of membrane-like structures that could isolate interior material from the external environment. Existence of membranous boundaries limited the diffusion of organic molecules and protected those inside from the possibly degradative influence of the environment. Currently the most attractive models for studying proto-biological membranes are lipid vesicles.

An important characteristic of early membranes was their permeability to those simple organic molecules and ions that were necessary for proto-biochemical processes. Understanding transport of these molecules across membranes requires an explanation of the transfer of polar molecules from a high dielectric aqueous solution to a nonpolar membrane environment. This process is energetically unfavorable, and usually requires some assistance. Contemporary cells exploit complex, highly evolved proteins even for passive transport. However, in studies of prebiotic evolution much simpler transport systems must be considered. One class of molecules that can participate in passive ion transport as mobile ion carriers are ionophores. This report presents our initial studies directed toward explaining the structural, thermodynamic, and kinetic properties of ionophore assisted transport across membranes. These studies focused on establishing what properties of an ion carrier enable it to capture an ion from aqueous medium.

Results presented here were obtained by computer simulation methods. Specifically, we used molecular dynamics (numerical integration of Newton's equations of motion) and Metropolis Monte Carlo methods. Both of these techniques allow the calculation of equilibrium thermodynamic properties of the system of interest. Molecular dynamics also provides the time-dependent characteristics of the system. An important feature of computer simulations is that they provide detailed, molecular level description of the behavior of the system studied.

In the first stage we studied the behavior of an ion in an aqueous film. These calculations allowed determination of such important characteristics influencing ion transport as the electric field gradient across interfaces between water and a nonpolar medium and the ability of an ion to approach a surface. The systems under study consisted of a film of 342 water molecules with one Na^+ ion. The film was approximately 23 Å wide and had two free liquid-vapor surfaces. Periodic boundary conditions were applied in the plane of the water layer. Results from molecular dynamics simulations show that the ion spends most of its time in the bulk liquid phase. The ion changes the structure of water in its solvation shell. The surface also causes reorientation of water molecules. Both structural changes, in turn, create the electric field gradient in the aqueous film and across the liquid-vapor interface. Both

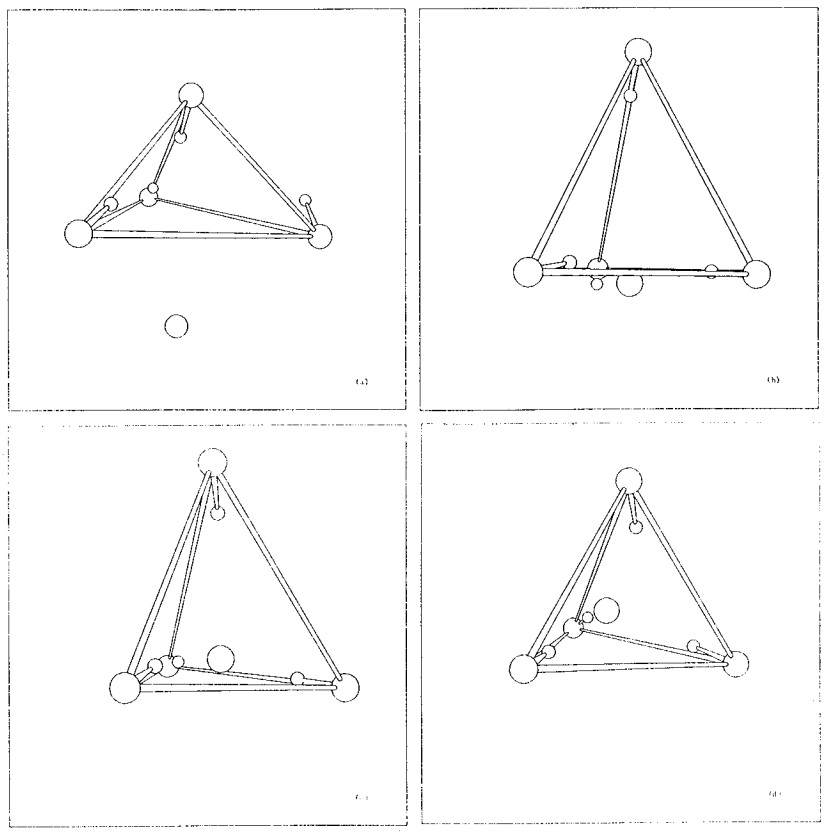

Fig. 1. Schematic view of ion capture by the cryptand SC24. Only the nitrogens (large spheres at the corners of the tetrahedron) with their attached hydrogens, and the Cl^- ion (free circle) are drawn. The distances between the Cl^- ion and the upper nitrogen are: (a) 5.6Å; (b) 5.0Å; (c) 4.1Å; and (d) 3.2Å. Notice how the charged hydrogens bend and move with the ion as it enters the cryptand cavity, and how the shape of the cryptand changes to accept the ion.

components of the electric field contribute to the inability of a positive ion to approach the surface. Our results also suggest that the approach to a surface by a negative ion may be somewhat easier because it would not require as much restructuring of water at the interface. The effects of the water liquid-vapor surface on an ion would also appear at a water-membrane surface since both water vapor and the membrane interior have dielectric constants close to zero.

The calculations described above underscore the energetical difficulties associated with dehydrating an ion and moving it across a surface. To understand how this process can be accomplished by an ionophore we studied a model ion capturing molecule, cryptand SC24. This molecule has a tetrahedral symmetry with nitrogen atoms in the vertices. Every pair of nitrogen atoms is connected by a $CH_2CH_2OCH_2CH_2$ chain. At low pH the nitrogens are pronated and the cryptand is very effective in trapping negative ions, such as Cl^- in the cavity of the molecule. The system that we studied consisted of a box of 319 water molecules with the cryptand and one Cl^- ion. Molecular dynamics simulations of this system gave us a detailed molecular description of ion capture by the cryptand. This process is schematically shown in Fig. 1. It was found that the key role in the capture of the ion is played by the charged $N\text{-}H^+$ groups of the cryptate which tilt towards the aqueous medium in order to assist dehydration. These results show that the two essential features of an ion capturing molecule are (1) the existence of atoms or groups that can interact favorably with an ion, and (2) structural flexibility of these groups which facilitates moving the ion across an energetically unfavorable region.

While the ionophore is an essential feature in initiating ion transport across an interface, fluidity of the surface plays an important role. Molecular dynamics simulations of a layer of undecanol molecules demonstrates how this flexibility arises, and explains how it can contribute to transport mechanisms.

The system studied here was composed of a film of 64 undecanol molecules ($CH_3(CH_2)_9COH$). This system had two free liquid-vapor surfaces and periodic boundary conditions were applied in the plane of the layer. The results of this work show that the -OH head groups of the undecanol molecules find the surface energetically favorable. As they move towards the surface, they compete with the *tails* of the molecules, which find the bulk liquid phase of the film energetically favorable. This competition causes constant fluctuations at the interface. *Heads* which become trapped under the surface by this motion tend to form clusters, indicative of inverse micelles. These clusters are free to diffuse through the membrane. Such clusters of polar head groups can have both sufficient partial charge and flexibility to help carry ions across low dielectric media. ■

MO STUDY OF TRANSITION STATE MODELS FOR RIBOZYME REACTION

R. Rein, M. McCourt and M. Shibata
Department of Biophysics, Roswell Park Memorial Institute, 666 Elm Street, Buffalo, New York 14263

The discovery of RNA enzymes provides a clue as to the possible source of enzymatic catalysis prior to the existence of an established translational apparatus. It has been shown that RNA exhibits similar types of catalytic activity in different systems including: (1) the self-splicing of precursor ribsomal RNA from the protozoan *Tetrahymena thermophila* (Cech *et al.*, 1981); (2) the catalytic reaction of M1 RNA of RNaseP from *E. coli* (Guerrier-Takada *et al.* 1983); and (3) the polymerization of polycytidilic acid by the shortened form (L-19) of the intron of *Tetrahymena thermophila* (Zaug and Cech, 1986). While the self-splicing reaction is inherently interesting, the importance of the polymerization reaction is not limited to the reaction itself but rather its significance is in its implication for prebiotic chemistry. The ability of RNA to polymerize nucleotide sequences using an internal template suggests a capability to use an external template for the polymerization. This is an important evolutionary link in that RNA molecules which could have been formed in the prebiotic environment, could act as the enzyme for the template copying and self-replication, thus setting off the molecular evolutionary process.

While significant information has been gathered on this reaction from various experimental studies (Cech and Bass, 1986), the details of the stereochemical arrangement of the catalytic site as well as the mechanistic details of the reaction have yet to be elucidated. We first start out with the modeling of the catalytic site with the ultimate goal of a 3-D model of the ribozyme complex. Our preliminary calculations have been performed to determine: (1) Does a transition state exist for models 1 or 2 (Figure 1)? The transition state is defined by the existence of one negative eigenvalue; (2) Given that a transition state exists for the models, which is the better choice for the ribozyme reaction? We based our choice on energy criteria.

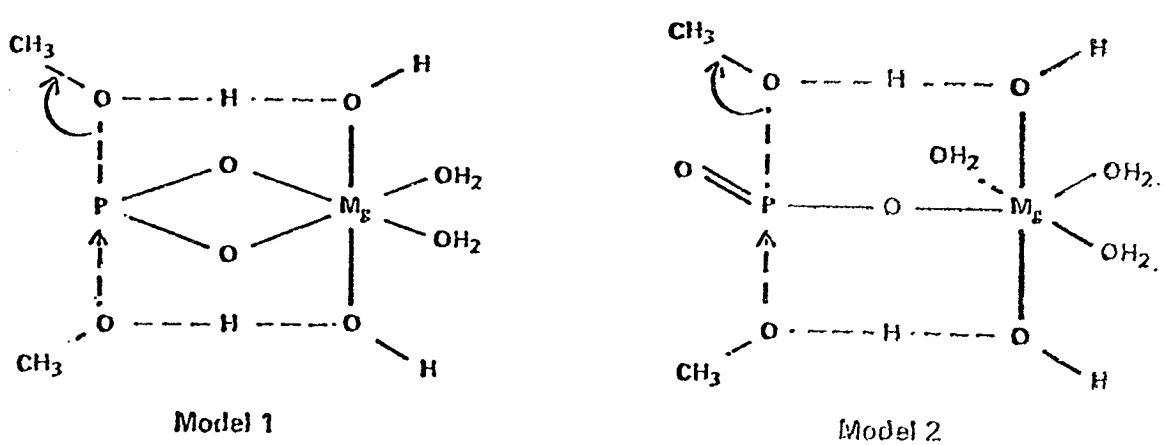

Figure 1. Model of transition state for ribozyme reaction.

As a first step we have performed quantum mechanical studies in an effort to gain insight into the nature of the transition state of the SN2 transphosphorylation reaction. To simplify the calculation we reduced the proposed model to a size reasonable for *ab initio* calculations while at the same time retaining the important chemical features of the transition state (Figure 1). Note that the models permit the study of the interaction of the hydrogen bonds of the axial ligands with the incoming nucleophile and exiting leaving group. Also, these preliminary models retain the fundamental features of the magnesium complex critical to the self-splicing reaction. Furthermore, the model permits flexibility for further calculations in which we will modify the phosphate backbone to introduce the 2'OH moiety determined to be another critical feature of the ribozyme reaction (Bass and Cech, 1984).

In addition to having determined the geometry that corresponded to the transition state of the ribozyme reaction for our simplified model, our calculations have give us insight into the ligands involved in proton transfer.

For our calculations, we used an IBM version of HONDO, which is an *ab initio* program permitting geometry optimization. Starting with a minimal basis set, which involved 92 basis functions, including d functions for phosphorus and magnesium, we performed geometry optimization on our model transition state. We followed the changes in charge density and bond orders along an appropriate reaction coordinate. By following the changes in the bond order matrix as well as the overlap populations and charge density as the transition state complex progressed along the reaction coordinate, we were able to study the polarization effects of the hydrated magnesium complex, including its impact on proton transfer involved in bond scission and formation. Having studied the complex with a minimal basis set to determine the appropriate geometry, we intend to continue our study using a more extensive basis set in an effort to further refine the stereochemical details of the transition state. ■

REFERENCES

Bass, B.L. and Cech, T.R. (1984) Nature 308, 820.
Cech, T.R. and Bass, B.L. (1986) Ann. Rev. Biochem. 55, 599.
Cech, T.R., Zaug, A.J. and Grabowski, P.J. (1981) Cell 27, 487.
Guerrier-Takada, C., Gardiner, K., Marsh, T., Pace, N. and Altman, S. (1983) Cell 35, 849.
Zaug, A.J. and Cech, T.R. (1986) Science 231, 470. ■

GC PROTOTYPE INSTRUMENTATION FOR THE CHEMICAL ANALYSIS OF TITAN'S ATMOSPHERE

G.C. Carle[1], D.R.Kojiro[1], B.J. O'Hara[1], J.R. Valentin[1], V.R. Oberbeck[2], T.W. Scattergood[3], D. O'Hara[4]
[1]*Solar System Exploration Branch, NASA/Ames Research Center, Moffett Field, California 94035*
[2]*Atmospheric Experiments Branch, NASA/Ames Research Center, Moffett Field, California 94035*
[3]*Department of Earth & Space Sciences, SUNY at Stony Brook, Stony Brook, New York 11794* [4]*San Jose State University Foundation, San Jose, California 95192*

During the next decade or so, NASA, in conjunction with the European Space Agency, plans to send a spacecraft to the Saturnian system so that local studies of Saturn and its satellite, Titan, can be made. Titan is of great interest to the exobiology community because of the belief that complex organic chemistry occurs there. This belief is based, in part, on the detection of many organic molecules, including hydrocarbons and simple C-N compounds, in Titan's atmosphere. These compounds, and others not yet detected, exist in two forms: gases and aerosols. In order to study these components of Titan's atmosphere, instrumentation for collection and gas chromatographic (GC) analysis of Titan atmospheric aerosols and gases from an entry probe is currently being developed. This paper will describe the analytical GC instrumentation under study. For the aerosols, a collection method employing wires will be used followed by a technique involving stepwise heating (pyrolysis) developed to prepare this material for analysis by gas chromatography. For the gases, a sampling system that will enable the collection and analysis of low pressure gases is being developed.

As the probe descends through Titan's atmosphere, aerosol materials will be periodically collected as liquids or solids. Previous work has show that thin wires are probably the best collectors for sampling Titan aerosols (Oberbeck *et al.*, 1987). This conclusion is based upon the fact that wires are very efficient from the standpoint of inertial impaction of high speed and low pressure under the aerodynamic conditions expected during the initial deployment of probe instruments in Titan's atmosphere. The particle collection efficiency on wires is directly proportional to the square of particle radius and entry velocity and inversely proportional to the collector diameter. Results for the collection of Titan's aerosol model by two types of collectors are shown in Figure 1. The cumulative mass of

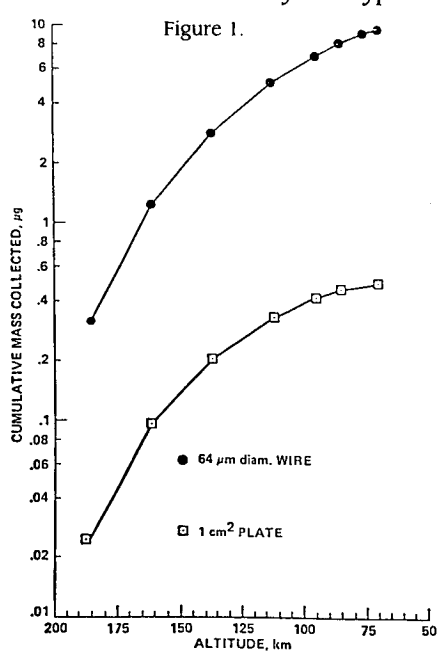

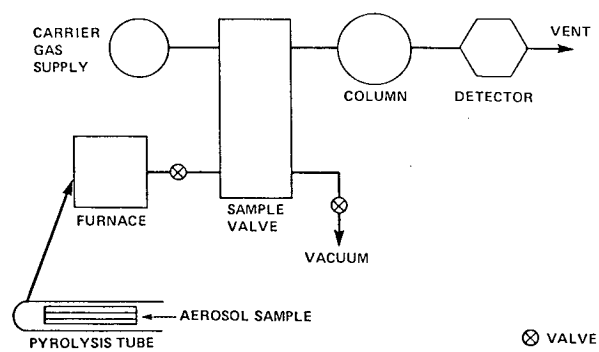

Figure 2.

aerosol collected as a function of altitude shows that only about 0.5 micrograms of aerosol is collected by a 1 cm^2 disc, but the cumulative mass collected by an array of 64 μm diameter wires spaced 3 diameters apart and occupying the same total area of 1 cm^2 is 10 μm. For this reason and because the aerosol sample can be easily pyrolized using resistant heating of the wires, we presently favor use of a thin wire array collector for collection of Titan aerosols.

The conversion of the aerosols to the gaseous form and subsequent transfer to the gas chromatograph is a reliable, simple way to prepare a chemically complicated sample for detailed analysis. The procedure will involve subjecting collected material to stepwise pyrolysis followed by gas chromatographic measurement of any volatiles produced. Analytical pyrolysis is a technique commonly used in many disciplines, *e.g.*, the study of lunar and meteoritic materials (Irwin, 1982) and of solid tholins (Khare *et al.*, 1981).

The length of heating required to allow quantitative release of volatiles at each selected temperature is dependent on the amount of sample and the type of pyrolyzer used. Of the pyrolytic techniques available, the pulse mode (Liebman *et al.*, 1984) will be used because smaller samples (ng to μg amounts) can be pyrolized in very short times (milliseconds). To best characterize the aerosol, the collected particles should be heated at several temperatures. Khare *et al.* (1981) found that in their tholins, nitrogen-containing compounds (nitriles) were released at 150 and 300° while hydrocarbons were not released until 450°C. The number of temperatures at which pyrolysis can be performed on an *in situ* sample will be limited by the chromatographic analysis time and the mission time constraints which are yet to be determined.

The GC system being studied for use in a Titan atmospheric probe incorporates modulated metastable ionization detectors, which can detect components at the parts per billion (ppb) levels in gas chromatographic samples (Woeller, *et al.*, 1984; Carle, *et al.*, 1985). This GC system, shown in Figure 2, has been used in our laboratory to pyrolyze 1-5 μg quantities of simulated Titan aerosols, which evolved volatiles in ppm concentrations. The results of this study, illustrated in Figure 3, show that compounds are released from the simulated aerosol when treated at 250, 450, and 700° C. Further work will include study of any modification of samples due to the collection process and the validity of the chemical analysis of the collected samples.

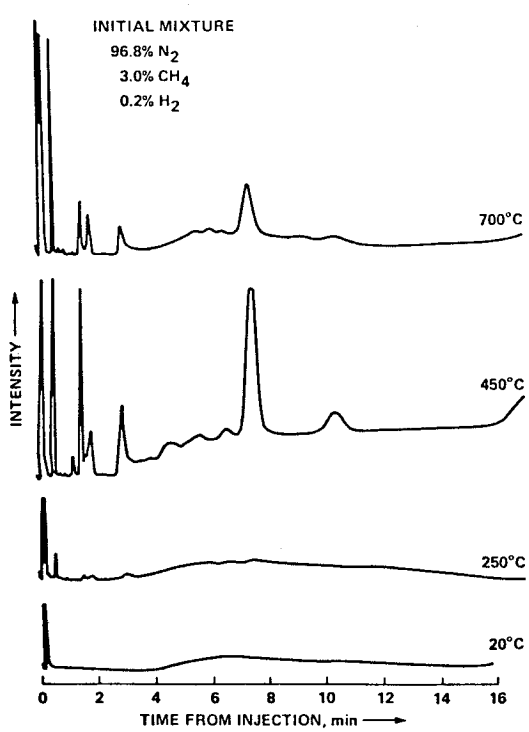

Figure 3.

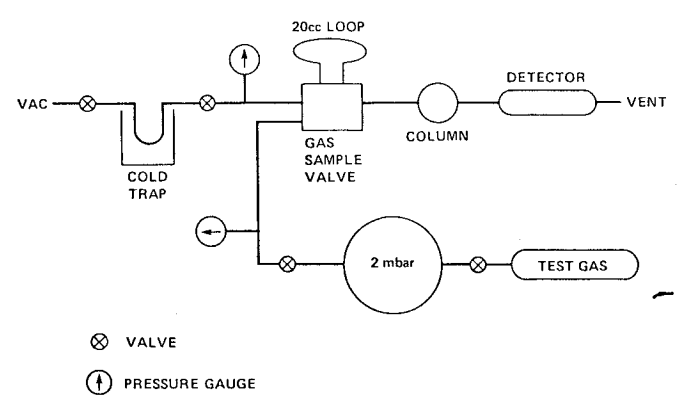

Figure 4.

In addition to collecting and analyzing aerosols in Titan's atmosphere, it is important to be able to accurately determine the gaseous components. The task of measuring the atmospheric components becomes challenging when conducted under the range of conditions expected for this mission. Current plans call for deployment of the science instruments after the probe becomes subsonic, somewhere near 200 km. The ambient pressure at this altitude, is expected to be less than 1 mbar (Lindal *et al.*, 1983). However, the effective atmospheric pressure will probably be closer to 2 mbar because of dynamic effects arising from the velocity of the probe.

The feasibility of analyzing Titan's atmosphere at altitudes up to 200 km was tested with a simple laboratory gas chromatographic system shown in Figure 4. This sampling system incorporated an evacuated 20 cm^3 sample loop in which gas was trapped from a reservoir of model Titan atmosphere at 2 mbar. The gas chromatograph was equipped with a miniature modulated metastable ionization detector. The chromatogram resulting from this study is shown in Figure 5. Clearly, detection of the

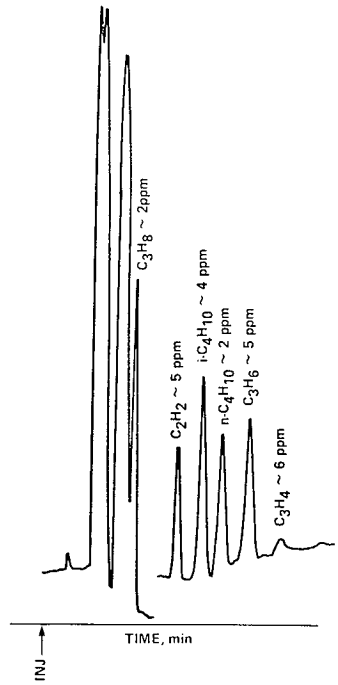

Figure 5.

ppm level components at 2 mbar total pressure was readily accomplished with this system. Furthermore, indications are that detection limits of 10 ppb or so can be achieved for most gases of interest. The detection limits of a gas chromatograph equipped with this type of inlet system are dependent on the ambient atmospheric pressure and temperature as well as the collected volume. The only parameter that can be adjusted is the volume. At 200 km in Titan's atmosphere, a sample volume of 150-300 cm^3 would be required to detect any component of the atmosphere that is at the ppb concentration level. Further research into increasing sample volume will be conducted in the future. ■

REFERENCES:

1. Carle, G.C. *et al.*, Modulated Voltage Metastable Ionization Detector, Patent #4,538,066 Aug. 27, (1985).
2. Irwin, W.J., "Organic Geopolymers" in *Analytical Pyrolysis*, Marcel Dekker, Inc., N.Y., pp 502-508 (1982).
3. Khare, B.N. *et al.*, Icarus, *48*, 290-297.
4. Liebman, S.A. *et al.*, H. High Res. Chromatog. and Chromatog. Comm. *7*, 172-184. (1984).
5. Oberbeck, V.R. *et al.*, J. Geophys. Res., in Press, 1987.
6. Woeller, F.H. *et al.*, Anal. Chem., *56*, 860-862 (1984).
7. Lindal, G.F., *et al.*, Icarus, *53*, 348-368 (1983).

SELF-ORDERING OF AMINO ACIDS AS THE SOURCE OF BIOMACROMOLECULAR INFORMATION: THE PRIMARY DARWINIAN PROCESS

S. W. Fox and T. Nakashima
Institute for Molecular and Cellular Evolution, University of Miami, Coral Gables, Florida 33134

The proteinoid flowsheet of origins stems from the laboratory-demonstrated self-ordering of amino acids to yield nonrandom thermal proteins (Fox, 1980). This process has explained (a) the source of biological information, (b) the origins of enzymic activity and metabolism (Rohlfing and Fox, 1969;

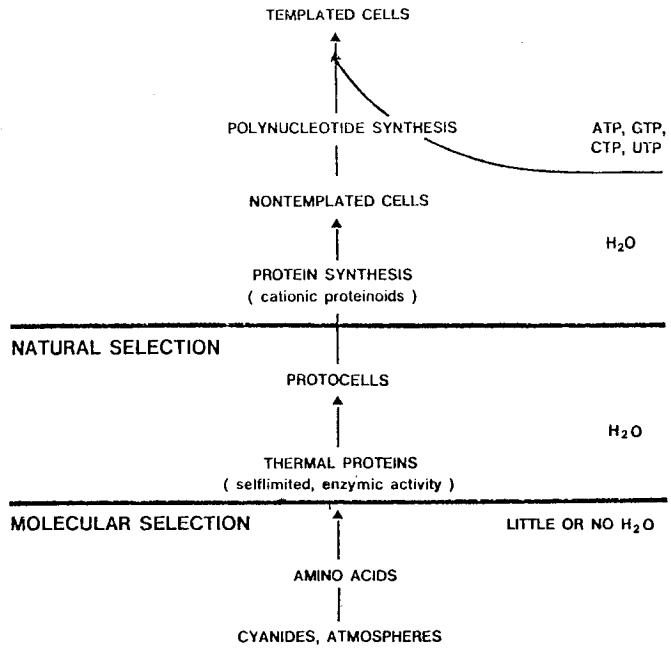

Nakashima, 1987), and (c) the selforganization of thermal proteins into protocells (Fox, 1986). Evolutionary relics of such a primordial process would help to validate the concept (Calvin, 1969) as the original source of biological information. Ivanov and Förtsch (1986), by using the whole protein base, report the cataloguing of such relics. Luque-Romero et al. (1986) have data that further establish the "direction-giving effect" (Mayr, 1981) of N-pyroglutamic acid in thermal polycondensation of amino acids (Fox, 1980). This source of information is plausibly simple for geological events, in contrast to a primodial genetic coding mechanism. The transfer of information from thermal proteins to a primitive nucleic acid mechanism has been partially modeled (Fox, 1981).

The fact the endogenously limited thermal proteins have biomemetic activities (Fox and Nakashima, 1980) further supports the self-ordering process as a source of biological information. The integration of nonrandom polymerization with the properties of the thermal proteins within laboratory protocells has yielded a revised theory of Darwinian evolution in which physical process takes precedence over survival by consequence. The primary process preceding natural selection (Szent-Györgyi, 1972) is in this view one of molecular selection (Ho and Saunders, 1984; Fox, 1986). ■

REFERENCES

Calvin, M. 1969. Chemical Evolution. Oxford University Press. Pages 155-170.
Fox, S.W. 1980. Life from an Orderly Cosmos. Naturwissenchaften 67:576-581.
Fox, S.W. 1981. A Model for Protocellular Coordination of Nucleic Acid and Protein Syntheses. In: Science and Scientists. M. Kageyama, K. Nakamura, T. Oshima, and T. Uchida, Eds. Japan Sc. Soc. Press, Tokyo. Pages 39-45.

Fox, S.W. 1986. Molecular Selection and Natural Selection. Quart. Rev. Biol. 61:375-386.
Fox, S.W. and Nakashima, T. 1980. The Assembly and Properties of Protobiological Structures: The Beginnings of Cellular Peptide Synthesis. BioSystems 12:155-166.
Ho, M.-W. and Saunders, P.T.: Eds. 1984. Beyond Neo- Darwinism/An Introduction to the New Evolutionary Paradigm. Academic Press, London. 376 + xi pages.
Ivanov C.O. and Förtsch B. 1986. Universal Regularities in Protein Primary Structure: Preference in Bonding and Periodicity. Origins of Life 17:35-49.
Luque-Romero, M.M., de Medina, L.S., and Blanco, J.M. 1986. Fractionation and Amino Acid Composition of an Aspartic Acid-Containing Thermal Proteinoid Population. BioSystems 19:267-292.
Mayr, E. 1980. Prologue: Some Thoughts on the History of the Evolutionary Synthesis. In: The Evolutionary Synthesis. Mary, E. and Provine, W.B., Eds. Harvard University Press. Page 3, Footnote 1.
Nakashima, T. 1987. Metabolism of Proteinoid Microspheres. Organic Geo- and Cosmochemistry. Topics in Current Chemistry 139:59-81.
Rohlfing, D.L. and Fox, S.W. 1969. Catalytic Activities in Thermal Polyanhydro -Amino Acids. Advances in Catalysis 20:373-418; Fox, S.W. 1980. Metabolic Microspheres. Naturwissenschaften 67 373-383.
Szent-Györgyi, A. 1982. The Evolutionary Paradox and Biological Stability. In: Molecular Evolution/ Prebiological and Biological. D. L. Rohlfing and A. I. Oparin, Eds. Plenum Press, New York. Pages 111-112.

ATMOSPHERIC OXYGEN IN THE PRECAMBRIAN

H. D. Holland and E. A. Zbinden
Harvard University, Department of Earth and Planetary Sciences, Hoffman Laboratory, 20 Oxford Street, Cambridge, Massachusetts 02138

A number of calculations have shown (Kasting and Walker, 1981) that molecular oxygen was essentially absent from the earth's atmosphere prior to the evolution of green plant photosynthesis. We do not know when green plant photosynthesis evolved. However, the paleontologic evidence for the presence of life on earth 3.5 b.y. ago is strong, and the sedimentologic evidence for the existence of life 3.8 b.y. ago is reasonably convincing. Life may therefore have evolved more than 3.8 b.y. ago. Green plant photosynthesis may be almost as ancient, but it is very difficult to establish this on the basis of paleontologic evidence since the fossil remains of Early Precambrian unicellular organisms which produced O_2 cannot be distinguished from those that did not.

The demonstration that O_2 was present in the early Precambrian atmosphere would be strong evidence in favor of the early development of green plant photosynthesis, and a well documented history of the O_2 level in the atmosphere would go far toward defining the evolution of the earth's biomass and its productivity. Several lines of inquiry suggest that a significant quantity of O_2 was present in the atmosphere more than 2.0 b.y. ago, but that P_{O_2} was much less than 0.2 atm between 2.0 and 3.0 b.y.b.p. During the development of soils on granitic rocks between 2.0 and 3.0 b.y. Fe^{2+} was oxidized to Fe^{3+} and retained as ferric oxides and/or hydroxides. During the development of soil on basaltic rocks during this period much of the Fe^{2+} released during soil formation was apparently not oxidized, and was either lost altogether from soil or was reprecipitated as a constituent of ferrous silicates in the lower soil horizons. Very few paleosols from this period of earth history have been studied thoroughly and the interpretation of their evolution is not straightforward, but their properties are best explained in terms of an atmosphere which contained ca. 10^{-2} atm CO_2 and ca. 10^{-3} atm O_2 (Holland Zbinden, 1987; Pinto and Holland, in press).Such a composition for the atmosphere 2.0 to 3.0 b.y.b.p. is consistent with other geologic evidence. The persistence of uraninite grains during weathering, and the accumulation of very large deposits of detrital uraninite in ores formed more than 2.0 b.y. ago demands a lower O_2 pressure than today (Grandstaff, 1980). The presence of very significant quantities of U, Mo, and V in 2.2 b.y. old black shales in Finland demands the presence of enough O_2 in the atmosphere to oxidize a significant fraction of these elements during weathering at that time (Holland,

1984, pp. 368-74). The presence of extensive sedimentary hematite ore deposits in banded iron formations older than 2.0 b.y. is also most easily explained in terms of an atmosphere of the type suggested by the paleosol evidence.

The paleosol record between 2.0 b.y.b.p. and the end of the Precambrian, some 0.6 b.y. ago, indicates that O_2 continued to be present in the atmosphere. The composition of a 1.7 to 1.8 b.y. old paleosol near Flin Flon, Manitoba suggests that P_{O_2} was significantly higher 1.7 b.y. than 2.3 b.y. ago. This suggestion is consistent with other geologic evidence, but is in need of corroboration. The nature of animal life during latest Precambrian time indicates that P_{O_2} was higher than ca. 0.02 atm (0.1 PAL) at that time.

The high O_2 pressure in the atmosphere today is needed to assure the oxidative destruction of all but a few tenths of a percent of the organic matter produced by the biosphere today. The lower O_2 content of the atmosphere during much of Precambrian time was probably a consequence of a lower rate of photosynthesis and a smaller marine biomass during this period of earth history. The apparent lower productivity of the oceans may have been related to a greater flux of iron and manganese from submarine hot springs. A significant fraction of the output of phosphorus from the oceans today can be ascribed to the precipitation of iron and manganese phosphates. Phosphorus may have been scavenged very efficiently from the oceans by this mechanism when the hydrothermal flux of iron and manganese to the oceans was greater than today. If the phosphate content of seawater was indeed lower in the Precambrian than it is today, the productivity of the oceans and the marine biomass were probably smaller as well. Hence, the oxygen pressure required to oxidize the excess organic matter produced by the marine biosphere would have been lower than P_{O_2} today. We find this hypothesis for the evolution of atmospheric O_2 in the atmosphere attractive, but it is obviously in need of more supporting evidence. ■

REFERENCES

Grandstaff D.E., 1980, Origin of uraniferous conglomerates at Elliott Lake, Canada, and Witwatersrand, South Africa: Implications for oxygen in the Precambrian atmosphere. Precamb. Res. 13:1-26.

Holland H.D., 1984, The Chemical Evolution of the Atmosphere and Oceans. Princeton University Press, 582 pp.

Holland H.D. and Zbinden E.A., 1987, Paleosols and the evolution of the atmosphere, Part I. In: Physical and Chemical Weathering in Geochemical Cycles, A. Lerman and M. Meybeck, eds, NATO ASI Institute.

Kasting J.F and Walker J.C.G., 1981, Limits on oxygen concentration in the prebiological atmoshere and the rate of abiotic fixation of nitrogen. J. Geophys. Res. 86:1147-58.

Pinto J.P. and Holland H.D., 1987, Paleosols and the evolution of the atmosphere, Part II. Geol. Soc. Amer. Special Publication (in press).

ISOTOPIC PERSPECTIVES ON THE PREBIOTIC SYNTHESIS OF ORGANIC MATTER IN THE EARLY SOLAR SYSTEM

J. F. Kerridge
Institute of Geophysics, University of California, Los Angeles, California 90024

The objective of this study is to constrain theories for the origin of organic matter in meteorites by means of the isotopic systematics of C, H and N in such material. Previously, it has been argued (1) that the C-isotopic data are consistent with an origin by Fischer-Tropsch-type catalysis on mineral grains in the solar nebula, but a more complex origin has since been invoked based on more detailed studies of C (2), H (3) and N (4) isotopes. This study focuses on the correlated distribution of C, H, and N isotopes in the insoluble organic fraction. This material is less susceptible to terrestrial contamination than is the soluble fraction, but nonetheless exhibits a range of internal variation in isotopic composition that is almost equivalent to that observed among the various soluble molecules. A key question, not resolved by previous work, is the relationship between soluble and insoluble material. Is the insoluble fraction analogous to terrestrial kerogen, which it generally resembles, *i.e.* was it made by diagenesis of a population of simpler organic molecules represented, at least in part, by the present soluble fraction? Alternatively, was it formed as a separate product of the synthesis that also made the soluble fraction? Or does it represent material synthesized by a totally separate process, perhaps even from a different reservoir of biogenic elements?

Stepwise extraction of C, H and N by both pyrolysis (5,6) and combustion (6,7) of acid-demineralized residues from several carbonaceous chrondrites reveals considerable isotopic inhomogeneity. The release profiles for these isotopic systems can be interpreted in terms of isotopic components, believed to represent structural moieties within the kerogen-like fraction. Based on the structural model for this material proposed by Hayatsu and coworkers (8,9), a minimum population of one aliphatic component, termed I, and two aromatic components, II and III, has been identified. The relative proportions of these components vary markedly among different samples, even of the same meteorite. These components are apparently unrelated to each other, though the possibility that secondary isotopic exchange may have affected one or more components, thereby masking intercomponent relationships, cannot be ruled out. With that caveat, origins for the different components may be discussed.

Little can be said about the aromatic components at this time. They share a common $\delta^{13}C$ value, -18.7‰ rel. PDB, so must have derived their C from the same source, but component II is substantially enriched relative to III in D, >1300 vs ~400‰ rel. SMOW, and modestly depleted in 15_N, -6 vs >40‰ rel. AIR. It is possible that II might consist of III to which has been added a trace of material enormously enriched in D, possibly depleted in ^{15}N, and with C not so different from "solar" isotopic composition as to perturb the bulk of $\delta^{13}C$ value, *i.e.* a hypothetical interstellar component (3,7,10). In fact, the structure postulated for components II and III resembles, at least superficially, that proposed for the interstellar polycyclic aromatic hydrocarbons, PAH, to which have been attributed the infrared emission bands associated with many celestial objects (11). If a significant fraction of the meteoritic aromatic material has an interstellar origin, it would imply, barring coincidence in ^{13}C contents, that interstellar PAH comprised a major part of the primordial solar C budget.

The aliphatic component, I, is characterized by a $\delta^{13}C$ value of >-12.4‰, a δD value that is probably around 1300 but may be as high as 1800‰, and a $\delta^{15}N$ value of >40‰. These values suggest that component I may be related to the polar soluble fraction, which shows roughly comparable enrichments in ^{13}C, D and ^{15}N (12-14). If the aliphatic component was derived from molecules such as are now present in the polar soluble fraction, useful constraints may be placed on the origin of the insoluble fraction. This follows because an origin on the meteorite parent body is indicated for the polar soluble material, based on the following argument. The monocarboxylic acids, which we take as representative of the polar fraction, were apparently derived as a homologous series utilizing as a C source CO_2 such as is now trapped in the meteorite (13). The difference in ^{13}C-content between that CO_2 and the inorganic carbonate in the meteorite (15,16) implies isotopic equilibration at around 273 K (17). This corresponds closely to the mineralization temperature, calculated from O-isotope systematics

(18), for the carbonates, which are known to have been formed on the meteorite parent body (19,20). Both the inorganic carbonates and the polar organics were therefore apparently made in the surface regions of the parent body using CO_2 presumably derived from the interior of the body. This took place very early in solar system history (21). At least the aliphatic component was thus apparently assembled into the macromolecular insoluble fraction soon after accretion of the meteorite parent body. Because this kerogen-like material is essentially immobile once formed, and because the spatial scale of its isotopic inhomogeneity seems to preclude synthesis *in situ*, it was presumably formed in a variety of regions in or on the planetesimal and subsequently mixed into its present configuration by impact-induced transport and brecciation.

The relatively straightforward scenario suggested by the C isotopes runs into difficulty, however, when the H isotopes are considered. Judging by the D-content of the apparently contemporaneous phyllosilicates, the water from which the carbonates crystallized was greatly depleted in D relative to the organic matter (5). Thus, it is difficult to understand how D-enriched soluble organics could have been synthesized in a low-D environment. However, it should be pointed out that this problem is not unique to the proposed model but is inherent in the observation of D-enriched soluble molecules coexisting with D-depleted hydrous silicates.

The presence of highly D-enriched H in aliphatic moieties and discrete molecules, such as amino acids (14), in addition to polycyclic aromatics, makes it likely that interstellar molecules survived formation of the solar system as reactive entities capable of participating in prebiotic syntheses, rather than simply as refractory, and presumably relatively unreactive, grains. Similarly, the chemical variety manifested by the D-distribution in meteoric organic matter suggests that the D-enrichment is not carried solely by an acetylinic or cyanoacetylinc polymer, as proposed (9). The most likely ultimate cause of the D-enrichment relative to galactic H remains the isotopic fractionation associated with ion-molecule reactions taking place at the temperatures of dense molecular clouds. (3,10). I thank S. Chang and R. Shipp for fruitful collaboration in this study. Support by NASA through the Exobiology Program is gratefully acknowledged. ■

REFERENCES

1. Lancet, M.S. and Anders, E. (1970) Science 170, 980.
2. Chang, S., Mack, R. and Lennon, K. (1978) Lunar Planet. Sci. IX, 157.
3. Kerridge, J.F. (1980) Lunar Planet. Sci. XI, 538.
4. Kung, C.-C. *et al.* (1979) Earth Planet. Sci.Lett. 46, 141.
5. Robert, F. and Epstein, S. (1982) Geochim. Cosmochim. Acta 46, 81.
6. Kerridge, J.F., Chang, S. and Shipp, R. (1987) Geochim. Cosmochim. Acta, subm.
7. Kerridge, J.F. (1983) Earth Planet. Sci. Lett. 64, 186.
8. Hayatsu, R. *et al.* (1977) Geochim. Cosmochim. Acta 41, 1325.
9. Hayatsu, R., Scott, R.G. and Winans, R.E. (1983) Meteoritics 18, 310.
10. Geiss, J. and Reeves, H. (1981) Astron. Astrophys. 93, 189.
11. Allamandola, L.J., Tielens, A.G.G.M. and Barker, J.R. (1985) Ap. J. Lett. 290, L25.
12. Becker, R.H. and Epstein, S. (1982) Geochim. Cosmochim. Acta 46, 97.
13. Yuen, G. *et al.* (1984) Nature 307, 252.
14. Epstein, S. *et al.* (1987) Lunar Planet. Sci. XVIII, 265.
15. Clayton, R.N. (1963) Science 140, 192.
16. Kvenvolden, K. *et al.* (1970) Nature 228, 923.
17. Bottinga, Y. (1969) Geochim. Cosmochim. Acta 33, 49.
18. Clayton, R.N. and Mayeda, T.K. (1984) Earth Planet. Sci. Lett. 67, 151.
19. DuFresne, E.R. and Anders, E. (1962) Geochim. Cosmochim. Acta 26, 1085.
20. Kerridge, J.F. *et al.* (1980) Meteoritics 15, 313.
21. Macdougall, J.D., Lugmair, G.W. and Kerridge, J.F. (1984) Nature 307, 249.

THE CHEMICAL BASIS FOR THE ORIGIN OF THE GENETIC CODE AND THE PROCESS OF PROTEIN SYNTHESIS

J. C. Lacey, Jr.
Department of Biochemistry, University of Alabama at Birmingham, Birmingham, Alabama

All cellular creatures store their genetic information in double stranded DNA, being encoded simply by variations in the sequence of four chemical nucleotide units abbreviated A,G,C, and T. Since DNA itself cannot carry out the functions it represents, it must be converted into proteins which are highly functional and are composed of strings of amino acids (20 total). This is done in two steps: (1) one strand of the DNA is copied to give an equivalent RNA and (2) that strand of RNA attaches to ribosomes which read the sequence of nucleotides and for each three nucleotides (codons) a particular amino acid is inserted into protein. The codons are "read" by base pairing of RNAs which carry the anticodons which are complementary to the codons. This consistent colinear compositional relationship between RNA and protein is called the genetic code. We have known the assignments (64 possible triplets given four letters) for all twenty amino acids since 1966; however, a fascinating question remained, "Just why does a particular triplet of nucleotides signify a particular amino?" This question is at the heart of our project. Some researchers hold the opinion that the development of the genetic code was due to a frozen accident. Others, including ourselves, believe the code origin was based on discernible physiochemical relationships. Our research has been guided by a further belief that the coding system is essentially buried in the process of protein synthesis and that in order to understand the code origin we must understand the origin of the process of protein synthesis. The three conceptual parts of protein synthesis are: (1) each amino acid must be chemically activated with enough energy to form the peptide bond; (2) while activated, the amino acids must be organized into a predetermined sequence; and (3) while thus activated and organized, they must be polymerized. To reach our objective, we must understand the principles which can accomplish each of these steps.

Not necessarily in chronological order, we will present a limited amount of our data which we believe supports the hypothesis that:

(1) the genetic code is not a random matrix but rather has in it a molecular logic which appears due to

(2) selective chemical reactions which are made selective by selective affinities between amino acids and their anticodonic nucleotides.

In Fig. 1, we show that there is a direct correlation between the hydrophobicity of amino acids and the hydrophobicity of their anticodonic nucleotides (1). This is sufficient evidence to justify the

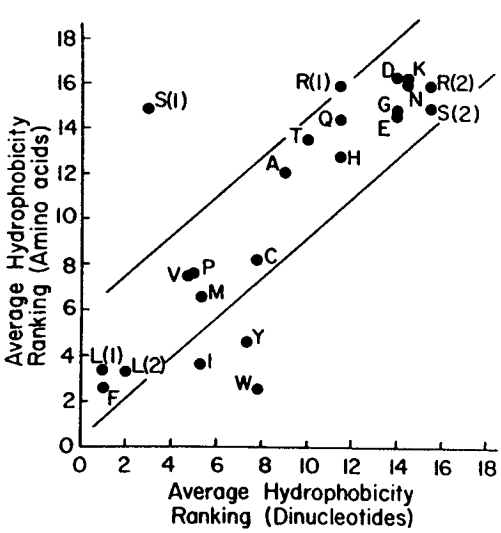

Figure 1. The average ranked hydrophobicity of the amino acids as a function of the average ranked hydrophobicity of their corresponding anticodonic dinucleoside monophosphates. The letters associated with the points are the single letter abbreviations for the amino acids (see Lacey and Mullins 1983).

5'-End	Middle Position: A	G	C	U	3'-End
A	Phe	Ser	Cys	Tyr	A
G	Phe	Ser	Cys	Tyr	
C	Leu	Ser	Trp	T	
U	Leu	Ser	T	T	
A	Leu	Pro	Arg	His	G
G	Leu	Pro	Arg	His	
C	Leu	Pro	Arg	Gln	
U	Leu	Pro	Arg	Gln	
A	Val	Ala	Gly	Asp	C
G	Val	Ala	Gly	Asp	
C	Val	Ala	Gly	Glu	
U	Val	Ala	Gly	Glu	
A	Ile	Thr	Ser	Asn	U
G	Ile	Thr	Ser	Asn	
C	Met	Thr	Arg	Lys	
U	Ile	Thr	Arg	Lys	

Decreasing Hydrophobicity →

TABLE I

The genetic anticode

The genetic anticode organized according to decreasing hydrophobicity of the mononucleotides. The assignments listed here are the anticodons predicted from Watson-Crick base pairing to the established codons. In reality, the anticodons found in tRNAs are seldom those shown. The variation is primarily in the wobble position (5'-end), where inosine is frequently found, and where A–U, G–C base pairing is not rigidly maintained. The major non-correlating assignments are shown in boxes.

conclusion that the genetic code is not due to a frozen accident. Even so, it is not sufficient to say just what the molecular basis for the code origin was. Because the correlation does show that hydrophobic amino acids tend to have hydrophobic anticodons and hydrophilic amino acids tend to have hydrophilic anticodons, one would think we might find selective affinities between amino acids and nucleotides. We first found such selectivities using thermal proteinoids and homopolyribonucleotides. In those experiments (2) Lys-rich, Gly-rich and Pro-rich thermal proteinoids preferentially precipitated with their anticodonic homopolynucleotides. Phe-rich thermal proteinoid only selected its anticodonic polynucleotide, Poly A, when the precipitation was carried out in the presence of 25% ethanol. This suggested that the hydrophobic Phe residues were folded inward and could not express themselves unless unfolded by a hydrophobic solvent. Subsequently, we showed, using NMR (3), that Phe has the highest binding constant for 5'-AMP, its anticodonic nucleotide (Table II).

Subsequent work with Phe, Leu, Val and Ile showed that their binding for 5'-AMP or Poly A central letter of their anticodon decreased as the hydrophobicity of the amino acid (4). This general principle, first noted by Reuben and Polk (5), holds true in all of our experiments. Given a hydrophobic moiety, the binding of a second moiety to the first declines as the hydrophobicity of the second moiety declines. While we continue to work on such selectivity in binding, which seems to be favoring the anticodonic

TABLE II

Binding constants of MeOPhe for the mononucleotides

5'-Nucleotide	Binding Constant, M^{-1}
AMP	6.6
GMP	3.5
CMP	2.2
UMP	1.1

Data from Khaled *et al.* (1983). Binding constants were calculated from changes in chemical shifts of nucleotide protons as MeOPhe concentration increased. 300 MHz NMR operated in pulse Fourier mode, pD 7 and room temperature.

model, binding itself only relates to recognition. We have, however, also found selectivity in reaction which parallels the binding preferences (6-8). I'll only give one example of that although we've found several cases. We studied the reaction of acetylphenylalanine imidazolide with 5'-AMP and 5'-UMP. The reaction with 5'-AMP proceeds much faster than does 5'-UMP (Fig. 2). As seen in Table II, the binding constant for 5'-AMP is $6.6M^{-1}$ and for 5'UMP is $1.1M^{-1}$ (3). Reaction rate correlates with binding suggesting that increased binding increases the reaction rate. By running the reaction at three different temperatures, we could calculate the energy and entropy of activation. The results showed that it was the entropy of activation which speeded up the reaction. Thus it does appear that positioning of the Ac-Phe-AMP pair was better than the ac-Phe-UMP pair.

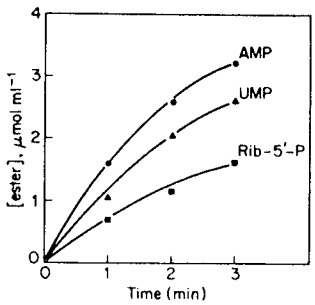

Figure 2. Reactions of Ac-Phe-imidazolide with 5'-AMP, 5'-UMP and ribose-5'-phosphate at -5 °C, pH 7 in 13% DMF. Nucleotide concentration 9.2 μmols/ml, initial imidazolide concentration 92 μmoles/ml.

As a result of these experiments and numbers of others which I do not report here, we believe as we proposed many years ago (9), that the origin of the genetic code (and the process of protein synthesis) was based on selective affinities between amino acids and their anticodonic nucleotides, the affinities giving rise to selective reactions (6-8). ■

REFERENCES

1. Lacey, J.C., Jr. and Mullins, D.W., Jr. (1983) Orig. Life 13, 3-42.
2. Lacey, J.C., Jr. Stephens, D.P. and Fox, S.W. (1979), Biosyst. 11, 9-17.
3. Khaled, M.A., Mullins, D.W., Jr. and Lacey, J.C., Jr. (1984) J. Mol. Evol. 20, 66070.
4. Khaled, M.A., Mullins, D.W., Jr., Swindle, M. and Lacey, Jr.C., Jr. (1983) Orig. Life 13, 87-96.
5. Reuben, J. and Polk, F.E. (1980) J. Mol Evol. 15, 103- 112.
6. Lacey, J.C., Jr. and Mullins, D.W., Jr. (1985) J. Theo. Biol. 115, 595-601.
7. Lacey, J.C., Jr., Hall, L.M. and Mullins, D.W., Jr. (1984) Orig. Life 20, 66-70.
8. Mullins, D.W., Jr. and Lacey, J.C., Jr. (1986) J. Mol. Evol. 23, 76-79.
9. Lacey, J.C., Jr. and Weber, A.L. (1976) in Protein Structure and Evolution (L. Fox, Z. Deyl, and A. Blazej, eds.) Marcel Dekker, Basel pp 213-222.

OXYGEN IN THE EARLY ATMOSPHERE

J. S. Levine
Atmospheric Sciences Division, NASA Langley Research Center, Hampton, Virginia 23665-5225

INTRODUCTION

Oxygen was a key gas in the early atmosphere due to its biological and atmospheric chemistry significance. The buildup of atmospheric oxygen led to the development of respiration in living systems and to the photochemical production of atmospheric ozone. Once ozone developed in the atmosphere and shielded the surface from biologically lethal solar ultraviolet radiation (200-300 nm), life was free to leave the protection of the oceans and go ashore for the first time in history. We have investigated the abiotic photochemical production of oxygen as a function of the level of incoming solar radiation (which initiates the photochemical production of oxygen) and atmospheric levels of carbon dioxide (a

source of oxygen atoms) and molecular hydrogen (which chemically destroys atmospheric oxygen) (Levine, 1985; Levine and Augustsson, 1985). In the present study, we have investigated the level and distribution of oxygen in the early atmosphere as a function of tropospheric water vapor and as a function of a possible surface source of oxygen, either abiotic of biotic.

THE ROLE OF WATER VAPOR

To assess the sensitivity of the photochemical production of oxygen to the level of water vapor (a source of oxygen atoms) in the troposphere, we have arbitrarily increased the "standard" temperature profile of the early troposphere by increments of 5°K, from 5°K to 20°K and then calculated the new H_2O vapor profile by assuming, near, but below saturation H_2O conditions. Our photochemical calculations indicate that contrary to intuition, surface levels of oxygen decrease with increasing levels of tropospheric water vapor. This is due to the fact that increased levels of tropospheric water vapor result in a significant decrease in the photolysis rate of H_2O, the source of oxygen atoms. Our calculations indicate that the photolysis rate of H_2O decreases by more than 10 orders of magnitude as the level of tropospheric water vapor increases by less than one order of magnitude.

THE ROLE OF A SURFACE OXYGEN SOURCE

To assess the sensitivity of the level and distribution of oxygen to a surface oxygen source, either abiotic or biotic, we have imposed an arbitrary surface source of molecular oxygen, with a flux varying from zero to 1×10^{12} oxygen molecules $cm^{-2}s^{-1}$, which corresponds to about 3×10^{14} moles of oxygen $year^{-1}$ (the present global production rate of oxygen via photosynthesis is about 10^{16} moles of oxygen $year^{-1}$). The level and distribution of oxygen was calculated with a prescribed surface oxygen flux in our

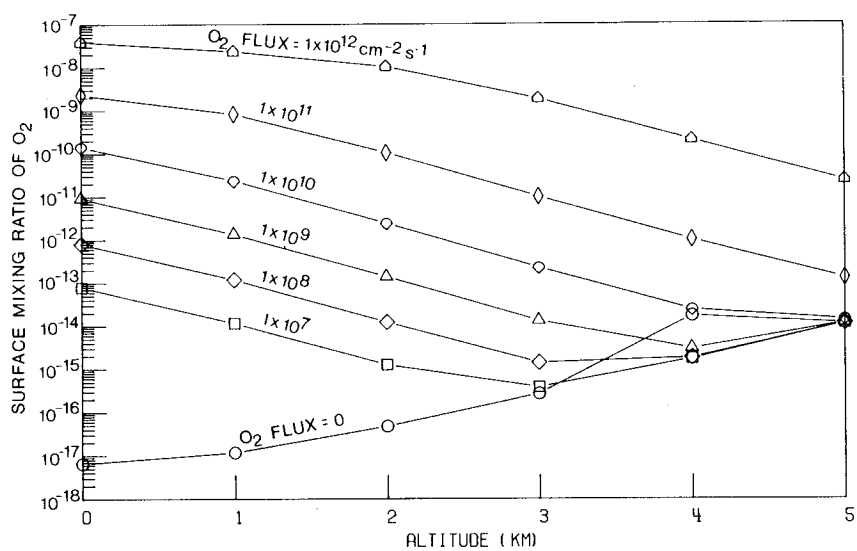

Figure 1. The vertical distribution of molecular oxygen from the surface to 5 km for a surface oxygen flux that varies from 0 to 1×10^{12} oxygen molecules $cm^{-2}s^{-1}$

photochemical model of the early atmosphere. For a zero surface flux of oxygen, the calculated surface mixing ratio of oxygen was found to be about 10^{-17}. For a surface flux of 1×10^{7} oxygen molecules $cm^{-2}s^{-1}$, the surface mixing was 10^{-13} and increased by about an order of magnitude for each order of magnitude increase in surface, reaching a mixing ratio of about 10^{-8} for a surface flux of 1×10^{12} oxygen molecules $cm^{-2}s^{-1}$ (see Fig. 1). ■

REFERENCES

Levine, J.S. The Photochemistry of Early Atmosphere. The Photochemistry of Atmospheres: Earth, the Other Planets, and Comets (J.S. Levine, ed.) Academic Press, Inc., 3-38, 1985.

Levine, J.S. and Augustsson, T.R. The Photochemistry of Biogenic Gases in the Early and Present Atmosphere. Origins of Life. 15, 299-318, 1985.

Figure 1. The vertical distribution of molecular oxygen from the surface to 5 km for a surface oxygen flux that varies from zero to 1×10^{12} oxygen molecules $cm^{-12}s^{-1}$

ABIOTIC SYNTHESIS OF ORGANIC GASES AND AEROSOLS IN THE ATMOSPHERE OF TITAN

T. W. Scattergood[1], C. P. McKay[2], W. J. Borucki[2], L. P. Giver[2], B. J. O'Hara[2], S. L. Miller[3]
[1]*State University of New York at Stony Brook, Stony Brook, New York 11794,* [2]*NASA - Ames Research Center, Moffett Field, California 94035,* [3]*University of California at San Diego, La Jolla, California 92093*

Saturn's satellite Titan has received much attention in recent years because of its extensive atmosphere and thick clouds. Ground-based and spacecraft (Voyager) observations of this satellite show it to possess a substantial atmosphere dominated by nitrogen, but also containing several simple hydrocarbons, nitriles, carbon monoxide and carbon dioxide (Hunten, *et al.*, 1984). At least three haze layers are present, one of which gives the satellite its red-orange color. The presence of these materials (and those which have not yet been detected) indicates the occurrence (past or present) of active chemical processes. Due to the lack of oxygen, Titan's atmosphere may represent a model for the atmosphere of the early earth (Owen, 1982). Thus the study of the nature and distribution of the materials present in Titan's atmosphere should provide important information for correlating the relationship between chemical evolution and planetary evolution in our solar system.

Titan's atmosphere may have been chemically different in the past, in particular, the concentration of CH_4 may have been higher than it is today. This suggestion was made based on the results of theoretical studies modeling the photochemistry of CH_4 in the atmosphere (Lunine, *et al.*, 1983). In these models, the CH_4 in the upper atmosphere is converted into ethane, hydrocarbons, and other simple organic compounds. These species can then coalesce into particles (droplets) which can fall through the atmosphere to collect on the surface. If ethane is indeed the dominant product, then the surface of Titan may be covered with an ethane 'ocean,' as the surface temperature is only 94 K. Because the troposhere below the visible cloud deck is invisible to remote observations in the infrared, not much is known about this region except that clouds of liquid methane may exist (Thompson and Sagan, 1984). This region may also be very rich in organic material transported down from the upper atmosphere and formed by lightning, if it occurs (Borucki *et al.*, 1984). Accumulation of these ultraviolet absorbing species over time would have changed the radiative properties of the atmosphere and, consequently, the temperature. This would effect the concentration of CH_4 and hence the rate of formation (and composition?) of the aerosols.

In order to study the chemistry and evolution of Titan's atmosphere, especially that of the troposphere, experiments are being carried out in which various mixtures of $N_2/CH_4/H_2$ representing Titan's atmosphere are subjected to electric discharge or ultraviolet light. Both gases and condensed phase materials were produced. When a nominal Titan mixture (96.8% N_2, 3% CH_4, .2% H_2) is subjected to electrical discharges the products are (in order of decreasing yield) C_2H_2, HCN, C_2H_6, C_2H_4, and C_3H_8, as shown in Figure 1. Note that except for the 1 spark case, which is most sensitive to analytical errors, the yields are essentially constant over a 20 fold range in energy (sparks). This order in yields is distinctly different from that for methane photolysis, where C_2H_6 is the primary product. In either case, however, all of the hydrocarbons so far observed on Titan can be made, but the distribution of such species may be different in the various regions of the atmosphere due to different formation mechanisms.

Experiments are also in progress to study the effect of varying the initial mole fraction of CH_4 on the production of HCN and C_2H_2. For these studies, laser supported detonations, simulating lightning (Borucki *et al.*, 1985), in the gas were used to initiate the chemical reactions. This technique has an advantage over the conventional spark methods due to the absence of foreign materials (*e.g.* electrodes) that may alter the chemistry being studied. Initial results show that the yield of acetylene increases monotonically with increasing mole fraction of methane, but that the yield of hydrogen cyanide increases until the mole fraction of methane is about 0.17. The yield of HCN then decreases with increasing mole fraction of CH_4. This behavior is not unexpected as the formation of HCN is limited by the availability of both N (from N_2) and C (from CH_4). Thus, the rate of formation of HCN in Titan's troposphere may have been higher in the past if the concentration of CH_4 was higher than it is today ($X \approx .03$).

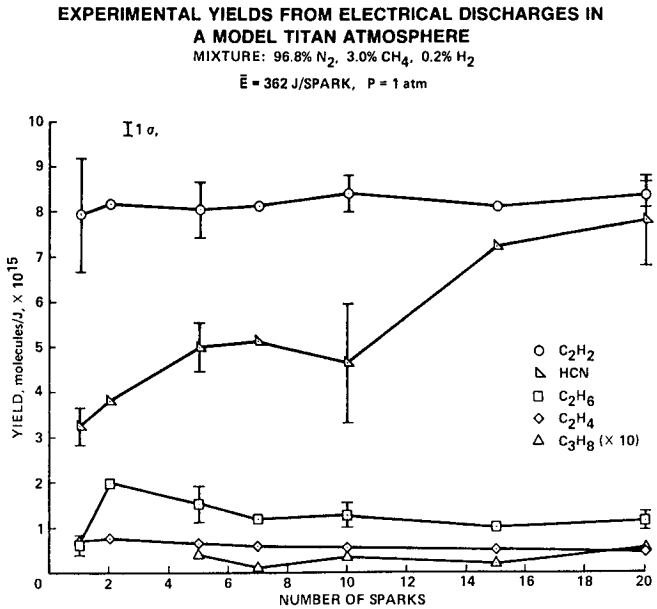

FIGURE 1

When the various gas mixtures are sparked long enough, a waxy reddish-brown solid is produced. This material was subjected to pyrolysis/gas chromatography, a technique that has been proposed as a method for analysis of Titan aerosols. Preliminary results, shown in Figure 2, reveal that the components of the material include simple hydrocarbons, HCN and CH_3CN, but little else. Since the material was

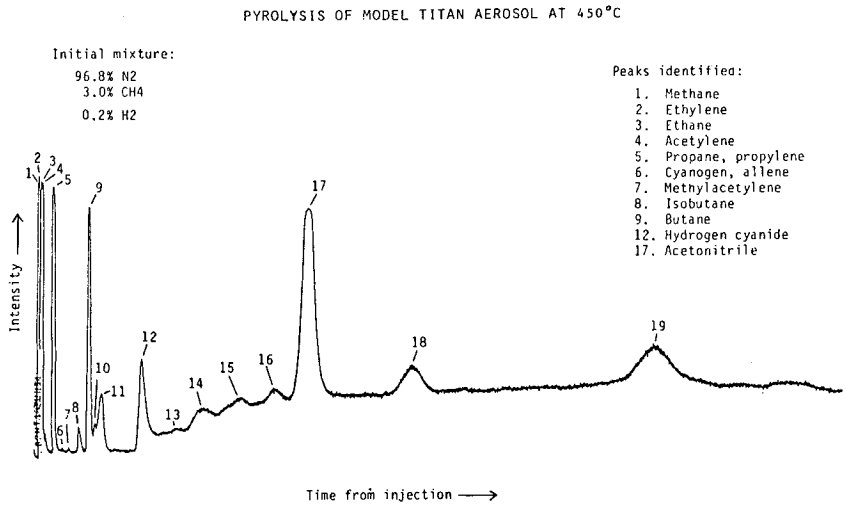

colored, solid, and at least part of it was not soluble in non-polar liquid ethane, compounds other than those mentioned above must be present. Studies of the variation of the composition and of the bulk elemental C/N/H ratios of the solid materials with composition (primarily the mole fraction of methane) of the gas mixtures are in progress and should provide information useful for the determination of the history of CH_4 in Titan's atmosphere. ■

REFERENCES
Borucki, W.J., McKay, C.P., and Whitten, R.C.: 1984, Icarus, *60*, 260.
Borucki, W.J., McKenzie, R.L., and McKay, C.P.: 1985, Icarus, *64*, 221.
Hunten, D.M., Tomasko, M.G., Flasar, F.M., Samuelson, R.E., Strobel, D.F., and Stevenson, D.J.: 1984, 'Titan,' in *Saturn*, Gehrels and Matthews, Eds., University of Arizona Press.
Lunine, J., Stevenson, D.J., and Yung, Y.L.: 1983, Science, *222*, 1229.
Owen,T.: 1982, Planet. and Spa. Sci., *30*, 833.
Thompson, W.R. and Sagan,C.: 1984, Icarus, *60*, 236.

ORIGIN OF GLYCOLYSIS: GLYCERALDEHYDE AS THE SUBSTRATE FOR EARLY GLYCOLYSIS AND PREBIOTIC POLYMER SYNTHESIS

A. L. Weber
The Salk Institute for Biological Studies, San Diego, California 92138

All organisms require a chemical form of energy for biopolymer synthesis. In contemporary life this chemical energy is obtained by the synthesis of the phosphoanhydride bonds of ATP. Although there are many biological processes that yield ATP, glycolysis is generally considered the most primitive because it is found in almost every living cell and operates under anaerobic conditions by a simple mechanism - substrate-level phosphosphorylation. In an effort to understand how useful chemical energy was obtained for the origin of life, we have studied nonenzymatic reactions resembling glycolysis that yield useful chemical energy.

Our early studies focused on the initial energy-yielding reaction of glycolysis. Since this glycolytic reaction involves the oxidation of glyceraldehyde-3-phosphate to give an "energy-rich" glyceroyl thioester which is used to drive the synthesis of ATP, we have 1) examined the nonenzymatic formation of thioesters from glyceraldehyde and a thiol, and 2) investigated thioester-driven phosphoanhydride synthesis. We showed that glyceraldehyde and a thiol could be converted to lactoyl thioester under anaerobic conditions and glyceroyl thioester synthesis in similar anaerobic reactions in the presence of oxygen (1, 2). We also obtained evidence of alanyl thioester synthesis in similar anaerobic reactions in the presence of ammonium ion (3). Our studies of thioester-driven phosphoanhydride synthesis demonstrated that thioesters can act as an energy source for the synthesis of pyrophosphate, tripolyphosphate, and phosphorylimidazole (4, 5). Phosphoanhydrides and phosphoamidates like these have been shown by others to act as condensing agents in prebiotic polymer synthesis (6, 7).

However, glyceraldehyde's role in prebiotic chemistry may not have been limited to its being an energy source for phosphoanhydride synthesis, since lactoyl, glyceroyl, and alanyl thioesters derived from glyceraldehyde are "activated" monomers which can form polyesters and polypeptides. This insight led to the development of a new hypothesis on the origin of life - the trioese model (8). In this model glyceraldehyde acts as a substrate for prebiotic polymer synthesis and the formation of "energy-rich" glyceroyl esters that drive the synthesis of phosphoanhydrides.

As shown in Figure 1, the triose model in its *simplest* form consists of three interconnected parts: the synthesis of glyceraldehyde from formaldehyde, an oxidative pathway that converts glyceraldehyde to polyglyceric acid, and autocatalysis by polyglyceric acid that includes rudimentary replication of the sequence of D- and L-residues in its structure. Also shown is phosphoanhydride synthesis (dashed arrow) which is driven by "energy-rich" glyceroyl esters of the C2-hydroxyl of residues of polyglyceric acid. The chemistry of the triose model is simple and resembles in some respects biological chemistry. The model also has the very attractive characteristic of uniting the origin of metabolism and polymer synthesis into a single process. This unification occurs because the oxidation of glyceraldehyde functions as the initial energy-yielding reaction of early glycolysis, and the polymerization reaction that yields polyglyceric acid - autocatalyst of the model.

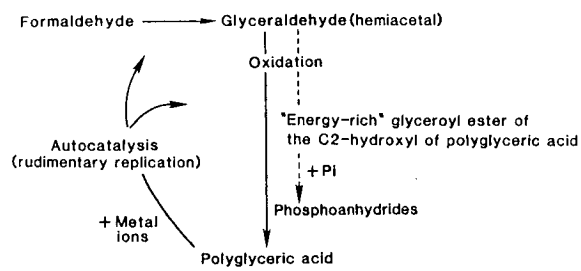

Fig. 1. Chemistry of the triose model.

In the model the synthesis of glyceraldehyde occurs by the condensation of formaldehyde in a manner that resembles the formose reaction (8-10). Formaldehyde has been synthesized under a variety of prebiotic conditions (11, 12). Furthermore, model studies that use an early earth atmosphere of N_2, H_2O, and CO_2 with trace amounts of H_2 and CO show the photochemical synthesis of formaldehyde in the atmosphere and its transport to the earth's surface by rain-out (13,14).

We began our studies of this new hypothesis - the triose model - by developing a thermal method for the synthesis of polyglyceric acid. We are now examining the hydrolytic stability of polyglyceric acid near neutral pH in order to access its stability in the prebiotic environment. We have also made preliminary measurements which indicate that α- and β-linked diglyceric acid are "energy-rich" esters. We are primarily interested in the glyceroyl ester of the C2- hydroxyl of glyceric acid (α-linked diglyceric acid) and are attempting to measure its standard free energy of hydrolysis. This energy value could be to estimate the standard free energy of hydrolysis ($\Delta G'$) of the glyceroyl ester of the C2-hydroxyl of residues of polyglyceric acid. Our earlier calculations indicate that this glyceroyl ester of polyglyceric acid is very "energy- rich" with a $\Delta G'$ of hydrolysis of -9.1 kcal/mol (8). ■

REFERENCES:

1. Weber, A.L.: 1984, J. Mol. Evol. *20*, 157-166.
2. Weber, A.L.: 1984, Origins of Life *15*, 17-27.
3. Weber, A.L.: 1985, J. Mol. Evol. *21*, 351-355.
4. Weber, A.L.: 1981, J. Mol. Evol. *18*, 24-29.
5. Weber, A.L.: 1982, Bio Systems *15*, 183-189.
6. Hulshof, J. and Ponnamperuma, C.: 1976, Origins of Life *7*, 197-224.
7. Oro, J. and Stephen-Sherwood, E.: 1976, Origins of Life *7*, 37-47.
8. Weber, A.L.: 1987, Origins of Life, in press.
9. Gable, N.W. and Ponnamperuma, C.: 1967, Nature *216*, 453-455.
10. Reid, C. and Orgel, L.E.: 1967, Nature *216*, 455.
11. Miller, S.L. and Schlesinger, G.: 1984, Origins of Life *14*, 83-90.
12. Getoff, N., Scholes, G. and Weiss, J.: 1960, Tett. Lett. 17-23.
13. Pinto, J.P., Gladstone, G.R. and Yung, Y.L.: 1980, Science *210*, 183-185.
14. Kasting, J.F. and Pollack, J.B.: 1984, J. Atmos. Chem. *1*, 403-428.

THE ROLE OF HUMAN FACTORS IN SPACE

J. W. Brown
Crew Interface Analysis Section, Man-Systems Division, SP34, Johnson Space Center, Houston, Texas 77058

Human factors have played an important role in spaceflight, since the very first flights. From the first suborbital Mercury flight, it was learned that the astronaut could and might have to use attitude controls during the flight and descent. The Mercury window was moved after the first flight showed that a more direct line of vision would enhance the astronaut's earth viewing capabilities, and give him better feedback on the craft's attitude. That these manual controls were more than "pacifiers" became evident in John Glenn's orbital flight, during which a yaw thruster malfunctioned, and telemetry problems interfered with ground spacecraft control. The mission was brought to a successful end by skillful astronaut intervention.

While the number of displays and controls grew rapidly with increasing space missions, it was during Skylab that the first systematic study of human factors in space took place. Some studies were combined with medical data gathering. Is analysis of the neutral body posture and the resulting comfortable working position a physiological question or a human factors question? In any event, it was documented and analyzed, and has strongly influenced the design of the Orbiter and Space Station. Other studies were clearly in the realm of human-system interfaces. Restraint systems may have generated more comments and analysis that any other single feature. The difficulty of writing and managing paper lists and documents stemmed partly from the design of the writing table, and its dual function as a food preparation center. However, a major complaint was that there was no way to keep books open to the right papers, and that loose papers or long scrolls such as came off the teletype were unmanageable. In the Orbiter, elastic restraint systems are provided.

The techniques of human factors data collection were primarily in-flight questionnaires and conversations with Mission Control, and post-flight debriefings. Some more quantitative data was collected through the analysis of movies and photographs taken in flight. These are still the techniques in use. One current in-house project is developing better requirements for in-flight videotape documentation of crew member performance. This project is simultaneously developing non-intrusive methods of monitoring such physiological indicators of workload as electrocardiographs and electromyographs.

During Orbiter design and construction, the Spacecraft Design Division maintained the Crew Station Design Branch which was particularly concerned to analyze the lessons from Skylab and apply them to the Space Shuttle. One example of this effort was the design of operator control modes of the Remote Manipulator System (RMS). The RMS can be controlled in a joint-by-joint manner. However, the more frequently used modes are ones that relate directly to what the operator sees looking out the window (orbiter coordinates) or to what he or she sees looking at the payload or the camera mounted on the RMS's tip. These provide a computer- aided augmentation of the operator's instructions, reducing them automatically to the joint-by-joint motion which is all the arm is capable of.

During the planning stages of Space Station, Johnson Space Center instituted a division whose name describes its function: the Man-Systems Division. The engineers and scientists in this division have as their goal increasing human productivity through better design of the spacecraft and its human interfaces. Research conducted in the Man- Systems Division is sponsored by OSSA and OAST, and centers on such questions as the physical fit between the spacecraft and its occupants, the enhanced productivity of engineers in spacecraft design when human factors requirements are made known in an interactive graphical mode, and the increased effectiveness of the crew when human-machine interfaces are well designed. ■

DATA COLLECTION FOR HUMAN WORK PERFORMANCE IN SPACE

M. C. Greenisen
Biomechanics Laboratory, University of Wisconsin- Milwaukee, Milwaukee, Wisconsin 53201

This investigation evaluated STS Space Suited (3.7 PSID) and unsuited astronaut dominant upper limb skeletal/muscle work performance with a *Cybex* Dynamometer during Zero Gravity (0-G) and Space Suited only performance testing during neutral buoyancy (NB). The purpose of this study was to determine the extent to which the Space Suit affects work performance and skeletal muscle force applications, in order to quantify future EVA dominant upper limb work performance expectations.

Subjects were five Mission Specialist astronauts, four male and one female. All subjects were right-hand dominant.

Zero-G data was collected while flying parabolas on board NASA/JSC modified KC-135 aircraft. Each parabolic trajectory maneuver flown by the aircraft provided three-dimensional 0- G for 20-25 seconds per maneuver. NB testing occurred underwater in NASA/JSC Weightless Environment Training Facility (WETF).

The test article, a *CYBEX* Dynamometer measures skeletal muscle force applied, through a circular range of motion, against the shaft of the dynamometer in foot pounds of torque. The test article was calibrated before each data collection period. The dynamometer is electrically powered by a square wave pulse width modulation signal averaging 35 volts DC.

In order to use the dynamometer underwater in JSC's WETF, a waterprooof container was engineered and fabricated. The dynamometer waterproof container is nitrogen charged and maintained at 4.0 PSID when submerged.

To standardize testing, data was collected during 0-G flights as well as NB with the dynamometer in the sealed, waterproof container and mounted on a dedicated stand.

The subject test conditions were designed to replicate typical upper limb EVA work requirements. In order to most accurately reflect actual dominant limb work performance parameters, all testing was performed without a stabilizing hand hold for the non-dominant upper limb. Subjects performed all tests while standing in EVA foot restraints. The foot restraints were secured to the platform of the test articles stand.

Each test condition was performed utilizing three different resistance velocities; each velocity received three trials.

The test conditions were: 1) EVA ratchet wrench crank, 135 degree range of motion clockwise, with resistance velocities of 60, 180, and 0 deg./sec.; 2) Handle turn, supination (clockwise); 3) Handle turn, pronation (counterclockwise), both handle turns had 180 degrees range of motion, with resistance velocities of 30, 120, and 0 deg./sec.; 4) EVA ratchet wrench push (counterclockwise); 5) EVA ratchet wrench pull (clockwise), both the push and pull had 90 degree range of motion, with resistance velocities of 60, 180, and 0 deg./sec.

Work performance abilities with the EVA ratchet wrench crank ranged from 84 ft. lbs. torque at 60 deg./sec. unsuited during 0-G to 15 ft lbs. at 180 deg./sec. Space Suited, also in 0-G. The Space Suit reduced performance in 0-G by 23 and 33 per cent at 60 and 180 deg./sec. during the dynamic movements. However, the Space Suit enhanced isometric (0 deg./sec.) ability by 8 per cent in 0-G. NB isometric performance was increased another 17 per cent over 0-G, Space Suited.

Handle turning performance ranged from 30 ft. lbs. of torque at 30 deg./sec. during pronation in 0-G, Space Suited, to 3 ft. lbs. at 120 deg./sec. during supination in 0-G, Space Suited. Individual supination values were remarkedly consistent across 0-G Space Suited, Unsuited and NB conditions, except 0-G Space Suited isometric supination force increased 10 per cent compared to 0-G Unsuited. However, the Space Suit enhanced pronation performance by 34, 37, and 47 per cent at 30, 120, and 0 deg./sec. NB results produced further increases in pronation performance ability compared to 0-G.

EVA ratchet wrench push values ranged from 69 ft. lbs. torque at 0 deg./sec. during NB to 12 ft. lbs. torque 0-G Space Suited at 180 deg./sec. Space Suited and Unsuited individual wrench pushing performance, in 0-G at 60 and 0 deg./sec. were similar. The Space Suit reduced 0-G pushing force by

17 per cent at 180 deg./sec. NB performance at 60 deg./sec. were similar to 0-G Space Suited and Unsuited ability. However, performance in NB at 0 deg./sec. was 40 per center greater than 0-G Space Suited and Unsuited push performance.

EVA ratchet wrench pull performance levels ranged from 84 ft. lbs. torque in NB at 0 deg./sec. to 12 ft. lbs. during 0-G Unsuited, 60 deg./sec. In 0-G, the Space Suit increased pulling ability by 21, 27 and 29 per cent at 60, 180 and 0 deg./sec. During NB pull force exceeded Space Suited 0-G force by 8 and 15 per cent at 60 and 0 deg./sec.

Only a limited number of subjects have been tested to date; however, some interesting trends are developing.

The effect of the Space Suit on performance was surprisingly uniform across all subjects in the per cent of reduction on enhancement compared to unsuited 0-G performance. These effects on performance occurred even though the subjects had distinctly different initial levels of skeletal muscle force production abilities.

In some cases the Space Suit impacts substantially on performance such as the EVA ratchet wrench crank. On the other hand, during handle turning pronation and EVA ratchet wrench pulling, the Space Suit seems to provide a distinct mechanical advantage enhancing performance. However, during dynamic handle turning supination and EVA ratchet wrench pushing, the Space Suit seemed to be neutral in effect. Curiously, the Space Suit provided an isometric mechanical advantage in every test but wrench pushing.

This testing indicates that when there is a need to understand Space Suited human work performance, absolute force levels, 0-G KC-135 flight data will be the most accurate.

These data also suggest that practice in the Space Suit learning to refine a variety of movement patterns in the WETF may be important for future EVA crew training considerations. ■

MODELING AND ANIMATING HUMAN TASK PERFORMANCE

N. I. Badler
Computer and Information Science Department, University of Pennsylvania, Philadelphia, PA 19104- 6389

With the widespread acceptance of three-dimensional modeling techniques, high-speed hardware, and relatively low-cost computation, modeling and animating one or more human figures for the purposes of design assessment, human factors, task simulation, and human movement understanding has become quite feasible. Though not recent, the demand for creating, modeling, and controlling one or more human figures in a 3-D world is expanding and the application base is growing. Human figure models have long been used in cockpit and automobile occupant studies; now they are finding application in vehicle and space station design, maintenance assessment, and product safety studies.

With the expansion of the 3-D CAD field to include a large number of competent and competitive products human figure modeling must be to fit into this environment rather that supplant it [3]. The human figure must become just one other object to the design system, albeit one with very special capabilities, requirements, and size variability.

We have designed, developed, and built a human figure modeling system which acts as an adjunct to a CAD system for human factors assessment. The principal functions of this system, called TEMPUS [1], are:

- Creating and selecting individual or statistical human figure models and body sizes.
- Providing interfaces to CAD object information for workplace descriptions.
- Positioning body segments and reaching workplace points.
- Providing fast and high quality graphics output for both bodies and objects.

We are currently extending TEMPUS into a *task analysis* tool for assessing the actions of one or more individuals in a given environment. For example, the tasks to be performed are enumerated and decomposed into simple, primitive tasks such as reach, view, grasp, transport, etc., each of which has an instantiation as a sequence of movements. Given an environment (3D workplace), agent(s) (human

or robotic figures to carry out task actions), and the task lists, the system will be able to evaluate the performance of the agents doing the tasks in that environment. By performance we mean

- Reach assessment. For an individual or a population, specify end effector(s) and fixed ends or restraints. Figure must reach a point in space or a workplace point. Show failure distance, reachable objects, and reachable space.
- View assessment. For an individual or a population, specify one or both eyes and the viewed point. Show the corresponding view and show or list visible objects.
- Collision and interference detection. Adjacent body segment collisions are checked by joint limits. Non-adjacent segment collisions depend on the particular geometric representation of the body. Collisions of body with environment need hierarchic bounding boxes for efficiency. A real-time display maybe used for simple visual assessment without computation.
- Strength or reaction force assessment. Determine the nominal or maximum force or torque achieved at a body part or end effector. Forces must be resisted, maintained, or reacted through restraints.
- Task load. Determine whether or not a task can be executed in some specific circumstances, whether two or more agents can work in parallel, whether fewer agents can get the jobs done, how much motor or psychomotor workload is imposed on each agent, and so on.

System Components

There are many components required to realize this task performance analysis system. The TEMPUS system and its evolving suite of programs is directly addressing large scale questions of effective, general purpose, flexible, and usable human factors analysis tools. Figure 1 is a block diagram of the structure of the task analysis system. In general, boxes denote processes and arrows denote data flow (structures or files) or access. Below we give a summary of the characteristics of each component.

Workplace models

Workplace geometry is obtained from an existing Computer- Aided Design System. Interfaces to CAD systems providing either boundary polygons or constructive solid geometry are available.

Figure models

Computer graphics figures with reasonable human-like appearance are provided in TEMPUS. There are at least four different levels of detail that can be used. The most detailed models are BUBBLE people: they look surprisingly life-like and yet are neither expensive nor difficult to move and display. The models are sized from anthropometric data and stored in a database (ADB).

Position control

An articulated figure is manipulated by specifying joint orientations or end effector goals, subject to known joint limits [7].

Motion playback

Articulated figures are animated in real-time so that motions may be assessed and tasks validated. The real-time playback is effected on a Silicon Graphics Iris Workstation.

Kinematics

A human or robot figure model must be kinematically- controlled so that goals and constraints may be used to position and orient the parts and end-effectors [4].

Constraint Language

A goal and constraint language may be used to communicate position and orientation information to the body or robot [5].

Dynamics

External or internal forces or torques may be applied to the articulated figure to produce motion. Dynamic control is most useful for fast motions, for response to external forces (such as gravity), and for incorporating strength models.

Task expert

An expert system shell transforms task descriptions into constraints, goal and dynamics. More than one agent may be utilized. The expert system handles task simulation, agent interaction, and possibly motion planning [6].

Agent models

Agent capabilities and responsibilities are modeled explicitly. This includes not only physical attributes, but also preferences, duties, limitations, etc.

Task definitions

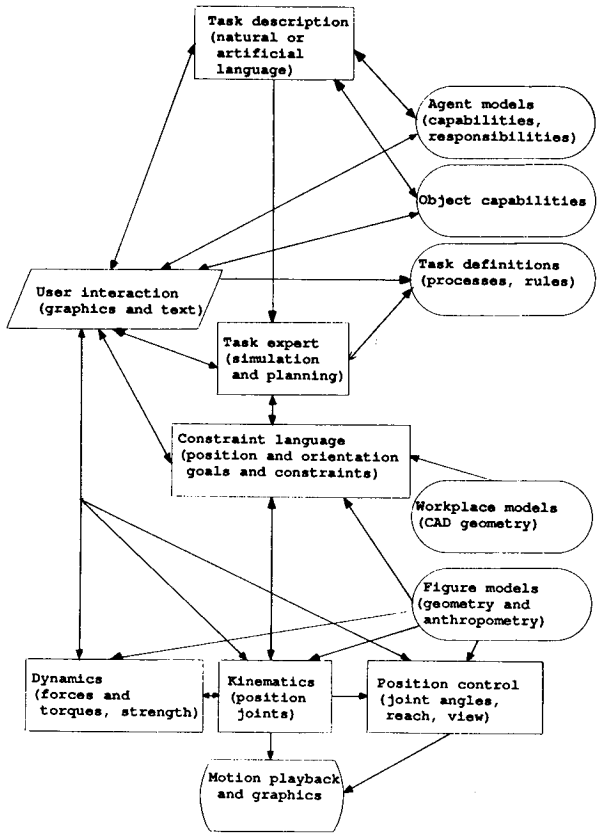

Figure 1. Block diagram of human factors assessment system.

Tasks are defined by rules or procedures, decomposed into simpler acts the system can interpret as goals, constraints, affected objects, paths, directions, etc. Task definitions are built from process models (scripts, Petri nets, data flow diagrams, production rules, or discrete or continuous simulation models) [6].

Task description

Tasks are provided by commands in a subset of natural language or in an artificial (such as NASA Flight Data File) command language [2].

Knowledge bases

Knowledge bases store information shared across system components, such as the geometry data, the anthropometric database, the agent models, the task descriptions, and object capabilities. Object capabilities are used to determine the meaningfulness of a task command and the results of the action on the workplace environment. Sample interaction with control panel objects and their inter-relationships have been investigated. Some of the databases reside in the DEC Relational Data Base system, including part of the task definition knowledge base.

User interaction

The user may interact with the task analysis system models at any level. It is expected that different tasks will require utilization of various parts (and maybe all) of the whole system. All interaction is through effective computer graphics interfaces or flexible language understanding processors.

Status

The TEMPUS project is a major software activity initiated and encouraged by the Crew Station Design Section of NASA Johnson Space Center. All of the system components in Figure 1 are functioning in some form. Almost all of the interfaces are functioning. Though significant efforts remain to broaden the scope of some of the components and build task vocabulary, agent models, and additional user interfaces, we are confident that feasibility is demonstrable. Moreover, any approach to human factors that fails to include all these processes can be shown to have significant weakness for certain analysis and assessment tasks. ■

REFERENCES
1. Badler, NI, Korein JD, Korein JU, Radack G, Brotman LS. Positioning and animating human figures in a task-oriented environment. The Visual Computer: The International Journal of Computer Graphics 1, 4(1985):212-20.
2. Badler NI and Gangel JS. Natural language input for human task description. Proc. Instrument Society of America ROBEXS '86: The Second International Workshop on Robotics and Expert Systems, June, 1986, pp. 137-48.
3. Badler NI. Modeling and animating human figures in a CAD environment. Proc. NCGA '87; Tutorials, Vol. 1, 1987, pp. 93-111.
4. Badler NI, Manoochehri K and Walters G. Articulated figure positioning by multiple constraints. IEEE Computer Graphics and Applications 7, 6 (June 1987).
5. Badler NI, Esakov J, Koelewyn L and Walters G. Animation using constraint-based kinematics. Dept. of Computer and Information Science, Univ. of Pennsylvania, Philadelphia, PA 1987 (Submitted to SIGGRAPH '87).
6. Fishwick PA. Hierarchical Reasoning: Simulating Complex Processes over Multiple Levels of Abstraction. Ph.D. Th., Dept. of Computer and Information Science, University of Pennsylvania, Philadelphia, PA 1986.
7. Korein JU. A Geometric Investigation of Reach. MIT Press, Cambridge, MA 1985.

CAE IN HUMAN FACTORS FOR SPACE

L. S. Orr
NASA/Johnson Space Center, SP34, Houston, Texas 77058

The Johnson Space Center's Man-Systems Division (MSD) uses a computer aided engineering (CAE) package called PLAID (not an acronym) as a tool for evaluating human factors issues in spacecraft design and mission task procedures. PLAID is an interactive three-dimensional solids modeling graphics program that runs on a VAX 11/785 and various high-performance graphics workstations. The package includes special features for NASA-MSD specific interests, such as a Remote Manipulator System (RMS) simulation capability, and a man-modeling program for automatic generation of computer "human" models based on anthropometrically correct body segment size and joint limit data.

PLAID plays a significant role as an evaluation tool for increasing the effectiveness of man-machine interactions in spacecraft design. Engineers use it to identify human factors issues and correct potential problems in the early stages of workstation design and mission planning. PLAID is especially useful in zero-gravity analyses of anthropometric issues, since it is cheaper and quicker to perform an analysis by computer than by other zero-gravity simulation techniques (*e.g.*, submersion in a neutral buoyancy water tank). Using PLAID, engineers can help create more productive and comfortable environments for living and working in space.

Specific examples of analyses performed with PLAID include viewing assessments, anthropometric evaluations of reach envelopes, clearance studies, and graphical depiction of mission planning scenarios. For Shuttle support, PLAID is used to study potential RMS operations, to help develop mission procedures, to aid cargo integration in the payload bay, to perform "fit checks" of human anthropometry for proposed crew escape systems, and to provide illustrations for crew training purposes. For Space Station support, PLAID is being used extensively for cupola and window viewing analyses, to evaluate the effect of zero-g anthropometry on crew quarters design, and to study other human factors concerns such as accessibility of equipment and traffic patterns within modules.

PLAID research and development efforts include an animation tract for real-time mission task planning evaluations, incorporation of strength and motion data into its computer-generated human models, and the addition of Artificial Intelligence features to the program for increasing the sophistication of its analyses. The presenter will include still photo examples of both PLAID analyses and their actual in-flight counterparts, and time permitting, will also show a short film clip of examples. ■

LIVING AND WORKING IN SPACE

W. R. Pogue
Space Station Program, Boeing Aerospace Company, 499 Boeing Blvd., Bldg. 6-6010, Huntsville, Alabama 35806

Developing an ability to anticipate the various human engineering implications of the weightless (or 0-g) environment of outer space poses a special problem for designers, planners, and engineers. This presentation consists of a film entitled "Living and Working in Space." The film is intended to serve as a training device to create an awareness of 0-g human factors issues.

During the ten-year period from 1964-1974 the U. S. Space Program developed rapidly in the complexity of operations conducted. There was an ever increasing sophistication of the hardware and an expanding role for crew members who were learning to cope in the weightless environment of space and reduced gravity on the lunar surface. Support personnel, such as flight controllers and procedure writers, maintained a close link with the flight crews. Each new discovery pertaining to the low-g working environment was shared by all and the supporting personnel attained an effective working awareness on par with the crew members. Through the normal course of planning meetings and design reviews, general human factor principles of spaceflight operations were also conveyed to managers, engineers, and designers. By the end of the Skylab program in 1974, NASA and its contractors had a work force with a large cross-section cognizant of the peculiar human engineering requirements of working in space. These people, capable of "thinking space," exerted influence at all levels and had the ability to improve planning, development, and decision making relevant to space operations.

Although some of these people still serve in positions of responsibility at NASA and within the aerospace industry, their number has been reduced by retirement, transfers and promotion, and work force reductions.

By the mid-1980's, NASA and its aerospace supporting contractors had a work force of senior employees who had matured with the space program and "new hires" who were just beginning their aerospace careers in support of manned space efforts.

During 1984, Jerry Carr and Bill Pogue, Commander and Pilot respectively of Skylab 4, identified in the aerospace industry the new employee's difficulty in becoming accustomed to think in terms of the weightless environment and the human factors implications. The former astronauts tried several approaches to generate an effective level of 0-g understanding. The most successful technique was the use of film and videotapes from Skylab and Shuttle operations. This effort was supported by the aerospace industry, and the result was the film, "Living and Working in Space." It incorporates scenes from Gemini, Apollo, Skylab, and Shuttle, and is intended to provide a wide scope general introduction to 0-g human factors/human engineering issues. Further, the film is designed to create an awareness of the basic 0-g considerations applicable to planning, engineering, and design work. The content is biased toward the special requirements of the Space Station effort and long-duration space flights, such as the 84-day Skylab mission the author participated in. ■

HUMAN PERFORMANCE MODELING AND DATA COLLECTION

B. Woolford
Crew Interface Analysis Section, Man-Systems Division, Johnson Space Center, Houston, Texas 77058

The Anthropometrics and Biomechanics Lab (ABL) at Johnson Space Center collects data for use in human modeling for spacecraft design. Types of data collected include static anthropometric data, reach envelopes, and dynamic measures of force capability. This presentation will describe the data collection purposes, techniques, and applications.

Static body measurements are collected on all individuals who are invited to the Center to be interviewed for positions as astronauts. This data base has been growing since 1977 Current measurements include stature, seated eye height, fingertip reach, and hand size, and other measurements needed for building the body models in TEMPUS. The ABL also obtains data from other sources. For example, the Japanese Space Station liaison office provided extensive anthropometric data on Japanese females to aid in specifying body sizes for Space Station design.

Currently the anthropometric data is collected with traditional instruments such as calipers and tape measure. However, in conjunction with Wright Patterson Air Force Base, the ABL is developing a 3-D digital mapping system which will permit acquiring a digital image of the body in a matter of minutes. This data can later be analyzed to provide the standard measurements, or can be used directly by CAD systems to represent the human. These measures are all taken in the lab, under one-g conditions. However, inflight measurements provide guidelines for predicting the changes in body size that will occur in 0-g. These percentage changes can be used to estimate inflight sizes for astronauts on their first flights. This data is available in tables, but is primarily accessed through TEMPUS to display specified percentile bodies in the spacecraft environment.

The ABL collects a great deal of reach data. These envelopes outline the 3-dimensional region in space in which a person can work. Two studies have been completed. One compared the reach envelopes of a large male subject with those of a small female subject. Envelopes were collected in shirt-sleeves and in pressurized space suits. All measurements were taken in one-g; however some support and weight relief was provided for the suited condition by suspending the suit's weight from an overhead crane. Another reach study compared the Shuttle Extravehicular Mobility Unit (EMU) with a prototype zero-prebreathe suit (ZPS). The EMU operates at 4.3 psi, while the ZPS is designed for 8 psi. Despite the higher operating pressure, the difference in design appeared to provide for greater mobility in the ZPS.

Reach data is collected by use of a commercially available Selspot System, which uses four cameras to obtain spatial coordinates of up to 30 LEDs.

The data from any non-colinear pair of cameras can be used to triangulate the three-dimensional location of the LED. LEDs are generally attached to the fingertips, the palm of the hand, and other points of interest in mapping. The digital data from each camera is recorded on tape during the test, and later played back to a VAX 11/785 for calculation of the 30D coordinates. Further processing is done through PLAID, which presents the points for a given "slice" or small vertical intervals, for the physiologist to examine. The physiologist draws a contour enclosing the points, smoothing where necessary for physical considerations, and after all slices are contoured, they are assembled into a 3- D solid which can be presented graphically, attached to the body, to demonstrate the intersection of the reach envelope and the workstation.

The ABL has begun collecting strength and force capability data in the last two years. A study of hand grip strength with the bare hand, with an unpressurized EVA glove, and with a pressurized EVA glove, was carried out last year. The data show significant differences in the various conditions, which must be taken into account when planning EVA tasks. The data was also collected as a function of elbow and wrist angles, to permit accurate man modeling.

A Cybex dynamometer was used in a study of the effect of surface type on the amount of torque that could be applied to a strut, to join it to a node, in a study in support of Space Station construction. The dynamometer allows the experimenter to control the speed with which the strut rotates. More force can generally be applied at lower speeds. The study showed that one of the four surfaces tested was significantly better than the other three.

Besides the hand and wrist, whole arm movements have been studied. A waterproof container and mounting stand was built for the Cybex, and data has been collected in the neutral buoyancy simulation of weightlessness, and in the true, but brief, periods of weightlessness experienced in parabolic flight. Data from those studies will be presented in a separate paper.

The Cybex allows primarily rotational motion. It is designed to enable physical therapists to place the center of rotation along the joint axis, and measure the strength of the specific joint. This data is needed for the TEMPUS man models, which will attempt to combine strengths as functions of positions of the individual joints into predictors of the strength of the whole arm. To collect total, resolved strength in a straight line, or in a rotation where several joints are working together, another device is being designed and constructed. It too will control the speed at which the subject can move. It is being designed to fit in a double locker space, in hopes of flying it in the Orbiter to collect true 0-g data as a function of time in flight.

Presentation of reach and strength data is a problem, as the data are inherently three and even four dimensional. Techniques are being worked out in TEMPUS to use contours and color coding to display the amount of force that can be exerted in a specific 3-D location by a person restrained in a specific place and manner.

This data collection, analysis, and presentation is an ongoing research project in the ABL, supported by OSSA Life Sciences RTOPs. ■

PAGE 295 INTENTIONALLY BLANK

PRECEDING PAGE BLANK NOT FILMED

ENVIRONMENTAL DETERMINANTS OF BEHAVIOR IN SPACE

Y. A. Clearwater
Space Human Factors Office, NASA/Ames Research Center, Moffett Field, California 94035

The primary mission of the Ames Habitability Research Program is to improve understanding of environmental influences on human behavior and, as an outgrowth of this understanding, to produce guidelines for designing habitable facilities which will promote crew productivity and well-being on long duration space missions. The major goals of this program are to: 1) understand and minimize the effects of acute and long-duration environmental stresses on human behavior, 2) develop guidelines for the design of habitable and functional environments, 3) develop tools for the generation of design solutions and operational policies with design impact, 4) evaluate design solutions as they evolve, and later in operational environments. Habitability research efforts currently underway at Ames include the development of human factors models for the determination of spatial habitability needs (physical and visual spaciousness), crew privacy requirements, functional decor concepts (color, lighting, spatial orientation aids, etc.), and efficient facility layouts. Other work includes the development of an operational computer simulation to provide a means for studying space crew activities, mission procedures, equipment usage, and other operational factors through simulation. In addition to these research efforts, in-house staff and grantees are developing "ideal design solutions" and architectural concepts to be tested for adherence to human factors requirements including a Space Station wardroom table, microgravity body restraints, and an EVA access facility. ■

CIRCADIAN AND RELATED FACTORS IN SPACE CREW WORK PERFORMANCE

R. C. Graeber
Aerospace Human Factors Research Division, NASA-Ames Research Center, Moffett Field, California 94035

The potential impact of circadian rhythmicity on space crew performance is derived from two sources. The first is the, sometimes unplanned, requirement to work at times near the nadir of the circadian performance cycle. The second is associated with the sleep loss which results from attempting to sleep in accordance with an altered circadian cycle. When combined, the effects of these two components have had serious effects on performance in both the U.S. and Soviet manned space programs.

A recent review of published accounts indicates that most reports of poor sleep in space can be attributed to altered sleep-wake cycles due to mission requirements, especially when comfort and noise interference can be ruled out. There are four types of space missions that raise different operational and biomedical concerns about planning for crew work schedules and sleep. These types include short-term shuttle flights, long-term space station habitats, lunar or planetary bases, and interplanetary flights. Each of these exposes the crews to different relationships among the environmental zeitgebers which moderate the human circadian system. Evidence from past missions can provide a framework for anticipating research needs for future missions. It is also clear that individual differences are important and may need to be seriously considered as selection criteria for long-term missions. Some guidance for such criteria and potential countermeasures may be forthcoming from parallel research on aircraft flight crews subjected to altered circadian working conditions. ■

THE POTENTIAL FOR HUMAN ERROR IN SPACE OPERATIONS

D. C. Nagel
NASA/Ames Research Center, Moffett Field, California

For all known systems in which humans interact with complex machinery, human error seems to play the predominant role in determining overall levels of safety. This is true not only in aviation, where the role of human error in aircraft accidents has been documented extremely well, but also in the nuclear power industry, marine systems, industrial systems, and various forms of surface transportation systems. For space operations, human error seems not to have contributed to the same degree as in other areas. There appear to be several reasons for this. First, space transportation systems are not yet as reliable as those in aviation, for example; most system failures represent "simple" hardware and software problems. For manned flight, unique approaches to the selection and training of flight and ground crews have no doubt played major roles in preventing human errors. For future space operations, some of the conditions which have prevented human error incidents and accidents may be altered to the degree that this will no longer hold. For instance, once space operations become more routine and crews more heterogeneous, very long duration training may simply not be as practical. Also, mission success will depend on the successful interplay of larger numbers of crewmembers; current training tends to be focused on the development of individual competence, not team effectiveness. In addition, if the experience in aviation is any guide, the increased use of and reliance on automated systems may play a role. New forms of automation in aviation are increasingly being implicated in new forms of human error.

In this paper, the role of human error in complex systems will be documented. What is known about the nature and cause of human error will be described, and, in particular, the scientific basis for the prediction of error will be reviewed in some detail. Finally, solutions to the error problem will be described as will the prescriptions for the prevention of human error in future long duration space missions. ■

HUMAN-MACHINE PERFORMANCE IN SPACE

R. Remington and E. Palmer
NASA/Ames Research Center, MS239-3, Moffett Field, California 94035

The complexity of manned spacecraft has increased steadily since the early Mercury spaceflights. The range of tasks for astronauts and ground crews has similarly grown as the capabilities of the spacecraft have increased, yet NASA crew and ground personnel have not increased to keep pace. Present levels of complexity have arisen primarily from increases in the number of subsystems and the diversity of in-flight tasks. However, future efforts, such as Space Station, will require significant amounts of automation to keep ground and space crews at reasonable levels, adding subsystem sophistication as another dimension of complexity. We will draw on laboratory studies and operational research on automation in civil aircraft to detail the problems associated with sophisticated, automated subsystems in dynamic environments. Our current approach focuses on providing operators with means of understanding and validating the performance of sophisticated subsystems. This will be illustrated using the development of a human interface to an expert system for the control of a space- borne thermal management system as an example. ■

THE PREDICTION AND MEASUREMENT OF MENTAL WORKLOAD DURING SPACE OPERATIONS

M. A. Vidulich and S. G. Hart
NASA/Ames Research Center, MS 239-3, Moffett Field, California

NASA formed a Workload Assessment Program at Ames in 1981. The initial focus of the program was on developing techniques to *assess* workload in aviation environments. The first phase of the program has been completed: a variety of measures has been developed, tested, and applied and criteria have been formulated to standardize the selection and application of workload measurement procedures that are appropriate for different applications. More recently, the focus has been on developing techniques to *predict* workload. Initially, this research element was focused on aircraft operations, as well.

The research results of both program elements have broad application beyond their initial vehicle-specific focus. The measures that have been developed and the conceptual framework of the predictive model can be applied to other environments, as well as aviation (given appropriate modifications), thereby capitalizing on the wealth of research already accomplished. The need for workload assessment and prediction procedures has been highlighted by two recent events in the aviation community: First, the Army has reversed an earlier decision that the next generation of scout-attack helicopters (LHX) would be operated by a single crewmember. This reversal reflects the results of numerous studies in which it was found that single-crewmember workload levels might be unacceptably high, regardless of the level of cockpit automation provided. Second, NASA/Ames is currently collaborating with the FAA, Douglas, and Boeing to select and validate workload assessment techniques appropriate for certifying commercial transport aircraft. This research program reflects the current level of concern in the civil sector over the impact of advanced cockpit technologies on pilot workload.

Despite the solid theoretical knowledge and methodological technology developed for the aviation environment, the extension of such workload measures and predictors to space applications presents a host of new challenges. For example, existing measures of workload may or may not adequately reflect the sources of workload that are typical of Space Station operations. Thus, the factors that will influence the workload of Space Station crewmembers must be determined and measures that are sensitive to these factors identified. Although many measures exist with which workload can be assessed, they have not been applied to the unique activities performed by Space Station crewmembers, operating for long durations in a microgravity environment. Task and time-line analyses provide a detailed description of what crewmembers will be required to accomplish, and when. But, they can not quantify the workload that performing these activities will impose on the human operations. Furthermore, little information is available about how to interpret the results of a workload analysis. That is, how much workload is optimal, excessively high, or excessively low. Without such evaluation criteria, the results of a workload analysis are of relatively limited value in determining crew schedules, deciding how many people are required to perform a specific task comfortably and efficiently, or selecting activities which will require partial or complete automation.

After several years of research on the structure of pilot workload and developing and applying workload assessment techniques, computer models to predict pilot workload in fixed wing and rotary-wing aircraft are being developed. Such predictive capabilities are essential so that the potential impact of design decisions on the human operators of advanced systems can be assessed early enough in the design process for modifications to be accomplished in a cost-effective manner. Laboratory research has provided the initial equations by which the workload levels of task elements can be measured and combined to predict the workload and more complex tasks. Here, it was found that the workload levels of subtasks performed individually, but concurrently, could be added together to predict the performance of the combined task. When functionally related subtasks that shared common information, processing, or response requirements were combined, on the other hand, the workload of the combined task was considerably less than would be predicted from a linear combination of the workload levels of the individual subtasks.

C-4

Experienced workload is the integrated product of many factors in addition to the objective demands that are placed on a pilot. Although workload predictions, particularly those made during the design of a new system, must necessarily focus on the objective demands that are imposed on an operator, there are a number of other types of information that might be included to enhance the predictive power of such a model. Our approach has been to start with nominal or typical mission elements. Information about their duration, workload, and visual, auditory, information processing, and manual control requirements are obtained. A data base of additional tasks or events that might occur are identified and the same information is obtained for them. The functional relationships among specific segments and additional tasks are defined so the model can select the appropriate combination algorithms to estimate the workload of a complex task.

A preliminary model has been developed to predict the workload of general aviation pilots based on this structure. The predictions of the model were tested in simulated flight, and they were found to correlate well with the objective and subjective measures of workload that were obtained. A more complete model is under development focused on the workload demands of current and advanced-technology helicopters. Although the structure of the model is equally applicable to the Space Station environment, considerable research will be required to: (1) identify nominal mission segments, (2) identify additional events that might occur or activities that will be performed, (3) quantify the workload of these activities, and (4) compare the workload predictions produced by the model to those obtained in part-task and full-mission simulations of Space Station operations.

This paper will review the accomplishments of the Workload Research Program at NASA/Ames and will describe our plans to extend this expertise into the domain of Space Station operations. ■

ADVANCED SPACE SUITS AND PORTABLE LIFE SUPPORT FOR ROUTINE OPERATIONS IN SPACE AND ON PLANET SURFACES

H. C. Vykukal and B. W. Webbon
NASA/Ames Research Center, Moffett Field, California 94035

Future manned space missions will require extensive extravehicular crew activity for both operational and scientific reasons. Protective systems must be developed to allow such activities to become both safe and routine. The requirements for long duration orbital, Mars, and lunar EVA equipment are in many ways different than those for systems currently in use or planned for the near future. These requirements and their effects on the EVA equipment, as well as several conceptual systems that might be developed to meet these requirements, will be presented. Advanced hard space suit and glove prototypes, a low cost suit testing facility, and technology developments in the area of manually powered dextrous end effectors will also be shown and discussed ■

MODELLING A MODULAR CONTROLLED ECOLOGICAL LIFE SUPPORT SYSTEM

J. D. Rummel[1] and T. Volk[2]
[1]*Life Sciences Division, NASA Headquarters, Washington, D.C. 20546 and* [2]*Department of Applied Science, 26 Stuyvesant St., New York University, New York, New York 10003*

In order to build a practical controlled ecological life support system (CELSS) the material flows essential to human survival within the biosphere have to be duplicated within a system without the buffering capacity allowed by the huge material reservoirs available on Earth. The lack of these buffers and the critical nature of the mass flows within a CELSS dictate the need for tight control to coordinate the movement of materials within the system. An operable CELSS will be made up of a series of processors that affect the state of materials within the system (taking in carbon dioxide and water and producing sugar and oxygen for example), processors whose rates of action may be widely different, yet whose actions must be complementary in order to allow the system to operate. The design of a CELSS must provide a suitable interface for these processors while allowing the possibility for system expansion.

The model presented handles both the coordination problem and the expansion issue in the same fashion. A suitable array of reservoirs is established representing the most likely storage elements of an operable CELSS (oxygen, carbon dioxide and water tankage, etc.) and those reservoirs that are a consequence of the life support function of the system (e.g., the crew's atmosphere). These are a standard set of reservoirs with which any manner of life support processors can be interfaced, and which can buffer those processors by their capacity for storage and release of materials. This model therefore has a modular structure, with processor modules being modelled independently (and potentially at varying levels of detail). These modules are freely interchangeable on a common reservoir structure.

Of course, long term system operation requires the presence of specific processors whose actions eventually counterbalance each other (plants vs. the crew, for example), but the need for coordination is much less stringent if the buffering capacity of the reservoirs is higher than a baseline level (investigated through the use of the model), and if each of the processors has excess capacity over that needed to maintain the steady state. Partial and complete failures of various system components, such as the plants or the waste processor, drive transient responses in the model system, allowing both control strategy testing and an assay of system design requirements.

As the system develops in complexity, the model can adjust to design changes and the level of detail within each module of the program can be enhanced to keep abreast of the monitoring and control capabilities of the system. By developing the model in this way, the model can become a representation of the system that can be run in a faster mode than real time. As such, the model can be used to determine overall system control strategies by acting, in effect, as a test for any conceivable strategy. One way to do this in a space system might be to interface a CELSS model with an expert system front end. The model could then generate the expertise to be used by the system to control the workings of the CELSS. A moderately parallel computing system would greatly enhance this capability. ■

MASS BALANCES FOR CELLS SIMULATION MODELS

T. Volk[1] and J. D. Rummel[2]
[1]*Department of Applied Science, New York University, New York, New York 10003 and* [2]*NASA/Life Sciences Division, Washington, D.C. 20546*

Design decisions to aid the development of future space-based controlled ecological life support systems can be made with simulation models. This work develops the biochemical stoichiometry in (1) protein, carbohydrate, fat, fiber, and lignin production in the edible and inedible parts of plants; (2) food consumption and production of organic solids in urine, feces, and wash water by the humans; and (3) operation of the waste processor. Flux values for all components are derived for a steady-state system with wheat as the sole food source; an extension of this methodology can explore multi-food systems and more complex biochemical dynamics while maintaining whole-system closure as a focus.

System mass closure occurs on the level of elements, not of compounds, and the focus here is on the elements that constitute most of the system's mass: carbon (C), hydrogen (H), oxygen (O), and nitrogen (N). These comprise the compounds, such as H_2O, O_2, and CO_2, that determine the activities of the processors. In simulating the plants and the humans choices must be made which, while simplifying the complex actual biochemistry of organisms, capture the large-scale products of metabolism. The edible food from the plant is tracked as the dietary necessities of protein, carbohydrate, and fat, while the inedible plant component is taken to consist of protein, fiber, and lignin, whose relative proportions will influence eventual further processing into other edible substances (see Figure 1). To these five plant-matter types are added three forms of human waste: urine solids, feces solids, and sweat solids.

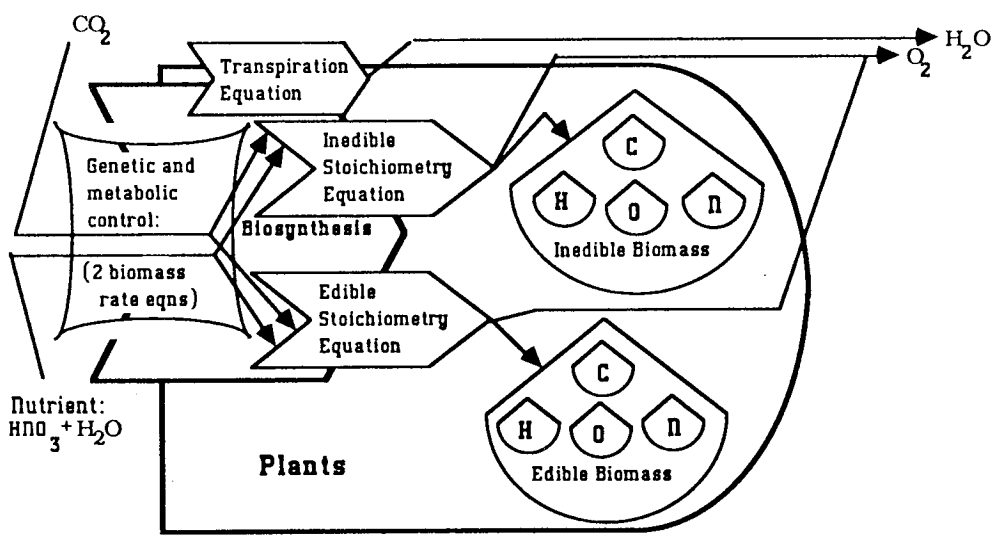

Figure 1

Canonical chemical formulas for all these have been developed elsewhere (Volk, T. and J.D. Rummel, Mass balances for a biological life support simulation model, Adv. Space. Res., in press, 1987); these formulas are summarized in Table 1.

The plants transform CO_2, HNO_3, and H_2O into O_2 and the various Table 1 matter types; the humans take the food and O_2 into CO_2, H_2O and wastes, and the waste processor will receive both the inedible

TABLE 1 Canonical Formulas and CHON Composition of Model Constituents

Type and Components	Symbol	C (%)	H(%)	O(%)	N(%)
Edible plant					
Protein	C_4H_5ON	57.8	6.0	19.3	16.9
Carbohydrate	$C_6H_{12}O_6$	40.0	6.7	53.3	-
Fat	$C_{16}H_{32}O_2$	75.0	12.5	12.5	-
Inedible plant					
Protein	C_4H_5ON	57.8	6.0	19.3	16.9
Fiber	$C_6H_{10}O_5$	44.4	6.2	49.4	-
Lignin	$C_{10}H_{11}O_2$	73.6	6.7	19.6	-
Human waste					
Urine solids	$C_2H_6O_2N_2$	26.7	6.7	35.6	1.0
Feces solids	$C_{42}H_{69}O_{13}N_5$	59.2 8.1	24.4	8.2	
Wash solids	$C_{13}H_{28}O_{13}N_2$	37.1	6.7	49.5	6.7

plant materials and the human wastes, and sometimes even the edible food. From these considerations, stoichiometric balances can be formed that serve as the matter-conserving equations for the operation of the processors:

Growth of edible plant matter:

$$n_1CO_2 + n_2H_2O + n_3HNO_3 \rightarrow n_4C_4H_5ON + n_5C_6H_{12}O_6 + n_6C_{16}H_{32}O_2 + n_7O_2 \tag{1}$$

Growth of inedible plant matter:

$$n_8CO_2 + n_9H_2O + n_{10}HNO_3 \rightarrow n_{11}C_4H_5ON + n_{12}C_6H_{10}O_5 + n_{13}C_{10}H_{12}O_2 + n_{14}O2 \tag{2}$$

Human metabolism of edible plant matter:

$$n_{15}C_4H_5ON + n_{16}C_6H_{12}O_6 + n_{17}C_{16}H_{32}O_2 \rightarrow n_{19}C_2H_6O_2N_2 + n_{20}C_{42}H_{69}O_{13}N_5 + n_{21}C_{13}H_{28}O_{13}N_2 + n_{22}CO_2 + n_{23}H_2O \tag{3}$$

Waste processing of edible plant matter:

$$n_{24}C_4H_5ON + n_{25}C_6H_{12}O_6 + n_{26}C_{16}H_{32}O_2 + n_{27}O_2 \rightarrow n_{28}CO_2 + n_{29}H_2O + n_{30}HNO_3 \tag{4}$$

Waste processing of inedible plant matter:

$$n_{31}C_4H_5ON + n_{32}C_6H_{10}O_5 + n_{33}C_{10}H_{11}O_2 + n_{34}O_2 \rightarrow n_{35}CO_2 + n_{36}H_2O + n_{37}HNO_3 \tag{5}$$

Waste processing of human waste:

$$n_{38}C_2H_6O_2N_2 + n_{39}C_{42}H_{69}O_{13}N_5 + n_{40}C_{13}H_{28}O_{13}N_2 + n_{41}O_2 \rightarrow n_{42}CO_2 + n_{43}H_2O + n_{44}HNO_3 \tag{6}$$

Equations (1-6) constitute a system for a biological life support system model if the rate coefficients, n_i in moles per unit time, are known. Four equations for the balance of C, H, O, and N can be written for each overall equation, making 24 equations in all for 44 unknown n_i's. Further constraints are

necessary. In fact, the system can be determined by specifying six rates: the plant growth rate, the harvest index, which is the fraction of edible growth to total growth, the rate of human food consumption, and the rates of waste processing of edible matter, inedible matter, and human waste. Data from wheat is used, but extension to multiple species is straightforward. More biochemical detail could be incorporated, guided by the principle that an entire operational model should be reasonably consistent in the level of internal detail in all parts. ■

DEVELOPMENT OF A MEMBRANE NUTRIENT SYSTEM

T. W. Dreschel[1], C. R. Hinkle[1], W. M. Knott[2], R. P. Prince[2], J. C. Sager[2]
[1]*The Bionetics Corporation and The National Aeronautics and Space Administration,* [2]*Biomedical Operations and Research Office, John F. Kennedy Space Center, Florida*

INTRODUCTION

The purpose of this project is to develop a plant support system for crop production under microgravity conditions. The use of a microporous, hydrophyllic membrane to contain an aqueous plant nutrient solution and act as a capillary interface between the plant roots and the nutrient solution was proposed by Wright and Bausch (1984). The application described was on a small scale for the support of plants for 8 to 10 days (as on a Space Shuttle flight). Their system utilized a membrane in a flat configuration, affixed to anodized aluminum plates with screen between to prevent the membrane from collapsing against the plate. The nutrient solution was pumped in a thin layer between the membrane and plate under a slight negative pressure. These were used vertically and in pairs with the membrane sides facing each other and the plant roots sandwiched between. A bubble removal system utilizing a hydrophobic membrane was also incorporated into the plates to prevent drying of the hydrophyllic membrane.

PROJECT IMPLEMENTATION

A membrane envelope was developed in this project as a first attempt to apply the membrane-capillary effect technique on a larger scale. The envelope was constructed from a rectangular sheet of membrane which was heat sealed to a black vinyl sheet at the edges, with several layers of nylon screen between. Manifolds were fabricated from vinyl at two opposing edges and tubing fittings were attached to the vinyl sides of the manifolds. Nutrient solution was drawn by suction from a reservoir to one manifold, flowed as a thin layer among the screens between the membrane and vinyl, and out the opposite manifold to the pump and returned to the reservoir. This membrane was folded to form an envelope with the manifolds at the top and wheat seeds were planted within the envelope at 3 centimeters (cm) from the top. Wheat was maintained in the envelope through one growth cycle from seed to harvest. The space requirements of the envelope, difficulty in maintaining a good seal between the membrane and vinyl, and the large area of membrane used led to further modifications.

A tubular membrane plant growth system (NASA 1986) was developed to solve some of the problems which arose with the membrane envelope. The tubular configuration was found to be more easily fabricated and could be built from readily available parts as presented in Figure 1. The membrane tube was formed by folding a strip and stitching the long edges together. This was supported by a cylinder of semi-rigid plastic screening inserted into the membrane tube. The support of the plants, shading and protection of the root mass and membrane were facilitated using polyvinyl chloride (PVC) pipe. This pipe was slightly larger than the membrane tube and had appropriate openings to accommodate shoot emergence. Pipe fittings were attached to each end of the supported membrane tube to facilitate connection of the units to a positive displacement pump and a reservoir. The nutrient solution was pumped through the system from the reservoir, through the membrane tube, to the pump and back to the reservoir. The nutrient solution was contained within the membrane tube by a slightly negative pressure.

RESULTS AND DISCUSSION

The initial trials with this system have shown that wheat can be grown at a rate equal to or better than in the field, with seed biomass produced at an amount per plant generally obtained in the field or other hydroponic systems. The initial trials also indicate that plant growth and production were dependent upon the amount of suction pressure applied to the solution within the membrane tube. This fact may give this system other applications in plant physiology research as well as its possible use in

Figure 1. Tubular membrane plant growth unit.

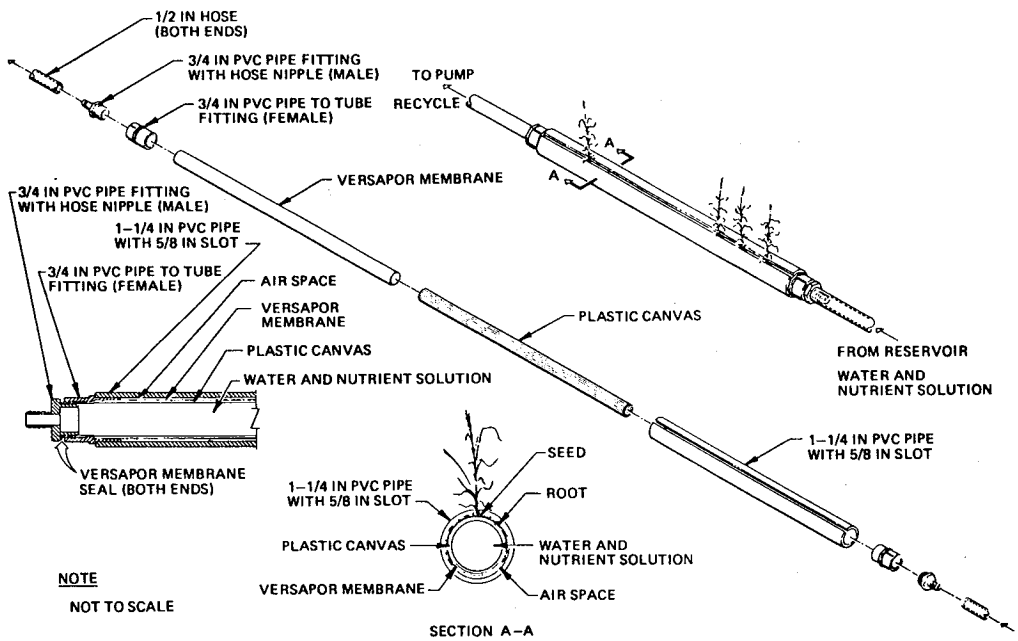

microgravity crop production. Rice and beans have also been grown in the system to seed production; thus it has potential for use with other crops. Its compact size, simplicity and low cost of fabrication suggest that it might have use as an alternative to conventional plant propagation systems. ■

REFERENCES

1. National Aeronautics and Space Administration (NASA). 1986. Tubular membrane plant growth system. In the Research and Technology 1986 Annual Report of the John F. Kennedy Space Center. NASA Technical Memorandum 89193.
2. Wright, B.D. and W. C. Bausch. 1984. A plant growth system for orbital plant experiments. Paper presented to the American Society of Agricultural Engineers, New Orleans, Louisiana.

NON-CONVENTIONAL APPROACHES TO FOOD PROCESSING IN CELSS. II. INCORPORATION OF ISOLATED ALGAL MACRONUTRIENTS AS DIET COMPONENTS IN CELSS

Z. Nakhost and M. Karel
Department of Applied Biological Sciences, Massachusetts Institute of Technology, Cambridge, Massachusetts

Utilization of photosynthetic micro-algae as components of the diet in CELSS is promising. Isolation, characterization, and incorporation in diet components of algal macronutrients is the subject of our study. The use of unpurified algal biomass is undesirable due to its intense color and flavor and we have developed methodologies to remove the undesirable components. Green alga *Scenedesmus obliquus* provided to us by Dr. Radmer (Martek Corp.) was used in this study. To optimize the removal of algal lipids and pigments and to minimize protein denaturation, we used supercritical fluid (SCF) extraction using carbon dioxide with and without ethanol as a cosolvent. This resulted in more efficient removal of

algal lipids and improved water solubility of protein isolate. Characterization of protein revealed a high content of essential amino acids leucine, valine and lysine. The algal lipids showed high content of total unsaturated fatty acids.

Work is underway to prepare sufficient amount of protein isolate from *S. obliquus* to be incorporated into model foods, which also contain wheat- and soybean-derived ingredients, since wheat and soybeans may also be part of CELSS biosystem. We have also conducted studies on chemical composition of blue-green alga cyanobacterium *Synechococcus 6311* provided to us by Dr. Packer (UC Berkeley). Cells grown under controlled conditions were ruptured by the method previously used for *S. obliquus*. Comparison of the scanning electron micrographs (SEM) of intact and homogenized cells

Table 1. Chemical composition. Calculated on a dry weight basis.

Algal Flour freeze dried	Proteins %	Nucleic acids %	Lipids and lipid-soluble pigments
Scenedesmus obliquus (green alga)	52.6	6.0	15.0
Synechococcus 6311 (blue-green alga)	54.0	5.0[(a)]	12.6

(a) cited in the literature

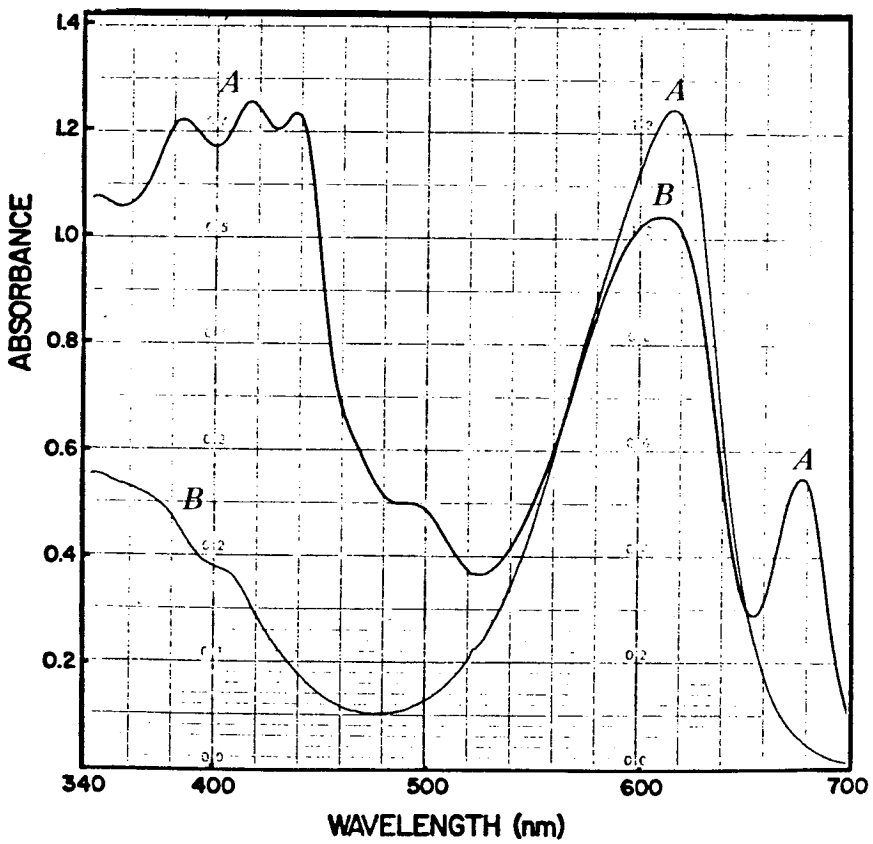

Figure 1. Absorption spectra of "water-extracted pigments" from *Synechococcus* 6311 algal flour (spectrum A) and of "water-extracted pigments" from ethanol-extracted residue (blue-gray powder) (spectrum B).

indicated the rupturing of the cell walls as a result of homogenization. Upon freeze-drying, the algal flour was used for determination of algal proteins and lipids. Microkjeldahl method gave a protein concentration value of 54% (dry weight basis, Table 1). The amount of proteins, nucleic acids, and lipids from *S. obliquus* and *Synechococcus 6311* are compared in Table 1. Extraction of lipids and pigments from blue-green algal flour was achieved using boiling ethanol in a Soxhlet apparatus. The presence of water-soluble blue pigment, the biliprotein phycocyanin resulted in the extraction residue having a blue-gray color while residue of *S. obliquus* had a light olive-green color. The absorption spectra of water-extracted pigments from algal flour (Spectrum A) and of water-extracted pigments from blue-gray residue (Spectrum B) are compared in Fig. 1. Spectrum B clearly shows the predominance of c-phycocyanin with absorption maximum at about 620 nm. Because chlorophylls are water- and lipid-soluble, the coelution of chlorophyll A (absorption maxima at about 410 and 670 nm) with phycocyanin is indicated by Spectrum A. Absorption spectra of ethanol-extracted pigments from water-extracted residue (Spectrum C) and from algal flour (Spectrum D) are shown in Fig. 2. Overlapping of the

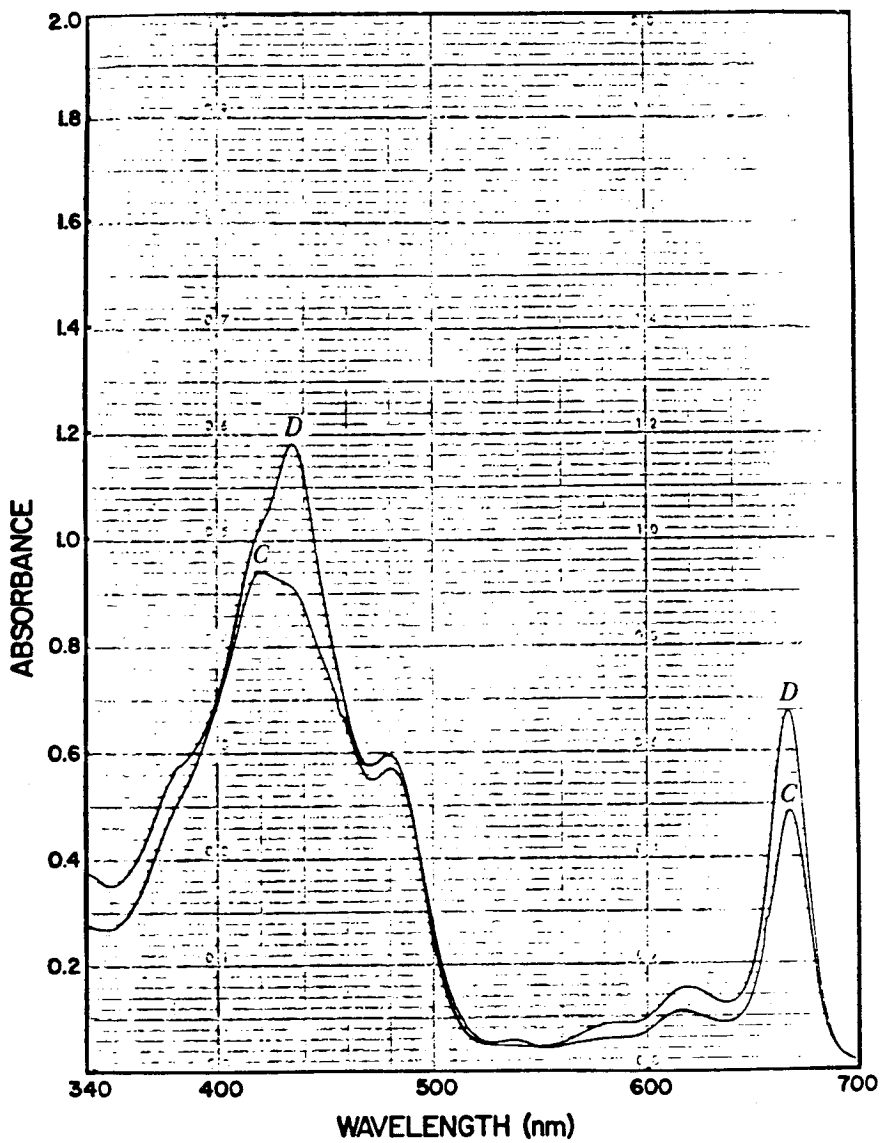

Figure 2. Absorption spectra of "ethanol-extracted pigments" from water-extracted residue (spectrum C) and of "ethanol-extracted pigments" from *Synechococcus* 6311 algal flour (spectrum D).

Table 2. Fatty acid composition (% total of fatty acids) of total lipids fraction of *Scenedesmus obliquus* and *Synechococcus 6311*

Fatty Acids	*Scenedesmus obliquus*[a]	*Synechococcus 6311*
12:0	0.98	0.12
14:0	0.81	1.27
14:1	0.43	1.58
16:0	17.31	38.21
16:1	9.18	46.74
16:2	3.87	-
16:3	9.52	-
16:4	6.97	-
17:0	-	0.24
17:1	-	0.45
18:0	0.82	2.35
18:1	10.94	9.04
18:2	22.20	-
18:3(ϑ)	1.05	-
18:3(α)	14.81	-
18:4	1.11	-
T.S.F.A.	19.92	42.19
T.U.S.F.A	80.08	57.81
EFA	38.060	

[a] From Choi K J, Nakhost Z, Barzana E, and Karel M 1987 Food Biotechnol in press

TSFA = Total saturated fatty acids
TUSFA = Total unsaturated fatty acids
EFA = Essential fatty acids

absorption maxima of these ethanol-extracted pigments resulted in a spectrum which is not specifically representative of any individual pigment. The amount of lipids and pigments extracted by boiling ethanol was 12.6% (Table 1) which is lower than what we previously reported for *S. obliquus*. Table 2 shows the fatty acid composition of total lipid fraction of *S. obliquus* and *Synechococcus*. The main fatty acids in *S. obliquus* were $C_{18:2}$, $C_{16:0}$, $C_{18:3(\alpha)}$, $C_{18:1}$, $C_{16:3}$, and $C_{16:1}$ and in *Synechococcus* were $C_{16:1}$, $C_{16:0}$, and $C_{18:1}$. We found lower amounts of total unsaturated fatty acids (TUSFA) for *Synechococcus* as compared to *S. obliquus*. Similar results on fatty acid composition of blue-green algae have been reported. ■

UNCONVENTIONAL FOOD REGENERATION IN SPACE: REQUIREMENTS FOR MICROBIAL FOOD PRODUCTION

G. R. Petersen[1], P. K. Seshan[1] and E. H. Dunlop[2]
[1]*Applied Sciences and Microgravity Experiments, Jet Propulsion Laboratory, California Institute of Technology, Pasadena, California 91109 and* [2]*Department of Chemical Engineering and Center for Biotechnology, Washington University, St. Louis, Missouri 63130*

In Controlled Ecological Life Support System (CELSS) technology, the major focus for food regeneration has been on conventional agronomical systems. Although the major portion of the NASA CELSS effort is directed towards growing plants in space, some attention has been paid to other or unconventional food regeneration processes. Work at JPL has focused on alternate food production processes involving microbial food sources. Microbial systems can serve as the biological portion of hybrid chemical/biological regeneration systems for primary food production, as a means to more fully utilize waste matter from conventional food production, and to provide supplements to the nutritional products derived from conventional plant foods. Examples will be given of each of these, all of which will require the use of biological fermentors which can operate in microgravity.

PRIMARY FOOD PRODUCTION BY MICROORGANISMS

Given that the carbon dioxide and water can be recycled by some physical chemical means into a simple C1 compound such as methanol, then microorganisms can be used to provide the biological synthesis of complex food components-carbohydrates, protein and lipids. Several years of research into this approach has yielded data that shows that microbial food sources are approximately equivalent in total food content (and overall carbon conversion efficiency) to that derived from plants. These results are shown Table I and will be discussed.

TABLE I
Edible fractions of *Hansenula polymorpha* and *Saccharomyces*

Subs	Yeast species and strains	Fraction of dry weight (as %)		
		EDIBLES		TOTAL EDIBLES
		Protein	Carbohydrates	
Methanol	*H. polymorpha*			
	Wild type	17.0	27.9	44.9
	#13 (High Glg)	24.4	34.7	59.1
	#84 (High Glg)	12.5	44.8	57.3
	#122 (Low Glg)	20.9	21.0	41.9
Glucose	*S. cerevisiae* *	48.0	13.4	61.4
	S. uvarum	55.0	20.4	75.4
	S. diastaticus	47.0	21.2	68.2

* FDA approved for human consumption

WASTE TO FOOD BY MICROORGANISMS

All efforts to maximally utilize conventional food sources will still result in carbon conversion losses due to inedible material such as cellulose, lignin and pentose sugars. Figure 1 shows possible routes for waste-to-food yeast systems. Data for microbial growth on alternate carbon sources such as xylose was obtained, shown in Table II and will be discussed.

SUPPLEMENTAL FOOD COMPONENTS PROVIDED BY MICROORGANISMS

The nutritional content of microbial food sources also permits their use as providers of necessary supplements to conventional food sources. Lysine is the most limiting of the essential amino acids in

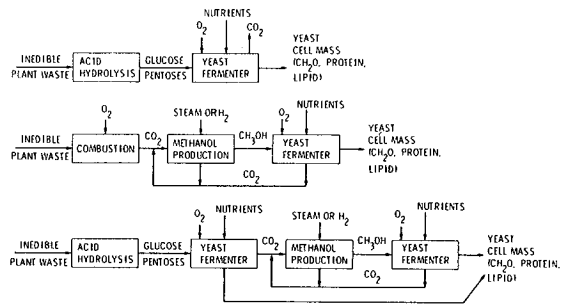

Figure 1. Waste to food yeast options in CELSS.

TABLE II
Utilization of Plant Waste Materials
Edible Fractions of *C. utilis* & *C. boidinii*

Subs	Yeast species	Fraction of dry weight (as %)		
		EDIBLES		TOTAL EDIBLES
		Protein	Carbohydrate	
	C.utilis			
Glc	CUG	17	38.9	55.9
Et	CUE	17	35.9	52.9
Xyl	CUX	16	40.2	56.2
	C.boidinii			
Me	CBM	15	36.3	51.3
Xyl	CBX	6.1	42.1	48.2

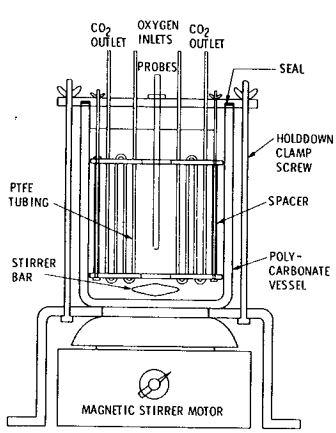

Figure 2. Prototype, terrestrial, phase separated membrane bioreactor test model.

the human diet followed by tryptophan and methionine. A quick survey of microbial food sources shows that most microbial sources can provide lysine at levels above that recommended by WHO-FAO guidelines. Most strains are equivalent to other food sources in tryptophan but all are deficient in methionine. If a need for a general protein supplement exists in CELSS, yeasts and/or bacteria can meet that need. If one or two essential amino acid supplements are needed, a specific microbe selected or genetically engineered to meet that need could be used.

FERMENTATIONS IN MICROGRAVITY

At JPL and Washington University, considerable effort was given to developing concepts for bioreactors that would operate in microgravity. It is clear that terrestrial reactors now in operation will not operate in microgravity and that significant effort must be expended to modify conventional reactors to operate in that environment. The alternative is to design systems that are independent of the presence or absence of gravity. Following this approach, two possible configurations were developed. One involves membrane technology and addresses only the fermentor operation without consideration of gas/liquid separation. The second involves a rotating packed bed that creates gas/liquid interfaces and is unique in that it also provides for gas/liquid separation as well. Based on simplicity of design, construction and testing, the phase-separated membrane reactor was chosen to undergo an initial engineering analysis. The first design is shown in Figure 2. Data on oxygen transfer capabilities were the first step in evaluating the design and data will be given on these initial experiments. ■

DESIGN AND ENGINEERING THE BIOMASS PRODUCTION CHAMBER

R. P. Prince
Biomedical Operations and Research Office, John F. Kennedy Space Center, Florida

The need to provide gas, liquid, and solid regeneration for crews on long duration space missions has been recognized by the scientific community for many years. Oxygen, carbon dioxide, and water recycling interested early investigators engaged in algal research. This work resulted in a food product which showed promise of providing reasonable efficiencies. The problems associated with short duration missions (14 to 90 days) did little to encourage outside investigators to pursue the regeneration concept vigorously.

A renewed interest in product regeneration by NASA was evident in the early 1970's with the creation of the Controlled Ecological Life Support System (CELSS) within the Life Sciences Division. Extramural research, conferences, panels, and seminars have been major efforts of this program. In 1985, CELSS initiated a "Breadboard" Project at the Kennedy Space Center to investigate, in an operational research mode, known principles and concepts involved with crop production atmospheric regeneration, waste management, food processing, analytical monitoring, engineering and control, product storage, and crew habitation. Central to the project has been the crop production facility or Biomass Production Chamber (BPC). This BPC, shown schematically in Figure 1, was designed to maintain an environment similar to commercial plant growth chambers. Its cylindrical shape, two levels, and vertical position necessitated new shelf and tray designs, air flow patterns, and lamp bank arrangements to be used. The primary difference between the BPC and commercial plant growth chambers is in the ability to seal the BPC. A good seal will be essential to assess the gas contaminant level. It became operational December 1, 1986, growing wheat in a semi-open mode. The improved nutrient delivery system and the gas and pressurized control systems will not be installed until the summer of 1987.

The block diagram in Figure 2 shows the subsystems specified for the BPC. The control and monitoring functions are treated as different subsystems and have separate sensors. A Programmable

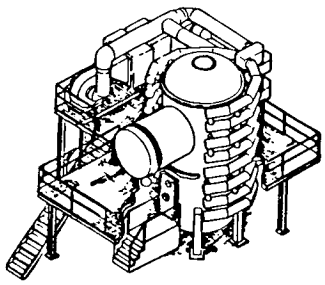

Figure 1. Biomass production chamber.

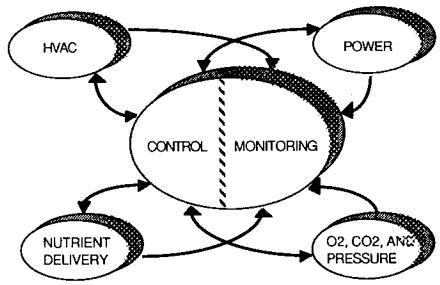

Figure 2. BPC subsystems.

Logic Controller (PLC) performs the computer control function, and an intelligent datalogger performs the acquisition of monitoring data. These two machines, along with other devices (printers, plotters, other computers, etc.), are integrated into an IEEE 488 General Purpose Interface Bus (GPIB) with one of the extended micro-computers serving as the bus controller.

Nutrient flow, nutrient temperature, and alarms will be controlled by the PLC. Each of the four shelves within the BPC contains 8 adjustable platforms with two plant growing trays per platform for a total of 64 trays for the chamber. A manifold will direct nutrient solution to each tray from the four sealed tanks (one tank for each shelf) located outside of the BPC. All tanks will be vented to the chamber to maintain atmospheric integrity. One half of the BPC (32 trays) are presently growing wheat in a continuous mode (2 trays harvested and 2 seeded every 4 days). The growing time for wheat is approximately 72 days.

Provision is being made to control oxygen at atmospheric level and carbon dioxide from 300 ul/l to 2500 ul/l with bottled gases; carbon dioxide, breathing air, oxygen, and nitrogen. Internal chamber pressure will be maintained at +12 mm H_2O referenced to ambient. Experience with controlling pressure, carbon dioxide, and oxygen with breathing air and CO_2 will determine if addition of bottled oxygen and nitrogen will be required.

Coupled with producing biomass with crops like sweet and white potatoes, wheat, soybeans, rice, beans, etc., the atmosphere and condensate water will be monitored regularly for contaminants. Samples will be taken for microbial count and identification. Periodic air samples taken since December 1, 1986 indicate the absolute (99.97% *0.3 micron*) filters are servicing the air stream as designed.

ACKNOWLEDGEMENT

Many individuals and groups in the Biomedical Operations and Research Office, in Engineering Design, and in The Bionetics Corporation at the Kennedy Space Center, other NASA centers, and outside advisory panels are acknowledged for their help and constructive encouragement. ■

PAGE 313 INTENTIONALLY BLANK

PRECEDING PAGE BLANK NOT FILMED

CONTINENTAL-SCALE VARIABILITY IN VEGETATION REFLECTANCE AND ITS RELATIONSHIP TO CANOPY MORPHOLOGY

D. S. Bartlett[1], M. A. Hardisky[2], R. W. Johnson[1], M. F. Gross[3], V. Klemas[3], J. M. Hartman[4]
[1]*Atmospheric Sciences Division, MS 483, NASA Langley Research Center, Hampton, Virginia 23665-5225*
[2]*Department of Biology, University of Scranton, Scranton, Pennsylvania* [3]*College of Marine Studies, University of Delaware, Newark, Delaware* [4]*Graduate School of Design, Harvard University Cambridge, Massachusetts*

Remote sensor studies of terrestrial vegetation have recently begun to address continental-sized geographic areas. If quantitative relationships between satellite- derived spectral indices and canopy parameters (e.g., phytomass, leaf area index—LAI, absorbed photosynthetically active radiation—APAR) can be extrapolated to these very large areas, important contributions to models of global production and biogeochemical cycles could result. However, little is known of the consequences of extending locally derived relationships to large areas. We have measured the spectral canopy reflectance, biomass, and horizontal LAI of widely dispersed plots of a North American coastal plant (salt marsh cord grass) in an attempt to identify potential impacts of continental-scale environmental variability on the assumptions underlying remote vegetation analysis.

We found that important, systematic changes in the canopy geometry and resultant near-infrared reflectance of this plant occurred within its 17-degree latitudinal range. Mean infrared canopy reflectances of canopies in the northern half of the range are nearly double those of the southern half despite almost identical total and green standing biomass in the two regions (Fig. 1). The transition from one regional canopy type to the other appears to occur quite abruptly near the center of the plant's latitudinal range. Continental assessment of green biomass using spectral indices would be

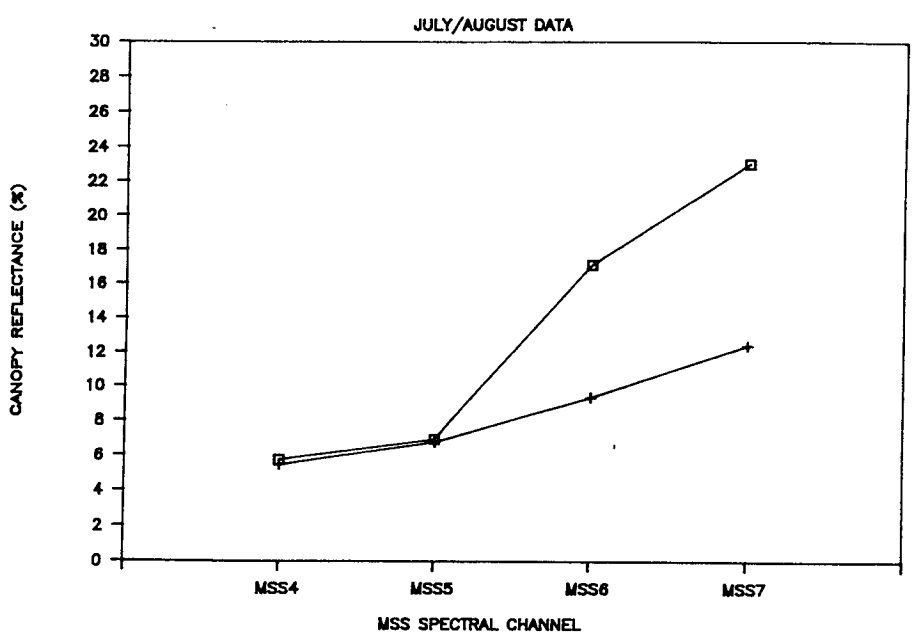

Figure 1. Mean canopy reflectance of cord grass North (□) and South (+) of 37°30′ N. MSS4—500-600 nm MSS5—600-700nm, MSS6—700-800nm MSS7—800-1100nm.

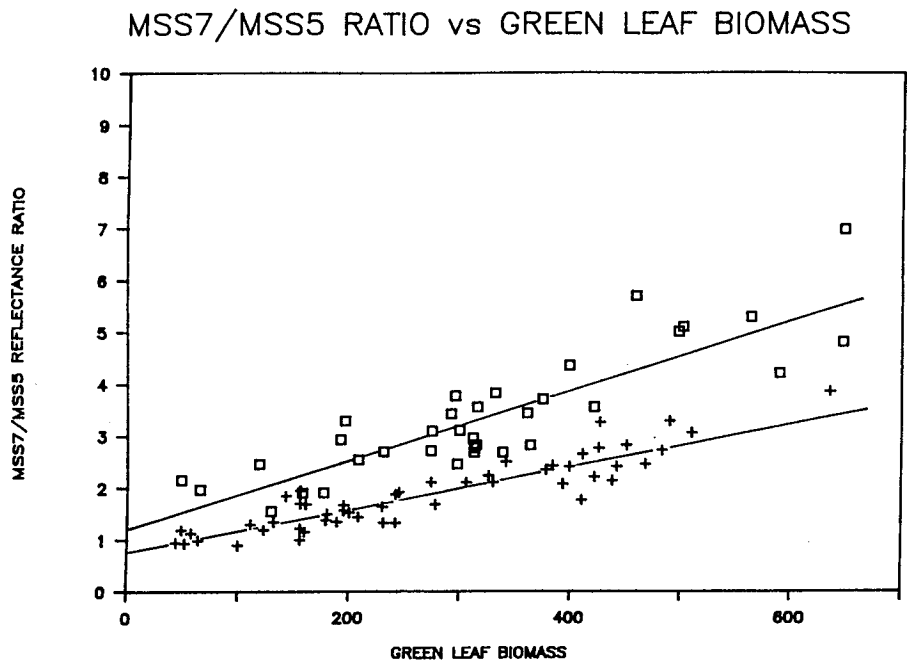

Figure 2. MSS7/MSS5 reflectance ratio vs. green leaf biomass (g dry wt/m^2) for cord grass canopies North (□) and South (+) of 37°30′ N.

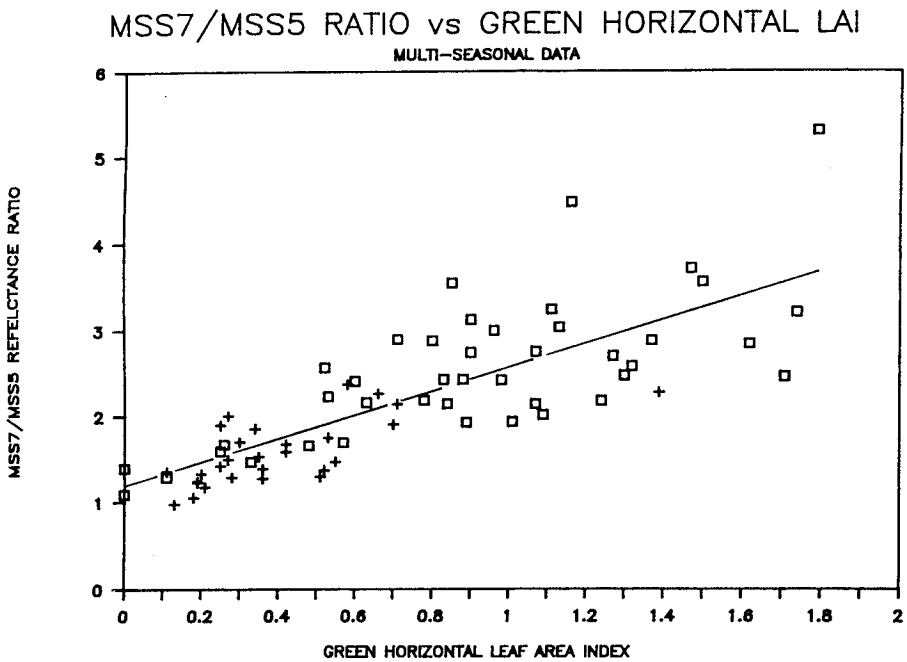

Figure 3. MSS7/MSS5 reflectance ratio vs. green leaf area index for cord grass canopies North (□) and South (+) of 37°30′ N.

severely affected by the observed differences (Fig. 2). Use of spectral indices to assess more fundamental radiative transfer properties of the canopy, such as horizontal LAI, is not subject to the observed latitudinal changes (Fig. 3), suggesting that large area studies can more reliably address canopy parameters such as APAR. The observed canopy changes also have potential functional consequences for the plant which would be of considerable ecological interest, particularly if similar trends are found for other plants and regions. ■

FACTORS CONTROLLING EMISSION OF DIMETHYLSULFIDE FROM SALTMARSHES

J. W. H. Dacey[1], G. M. King[2], S. G. Wakeham[1]
[1]*Woods Hole Oceanographic Institution, Woods Hole, Massachusetts 02543;* [2]*I. C. Darling Center, University of Maine, Walpole, Maine 04573*

Saltmarshes have been identified as a system with high area-specific sulfur gas emission. Dimethylsulfide (DMS) and hydrogen sulfide (H_2S) constitute the bulk of the flux from saltmarshes, with DMS predominating in vegetated areas of the marsh. Since H_2S arises directly from anaerobic decomposition in sediments, it has been mistakenly assumed that other sulfur gases emitted from saltmarshes share a similar source. We have investigated the distribution of DMS and dimethylsulphoniopropionate (DMSP) in saltmarshes, and conclude that DMS arises from physiological processes, primarily in one species of grass, *Spartina alterniflora*. Measurements of emission from *S. alterniflora* cannot be extrapolated to estimate the global flux of DMS from saltmarshes without accounting for species composition in the marshes.

The sources and controls of the two major sulfur gas emissions from saltmarshes differ markedly. The observed flux of H_2S (~150 umol $m^{-2}d^{-1}$) from saltmarsh sediments represents a flux of only 0.001 d^{-1} for the 0-2 cm porewater pool (500 umol L^{-1}). In contrast, the emission rates for DMS (1-246 umol $m^{-2}d^{-1}$) would require the 0-2 cm porewater pool of DMS (50 nmol L^{-1}) to turn over 1-300 times per day.

Our research on DMSP suggests an alternative explanation for DMS fluxes. We have investigated the concentration of DMSP in a variety of higher plants inhabiting the intertidal saltmarshes of eastern North America. The pool of DMSP to be especially high in the tissues of *S. alterniflora*, with concentrations exceeding 100 umol per g dry weight. We have not measured DMSP at concentrations greater than 0.1 umol per g dry weight in tissues of any other marsh species. Perhaps coincidentally, there are no published reports of measurements of DMS emission from any other marsh species or from marshes without *S. alterniflora*.

Concentrations of DMSP in *S. alterniflora* are highest in leaves (80-300 umol per g dry weight) and lowest in roots and rhizomes (20-60 umol per g dry weight). Based on conservative estimates of leaf and root concentrations of 120 and 40 umol per g dry weight respectively, the total amount of DMSP integrates to about 60 mmol DMSP m^{-2} in porewater from the 0.2 cm depth interval in Great Sippewissett Marsh. The fact that DMSP is at least 30000 times more abundant than DMS, and that DMSP degrades physiologically to DMS, suggests that a very small turnover of plant DMSP is responsible for the observed DMS flux. In fact, a daily turnover of only 0.4% per day would release sufficient DMS to support the highest DMS emission rates measured in salt marshes. Such a low rate of DMSP turnover is consistent with previously observed DMS production rates in marine algae where less than 1% of DMSP is converted to DMS per day.

In spite of its likely osmotic role, the concentration of DMSP in leaves of *S. alterniflora* does not show a strong link to sediment salinity, either between or within marshes. The concentration of DMSP in *S. alterniflora* is influenced by the nutritional status of the grass. Plants fertilized with nitrogen have less DMSP and more glycine betaine (another osmotic effector in marsh grass) in their tissues.

To evaluate the role of plant species on DMS emission from salt marshes, we collected a core of each of *S. alterniflora*, *S. patens*, and *Distichlis spicata*. Measurable and significant accumulation of DMS occurred in the headspace over *S. alterniflora*, while emission rates from the other two species were more than 100 times smaller. Further investigation of the accumulation of DMS in the headspace of the *S. alterniflora* core indicated that the DMS must originate from the leaves. When the surface of the sediment in the core was covered with 2 cm of seawater, rates of DMS accumulation in the headspace of the core were significantly higher than when the sediment was exposed. Furthermore, the concentration of DMS in the headspace reached levels three times higher than equilibrium with surface water, and two times higher than sediment porewater. In other words, DMS entered the headspace from the leaves. It could not have diffused or bubbled out of the sediment.

These data suggest that more attention must be directed towards the method of gas emission measurement. The factors controlling DMS and H_2S emission are distinct. It follows that procedures employed to measure the rates of emission of each may require different methods. Most of the H_2S emitted from saltmarshes probably passes directly across the sediment surface. On the other hand, the emission of DMS requires that the physiology of DMSP in the marsh grasses be taken into account. Since DMSP may play an important role in osmotic adjustment in these plants, the dynamics of DMSP in leaves may be affected by short-term changes in the heat and water balance of leaves. As a result, the common practice of enclosing marsh plants in a chamber may lead to erroneous estimates of DMS emission.

Reports of previous measurements of DMS emission have reported a high level of spatial variability. This may be due to the fact that different plant species dominate in neighboring sites, or that plants in the different sites differ in their physiological state. Previous estimates for global DMS emission from saltmarshes are almost certainly overestimates, since they have been based on fluxes from *S. alterniflora* marshes which were extrapolated to global marsh area without considering the plant species present in the marshes. Understanding the mechanisms of DMSP conversion to DMS will greatly enhance our ability to measure DMS emissions accurately and to establish the significance of saltmarshes to global sulfur emissions. ■

A ROLE FOR MARINE HERBIVORES IN THE FORMATION OF MARINE DIMETHYLSULFIDE

J. W. H. Dacey
Woods Hole Oceanographic Institution, Woods Hole, Massachusetts 02543

Dimethylsulfide (DMS) is ubiquitous in surface waters of the ocean and appears always to be present in concentrations far in excess of concentrations expected at atmospheric equilibrium. This large concentration gradient between the oceans and the atmosphere drives a major portion of the biogenic sulfur flux to the earth's atmosphere.

Exact mechanisms and factors controlling DMS formation in the ocean remain unknown. It has been generally recognized that many marine algae produce DMS in the normal course of metabolism, most likely by way of decomposition of dimethylsulfoniopropionate (DMSP) via an enzymatically catalyzed elimination reaction.

There is widespread evidence that zooplankton and other filter-feeding invertebrates ingest DMSP-containing plants. Accumulation of DMSP in food chains has been implicated in flavor-tainting in certain fish species. Sieburth has reported high concentrations of acrylic acid in guts of penguins, and pointed to DMSP in food species as the source. The presence of acrylic acid suggests that DMS must have been produced somewhere in the food chain. I have investigated a range of marine herbivores (zooplankton, fish, snails, and birds) for their potential for DMS formation. All appear to accelerate the formation of DMS by DMSP-containing food species. The exact mode and site of DMS formation is uncertain, although release of DMS from feces occurred in all species tested (when food contained substantial DMSP).

Experiments show that ingestion of phytoplankton by zooplankton releases DMS into the water column. Bottles containing zooplankton alone and seawater without organisms were run as controls, and showed no significant DMS production. Phytoplankton (alone) produced DMS at a measurable rate. Assuming that DMS formation in phytoplankton is a breakdown product of DMSP, it is possible to generate a DMSP-specific DMS production rate. This ratio represents a first attempt at direct comparison of DMS production by phytoplankton across broad taxonomic groups, sizes, and physiological states. Using the limited data available, the author estimates that the typical turnover rate for DMSP (releasing DMS) in DMSP-containing cells is less than 1% per day.

In the zooplankton grazing experiments, it was possible to measure the amount of phytoplankton DMSP ingested and compare that amount with the amount of DMS released. These calculations suggest that roughly one-third of ingested DMSP is liberated as DMS. Some DMS may be oxidized before measurement to DMSO, and therefore remain undetected in this research. Preliminary investigation suggests that during herbivory, significant amounts of DMSP may be released into seawater. This finding suggests a source for high concentrations of DMSP commonly found in seawater samples. The geochemical fate of this soluble DMSP in the DMS cycle remains uncertain.

In an effort to estimate the potential significance of this mechanism to the marine DMS cycle, several assumptions were necessary. I assumed that DMS is produced at a daily rate equal to 1% of the DMSP pool, and that when cells are ingested by zooplankton (regardless of species), one-third of each cell's DMSP would be released to the water as DMS. Under these circumstances, whenever more than 3% of DMSP- bearing phytoplankton in a parcel of water is ingested by zooplankton per day, the amount of DMS produced by ingestion should equal that produced by phytoplankton alone.

The extent of zooplankton grazing in oceans has been a long-standing focus of research and debate, but it is almost certain that considerably more than 3% of phytoplankton cells are consumed on most days. In oceanic systems, zooplankton grazing usually matches phytoplankton production, keeping phytoplankton biomass in approximate steady state. At steady state, a phytoplankton production rate of 0.2 per day would require that about 20% of cells be ingested each day. Under these circumstances, production of DMS during grazing should be 6 times higher than the rate of DMS production by the phytoplankton alone. In other words, zooplankton grazing may account for more than 80% of DMS production in open ocean environments. In coastal environments, zooplankton grazing may be less efficient at consuming primary production, and if so, zooplankton would play a less important role in DMS production than in areas of open ocean.

This mechanism for DMS production should explain some of the weakness in the relation between DMS concentrations and phytoplankton biomass. In general, DMS concentrations are higher where phytoplankton biomass is higher. Adding a component of grazing to these relations should improve our understanding of vertical profiles and diurnal dynamics in DMS in the water column.

Evaluation of this mechanism of DMS release into ocean water requires a better understanding of the physiology of phytoplankton and the factors controlling release of DMS by phytoplankton. The mechanisms of DMS release during ingestion by zooplankton also require further study. Dimethylsulfide may be released during capture and handling of phytoplankton cells by zooplankton, it may be excreted from or diffuse out of zooplankton, and it may be produced in fecal pellets. The relative importance of these mechanisms may influence the depth distribution of DMS production resulting from zooplankton grazing. ■

ESTIMATION OF ABOVEGROUND MARSH BIOMASS USING LANDSAT TM AND SPOT IMAGERY

M. F. Gross, M. A. Hardisky, V. Klemas and P. L. Wolf
College of Marine Studies, University of Delaware, Newark, Delaware 19716

Remote sensing from high spatial resolution satellites is a useful means of monitoring highly productive, and yet spatially variable, coastal zone waters and wetlands vegetation. A Landsat Thematic Mapper image was used to quantify and map the distribution of live aerial biomass of the dominant grass *Spartina alterniflora* in a Delaware salt marsh. Total *S. alterniflora* live aerial biomass for the marsh was estimated from satellite-gathered radiance data to be 1.55×10^9 dry weight distributed over 527 ha, for a mean of 294g dry weight/m^2 (one standard deviation of the mean = 76 gdw/m^2). Such biomass estimates were within 13% of those derived from ground- gathered radiance data.

To assess and compare the abilities of Landsat and SPOT imagery for this purpose, a 21 September, 1984 Landsat Thematic Mapper (TM) and 13 September, 1986 SPOT multispectral image of the Lewes,

Delaware, area were analyzed. Many distinct Delaware Bay water features were evident on the SPOT image. These patterns were not apparent on the TM image, presumably because of extensive horizontal striping. Thus, SPOT imagery's superior radiometric quality makes it preferable to bands 2, 3, and 4 of Landsat TM data for analysis of coastal water masses. The wetland portions of both images were used to compute changes in the vegetation index (VI) from 1984 to 1986 for pixels representing the dominant salt marsh grass *Spartina alterniflora*. This procedure revealed substantial variation in relative VI, and presumably also productivity for similar pixels between years. For monitoring wetland vegetation, SPOT's better spatial resolution facilitates discrimination between areas of vegetation and water, and permits enhanced detection of productivity changes occurring on a small spatial scale. The TM collects data in a blue band and two near infrafred bands not covered by SPOT. This may make TM data more useful for distinguishing vegetation types and certain water features. ■

LATITUDINAL VARIATION IN BELOWGROUND BIOMASS AND CANOPY REFLECTANCE OF *SPARTINA ALTERNIFLORA*

M. A. Hardisky[1], M. F. Gross[2], V. Klemas[2], and P. L. Wolf[2]
[1]*Biology Department, University of Scranton, Scranton, Pennsylvania 18510 and* [2]*College of Marine Studies, University of Delaware, Newark, Delaware 19716*

Of fundamental importance to understanding energy flow in an ecosystem is the quantification of carbon fixation through photosynthesis. All heterotrophic biological activity, including biogenic gas formation, is dependent on this supply of fixed energy. Traditional surveys of wetlands biomass (a measure of net carbon fixation) have focused on the aboveground canopy because of its accessibility and relative ease of quantification. Scientists have long recognized the importance of the belowground (root) component in the total productivity of the emergent plants, but because of the difficulty in sampling and processing these samples, few reliable estimates of belowground biomass exist. In support of the biogenic gas flux studies and simply as a fundamental question that needs to be addressed, we have embarked upon a series of studies to relate aboveground biomass (quantifiable using remote sensing techniques) to the belowground biomass. The scope of our work also includes a quantification of latitudinal differences in the above- to belowground biomass relationship.

Initial results have shown a positive and highly significant relationship to exist between above- and belowground biomass (correlation coefficients 0.60-0.70). Difficulty in sampling, as well as in parameters other than aboveground biomass itself, likely account for the scatter observed in the relationship. For example, we suspect that various edaphic factors such as soil porosity, nutrient concentrations, anaerobiosis and soil composition may also influence belowground biomass development.

Other published studies have shown a latitudinal disparity in the canopy architecture of *Spartina alterniflora*. This intrinsic growth difference will affect our ability to estimate the aboveground component of *S. alterniflora*. This observation may also be indicative of a similar difference in the development of the belowground component of *S. alterniflora*.

Remote sensing of belowground biomass over large regional areas depends on accurate estimation of the aboveground component. We have accomplished this for the Delaware area and will extend this as our work progresses. The use of satellite imagery as a large-scale estimator of above- and belowground biomass remains an exciting and highly promising technique. ■

BIOGEOCHEMISTRY AND GASEOUS SULFUR RELEASE IN TIDAL WETLANDS

M. E. Hines
University of New Hampshire, Institute for the Study of Earth, Oceans and Space, Science and Engineering Research Building, Durham, New Hampshire 03824

The production and flux of biogenic gases from terrestrial ecosystems is a function of several interrelated conditions and processes including floral speciation and physiology, soil chemistry, salinity, temperature and the duration and vigor of the growing season. Tidal wetlands are especially influenced by the physical environment, since they act as an interface and buffer between the aquatic and terrestrial environments. Hence, these ecosystems are unusually complex and productive and can act as a source of biogenic compounds which greatly exceeds an averaged ecosystem.

Because of the juxtaposition to the sea and the varying redox gradients, salt marshes have an abundant source of sulfur and potentially can generate an unusually large quantity of biogenic sulfur gases. To fully understand the role of wetlands in atmospheric chemical budgets it is necessary to study the total environment, including the soil, to clarify the effects of physical factors on gaseous emissions. The present study has been examining the short- and long-term changes in the biogeochemistry of tidal wetlands in terms of sulfur cycling and the production and flux of sulfur gases to the atmosphere.

Two temperate East Coast marsh systems have been studied during the past three years. The New Hampshire marsh under investigation is dominated by *Spartina* plant species particularly *S. patens*, with a narrow but productive stand of *S. alterniflora* along river and creek banks. The Great Marsh in Lewes, Delaware, was investigated during June of 1986 as part of an interdisciplinary study to examine the flux of various gases from tidal wetlands along a salinity gradient. The Delaware marsh contained a variety of grass species but was dominated by *S. alterniflora* and *S. patens*.

Sedimentary pore water samples were collected using *in situ* samplers which were deployed several days prior to use and which minimize disturbance to the plant root-rhizome system. Rates of bacterial sulfate reduction were determined using radioisotopes. Solid phase analyses were conducted on core samples which were handled anoxically. Emission rates of the gaseous sulfur compounds methane thiol (CH_3SH), hydrogen sulfide (H_2S), dimethyl sulfide (DMS), carbonyl sulfide (COS) and carbon disulfide (CS_2) were determined using a dynamic flow-through teflon flux chamber. Gas samples were concentrated in cryogenic traps and, after remobilization, were analyzed using a gas chromatographic system with a flame photometric detector.

The sedimentary biogeochemistry of the New Hampshire marsh was influenced primarily by the growth of marsh plants and the desiccation of marsh soils by periodic precipitation events and the cycling of the tide. Rapid bacterial anaerobic activity occurred only during periods of rapid plant growth. However, this vigorous growth of marsh vegetation also caused an oxidation of marsh soils which enhanced the turnover of sulfide in the sediments. The high marsh soils were subjected to severe desiccation during neap tides and periods of drought which caused a reoxidation of iron and the recycling of iron and sulfur. This prevented the accumulation of reduced sulfur compounds in the high marsh soils.

Diel measurements of sulfur gas fluxes revealed that the total S flux rate was similar at *S. alterniflora*-containing locations which differed tremendously in terms of sedimentary chemistry. A large portion of the Delaware marsh contained sediments which were oxidizing and low in pH due to sulfur oxidation within the soil. However, the flux of DMS from these sites was similar in magnitude to the flux noted at a site which exhibited reducing, neutral soils rich in dissolved sulfide. Conversely, H_2S fluxes were influenced strongly by subsurface chemistry, and a rapid flux was noted only at sites rich in dissolved sulfide.

Sulfur gas fluxes varied greatly throughout the day. DMS flux rates were most rapid at night and appeared to be enhanced by the condensation of water on grass leaves. H_2S fluxes also increased at night but decreased rapidly at dawn, presumably because of the pumping of photosynthetically-generated oxygen to roots. H_2S fluxes also increased very quickly as a result of tidal pumping of sedimentary pore waters. The fluxes of CS_2, COS and CH_3SH were much slower than the fluxes of DMS

and H_2S and fluxes of the former gases varied throughout the day. DMS was the major S gas emitted for *S. alterniflora*-containing soils. However, DMS fluxes from *S. patens* were slow. The results suggested that DMS is emitted from the leaves of marsh plants while H_2S is emitted directly from soils. Although the sites studied were marine, the flux of sulfur gases amounted to ~ 2% of the flux of methane from the same locations.

Extrapolation of flux data revealed that salt marshes contribute ~ 1.5 Tg of S globally to the atmosphere. This estimate is a maximum since measurements were made during an active period of the year and only rates for *S. alterniflora* were considered in the calculation. ■

METHANE PRECURSORS IN MARINE AND OTHER SALINE ENVIRONMENTS

G. M. King
Darling Marine Center, University of Maine, Walpole, Maine 04573

Methane production in marine or other saline environments containing sulfate is limited by competition with sulfate-reducing bacteria. Typically, sulfate reducers dominate the metabolism of hydrogen and acetate, which are the primary methane precursors in nonsaline environments. Other substrates, such as trimethylamine, are utilized by methanogens, however. In fact, the presence of trimethylamine may explain a major fraction of the methane produced in surface, sulfate-rich sediments of a variety of systems, including nearshore sediments, salt marshes, and hypersaline systems.

During the past three years, a research effort has been devoted to determining the distribution and metabolism of trimethylamine and its relationship to methanogenesis. Particular emphasis has been placed on measurements of trimethylamine precursors, such as glycine betaine (GBT), as well. Both trimethylamine and GBT have been commonly observed in intertidal mudflats, salt marshes, and hypersaline algal flats. In an intertidal mudflat, trimethylamine was observed to account for 35-61% of surface (0-10 cm depth) methane production. The pool sizes of trimethylamine in this system were 0-3 μmol/l.

In salt marshes a variety of experiments have also implicated trimethylamine as an important methane precursor. First, GBT, the major trimethylamine precursor, has been found in the predominant salt marsh flora and fauna at concentrations typically between 50-300 μmol/g dry weight of tissue. The primary pool of GBT occurs in the halophyte *Spartina alterniflora*. Concentrations are greatest in the plant shoots, but about two-thirds of the total plant inventory occurs belowground due to the large biomass of roots. Plant concentrations were sensitive to the availability of nitrogen as indicated by increases after fertilization with ammonium chloride. GBT concentrations are also sensitive to salinity regimes as indicated by analyses of plants occurring over a gradient from about 10-65 ‰; over the gradient, GBT tended to increase markedly.

Second, radiotracer studies have demonstrated that both GBT and trimethylamine are converted to methane. Ratios of methane to CO_2 production indicated that an oxidative process, probably sulfate reduction, competed to some extent with methanogenesis for trimethylamine. In general, however, methogenic bacteria were responsible for at least 50% of the substrate metabolism. Relatively more important roles for methanogens were observed in sediments containing plants with increased GBT due to fertilization.

Third, fluxes of methane were greater in experimental field plots of *S. alterniflora* that had been fertilized with nitrogen. Increased fluxes were presumably due to increased plant GBT which in turn resulted in increased trimethylamine concentrations in the sediment. A close association of methane production in surface marsh sediments with trimethylamine supplied from the plant roots may explain the enhanced flux of methane to the atmosphere observed by Chanton, Bartlett and others.

An important role for GBT and trimethylamine has also been noted for sediments from a hypersaline algal mat. A *Spirulina*-dominated algal mat occurring in a pond with a salinity of >180 ‰ contained

very high GBT and trimethylamine concentrations. These substrates appeared to support extremely high rates of methanogenesis near the sediment surface, in spite of the co-occurrence of high rates of sulfate reduction. The observed rates of methanogenesis were sufficient to form gas bubbles containing about 35% methane. Additions of GBT, choline, trimethylamine, trimethylamine oxide and methanol all strongly stimulated methanogenesis while hydrogen, acetate, or inhibition of sulfate reduction had little effect. These results contrast to some extent with most marine systems, but are consistent with the characteristics of methylotrophic methanogens.

An additional analysis of methanogenesis in sediments from hypersaline Mono Lake provided different results. In this system, methanogenesis appeared dominated by CO_2 reduction and not by methylamine metabolism as in other saline systems. This difference was probably due to the lack of significant sources of methlyamines in Mono Lake sediments; in salt marshes and hypersaline algal mats, methylamine sources occur in close association with methanogenic environments.

In summary, the results of these studies illustrate the importance of trimethylamine and its precursors for methanogenesis in saline, sulfate-rich ecosystems. Controls of amine distribution and metabolism as well as methane production in these systems are the result of complex interactions between salinity, nitrogen availability, osmoregulation, and microbial physiology. ■

BIOGEOCHEMICAL CYCLE OF DIMETHYLSULFIDE IN A STRATIFIED COASTAL SALT POND

S. G. Wakeham
Skidaway Institute of Oceanogaphy, Post Office Box 13687, Savannah, Georgia 31416

The global atmospheric sulfur cycle requires a substantial flux of biogenic sulfur from the ocean to the atmosphere. Dimethylsulfide (DMS) is the most abundant biogenic volatile sulfur compound in the ocean. Investigations into the distribution of DMS in surface seawater and in the marine atmospheric boundary layer indicate that the DMS flux constitutes some 90% of annual oceanic flux of biogenic sulfur and may be roughly equivalent to 50% of the global biogenic sulfur flux to the earth's atmosphere. Considerable attention has therefore been focused on the distribution and dynamics of DMS in the marine environment in an effort to understand the mechanisms controlling its production and flux to the atmosphere. We have been investigating the biogeochemsitry of DMS in a coastal salt pond as part of a study to characterize the processes which produce and consume DMS in the aquatic environment. Salt Pond is a shallow (5.5m) eutrophic coastal marine basin on Cape Cod, MA. During summer, the pond becomes thermally stratified and bottom waters are highly anoxic. Thus aerobic processes dominate the epilimnion, but sulfate reduction in the hypolimnion leads to bottom water concentrations of H_2S upwards of 3 nmol/L. The oxic-anoxic interface in late summer rises to within 2-3 m of the pond surface, and steep biogeochemical gradients develop in the metalimnion. The water column of the pond

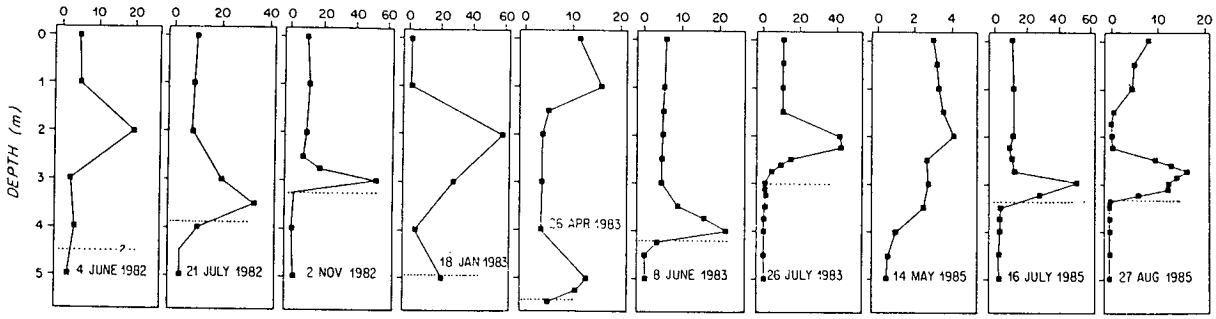

Figure 1.

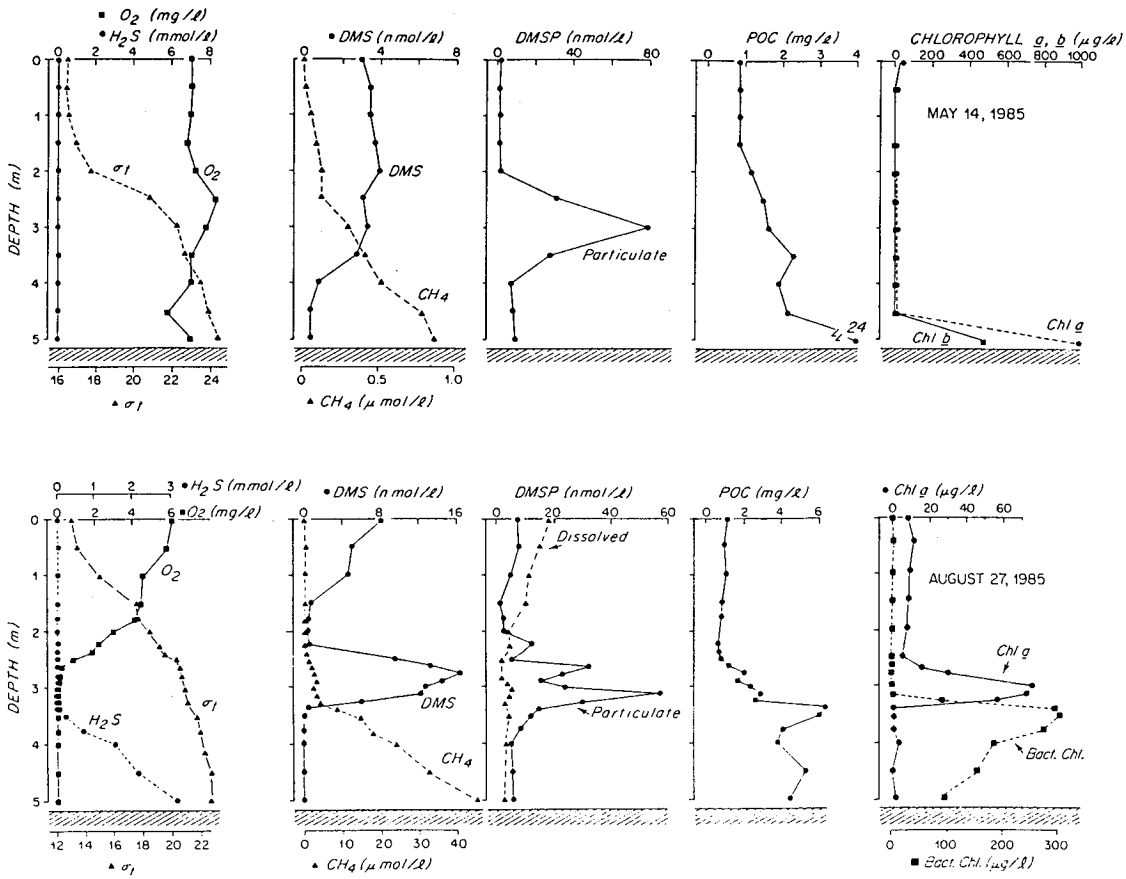

Figure 2.

therefore exhibits a diversity of biological and geochemical environments making it an ideal site to investigate biogeochemical cycling.

Seasonal distributions of DMS in the water column of Salt Pond have been determined over several years (Fig. 1) and have been coupled with simultaneous measurements of other water column geochemical and biological parameters (Fig. 2). Concentrations of DMS in summer were on the order of 10 nmol/L in the oxic epilimnion, peaked at up to 60 nmol/L in the oxygen-depleted metalimnion, and decreased sharply at the top of the sulfidic hypolimnion to less than 0.2 nmol/L. Often there was poor correspondence between DMS vertical concentration profiles and algal biomass as indicated by chlorophyll *a* measurements. DMS concentrations in the epilimnion were generally higher than typical ocean values of 5 nmol/L or less, but were similar to concentrations in coastal upwelling areas. The absence of a DMS-chlorophyll *a* relationship in the pond also contrasts with oceanic DMS distributions which do tend to show a general relationship with phytoplankton productivity and biomass, an observation which has been taken as indicating a phytoplankton source for DMS in seawater.

Nevertheless, as in the ocean, the primary source of DMS in Salt Pond appears to be the breakdown of algal dimethylsulfoniopropionate (DMSP). DMSP is a natural product in many species of phytoplankton and may be involved in regulating cellular osmotic pressure. DMSP concentrations are highest in the epilimnion and metalimnion of the pond, reaching levels of about 100 nmol/L (Fig.2). The hypolimnion contains only a few nmol/L DMSP. Enzymatic cleavage of DMSP yields DMS and acrylic acid. Intercellular conversion of DMSP (or other similar sulfonium compounds) to DMS may lead to direct release of DMS by alga in the epilimnion, or DMSP itself may be released and its decomposition may be extracellular. DMS may also be released as algal cells are grazed by herbivorous zooplankton. It is, however, the oxygen-depleted metalimnion which appears to be the major site of DMS production. Physiological stress on otherwise healthy cells resulting from depressed oxygen tensions may lead to release of DMS. A more likely mechanism, however, involves microbially-mediated breakdown of DMSP

during decomposition of organic material near the oxic-anoxic interface. DMSP concentrations and particulate organic carbon turnover times in the pond have been used to estimate a DMS production rate of 20 umol/m^2 d in the epilimnion and metalimnion. Production of DMS does not appear to be associated with microbial decomposition related to sulfate reduction which occurs in the hypolimnion because DMS concentrations in the hypolimnion were always extremely low. Anoxic sediments also are not a significant source of DMS in the water column (in contrast to methane; Fig. 2) since concentrations do not increase toward the sediment bed.

In the summer, the pond appears to be in quasi-steady state with respect to DMS distributions and inventory, so there must be a balance between rates of production of DMS and its removal from the water column. We have identified the major processes which remove DMS from the pond as being gas exchange across the pond surface into the atmosphere, tidal exchange to coastal seawater in adjacent Vineyard Sound, and metabolism of DMS in the epilimnion or at the top of the hypolimnion. It is possible to estimate removal rates for the individual processes. The flux of DMS out of the pond via gas exchange may be predicted from the two-film model to be about 4 umol DMS/m^2 d. Tidal exchange is minimal and may remove an additional 0-2 umol DMS/m^2 d. It is the sharp concentration gradient for DMS at the metalimnion-hypolimnion boundary where a lens of photosynthetic bacteria occurs (bacterial chlorophyll *d* in Fig. 2) which suggests that consumption of DMS by anaerobic bacteria at the top of the hypolimnion may be the major removal process. Microbial metabolism at the top of the hypolimnion could consume some 30 umol DMS/m^2 d.

Laboratory experiments have shown that some components of the microbial population indigenous to Salt Pond are capable of decomposing DMSP to DMS. Microbial activity towards DMSP decomposition increases toward the metalimnion. There is also laboratory evidence that some of the microorganisms in the hypolimnion can anaerobically degrade DMS. The photosynthetic bacterial plate at the top of the hypolimnion is composed of phototrophic purple and green sulfur bacteria and is responsible for the elevated concentrations of particulate organic carbon and bacterial chl *d* immediately below the oxic-anoxic interface (Fig.2). Enrichment cultures of photosynthetic purple bacteria from the pond are able to oxidize DMS to dimethylsufoxide (DMSO). DMS supports growth of these bacteria by serving as an electron source of photosynthesis, with electrons released during oxidation of DMS to DMSO being quantitatively used to reduce CO_2 biomass. Certain cultures of bacteria from the pond were also able to use DMSO as an electron acceptor in a light-independent reduction of DMSO back to DMS. Thus there appears to be a sulfur cycle involving anaerobic interconversions between DMS and DMSO. ■

PAGE 325 INTENTIONALLY BLANK

PRECEDING PAGE BLANK NOT FILMED

REMOTE SENSING STUDIES OF THE FLORIDA EVERGLADES CONDUCTED IN SUPPORT OF THE METHANE FLUX STUDY

D. Dow[1], R. Pelletier[1], C. Clark[1], D. Brannon[1], and L. Gunderson[2]
[1]*NASA/Earth Resources Laboratory, National Space Technology Laboratories, NSTL, Mississippi 39529 and*
[2]*U. S. National Park Service, South Florida Research Center, Everglades National Park, Homestead, Florida 33030*

Remote sensing analysis has proven to be a valuable tool in supporting biogeochemical studies in wetlands. Remote sensing investigations allow one to identify the area occupied by different vegetation types and the ratio of land-to-water area within the watershed. In the methane flux project a geographic information system (GIS) approach has been employed to combine data bases generated in the field with those developed from remote sensing analysis. The major goals of the remote sensing investigations are to provide an estimate of the vegetative area occupied by classes with distinctly different methane flux rates and to estimate the extent of inundation in the Florida Everglades on a seasonal basis. Since methane production is an anaerobic process carried out in waterlogged soils, the extent of inundation is a key environmental variable influencing methane flux rates. In the Florida Everglades the extent of inundation of each vegetative type varies seasonally due to the manipulation of the system's hydrology by man and seasonal changes in the balance of precipitation and evapotranspiration. Minimum water levels in the Everglades National Park occurs in May, while maximum water depth occurs in September.

The Thematic Mapper (TM) with a 30 meter pixel size and the Advanced Very High Resolution Radiometer (AVHRR) sensor with a 1 kilometer spatial resolution have been utilized in this study. The

Table 1. Thematic Mapper Land Cover Classification of Shark River Slough, Florida (December 20, 1984 Data).

Land Cover Type	Area in Ha.	% of Total	Classification Accuracy (%)	Object Accuracy (%)
Sawgrass/Muhly Prairie	28007	20.2	62	90
Sawgrass Marsh (wet)	22902	16.5	95	90
Dwarf Cypress Prairie	18664	13.5	81	85
Sawgrass Marsh (dry)	12554	9.1	85	85
Sparse Sawgrass, Rock	12335	8.9	89	85
Marsh Complex	8999	6.5	91	100
Dense, Tall Sawgrass	8555	6.2	95	95
Slough (periphyton)	7722	5.6	100	90
Slough (water)	5439	3.9	100	80
Wetland Hardwoods	5178	3.7	81	85
Dwarf Red Mangrove	4533	3.3	100	95
Red Mangrove	3246	2.3	100	84
Upland Hardwoods	333	0.2	100	90
TOTAL	138469	100.0	x = 91	89

Classification Accuracy: % of remote sensing derived classes that is actually the land cover class in question (as identified on the ground).

Object Accuracy: % of the ground truth derived class that is accurately identified by the remote sensing class.

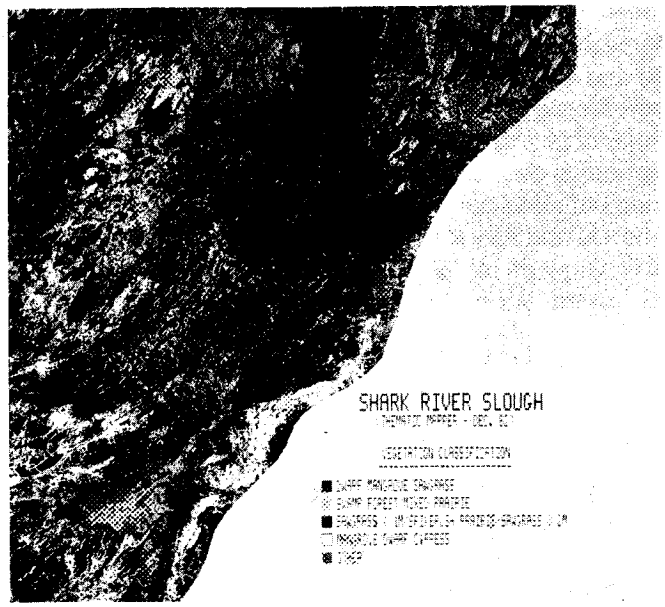

Figure 1. Classified Thematic Mapper Data Over Shark River Slough, Florida (December, 1984).

initial TM scene processed utilized bands 3, 4, 5, and 6 in an unsupervised classification for a data set from December 1984. Due to the cloud cover over parts of the Everglades National Park (ENP) and the inability to spectrally separate pines from mangroves at this time of the year, the initial remote sensing analysis was limited to the Shark River Slough area. A 13 class vegetation cover map was produced which had an acceptable classification accuracy (see Table 1) of 91% and object accuracy of 89%. Methane flux measurements in the field resulted in 5 statistically significant land cover types, so that the 13 class land cover map was condensed to the 5 class product illustrated in Figure 1. A November, 1985 TM scene with minimum cloud cover over the ENP has been obtained and is being examined for its potential to produce a land cover map of the entire ENP that can detect the 5 distinctly different methane flux land cover types.

AVHRR data has been collected from March, April, May and October of 1986 and February of 1987. Figure 2 illustrates the 12 class land cover map produced from an unsupervised classifier using bands 1,

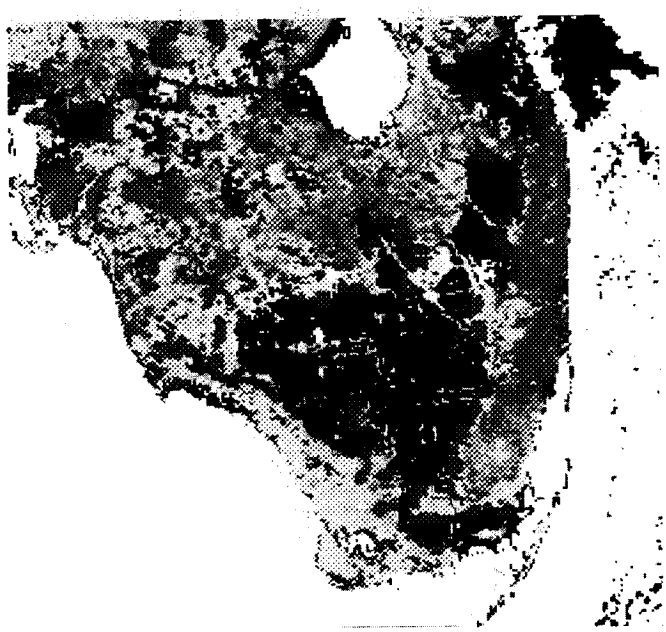

Figure 2. Classified Advanced Very High Resolution Radiometer Data Over South Florida (October, 1986).

2, and 4 from the October, 1986 data set. The CAUSE classifier utilized has produced similar land cover maps for the other dates in 1986. Nighttime AVHRR data in February, 1987 and October, 1986 is being examined using bands 3 (mid-IR) and 4/5 (thermal) to produce an inundation mask for the ENP. The AVHRR data can be gathered more frequently than TM data and offers the possibility of region wide coverage with a reasonable number of pixels, but suffers from the disadvantage that AVHRR data integrates vegetation spectral signatures over a large pixel size (1 km) (creating many mixed pixels and thus creating difficulties in carrying out an accuracy assessment).

By combining the benefits of the TM and AVHRR data, we hope to produce a vegetation cover/ inundation extent product that will supplement the methane flux measurements made in the field and aid in the construction of the GIS system for estimating the methane flux from the Everglades National Park. ■

METHANE FLUXES FROM ORGANIC-RICH ENVIRONMENTS: RADON TRACING OF TRANSPORT AND SEASONAL VARIATION IN ISOTOPIC COMPOSITION

C. S. Martens and J. P. Chanton
Marine Sciences Program, 12-5 Venable Hall 045A, University of North Carolina, Chapel Hill, North Carolina 27514

Methane and other reduced biogenic gases are known to have important roles in atmospheric chemical and radiative heat transfer processes. Recent observations of systematic increases in the atmospheric concentration of methane and other biogenic gases have led to intensified efforts to quantify their fluxes from potential sources which include organic-rich sediments and flooded soils. Mechanisms of gas transport from these environments include molecular diffusion, advection through plants, and ebullition of methane-rich gas bubbles. Recent studies of methane fluxes from central Amazonian floodplain lakes and wetlands suggest that gas bubble ebullition may be the dominant transport mode among these on a worldwide basis.

Ebullition from methane-saturated sediments also represents a potentially important delivery system to overlying waters and the troposphere for many other dissolved gases, some of which are known to be stripped from surrounding pore waters by upward migrating bubbles. Marine and tidal freshwater systems, the latter comprising over 164,000 ha on the U.S. Atlantic Coast, contain tremendous inventories of buried gas, typically over 15 liters per m^3 during warm summer months. The inventory changes seasonally in response to temperature-controlled microbial production rates. In such systems we have found that ebullition is triggered by tidal hydraulics: as the tidal cycle reaches its nadir, water

Figure 1.

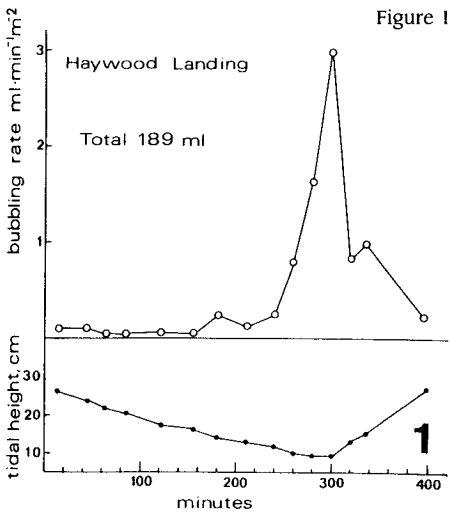

Figure 2.

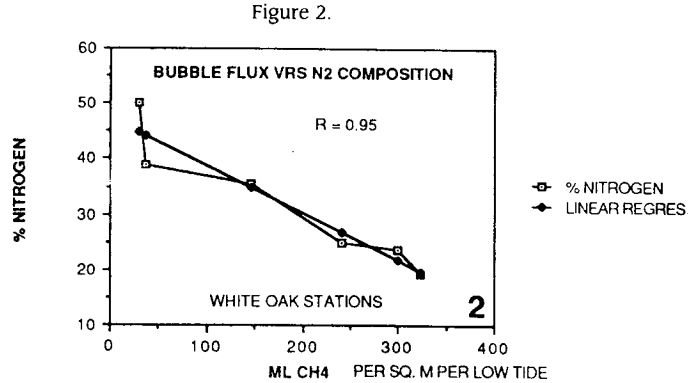

column hydrostatic pressure is decreased. This pertubation causes an intense pulsed release of reduced gases as shown in Figure 1. The major gas in released bubbles is generally methane, with the balance comprised of N_2, CO_2 and other trace gases, including radioactive radon-222. Ebullition rate controls bubble N_2 composition as illustrated in Figure 2; such compositional variation may be a useful indicator of relative methane flux rates from wetlands.

Measurements of radon activity in gas bubbles can be used to quantify dissolved gas equilibration and stripping rates from ebullating sediments as illustrated by measurements over the past three years at our coastal study site (Figure 3). These results prove that gas bubbles are rapidly equilibrated with dissolved gases in surrounding sediments by diffusion. Seasonal variations in radon-222 activity exactly follow temperature-dependent solubility predictions. The ebullative radon flux divided by sediment radon inventory yields a stripping efficiency which can be directly applied to other reducing gases. Since radon is a radioactive conservative tracer, it can also be used to help distinguish processes following ebullition such as oxidation or dissolution in overlying waters.

We have begun systematic measurements of carbon isotopic values in methane from a series of well-characterized, temperate and subtropical marine and freshwater sites, including the Everglades, in conjunction with NASA-Langley scientists. The most important findings from this work to date are large seasonal variations at all three of our temperate sites (Figure 4) which are on the order of 10‰. These

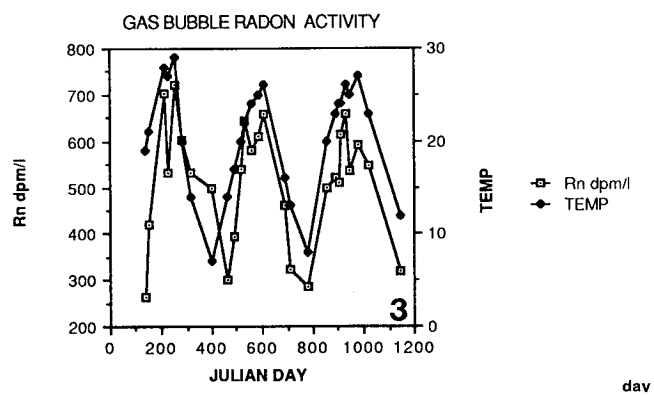

Figure 3.

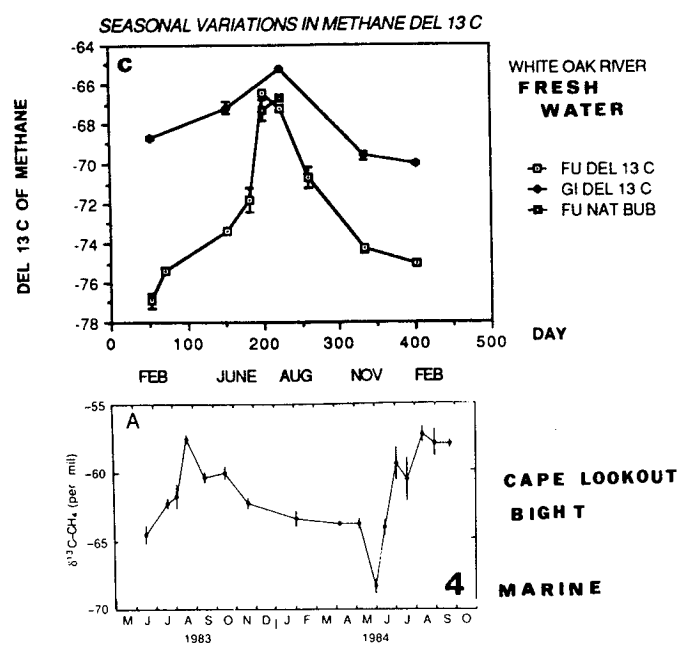

Figure 4.

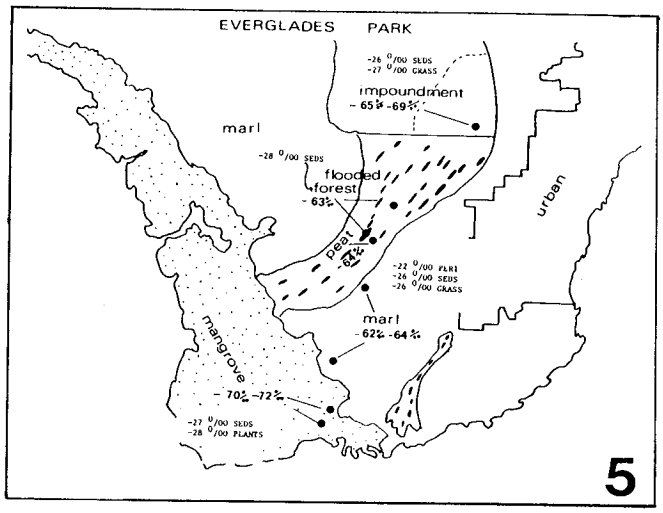

Figure 5.

variations may be controlled by changes in microbial methane production pathways. Two recent publications in *Science* describe the significance of our findings. Attempts to establish a global isotopic mass balance for atmospheric methane must account for such variation.

Figure 5 shows the carbon isotopic composition of sedimentary methane in gas bubbles at sites typical of four major wetland ecosystems in the Florida Everglades identified by remote sensing. The ecosystems and their methane isotopic composition are: (1) wet prairie and sawgrass marsh, -62 to -64‰, (2) wetland forest, -63‰, (3) mangrove swamp, -70 to -72‰, and (4) man-made impoundments, -65 to -69‰. The carbon isotopic composition of plants and sediments (Figure 5) varies only by 3 ‰, while that of associated methane varies by a factor of 10 ‰, which suggests an important role for plant oxidative processes. Using a weighted average approach based upon the aeral extent of each ecosystem, we calculate a weighted average CH_4 isotopic composition of -65 ‰ for the Everglades system. Flux chamber experiments indicate an isotopic enrichment on the order of 5‰ due to oxidation during transport to the troposphere.

ISOTOPIC COMPOSITION OF METHANE IN PLANTS

	% CH_4 IN STEM		PLANT DEL ^{13}C	BUBBLE DEL ^{13}C
EVERGLADES				
P.H. PELTANDRA	2.3		-51.1 (.1)	-63.1 (.3)
PHO ARROWHEAD	2.0		-59.7 (0.1)	-63.8 (.1)
P-33 NYMPHAEA	0.8		-74.4	-63.8 (.1)
WHITE OAK				
21 JULY CATTAIL	0.4		-64.3 (2.1)	-65.3 (.1)
13 AUG CATTAIL	0.7		-51.8 (17.1)	-62.6 (.3)
		OR	-61.6 (1.7)	
13 AUG PONTIDERIA	0.3		-47.1 (3.3)	-62.6 (.3)

Rooted aquatic plants have been shown by other workers to be important conduits for methane transported from sediments to the atmosphere. Our initial isotopic investigations of isotopic fractionation occurring during such transport (Table 1) show that heavier $^{13}CH_4$ is preferentially delivered to the atmosphere. No such fractionation is observed for methane transported by ebullition. ■

GIS IMPLEMENTATION FOR METHANE FLUX ESTIMATES FROM THE SHARK RIVER SLOUGH OF THE FLORIDA EVERGLADES

R. Pelletier[1], D. Dow[1], C. Clark[1], D. Brannon[1], D. Bartlett[2], K. Bartlett[2], R. Harriss[2], and D. Sebacher[2]
[1]*NASA/Earth Resources Laboratory, NSTL, Mississippi 39529 and* [2]*NASA/Langley Research Center, Hampton, Virginia 23665*

The concentration of atmospheric methane has been observed to be steadily increasing during the past decade. Historical records indicate a gradual rise even over the last 400 years. During that length of time, atmospheric concentration has nearly tripled from 0.6 ppm to 1.6 ppm. Such levels may seem small, but the effect from these and expected future changes, if trends continue, could have a great impact on atmospheric chemistry and radiative properties and thus climate. While the increase in CO_2 is generally thought to be the cause for the "greenhouse effect" other trace gases, among which CH_4 is quite important, play significant roles.

Most CH_4 sources are biogenic in origin and due to microbial anaerobic processes. A major source of methane flux to the atmosphere are natural wetlands which produce CH4 through the anaerobic decomposition of organic material in waterlogged soils and sediments. In this paper we examine one of the world's significant wetland regions, the Florida Everglades, and attempt to estimate large scale CH_4 flux through the extrapolation of measured flux rates in a Geographical Information System (GIS).

The Everglades cover most of the southern third of the state of Florida; and water flow out of the marsh system is dominated by the Shark River Slough, which extends from below Lake Okechobee southwest to the Gulf of Mexico. Approximately 80% of the average annual 1375 mm of precipitation falls between June and September with the winter representing the dry season. Saw-grass marsh is the dominant vegetation accounting for perhaps 70% of vegetation cover.

Landsat Thematic Mapper data were acquired from a December overpass and processes to delineate 13 vegetation categories. Using these categories as a sampling guide *in situ* CH4 flux measurements were collected. Based on these flux readings the vegetation categories were recombined into five new composite categories that represented vegetation types and sizes that displayed similar flux results. Following from the known hydroperiod of the original vegetation classes, inundated vs. non-inundated classifications were developed for both the dry and the wet seasons. Vegetation which was located in a "non-inundated" area was assumed to contribute negligibly as a CH_4 source since conditions were unlikely to be anaerobic enough for methanogenesis. (Vegetation located in saline environments, *e.g.*, mangroves, were similarly classified as a negligible source of CH4 due to the inhibition of methanogenesis by the presence of sulfur). Vegetation located in "inundated" areas were assigned CH_4 flux values based on the *in situ* measurements from its composite vegetation category.

Table 1 lists the five composite vegetation categories and respective areal coverages. Table 2 lists the vegetation/flux classes for the wet season with the respective areal coverages, flux rate per day, extrapolated flux amount per class per day, and the total daily flux amount for the Shark River Slough

TABLE 1. Vegetation Classification for the Shark River Slough

Vegetation Class	% Area	Hectares
1—Dwarf mangrove/Sawgrass	20	27381
2—Swamp forest/Mixed prairie	8	11546
3—Sawgrass <1M/Spikerush prairie/ Sawgrass >2M	54	74504
4—Mangrove/Dwarf cypress	16	21884
5—Other	2	2938
Total		138253

TABLE 2. CH_4 Flux Classification for the Shark River Slough (Wet Season).

Vegetation/Flux Class	% Area	Hectares	Flux (g/ha/day)	Category Flux (g/day)
1—Dwarf mangrove/Sawgrass	20	27381	1020	2.79×10^7
2—Swamp forest/Mixed prairie	8	11546	720	8.31×10^6
3—Sawgrass <1m/Spikerush prairie/Sawgrass >2m	45	61978	386	2.39×10^7
4—Mangrove/Dwarf cypress	16	21884	62	1.36×10^6
5—Other/negligible flux	11	15464	0	0
Total				6.15×10^7

TABLE 3. CH_4 Flux Classification for the Shark River Slough (Dry Season).

Vegetation/Flux Class	% Area	Hectares	Flux (g/ha/day)	Category Flux (g/day)
1—Dwarf mangrove/Sawgrass	20	27381	1020	2.79×10^7
2—Swamp forest/Mixed prairie	8	11546	720	8.31×10^6
3—Sawgrass <1m/Spikerush prairie/Sawgrass >2m	25	33998	386	1.31×10^7
4—Mangrove	2	3246	62	2.01×10^5
5—Other/Negligible flux	45	62082	0	0
Total				4.95×10^7

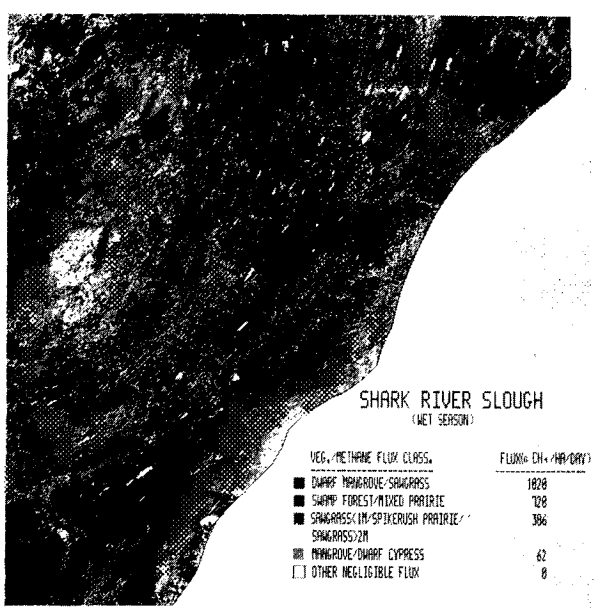

Figure 1. Methane flux classification for the Shark River Slough (wet season).

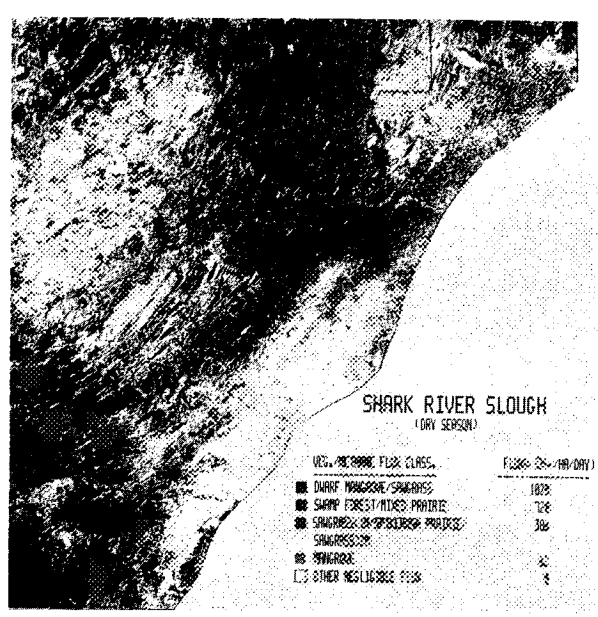

Figure 2. Methane flux classification for the Shark River Slough (dry season).

region under study. Figure 1 illustrates the spatial distribution of the five flux classes for the wet season. Table 3 lists the same information for the dry season as Table 2 did for the wet season. Figure 2 spatially illustrates the dry season flux classes.

Geographical Information Systems have much to offer in modelling local, regional and global estimates of methane flux and other biogeochemical concerns. Thirty meter Thematic Mapper data was used as the land cover classification source in this case, but for larger scale analysis a coarser resolution data source such as AVHRR (Advanced Very High Resolution Radiometer), with a 1 km cell size, may prove more cost efficient while possibly still working as effectively as a classification source. Research is continuing to evaluate such use of AVHRR data in global biogeochemical modelling. ■

ROLE OF SPACECRAFT IMAGING RADAR IN VECTOR-BORNE DISEASE STUDIES

J. F. Paris
Jet Propulsion Laboratory

Recent advances in the understanding of the interactions between microwaves and elements (vegetation and its substrates) of terrestrial scenes have provided the basis for the development of spacecraft imaging radar technology for vector-borne disease studies. Using 23-cm (L-band) synthetic aperture radar (SAR) image data from the Seasat mission in 1978 and from the Shuttle Imaging Radar (SIR) missions in 1981 and 1984, environmental scientists discovered that vegetated wetlands (*e.g.*, marshes, swamps, rice fields, and temporarily-flooded areas) always appear on L-band SAR images as distinctly bright regions. In contrast, open water areas are very dark. Public health organizations can use these distinct signatures to locate and characterize the condition of vector habitats in relationship to human habituations as involved in the transmission of certain diseases. The SAR technology provides the additional capability of obtaining this information under cloudy conditions (that often occur in endemic areas). Thus, one can make assessments of changes in habitat environmental conditions during a season with high reliability. In the coming decade, several countries will put operational SAR systems on earth-orbiting spacecraft of long duration. These include the first European Remote Sensing Satellite (ERS-1) SAR in about 1990, the first Japanese Earth Resources Satellite (JERS-1) in 1991, the Canadian Radar Satellite (RADARSAT) in 1991, and the joint U.S. and European Space Agency SAR on the Polar Platform of the Space Station in the mid-1990's. These systems will provide L-band, C-band (6 cm) and/or X-band (3 cm) SAR images. The combination of multiwavelength, multipolarization, multiangle and multidate SAR data should add to the proven capability of the L-band SAR. Thus public health organizations should be able to exploit these sources of satellite-borne information in their continuing struggle against vector-borne diseases. ■

VECTOR BORNE DISEASE MODELING UTILIZING REMOTE SENSING AND RELATED GROUND DATA: THE CALIFORNIA STUDY

R. K. Washino and J. G. Lawless
University of California and NASA/Ames Research Center

On a global basis some 92 to 98 million new cases of malaria are estimated to occur every year (WHO 1986a; 1986b), and this very large number of cases is further burdened by the morbidity from other diseases (many of them vector-borne) in the tropical areas of the world. Gratz (1987) states that in the majority of the malarious countries of Asia, a reduced level of malaria is maintained by widespread antimalaria measures including residual application of insecticides, some mosquito

larviciding and the widespread use of antimalarial drugs. However, parasite drug resistance in *Plasmodium falciparum* is widespread, and combined with the problem posed by vector resistance to insecticides, severely hampers the control of malaria transmission.

Principal difficulties associated with the logistics of controlling mosquito vectors of malaria in most disease-ridden areas are in the monitoring and predicting of vector abundance in a geographic area with any degree of precision. Successful application of remote sensing to predict spatial and temporal distribution of mosquito larvae in permanent and semi-permanent breeding habitats would be a major breakthrough in the technology of controlling malaria vectors in tropical and semi-tropical areas of the world. The initial phase to determine the feasibility of such a study was implemented in the Sacramento Valley of California. During the summer of 1985, approximately 46 rice fields were examined at regular intervals. These fields were surveyed for two species of mosquitoes along with possible association with aquatic plants including 19 aquatic emergent and four submerged plants as well as seven species of algae. Simultaneously, 11 imaging missions were flown by U2 aircraft to coincide with the ground examinations of the 46 rice fields. Information was collected by sensors detecting 12 spectral bands including visible, infrared, and thermal regions to determine whether seasonal color changes in the imagery could reflect varying abundance levels in the mosquito population delineated by the associated changes in the aquatic flora.

The results of this study showed that *Anopheles freeborni*, the western malaria mosquito, appeared to be associated with specific vegetative characteristics of rice fields, and that the abundance of larvae showed a significant correlation with reflectance data acquired with the Daedalus Thematic Mapper Simulator (TMS) between June and October 1985. TMS data, specifically the infrared/red ratio, were used to monitor plant biomass and crop development over time. The TMS spectral data showed that those fields with low numbers of mosquito larvae tended to develop slower than those that had high mosquito abundance. This suggested that vegetative characteristics, identified and tracked with aircraft or satellite-borne sensors during early season rice development, could be used to predict larval mosquito production in late summer. Because of these encouraging results, an expanded study, consisting of a much expanded monitoring system, will be executed in 1987. The objective of this more comprehensive study is to develop a predictive model using remote sensing data identifying continuously flooded rice fields having no, low or high mosquito production. The present study will also provide an excellent opportunity to better define the functional relationship between the remote sensing data and development of the vector mosquito habitat, and if successful, will offer a more precise basis to work out strategies for controlling anopheline vectors of malaria in afflicted areas of the world. ■

REFERENCES

WHO. 1986a. WHO Expert Committee on malaria. 18th report. Tech. Rpt. Ser. No. 735. World Health Organization, Geneva.

WHO. 1986b. World malaria situation. 1984. Wld. Hlth. Statist. Quart. 39:171-205. World Health Organization.

Gratz, N.G. 1987. Ricefields, vectors and vector-borne diseases. An assessment of the problems and priorities. Workshop on Research and Training Needs in the Field of Integrated Vector-borne Disease Control in Riceland Agroecosystems of Developing Countries. 9-14 March 1987. IRRI, Manila, Philippines. 9 pp.

PAGE 335 INTENTIONALLY BLANK

PRECEDING PAGE BLANK NOT FILMED

THIOREDOXIN-LINKED ENZYME REGULATION AS A PROBE FOR STUDYING THE EVOLUTION OF PHOTOSYNTHESIS

B. B. Buchanan
Division of Molecular Plant Biology, 305 Hilgard Hall, University of California, Berkeley, California 94720

The aim of our NASA project is to study the structure (amino acid sequence) of thioredoxins and the role of these proteins as regulators of enzymes in primitive photosynthetic organisms. The overall goal of the research is to gain insight into the early stages of the evolution of photosynthesis.

Thioredoxins are low molecular weight (typically ca. 12 kDa) disulfide proteins that appear to function ubiquitously in enzyme regulation in plants, animals and microorganisms. All authentic thioredoxins have an active site consisting of four amino acids — Cys-Gly-Pro-Cys — and undergo reversible oxidation and reduction changes in their functional thiol groups (S-S 2SH). The amino acid sequence of thioredoxins from three photosynthetic bacteria — *Chlorobium thiosulfatophilum, Chromatium vinosum*, and *Rhodospirillum rubrum* — have been completed as a part of the research program in collaboration with Prof. K. Biemann of MIT. These findings are providing a basis for constructing an evolutionary tree based on the structure of these seemingly ancient proteins.

Thioredoxins are important in the regulation of photosynthesis, and there is now extensive evidence that the major pathways of CO_2 assimilation of higher plants (C_3, C_4, and crassulacean acid metabolism or CAM pathways) are regulated by thioredoxins. In our recent research, thioredoxins have been found to play a similar role in oxygenic photosynthetic prokaryotes and eukaryotic algae. Here, as in chloroplasts of higher plants, thioredoxins are part of the ferredoxin/thioredoxin system—a mechanism for the regulation of photosynthetic enzymes (Fig. 1). Knowledge of thioredoxins is important not only because it adds completeness to our understanding of the structure and function of these proteins and their role in primitive types of cells, but also (and as significantly) because it could give clues about the origin of photosynthesis and help toward elucidating the evolution of this fundamental process.

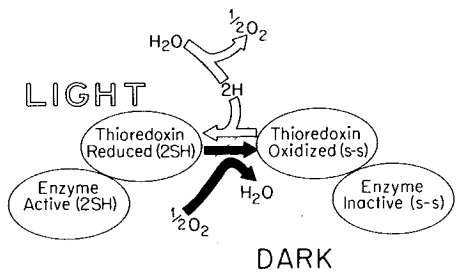

Figure 1. Light activation/dark deactivation enzymes by the ferredoxin/thioredoxin system.

In the ferredoxin/thioredoxin system, thioredoxins are reduced via ferredoxin-thioredoxin reductase by ferredoxin, which itself is reduced by illuminated photosystems of the chloroplast thylakoid membranes (equations 1 and 2). Thioredoxins can also be reduced chemically *in vitro* in the dark by the nonphysiological reagent dithiothreitol (DTT) in the absence of chloroplast membranes, ferredoxin (Fd), and ferredoxin-thioredoxin reductase (FTR) (equation 3).

$$4\ Fd_{ox} + 2\ H_2O \text{ Light } 4\ Fd_{red} + O_2 + 4\ H^+ \qquad (1)$$

Chloroplast thylakoids

$$2\ FD_{red} + 2H^{+} + Thioredoxin_{ox}\ \xrightarrow{FTR}\ 2\ Fd_{ox} + Thioredoxin_{red} \quad (2)$$

$$Thioredoxin_{ox} + DTT_{red}\ \rightleftharpoons\ Thioredoxin_{red} + DTT_{ox} \quad (3)$$

The two thioredoxins, *f* and *m*, are part of the ferredoxin/thioredoxin system, not only in chloroplasts, but also, as found in our NASA research, in cyanobacteria and eukaryotic green algae. In the reduced state, these thioredoxins selectively activate enzymes of biosynthesis and deactivate enzymes of degradation. Recently, we have been able to clone the gene for one of these thioredoxins, thioredoxin *m*, from a cyanobacterium, *Anacystis nidulans* R2. Characterization of this gene is now being completed. Evidence obtained so far from transformation experiments have provided evidence that thioredoxin *m* is essential for growth. This is the first demonstration of such a requirement for thioredoxin in any organism.

We have found that the ferredoxin/thioredoxin system is apparently absent in anoxygenic photosynthetic organisms — *i.e.*, the purple photosynthetic bacteria. Here, enzymes of photosynthetic carbon dioxide assimilation are regulated not by light-actuated reduction, but rather by metabolite changes that fundamentally are independent of light. Photosynthetic bacteria of this type contain a system in which thioredoxin is reduced by NADPH in the presence of thioredoxin reductase — *i.e.*, in the NADP/thioredoxin system (equation 4). In this respect the photosynthetic bacteria, which are anaerobes, resemble aerobic cells of animal, plant and bacterial origins.

$$NADPH_2 + Thioredoxin_{ox}\ \xrightarrow[\text{reductase}]{\text{NADP-Thioredoxin}}\ NADP + Thioredoxin_{red} \quad (4)$$

In summary, our results support the view that thioredoxins play an essential role in regulating the reductive pentose phosphate cycle in oxygenic photosynthetic organisms, both eukaryotes and prokaryotes but not in the anoxygenic photosynthetic organisms that have been examined (Fig. 2). The

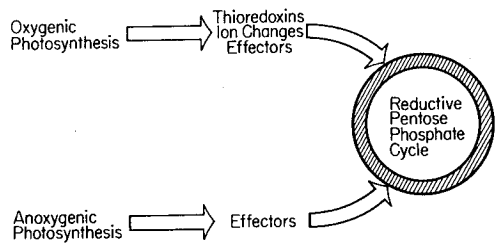

Figure 2. Regulation of the reductive pentose phosphate cycle in oxygenic and anoxygenic photosynthesis.

question arises as to why enzymes catalyzing the same reactions of photosynthetic carbon dioxide assimilation are subject to differential regulation in oxygenic and anoxygenic photosynthesis. While a firm answer to this question awaits further experiments, the data presently available suggest that this difference is related to oxygen availability and function. Thus, oxygenic photosynthetic organisms, characterized by a ferredoxin/thioredoxin system, have oxygen readily available to reverse activation effects of reduced thioredoxin, whereas anoxygenic organisms by the NADP/thioredoxin system, do not have that option because of their need for anaerobiosis for photosynthetic growth. On this premise, it would seem that thioredoxin became important in regulating the reductive pentose phosphate cycle only after oxygenic photosynthesis developed and oxygen was built up in the earth's atmosphere during the course of evolution. ■

THE MEMBRANE-BOUND ATPase FROM *HALOBACTERIUM SACCHAROVORUM* IS COMPOSED OF FOUR SUBUNITS

L. I. Hochstein
Planetary Biology Branch, 239-4, Ames Research Center, Moffett Field, CA 94035

Light and respiration-driven DCCD sensitive ATP synthesis has been reported in whole cells of *Halobacterium halobium* as has ATP hydrolysis (*i.e.*, ATPase activity) in cell-free extracts. However, the operation of an F_OF_1 ATP Synthase in the Halobacteria, or for that matter in any Archaebacterium, has yet to be demonstrated. The apparent absence of such an enzyme raises several interesting questions concerning the origin and evolution of this energy transducing enzyme, whose otherwise ubiquitous distribution, as well as the structural and functional similarities, have been suggested to imply an early origin in the evolution of life.

H. saccharovorum contains a membrane-bound ATPase which is inhibited by DCCD. Such inhibition is accompanied by the covalent binding of this inhibitor to a 60 kDa polypeptide. The enzyme possesses several properties which suggest it may be an F_OF_1-type of ATP Synthase such as: inhibition by DCCD; competitive inhibition by ADP which suggests that, unlike E_1E_2-ATPases, the reaction mechanism proceeds via an enzyme-ADP complex; and the absence of vanadate inhibition. However, the subunit structure of the halobacterial enzyme is unlike that of either and F_OF_1- or E_1E_2-type enzyme. There were a number of polypeptides: two, M_r 87kDa and 60 kDa, constituted about 90% of the Coumassie-blue staining material. In addition there were several "minor" bands. We had concluded earlier that the halobacterial ATPase was a 2- subunit enzyme. During studies on the cold-inactivation of the halobacterial ATPase, the loss of enzyme activity was associated with the dissociation of the enzyme into subunits. Fortuitously, this dissociation process provided a means for determining a minimum subunit structure for the halobacterial enzyme. This communication will summarize the purification of the halobacterial ATPase and structural studies related to cold inactivation.

Membranes were suspended in octylglucoside and the detergent-treated membranes were separated from the solubilized material by gel filtration through a Sepharose 6B column. The detergent-extracted membranes were suspended in a mixture consisting of Zwittergent 3-10 and sodium deoxycholate and subsequently passed through a Sepharose 6B column. The soluble enzyme was further purified by hydrophobic chromatography on phenyl separose followed by ammonium sulfated-mediated chromatography on Bio-Gel DEAE. This relatively simple procedure resulted in a preparation which hydrolyzed 3.5 umols of ATP/min/mg of protein. There were at least 2 contaminants still associated with the ATPase. One copurified with the ATPase and was the source of the 49 kDa subunit frequently associated with the ATPase.

The enzyme had a molecular mass of 350 kDa as determined by gel filtration in the presence of 4 M NaCl. A number of polypeptides were observed following gel electrophoresis in the presence of sodium dodecyl sulfate. There were two principal ones (87 kDa and 60 kDa) in addition to several minor components. When gel filtration was carried out in the presence of 0.2 M NaCl, the enzyme was rapidly and irreversibly denatured. A series of complex structural changes took place since virtually all of the inactivated enzyme eluted in a volume corresponding to M_r 220 kDa and 480 kDa. Whether this represented aggregation or changes in Stokes radii is not known at this time.

The halobacterial ATPase was markedly cold-labile. When incubated at -13°C, no ATPase activity was detected after about 2 hours. When the cold-inactivated enzyme was examined by gel filtration, the component which eluted in a volume corresponding to M_r 350 kDa had considerably diminished in quantity and was replaced by a material which eluted in a volume corresponding to M_r 65 kDa. SDS-gel electrophoresis of this material indicated the presence of 4 components corresponding to 87, 60, 29, and 20 kDa subunits. The column used for gel filtration, while unable to resolve 87 and 60 kDa molecular mass standards was able to resolve the 60 kDa and 29 kDa standards. Thus, the inability to resolve the lower molecular mass components from the higher ones appears unreasonable. The 29 and 20 kDa components could have exhibited non-ideal behavior during gel filtration so that their elution volume was not related to their apparent molecular masses. Another possibility is that these minor

components were artifacts generated after gel filtration and/or during electrophoresis. While these explanations cannot be ruled out at this time, a simpler interpretation suggests that cold inactivation generated 3 components: the 87 and 60 kDa subunits, and a third, a dimer composed of 29 and 20 kDa subunits (*i.e.*, a 49 kDa dimer) which was not resolved by gel filtration. Thus, the 65 kDa peak was a composite of 3 overlapping components and the dissociation of this dimer by sodium dodecylsulfate accounted for the anomalous presence of the 29 kDa and 20 kDa subunits. The mole ratio of the 2 major subunits was probably the same, since their staining intensities appeared equal. Taking this into account, the minimum ratio of these subunits, consistent with the M_r of 350 kDa observed for the native enzyme, would be 2:2:1:1, which gives an apparent M_r of about 343 kDa.

While the halobacterial enzyme exhibits a number of enzymatic properties which are consistent with its being an $F_OF_1$4ATPase-Synthase, the enzyme's structural properties suggest something else. Whether the enzyme is a novel ATP Synthase, as has been suggested, or possesses a different function has yet to be determined. If so, the question as to whether the Halobacteria, and by extension the Archaebacteria, possesses an F_OF_1-ATP Synthase is yet to be resolved. ■

THE EFFECTS OF OXYGEN ON BIOLOGICAL EVOLUTION: STEROL SYNTHESIS IN PROKARYOTIC AND EUKARYOTIC ORGANISMS

L. L. Jahnke
Planetary Biology Branch, NASA/Ames Research Center, M/S 239-4, Moffett Field, California 94035

An understanding of the origins of life and early biological evolution necessarily involves an understanding of the interaction of the earth's biota with its changing physical environment. One of the key elements of this interaction is oxygen. The atmosphere of early earth was initially anoxic, and only after the evolution of oxygenic photosynthesis did sufficient quantities of oxygen result in the transition, first of the hydrosphere and then the atmosphere, to an oxidizing one. The first organisms must almost certainly have been anaerobes, and thus the initial metabolic pathways responsible for the maintenance and development of these organisms must also have been anaerobic. Increasing levels of oxidative involvement can be correlated with the evolution of a number of metabolic pathways including the biosynthesis of porphyrins, carotenoids, quinones, steroids and unsaturated fatty acids. The initial reaction steps of such pathways are anaerobic and characteristic of all organisms, including the most primitive anaerobes; however, as biologically produced oxygen entered the environment, organisms developed mechanisms to biosynthetically utilize oxygen. Some of the intriguing questions in this context are: when did oxygen-requiring processes first appear and how did the development of these metabolic pathways influence biological evolution?

Eukaryotes are generally viewed as highly evolved aerobic, respiring organisms, requiring the development of an oxygen-rich environment for evolution. However, a number of primitive eukaryotes are capable of growth in "semianaerobic" environments and many questions involving the relationship of eukaryotic evolution and the level of oxygen prevalent during that period of geologic history remain to be answered. Indeed, recent evidence has shown that the genetic diversity in eukaryotic lines of descent appear to exceed that displayed within either the eubacterial or archaebacterial lines and again raise the question as to the antiquity of the eukaryotic line.

Our laboratory has focused upon the use of atmospheric oxygen in the biological formation of compounds as a possible indicator of the sequence of appearance and phylogenetic relationships of different organisms, and has recently begun a study involving the synthesis of sterol in both eukaryotes and prokaryotes. Essential to the viability of all extant eukaryotic cells is the ability to synthesize sterol or, lacking in this synthetic potential, an exogenous source of this lipid during growth. Indeed, the importance of cholesterol to the maintenance of membrane fluidity is well documented. The synthesis of sterols involves a number of oxygen-requiring enzymes. In *Saccharomyces cerevisiae*, although a number of oxygen-requiring enzymes are involved in the biosynthetic reactions necessary for

fermentative growth (anaerobic energy production), sterol synthesis requires the highest concentration of oxygen (1×10^{-2} of present atmospheric level, PAL) and, therefore, establishes a minimal growth requirement. In order to extend this work and address the question of the minimal growth requirements of more primitive eukaryotes, we have recently begun a study of sterol synthesis in prokaryotes.

Until recently, it was believed that one major difference between prokaryotic and eukaryotic organisms was the inability of prokaryotes to synthesize sterols. However, the synthesis of sterols by several prokaryotes has now been demonstrated and presumably evolved in this group. This is of particular interest since another class of membrane-modulating compounds, the hopanoids, are synthesized by a diverse group of prokaryotic organisms. The synthesis of sterol and hopane involves the cyclization of a common substrate, squalene; however, in the case of sterol synthesis, the oxygen-dependent epoxidation of squalene is first required, while hopane synthesis involves the direct cyclization of squalene and is an anaerobic process.

Methane-oxidizing bacteria are known to synthesize both types of cyclic triterpenes: methyl sterols and hopanoids, principally bacteriohopane polyol (BHP). In the case of *Methylococcus capsulatus* large amounts (300 μg/gm dry weight) of both 4α-methyl and 4.4-dimethyl sterol are synthesized. We have previously shown that when *M. capsulatus* is grown with very low levels of oxygen, 4×10^{-3} PAL, the cellular content of sterol is reduced by 50%. Concomitant with the decrease in sterol content was a dramatic increase in the synthesis of an unidentified compound which we believed to be bacteriohopane polyol. Analysis of BHP requires periodate oxidation of the polyol side chain and borohydride reduction of the resulting aldehyde prior to TLC separation and GC analysis. After applying the techniques developed by Rohmers' group in France and analyzing the resulting derivates by GCMS, these compounds have indeed proven to be a mixture of BHP. When *M. capsulatus* was grown with different oxygen concentrations, BHP content increased with decreasing oxygen (3380 μg/gm at 10% O_2 and 5600 μg/gm at 0.1% O_2). Since hopanoids are not known to require oxygen for synthesis, this result reflects the previous decrease in sterol synthesis noted and implies a direct relationship of oxygen to the synthesis of methyl sterols in this prokaryotic organism.

Although the synthesis of hopanoids by methane-oxidizing bacteria is well documented, few reports of methyl sterol have appeared. In addition to *M. capsulatus*, methyl sterols have been reported to be present in *Methylobacterium organophilum*, however, only at negligible concentrations (308 ng/g dry wt). At the present time, we have analyzed three additional methanotrophic organisms for sterol, and detected only low levels in extracts of *Methylomonas methanica* and *Methylomonas albus* (6 and 13 μg/gm dry wt, respectively). No sterol was detected in *Methylosinus trichosporium*, however, the sample size would have obviated detection below 400 ng/g dry weight. Therefore, although the presence of large quantities of sterol are unique to *M. capsulatus* at the present time, the detection of these compounds in other methanotrophs raises the question of the evolutionary relationship to hopane and sterol synthesis. Hopanoids are common in a variety of phylogenetically diverse bacteria while sterol synthesis apparently is not. What are the unique characteristics of this group of organisms that may have led to the evolution of the biosynthetic steps involved in sterol synthesis and how might this relate to the evolution of sterol synthesis in eukaryotic organisms? ■

CHLORIDE TRANSPORT BY HALORHODOPSIN, AN ARCHAEBACTERIAL RETINAL PROTEIN

J. K. Lanyi
Department of Physiology and Biophysics, University of California, Irvine, California 92717

Halorhodopsin is one of several retinal proteins found in the cytoplasmic membrane of many halobacteria. Its function is the electrogenic transport of chloride ions into the cells upon illumination (Schobert and Lanyi, 1982), probably to facilitate volume maintenance during growth (Mehlhorn *et al.*, 1985). The pigment is a small integral membrane protein: its MW is about 25 kda (Lanyi and Oesterhelt, 1982), similar to that of bacteriorhodopsin, a light-driven proton pump in the same organism (reviewed in Lanyi, 1984b). The absorption maximum of halorhodopsin is at 578 nm (Steiner and Oesterhelt, 1983), which is about 10 nm red-shifted from that of bacteriorhodopsin.

Any chloride pump should contain binding sites for chloride, which are in equilibrium with the aqueous compartments separated by the membrane. Such binding of chloride might be expected to influence the chromophore through electrostatic interactions with the retinal, in the manner intrinsic protein residues carrying charges are postulated to do in other rhodopsins (*e.g.*, Honig *et al.*, 1979; Warshel, 1979). Indeed, anions do affect the spectrum of halorhodopisn (Schobert *et al.*, 1986), and the effects have been interpreted in terms of two distinct anion binding sites: (a) Site I, whose occupancy causes a small blue-shift and a rise of the pK of the retinal Schiff-base. This nonspecific site will bind many anions including chloride and bromide, and shows only weak preference towards these and other small hydrated anions, such as nitrate and thiocyanide (Schobert and Lanyi, 1986), and (b) Site II, whose occupancy causes a small red-shift, but no change in the pK. This site binds only chloride and bromide, thus its specificity agrees with that of the transport (Schobert and Lanyi, 1986). It has been argued that the simplest explanation for the observed consequences of anion binding is that the negative charge of the anions at Site I influences the Schiff-base (Schobert *et al.*, 1986); Lanyi, 1986). Such localization of the two sites relative to the retinal is consistent with their effects on the Schiff-base pK.

Halorhodopsin exhibits a photocycle on a millisec time-scale (Weber and Bogomolni, 1981; Schobert *et al.*, 1983), but the kind of photointermediates produced, and the rate of their interconversions, depend on the presence and concentration of chloride (Schobert *et al.*, 1983). A recently proposed photycycle scheme (Figure 1) is based on results of a combination of experiments using flash and continuous

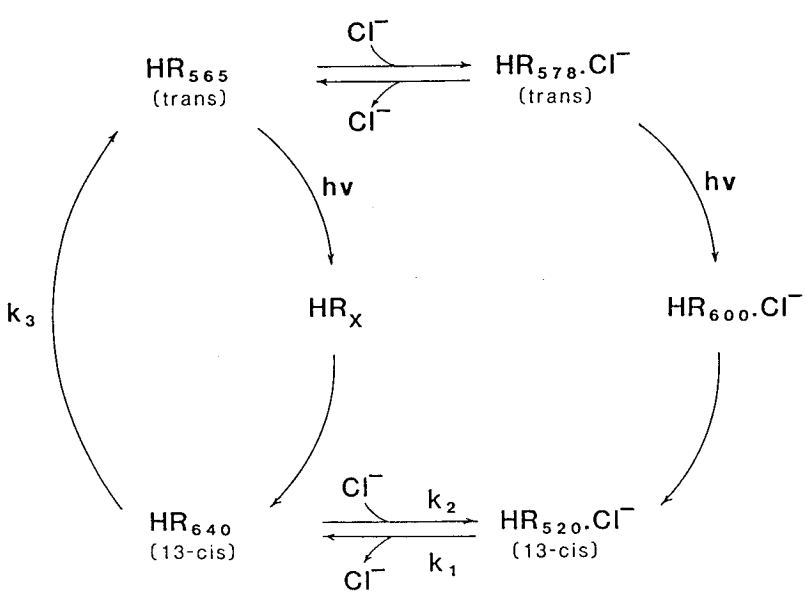

Figure 1. Photocycle scheme proposed by Oesterhelt et al. (1985), with a photoreaction for HR(565) added (Lanyi and Vodyanoy, 1986)

illumination (Oesterhelt *et al.*, 1985), and from kinetic analysis of the rise and decay of photointermediates HR(520).Cl and HR(640), using numerical solutions to their rate equations (Lanyi and Vodyanoy, 1986). The latter yielded a unique set of rate constants, k1, k2, and k3, which predicted the shape of the flash-induced absorption changes over a large chloride concentration range.

The photocycle scheme contains two chloride-dependent equilibria, which correspond to binding of the chloride to Site II, for HR(565) ⟷ HR(578).Cl, and to another site termed Site IIa, for HR(640) ⟷ HR(520).Cl. The chloride binding constant for Site II was determined to be 10 - 20 mM (Steiner *et al.*, 1984), but for Site IIa it was k1/k2 = ca. 0.5 M. Because of the diminished affinity for chloride, and because of the irreversible step, k3, which follows loss of chloride from Site IIa, chloride will cyclically debind and rebind during the photocycle, even at physiological (*i.e.*, > 4 M) chloride concentrations. This kind of cyclic binding of the chloride to halorhodopsin would lead to chloride translocation across the protein (and the membrane) if access of medium chloride to Site II were from one side of the membrane, and to Site IIa from the other side. Site II indeed communicates with the side from which chloride is transported (Schobert *et al.*, 1983; Bogomolni *et al.*, 1984), but no such topological information is available for Site IIa as yet.

In bacteriorhodopsin, light-energy is conserved by the conversion of the all-trans chromophore to the 13-cis, and the proton translocation takes place during the subsequent thermal relaxation back to the all-trans state (reviewed in Stoeckenius *et al.*, 1979). This kind of mechanism seems to be operating in halorhodopsin also. All-trans → 13-cis isomerization in this pigment was demonstrated by flash-induced absorption changes in the near UV, where the characteristic "cis-peak" at 335 nm arises and decays simultaneously with HR(520).Cl and HR(640), under experimental conditions designed so that either one or the other of these intermediates is produced (Lanyi, 1984a; Lanyi and Vodyanoy, 1986).

The complete amino acid sequence of halorhodopsin is now available (Blanch and Oesterhelt, 1987), and the observed significant similarity with the bacteriorhodopsin sequence suggests a plausible secondary (and perhaps also tertiary) structure common for the two proteins. Preliminary results from reconstitution of halo-opsin with retinal analogues suggest that the distribution of charged residues near the retinal is similar to that proposed earlier for bacteriorhodopsin (Spudich *et al.*, 1986). Indeed, comparison of acidic and basic residues in the sequence of the two proteins reveals conservation of those charges thought to influence the retinal. The current investigations of the similarities and differences in the two retinal proteins will be useful not only in describing the way the photoreaction of the pigments is coupled to the two different ion transport functions, but also in gaining understanding of the evolution of energy transforming systems in archaebacteria. ■

REFERENCES

Blanck, A. and Oesterhelt, D. (1987) EMBO J. (in press)
Bogomolni, R.A., Taylor, M.E. and Stoeckenius, W. (1984) Proc.Nat.Acad.Sci.U.S.A. 81, 5408-5411.
Honig, B., Dinur, U., Nakanishi, K., Balogh-Nair, V., Gawinowitz, M.A., Arnaboldi, M. and Motto, M. (1979) J.Am.Chem.Soc., 101, 7084-7086.
Lanyi, J.K. (1984a) FEBS Lett. 175, 337-342.
Lanyi, J.K. (1984b) in Comprehensive Biochemistry (L. Ernster, ed.) pp. 315-350, Elsevier, Amsterdam.
Lanyi, J.K. (1986) Biochemistry 25, 6706-6711.
Lanyi, J.K. and Oesterhelt, D. (1982) J.Biol.Chem. 257, 2674-2677.
Lanyi, J.K. and Vodyanoy, V. (1986) Biochemistry 25, 1465- 1470.
Mehlhorn, R.J., Schobert, B., Packer, L. and Lanyi, J.K. (1985) Biochim.Biophys.Acta 809, 66-73.
Oesterhelt, D., Hegemann, P. and Tittor, J. (1985) EMBO J. 4, 2351-2356.
Schobert, B. and Lanyi, J.K. (1982) J.Biol.Chem.257, 10306- 10313.
Schobert, B. and Lanyi, J.K. (1986) Biochemistry 25, 4163- 4167.
Schobert, B., and Lanyi, J.K. and Cragoe, E.J. (1983) J.Biol.Chem. 258, 15158-15164.
Schobert, B., Lanyi, J.K. and Oesterhelt, D. (1986) J.Biol. Chem. 261, 2690-2696.
Smith, S.O., Marvin, M.J., Bogomolni, R.A. and Mathies, R.A. (1984) J.Biol.Chem. 259, 12326-12329.
Spudich, J.L., McCain,D.A., Nakanishi, K., Okabe, M., Shimizu, N., Rodman, H., Honig, B. and Bogomolni, R.A. (1986) Biophys.J. 49, 479-483.

Steiner, M., Oesterhelt, D., Ariki, M. and Lanyi, J.K. (1984) J.Biol. Chem. 259, 2179-2184.
Stoeckenius, W., Lozier, R.H. and Bogomolni, R.A. (1979) Biochim.Biophys.Acta 505, 215-278.
Warshel, A. (1979) Photochem.Photobiol. 30, 285-290.
Weber, H.J. and Bogomolni, R.A. (1981) Photochem.Photobiol. 33, 601-608.

CRYPTOENDOLITHIC MICROBIAL LIFE AND FOSSILIZATION: A SCENARIO FOR EVIDENCE OF PAST LIFE ON MARS

M. A. Meyer and E. I. Friedmann
Polar Desert Research Center, Department of Biological Science, Florida State University, Tallahassee, Florida 32306-2043

In sharp contrast to the apparently abiotic landscape of the ice-free age of the Antarctic (Ross Desert), diverse cryptoendolithic microbial communities live sheltered under the surface, inside porous sandstone rocks (Friedmann, 1982). The Ross Desert has long been considered the closest terrestrial analogue to the environment of Mars. Yet, results from the Viking missions have shown that no life forms, including those similar to Antarctic cryptoendolithic microorganisms, can survive in the extreme hostile environment of present day Mars.

Life may have existed, however, on early Mars: There is a likelihood that the planet possessed atmosphere and water (Carr, 1987), resulting in temperatures conducive to the development of life during the same time that life evolved on earth (McKay, in press). The loss of Martian atmosphere and water, with concomitant cooling, could have resulted in conditions not unlike the present terrestrial cold desert, forcing newly evolved life to take refuge in the last habitable niches of a deteriorating environment. In the higher elevations of the Ross Desert, the mean annual temperature is -22°C and the precipitation is minimal, but insolation can warm colonized rocks to over 15°C, enabling cryptoendolithic microbial activity (Friedmann *et al.*, in press). Thus, the Antarctic cryptoendolithic ecosystem may serve as a paradigm for microorganisms in the twilight of life on Mars.

The likelihood that such early Martian life forms have left behind fossil traces conflicts with the generally assumed unsuitability of the cold desert environment to form fossils. Even if present, the detection of microfossils requires an involved technique (preparation of petrographic thin section and transmission light microscopy), which in the context of exobiology implies sample return in substantial quantities.

The recent discovery of trace fossils of cryptoendolithic microbial communities in the Ross Desert (Friedmann and Weed, in press) now suggests a scenario that overcomes these problems (Friedmann, in press).

Trace fossils are formed in the Antarctic desert when cryptoendolithic microbial life terminates, due to deterioration of the physical environment, and the porous rocks become silicified. Although cellular structures may disappear, the characteristic changes in the rock substrate caused by microbiological activity, such as the surface exfoliation pattern and the iron-leached zone under the surface, are well preserved.

Comparable features could have been formed on early Mars and still be preserved, due to geological quiescence of the surface for the last three billion years (Carr 1981). Studies of Ross Desert trace fossils suggest that signatures of early Martian life could be detected by searching for the following signs in rocks: (1) patterns in the scale of centimeters or less, (2) discontinuities in physical or chemical composition, (3) features that cross physical gradients, and 4) structures unaccounted for by physical or chemical processes.

The above features can be detected on site, without sample return, and by unmanned remote control instruments. ■

REFERENCES
1. Carr, M.H. 1981. The Surface of Mars. Yale Press, New Haven.
2. Carr, M.H. 1987. Water on Mars. Nature 326:30-35.
3. Friedmann, E.I. 1982. Endolithic microorganisms in the Antarctic cold desert. Science 215:1045-1053.
4. Friedmann, E.I. (in press). The Antarctic cold desert and the search for traces of life on Mars. Journal of Advances in Space Research.
5. Friedmann, E.I. and R. Weed. (in press). Microbial trace- fossil formation: Biogenous and abiotic weathering in the Antarctic cold desert. Science.
6. Friedmann, E.I., C.P. McKay, and J.A. Nienow. (in press). The cryptoendolithic microbial environment in the Ross desert of Antarctica: Satellite transmitted continuous nanoclimate data, 1984 to 1986. Polar biology.
7. McKay, C.P. (in press). Exobiology and future Mars missions: The search for Mars' earliest biosphere. Journal of Advances in Space Research.

ENERGY YIELDS IN THE PREBIOTIC SYNTHESIS OF HYDROGEN CYANIDE AND FORMALDEHYDE ON THE PRIMITIVE EARTH, JUPITER AND THE SOLAR NEBULA: ANCESTORS TO THE PYRIMIDINES AND RIBOSE IN RNA

S. L. Miller and R. Stribling
Department of Chemistry, B-017, University of California, San Diego, La Jolla, California 92093

Prebiotic experiments are usually reported in terms of carbon yields, *i.e.*, the yield of product based on the total carbon in the system. These experiments involve a large input of energy and are designed to maximize the yields of product. However, large inputs of energy result in multiple activation of the reactants and products. A more realistic prebiotic experiment is to remove the products of the activation step so they are not exposed a second time to the energy source. This is equivalent to transporting the products synthesized in the primitive atmosphere to the ocean, and thereby protecting them from destruction by atmospheric energy sources. Experiments of this type, using lower input of energy, give energy yields (moles of products J^{-1}) which can be used to estimate the relative importance of the different energy sources on the primitive earth.

Simulated prebiotic atmospheres containing either CH_4, CO or CO_2 with N_2, H_2O and variable amounts of H_2 were subjected to a high frequency Tesla coil. The samples were analyzed for HCN with the cyanide electrode and for H_2CO by chromotropic acid. The energy yields for HCN production are about 10 n moles J^{-1} with CH_4 ($H_2/CH_4 = 1$), 5 no moles J^{-1} with CO ($H_2/CO=2$), and 0.3 n moles J^{-1} with CO_2 ($H_2/CO_2 = 3$).

These results will be compared with HCN production rates calculated for lightning, calculated for photochemically produced N atoms, and preliminary experiments using an artificial lightning source. The H_2CO results will be compared with calculated and experimental photochemical yields. The energy yields can be used to estimate the HCN concentration in the primitive ocean as well as the rate of synthesis of amino acids. The steady state amino acid concentration is calculated very approximately to have been 3×10^{-4}. This is based on the rate of synthesis and the rate of decomposition of the amino acids on passing through the submarine vents.

HCN was detected in the atmosphere of Jupiter in 1981. Several possible sources of this HCN have been proposed, including upwelling from lower in the Jovian atmosphere, photolysis of methylamine or aziridine, and lightning. Corona discharges, however, have not been proposed as a possible energy source.

Since corona discharges have been shown to be effective in producing organic molecules, including HCN, in reducing atmospheres, we determined energy yields for the production of HCN under the very high H_2/CH_4 mixing ratios found on Jupiter. These yields, combined with estimates of the energy available as corona discharge, can be used to calculate the contribution of this mechanism to the HCN observed on Jupiter.

It would be expected that corona discharges on Jupiter would accompany lightning as on the Earth where the ratio of corona to lightning is about 3:1. Using this ratio and estimates of the energy available as lightning, together with estimates of the survival time of HCN, indicate that corona discharge may play a significant role in HCN production.

These data on the synthesis of HCN at high H_2/CH_4 ratios are also be applicable to the synthesis of HCN in the solar nebula, where H_2/CH_4 ratios were high, and may account for some of the organic material found in the carbonaceous chondrites. This may have been a mechanism for the retention of carbon on the planetary bodies.

Energy yields for the corona discharge synthesis of HCN and H_2CO have also been measured in H_2, CH_4, NH_3 mixtures. The H_2CO yields are comparable to the HCN yields. The synthesis would have taken place in the region of the solar nebula where H_2, CO and N_2 predominated.

Experiments in this laboratory are also concerned with the steps closer to the origin of life. Although the pyrimidines cytosine and uracil can be synthesized under primitive earth conditions, they may not have occurred in the first nucleic acids. The principal reasons are that there is no prebiotic synthesis of pyrimidine nucleoside, as there is for purine nucleosides, and the activated pyrimidine nucleotides do not undergo template directed polymerizations in contrast to the activated purine nucleotides. We are considering alternative basis that might have substituted initially for the pyrimidines. These include the quinazoline analog of uracil and xanthine riboside with the ribose on the 3-nitrogen.

Although the first living systems are currently thought to have been self-replicating RNA molecules, there are a number of difficulties with this proposal, particularly with the synthesis of the ribose and the ribonucleotides. It seems more likely that the first self-replicating molecules were RNA like, but with the ribose replaced by acyclic, flexible, and probably prochiral nucleotide analogs. Experiments are being conducted to determine which ribonucleotide analogs have plausible prebiotic syntheses and whether such analogs will undergo template polymerizations. ■

COLORATION AND DARKENING OF METHANE CLATHRATE AND OTHER ICES BY CHARGED PARTICLE IRRADIATION: APPLICATIONS TO THE OUTER SOLAR SYSTEM

W. R. Thompson, B. G. J. P. T. Murray, B. N. Khare and C. Sagan
Laboratory for Planetary Studies, Cornell University, Ithaca, New York 14853

Methane clathrate is expected to be an important carbon-containing ice in the outer solar system. We investigate the effect of charged particle irradiation by coronal discharge on several simple hydrocarbons enclathrated in or mixed with H_2O or H_2O+NH_3 in simulation of the effects of the solar wind, planetary magnetospheric particles, and cosmic rays on surfaces containing these ices in the outer solar system and interstellar space. CH_4+H_2O clathrate, $C_2H_6+H_2O$, $CH_4+H_2O+NH_3$, $C_2H_6+H_2O+NH_3$, $C_2H_2+H_2O$ and $C_6H_{14}+H_2O$ are all initially white ices, and all produce yellowish to brownish organic products upon charged particle irradiation. Significant coloration occurs with doses corresponding to short interplanetary irradiation times, $\leq 10^4$ yr of solar wind or cosmic rays at Uranus, and even shorter magnetospheric irradiation times. Progressive darkening toward brownish or gray occurs upon continued irradiation of the ices or their involatile residues. We characterize the ultraviolet to infrared spectral properties of the copious involatile organic residues by transmission and reflection spectroscopy (residue left after $CH_4 \cdot nH_2O$ irradiation exhibits IR bands which we tabulate and identify with alkane, aldehyde, alcohol and perhaps alkene and substituted aromatic functional groups); make general comparisons with the spectra of the satellites of Saturn and Uranus, Triton, Pluto and cometary nuclei; and argue that pre- and post-accretional ice irradiation is an important source of the abundant dark organic chromosphere in the outer solar system ■

TAPHONOMIC AND TAXONOMIC STUDIES OF MICROBIAL MATS

M. Enzien and L. Margulis
Boston University, Department of Biology, 2 Cummington Street, Boston, Massachusetts 02215

Extant laminated microbial mats are analogous to stratiform stromatolites in Archean and Proterozoic sedimentary rocks. Occasionally chert layers or lenses associated with these stratiform stromatolites contain well preserved microfossils. Many mechanisms for microfossil preservation have been proposed and indeed many may have existed. One model suggests silcification occurs selectively in buried microbial mat sediments having high local concentrations of organic matter and high sediment permeability allowing silica-rich groundwaters to easily flow into the sediments. We are investigating the importance of organic matter acting as either a template for silica precipitation or as substrate for fermentative and anaerobic respiratory processes that by lowering local pH promote silica precipitation.

Two possible models for silcification of extant microbial mat sediments are being tested: (1) transport of silica into anaerobic sediments from an external source with subsequent precipitation induced by microbial processes and (2) mobilization of silica during early diagenesis from within the laminated microbial mat sediments followed by local advection or diffusion to a zone of precipitation. Flow-through core reactors have been designed to monitor and sample continuously incubated anaerobic sediments and their porewaters without disruption. Changes in silica concentration in porewaters will be monitored while silica and nutrient concentration of influent are independently varied. Porewater chemistry and identification of the clay-sized mineral fraction with powdered X-ray diffraction of *in situ* microbial mat sediments will also be studied.

Recently discovered microbial mats in Hawaii have provided us with an excellent opportunity to study the ecology and biogeochemistry of microbial mats in a volcaniclastic setting. Devitrification of volcanic sediments frequently has been proposed as the source of silica in silicified sediments. Studying the early diagenesis in mats from Hawaii might help elucidate mechanisms and paleoenvironments of silicification.

We have isolated a new desiccation-resistant cyst forming marine chlorella (*C. desiccata*) and another cyst forming eukaryote, *Paratetramitus jugosus* from microbial mats in Baja California, Mexico. Cysts from these organisms may have been preserved as acritarchs in Proterozoic stromatolitic cherts. An unusual type of reproduction (*i.e.*, formation of small propagules) of the amoebomastigote, *P. jugosus* is under investigation. Using fluorescent nuclear stains (DAPI, mithramycin) and nuclease treatment, irregularly shaped DNA-containing bodies (propagules?) have been found in culture slides which do not resemble the bacteria upon which the amoebomastigote feeds. ■

EVOLUTION OF ANTICODONS; VARIATIONS IN THE GENETIC CODE

T. H. Jukes
Space Sciences Laboratory, University of California, Berkeley, California 94720

The codons in the genetic code are fixed both in number and composition. The number is 64 and the composition is all the possible arrangements of U, C, A and G, taken three at a time. Evolution of the code may be studied through the composition of anticodons that translate the 64 codons. At first, there were probably fewer amino acids in the code, and therefore fewer anticodons. Also, it is likely that an archetypal code contained only 15 amino acids and 15 anticodons.

Each anticodon had U in the first position and paired with four codons for one amino acid, and the other four codons were stop signals.

The code expanded by adding "new" amino acids, and each new amino acid had its own anticodon. As a result, the expanded "early" code consisted of GNN and UNN anticodons (N = U, C, A or G).

We propose that the number of anticodons has increased and that evolution continued until three existing forms of the universal code were produced: eukaryotic, eubacterial and the code for halobacteria and methanococci. These three codes are distinguished from each other by their anticodon pattern. The eukaryotic code contains eight INN (ANN) anticodons which have replaced GNN anticodons as a result of AT pressure. Mitochondrial and chloroplast codes have evolved from the eubacterial code through genomic economization and AT pressure, leading to losses of GNN and CNN anticodons. The mitochondrial code uses "four-way wobble" with UNN anticodons in 8 family boxes, and there are three examples of this in the chloroplast code. The code is still evolving except for its content of the present 20 amino acids, from which no exceptions are known. The wobble rules of codon-anticodon pairing were fundamental in evolution of the code.

Some earlier hypotheses said that methionine and tryptophan have only one codon apiece because they are the last amino acids to be added to the code. In support of this, their structures are too complex to be formed in abiotic synthesis of the Miller-Urey type. We propose that, in earlier codes, methionine and tryptophan had two codons apiece, and that methionine lost AUA to isoleucine, and that the early UGA code for tryptophan became a stop codon. In support of this viewpoint, methionine and tryptophan each have two codons in the mitochondrial code, which is seen as a return to a more primitive code. Also, in a common microorganism, *Mycoplasma*, UGA is no longer a stop codon, but has been "captured" by tryptophan as a result of high AT content in genomic DNA.

The effects of biased mutational pressure towards high AT content of DNA, or, conversely, high GC content, will be traced with respect to their effects on evolution of the genetic code, and it will be shown that the code is still evolving. ■

ORIGIN OF UNDULIPODIA FROM SPIROCHETES?

L. Margulis, D. Bermudes, R. A. Laursen, R. Obar and G. Tzertzinis
Boston University Department of Biology, 2 Cummington Street, Boston, Massachusetts 02215

We have hypothesized the origin of undulipodia (cilia, eukaryotic flagella) via motility symbioses from prokaryotes (*e.g.*, spirochetes). This hypothesis has led to the search for axonemal proteins in *Spirochaeta bajacaliforniensis*, a free-living microbial mat spirochaete that shows immunoreactivity to antiserum made against bovine brain tubulin. Two tubulin-like proteins (S1 and S2) copurify in spirochete lysates. The 64kD protein S1 has been isolated and purified by preparative gel electrophoresis and column chromatography. Antibodies (that crossreact with each other) have been made against both spirochete proteins. Antibody to bovine brain tubulin binds to the *in vitro* fibers presumably by reacting with S1 protein. Attempts to sequence the spriochete proteins are in progress. Our results, which indicate that fibrous spirochete protein share at least one epitome with bovine brain tubulin, are consistent with the motility symbiosis hypothesis. ■

ORGANIC CHEMISTRY OF CARBONACEOUS METEORITES

J. R. Cronin, G. U. Yuen, and S. Pizzarello
Department of Chemistry and Center for Meteorite Studies, Arizona State University, Tempe, Arizona 85287

Carbonaceous chrondrites have been known for almost as long as meteorites have been recognized as extraterrestrial materials, *i.e.*, since early in the nineteenth century. Meteorites of this class have an elemental composition very similar to that of the solar system as a whole, are of similar ages as the sun and planets, and show but slight effects of chemical or physical alteration. They thus appear to be an aggregrate of little-altered solar nebular matter.

It was recognized quite early that these primitive extraterrestrial material contain their complement of carbon mainly in the form of organic compounds (Berzelium, 1834). However, only within the last 30 years has it been possible to determine exactly what compounds are present and their amounts.

Much (~ 70 percent) of the organic carbon on carbonaceous chrondrites occurs as an insoluble macromolecular material that has been only partially characterized. It occurs in the meteorite matrix as a film coating mineral grains and as particles that either lack regular structure or are composed of randomly stacked two-dimensional layers (Lumpkin, 1986). In terms of chemical structure, it is comprised of condensed aromatic, heteroaromatic, and hydroaromatic ring systems, cross-linked by short methylene chains, ethers, sulfides, and biphenyl groups (Hayatsu *et al.*. 1983). This material is structurally similar in some respects to certain terrestrial kerogens.

The soluble organic compounds of the CM and probably the CI type carbonaceous chrondrites comprise a complex mixture. The principal classes of soluble compounds, the number of discrete molecular species, and their amounts in a representative specimen, *i.e.*, the Murchison meteorite, are given in Table 1.

The amino acids of carbonaceous chrondrites have been of particular interest because of their potential importance in the origin and evolution of life. Seventy-four amino acids have now been

TABLE 1

Class	Concentration (ppm)	Compounds Identified
Amino acids	60	74
Aliphatic hydrocarbons	>35	140
Aromatic hydrocarbons	15-28	87
Alkanoic acids	>300	15
Alkandioic acids	>30	17
Hydroxyalkanoic acids	15	7
Purines and pyrimidines	1.3	5
Basic N-heterocycles	7	32
Amines	8	10
Amides	55-70	>2
Alcohols	11	8
Aldehydes and ketones	27	9
Total	564-592	406

identified in extracts of the Murchison meteorite, of which 55 are uniquely extraterrestrial. The meteorite amino acids fall into two general classes: (1) cyclic and acyclic monoamino alkanoic acids and (2) monoamino alkandioic acids. As a group, they exhibit general structural characteristics that appear to be common to many of the other classes of organic compounds found in carbonaceous chrondrites. These are (1) complete structural diversity, (2) no enantiomeric preference, (3) an exponential decline in concentration with increasing carbon number within homologous series, and (4) a predominance of branched chain isomers.

A goal of studies of meteorite organic compounds has been to elucidate their origin in terms of location and a plausible synthetic mechanism. Processes believed to occur in the solar nebula, *e.g.*, electrical discharge in a reduced gas atmosphere (Wolman *et al.*, 1972) have been proposed. However, certain characteristics of the amino acids suggest a presolar synthesis (Cronin and Pizzarello, 1986). Stable isotope analyses of hydrogen extracted from the interstellar processes that are known to enrich certain organic compounds in deuterium, *i.e.*, ion-molecule reactions. Recently amino acids obtained from the Murchison meteorite have also been found to be deuterium-rich (Epstein *et al.*, 1987). The amino acids and perhaps other soluble compounds of carbonaceous chrondrites (carboxylic acids are also enriched in deuterium, but to a lesser extent) or perhaps their precursors may have been formed in an interstellar cloud and thus may predate the solar nebula. ■

REFERENCES

1. Berzelius, J.J. (1834) Ueber Meteorstein. *Ann. Phys. Chem.* 33:113-148.
2. Cronin, J.R. and Pizzarello, S. (1986) Amino acids of the Murchison meteorite. III. Seven carbon acyclic primary α-amino alkanoic acids. *Geochim. Cosmochim. Acta* 50: 2419-2427.
3. Epstein, S., Krishnamurthy, R.V., Cronin, J.R., Pizzarello, S., and Yuen, G.U. (1987) Unusual stable isotope ratios in amino acid and carboxylic acid extracts from the Murchison meteorite. *Nature*, in press.
4. Hayatsu, R. and Anders, E. (1981) Organic compounds in meteorites and their origins. *Topics in Current Chemistry* 99:1-37.
5. Hayatsu, R., Scott, R.G., and Winans, R.E. (1983) Comparative structural study of meteoritic polymer with terrestrial geopolymers coal and kerogen. *Meteoritics* 18:310.
6. Lumpkin, G.R. (1986) High resolution electron microscopy of carbonaceous material from CI, CM, CV,and H chrondrites. *Lunar and Planet. Sci.* 17:502-503.
7. Wolman, Y., Haverland, W.J., and Miller, S.L. (1972) Nonprotein amino acids from spark discharges and their comparison with the Murchison meteorite amino acids. *Proc. Natl. Acad. Sci. USA* 69:809-811.

CHARACTERIZATION OF CARBONACEOUS MATERIALS IN INTERPLANETARY DUST PARTICLES UTILIZING LASER MICROPROBE MASS SPECTROMETRY

E. K. Gibson, Jr.[1] and R. H. Carr[2]
[1]*Experimental Planetology Branch, NASA/Johnson Space Center, Houston, Texas 77058 and* [2]*Former NRC-NAS Research Associate, presently at I.C.I. Europa, Kortenberg, Belgium*

The study of cosmic dust or interplanetary dust particles (IDP) can provide vital information about primitive materials derived primarily from comets and asteroids along with a small unknown fraction from the nearby interstellar medium. The study of these particles can enhance our understanding of comets along with the decoding of the history of the early solar system. The study of the cosmic dust or IDP particles can assist in the elucidation of the cosmic history of the organogenic elements (*i.e.*, H, C, N, O, S etc.) which are vital to life processes. Studies to date on these particles have shown that they are complex, heterogeneous assemblages of both amorphous and crystalline components. Carbonaceous material in chondritic interplanetary dust particles (IDP's) constitutes the embedding medium for fine-

grained minerals that include silicates, sulphides, oxides, and metallic phases. In general, this carbonaceous material is present as polymerized hydrocarbons and amorphous carbon, although in the ore fluffy particles, carbon occurs predominantly in a poorly graphitized form. This diversity makes the characterization of these carbonaceous species an important task in elucidating the origins of IDP's.

In order to understand the nature of these particles, any analytical measurement must be able to distinguish between the possible sources of these particles. We have undertaken a study using the laser microprobe interfaced to a quadrupole mass spectrometer for the direct analysis of the volatile components present in cosmic dust particles, terrestrial contaminants present in the upper atmosphere along with the primitive carbonaceous chondrites (CI, CM, CV). The studies have been supplemented with stable isotope measurements using static mass spectrometry techniques. From the study of the volatiles released from the carbonaceous materials, it is hoped that one can distinguish between components and sources in the IDP's.

Studies with the laser microprobe-mass spectrometer system show that the volatile species produced by "ZAPPING" a Type C IDP particle (W7027B8) are similar to those seen during analyses of the matrices of the carbonaceous chondrite meteorites Orgueil, Murchison and Allende and include CO_2, H_2O, $CO + N_2$, CH_4 and CS_2. Semiquantitative measurements give values of *ca.* 1% water and 1% carbon dioxide from the IDP particle. Analysis of an aluminum (or TCA type) type particle W7027C7 showed the expected low volatile content.

Refractory components in carbonaceous chondrites show anomalous carbon isotopic compositions which can be measured on as little as 150 pgC. To establish whether similar components are present in IDP's, a sample of five 10-micron- sized particles was subjected to stepped combustion analysis. Since high temperature phases should have survived heating during entry into the Earth's atmosphere, any "interstellar" carbon present in the grains would be evident by an elevated del ^{13}C value. The experiment revealed no isotopic values greater than -30% at temperatures above 600°C; the bulk isotopic value measured was only just distinguishable from the blank by *ca.* 2%. Within the limits of detection, no isotopically heavy carbon from interstellar grains could be recognized in the cosmic dust—a result similar to those seen previously by ion probe.

Pursuing the measurement of carbon isotopes in cosmic dust, a single 35-micron chondritic particle (U2022C13) was selected for study because of the high bremsstrahlung background in its bulk energy dispersive spectrum. Preliminary analytical electron microscope results from a fragment (U2022C26) of the parent showed that chemical variations of Mg-rich silicates and low-Ni iron-sulphides are similar to those for ultra-fine-grained silicates and sulphides in the microcrystalline matrix of the chondritic porous (CP) IDP's W7010*A2 and U2015*B. The carbonaceous material in the matrices of these IDP's occurs predominantly as hydrocarbons and amorphous carbon, with minor amounts of poorly graphitized carbon. Stepped combustion analysis of the parent particle again revealed no evidence of isotopically heavy carbon at high release temperatures and the bulk isotopic value was indistinguishable from the blank. ■

CHEMISTRY OF THE BIOGENIC ELEMENTS IN DENSE INTERSTELLAR CLOUDS: RECENT RESULTS

W. M. Irvine, S. C. Madden, and L. M. Ziurys
Department of Physics and Astronomy and Five College Radio Astronomy Observatory, University of Massachusetts, Amherst, Massachusetts 01033

It is now well established that stars, and presumably planetary systems, form in dense interstellar clouds of gas and "dust." In individual cases, such clouds may contain as much material as millions of suns, making them the most massive objects in the galaxy. Approximately 70 molecular species, the vast majority of them organic, have been identified in the gas phase, and the particulate matter may also be rich in complex organics. These "molecular clouds" thus play a crucial role in the history of the

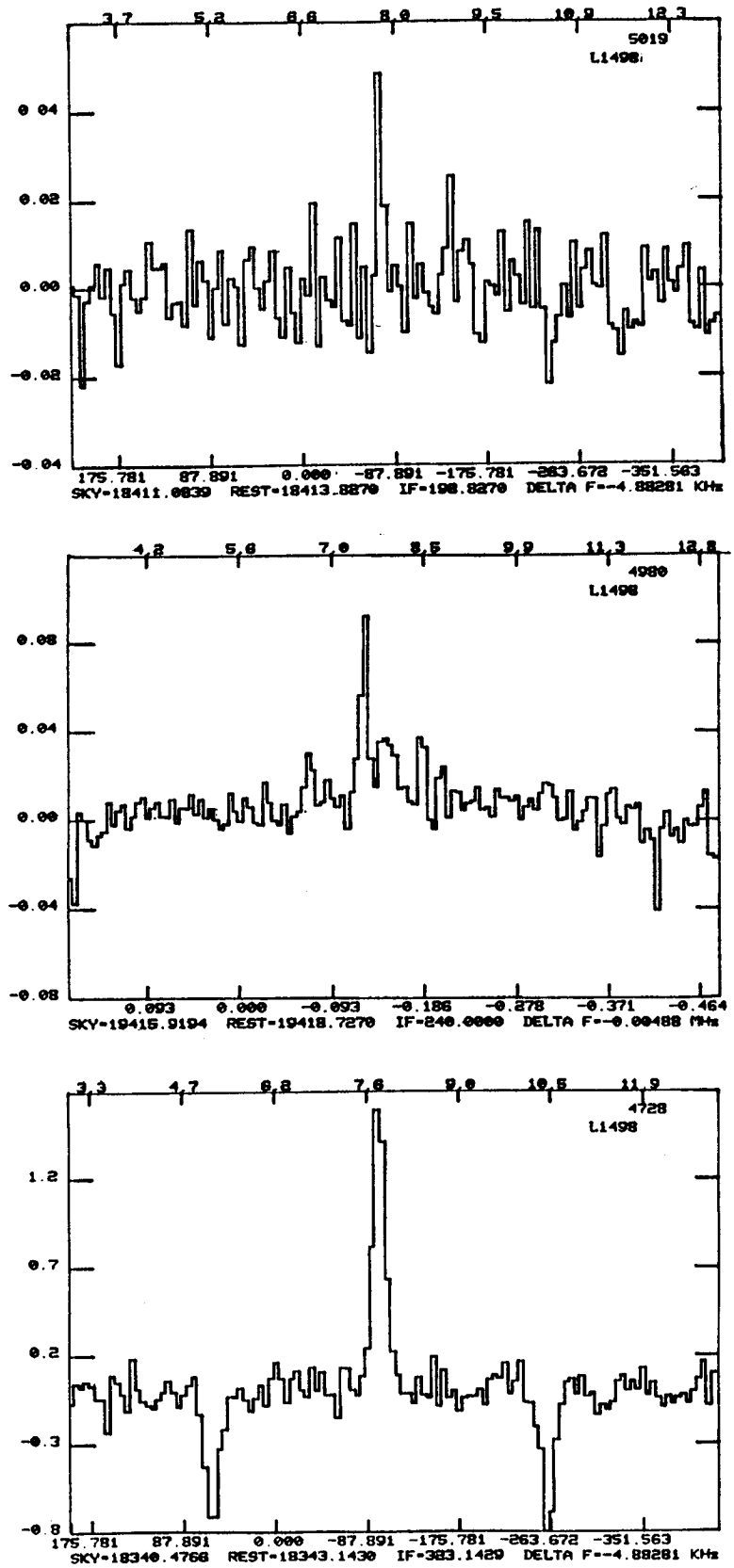

Figure 1. Rotational transitions of three isotopic forms of cyclopropenylidene observed in the cold, dark interstellar cloud L1498. In each case the transition is 1(1,0)-1(0,0). Top: $CC^{13}CH_2$; Middle C_3HD; Bottom: C_3H_2 (principal isotope for each element given without superscript). Structure in spectrum of C_3HD due to hyperfine splitting by deuterium nucleus, an effect never observed in the laboratory for this molecule.

biogenic elements, intermediate between the diffuse interstellar gas which is primarily atomic in composition, and the solar nebula itself, in which the sun and planets actually formed. The present research includes searches for important new interstellar constituents; observations relevant to differentiating between different models for the chemical processes that are important in the interstellar environment; and coordinated studies of the chemistry, physics, and dynamics of molecular clouds which are the sites or possible future sites of star formation.

A detailed study has been made of the abundance and distribution of the only known interstellar hydrocarbon ring, cyclopropenylidene (C_3H_2), using radio telescopes at the University of Massachusetts and at the Nation Radio Astronomy Observatory. In addition to the principal isotopic species, we have observed the singly deuteriated isotope (C_3HD) and the ^{13}C-isotopic form in a number of interstellar clouds. A very high degree of deuterium fractionation is found, up to about $C_3HD/C_3H_2 \sim 0.05$ in some cold clouds, which is a factor of 5000 larger than the cosmic D/H ratio. This is among the highest degrees of fractionation ever observed in interstellar chemistry, and places severe constraints on models for the formation of C_3H_2.

In order to make the first determinations of the CO_2/CO abundance ratio in interstellar sources, we have carried out observations of protonated $CO_2(HCO_2^+)$, since CO_2 itself has no allowed rotational transitions. The results are consistent with models based on ion-molecule chemistry, which predict that the ratio $CO_2/CO \ll 1$. In fact, HCO_2^+ is observed in only one molecular cloud, near the center of our galaxy.

In quiescent interstellar clouds there is substantial evidence that the chemistry is dominated by ion-molecule reactions which are ultimately powered by cosmic rays. In these regions the kinetic temperature is in the range 10-50K, and densities are from 10^3 to 10^{-6} molecules per cc. In certain regions, however, "high temperature processes" seem to occur which change the character of the chemistry. A particularly interesting source in this regard is the supernova remnant IC443, where it appears that the supernova blastwave has created dense, shocked regions in the ambient gas. The chemistry of these clumps shows interesting anomalies with respect to that in quiescent clouds, and is being actively investigated. Similar high temperature processes seem to occur in the vicinity of imbedded infrared sources (protostars?) in dense molecular clouds. Such regions are being investigated through the study of vibrationally excited molecules and emission from silicon-containing molecules, whose abundance is vastly enhanced under these conditions. ■

A GAS-GRAIN SIMULATION FACILITY FOR SPACE STATION

D. E. Schwartz, C. P. McKay and C. R. Stoker
Solar System Exploration Branch, NASA/Ames Research Center, Moffett Field, California 94035

Space platforms in earth orbit provide a unique capability to do experiments in the space environment. Because of the very low apparent gravitational acceleration (microgravity) experienced by objects in orbit, many experiments that are impractical or impossible on earth become feasible in space. These experiments are those in which gravity either interferes directly with the phenomenon under study (*e.g.* gravitational convection masking diffusional processes) or precludes the establishment of the proper experimental conditions (*e.g.* by accelerating test objects to unacceptable velocities). This reduction in the forces required to suspend particles during an experiment can be reduced by as much as six orders of magnitude and enables us to perform many new experiments in a variety of disciplines (Squyres *et al.*, 1985). A representative range of particle sizes of importance for different astrophysical systems is shown in Figure 1 (McKay *et al.*, 1987).

Exobiology is one of the key scientific areas that can benefit from an orbital gas-grain simulation facility. Exobiology is the study of life in the universe (DeVincenzi, 1984). It is concerned with the origin and distribution of the biogenic elements (C,H,N,O,P,S) and the relationship between the physical and chemical evolution of the solar system and the appearance of life. Many of the current research

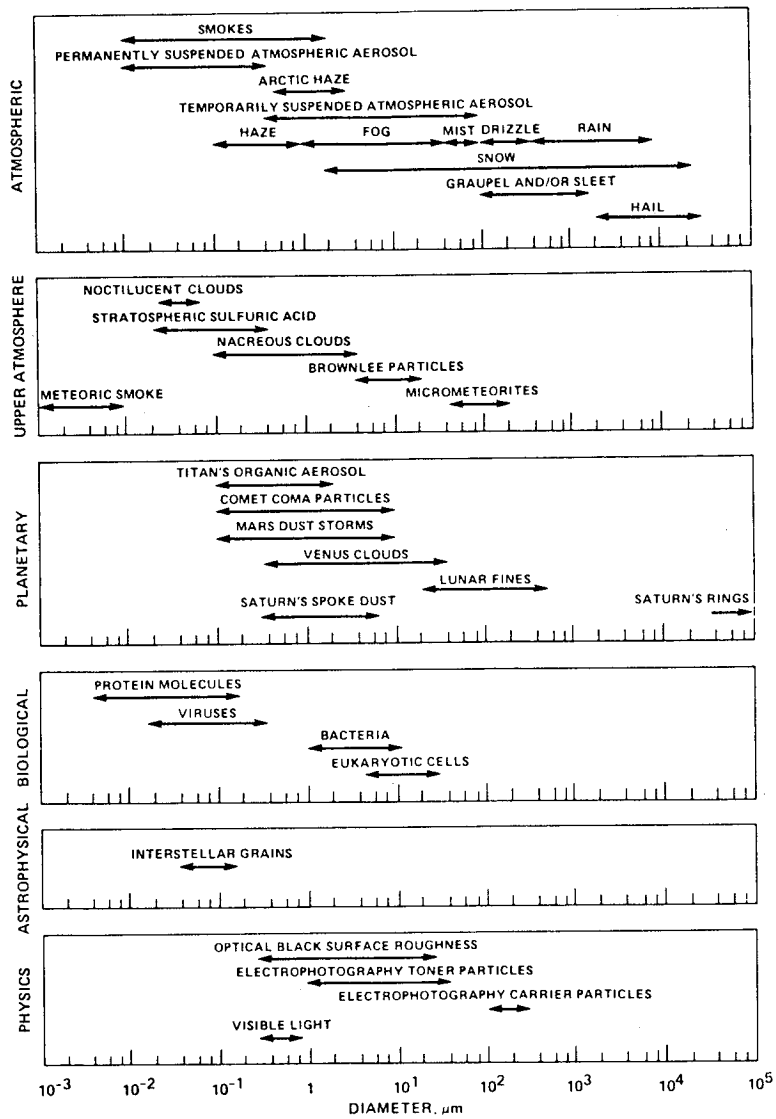

Fig. 1. Typical sizes of particles for a variety of astrophysical systems that may be applicable to a space station gas–grain simulation facility, from McKay *et al.* (1987).

problems in exobiology concern the behavior of small grains and particles. The processes that govern the interactions of these grains occur in environments that cannot be adequately simulated on earth because of the presence of gravity. Nonetheless, laboratory simulations are desirable since they provide a powerful tool in studying the behavior of cosmic systems for which there are no terrestrial analogs. Several exobiology experiments that might make use of a gas-grain simulation facility on the Space Station are listed in Table 1.

We have concluded that access to a space vacuum is not an absolute requirement for a microgravity particle facility in light of possible no-dump requirements, suitable laboratory vacuums systems, and no clear experimental requirement for ultrahigh vacuum or pump rates (see McKay *et al.*, 1987).

The earth orbital environment is often described as "zero" gravity. This is a misnomer in two important ways. First, the gravitational acceleration of the earth as the space station altitude (~500 km) is ~8.5 ms^{-2}, clearly not zero. A point particle in orbit in a vacuum, however, doesn't "feel" this gravitational acceleration because it is free to move in response to the gravitational force; it is in free fall. Regions of an earth-orbital platform distant from the center of mass will feel small resudual

Table 1. Exobiology Experiments for a Gas-Grain Simulation Facility

- Laboratory simulations to characterize the condensation of carbon in the interstellar medium and stellar atmospheres.
- Investigate the chemistry of surface reactions on interstellar grains that may form the complex molecules (C9 and above) that have been detected in the interstellar medium.
- Investigate the thermodynamic and hydrodynamic states of particles and grains in the solar nebula and the implication of these characteristics for the survival of interstellar organic material during the formation of the solar system.
- Simulate the formation of comet coma particles in order to determine the contribution comets make to the volatile and organic inventories of the terrestrial planets.
- Investigate the abiotic production of organic material and the condensation of this material into solid particles under varying conditions.
- On-site analysis of the extraterrestrial particles collected on the space station.

acceleration forces; these are essentially tidal forces (see McKay *et al.*, 1987). A complete analysis of magnitude of these forces, including absolute rotation of the spacecraft, atmospheric drag and other secular accelerations yield values of the gravity gradient of ~0.44 $\mu g\ m^{-1}$ radial to the direction of motion of the spacecraft, ~0.13 $\mu g\ m^{-1}$ along the direction of motion and ~0.38 $\mu g\ m^{-1}$ transverse to it. The gas-grain simulation facility will therefore be subjected to secular gravitational accelerations of about 1 μg. For these levels of residual force, the time required for the particle to move across the dimensions of a simulation facility are surprisingly short. At 1 μg it takes less than 8 minutes to move across a one meter chamber, and less than 2.5 minutes if the chamber dimension is 10 cm (McKay *et al.*, 1987).

The effect of this acceleration on the gas-grain simulation facility depends strongly on the relative properties of the gas and the grains in the facility. The results for a detailed analysis of the gas particle interactions (McKay *et al.*, 1987) show that the presence of gas in the gas-grain simulation facility induces Brownian motion of the particle but, even at low pressure, acts to damp the particles' motion in response to residual acceleration.

There are a variety of methods available that can provide the levitation forces required to overcome the gravity gradient forces and maintain the particle in the desired location against the disturbing force of Brownian motion and residual acceleration. We have considered four types of particle control methods: radiation, acoustic, electrostatic, and electromagnetic. Each of these has applications for certain particle sizes and compositions and each presents some degree of difficulty (McKay *et al.*, 1987).

Levitation and control requirements for experiments involving single particles can be readily achieved. Experiments that require the suspension and control of clouds of particles pose new difficulties in at least three major areas: electric effects of particle charging, coalescence of the cloud by the levitation mechanism, and wall effects. Preliminary analysis indicates that particle charging can be controlled by the introduction of radioactive emmiters into the chamber or by the introduction of certain chemicals that can reduce static buildup. Forced coalescence of the cloud of particles and wall effects may be minimized by scaling up the dimensions of the chamber.

We have selected the simulation of organic haze production on Titan as an example experiment for detailed study. The objective of this experiment is to simulate the photolysis of methane and the subsequent formation of organic haze particles in the upper atmosphere of Titan. The experiment would attempt to follow the growth of a single particle as it grows from an initial organic polymer to a micron-size particle. The shape and scattering properties of the particle would be determined. ■

REFERENCES

DeVincenzi, D.L., NASA's Exobiology Program, *Origins of Life* 14, 793-799 (1984).

McKay, C.P., Stoker, C.R., Morris, J., Conley, G., and D. Schwartz, Space Station Gas-Grain Simulation Facility: Application to Exobiology, submitted to *Space Research* (1987).

Squyres, S.W., McKay, C.P. and D.E. Schwartz, Microgravity Particle Research on the Space Station, unpublished report of a workshop held at NASA Ames 22-24 August 1985.

HYPERVELOCITY INTACT CAPTURE OF INTERPLANETARY COSMIC DUST

P. Tsou[1], D. E. Brownlee[2] and A. L. Albee[3]
[1]*Jet Propulsion Laboratory, Pasadena, California 91109,* [2]*Washington University, Seattle, Washington 98195, and* [3]*California Institute of Technology, Pasadena, California 91125*

INTRODUCTION

Knowledge of the phase, structure, and crystallography of cosmic particles, as well as, possibly, their molecular composition, would be very valuable information toward understanding the nature of extraterrestrial material and biogenic elements and compounds. This information can be obtained from the intact capture of large grains of cosmic dust particles in Earth orbiting platforms and from hypervelocity flyby missions to comets [1]. Hypervelocity experiments of intact capture in underdense media have indicated realistic potential in this endeavor [2,3]. Passive underdense media will permit relatively simple and inexpensive missions to capture cosmic dust particles intact.

The relative speed between the collector and cosmic dust particles is in the hypervelocity range, 8 km/s or higher. To enable such a sample return mission, development work in hypervelocity capture of particles has been conducted. Surprising success has been achieved with commercially available polymer foams as intact capture media. More than 60% of the aluminum projectile has been captured at 7.9 km/s. For a simulated cometary-like projectile, intact capture has been achieved at greater than 4 km/s. This paper reports the hypervelocity intact capture experiment data and plans for organic recovery experiments.

FOAM CAPTURE EXPERIMENTS

A wide range of polymer underdense foam media was used as capturing targets. The foam densities varied from 9 to 528 mg/cc. Most of the capturing experiments were performed under vacuum. The projectiles were mostly polished aluminum spheres of 1.5 to 3.2 mm diameter and were accelerated with a two-stage light-gas gun from 1 to 7.9 km/s. In order to assess the effect on more realistic, fragile, and comet-like particles, projections of Pyrex glass, Wellman meteorite, Epoxy-bonded Allende meteorite powder, Epoxy-bonded olivine/FeS/glass microspheres, and organic spiked projections were used.

RESULTS The experiments seemed to show that polymer underdense media were quite effective in capturing intact projectiles up to about 5 km/s. The typical track left in the underdense medium is characteristically carrot-shaped. The track has two distinct sections: the burn section, and the shear section. The burn track is marked distinctly with black residues from foam pyrolysis or melt, and the burn track diameter is very much larger than the projectile diameter. The width of the shear track, on the other hand, is nearly the same as the projectile diameter and is devoid of any burnt residues. The entry hole size is on the order of one to three times the projectile diameter. For a given foam density the maximum track diameter seems to be proportional to the projectile speed; and for a given speed, the maximum track diameter seems to increase with foam density, while the stopping distance shortens with increased foam density.

The projectiles' captured-mass to original-mass ratio for aluminum projectiles becomes less than one for projectile speeds greater than about 2 km/s for a 16 mg/cc expanded polystyrene foam. The capture ratio decreases with increased speed. Up to 83% of the projectiles' original mass has been captured at 6.3 km/s for 3.2 mm size projectiles. About 60% has been captured at 7.9 km/s for 1.5 mm size projectiles.

FINDINGS

These intact capture experiments provide very positive and encouraging results for the intact capture of cosmic dust at speeds less than 15 km/s. As increased understanding of intact capture in underdense media is gained, an optimum underdense medium can be designed to achieve the desired captured ratio at a specific hypervelocity and for a specific particle. The ability to capture conglomerated fragile cometary-like particles, the development of methods to detect small particles in the underdense media, and the characterization of organic recovery are some of the near-term objectives to be achieved.

ACKNOWLEDGMENTS

Without the cooperative support of the NASA Ames Vertical Gun Range, this research would not have been possible. This work was carried out, in part, by the Jet Propulsion Laboratory, California Institute of Technology, under NASA contract. ■

REFERENCES

[1] Tsou, P. et al. (1985) Comet Coma Sample Return via Giotto II, J. British Interplanetary Soc. 38:232-9.

[2] Tsou, P. et al. (1984) Experiments on Intact Capture of Hypervelocity particles, Lunar and Planet. Sci. XV:866-7.

[3]Tsou, P. et al. (1986) Comet Coma Sample Return, 20th ESLAB Symposium on the Exploration of Halley's Comet, 1986.

PAGE 357 INTENTIONALLY BLANK

PRECEDING PAGE BLANK NOT FILMED

FERTILITY GRADIENTS IN CONIFEROUS ECOSYSTEMS: FOLIAR CHEMISTRY AND NUTRIENT FLUX

P. A. Matson and N. Swanberg
NASA/Ames Research Center, Ecosystem Science and Technology Branch, Moffett Field, California 94035

Forest ecosystems vary widely in biogeochemical cycling characteristics and in production of trace gases. The identification of forests that are important sources of trace gases requires an understanding of the factors that control flux. We are examining the relationships among forest fertility, nutrient cycling, and nitrous oxide flux, and the extent to which foliar chemical composition reflects ecosystem processes. We are also examining the remote detection of differences in canopy biochemical status using the Airborne Imaging Spectrometer (AIS) and the Airborne Visible and Infrared Imaging Spectrometer (AVIRIS).

A fertilization study was established in even-aged Douglas fir forests in northwestern New Mexico. Treatments included fertilization, irrigation, carbon additions (to cause severe nutrient limitation), and control. One year after treatment, nitrate production (measured with *in situ* incubations) was significantly higher in the fertilized plots than control (16.5 ug/g/2 month vs. 1.4 respectively, in forest floor; 1.9 ug/g/2 month vs. .4 respectively, in mineral soil). Nitrous oxide flux was also significantly higher in the fertilized plots, but only in July (5 $ng/cm^2/hr$ vs. .2, respectively).

As with nitrogen cycling processes and nitrous oxide flux measurements, foliage samples were collected once monthly from May-October, 1986. Foliar chemical concentrations also responded to treatments. For all foliage age classes, total nitrogen, protein, amino acids, and chlorophyll concentrations were significantly higher in the fertilized treatment than in control (*e.g.* total N:11.3 mg/g vs. 8.2 mg/g for June 1+2 year old needle age class). Starch concentrations were reduced in the fertilizer treatments in June, during the period of new growth, presumably because carbohydrates were in greater demand in trees growing with adequate nutrients.

In September, 1986, AIS spectral data were collected. Intensity values are being extracted for each plot and are being used to generate spectra which can then be related to actual chemical content measured by the ground-based sampling. ■

THE RELATIONSHIP OF AVHRR DATA TO THE LEAF AREA INDEX OF WESTERN CONIFEROUS FORESTS

M. A. Spanner[1], D. L. Peterson[2], S. W. Running[3] and L. Pierce[3]
[1]TGS Technology, Inc., Ecosystem Science and Technology Branch, Mail Stop 242-4, NASA/Ames Research Center, Moffett Field, California 94035, [2]Ecosystem Science and Technology Branch, NASA/Ames Research Center, Moffett Field, California 94035 and [3]School of Forestry, University of Montana, Missoula, Montana 59812

The objective of this research is to analyze the relationship between the leaf area index (LAI) of coniferous forests and data acquired by the Advanced Very High Resolution Radiometer (AVHRR) to permit the determination of the spatial distribution of the LAI of coniferous forests throughout the western United States. Coniferous forests occupy approximately one-third of the land of the western United States, mostly in mountainous regions. Leaf area index is functionally related to the exchange of carbon dioxide, water and oxygen, and is valuable in estimating the rate of canopy photosynthesis and evapotranspiration. In coniferous forests of the Pacific Northwest, leaf area index has been shown to be

linearly related with site water balance and net primary productivity (Grier and Running, 1977; Gholz, 1982).

Recent studies have demonstrated the relationship between the LAI of coniferous forests and remote sensing data acquired by the Thematic Mapper (TM) and a Thematic Mapper Simulator (TMS) (Running *et al.* 1986). A strong positive relationship was observed between the ratio of near infrafred (IR) to red radiance measured by the TMS and the LAI of eighteen coniferous forest stands across a temperature-moisture gradient in Oregon. Additional sites were established in the Seeley-Swan Valley in western Montana and at Sequoia National Park to provide a regional representation of LAI. A positive relationship was observed between the near IR/red ratio of the TM data and the LAI of 73 sites, however, the relationship was not as strong as was observed in Oregon alone.

The spatial resolution of the Thematic Mapper is 30 meters. Fine spatial resolution increases variability between pixels because of the variable arrangement of trees at a 30 meter scale. This tends to weaken a relationship between remote sensing data and forest structure at high spatial resolution. A problem with the estimation of the LAI of western coniferous forests from TM data is that complete coverage of the western United States is expensive in terms of data acquisition and image processing. Data acquired by the Advanced Very High Resolution Radiometer (AVHRR) on the NOAA-7 and NOAA-9 satellites are amenable to regional scale estimation of leaf area index. The AVHRR provides spectral coverage similar to that of the Thematic Mapper. With a spatial resolution of approximately 1 kilometer at nadir, the spatial variability between pixels is reduced and coverage of the entire western United States can be obtained from one overpass. Drawbacks to the AVHRR include spatial averaging of clearcuts and mature forests, and the effect of large scan angles and differing atmospheres over large areas.

In our current research, the relationship between AVHRR data and LAI for a series of AVHRR acquisitions from the summer of 1984 were analyzed. Approximately twenty-five AVHRR scenes were acquired for this time period. Eighteen coniferous forest stands at least two kilometers on a side and relatively homogeneous with respect to crown closure and composition were established in the western United States. Seven of the sites were from the Oregon transect and one was from Sequoia National Park. LAI for these sites were calculated from measurements made from the previous studies. In addition, measurements were obtained at forest stands from six new sites in Montana and four at Mt. Rainier National Park. The projected LAI of the large stands ranged from .7 to 12.8. The relationships between LAI and the near IR/red ratio measured at each site from a cloud-free AVHRR scene from July, August, and September were analyzed. Significant positive relationships were observed for all three scenes. The strongest relationship between LAI and the near IR/red ratio existed for the September scene, with a coefficient of determination of .85, significant at the .001 level. The strong relationship for the September scene is attributed to senescence of both the understory grasses and the deciduous component of some of the stands. Understory vegetation and the deciduous component of the forest stands adversely affected the LAI-TM relationship developed from Thematic Mapper imagery acquired in July and August. The effect of scan angle variations on the ratio tended to improve the relationship slightly; conversely, varying atmospheric conditions tended to degrade the relationship.

A maximum value composite consisting of the maximum near IR/red ratio for each site calculated from all of the available AVHRR data for each of the summer months was derived. The maximum value composite reduces sun angle, scan angle and atmospheric effects on the near IR/red ratios. The maximum value composite for each month displayed the same positive relationship to LAI. The coefficients of determination, however, were slightly lower for the maximum value composite near IR/red ratio and LAI than for the single scene near IR/red ratio and LAI. Not all of the scenes required for a monthly maximum value composite were acquired, possibly reducing the effectiveness of the composite.

AVHRR data for 1986-87 are currently being analyzed. Analysis of a May cloud-free scene and the May maximum value composite near IR/red ratio confirm the positive relationship with LAI. These initial results indicate the potential for regional estimation of the leaf area index of western coniferous forests using data acquired by the Advanced Very High Resolution Radiometer. ■

REFERENCES:

1. Gholz, H.L. (1982), Environmental limits on aboveground net primary production, leaf area, and biomass in vegetation zones of the Pacific Northwest, Ecology 63(2):469-481.
2. Grier, C.C. and S.W. Running, (1977), Leaf area of mature Northwestern coniferous forests: relation to site water balance, Ecology 58(4):893-899.
3. Running, S.W., D.L. Peterson, M.A. Spanner and K.B. Teuber, (1986), Remote sensing of forest leaf area, Ecology 67(1):273-275.

METHANE FLUX FROM THE CENTRAL AMAZONIAN FLOODPLAINS

K. B. Bartlett[1], P. M. Crill[2], D. I. Sebacher[3], R. C. Harriss[3], J. O. Wilson[2], and J. M. Melack[4] / [1]*Department of Biology, The College of William and Mary, Williamsburg, Virginia 23185* [2]*National Research Council, Resident Research Associate, NASA/Langley Research Center, Hampton, Virginia 23665* [3]*Atmospheric Sciences Division, NASA/Langley Research Center, Hampton, Virginia 23665* [4]*Department of Biological Sciences, University of California, Santa Barbara, California 93106*

A total of 186 methane measurements from the three primary Amazon floodplain environments of open water lakes, flooded forests, and floating grass mats were made over the period 18 July through 2 September, 1985. These data indicate that emissions were lowest over open water lakes, where flux averaged 27 ± a standard error of 4.7 $mgCH_4/m^2/d$ (n=41). Flux from flooded forests and grass mats was significantly higher. Emissions from flooded forests averaged 192 ± 26.8 $mgCH_4/m^2/d$ (n=90), while those from floating grass mats averaged 230 ± 72.2 $mgCH_4/m^2/d$ (n=55). At least three transport processes contribute to tropospheric emissions: ebullition from sediments, diffusion along the concentration gradient from sediment to overlying water to air, and transport through the roots and stems of aquatic plants. Measurements indicate that the first two of these processes are most significant. Diffusive flux from flooded forests averaged 50.5 ± 11.0 $mgCH_4/m^2/d$, while that from floating mats averaged 43.7 ± 11.8 $mgCH_4/m^2/d$. Diffusive flux from open waters averaged 8.3 ± 1.9 $mgCH_4/m^2/d$. Emissions through bubbling were 168 ± 32.2 (flooded forest), 346 ± 128 $mgCH_4/m^2/d$ (floating grasses), and 17.3 ± 5.2 (open water). We estimate that on the average bubbling makes up 49% of the flux from open water, 54% of that from flooded forests, and 64% of that from floating mats. If we apply our measurements to the entire Amazonian floodplain, we calculate that the region could supply up to 12% of the estimated global natural sources of methane. ■

PAGE 361 INTENTIONALLY BLANK

PRECEDING PAGE BLANK NOT FILMED

CLIMATE EVOLUTION OF VENUS, EARTH, AND MARS

J. F. Kasting
Space Science Division, 245-3, NASA/Ames Research Center, Moffett Field, California 94035

The distribution of life in the universe may be highly dependent on the availability of suitable planetary environments to support it. In our own solar system only earth, with a mean surface temperature of 288 K, has a climate that permits the presence of liquid water at the planet's surface—a necessary prerequisite for life as we know it. Venus is so hot (730 K) that water can exist only as steam, whereas Mars is sufficiently cold (212 K) that water exists almost exclusively as ice. The observed trend does not result simply from the planets' respective distances from the sun. It depends equally strongly on the greenhouse effect of their atmospheres and on the amount of sunlight scattered back to space by gases, aerosols, and clouds. Atmospheric density and composition have almost certainly varied with time on each of the terrestrial planets, resulting in changes in the amount of greenhouse warming. At the same time, solar luminosity has gradually increased, starting from approximately 25 to 30% below its present value around 4.6 billion years ago. Given such evolutionary changes within our own solar system, and given that other star systems may have somewhat different distributions of planetary orbits, an important goal for exobiology is to estimate the width of the continuously habitable zone (CHZ) around a star in which planets may maintain an earth-like climate over time periods long enough for life to evolve and proliferate.

The first challenge is to understand why earth itself has remained habitable in spite of the large increase in solar luminosity over geologic time. If the composition of earth's atmosphere had remained unchanged, climate models predict that earth's oceans would have been completely frozen over prior to about 2 billion years ago. This so-called "faint young sun paradox" can be resolved if one assumes that the early atmosphere contained at least 100 to 1000 times its present content of carbon dioxide. This assumption is not as *ad hoc* as it might at first seem. Over time periods longer than 10^5 years, the concentration of CO_2 in earth's atmosphere is controlled by exchange with carbonate rocks via the carbonate-silicate geochemical cycle. CO_2 is lost by weathering of silicates—a process that is highly sensitive to temperature because it depends on the rates of precipitation and runoff. CO_2 is restored to the atmosphere by carbonate metamorphism, which occurs when carbonate sediments on the ocean floor are subducted downwards and exposed to higher temperatures and pressures. The CO_2 given off by this process reenters the atmosphere through volcanic outgassing at the plate margins.

The net effect of this CO_2 cycle is to provide an effective mechanism for buffering earth's climate over long time scales. If the mean surface temperature had ever approached the freezing point of water, silicate weathering would have been strongly inhibited, and CO_2 would have begun to accumulate in the atmosphere. This would have enhanced the greenhouse effect, thereby helping to restore warmer conditions. Conversely, if the surface temperature had become too hot, the rate of silicate weathering would have increased, drawing down atmospheric CO_2 levels and decreasing the amount of greenhouse warming. Thus, earth's climate has remained reasonably temperate despite large changes in solar insolation over the planet's history.

By contrast, Mars appears to have been relatively warm during its early history, but is now too cool to support most terrestrial forms of life. Images of Mars from Mariner 9 and Viking show fluvial gullies and valley networks that were clearly produced by running water. Some of these features imply the existence of an earth-like hydrological cycle and, hence, a much warmer and denser atmosphere at some previous time. One-dimensional, radiative-convective climate calculations show that a surface CO_2 pressure of between 1 and 5 bars would have been required to elevate the Martian surface temperature above freezing early in that planet's history (Figure 1). These estimates correspond to effective solar fluxes of 1.3 and 0.7 times the present flux at Mars' orbit (S_o). The lower value of S_o represents globally and orbitally averaged conditions; the higher value is for conditions at the equator

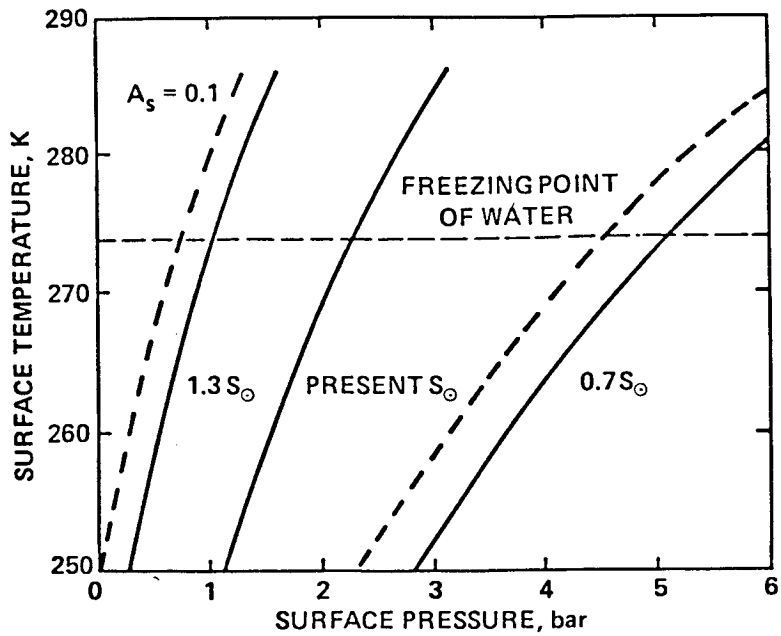

Figure 1.

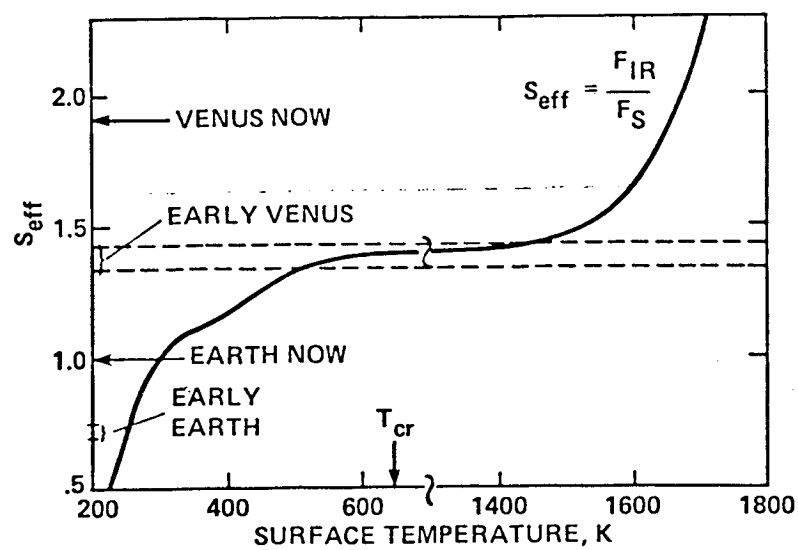

Figure 2.

during perihelion. Such a dense CO_2 atmosphere could have been maintained for a geologically significant time period if tectonic activity on early Mars was sufficiently vigorous to recycle carbonate rocks. Mars, however, is much smaller than earth and should therefore have lost its internal heat more rapidly. As the heat flux from Mars' interior diminished and tectonic activity subsided, the CO_2 in Mars' atmosphere was irreversibly converted into carbonates and adsorbed onto the regolith. Eventually, the Martian climate approached its present frozen state.

Venus, because of its position nearer to the sun, faced the opposite climatic problem: its surface temperature was always high enough so that it could lose water rapidly by photodissociation followed by escape of hydrogen to space. Venus is currently deficient in water by a factor of 10^5 compared to earth. Theoretical models of planetary accretion suggest, however, that Venus' original complement of water was roughly comparable to that of earth. One-dimensional climate calculations indicate that liquid water may have been present on Venus' surface at one time. For a cloud-free atmosphere, the critical solar flux at which a runaway greenhouse would have occurred, that is, at which the oceans would have evaporated completely, is 1.4 times the present solar flux at earth's orbit (Figure 2). By

comparison, the flux expected at Venus' orbit early in solar system history was 1.34 to 1.43 times this value (horizontal dashed lines), assuming a 25 to 30% decrease in solar luminosity at that time. If clouds cooled the planet's surface, as seems likely, then oceans may originally have been present. They would have been short-lived, however, since even an ocean- covered early Venus would have lost its water rapidly by photodissociation followed by escape of hydrogen to space. This process becomes very efficient at solar fluxes exceeding 1.1 times the present terrestrial value.

This last calculation implies that the inner edge of the continuously habitable zone lies at ~0.95 AU, not far from the orbit of earth. The outer edge of the CHZ, however, may lie as far out as the orbit of Mars, since an earth-sized planet at that distance would presumably be kept warm by the feedback between atmospheric CO_2 levels and climate. This result suggests that the liklihood of finding earth-like planets around other stars is very good, thereby increasing the possibility that life may have evolved elsewhere. ■

EXTRATERRESTRIAL CAUSES OF EXTINCTION: AN UPDATE

D. M. Raup
Department of Geophysical Sciences, University of Chicago, Chicago, Illinois 60637

The classic paper by Alvarez *et al.* (1980) on iridium anomalies at the Cretaceous-Tertiary ("K-T") boundary touched off a controversy about the causes of biological extinction which continues unabated to the present. In this paper, I will summarize the main features of the extinction debate and attempt to point directions for future research.

The iridium anomalies were interpreted by the Alvarez group as indicative of large-body impact (asteroid or comet) because of the similarities in trace element chemistry with certain meteorites (especially carbonaceous chrondrites). The causal link to mass extinction was based on a probabilistic argument: it was argued that major mass extinctions and large impacts are both rare events in geologic history and that their coincidence thus indicates cause and effect. The argument was strengthened by models of the atmospheric and other effects of large body impact which suggested that the environmental consequences of such an impact would suffice to cause global extinctions of species.

Since 1980, several lines of evidence from many laboratories have contributed to the impact-extinction theory. These include work on osmium isotope ratios, microtektites, and shock-metamorphosed quartz, among others. In each case, indicators of extraterrestrial influence in association with the K-T iridium were reported. Also since 1980, there has been a quantum increase in detailed field work on the fossil record near the K-T boundary so that the chronology of the extinctions is far better known than before.

The impact-extinction theory has been challenged by a number of workers. It has been argued, for example, that the iridium anomalies result from mantle volcanism, that the spherules identified as microtektites are not related to impact, and that some of the other geochemical and geophysical evidence has been misinterpreted. On the paleobiological side, it has been argued that the extinctions are too dispersed in time for the impact hypothesis to be credible and that conventional earth-bound explanations, such as those based on climate and sea level, are adequate to explain the terminal Cretaceous mass extinction. Of these counterarguments, that based on volcanism is perhaps the most cogent. Indeed, there are strong suggestions in the total geologic record of persistent associations between pulses of extinction and extensive flood basalt volcanism. For some investigators, this opens the way to suggest that comet or asteroid impact may have triggered mantle volcanism.

Because the original Alvarez proposal was based primarily on the coincidence in timing of extinction and impact, and because this was based only on a single case (the K-T event), it is important to determine whether the temporal association between impact and extinction is found elsewhere in geologic history. To this end, reports of a similar association have been published for five other cases but each has controversial elements.

An important added element is the question of the spacing in time of both impact events and extinction pulses. Several periodicities have been reported for the record of the past 250 million years. These include the timing of (a) major extinctions, (b) dated impact craters, and (c) pulses of reversals of the earth's magnetic field. All three kinds of data have been interpreted to show coincident periodicities in the range of 26-30 million years, and several astronomers have proposed driving mechanisms involving solar system or galactic periodicities. This general subject is especially controversial because of questions about the statistical analyses of the geologic data and because of challenges to the astronomical explanations.

Fortunately, the data critical for resolving the foregoing questions are reasonably accessible. The following areas are most important:

(1) High-resolution paleontological data on biological extinction throughout the Phanerozoic. Collection of these data must be coordinated with the best possible radiometric dating.

(2) Comprehensive sampling of large portions of the geologic column for trace element and isotopic analysis. For iridium, the new instrument now operating at Lawrence Berkeley Laboratory is beginning to revolutionize the data base.

(3) Systematic data collection on the distribution of major episodes of volcanism in earth history.

(4) Further exploration for and documentation of impact craters on earth.

(5) Intensive research on the biological selectivity of extinction, especially mass extinction. Although atmospheric and other modeling is valuable in assessing the environmental effects of large-body impacts, our ultimate understanding of the causes of extinction can only come from detailed investigations of the physiological and ecological characteristics of the victims and survivors of the principal events of mass extinction.

The last of these, selectivity of extinction, is the principal objective of the PI's current NASA-supported research. ■

PERIODICITY IN MASS EXTINCTION: NEW DATA AND OBSERVATIONS

J. J. Sepkoski, Jr.
Department of the Geophysical Sciences, University of Chicago, 5734 South Ellis Avenue, Chicago, Illinois 60637

Mass extinctions are brief intervals of geologic time, less than several million years (Ma) long, during which unusually large numbers of species and higher taxa disappear. Approximately 25 such events have been identified in the fossil record of the last 700 Ma. Five of these mass extinctions were extraordinarily large, eliminating anywhere from 67 to 95% of species in both marine and terrestrial ecosystems. These large events may be very important in the history of advanced life, eliminating armchair taxa and vacating ecospace into which new taxa can diversify.

Two discoveries over the past decade have linked mass extinction with astronomical phenomena: (1) the finding of iridium anomalies and other indicators of a large-body impact at the Cretaceous-Tertiary Boundary, coincident with one of the five largest mass extinctions; and (2) the observation of a 26.2±1 Ma periodicity in mass extinctions, suggesting a cyclic forcing inconsistent with known terrestrial processes. Several models have been proposed that attempt to combine these two discoveries; these implicate impacts during comet showers as the cause of all or most mass extinctions, with the periodic forcing resulting from z-oscillation of the solar system through the galactic plane, precession of an unobserved tenth planet ("Planet X") into the inner edge of the Oort Cloud, or orbital dynamics of an undetected solar companion ("Nemesis"). These models are speculative and have been the subject of some controversy, as have the basic observations. In particular, critics have questioned the empirical basis for the 26-Ma periodicity, arguing that the data base (times of extinction of 3500 fossil taxonomic families) is too noisy to permit rigorous statistical conclusions and that different treatments of the data result in different apparent patterns of extinction.

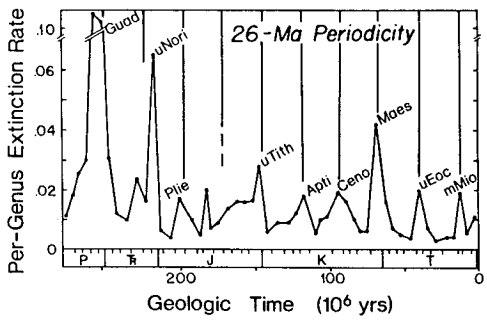

Figure 1. Per-genus rate of extinction (in units of extinctions per genus per million years) for marine mammals from the Middle Permian (270 Ma ago) to the present. Labelled maxima correspond to mass extinctions, which exhibit an approximate 26-Ma periodicity, as indicated by the vertical lines. Labels for the peaks are Guad: Guadalupian (Late Permian); uNori: Upper Norian; Plie: Pliensbachian; uTith: Upper Tithonian; Apti: Aptian; Ceno: Cenomanian; Maes: Maestrichtian; uEoc: Upper Eocene; mMio: Middle Miocene. Geologic systems (Permian, Triassic, Jurassic, Cretaceous, and Tertiary) are indicated by standard abbreviations along the abscissa. Points along the time series indicate measured values, computed for 51 stratigraphic stages and substages averaging 5.5 Ma in duration.

In response to these criticisms, I have been developing a data base on times of extinction of marine animal genera. This data base, compiled from the primary paleontologic literature, now contains information on nearly 30,000 fossil genera, with an average resolution of better than 10 Ma on times of extinction (and better than 5 Ma for over half of the genera). Time series computed from these data provide much clearer displays of fluctuations in extinction intensity over geologic time than did the older familial data. Local maxima of extinction are much more distinct from background, and questionable maxima in the familial data are resolved either into definite extinction peaks or into minor variations in background.

Figure 1 illustrates a time series for the per-genus rate of extinction (= probability of generic extinction) computed for the last 270 Ma of geologic time. Nine definite maxima of extinction are evident in the time series, including an event in the Aptian Stage of the mid-Cretaceous which was not evident in previous data. As shown by the vertical lines, the fit of these maxima to a 26-Ma periodicity is excellent; extinction maxima over the well-dated last 100 Ma fall almost precisely on the periodicity, and all periods, except one in the Middle Jurassic, are represented by extinction maxima.

Two aspects of the generic data in Figure 1 are somewhat surprising. First, many of the extinction maxima span several stratigraphic stages, suggesting they have durations of more than 5.5 Ma (the average length of a sampling interval); thus, these maxima may represent long-termed positive fluctuations in extinction intensity rather than short-termed, catastrophic events. Second, the amplitudes of most of the maxima are very similar and cannot be distinguished within the resolution of the data; only three events (Guadalupian, upper Norian, and Maestrichtian) have much larger magnitudes, appearing as outliers in the time series. These observations suggest that attempts to link all periodic mass extinctions directly to impacts of variable number, mass, and velocity during comet showers may not be correct. Instead, other processes and phenomena associated with occasional large body impacts (such as, perhaps, cometary dust generated during showers which may affect the earth's albedo and, thus, heat budget) should be explored. ■

COMETARY ICE AND DUST EXPERIMENT FOR THE COMET RENDEZVOUS ASTEROID FLYBY MISSION

G. C. Carle[1], B. J. O'Hara[1], B. C. Clark[2]
[1]*NASA/Ames Research Center, Moffett Field, California 94035,* [2]*Martin Marietta Denver Aerospace, Planetary Sciences Laboratory, Denver, Colorado 80201*

The Cometary Ice and Dust Experiment (CIDEX) is one of thirteen experiments selected for the Comet Rendezvous Asteroid Flyby (CRAF) mission. The CIDEX will determine the molecular and elemental composition of the comet nucleus (ice and dust grains and gases released from the nucleus), and the physical properties of the nucleus (ice to dust ratio, physical properties of the dust, active regions). It will

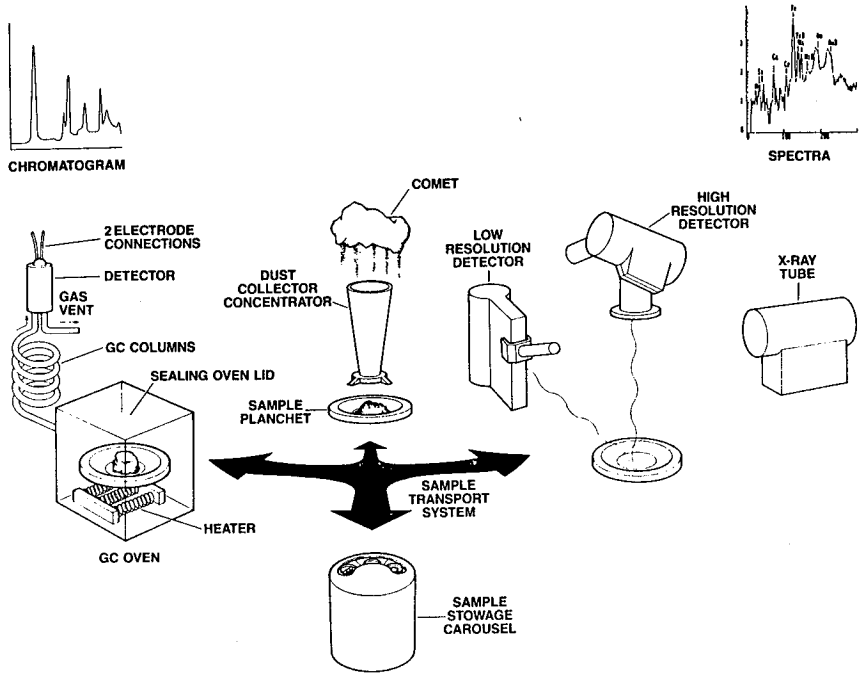

Figure 1. Cometary ice-and-dust experiment CIDEX concept.

characterize changes in the nucleus as a function of time and orbital position (dust flux and compositional variations in the grains and gases released from the nucleus). In addition, the CIDEX will characterize the chemical and physical nature of the atmosphere of the comet (gas composition and grain composition, and momentum and directionality distributions) and the development of the coma as a function of time and orbital position (variations in composition and flux of gases and grains).

The results from CIDEX will bear directly upon major scientific issues of the origin and evolution of comets, as well as the evolution of the solar system, planets and life itself. The data obtained from the CIDEX will increase our knowledge in several areas, including the composition of dust and inventory of volatiles in the comet nucleus, the relationships between comets and the meteorites, interstellar grains, and interplanetary dust particles, and the abundances and distribution of the biogenic elements and their compounds.

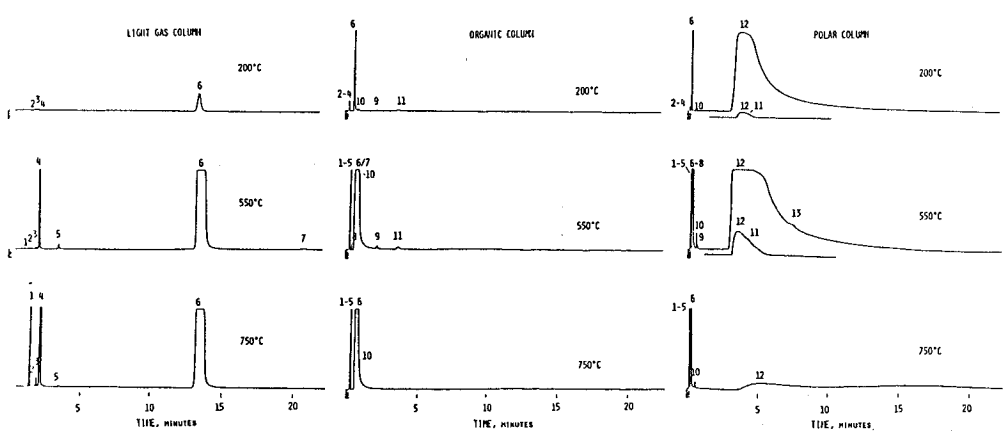

115 µg sample heated for 3 minutes at 200, 550 and 750°C. The evolved gases are: (1) H_2, (2) N_2, (3) O_2, (4) CO, (5) CH_4, (6) CO_2, (7) CH_2CH_2, (8) CH_3CH_3, (9) CH_2CHCH_3, (10) OCS, (11) CS_2, (12) H_2O, (13) CH_3CN.

Figure 2. Gases evolved upon heating Orgueil Meteorite.

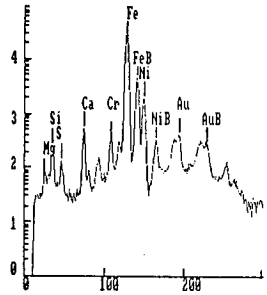

Figure 3. XRF spectrum of Allende Meteorite 0.5 monolayer (500μg/cm^2).

The CIDEX instrument (Figure 1) includes a sample collector, a gas chromatograph (GC) and an X-ray fluorescence spectrometer (XRFS). The sample collection subsystem is designed to efficiently collect cometary gases, ices and dust grains on a number of different collection planchets and at several collection stations. The design includes a planchet storage facility and a sample transporter mechanism for moving planchets between collector stations and storage stations.

The GC employs helium ionization detectors and three columns designed to separate light gases (*i.e.*, N_2, CO, CO_2), polar gases (*i.e.*, H_2O) and hydrocarbons (below C_5) to measure the volatile compounds of the biogenic elements (C,H,O,N,S) thermally released from dust grains. The sensitivity of the GC for compounds of interest is at the picogram level.

The XRFS utilizes cooled Si(Li) solid state detectors of nominal 150 eV resolution at 5.9 keV. Excitation is by x- rays from Fe-55 radioisotope and alpha particles/x-rays from Cm-244 radioisotope sources. The XRFS measures the elemental composition of the collected dust at a detection limit of 100 nanograms per square centimeter for elements such as Si, Fe, O, S, Ca, and C.

Based on laboratory work with carbonaceous meteorites, both the GC and XRFS can perform meaningful analyses on less than 0.01 monolayers or a few micrograms of collected comet dust (Figures 2-3). ■

ANALYTICAL INSTRUMENTATION FOR FUTURE SOLAR SYSTEM EXPLORATION MISSIONS UTILIZING ION MOBILITY SPECTROMETRY

D. R. Kojiro and G. C. Carle
NASA/Ames Research Center, Mail Stop 239-12, Moffett Field, California 94035

Future solar system exploration missions will require instrumentation capable of providing identification and quantitation of a multitude of molecular species over a wide range of concentrations. As an example, the complete analysis of the atmospheric components of Titan, both gaseous and in aerosols, will tax the limits of current analytical technology. A combination Gas Chromatograph/Ion Mobility Spectrometer (GC/IMS) can provide the sample separation, identification and quantitation required for such an analysis.

The Ion Mobility Spectrometer (MS) is an ion molecule reactor coupled with an ion drift spectrometer. In the reactant region of the instrument, beta particles from a Ni^{63} source create a reservoir of reactant ions, both positive and negative ions, from a reactant gas. The reactant ions ionize sample molecules through various charge transfer mechanisms, (generally ion-molecule reactions involving electron transfer, proton transfer or dissociative attachment reactions), forming positive and negative product ions. These relatively benign sample ionization processes produce molecular ions and clusters of simple additives from the reactant ions rather than the more complex fragments commonly produced in mass spectrometers.

The product ions, and any residual reactant ions, are admitted into an ion drift chamber at fixed intervals. An electric field moves the ions through this drift chamber, against the flow of a drift gas,

where they are separated according to their size, structure and charge distribution. As they exit the drift chamber, the ions are detected by a sensing electrode. The concentration profile, or "spectrum" produced by measuring the detected ion density vs. drift time, can be used as a fingerprint to characterize and identify the sample, in a manner similar to mass spectrometer sample identification. The rational for developing IMS as a detector for a flight GC is based on the fact that the IMS is a pressure instrument. This means that there is essentially no interface needed between the IMS and the GC. The separated sample components eluting from the GC column and all the carrier gas are vented directly into the reactant region of the IMS. The GC/IMS can thus provide primary sample identification without the interfacing difficulties inherent in GC/MS systems.

Current versions of IMS have not yet been developed specifically for flight experiments, however, and further research is necessary in several important areas.

Expanding the response range to include ppb to percent range: Although the IMS is very sensitive to many chemical species, it is easily saturated, which results in a very short linear response range. Methods to increase the response range of the instruments are necessary if it is to be utilized for future missions. Some techniques now being considered include the use of specialized reagent gases, to generate different types of reactant ions, and the use of alternate means of sample ionization such as photo ionization and metastable ionization.

Optimizing the reactant ion population for the chemical species anticipated for Titan or any other specific analysis: The research in this area is along the same lines as those for expanding the response range and include alternate means of sample ionization and the use of specialized reagent gases.

Miniaturization and other alterations to make IMS a flight-ready instrument: The commercial IMS is, of course, too large for a flight type instrument. However, smaller versions of the IMS have been developed by others. Although these miniature IMS designs are highly specialized and fall short of the capabilities required for future missions, they do demonstrate the feasibility of miniaturizing the IMS. Combining the use of resistive coated ceramic tubes for the construction of the IMS cell with a unidirectional flow design can reduce system contamination and allow for a more efficient flushing out of the IMS. This can result in the use of much lower drift flow rates than the 500 ml/min flow rates used in the commercial IMS. By using ultra-high-purity gases and careful elimination of sources for system contamination, successful IMS analysis has been conducted in our laboratory using a commercial version of the IMS at much lower drift flow rates. Miniature versions of the IMS are now being developed in our laboratory. ■

THE *IN VIVO* EFFECTS OF LOW PARTIAL PRESSURES OF DINITROGEN ON BIOLOGICAL ACTIVITY—A MARS PERSPECTIVE

R. L. Mancinelli
Solar System Exploration Branch, Mail Stop 239-12, NASA/Ames Research Center, Moffett Field, California 94035

There is considerable evidence which suggests that primitive Mars had a clement environment. Large valley networks and outflow channels indicate that liquid water once flowed over the Martian surface (*e.g.*, Carr, 1981; Squyres, 1984). This in turn implies that Martian surface temperatures were considerably warmer than today, with concomitant higher atmospheric pressure (1 bar), consisting primarily of CO_2 and N_2 (Pollack *et al.*, 1987). Early earth and early Mars were not that dissimilar. One of the most striking differences between the two planets was the low partial pressure of dinitrogen (pN_2) on early Mars *i.e.*, 18 mb, which was still greater than the 0.2 mb found on present day Mars (Fox and Dalgarno, 1983). Nitrogen is a key biological element and in many earth ecosystems the ability to transform N_2 into biologically useful forms is the main factor limiting growth. The ability of the nitrogenase enzyme to fix N_2 at extremely low partial pressures is uncertain. Laboratory investigations suggest that the nitrogenase enzyme follows Michalis-Menten kinetics. *In vitro* studies of nitrogenase from *Clostridium, Azotobacter,* and *Klebsiella* have reported K_m values for the reduction of N_2 to NH_3, of

pN_2 at 130 mb, 140 mb and 210 mb respectively (Hardy, 1979). *In vivo* studies using the cyanobacteria *Anabaena* and *Calothrix* have shown that the K_m for nitrogenase to be 121 mb, and 110 mb, respectively (Jensen and Cox, 1983; Stewart, 1967). In fact *Calothrix* was reported to be able to fix N_2 at a pN_2 of 50 mb. Ohomori and Hattori (1972) speculated that N_2 at a pN_2 of 0.1 mb or lower should induce the formation of nitrogenase. It is interesting to speculate what role nitrogen limitation may have played in the development and evolution of any possible early Martian biota. Nitrogen could have been rapidly removed from the atmosphere by two processes: 1) nonthermal escape of N-atoms to space (McElroy *et al.*, 1977; Fox and Dalgarno, 1983); and 2) burial deep within the regolith as nitrates (Yung *et al.*, 1977) (perhaps in conjunction with the burial of CO_2 as carbonates). The decrease of atmospheric nitrogen may have played a determining role in the deterioration of the environment that led to the extinction of any possible Martian life.

Pure cultures of *Azotobacter vinelandii* (ATCC#12837), *Azomonas agilis* (ATCC#7494), and *Beijerinckia indica* (ATCC#9030) were maintained on nitrogen-free mineral salts agar. Cells were grown in a nitrogen-free synthetic liquid medium under a one bar total pressure atmosphere containing oxygen (180 mb), nitrogen at partial pressures (pN_2) of 780 mb, 400 mb, 100 mb, 50 mb, 20 mb, or 10 mb, and the balance helium. An additional set of control flasks was run under a standard air atmosphere. The composition of the atmosphere was checked by gas chromatography. Growth was monitored using a Klett-Summerson colorimeter equipped with a red #66 filter. The spent growth medium was analyzed for NH^+_4. No effect was observed at a pN_2 of 400 mb for any organism. However, the growth rate of each organism began to decrease at pN_2=100 mb, and steadily declined with each successive lower pN_2. At pN_2 equal to 20 mb and 10 mb growth could be detected for each organism, but the total number of organisms in stationary phase was statistically significantly less than at higher pN_2's. In addition, no free NH^+_4 could be detected in the spent medium at either 10 mb or 20 mb pN_2.

The results of this study indicate that nitrogen fixing organisms belonging to the genera *Azomonas, Beijerinckia,* and *Azotobacter* have the ability to fix dinitrogen at a partial pressure as low as 10 mb, and possibly lower. However, the growth rates at these lower pN_2 values are much slower. This data suggests then that the low pN_2 on primitive Mars would not have been a significant limitation to the development of a biological system capable of fixing N_2. These data alone are insufficient to conclude that nitrogen was not a limiting factor on primitive Mars, because on earth, even with 800 mb of nitrogen, many ecosystems are nitrogen limited by a variety of mechanisms. ■

REFERENCES

Carr, M.H., The Surface of Mars. Yale University Press, New Haven, CT. (1981).

Fox, J.L. and A. Dalgarno, Nitrogen escape from Mars. J. Geophys. Res. 88, 9027-9032 (1983).

Hardy, R.W.F., Reducible substrates of nitrogenase. In: *A Treatise on Dinitrogen Fixation*, R.W.F. Hardy ed., pp. 515-568, John Wiley & Sons, London, England (1979).

Jenson, B. and R. Cox, Direct steady state kinetics of cyanobacteria n_2 uptake by membrane-leak mass spectrometry, and comparisons between nitrogen fixation and acetylene reduction. Appl. Env. Microbiol. 45, 1331-1337 (1983).

McElroy, M.B., T.Y. Kong, and Y.L. Yung, Photochemistry and evolution of Mars' atmosphere: A Viking perspective, J. Geophys. Res. 82, 4379-4388 (1977).

Ohomori, M. and A. Hattori, Effect of nitrate on nitrogen fixation by the blue green algae *Anabaena cylindrica*. Plant Cell Physiol. 13, 589-599 (1972).

Stewart, W.D.P., Nitrogen turnover in marine and brackish habitats. II. Use of ^{15}N measuring nitrogen fixation in the field. Ann. Bot 31, 385-407 (1967).

Pollack, J.B., J.F. Kasting, S.M. Richardson, and K. Poliakoff, The Case for a Wet, Warm Climate on Early Mars. Icarus, In press (1987).

Squyres, S.W., The History of Water on Mars. Ann. Rev. Earth Planet. Sci., 12, 83-106 (1984).

Yung, Y.L., D.F. Strobel, T.Y.Kong, and M.B. McElroy, Photochemistry of nitrogen in the Martian atmosphere. Icarus 30, 26-41 (1977).

CRAF MISSION EXOBIOLOGY INTERDISCIPLINARY SCIENCE: STABILITY OF ORGANIC MOLECULES IN COMETS

C. P.McKay
Solar System Exploration Branch, Life Science Division, NASA/Ames Research Center, Moffett Field, California 94035

INTRODUCTION

The recent spacecraft encounters with Comet Halley have provided further evidence that comets may have played an important role in the distribution of organic material in the early solar system. Of particular interest is the evidence that comets have dark mantles (Keller *et al.*, 1987) presumably composed of organic material, and the discovery of a population of comet particles, known as "CHON" particles (Clark *et al.*, 1987) rich in light elements.

The Comet Rendezvous Asteroid Flyby mission provides an opportunity to study in detail the organic chemistry of a comet. Of considerable interest is the stability of organic compounds in a cometary nucleus. To investigate this, I have computed the stability criteria and timescale for loss of a variety of organic molecules. The list considered (plus water) is shown in Table 1. This list includes the normal hydrocarbons through C_6, aromatics up to naphthalene, and all of the organic molecules detected in the atmosphere of Titan. The compounds considered represent a variety of degrees of volatility.

Table 2 shows the conditions under which each of the compounds listed begins to be lost from the nucleus. To obtain this calculation we begin with the energy balance of the nucleus. When the nucleus

Table 1. Compounds Considered

Index	*Formula*	*Name*	*Heat of Vaporization* cal gm-mole^{-1}	*T* (°C) (*P* = 1 torr)
1	H_2O	water	12186.0	-17.4
2	CO	carbon monoxide	1613.3	-222.0
3	CO_2	carbon dioxide	5539.0	-134.3
4	CH_4	methane	2128.8	-205.9
5	C_2H_6	ethane	3739.5	-159.5
6	C_3H_8	propane	4550.0	-128.9
7	n-C_4H_{10}	butane	5801.2	-101.5
8	n-C_5H_{12}	pentane	6595.1	-76.6
9	n-C_6H_{14}	hexane	7627.2	53.9
10	C_2H_2	acetlyene	4665.8	-142.9
11	C_6H_6	benzene	10254.0	-36.7
12	$C_{10}H_8$	naphthalene	17065.0	52.6
13	C_2H_4	ethene	3453.7	-168.3
14	HCN	hydrogen cyanide	7338.8	-70.8
15	C_4H_2	1,3-butadiene	7761.0	-70.8
16	C_3H_4	propyne	5632.0	-111.0
17	C_2N_2	cyanogen	6597.3	-95.8

Table 2. Sublimation Distance and Loss Rates for Different Organics and Water in a Cometary Nucleus.

Index	*Compound*	R_o[a] AU	Z_o[b] mol cm^{-2}s^{-1}	τ_o[c] years	N[d]
1	H_2O	3.0	$456. \times 10^{13}$	1400	280
2	CO	159.4	1.	540000	270
3	CO_2	13.4	49.	13000	270
4	CH_4	86.3	3.	210000	260
5	C_2H_6	25.6	20.	32000	250
6	C_3H_8	15.7	44.	15000	240
7	n-C_4H_{10}	9.8	88.	7400	240
8	n-C_5H_{12}	7.3	140.	4700	240
9	n-C_6H_{14}	3.4	568.	1100	190
10	C_2H_2	17.2	36.	18000	260
11	C_6H_6	3.8	330.	2000	270
12	$C_{10}H_8$	1.6	1083.	600	290
13	C_2H_4	30.6	15.	43000	250
14	HCN	6.3	167.	3900	240
15	C_4H_2	6.0	176.	3700	250
16	C_3H_4	10.9	74.	8800	250
17	C_2N_2	8.3	108.	6000	250

[a] R_o is the heliocentric distance within which vaporization of the specified volatile material occurs. At R_o 2.5% of the solar flux incident on the comet surface goes into sublimation (see *e.g* Delsemme, 1982).
[b] Z_o is the flux of the specified volatile material from the subsolar point of the comet for a perfectly absorbing nucleus at the distance R_o from the sun.
[c] τ_o is the timescale to lose 10% of the mass of a 10^{16}g comet nucleus with a density of 1 g cm^{-3} at the rate Z_o.
[d] N is equal to τ_o/P, where P is the orbital period corresponding to R_o.

is far from the sun, there is no coma and the surface energy balance (see *e.g.* Squyres *et al.*, 1985; McKay *et al.*, 1986) can be expressed as:

$$(1-A)\frac{S}{r^2} = \epsilon\sigma T^4 + P(T)L\left[\frac{\mu}{2\pi RT}\right]^{\frac{1}{2}} \qquad (1)$$

where S is the solar constant at 1 AU, r is the sun-comet distance, A is the nucleus albedo, ϵ is the emissivity, σ is the Stefan-Boltzmann constant, T is the surface temperature, $P(T)$ is the vapor pressure of the compound under consideration, L is the heat of vaporization, μ is the molecular weight and R is the gas constant. The last term in Eq. (1) represents the energy that is used to sublimate the nucleus material. Following Delsemme (1982) we define the stability criteria as that sun-comet distance at which the sublimation of a compound, exposed upon the surface, would require 2.5% of the mean incident solar flux. This distance is a rough measure of the point at which a volatile component of a nucleus would be lost to sublimation.

Vapor pressures for the compounds listed in Table 1 were computed using the following expression:

$$P = P_1 \exp\left(-\frac{\mu L}{R}\left[\frac{1}{T} - \frac{1}{T_1}\right]\right) \qquad (2)$$

where P_1 is the reference pressure (1 torr) and T_1 is the temperature that corresponds to that reference pressure. Table 1 lists the values of the heat of vaporization and the reference temperature for the compounds considered.

MAJOR CONCLUSIONS

Organic compounds listed in Table 1 are lost from the nucleus after ~ 200 orbits, independent of the distance at which they sublime. This is probably also true for other organic compounds not considered as part of this study and provides a useful rule for estimating loss of organics.

- Many volatile organic compounds are lost long before a comet reaches the inner solar system.
- Many of the organics are still retained to within a few AU and hence could be a component of the observed short period comets. ■

REFERENCES

Clark, B., L.W. Mason, and J. Kissel (1987) *Proceedings of the 20th ESLAB Symposium on the Exploration of Halley's Comet*, ESA SP-250.

Delsemme, A.H. (1982) in *Comets*, (L. Wilkening, ed.), pp 131-163, Univ. of Ariz. Press, Tucson, Arizona.

Keller, H.U. *et al.* (1986) *Nature, 321*, 320-326.

McKay, C.P., S.W. Squyres, and R.T. Reynolds (1986) *Icarus, 66*, 625-629.

Squyres, S.W., C.P. McKay, and R.T. Reynolds (1985) *JGR, 90*, 12381-12392.

POSSIBLE FORMATION OF CARBONATES IN ANCIENT LAKES IN THE VALLES MARINERIS, MARS

S. S. Nedell, C. P. McKay

Solar System Exploration Branch, Life Science Division, NASA/Ames Research Center, Moffett Field, California 94035

Scientific evidence from geologic, climatologic, and planetary formation studies suggest that the climate of early Mars may have been warm due to a thick carbon dioxide atmosphere, with liquid water at the surface, which is similar in many ways to primordial Earth. During this epoch, billions of years ago, the surface of Mars could have been conducive to the origin of life. The record of the origin and early evolution of life on Earth has been obscured by extensive surface activity. On Mars, however, large fractions of the surface date back to this early time period. Hence, it is possible that even if no life exists on Mars today, it holds the best record of the chemical and biological events that lead to the origin of life.

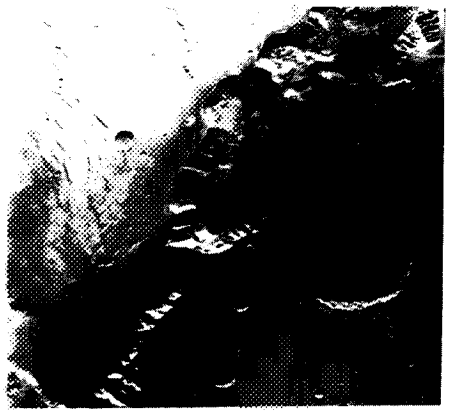

Figure 1. Hebes Chasma showing the central plateau of layered deposits. Many workers have suggested that these and similar deposits in the canyons to the south formed in lakes early in Mars' history.

One set of features that is particularly interesting from an exobiology perspective is the putative lake sediment on the floors of the equatorial canyons. The lakes that may have once filled these basins have been compared to the perennially ice-covered lakes in the Antarctic dry valleys, which are reservoirs of life in those cold deserts. In many of the Antarctic lakes there are copious amounts of calcite precipitation, and the presence of microbial mats accelerates this calcite formation. An interesting feature of these benthic mats is that they develop into modern, cold water stromatolites (1). Thus, identification of carbonates in the putative Martian paleolake deposits would imply that it might also be useful to search for microfossil remnants of an early Martian biosphere in the same deposits. We therefore examined the equatorial lake deposits on Mars as possible future targets for exobiologic investigations.

The canyons of Valles Marineris contain thick sequences of horizontally layered deposits. Recent mapping by Nedell *et al.* (2) shows that they form plateaus of rhythmically layered material whose bases are in the lowest elevations of the canyon floors, and whose tops are commonly within a few hundred meters of the surrounding plateaus. The greatest thickness of these deposits are found in the central canyons, which include Hebes (see Fig. 1), Ophir, Candor, and Melas chasmata. Several workers have suggested that the layered deposits were formed in lakes that existed in these depressions early in Mars' history (3,4,5). If standing bodies of water did exist in the Valles Marineris, they were almost certainly ice-covered in their later stages. Nedell *et al.* (2) suggested that sediment could have migrated through the ice cover by Rayleigh-Taylor instabilities or foundering, or entered by subaqueous volcanic eruptions on the lake floors. We suggest that a considerable fraction of these sediments could also be carbonate deposits precipitated in the lake water under conditions of high CO_2 atmospheric pressure.

Kahn (6) proposed that the formation of carbonate rocks due to chemical reactions in liquid water has continued over much of the lifetime of the planet, and consequently has limited the partial pressure of CO_2 to a value close to the triple point pressure of water (6.1 mbar). Pollack *el al.* (7) developed a detailed model for the formation of carbonates over an estimated timescale of tens of millions of years, which included the recycling of CO_2 by burial. A major problem with carbonate formation on early Mars is being able to maintain significant bodies of liquid water after the mean temperature falls below 273 K, which would occur when the atmospheric pressure drops below a few bars (7). Ice-covered lakes in the Valles Marineris could provide stable bodies of liquid water. The water in the lakes would still contain atmospheric gases carried in through groundwater flow, and possible melting of surface snowpacks (8).

Perennially frozen lakes represent, in many ways, the ideal environment for precipitating carbonate on the early Mars. Liquid water can remain in the lake long after the mean surface temperatures fall well below freezing (9), and snowmelt and groundwater flow into the lake would carry in CO_2 and cations leached from the adjacent rocks. The ions and gases would be concentrated in the lake water due to dissolution upon freezing. Thus the process of inflow of water, freezing, followed by ablation at the ice surface would concentrate gases and ions in the water column and enhance carbonate formation. This mechanism is known to operate in the Antarctic dry valley lakes where the relatively complete seal of the perennial ice covers results in supersaturated levels of dissolved gases. For example, Lake Hoare in Taylor Valley has ~ 300% more O_2 and ~ 160% more N_2 than would be at equilibrium with the atmosphere (10).

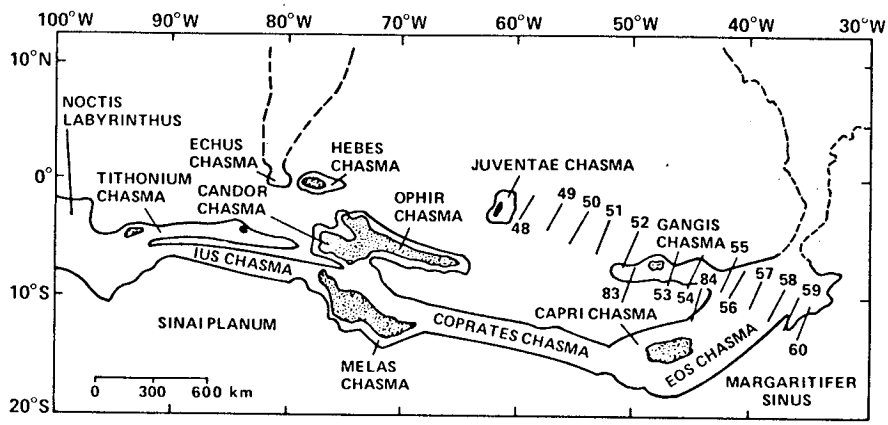

Figure 2. Location of all the Mariner 6/7 infrared spectrometer data that lie near the region of the Valles Marineris. Stippled areas mark the locations where layered deposits have been identified by Nedell et al. (1987). The record numbers correspond with those given in the dataset.

Carbonate precipitation could provide enough material to account for the layered deposits. If all the sedimentary material identified by Nedell *et al.* (2) in Coprates northwest quadrangle ($1.29 \times 10^5 km^3$) consisted of calcite with a bulk density of $2\ g\ cm^{-3}$, it would represent a total CO_2 amount equal to an atmospheric pressure of 30 mbar, which is not unreasonable for an early Mars atmosphere. Therefore, carbonate precipitation is an alternative to direct sedimentation of solid material.

We searched the Mariner 6/7 Infrared Spectrometer (IRS) dataset that lie in the region of the putative paleolakes in an attempt to identify a carbonate component in the deposits. These sixteen spectral footprints lie near Gangis Chasma (see Fig. 2). Spectra that lie on the surrounding uplands where there are no layered deposits were combined to obtain an average "background" spectral profile. About 25% of the remaining spectra overlie the canyons where layered deposits may exist. These "target" spectra were individually compared to the background spectra between wavelengths 1.9 to 6.0μm. Any material present in the target spectra and not present in the background spectra would be detected. Material equally present in both spectra would not be determined by this method. We found that there does not appear to be significant differences between the target spectra and the background spectra. No evidence for carbonates was found in any of the spectra that overlie the layered deposits. However, there are serious limitations in the coverage of this dataset. The vast majority of the layered deposits lie in the central canyons, to the west of Gangis Chasma. Furthermore, a relatively thin eolian mantle could obscure any underlying carbonate material.

We feel that the canyon deposits are still a prime site for future searches for carbonates on Mars, and that extensive coverage of the Valles Marineris by the Mars Observer could reveal the presence of carbonates in regions where surface weathering has exposed fresh material. Future studies of this primordial Martian sediment could yield detailed information on past Martian organisms and the processes instrumental for the origin of life. ■

REFERENCES:

1. Wharton, R.A., Jr., Parker, B.C., Simmons, G.M., Jr. (1983) *Phycologia, 22*, 355-365.
2. Nedell, S.S., Squyres, S.W., and Andersen, D.W. (1987) *Icarus*, in press.
3. McCauley, J.J. (1978) *USGS Misc. Inv. Series Map I- 897.*
4. Lucchitta, B.K. and Ferguson, H.M. (1983) *JGR, 88*, 553-568.
5. Carr, M.H. (1986) *Icarus, 68*, 187-216.
6. Kahn, R. (1985) *Icarus, 62*, 175-190.
7. Pollack, J.B. and Kasting, J.F. (1987), *Icarus*, in press.
8. Clow, G.D. (1987) submitted to *Icarus* 9. McKay, C.P., Clow, G.D., Wharton, R.A., and Squyres, S.W. (1985) *Nature, 313*, 561-562.
10. Wharton, R.A., Jr., McKay, C.P., Mancinelli, R.L., and Simmons, G.M., Jr. (1987) *Nature*, in press.

EXOBIOLOGY SITE SELECTION FOR FUTURE MARS MISSIONS: MARTIAN PALEOLAKE SEDIMENTS AND TERRESTRIAL ANALOGS

R. A. Wharton, Jr.[1], C. P. McKay[2]
[1]*Desert Research Institute, Atmospheric Sciences Center, P. O. Box 60220, Reno, Nevada 89506;* [2]*Solar System Exploration Branch, Mail Stop 239-12, NASA/Ames Research Center, Moffett Field, California 94035*

There is a confluence of scientific evidence from geology, climatology, and planetary studies which suggests that in the past, conditions on Mars were quite different from what they are today. Four billion years ago the surface of Mars could have been conducive to the origin of life (1. McKay, C.P. Exobiology and future Mars missions: the search for Mars' earliest biosphere. submitted to *J. Adv. Space Res.*). Photogeological evidence from high-resolution Viking images suggests that sediments in the equatorial Valles Marineris canyon system on Mars were deposited in lakes which were probably ice-covered (2. Nedell, S.S., Squyres, S.W., and Andersen, D.W. Origin and evolution of the layered deposits in the Valles Marineris, Mars. *Icarus:in press.*). These sediments could contain chemical, isotopic or actual fossil evidence of ancient martian life. The only terrestrial analog of ancient ice-covered martian lakes are the perennially ice-covered lakes of Antarctica.

The goal of our research is to develop the scientific framework for the exobiological study of sediments on Mars and to motivate the selection of these sediment beds as sites of future Mars missions, such as the Mars Network or Sample Return Missions. To this end, we are studying perennially ice-covered Antarctic lakes in order to develop quantitative models that relate the environmental factors to the nature of the biological community and the sediment forming processes. We are currently identifying the key chemical signatures in the sediments that preserve information on the nature of the environment and the biological community. The models which we are developing for the Antarctic lakes will be applied to the Mars paleolakes to establish the scientific rationale for the exobiological study of ancient martian sediments. In addition, the information gained from our Antarctic experiences will be utilized to aid in the conceptual design of instruments/experiments for *in situ* analysis of martian sediments.

Using data from perennially ice-covered Antarctic lakes, we have developed a model for determining the thickness of ice on perennially ice-covered lakes and applied this model to Mars paleolakes (3. McKay, C.P., Clow, G., Wharton, R.A., Jr., and Squyres, S.W. 1985. The thickness of ice on perennially frozen lakes. *Nature* 313:561-562.). Ice cover thickness on the equatorial lakes could be as low as 65 m under the present martian equatorial climate, assuming an ablation rate of 10 cm/yr. The ice covers on the martian paleolakes were probably thinner as a result of warmer temperatures on early Mars and relatively higher ablation rates due to downslope winds along the canyon walls (1).

An important feature of an ice cover is its capacity to thermally buffer the underlying water from the relatively cold external temperature (4. Wharton, R.A., Jr., Simmons, G.M., Jr., and McKay, C.P. Lake Hoare, southern Victoria Land, Antarctica: an analog of the past, a prolog of the future. submitted to *Hydrobiologia.*). The mean annual temperature in the Antarctic dry valleys is -20°C, yet the water in an ice-covered lake does not drop below freezing except at the ice/water interface. Consequently, microorganisms are capable of thriving in these thermally stable lakes in spite of the cold external environment. Similarly, it is possible that ice-covered lakes on early Mars provided a relatively warm, liquid water environment for early martian biota.

The relatively complete seal of a perennial ice cover on a lake is reflected in the gases dissolved in the water. For example, we have shown that Lake Hoare, Antarctica has *ca.* 300% more oxygen and *ca.* 160% more nitrogen than would be at equilibrium with the atmosphere (5. Wharton, R.A., Jr., McKay, C.P., Simmons, G.M., Jr., and Parker, B.C. 1986. Oxygen budget of a perennially ice-covered Antarctic lake. *Limnol. Oceanogr.* 31:437-443. 6. Wharton, R.A., Jr., McKay, C.P., Mancinelli, R.M., and Simmons, G.M., Jr. 1987. Perennial nitrogen supersaturation in an Antarctic lake. *Nature* 325:343-345.). Both biological and abiological processes contribute to the enhanced gas concentrations. Sedimentation and loss through the ice cover of organic carbon represent a biological source of oxygen. Also, the incoming

meltstream carries air in solution into the lake which is concentrated when the water freezes to the bottom of the ice cover. We have shown that both processes are effective in controlling the gas concentration in the lake water. These concentration mechanisms may have operated in the ice-covered martian paleolakes, possibly enhancing the concentrations of biologically important gases (*e.g.* nitrogen) from a thin martian atmosphere.

It is possible that a considerable fraction of the martian paleolake sediments could be carbonate deposits precipitated in Lake water under conditions of high atmospheric pressures of carbon dioxide (7. McKay, C.P. and Nedell, S.S. Are there carbonate deposits in the Valles Marineris, Mars? submitted to *Icarus*). Perennially ice-covered lakes represent an ideal environment for precipitating carbonate in the early Mars. Liquid water can remain in an ice-covered lake long after the mean surface temperature falls well below freezing. Groundwater flow into these lakes would carry in carbon dioxide and cations leached from the adjacent rocks. As suggested above, the gases and ions that enter the lake would be concentrated in the lake water due to dissolution upon freezing. Thus, the process of inflow of water, then freezing at the ice/water interface, followed by ablation at the ice surface would concentrate gases and ions in the water column and enhance carbonate formation.

A major focus of our research for the next several years is to document and model the carbon/carbonate budget of an Antarctic lake in order to apply this information to the martian paleolakes. Our studies will include an analysis of the stratigraphy of sediment cores, including the distribution of organic carbon and carbonates. We will also be looking at the nature of gases trapped within the crystalline carbonate structure. We will continue our modeling effort to determine the factors that control the environment within the lake and their dependence on the ice-cover and microbial activity. Using this information, we intend to establish a scientific framework for the study of sediments on Mars and to motivate the selection of these sediment beds as sites for future Mars missions. ■

PAGE 372 INTENTIONALLY BLANK

PRECEDING PAGE BLANK NOT FILMED

REAL TIME DATA ACQUISITION AND PROCESSING FOR FIELD TESTS OF THE PROTOTYPE SETI MCSA

P.R. Backus[1], D.G. Harper[1], and J.C. Jordan[2]
[1]*The SETI Institute, Los Altos, California 94022 and* [2]*Sterling Software, 1121 San Antonio Road, Palo Alto, California 94303*

The Search for Extraterrestrial Intelligence (SETI) presents a unique challenge for data acquisition and analysis. During the proposed Microwave Observing Project each MultiChannel Spectrum Analyzer (MCSA) system will process more than 60 million bytes of information every second. In order to keep up with this data rate, the data must be processed in real time. This processing involves a number of stages including the removal of the spectrum baseline variations, excision of radio frequency interference (RFI), thresholding the data for pulse detection, and compression of the data for archival storage. The performance of the system must be monitored to assure the maximum sensitivity and most efficient use of observing resources.

As part of the SETI Research and Development Program, a prototype data acquisition system has been developed. This system, the Virtual Emulation for Rendezvous and Acquisition (VERA), is implemented as a set of virtually concurrent, communicating software processes. Coordination of the activities of these processes and monitoring of system performance are accomplished through a supervisor process. This software architecture has provided a flexible environment for conducting field tests of the prototype MCSA and software implementations of signal detection algorithms. It also serves as a model for the multiprocessor MCSA system that is planned for the Microwave Observing Project.

The observational phase of the SETI MOP will span from five to seven years and will use existing DSN and national telescope facilities. In order to use the available telescope time most efficiently with the least amount of retraining of SETI observers, the VERA system will present a site-independent user interface. This is possible because the basic observation control logic is contained in one process in the VERA system. This process communicates with the observatory's control computer through a site-specific interface process. This minimizes the burden on the observer and allows the VERA system to follow equipment changes and upgrades at each observatory without impacting the other SETI MCSA observing systems.

In order to effectively conduct the search in an environment with unknown and unpredictable RFI, an independent, relatively narrow band spectrum analyzer will be part of the observing system. This RFI Subsystem will be controlled by its own computer with an "expert system" and RFI database. The expert system will attempt to identify signals detected by the small spectrum analyzer with known sources of RFI in the database. It will communicate its findings to the main SETI control computer so that channels contaminated with interference may be eliminated from further processing.

A second expert system will monitor overall system performance with the goal of achieving as close to maximum sensitivity as possible with the minimum contamination by RFI. This system will have to dynamically reschedule observations based on real time experience with RFI and equipment performance.

Results of the field tests with VERA at the Goldstone tracking station will be discussed. Preliminary plans for the next generation of real time acquisition and control software for the NASA SETI observing system will be presented. ■

NEW INSTRUMENTATION FOR SETI

J.B. Burr, I.R. Linscott, and A.M. Peterson
Center for Radar Astronomy, Stanford University, Stanford, California 94035

A new generation of instrumentation is being developed to perform spectral analysis and pattern detection for SETI. This activity includes design, packaging, and testing of multichip, multiboard systems based on a mixture of commercial and custom VLSI components.

The MCSA was designed to be extended to 10 MHz through subsystem replication. Its most frequently used component is the DFT Processor board, which has been redesigned as a custom VLSI chip called the SETI DSP Engine.

The chip is five times faster and requires one eighth the space of the board it replaces. It achieves an effective computation rate of 80 million 16 bit fixed point operations per second, executing a 1040 point Fourier Transform in 630 microseconds.

Mainly as a result of the SETI DSP Engine, the new MCSA will have one twelfth the number of circuit boards originally projected.

Architectures based on custom VLSI are also under development which implement algorithms to detect pulse trains and drifting cw signals embedded in the noise background. ■

ANTENNAS AND RECEIVING SYSTEMS FOR THE SETI MICROWAVE OBSERVING PROJECT

R. B. Crow, M. J. Klein, S. Gulkis and C. F. Foster
Jet Propulsion Laboratory, California Institute of Technology, Pasadena, California 91109

The NASA SETI program plans to use existing radio telescope facilities to carry out the Microwave Observing Project. The special purpose signal processing systems developed for SETI are designed for use at a variety of observatory sites to take advantage of the unique capabilities of each site. For example, the prime candidate to meet the high sensitivity requirement of the Targeted Search is the world's largest microwave antenna, the 300-meter diameter radio telescope at Arecibo, Puerto Rico, which is operated by the National Astronomy and Ionospheric Center. The large antennas and sensitive receiving systems of the NASA Deep Space Network (DSN) will be the primary sites for the Sky Survey component of the project. The DSN complex in Australia will play a key role to complete the Sky Survey in the southern sky and the 70-m antenna located there will be used to observe targeted stars too far south to be visible from Arecibo. Radio observatories in other countries will be invited to participate in the search. Interest has already been expressed by researchers in Australia and France.

To take maximum advantage of these several radio telescopes, SETI will provide an equipment package that will connect directly to the antenna feeds. This equipment will provide for the broadband low noise amplifiers, RF to baseband conversion, spectrum analysis and special signal processing equipment. The equipment will be capable of connecting to the controls of the radio telescope so that automated searches will be possible. This equipment will provide consistent instrumentation and easy integration.

A primary objective of both the Targeted Search and the Sky Survey is to optimize the sensitivity of each system to detect very weak, narrow band signals. Because the search will be conducted in frequency bands already used for terrestrial communication purposes, the SETI detection system must be able to discriminate between candidate signals of extraterrestrial origin from the multitude of signals transmitted on earth and from orbiting satellites. These terrestrial signals, which are likely to possess some of the characteristics that the SETI system is designed to detect, will interfere with the SETI

search process. If the interfering signals are strong and cannot be circumvented by careful scheduling, certain frequency bands and some parts of the sky will be lost to the search. The impact of radio frequency interference (RFI) on SETI is being studied. Results indicate that the RFI problem is serious now, that it will most likely become a greater problem in the future, and that it is important to begin the search as soon as possible before the RFI problem gets any worse. ■

DEVELOPMENTS IN SIGNAL PROCESSING STRATEGY FOR THE NASA ALL SKY SURVEY

W. T. Deich, E. T. Olsen, and R. A. Brady
Jet Propulsion Laboratory, Pasadena, California 91109

The NASA SETI (Search for Extraterrestrial Intelligence) All Sky Survey is expected to search the entire celestial sphere for narrowband signals throughout the terrestrial microwave window (1GHz to 10 GHz) over the period of a few years. The problems which must be solved to achieve this goal are distinct from those presented by other strategies for SETI. The sky is divided into a patchwork quilt, each element of which can be observed in a few hours by rapidly scanning the radio telescope beam. During the time in which the beam moves a small fraction of its width across the sky, spectral data from each beam area must be analyzed for the presence of narrowband signals, which are stored for confirmation and reobservation. A key issue is the identification and removal of signals which are due to radio frequency interference (RFI) generated by terrestrial intelligence.

The focus of the sky survey development effort at the Jet Propulsion Laboratory is the construction of a prototype sky survey system known as the Engineering Development Model (EDM). This prototype two-million channel signal processor will be ready for field tests in mid-1989 and will provide the functionality required to test and verify the observation and signal detection strategies to be employed in the all Sky Survey. ■

STRATEGIES FOR THE DETECTION AND STUDY OF INTERMITTENT EXTRATERRESTRIAL RADIO SIGNALS

R. S. Dixon and J. L. Bolinger
The Ohio State University Radio Observatory, 2015 Neil Avenue, Columbus, Ohio 43210

INTRODUCTION AND PHILOSOPHICAL BACKGROUND

It is desirable that man be aware in detail of all electromagnetic (and other) radiation arriving at the earth, so that we may better understand the extraterrestrial environment. Unfortunately, technological and financial constraints limit our knowledge of this radiation to only a tiny fraction of that which arrives. It is not possible today to monitor all wavelengths in all directions at all times with a useful degree of sensitivity. Virtually all astronomical observations are of an extreme generalized telephoto type, restricted to a relatively tiny wavelength range, a relatively tiny portion of the sky, and a relatively tiny time period. The trade off however, is that great sensitivity is obtained.

Of the various observation dimensions, time is generally the most restricted. Time-varying and intermittent phenomena are of great interest, yet are often discovered only accidentally or incidentally (pulsars, distant supernovae, aperiodic comets, etc.). Astronomical instruments are typically designed and administered for short-term observations, thereby decreasing the likelihood of discovering intermittent phenomena. As technology improves, it is important to relax the restrictions on the

TABLE 1. OSU Radio Cameras

Current Status	Mark I Under construction	Mark II In planning stage	Mark III In thinking stage
Date of Operation	1987	1988-89	1989-90
Picture Dimensions	1	2	2
Frequency	162.4 MHz	3.7-4.2 GHz	1-2 GHz
Bandwidth	10 kHz	500 MHz	1 GHz
Elements	$\lambda/4$ monopole	horn	multifilar helix
Array	8 elements on .95λ diameter circle	16-64 elements or arms of spiral	?
Polarization	Vertical	Linear	Dual circular
Receivers	Ham-type	Home TV dish-type	Broadband GASFET
Known detectable	Weather stations	TV Satellites and continuum radio sources	Many

observation dimensions and move toward more generalized wide angle methods. Two such approaches being implemented now at Ohio State University are described below.

AN ADAPTIVE TELEPHOTO APPROACH

For the past 14 years, the Ohio State University Radio Telescope (53m equivalent diameter) has been dedicated to a sky survey for narrow band extraterrestrial radio signals, in the vicinity of the Hydrogen Line at 1420 MHz, with the idea that such signals might be transmitted by other civilizations. A 500-KHz-wide-band is examined at any instant of time, and the center of the band is continuously doppler-corrected to track the hydrogen frequency with respect to the galactic standard of rest. Although many signals have been detected in the survey, none have ever been present when reobservations were made days or months later. Almost all current and planned SETI programs (NASA, Harvard, OSU) are of the automated survey type, and highly telephoto. The microwave frequency range and the sky are basically combed very slowly and systematically for relatively narrowband signals. If a signal should be present at any time other than its frequency and direction are being examined, it will not be detected, even though it could be very strong. This strategy is forced primarily by technological constraints, but is nevertheless the best starting point.

In an attempt to learn more about intermittent signals and reduce the degree of telephotoness, the OSU program is being improved and modified in several ways. The most fundamental change involves changing from the continuous survey mode to an adaptive mode in both the time and frequency domains. Previously the telescope would simply record the frequency, intensity, and sky positions of any signals detected, with a constant receiver bandwidth, and continue on with the survey at a constant rate. The new strategy will temporarily stop the survey whenever a signal is detected, track that sky position for a 1- to 2-hour period of detailed immediate study, narrow the receiver bandwidth by a factor of 10 to more precisely determine the signal frequency, activate more detailed data analysis algorithms, and make audio recordings of the signal as detected by a variety of methods (AM, FM, SSB, CW). The philosophy here is that it is more profitable to spend time immediately studying a signal that is present, than to continue searching for other signals that are only rarely present.

In addition, the survey bandwidth is being expanded from 500 KHz to 300 MHz, to cover the entire Water Hole region. An intentional trade off is being made to increase the frequency coverage at the expense of sensitivity to weak signals.

A WIDE ANGLE RADIO CAMERA APPROACH

It is well known that an array of small antenna elements can be phased together to create an antenna beam comparable to that of a single large antenna of equivalent total size, and that beam may be electronically scanned rapidly to any desired direction. Less well known is the fact that the outputs of the antenna elements can be processed so as to create all beam positions simultaneously, providing a

continuous image of the entire field of view of the antenna. Such an array has the same sensitivity as a single large antenna, but eliminates the need to scan and hence can see the entire sky at once.

A sequence of successively more capable radio cameras is being designed and constructed now to illustrate the principle and investigate the practical problems involved in their use. The beam-forming operation is computer intensive, but rapid advances in computer technology are bringing the day of a large radio camera closer to reality. Table 1 summarizes the current cameras under consideration. ■

OPTIMIZATION OF SETI'S TARGETED SEARCH SIGNAL DETECTORS

D. G. Harper and D. K. Cullers
The SETI Institute, Los Altos, California 94022

As part of NASA's studies into the question of life in the universe, the SETI project is designing a computer system that will conduct, with a high degree of automation, a search for evidence of other technological civilizations in the galactic neighborhood. The task involves observing approximately 1000 stars, each over 2 gigahz bandwidth at 10 million Hz per observation. This requires 200,000 observations, 1000 seconds at a time. The currently planned search procedure will generate 60e9 words of data in each observation.

Thus the success of SETI's ambitious search for nonhuman artificial radio signals depends on use of leading edge computer hardware and very efficient data processing algorithms. The software group of the SETI Institute has designed economical, high speed logic that when implemented in hardware will detect these signals in real time. The sensitivity of the pulse train detector is within 1 dB of the optimal coherent case. This was accomplished by discovering a number of design optimization techniques over the past two years that have yielded: in continuous signal detection, a 40-fold increase in computation efficiency, in pulse train detection, more than 1000-fold reduction in memory requirements, and approximately 200-fold increase in computation efficiency.

Besides speed and memory-use improvements, these detectors provide a number of other attractive features. They are online data processors. This is important to facilitating signal verification procedures and eliminating storage requirements for raw data. The pulse train detector has the flexibility of being programmed to run any of the proposed detection algorithms. The data flow can be adjusted by the operator, or automatically, during the observations, to increase or decrease the computation load in response to changing noise and RFI conditions. The designs also have a build-in redundancy for discovering the characteristic patterns. This aids the automatic signal verification processes.

A brief overview of the general SETI system is provided to show how the signal detectors fit in and complement the other stages of data processing. ■

THE SEARCH FOR EXTRATERRESTRIAL INTELLIGENCE MICROWAVE OBSERVING PROJECT

H. W. Jones[1] B. M. Oliver[1], M. J. Klein[2], J. C. Tarter[3], and P. R. Backus[3]
[1]SETI Office, N229-8, NASA/Ames Research Center, Moffett Field, California 94035, [2]Space Physics and Astrophysics, 264-802, Jet Propulsion Laboratory, Pasadena, California 91109, and [3]SETI Institute, N229-8, NASA/Ames Research Center, Moffett Field, California 94035

INTRODUCTION

The Search for Extraterrestrial Intelligence (SETI) will gather data concerning one of the most interesting and fundamental questions ever posed, "Is there intelligent life elsewhere in the universe?"

Current scientific thought overwhelmingly indicates that there is extraterrestrial intelligent life, and public opinion is strongly in agreement.

The SETI Microwave Observing Project is an element of the Exobiology Program being managed by the Life Sciences Division of the Office of Space Science and Applications at NASA Headquarters. The Microwave Observing Project is the only practical and logically justified approach to gathering data on this question, which has unequaled importance for science. In addition, the SETI Project will develop new signal processing technology and acquire significant radio astronomy data.

The first serious proposal for SETI was made in 1959, by Cocconi and Morrison, and many scientific studies have followed. SETI has been recommended by several Science Advisory Groups, most recently the National Commission on Space, chaired by Thomas O. Paine. The SETI Science Working Group was established in 1980 and meets regularly to assess SETI ideas and progress, and to critique planning.

Many studies have come to the conclusion that electromagnetic radiation is the most efficient means for interstellar signaling, since radio waves travel at the speed of light and consist of low energy photons. In all the electromagnetic frequency range, the microwave frequencies between roughly 1 and 10 GHz are easiest to detect because the background noise is least.

The SETI Microwave Observing Project will search for microwave transmissions of intelligent origin using two complementary approaches, a Targeted Search of nearby solar-type stars and a complete Sky Survey. The Targeted Search will be carried out by Ames Research Center (ARC), and the Sky Survey will be carried out by the Jet Propulsion Laboratory (JPL). The Microwave Observing Project has developed out of a continuing SETI R&D effort.

TARGETED SEARCH

The Targeted Search will examine all known solar-type stars within 80 light years of earth (nearly 800 stars) in the 1 to 3 GHz band, with a frequency resolution of 1 Hz. A unique wide bandwidth Multichannel Spectral Analyzer (MCSA) will be developed and deployed at several existing radio astronomy observatories with very large antennas. An automatic data analysis subsystem will detect the presence of fixed-frequency or drifting continuous wave (CW) signals or sequences of pulses. Particular emphasis will be placed on solar-type stars within 20 light years of earth, because civilizations on planets circling those stars may have already detected our television signals and sent a response that could be reaching earth now.

The Targeted Search sensitivity is comparable to that of the most sensitive past search, but it will increase the number of nearby solar type-stars examined by a factor of four. Past searches have been restricted to a limited number of fixed-frequency, continuous wave signals in narrow bandwidths of a few kHz. The Targeted Search will examine a 2 GHz microwave bandwidth, using bandwidths as small as 1 Hz, and will detect continuous or pulse signals, either fixed in frequency or drifting at rates produced by celestial acceleration.

SKY SURVEY

The Sky Survey will search the entire sky between 1 and 10 GHz with resolution of 30 Hz. A very wide bandwidth spectrum analyzer will be deployed at one northern hemisphere site and one southern hemisphere site of the Deep Space Network (DSN). An automatic pattern recognition system will detect fixed or slowly drifting continuous signals. The entire sky will be examined in a systematic way.

The Sky Survey will be 300 times more sensitive than previous surveys, and will be the most detailed survey to examine the entire sky systematically. Past surveys have covered less than 1 Mhz; the Sky Survey will cover 9 GHz, examining 300 Mhz on each scan.

The observation systems for the Targeted Search and the Sky Survey are similar in concept. Both consist of an antenna, a microwave subsystem, a multichannel spectrum analyzer, a signal processor, a control subsystem, and a radio frequency interference subsystem.

OPERATIONS

Principal Investigators (PI's) will be invited to propose to participate in the execution of the Microwave Observing Project, or in other uses of the SETI observing system. An Investigators Working Group will review SETI plans and progress to insure that the scientific goals and objectives of the Microwave Observing Project are met.

The SETI observation systems will be deployed, operated, and maintained at several observing sites. The Targeted Search will use astronomical observatories, such as those at Arecibo, Green Bank, and

Ohio State, by arrangement with their managing institutions. The Sky Survey will use Deep Space Network sites, under the management of NASA's Office of Space Operations. Data analysis will be automated, and only very limited archival data will be maintained, except for the Sky Survey radio source data. ■

Supplementary Abstracts

PARTITIONING OF ORGANIC ASSIMILATES IN A STRESSED CYANOBACTERIUM

L. E. Shubert
NASA/Ames Research Center, Moffett Field, California 94035 and Department of Biology, University of North Dakota, Grand Forks, North Dakota 58202

Photosynthetic organisms that are cultured in environmentally stressed conditions exhibit physiological and biochemical adaptations. These alternative pathways change the nutritional quality of these autotrophic organisms. Since photoautotrophs are components of a bioregenerative system, organic partitioning is relevant to the Controlled Ecological Life Support System (CELSS).

An axenic culture of *Spirulina platensis* Nordst. Geitl. (UTEX 2340) was cultured in a 14 L fermenter, and monitored for pH, temperature, DO, nutrient flux, chlorophyll *a*, phycobilins, and C-H-N. Aliquots of cells were decolorized with DMSO and analyzed for protein (Lowry method), carbohydrates (phenol-sulfuric acid method), lipids (chloroform:methanol method), and nucleic acids (diphenylamine reaction method).

Results of experiments demonstrating shifts in the ratios of protein:carbohydrate:lipid:nucleic acid in *S. platensis* when stressed with high light (>100 μEm-2s-1), high salt (>0.05M Na), or a nitrogen deficiency will be discussed. Specific effects on metabolism due to environmental stress will be described. Studies such as these may provide a "model" for evaluating the potential of algal species as candidates for CELSS based on their nutritional qualities and growth characteristics. ■

OPTIMIZATION OF GROWTH FOR CELSS

J. D. Goeschl[1], C. E. Magnuson[1], Y. Fares[1], C. J. McKinney[1], C. H. Jaeger[1], H. W. Scheld[1] and R. D. MacElroy[2]
[1]PhytoResource Research, Inc., College Station, Texas 77840 and [2]NASA/Ames Research Center, Moffett Field, California 94035

The design of facilities and selection of plant species and genotypes for growth in space habitats can take a number of possible directions. One approach is to assume that plant growth conditions will be dictated by existing space habitat design constraints (*i.e.,* atmospheric pressures, gas composition, water supply, temperatures, habitat volume, *etc.*) A second approach would be to examine the range of possible operating conditions for plants and humans to set new design criteria, perhaps radically different from present designs, but which would be optimal for habitats which are larger, simpler, and/or less power consuming.

The research reported here is designed to examine plant responses to environmental inputs in order to optimize either of the above approaches. Specifically the underlying physiological basis for plant responses to temperature, humidity, CO_2, O_2, pollutants, and other environmental inputs can be measured and expressed quantitatively (*i.e.,* in the sense of systems engineering principals). Thus plants can be selected for specific conditions, or environmental conditions can be specified to optimize plant performance.

The experimental technology consists of an integrated, computer driven instrumentation system which simultaneously measures several physiological parameters in live, intact plants (Figure 1). The key technical feature is application of a square wave pulse of a short lived isotope labelled molecule (*e.g.* $^{11}CO_2$ or $^{13}N_2$) in a unique "Extended Square Wave" (ESW) pattern with kinetic analysis of tracer-metabolite transport within the plant. These tracer techniques capitalize on the tissue penetrating

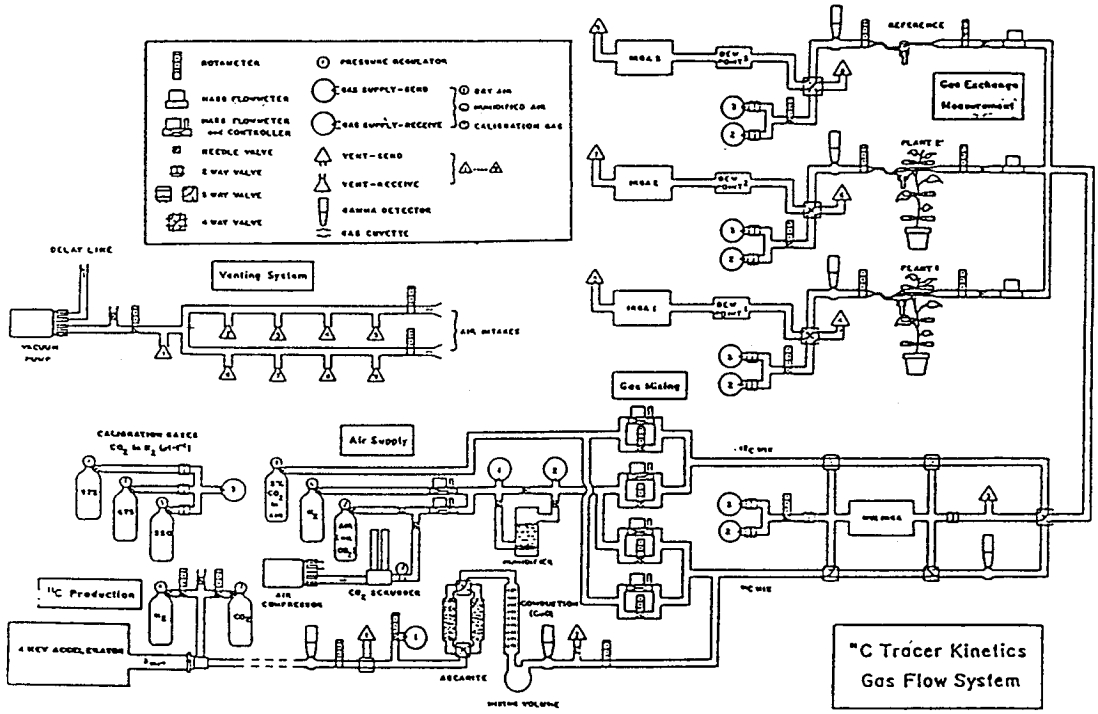

Figure 1. Schematic of the existing ^{11}C system. Lower left - beam line and target chamber; Lower center - chemical processing system; center - gas mixing and measurement; Upper right - plants with leaf chambers and detectors. (Electronics and computer are not shown); Upper center - output gas measurement and calibration system.

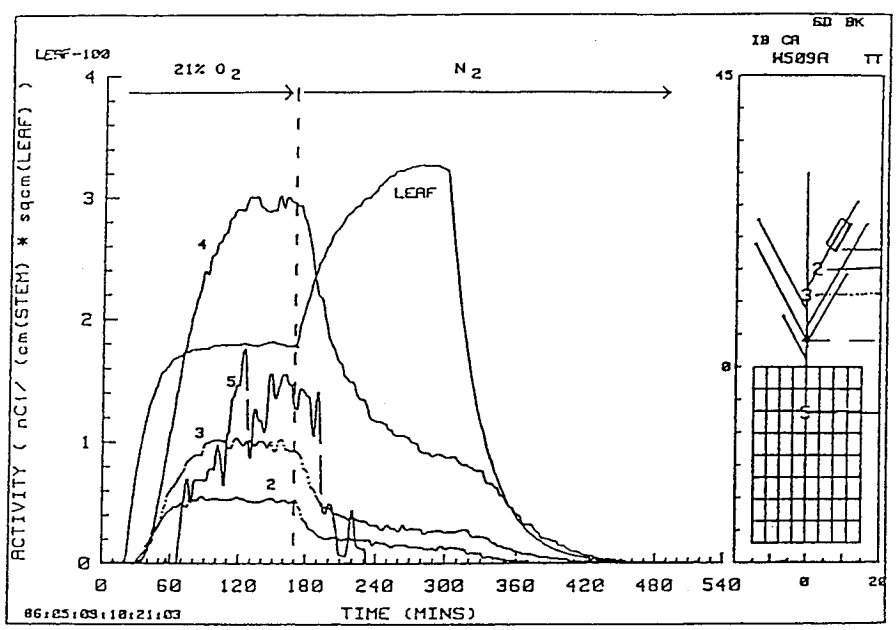

Figure 2. Levels of ^{11}C activity at different positions on the wheat plant shown in the diagram, before and during a change in O_2 concentration from 21% to 0%. Note that activity in the labelled portion of the leaf (LEAF) increased as O_2 was removed, partly because CER increased and partly because of an increase in the rate of photosynthate storage. The concurrent decrease in the rate of photosynthate export from the leaf resulted in a decline in ^{11}C activity at detector positions 2 (region of the leaf basipetal to the labelled area), 3 (leaf sheath), 4 (stem tissue where much of the recent photosynthate appears to be stored) and 5 (roots). These data are smoothed (see SD in upper right corner) and corrected for background (BK) induced background (IB) detector calibration (CA) and mean transit time of the ^{11}C tracer to each detector location (TT). The designation W509A refers to the file on which data is stored, and indicates that the experiment was conducted on wheat on 5/9/86 in the "A" position of the ^{11}C apparatus.

capability of high energy gamma emissions to measure the level and rate of flow of photosynthetic products in real time as plants are subjected to various environmental manipulations, especially the absolute and partial pressures of atmospheric gases. The physiological parameters measured include:

1. Leaf Temperature
2. Transpiration
3. Carbon exchange rate
4. Photosynthate Storage Rate
5. Photosynthate Export Rate (*i.e.,* phloem loading)
6. Export pool size
7. Transport speed
8. Relative Concentration of transported products
9. Unloading rate into metabolic sinks (*e.g.* roots, stems, fruit, immature leaves).

Results will be presented showing; a) the minute by minute responses time of these parameters in response to step changes in atmospheric gas concentration (Figure 2), b) the long term adaptation of plants to the same environmental factors, and c) the genetically determined differences of plant cultivars (*e.g.* wheat cultivars) as measured under given environmental conditions.

The goal is to express these parameters in a manner similar to that used in systems engineering so that selection of plants and design of growth conditions can be accomplished in a manner consistent with other aspects of space hardware design, construction, and testing. ■

LOW COST MODULAR HARDWARE FOR SUPPORT OF BIOSCIENCE INVESTIGATIONS

H. W. Scheld[1], J. W. Magnuson[1], R. R. Scruby[1], C. E. Magnuson[1], R. L. Sauer[2], D. R. Morrison[2] and A. D. Krikorian[3]

[1]PhytoResource Research, Inc., College Station, Texas 77840, [2]NASA/Johnson Space Center, Houston, Texas 77058, and [3]Department of Biochemistry, State University of New York, Stony Brook, New York 11794

The development of flight experiments to probe basic gravitational biology has suffered from the chicken vs. egg syndrome: design of an effective experiment is best accomplished when something is known about the nature and possibilities of the apparatus which will be available, while according to NASA science experiment support rules, equipment cannot be developed until there is a specific experiment that requires it. There is inadequate recognition of the difficulties inherent in designing biological test apparatus for space experimentation, and particularly in the case of flight experiments, there has been a failure to recognize that the effort to develop adequate hardware is, in itself, an experiment because of the many unknowns with regard to the interaction of the organism and the space environment and of the organism and the hardware.

This investigation was undertaken in the development of a series of modular small flight instruments which are designed to support a variety of inflight experiments with small plants and tissue or cell cultures. Sheet metal containers sized to the Shuttle Mid-deck locker and half locker dimensions as well as a framework support for unmanned flight apparatus have been designed with a variety of internal fixtures to allow support of several different experimental hardware items. Hardware items designed to be used within the support containers include a series of modular Lexan chambers configured to support a variety of seed germination and small plant growth experiments. These incorporate the capability for aeration as well as for thermal environment control of the experimental materials through the use of water or air jackets. A color schlieren optics system mounted on an optical breadboard is being designed for use in studies of the effect of the non-convective micro-g environment upon heat and gas exchange between plant leaves and the surrounding atmosphere. ■

DEVELOPMENT OF AN IN-SUIT DOPPLER BUBBLE DETECTOR

M. Macecek
Techno Scientific Inc., 60 Caster Avenue, Woodbridge, Ontario L4L 4X2, Canada

Prevention of decompression sickness can be accomplished by the development of effective procedures and proper monitoring of subjects using an ultrasonic precordial bubble detector (UPBD). This is especially applicable for the preparation of crews for extravehicular activities (EVA).

The methodology is based on acoustical monitoring of intracardial gas bubbles by the precordial Doppler ultrasound technique, and recording on a tape recorder. A technician or the subject himself holds the ultrasonic transducer in the precordial area. The presence of bubbles is revealed by the swishing or higher frequency chirping sound during systole. While the technique is subjective, experiments show an excellent agreement between data obtained by trained technicians.

The unit uses continuous wave (CW) Doppler monitoring of gas bubbles. Doppler frequency shift is directly proportional to reflector velocity.

The main challenge of an in-suit Doppler monitor is the need for completely remote operation, maintenance of acoustical coupling, and data collection capability for periods of up to 14 hours. In addition, accommodation must be made for movement of internal organs in a zero G environment.

This project is supported by NASA contract No. NAS9 17697, with Mr. Dave of Horrigan of JSC Houston as Technical Monitor. ■

Adams, J.D. POSTER: SPACE BIOMEDICINE; 59
Albee, A.L. EXOBIOLOGY-IV; 355
Albertine, K.H. DECOMPRESSION SICKNESS; 153
Alberts, J.R. LIFE SCIENCE AND THE SPACE STATION; 240
Alkon, D.L. POSTER: SPACE BIOMEDICINE; 98
Ambrosia, V.G. POSTER: BIOSPHERICS; 2
Arnaud, S.B. POSTER: SPACE BIOMEDICINE; 114
Arnaud, S.B. CALCIUM AND BONE PHYSIOLOGY-II; 226
Arnaud, S.B. POSTER: SPACE BIOMEDICINE; 59
Arnett, K. BIOMASS PRODUCTION-II; 256
Arrhenius, G. EXOBIOLOGY-I; 260
Arrott, A.P. NEUROSCIENCE-II; 218
Aufdemorte, T.B. POSTER: SPACE BIOMEDICINE; 88
Babij, P. MUSCULOSKELETAL SYSTEM; 160
Backus, P.R. EXOBIOLOGY-VI; 378
Backus, P.R. EXOBIOLOGY-VI; 382
Badler, N.I. HUMAN FACTORS-I; 288
Bain, J.L.W. MUSCULOSKELETAL SYSTEM; 163
Baldwin, K.M. POSTER: SPACE BIOLOGY; 57
Banin, A. POSTER: EXOBIOLOGY; 28
Bank, B. POSTER: SPACE BIOMEDICINE; 98
Barker, P. POSTER: SPACE BIOLOGY; 49
Barlow, G.H. CELL BIOLOGY; 186
Barnett, J.G. MUSCULOSKELETAL SYSTEM; 163
Barnicott, P.T. POSTER: SPACE BIOMEDICINE; 129
Bartlett, D.S. BIOSPHERICS-I; 314
Bartlett, D.S. BIOSPHERICS-II; 331
Bartlett, K.B. BIOSPHERICS-III; 360
Bartlett, K.B. BIOSPHERICS-II; 331
Bascom, D. CARDIOPULMONARY PHYSIOLOGY-II; 143
Battles, A.H. POSTER: SPACE BIOLOGY; 38
Behrens, P. BIOMASS PRODUCTION-II; 256
Benjaminson, M.A. POSTER: SPACE BIOLOGY; 38
Benton, E.V. POSTER: SPACE BIOLOGY; 53
Bermudes, D. EXOBIOLOGY-IV; 347
Bernauer, E. POSTER SPACE BIOMEDICINE; 59
Berry, P. POSTER: SPACE BIOMEDICINE; 59
Berthoz, A. NEUROSCIENCE-II; 216
Black, S.D. POSTER: SPACE BIOLOGY; 41
Blackwell, C.C. POSTER: CELSS; 8
Blackwell, A.L. POSTER: CELSS; 8
Blanks, R.H.I. MICRO-G: UNDERSTANDING G-RECEPTORS; 193
Block, J. E. CALCIUM AND BONE PHYSIOLOGY-I; 140
Block, J. E. CALCIUM AND BONE PHYSIOLOGY-I; 140
Blomqvist, C.G. POSTER: SPACE BIOMEDICINE; 62
Blomqvist, C.G. POSTER: SPACE BIOMEDICINE; 60
Bolinger, J.L. EXOBIOLOGY-VI; 380
Bologna, N. POSTER: SPACE BIOMEDICINE; 76
Bond, M. POSTER SPACE BIOMEDICINE; 59
Booth, F.W. MUSCULOSKELETAL SYSTEM; 160
Borucki, W.J. EXOBIOLOGY-II; 282
Boyce, B.F. POSTER: SPACE BIOMEDICINE; 88
Brady, R.A. EXOBIOLOGY-VI; 380
Brannon, D. BIOSPHERICS-II; 326
Brannon, D. BIOSPHERICS-II; 331
Brass, J.A. POSTER: BIOSPHERICS; 2
Brooks, G. CALCIUM AND BONE PHYSIOLOGY-I; 140
Brown, A.H. POSTER: SPACE BIOLOGY; 44
Brown, J.W. HUMAN FACTORS-I; 286
Brownlee, D.E. EXOBIOLOGY-IV; 355
Bubenheim, D.L. POSTER: CELSS; 27
Buchanan, P. MUSCULOSKELETAL SYSTEM; 161
Buchanan, B.B. EXOBIOLOGY-III; 336
Buckey, J.C. POSTER: SPACE BIOMEDICINE; 62

Buckey, J.C. POSTER: SPACE BIOMEDICINE; 60
Bugbee, B. BIOMASS PRODUCTION-I; 248
Bugbee, B. BIOMASS PRODUCTION-I; 246
Bula, R.J. POSTER: CELSS; 9
Bula, R.J. POSTER: CELSS; 16
Bull, R.J. SPACE STATION ENVIRONMENTAL FACTORS; 178
Burr, J.B. EXOBIOLOGY-VI; 379
Burton, R.R. POSTER: SPACE BIOMEDICINE; 63
Butler, B.D. DECOMPRESSION SICKNESS; 148
Callahan, P.X. POSTER: SPACE BIOLOGY; 43
Campbell, W.F. BIOMASS PRODUCTION-I; 248
Campbell, W.F. POSTER: SPACE BIOLOGY; 47
Cannon, S.R. CARDIOPULMONARY PHYSIOLOGY-I; 146
Carle, G.C. EXOBIOLOGY-II; 270
Carle, G.C. POSTER: EXOBIOLOGY; 34
Carle, G.C. POSTER: EXOBIOLOGY; 28
Carle, G.C. EXOBIOLOGY-V; 368
Carle, G.C. EXOBIOLOGY-V; 366
Carman, J.G. BIOMASS PRODUCTION-I; 248
Carman, J.G. POSTER: SPACE BIOLOGY; 47
Carr, R.H. EXOBIOLOGY-IV; 349
Carter, V.H. POSTER: SPACE BIOMEDICINE; 64
Chang, S. POSTER: EXOBIOLOGY; 28
Chanton, J.P. BIOSPHERICS-II; 328
Chapman, D.K. POSTER: SPACE BIOLOGY; 44
Charles, J.B. POSTER: SPACE BIOMEDICINE; 60
Chelly, J. POSTER: SPACE BIOMEDICINE; 111
Chen, Y.M. POSTER: SPACE BIOMEDICINE; 65
Chidester, T.R. CREW FACTORS; 234
Chryssanthou, C.P. DECOMPRESSION SICKNESS; 149
Cintron, N.M. POSTER: SPACE BIOMEDICINE; 65
Cintron, N.M. SPACE STATION ENVIRONMENTAL FACTORS; 182
Cintron, N.M. FLUIDS AND ELECTROLYTES; 202
Clark, B.C. EXOBIOLOGY-V; 366
Clark, C. BIOSPHERICS-II; 326
Clark, C. BIOSPHERICS-II; 331
Clarke, B. POSTER: SPACE BIOLOGY; 45
Clearwater, Y.A. HUMAN FACTORS-II; 296
Clement, G. NEUROSCIENCE-II; 216
Cogoli, A. CELL BIOLOGY; 184
Cogoli, A. CELL BIOLOGY; 186
Cohen, B. NEUROSCIENCE-I; 211
Cohen, M. POSTER: SPACE BIOMEDICINE; 59
Cohen, R. J. CARDIOPULMONARY PHYSIOLOGY-II; 198
Conkin, J. POSTER: SPACE BIOMEDICINE; 68
Convertino, V.A. CARDIOPULMONARY PHYSIOLOGY-II; 200
Convertino, V.A. MUSCULOSKELETAL SYSTEM; 161
Coohill, T.P. POSTER: SPACE BIOLOGY; 53
Corey, R.B. POSTER: CELSS; 9
Coyne, L.M. POSTER: EXOBIOLOGY; 28
Coyne, L.M. EXOBIOLOGY-I; 261
Crampton, G.H. NEUROSCIENCE-I; 210
Crill, P.M. BIOSPHERICS-III; 360
Cronin, J.R. EXOBIOLOGY-IV; 348
Crow, R.B. EXOBIOLOGY-VI; 379
Cuellar, M.D. POSTER: CELSS; 11
Cullers, D.K. EXOBIOLOGY-VI; 382
Cutchis, P.N. POSTER: SPACE BIOMEDICINE; 71
D'Amelio, F. NEUROSCIENCE-I; 204
Dacey, J.W.H. BIOSPHERICS-I; 316
Dacey, J.W.H. BIOSPHERICS-I; 317
Dalton, B.P. POSTER: SPACE BIOLOGY; 45
Danellis, J. POSTER: SPACE BIOMEDICINE; 59
Dant, C. POSTER: SPACE BIOLOGY; 47

Daunton, N.G. NEUROSCIENCE-I; 204
DeRoshia, C. POSTER: SPACE BIOMEDICINE; 59
Deamer, D.W. EXOBIOLOGY-I; 263
Deich, W.T. EXOBIOLOGY-VI; 380
Demer, J. L. POSTER: SPACE BIOMEDICINE; 69
Diamond, S.G. POSTER: SPACE BIOMEDICINE; 95
Dillaman, R.M. CALCIUM AND BONE PHYSIOLOGY-II; 227
Dintenfass, L. POSTER: SPACE BIOMEDICINE; 75
Dintenfass, L. POSTER: SPACE BIOMEDICINE; 73
Ditunno, Jr., J.F. POSTER: SPACE BIOMEDICINE; 91
Dixon, R.S. EXOBIOLOGY-VI; 380
Dobie, T.G. POSTER: SPACE BIOMEDICINE; 76
Doerr, D.F. POSTER: SPACE BIOMEDICINE; 77
Dolkas, C. MUSCULOSKELETAL SYSTEM; 170
Dow, D. BIOSPHERICS-II; 331
Dow, D. BIOSPHERICS-II; 326
Dreschel, T.W. CELSS TECHNOLOGY; 304
Dudley, G. MUSCULOSKELETAL SYSTEM; 161
Duke, J. POSTER: SPACE BIOLOGY; 50
Dunlop, E.H. CELSS TECHNOLOGY; 309
Duvoisin, M. MUSCULOSKELETAL SYSTEM; 161
Dwyer, A. POSTER: SPACE BIOMEDICINE; 96
Eberhart, R.C. POSTER: SPACE BIOMEDICINE; 71
Eckberg, D.D. CARDIOPULMONARY PHYSIOLOGY-II; 198
Edgerton, V.R. MUSCULOSKELETAL SYSTEM; 172
Edgerton, V.R. MUSCULOSKELETAL SYSTEM; 161
Edwards, B.F. POSTER: SPACE BIOMEDICINE; 68
Ellis, S. POSTER: SPACE BIOMEDICINE; 106
Ellis, S. MUSCULOSKELETAL SYSTEM; 163
Ellis, S. POSTER SPACE BIOMEDICINE; 59
Ellis, S. MUSCULOSKELETAL SYSTEM; 168
Enzien, M. EXOBIOLOGY-IV; 346
Etlinger, J.D. POSTER: SPACE BIOMEDICINE; 135
Fares, Y. POSTER: CELSS; 386
Farhi, L.E. CARDIOPULMONARY PHYSIOLOGY-I; 145
Farhi, L.E. CARDIOPULMONARY PHYSIOLOGY-II; 143
Farley, J. MICRO-G: UNDERSTANDING G-RECEPTORS; 193
Fast, T.N. NEUROSCIENCE-I; 204
Fast, T.N. POSTER: SPACE BIOMEDICINE; 82
Fell, R.D. MUSCULOSKELETAL SYSTEM; 165
Ferris, J.P. EXOBIOLOGY-I; 264
Fisher, J. POSTER: SPACE BIOMEDICINE; 81
Fisher, W. POSTER: SPACE BIOMEDICINE; 76
Fitts, R.H. MUSCULOSKELETAL SYSTEM; 167
Flores, D. DECOMPRESSION SICKNESS; 153
Flores, J.F. MUSCULOSKELETAL SYSTEM; 161
Foster, C.F. EXOBIOLOGY-VI; 379
Foushee, H.C. CREW FACTORS; 234
Fox, S.W. EXOBIOLOGY-II; 273
Frey, M.A.B. MUSCULOSKELETAL SYSTEM; 161
Frey, M.A.B. CARDIOPULMONARY PHYSIOLOGY-II; 200
Frey, M.A.B. CARDIOPULMONARY PHYSIOLOGY-I; 142
Friedmann, E.I. EXOBIOLOGY-III; 343
Fritsch, J.M. CARDIOPULMONARY PHYSIOLOGY-II; 198
Fry, I.V. BIOMASS PRODUCTION-II; 258
Fuller, C.A. LIFE SCIENCE AND THE SPACE STATION; 240
Funk, G.A. POSTER: SPACE BIOLOGY; 43
Funk, G.A. POSTER: SPACE BIOLOGY; 48
Furman, J.M.R. POSTER: SPACE BIOMEDICINE; 128
Gaffney, F.A. POSTER: SPACE BIOMEDICINE; 62
Gallagher, J.P. NEUROSCIENCE-I; 206
Gardetto, P.R. MUSCULOSKELETAL SYSTEM; 167
Gasset, G. CELL BIOLOGY; 189
Genant, H.K. CALCIUM AND BONE PHYSIOLOGY-I; 140

Genant, H. K. CALCIUM AND BONE PHYSIOLOGY-I; 140
Gernhardt, M. DECOMPRESSION SICKNESS; 151
Gerth, W.A. DECOMPRESSION SICKNESS; 154
Gerth, W.A. DECOMPRESSION SICKNESS; 151
Gibson, Jr., E.K. EXOBIOLOGY-IV; 349
Gibson, L.A. IMMUNOLOGY AND HEMATOLOGY; 156
Gifford, R.M. PLANTS AND GRAVITY-I; 224
Gingoza, H.J. POSTER: SPACE BIOLOGY; 41
Ginnett, R.C. CREW FACTORS; 235
Giver, L.P. EXOBIOLOGY-II; 282
Goble, R.L. POSTER: SPACE BIOMEDICINE; 60
Goeschel, J.D. POSTER: CELSS; 386
Goldberg, J. POSTER: SPACE BIOMEDICINE; 69
Goldberger, A.L. POSTER: SPACE BIOMEDICINE; 78
Goldstein, G. DECOMPRESSION SICKNESS; 149
Graeber, C.R. HUMAN FACTORS-II; 296
Grams, R.R. POSTER: SPACE BIOMEDICINE; 81
Greenisen, M.C. HUMAN FACTORS-I; 287
Greenleaf, J. POSTER: SPACE BIOMEDICINE; 59
Grindeland, R.E. POSTER: SPACE BIOLOGY; 52
Grindeland, R.E. NEUROSCIENCE-I; 204
Grindeland, R.E. POSTER: SPACE BIOMEDICINE; 82
Grindeland, R.E. MUSCULOSKELETAL SYSTEM; 173
Grindeland, R.E. POSTER: SPACE BIOLOGY; 43
Groschel, D.H.M. SPACE STATION ENVIRONMENTAL FACTORS; 179
Gross, M.F. BIOSPHERICS-I; 319
Gross, M.F. BIOSPHERICS-I; 314
Gross, M.F. BIOSPHERICS-I; 318
Grover, L.M. MICRO-G: UNDERSTANDING G-RECEPTORS; 193
Gulkis, S. EXOBIOLOGY-VI; 379
Gunderson, L. BIOSPHERICS-II; 326
Gutkowska, J. POSTER: SPACE BIOMEDICINE; 111
Guy, H.J.B. POSTER: SPACE BIOMEDICINE; 84
Guy, H.J.B. POSTER: SPACE BIOMEDICINE; 102
Hackman, J.R. CREW FACTORS; 237
Hagan, Jr., W.J. EXOBIOLOGY-I; 264
Hall, C.R. POSTER: BIOSPHERICS; 3
Hardisky, M.A. BIOSPHERICS-I; 319
Hardisky, M.A. BIOSPHERICS-I; 314
Hardisky, M.A. BIOSPHERICS-I; 318
Harm, D.L. POSTER: SPACE BIOMEDICINE; 86
Harm, D.L. POSTER: SPACE BIOMEDICINE; 84
Harper, D.G. EXOBIOLOGY-VI; 378
Harper, D.G. EXOBIOLOGY-VI; 382
Harris, B.A. POSTER: SPACE BIOMEDICINE; 59
Harris, B.A. POSTER: SPACE BIOMEDICINE; 114
Harriss, R.C. BIOSPHERICS-III; 360
Harriss, R.C. BIOSPHERICS II; 331
Hart, S.G. HUMAN FACTORS-II; 298
Hartman, J.M. BIOSPHERICS-I; 314
Harvey, W.T. POSTER: SPACE BIOMEDICINE; 60
Hashiba, M. NEUROSCIENCES-II; 212
Hashim, Z.N. BIOMASS PRODUCTION-I; 248
Hashim, Z.N. POSTER: SPACE BIOLOGY; 47
Hauschka, E.O. MUSCULOSKELETAL SYSTEM; 172
Hauschka, E.O. MUSCULOSKELETAL SYSTEM; 161
Hayes, C. POSTER: SPACE BIOLOGY; 52
Helmreich, R.L. POSTER: SPACE BIOMEDICINE; 87
Henderson, R.F. SPACE STATION ENVIRONMENTAL FACTORS; 179
Henninger, D.L. POSTER: CELSS; 23
Herbert, M. MUSCULOSKELETAL SYSTEM; 161
Herbison, G.J. POSTER: SPACE BIOMEDICINE; 91
Herrick, R.E. POSTER: SPACE BIOLOGY; 57
Heywood-Cooksey, A.L. MUSCULOSKELETAL SYSTEM; 167

Himi, T. NEUROSCIENCE-I; 208
Hinds, K.L. POSTER: SPACE BIOLOGY; 48
Hinds, W.E. POSTER: SPACE BIOLOGY; 48
Hines, M.E. BIOSPHERICS-I; 320
Hinkle, C.R. CELSS TECHNOLOGY; 304
Hinkle, C.R. POSTER: BIOSPHERICS; 3
Hochstein, L.I. EXOBIOLOGY-III; 338
Hodgson, J.A. POSTER: SPACE BIOLOGY; 49
Hoffler, G.W. CARDIOPULMONARY PHYSIOLOGY-II; 200
Hogan, R. POSTER: SPACE BIOLOGY; 45
Holland, H.D. EXOBIOLOGY-II; 274
Hollick, M.F. POSTER: SPACE BIOMEDICINE; 124
Holt, G.R. POSTER: SPACE BIOMEDICINE; 88
Horrigan, D.J. POSTER: SPACE BIOMEDICINE; 68
Houtchens, B.A. POSTER: SPACE BIOMEDICINE; 89
Hrabeta, J. BIOMASS PRODUCTION-II; 258
Huang, C.H. EXOBIOLOGY-I; 264
Hullinger, R. L. POSTER: SPACE BIOMEDICINE; 124
Hymer, W.C. POSTER: SPACE BIOLOGY; 52
Igarashi, M. NEUROSCIENCE-I; 208
Irvine, W.M. EXOBIOLOGY-IV; 350
Ishii, M. NEUROSCIENCE-I; 208
Jaeger, C.H. POSTER: CELSS; 387
Jahnke, L.L. EXOBIOLOGY-III; 339
Jarisch, W.R. POSTER: SPACE BIOMEDICINE; 78
Jauchem, J.R. POSTER: SPACE BIOMEDICINE; 129
Jaweed, M.M. POSTER: SPACE BIOMEDICINE; 91
Jee, W.S.S. CALCIUM AND BONE PHYSIOLOGY-II; 229
Jefferson, N.E. BIOMASS PRODUCTION-I; 248
Jenkins, H. A. POSTER: SPACE BIOMEDICINE; 69
Jin, Z.M. POSTER: SPACE BIOMEDICINE; 81
Johnson, R.W. BIOSPHERICS-I; 314
Johnson, W.H. POSTER: SPACE BIOMEDICINE; 95
Johnson, Jr., P.C. FLUIDS AND ELECTROLYTES; 202
Johnson, Jr., P.C. IMMUNOLOGY AND HEMATOLOGY; 156
Johnson, Jr., P.C. IMMUNOLOGY AND HEMATOLOGY; 156
Jones, J.B. IMMUNOLOGY AND HEMATOLOGY; 156
Jones, H.W. EXOBIOLOGY-VI; 382
Jordan, J.C. EXOBIOLOGY-VI; 378
Jukes, T.H. EXOBIOLOGY-IV; 346
Kalla, L.M. POSTER: SPACE BIOLOGY; 38
Kanavarioti, A. POSTER: EXOBIOLOGY; 31
Karel, M. CELSS TECHNOLOGY; 305
Kasting, J.F. EXOBIOLOGY-V; 362
Kasting, G.A. CARDIOPULMONARY PHYSIOLOGY-II; 198
Katz, D. POSTER: SPACE BIOMEDICINE; 93
Katz, J. DECOMPRESSION SICKNESS; 148
Keefe, J.R. LIFE SCIENCE AND THE SPACE STATION; 241
Keil, L. POSTER: SPACE BIOMEDICINE; 59
Kendall, M. POSTER: SPACE BIOLOGY; 52
Kennedy, M.J. POSTER: SPACE BIOLOGY; 58
Kerridge, J.F. EXOBIOLOGY-II; 277
Khare, B. N. EXOBIOLOGY-III; 345
Kila, R. POSTER: CELSS; 8
King, G.M. BIOSPHERICS-I; 321
King, G.M. BIOSPHERICS-I; 316
Kirby, E.E. POSTER: SPACE BIOMEDICINE; 123
Kirienko, N.M. POSTER: SPACE BIOMEDICINE; 95
Klein, M.J. EXOBIOLOGY-VI; 379
Klein, M.J. EXOBIOLOGY-VI; 382
Klemas, V. BIOSPHERICS-I; 319
Klemas, V. BIOSPHERICS-I; 318
Klemas, V. BIOSPHERICS-I; 314
Knott, W.M. POSTER: CELSS; 23

Knott, W.M. POSTER: SPACE BIOLOGY; 38
Knott, W.M. POSTER: BIOSPHERICS; 3
Knott, W. M. POSTER: CELSS; 12
Knott, W.M. CELSS TECHNOLOGY; 304
Koch, K.L. POSTER: SPACE BIOMEDICINE; 96
Koch, K.L. POSTER: SPACE BIOMEDICINE; 86
Kohl, R.L. POSTER: SPACE BIOMEDICINE; 97
Kojiro, D.R. EXOBIOLOGY-II; 270
Kojiro, D.R. EXOBIOLOGY-V; 368
Kojiro, D.R. POSTER: EXOBIOLOGY; 36
Koller, A.M. POSTER: BIOSPHERICS; 3
Krauhs, J.M. FLUIDS AND ELECTROLYTES; 202
Krikorian, A.D. POSTER: CELSS; 388
Krikorian, A.D. LIFE SCIENCE AND THE SPACE STATION; 243
Kulecz, W.B. NEUROSCIENCE-I; 208
Lacey, Jr., J.C. EXOBIOLOGY-II; 278
Lambertsen, C.J. DECOMPRESSION SICKNESS; 153
Lane, L.D. POSTER: SPACE BIOMEDICINE; 60
Lane, L.D. POSTER: SPACE BIOMEDICINE; 62
Lang, M.T. POSTER: SPACE BIOLOGY; 38
Lange, R.D. IMMUNOLOGY AND HEMATOLOGY; 156
Lanyi, J.K. EXOBIOLOGY-III; 341
Laursen, R.A. EXOBIOLOGY-IV; 347
Lawless, J.G. BIOSPHERICS-II; 333
Leach, C.S. FLUIDS AND ELECTROLYTES; 202
Leatherman, N.E. DECOMPRESSION SICKNESS; 154
Leatherman, N.E. DECOMPRESSION SICKNESS; 151
Lederhendler, I.I. POSTER: SPACE BIOMEDICINE; 98
Lee, P.L. MUSCULOSKELETAL SYSTEM; 168
Lee, P.L. POSTER: SPACE BIOMEDICINE; 59
Lee, P.L. POSTER: SPACE BIOLOGY; 49
Legters, L. POSTER: BIOSPHERICS; 4
Leifeste, W.S. POSTER: SPACE BIOLOGY; 50
Leifeste, N.P. POSTER: SPACE BIOLOGY; 50
Lencki, W. POSTER: SPACE BIOLOGY; 43
Leon, H. POSTER: SPACE BIOLOGY; 45
Lestienne, F. NEUROSCIENCE-II; 216
Levine, J.S. EXOBIOLOGY-II; 280
Lewis, M.L. CELL BIOLOGY; 186
Lewis, M.R. NEUROSCIENCE-I; 206
Linscott, I.R. EXOBIOLOGY-VI; 379
LoTurco, J. POSTER: SPACE BIOMEDICINE; 98
Loyd, O.H. POSTER: SPACE BIOMEDICINE; 119
Lucot, J.B. NEUROSCIENCE-I; 210
Ludemann, R. POSTER: SPACE BIOMEDICINE; 135
Lujan, M.S. CARDIOPULMONARY PHYSIOLOGY-I; 146
MacElroy, R.D. EXOBIOLOGY-I; 266
MacElroy, R.D. POSTER: CELSS; 387
Macecek, M. POSTER: SPACE BIOMEDICINE; 389
Mack, H.M. POSTER: SPACE BIOLOGY; 41
Madden, S.C. EXOBIOLOGY-IV; 350
Magnuson, C.E. POSTER: CELSS; 387
Magnuson, C.E. POSTER: CELSS; 386
Magnuson, J.W. POSTER: CELSS; 386
Maguire, Jr., B. POSTER: CELSS; 13
Mancinelli, R.L. POSTER: EXOBIOLOGY; 33
Mancinelli, R.L. EXOBIOLOGY-V; 369
Mandel, A.D. POSTER: SPACE BIOMEDICINE; 116
Mandell, A.J. POSTER: SPACE BIOMEDICINE; 78
Manning, W.J. POSTER: SPACE BIOMEDICINE; 78
Manno, B.R. POSTER: SPACE BIOMEDICINE; 133
Manno, J.E. POSTER: SPACE BIOMEDICINE; 133
Mantel, S. POSTER: SPACE BIOMEDICINE; 71
Marcus, R. CALCIUM AND BONE PHYSIOLOGY-II; 229

Margulis, L. EXOBIOLOGY-IV; 346
Margulis, L. EXOBIOLOGY-IV; 347
Markham, C.H. POSTER: SPACE BIOMEDICINE; 95
Marshall, T. POSTER: SPACE BIOLOGY; 53
Martens, C.S. BIOSPHERICS-II; 328
Martin, B.G. POSTER: SPACE BIOMEDICINE; 123
Martin, T.P. MUSCULOSKELETAL SYSTEM; 161
Martinez, D. MUSCULOSKELETAL SYSTEM; 173
Matson, P.A. BIOSPHERICS-III; 358
May, J.G. POSTER: SPACE BIOMEDICINE; 76
McClellan, R.O. SPACE STATION ENVIRONMENTAL FACTORS; 179
McCourt, M. EXOBIOLOGY-I; 268
McFeters, G.A. SPACE STATION ENVIRONMENTAL FACTORS; 180
McGuire, T.F. SPACE STATION CREW FACTORS; 244
McKay, C.P. EXOBIOLOGY-V; 372
McKay, C.P. EXOBIOLOGY-V; 375
McKay, C.P. EXOBIOLOGY-II; 282
McKay, C.P. EXOBIOLOGY-IV; 352
McKay, C.P. POSTER: EXOBIOLOGY; 33
McKay, C.P. EXOBIOLOGY-V; 371
McKinney, C.J. POSTER: CELSS; 386
Meeker, L.J. POSTER: SPACE BIOMEDICINE; 63
Meyer, M.A. EXOBIOLOGY-III; 343
Mietus, J. POSTER: SPACE BIOMEDICINE; 78
Miller, A.D. POSTER: SPACE BIOMEDICINE; 101
Miller, S.L. EXOBIOLOGY-III; 344
Miller, S.L. EXOBIOLOGY-II; 282
Mitchell, C.A. POSTER: CELSS; 27
Mitchell, C.A. POSTER: CELSS; 11
Mondon, C.E. MUSCULOSKELETAL SYSTEM; 170
Money, K.E. NEUROSCIENCES-II; 222
Money, K.E. POSTER: SPACE BIOMEDICINE; 95
Moore, J. POSTER: SPACE BIOLOGY; 50
Moore, W.E. POSTER: SPACE BIOMEDICINE; 62
Morey-Holton, E. CALCIUM AND BONE PHYSIOLOGY-II; 226
Morrison, D.R. POSTER: CELSS; 388
Morrison, D.R. CELL BIOLOGY; 186
Morrison, P.R. MUSCULOSKELETAL SYSTEM; 160
Morrow, R.C. POSTER: CELSS; 16
Motter, K. POSTER: SPACE BIOLOGY; 52
Moyer, J.L. POSTER: SPACE BIOLOGY; 38
Muller, G. MUSCULOSKELETAL SYSTEM; 160
Mundy, G.R. POSTER: SPACE BIOMEDICINE; 88
Munsey, W.R. POSTER: CELSS; 23
Munsey, W.R. POSTER SPACE BIOLOGY; 38
Murray, B.G.J.P. EXOBIOLOGY-III; 345
Musacchia, X.J. MUSCULOSKELETAL SYSTEM; 165
Myers, K.J. POSTER: SPACE BIOMEDICINE; 119
Nagaoka, T. NEUROSCIENCES-II; 212
Nagel, D.C. HUMAN FACTORS-II; 297
Nakashima, T. EXOBIOLOGY-II; 273
Nakhost, Z. CELSS TECHNOLOGY; 305
Nedell, S.S. EXOBIOLOGY-V; 372
Nelson, G.A. POSTER: SPACE BIOLOGY; 53
Obar, R. EXOBIOLOGY-IV; 347
Oberbeck, V.R. EXOBIOLOGY-II; 270
O'Hara, B.J. EXOBIOLOGY-II; 282
O'Hara, B.J. EXOBIOLOGY-V; 366
O'Hara, B.J. EXOBIOLOGY-II; 270
O'Hara, D. Exobiology II; 270
Oliver, B.M. EXOBIOLOGY-VI; 382
Olsen, E.T. EXOBIOLOGY-VI; 380
Oman, C.M. POSTER: SPACE BIOMEDICINE; 103
Oman, C.M. POSTER: SPACE BIOLOGY; 55

Orenberg, J.B.	POSTER: EXOBIOLOGY; 28
Orr, L.S.	HUMAN FACTORS-I; 291
Owenson, B.	EXOBIOLOGY-I; 266
Packer, L.	BIOMASS PRODUCTION-II; 258
Palaia, T.	DECOMPRESSION SICKNESS; 149
Palmer, E.	HUMAN FACTORS-II; 297
Paris, J.F.	BIOSPHERICS-II; 333
Parker, D.E.	NEUROSCIENCE-II; 218
Parker, D.E.	NEUROSCIENCE-II; 220
Patel, S.	NEUROSCIENCE-I; 208
Patterson, C.O.	POSTER: CELSS; 18
Patterson-Buckendahl, P.	CALCIUM AND BONE PHYSIOLOGY-II; 226
Peck, G.	POSTER: SPACE BIOMEDICINE; 81
Pelletier, R.	BIOSPHERICS-II; 331
Pelletier, R.	BIOSPHERICS-II; 326
Pendergast, D.R.	CARDIOPULMONARY PHYSIOLOGY-II; 143
Pendergast, D.R.	CARDIOPULMONARY PHYSIOLOGY-I; 145
Peters, E.J.	POSTER: SPACE BIOMEDICINE; 117
Petersen, G.R.	CELSS TECHNOLOGY; 309
Peterson, A.M.	EXOBIOLOGY-VI; 379
Peterson, D.L.	BIOSPHERICS-III; 358
Peterson, D.L.	POSTER: BIOSPHERICS; 5
Phelan, K.D.	NEUROSCIENCE-I; 206
Phillips, J.B.	POSTER: EXOBIOLOGY; 34
Philput, C.	POSTER: SPACE BIOMEDICINE; 93
Pierce, C.M.	SPACE STATION CREW FACTORS; 244
Pierce, L.	BIOSPHERICS-III; 358
Pierce, L.	POSTER: BIOSPHERICS; 5
Pierson, D.L.	SPACE STATION ENVIRONMENTAL FACTORS; 182
Pierson, D.L.	SPACE STATION ENVIRONMENTAL FACTORS; 181
Pisarello, J.	DECOMPRESSION SICKNESS; 153
Pizzarello, S.	EXOBIOLOGY-IV; 348
Planel, H.	CELL BIOLOGY; 189
Pogue, W.R.	HUMAN FACTORS-I; 292
Pohorille, A.	EXOBIOLOGY-I; 266
Porter, F. I.	POSTER: SPACE BIOMEDICINE; 69
Prince, R.P.	CELSS TECHNOLOGY; 311
Prince, R.P.	CELSS TECHNOLOGY; 304
Prince, M.J.	POSTER: SPACE BIOMEDICINE; 117
Prisk, G.K.	POSTER: SPACE BIOMEDICINE; 102
Prisk, G.K.	POSTER: SPACE BIOMEDICINE; 84
Propert, D.	POSTER: SPACE BIOMEDICINE; 93
Provancha, J.A.	POSTER: BIOSPHERICS; 3
Provancha, M.J.	POSTER: BIOSPHERICS; 3
Putcha, L.	POSTER: SPACE BIOMEDICINE; 65
Pyle, B.H.	SPACE STATION ENVIRONMENTAL FACTORS; 180
Radin, E. L.	CALCIUM AND BONE PHYSIOLOGY-II; 231
Radmer, R.	BIOMASS PRODUCTION-II; 256
Rague, B.W.	POSTER: SPACE BIOMEDICINE; 103
Raper, Jr., C.D.	BIOMASS PRODUCTION-1; 254
Raphan, T.	NEUROSCIENCE-I; 211
Raup, D.M.	EXOBIOLOGY-V; 364
Reaven, G.	MUSCULOSKELETAL SYSTEM; 170
Redetzki, H.M.	POSTER: SPACE BIOMEDICINE; 133
Rein, R.	EXOBIOLOGY-I; 268
Remington, R.	HUMAN FACTORS-II; 297
Reschke, M.F.	NEUROSCIENCE-II; 218
Reschke, M.F.	NEUROSCIENCE-II; 220
Reschke, M.F.	POSTER: SPACE BIOMEDICINE; 84
Rice, A.	EXOBIOLOGY-I; 261
Richards, K.L.	CARDIOPULMONARY PHYSIOLOGY-I; 146
Richoilley, G.	CELL BIOLOGY; 189
Riggan, P.	POSTER: BIOSPHERICS; 2
Rigney, D.R.	POSTER: SPACE BIOMEDICINE; 78

Riley, D.A. POSTER: SPACE BIOMEDICINE; 106
Riley, D.A. MUSCULOSKELETAL SYSTEM; 163
Robinson, E. POSTER: SPACE BIOLOGY; 45
Rodnick, K. MUSCULOSKELETAL SYSTEM; 170
Roer, R.D. CALCIUM AND BONE PHYSIOLOGY-II; 227
Rossberg, K. POSTER: SPACE BIOLOGY; 57
Roy, R.R. MUSCULOSKELETAL SYSTEM; 161
Roy, R.R. MUSCULOSKELETAL SYSTEM; 172
Rummel, J.D. CELSS SYSTEMS ENGINEERING; 301
Rummel, J.D. CELSS SYSTEMS ENGINEERING; 300
Running, S.W. POSTER: BIOSPHERICS; 5
Running, S.W. BIOSPHERICS-III; 358
Russo, D.M. SPACE STATION ENVIRONMENTAL FACTORS; 181
Russo, D.M. SPACE STATION ENVIRONMENTAL FACTORS; 182
Rutherford, E. CALCIUM AND BONE PHYSIOLOGY-II; 227
Sagan, C. EXOBIOLOGY-III; 345
Sager, J.C. CELSS TECHNOLOGY; 304
Sager, J.C. BIOMASS PRODUCTION-I; 250
Salisbury, F.B. BIOMASS PRODUCTION-I; 246
Sampson, O. POSTER: SPACE BIOMEDICINE; 108
Sanders, K.H. POSTER: SPACE BIOMEDICINE; 71
Santy, P.A. SPACE STATION CREW FACTORS; 245
Satyanaranyana, T. POSTER: SPACE BIOMEDICINE; 82
Sauer, R.L. SPACE STATION ENVIRONMENTAL FACTORS; 182
Sauer, R.L. POSTER: CELSS; 388
Scattergood, T.W. EXOBIOLOGY-II; 270
Scattergood, T.W. POSTER: EXOBIOLOGY; 28
Scattergood, T.W. EXOBIOLOGY-II; 282
Scheld, H.W. POSTER: CELSS; 386
Scheld, H.W. POSTER: CELSS; 388
Schimmerling, W. POSTER: SPACE BIOMEDICINE; 121
Schmalzer, P.A. POSTER: BIOSPHERICS; 3
Schmedtje, Jr., J.F. POSTER: SPACE BIOMEDICINE; 111
Schmidt, K. POSTER: SPACE BIOMEDICINE; 69
Schubert, W.W. POSTER: SPACE BIOLOGY; 53
Schwartz, D.E. EXOBIOLOGY-IV; 352
Scott, K.W. POSTER: CELSS; 20
Scruby, R.R. POSTER: CELSS; 388
Sebacher, D.I. BIOSPHERICS-III; 360
Sebacher, D.I. BIOSPHERICS II; 331
Sebesta, P.D. POSTER: BIOSPHERICS; 7
Sebesta, P.D. POSTER: BIOSPHERICS; 4
Sedlak, F.R. POSTER: SPACE BIOMEDICINE; 106
Selzer, R.H. POSTER SPACE BIOMEDICINE; 59
Selzer, R.H. MUSCULOSKELETAL SYSTEM; 168
Sepkoski, J. J. EXOBIOLOGY-V; 365
Seshan, P.K. CELSS TECHNOLOGY; 309
Shangraw, R.E. POSTER: SPACE BIOMEDICINE; 117
Shaw, S. MUSCULOSKELETAL SYSTEM; 173
Shen, Y.Z. POSTER: SPACE BIOMEDICINE; 81
Sheridan, P.J. POSTER: SPACE BIOMEDICINE; 88
Sherrill, D.L. CARDIOPULMONARY PHYSIOLOGY-I; 147
Shibata, M. EXOBIOLOGY-I; 268
Shinnick-Gallagher, P. NEUROSCIENCE-I; 206
Shipp, R. EXOBIOLOGY-I; 261
Shubert, L.E. POSTER: CLESS; 386
Silver, B.B. POSTER: SPACE BIOMEDICINE; 114
Silver, G. POSTER: SPACE BIOMEDICINE; 135
Skinner, J.E. POSTER: SPACE BIOMEDICINE; 111
Slocum, G.R. POSTER: SPACE BIOMEDICINE; 106
Smead, K.W. POSTER: SPACE BIOMEDICINE; 129
Smith, R. CALCIUM AND BONE PHYSIOLOGY-I; 140
Sonnenfeld, G. POSTER: SPACE BIOMEDICINE; 116
Souza, K.A. POSTER: SPACE BIOLOGY; 41

Spangenberg, D.B. POSTER: SPACE BIOLOGY; 55
Spangenberg, D. POSTER: SPACE BIOLOGY; 57
Spanner, M.A. POSTER: BIOSPHERICS; 5
Spanner, M.A. BIOSPHERICS-III; 358
Steffen, J.M. MUSCULOSKELETAL SYSTEM; 165
Steiger, P. CALCIUM AND BONE PHYSIOLOGY-I; 140
Steiger, S. CALCIUM AND BONE PHYSIOLOGY-I; 140
Steiger, P. CALCIUM AND BONE PHYSIOLOGY-I; 140
Stenger, R.J. DECOMPRESSION SICKNESS; 149
Stern, R.M. POSTER: SPACE BIOMEDICINE; 96
Stern, R.S. POSTER: SPACE BIOMEDICINE; 86
Stevens, B.R. POSTER: SPACE BIOLOGY; 38
Stoker, C.R. EXOBIOLOGY-IV; 352
Stribling, R. EXOBIOLOGY-III; 344
Stuart, C.A. POSTER: SPACE BIOMEDICINE; 117
Surdyka, D. POSTER: SPACE BIOLOGY; 57
Swales, S.M. POSTER: SPACE BIOLOGY; 41
Swanberg, N. BIOSPHERICS-III; 358
Swanson, G.D. CARDIOPULMONARY PHYSIOLOGY-I; 147
Takabayashi, A. NEUROSCIENCES-II; 212
Takagi, S. NEUROSCIENCES-II; 212
Takeuchi, N. POSTER: EXOBIOLOGY; 36
Tanaka, M. NEUROSCIENCES-II; 212
Tarter, J.C. EXOBIOLOGY-VI; 382
Taylor, A.A. POSTER: SPACE BIOMEDICINE; 111
Templier, J. CELL BIOLOGY; 189
Thomason, D.B. POSTER: SPACE BIOLOGY; 57
Thompson, W. R. EXOBIOLOGY-III; 345
Thornton, W. POSTER: SPACE BIOMEDICINE; 78
Tibbitts, T. W. BIOMASS PRODUCTION-I; 252
Tibbitts, T.W. POSTER: CELSS; 26
Tibbitts, T.W. POSTER: CELSS; 16
Tibbitts, T.W. POSTER: CELSS; 9
Tietjen, G. POSTER: SPACE BIOLOGY; 52
Tietjen, G. CALCIUM AND BONE PHYSIOLOGY-II; 226
Timm, M.G. POSTER: CELSS; 23
Tipton, D.A. POSTER: SPACE BIOMEDICINE; 119
Tixador, R. CELL BIOLOGY; 189
Todd, P. CELL BIOLOGY; 186
Tolley-Henry, L. BIOMASS PRODUCTION-1; 254
Tollinger, C.D. POSTER: SPACE BIOLOGY; 48
Townsend, L.W. POSTER: SPACE BIOMEDICINE; 121
Tredici, T.J. POSTER: SPACE BIOMEDICINE; 123
Tripplett, R.G. POSTER: SPACE BIOMEDICINE; 88
Tschopp, A. CELL BIOLOGY; 186
Tsou, P. EXOBIOLOGY-IV; 355
Tzertzinis, G. EXOBIOLOGY-IV; 347
Unsworth, B.R. MUSCULOSKELETAL SYSTEM; 167
Vailas, A.C. MUSCULOSKELETAL SYSTEM; 173
Valentin, J.R. POSTER: EXOBIOLOGY; 34
Valentin, J.R. EXOBIOLOGY-II; 270
Vandenburgh, H.H. MUSCULOSKELETAL SYSTEM; 175
Vanderploeg, J.M. POSTER: SPACE BIOMEDICINE; 65
Vanderploeg, J.M. NEUROSCIENCE-II; 220
Vann, R.D. DECOMPRESSION SICKNESS; 151
Vann, R.D. DECOMPRESSION SICKNESS; 154
Vasey, M. POSTER: SPACE BIOMEDICINE; 96
Vasques, M. POSTER: SPACE BIOMEDICINE; 82
Vasques, M. POSTER: SPACE BIOLOGY; 52
Vecera, T. POSTER: CELSS; 8
Vellinger, J. C. POSTER: SPACE BIOMEDICINE; 124
Venketeswaran, S. POSTER: CELSS; 23
Vidulich, M.A. HUMAN FACTORS-II; 298
Vieville, T. NEUROSCIENCE-II; 216

Volk, T. CELSS SYSTEMS ENGINEERING; 301
Volk, T. CELSS SYSTEMS ENGINEERING; 300
Volkweiss, S.J. POSTER: CELSS; 9
Volz, P.A. POSTER: SPACE BIOLOGY; 58
Vykukal, H.C. HUMAN FACTORS-II; 299
Wade, C. POSTER SPACE BIOMEDICINE; 59
Wade, T.D. POSTER: SPACE BIOMEDICINE; 126
Wakeham, S.G. BIOSPHERICS-I; 316
Wakeham, S.G. BIOSPHERICS-I; 322
Waligora, J.M. POSTER: SPACE BIOMEDICINE; 68
Wall, C. POSTER: SPACE BIOMEDICINE; 128
Washino, R.K. POSTER: BIOSPHERICS; 7
Washino, R.K. BIOSPHERICS-II; 333
Watanabe, S. NEUROSCIENCES-II; 212
Watenpaugh, D.E. POSTER: SPACE BIOMEDICINE; 60
Watenpaugh, D.E. POSTER: SPACE BIOMEDICINE; 62
Watt, D.G.D. POSTER: SPACE BIOMEDICINE; 95
Watt, D.G.D. NEUROSCIENCES-II; 222
Webb, J.T. POSTER: SPACE BIOMEDICINE; 129
Webbon, B.W. HUMAN FACTORS-II; 299
Weber, A.L. EXOBIOLOGY-II; 284
Webster, L. POSTER: SPACE BIOMEDICINE; 130
West, J.B. POSTER: SPACE BIOMEDICINE; 84
West, J.B. POSTER: SPACE BIOMEDICINE; 102
Wharton, R.A. EXOBIOLOGY-V; 375
Whedon, G.D. CALCIUM AND BONE PHYSIOLOGY-I; 141
Wheeler, R.M. POSTER: CELSS; 26
Wheeler, R.M. BIOMASS PRODUCTION-I; 60
White, D.H. POSTER: EXOBIOLOGY; 31
Whitesides, S.K. BIOMASS PRODUCTION-I; 248
Wilhelm, J.A. POSTER: SPACE BIOMEDICINE; 87
Williams, J. POSTER: SPACE BIOMEDICINE; 116
Williams, P. POSTER: SPACE BIOMEDICINE; 93
Williams, M.R. POSTER: SPACE BIOLOGY; 58
Wilmot, C. CALCIUM AND BONE PHYSIOLOGY-I; 140
Wilson, J.W. POSTER: SPACE BIOMEDICINE; 121
Wilson, J.O. BIOSPHERICS-III; 360
Woeller, F.H. POSTER: EXOBIOLOGY; 36
Wolf, P.L. BIOSPHERICS-I; 319
Wolf, P.L. BIOSPHERICS-I; 318
Wolfe, R.R. POSTER: SPACE BIOMEDICINE; 117
Wong, M. POSTER: SPACE BIOMEDICINE; 121
Wood, B. POSTER: BIOSPHERICS; 7
Wood, B. POSTER: BIOSPHERICS; 4
Wood, C.D. POSTER: SPACE BIOMEDICINE; 133
Wood, M.J. POSTER: SPACE BIOMEDICINE; 133
Woolford, B. HUMAN FACTORS-I; 293
Yeh, H.C. SPACE STATION ENVIRONMENTAL FACTORS; 179
Yost, B.D. POSTER: CELSS; 23
Young, L.R. NEUROSCIENCE-I; 214
Yu, F.S. POSTER: SPACE BIOMEDICINE; 81
Yuen, G.U. EXOBIOLOGY-IV; 348
Zbinden, E.A. EXOBIOLOGY-II; 274
Zeman, R.J. POSTER: SPACE BIOMEDICINE; 135
Zernicke, R.F. MUSCULOSKELETAL SYSTEM; 173
Ziurys, L.M. EXOBIOLOGY-IV; 350

END DATE FEB 2, 1993